POLITECNICO DI MILANO

DEPARTMENT OF CIVIL AND ENVIRONMENTAL ENGINEERING – Environmental Section

AWARE – *Assessment on Waste and Resources – Research group*

Assessment on WAste and REsources

LITERATURE REVIEW ON THE ASSESSMENT OF THE CARBONATION POTENTIAL OF LIME IN DIFFERENT MARKETS AND BEYOND

Customer: EuLA – the European Lime Association

Authors:

Prof. Mario Grosso (Principal Investigator)

Eng. Laura Biganzoli, Francesco Pietro Campo, Sara Pantini, Camilla Tua

July 2020

Report n. 845.0202.70.02

To refer to this report, please use the following reference:

Grosso M., Biganzoli L., Campo F. P., Pantini S., Tua C. 2020. Literature review on the assessment of the carbonation potential of lime in different markets and beyond. Report prepared by Assessment on Waste and Resources (AWARE) Research Group at Politecnico di Milano (PoliMI), for the European Lime Association (EuLA). Pp. 333.

CHAPTER	AUTHORS
1 EXECUTIVE SUMMARY	F. P. Campo, C. Tua, M. Grosso
2 METHODOLOGY AND SCOPE OF THE WORK	F. P. Campo, M. Grosso
3 INTRODUCTION: LIME USE AND APPLICATIONS	F. P. Campo, M. Grosso
3.1 USE OF LIME IN IRON AND STEEL INDUSTRY	L. Biganzoli, M. Grosso
3.2.1 USE OF LIME IN SAND LIME BRICK APPLICATION	C. Tua, M. Grosso
3.2.2 USE OF LIME IN LIGHT-WEIGHT LIME CONCRETE	C. Tua, M. Grosso
3.2.3 USE OF LIME IN MORTARS	F. P. Campo, M. Grosso
3.2.4 USE OF LIME IN HEMP LIME	F. P. Campo, M. Grosso
3.2.5 USE OF LIME IN OTHER CONSTRUCTION MATERIALS	F. P. Campo, M. Grosso
3.3.1 USE OF LIME IN SOIL STABILISATION	F. P. Campo, C. Tua, M. Grosso
3.3.2 USE OF LIME IN ASPHALT PAVEMENTS	F. P. Campo, M. Grosso
3.4.1 USE OF LIME IN DRINKING WATER TREATMENT	C. Tua, M. Grosso
3.4.2 USE OF LIME IN WASTEWATER TREATMENT PLANT	C. Tua, M. Grosso
3.4.3 USE OF LIME IN SLUDGE TREATMENT	C. Tua, M. Grosso
3.4.4 USE OF LIME IN FLUE GAS CLEANING SYSTEMS	L. Biganzoli, C. Tua, M. Grosso
3.4.5 USE OF LIME IN OTHER ENVIRONMENTAL PROTECTION APPLICATIONS	C. Tua, F. P. Campo, M. Grosso
3.5.1 USE OF LIME IN FERTILISER	C. Tua, M. Grosso
3.5.2 USE OF LIME IN OTHER AGRICULTURE APPLICATIONS	F. P. Campo, M. Grosso
3.6.1 USE OF LIME IN CALCIUM CARBIDE	F. P. Campo, M. Grosso
3.6.2 USE OF LIME IN OTHER CHEMICAL INDUSTRY APPLICATIONS	F. P. Campo, M. Grosso
3.7.1 USE OF LIME IN THE NON-FERROUS METALLURGY	L. Biganzoli, M. Grosso
3.7.2 USE OF LIME IN THE TREATMENT OF THE RED GYPSUM FROM TITANIUM DIOXIDE INDUSTRY	L. Biganzoli, M. Grosso
3.7.3 USE OF LIME IN THE ALUMINIUM PRODUCTION PROCESS	L. Biganzoli, M. Grosso
3.7.4 USE OF LIME IN OTHER INDUSTRIAL CONSUMERS APPLICATIONS	F. P. Campo, M. Grosso
3.8 USE OF LIME IN THE PULP AND PAPER	S. Pantini, M. Grosso
4. CONCLUSIONS OF THE LITERATURE REVIEW ON LIME CARBONATION	F. P. Campo, C. Tua, M. Grosso
ANNEX A – APPLICATIONS WITH CONCLUSIVE INFORMATION ON CARBONATION	F. P. Campo, M. Grosso
ANNEX B – LIST OF OPTIMAL pH-RANGE IN SOIL	C. Tua, M. Grosso
ANNEX C - LITERATURE REVIEW ABOUT THE EFFECT OF LIMING ON SOC LEVELS FOR THE EUROPEAN CONTEXT	C. Tua, M. Grosso
ANNEX D - CARBONATION OF CEMENT	F. P. Campo, M. Grosso

TABLE OF CONTENTS

LIST OF ABBREVIATIONS 1
LIST OF DEFINITIONS 4
1 EXECUTIVE SUMMARY 6
2 METHODOLOGY AND SCOPE OF THE WORK 12
3. INTRODUCTION: LIME USE AND APPLICATIONS 16
3.1 USE OF LIME IN IRON AND STEEL INDUSTRY 18
3.2 USE OF LIME IN CONSTRUCTION MATERIALS 61
3.2.1 USE OF LIME IN SAND LIME BRICK 61
3.2.2 USE OF LIME IN LIGHT-WEIGHT LIME CONCRETE - AUTOCLAVED AERATED CONCRETE 66
3.2.3 USE OF LIME IN MORTARS 76
3.2.4 USE OF LIME IN HEMP LIME 80
3.2.5 USE OF LIME IN OTHER CONSTRUCTION MATERIALS 92
3.3 USE OF LIME IN CIVIL ENGINEERING 93
3.3.1 USE OF LIME IN SOIL STABILISATION 93
3.3.2 USE OF LIME IN ASPHALT PAVEMENTS 102
3.4 USE OF LIME IN ENVIRONMENTAL PROTECTION 106
3.4.1 USE OF LIME IN DRINKING WATER TREATMENT 106
3.4.2 USE OF LIME IN WASTEWATER TREATMENT PLANT - BIOSOLIDS AND INDUSTRIAL SLUDGE APPLICATIONS 113
3.4.3 USE OF LIME IN SLUDGE TREATMENT - DREDGING SEDIMENTS TREATMENTS 121
3.4.4 USE OF LIME IN THE FLUE GAS CLEANING SYSTEMS 127
3.4.5 USE OF LIME IN OTHER ENVIRONMENTAL PROTECTION APPLICATION 148
3.5 USE OF LIME IN AGRICULTURE APPLICATIONS 153
3.5.1 USE OF LIME IN FERTILISERS 153
3.5.2 USE OF LIME IN OTHER AGRICULTURE APPLICATIONS 173
3.6 USE OF LIME IN THE CHEMICAL INDUSTRY 174
3.6.1 USE OF LIME IN CALCIUM CARBIDE 174
3.6.2 USE OF LIME IN OTHER CHEMICAL INDUSTRY APPLICATIONS 177
3.7 USE OF LIME IN OTHER INDUSTRIAL CONSUMERS 178
3.7.1. USE OF LIME IN THE NON-FERROUS METALLURGY 178
3.7.2. USE OF LIME IN THE TREATMENT OF THE RED GYPSUM FROM TITANIUM DIOXIDE INDUSTRY 225
3.7.3. USE OF LIME IN THE ALUMINIUM PRODUCTION PROCESS 237
3.7.4 USE OF LIME IN OTHER INDUSTRIAL CONSUMERS APPLICATIONS 258
3.8. USE OF LIME IN THE PULP AND PAPER - PRECIPITATED CALCIUM CARBONATE (PCC) PRODUCTION 259

4. CONCLUSIONS OF THE LITERATURE REVIEW ON LIME CARBONATION 285
ANNEX A – APPLICATIONS WITH CONCLUSIVE INFORMATION ON CARBONATION 305
ANNEX B - LIST OF OPTIMAL pH-RANGE IN SOIL 315
ANNEX C - LITERATURE REVIEW ABOUT THE EFFECT OF LIMING ON SOC LEVELS FOR THE EUROPEAN CONTEXT 316
ANNEX D – CARBONATION OF CEMENT 321

LIST OF ABBREVIATIONS

AAC: Autoclaved Aerated Concrete

AC: Accelerated Carbonation

ACBF: Air Cooled Blast Furnace

ACC: Accelerated Carbonation Curing

ACT: Accelerated Carbonation Technology

AMD: Acid Mine Drainage

ANC: Acid Neutralization/Neutralizing Capacity

AOD: Argon Oxygen Decarburization

APCR: Air Pollution Control Residues

BAT: Best Available Techniques

BF: Blast Furnace

BFS: Blast Furnace Slag

BHC: Blended Hydraulic slag Cement

BOD: Biochemical Oxygen Demand

BOF: Basic Oxygen Furnace

BOS: Basic Oxygen Steel

BREF: Best Available Techniques Reference Document

CAH: Calcium-Aluminate-Hydrates

CAPCON: CAPture and CONversion

CCE: Calcium Carbonate Equivalent

CCM: Carbon Capture Machine

CL: Carbide Lime

CLSM: Controlled Low-Strength Material

COD: Chemical Oxygen Demand

CR: Carbonation Rate

CS: Carbon Steel

CSH: Calcium-Silicate-Hydrates

De-S slag: Desulphurization slag

DM: Dry Matter

EAACA: European Autoclaved Aerated Concrete Association

EAF C: Electric Arc Furnace for Carbon steel production

EAF: Electric Arc Furnace

EC: Enhanced Carbonation

ENEA: Agenzia nazionale per le nuove tecnologie, l'energia e lo sviluppo economico sostenibile (Italian National Agency for new technologies, energy and sustainable economic development)

EU: European Union

EuLA: European Lime Association with members across European Union including the United Kingdom

FA: Fly Ash

FGC: Flue Gas Cleaning

FGD: Flue Gas Desulphurization

FGT: Flue Gas Treatment

GCC: Ground Calcium Carbonate

GGBF: Ground Granulated Blast Furnace

GGBS: Ground Granulated Blast-furnace Slag

GHG: Greenhouse Gas

HDS: High-Density Sludge

HG: Hydrogarnet

HMA: Hot Mix Asphalt

ICL: Initial Consumption of Lime

IPCC: Intergovernmental Panel on Climate Change

ISC: Indoor Standard Condition

JRC: Joint Research Centre

KoM: Kick Off Meeting

L/S: Liquid/Solid

LCA: Life Cycle Assessment

LCO_2: Loss of CO_2

LD: Linz Donawitz

LF: Ladle Furnace

LHC: Lime Hemp Concrete

M-LS: Manufactured-Limestone

NC: Natural Carbonation

OC: Organic Carbon (for chapter 3.5 and ANNEX C)

OC: Outdoor exposed Condition (for chapter 3.2.4)

OPC: Ordinary Portland Cement

P: Pressure

PC: Portland Cement

PCA: Principal Component Analysis

PCC: Precipitated Calcium Carbonate

PCC-A: Precipitated Calcium Carbonate Admixture

PGM: Platinum Group Metals

PoliMI: Politecnico di Milano

PP: Polypropylene

RH: Relative Humidity

S/S: Stabilization/Solidification

SAS: Sodium Aluminosilicates

SCC: Speciality Calcium Carbonate

SCM: Supplementary Cementitious Materials

SEM: Scanning Electron Microscope

SLB: Sand Lime Brick

SOC: Soil Organic Carbon

SS: Stainless Steel

T: Temperature

TCA: Tri-Calcium Aluminate

TGA: Thermo-Gravimetric Analysis

TOC: Total Organic Carbon

UK: United Kingdom

US: United States

VOD: Vacuum Oxygen Decarburization

WWTP: Wastewater Treatment Plant

XRD: X-Ray Diffraction

LIST OF DEFINITIONS

Applications with conclusive scientific data on carbonation: those where the amount of literature published on carbonation allows for statistical treatment or the results presented are consistent throughout these publications/reports to establish the carbonation rate being natural or enhanced.

Applications with less conclusive scientific data on carbonation: those where the amount of literature published on carbonation is insufficient to allow data comparability, thus the outcome is less conclusive to establish any carbonation rates (natural or enhanced).

Calcination: the heating of a substance at controlled high temperature. In this report, the term calcination is referred to the heating of limestone or other rocks composed mainly of calcium carbonate ($CaCO_3$) to produce quicklime or burnt lime, i.e. calcium oxide (CaO). During the thermal decomposition (calcination) of $CaCO_3$ two product are produced being CaO and CO_2.

Carbonated lime: the part of lime which has been transformed to $CaCO_3$ (carbonates) through reaction with carbon dioxide (CO_2).

Carbonation constant (K): parameter of the equation which expresses the progression of the carbonation by its depth related to time (t) for construction materials: $carbonation\ depth = K\sqrt{t}$.

Carbonation depth: the distance from the surface of lime to where the lime is low or not carbonated. It is measured through the phenolphthalein solution test and is expressed in mm.

Carbonation rate: the percentage ratio between the amount of CO_2 absorbed during carbonation and the amount of process CO_2 emitted during calcination.

Enhanced carbonation: the process by which the carbonation is fostered under enhanced carbon dioxide concentration, and/or by optimized process parameters such as the temperature, the relative humidity, the surface reactivity area, the pH and others, depending on the reaction matrix in the solid, water or gaseous phase. Thus, the time of carbonation is reduced.

Lime: in this report, it refers to both quicklime and slaked lime.

Natural carbonation: the process by which lime reacts spontaneously with carbon dioxide producing calcium carbonate ($CaCO_3$) which stores it permanently. The reaction is exothermal and therefore thermodynamically favourable. Depending on the reaction matrix solid, water of gaseous, the CO_2 can come from the atmosphere, from water or from any other source.

Process CO_2: is the CO_2 released by the decomposition of $CaCO_3$ in CaO and CO_2. When referring to process CO_2 the release from fuels combustion is not taken into account, since this is strongly dependent on the type of energy used.

Quicklime or burnt lime: calcium oxide (CaO), the product of calcination.

Slaked lime or hydrated lime: calcium hydroxide ($Ca(OH)_2$), the product of the reaction between quicklime and water.

1 EXECUTIVE SUMMARY

The lime sector is facing multiple market, policy and customer challenges. To be able to address these challenges EuLA has developed a 2050 vision, 'Lime sector will be Carbon Negative by 2050' (EuLA 2020, Annual report. Pp. 31-33). To address Pillar 2 of this vision, EuLA's objective is to map the CO_2 carbonated during the use of lime products in multiple applications. To be able to provide robust scientific and technical evidence to these challenges, EuLA has requested Politecnico di Milano, Department of Civil and Environmental Engineering, to conduct an extensive literature review (peer-review, publications, industry reports, BREFs, …) to assess the overall carbonation rate for all the applications using lime. This vision is consistent with the "European Green Deal" Communication and the consequent "Proposal for a Regulation of the European Parliament and of the Council establishing the framework for achieving climate neutrality and amending Regulation (EU) 2018/1999" which sets the climate neutrality around 2050 as a long-term goal for the European Union, i.e. the balance between emissions and removals compensating not only the remaining emission of CO_2 but also of all greenhouse gases.

The scope of the work is to assess the carbonation rate of lime in different applications by reviewing the available literature on the topic.

Carbonation is the reaction of lime with CO_2 forming calcium carbonate ($CaCO_3$), thus allowing to remove CO_2 from the atmosphere and store it permanently. The reaction is exothermic and therefore thermodynamically favourable. Through carbonation, lime can reabsorb part of the CO_2 previously emitted during calcination. The ratio between the amount of CO_2 absorbed during carbonation and the amount emitted during calcination is the carbonation rate. In the applications where lime gets fully carbonated, the carbonation rate is 100% and the lime application can be considered carbon neutral since the CO_2 emitted during calcination, excluding fuel combustion emission, is completely reabsorbed. In this work, the carbonation potential rate is assessed in natural conditions (i.e. under ambient carbon dioxide concentration) and in enhanced conditions (i.e. under enhanced carbon dioxide concentration and by optimising other parameters such as the temperature and the relative humidity).

Following the kind invitation received by EuLA (European Lime Association), the AWARE Group of Politecnico di Milano (Department of Civil and Environmental Engineering) performed a comprehensive review about the carbonation potential of lime in its main market sectors. The final objective of the work is to understand to what extent the unavoidable CO_2 emission in the production of lime due to the calcination process (assumed equal to 786 kg per tonne of CaO, excluding those

associated with the consumption of fuel) is later captured by recarbonation during the lifetime of the products where lime is used.

The market share of the applications where lime (CaO) is used was provided by EuLA for the European Union including the United Kingdom (UK) in 2018 as shown in Figure 1.1. These main applications are subdivided in sub-applications as reported in Table 1.1, with their respective lime consumption. The total amount of lime produced in 2018 in Europe including UK is about 20 million tonnes.

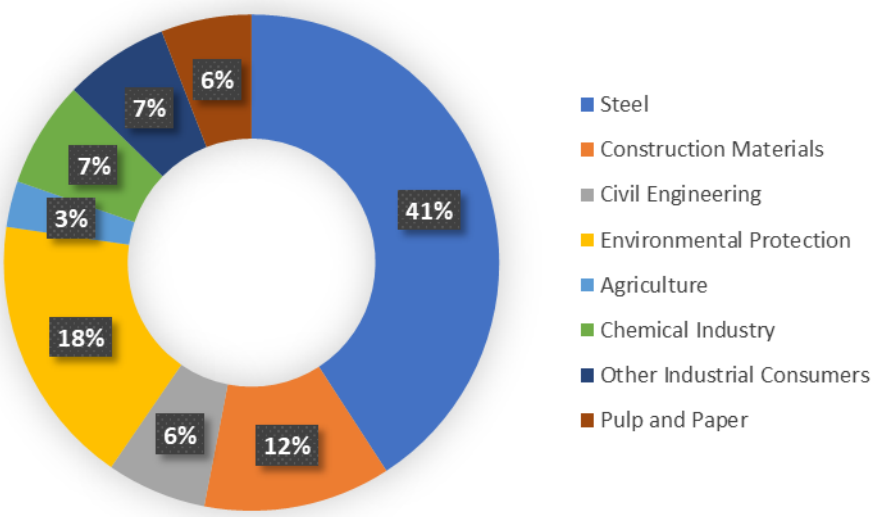


Figure 1.1. EuLA 2018 market share among the applications of lime.

Table 1.1. Lime applications and sub-applications with their respective lime (CaO) consumed in Europe in 2018 and the level of the information identified in literature about lime carbonation (**conclusive**, **less conclusive**, **not available** or **not assessed**).

Lime applications (Adapted from EuLA database)	Lime sub-applications (Adapted from EuLA database)	Lime amount (thousands of tonnes of CaO)	Information about lime carbonation in literature
Iron & Steel industry	Iron & Steel industry	**8,325**	**Conclusive**
Construction Materials	Sand lime brick (Silica brick)	**596**	**Less conclusive**
	Light-weight lime concrete	**894**	**Less conclusive**
	Pure air lime mortars	**86**	**Conclusive**
	Mixed air lime mortars (90%)	**588**	**Conclusive**
	Hemp lime	**10**	**Conclusive**
	Other (paints, natural fibres...)	**318**	**Not assessed**
Civil Engineering	Soil stabilisation	**1,308**	**Less conclusive**
	Asphalt pavements	**23**	**Not available**
Environmental Protection	Drinking water	**424**	**Conclusive**
	Wastewater treatment	**874**	**Less conclusive**
	Sludge treatment	**593**	**Less conclusive**
	Flue gas cleaning systems	**1,595**	**Conclusive**
	Other (Acid Mine Drainage – AMD, lake liming...)	**127**	**Not available**
Agriculture	Fertiliser	**331**	**Not available**
	Other (sanitation, aquafarming, ...)	**280**	**Not available**
Chemical Industry	Calcium carbide	**63**	**Less conclusive**
	Soda	**19**	**Not available**
	Petrochemical	**318**	**Not available**
	Other (salts, leather tanning, ...)	**1,017**	**Not assessed**
Other Industrial Consumers	Sugar	**35**	**Not assessed**
	Glass	**158**	**Not assessed**
	Non-ferrous metal industry without aluminium	**315**	**Not available**
	Aluminium	**276**	**Conclusive**
	Other	**608**	**Not assessed**
Pulp & Paper	Pulp and Paper	**1,204**	**Conclusive**

For each application, a review was performed about the carbonation potential rate of lime in terms of natural as well as enhanced carbonation (the latter, only for the applications where it is performed). The assessment was mainly based on peer-reviewed papers, on technical reports from research or institutional bodies (such as the Joint Research Centre or the Environmental Protection Agency), on the Best Available Techniques Reference (BREFs) Documents, on patent documents, Master and Doctoral theses, and industrial company websites.

Dedicated chapters were written for each sector, following the same overall structure. First of all, an introduction about the role and consumption of lime in the specific application is reported, together with a complete list of the documents consulted for the assessment (reference authors, title, year of

publication, and type of source). Then, the quantitative results about carbonation potential are reported, separately for the natural and accelerated process. In particular, each value found about CO_2 uptake is reported in a summary table together with the corresponding indications on the type of assessment (e.g., experimental assessment at the laboratory/pilot/full scale, modelling assessment), on the geographical and temporal scope, on the test duration and its operating conditions. The average, minimum and maximum CO_2 uptake of the collected data is indicated and, in some cases, dedicated statistical analyses were performed with the software *SPSS Statistics* in order to check the influence of the test operating conditions or of the material composition and mineralogy on the final CO_2 uptake. The last part of the report is dedicated to the conclusions of the study with the description of the main findings and of future research needs. Table 1.2 reports the average carbonation rate of lime for all the applications assessed in the study.

The sub-applications are grouped on the basis of the robustness of the information about carbonation found in the assessed literature, as shown by colours in Table 1.2. A sub-application is defined conclusive when a lot of information is available from the literature, thus yielding more robust conclusions, i.e. either the number of data found about carbonation allows a statistical analysis or there is consistency among the data. The results are considered less conclusive when shortcomings were reported in the existing literature, i.e. results reported only for laboratory or pilot scale assessment, or based only on few, old (more than 20 years old) literature sources or referring to non-EU data sources or without consistency among the few data. The remaining applications are characterized by a severe lack of information that does not allow any estimate of the carbonation.

Table 1.2. Average carbonation rate of lime derived from the literature assessment for all the covered applications, for both natural and accelerated processes. NOTE: the carbonation rate is expressed as a percentage of the CO_2 emitted during the production of lime (786 kg/t of lime, excluding CO_2 from fuel combustion, according to the BREF document for Cement, Lime and Magnesium Oxide Manufacturing Industries). The colour indicates the data robustness: **applications with conclusive scientific data, applications with less conclusive scientific data** and **no information available.**

Application	**Potential carbonation rate from the literature assessment**	
	Natural carbonation (%)	**Enhanced carbonation (%)**
Iron and steel industry		
Iron industry	Negligible even after 100 years	7% direct route 31% indirect route
Steel industry	5% (4 months) - 28% (1 year)	39-56% (direct route)
Construction materials		
Sand lime bricks	30% (reference time not reported)	No information identified in literature
Light-weight lime concrete / Autoclaved aerated concrete	30% (10 years) - 60% (30 years)	No information identified in literature
Pure air lime mortars	80-92% (after 100 years; depth 191 mm)	-
Mixed air lime mortars	20-23% (after 100 years; depth 191 mm)	-
Hemp lime	55% (after 91 days; depth 50 mm)	65%
Civil engineering		
Soil stabilisation	37% (after 34 years; field research)	Only lab-scale
Asphalt pavements	No information identified in literature	No information identified in literature
Environmental protection		
Drinking water – softening process	100% instantaneous	No information identified in literature
Wastewater treatment - Biosolids	40-50% (reference time not reported)	No information identified in literature
Sludge treatment - dredging sediments	35% (after 30 years)	No information identified in literature
Flue gas cleaning systems[1]	32% instantaneous	59-66% (full-scale)
Acid mine drainage	Negligible	No information identified in literature
Agriculture	No conclusive outcome	No information identified in literature
Chemical industry		
Calcium Carbide	Depending on the next use of carbide lime	No information identified in literature
Non-ferrous industry		
Aluminium production	11.5% (fresh sample) no information about time	11.5%
Titanium dioxide production	No information identified in literature	10-25% direct route 60% indirect route
Other non-ferrous metals prod.	No information identified in literature	No information identified in literature
Pulp and paper		
Precipitated calcium carbonate (PCC)	85%-93% instantaneous	No information identified in literature

NOTE: [1]Natural carbonation takes place inside the flue gas, while the enhanced carbonation on the APCR (Air Pollution Control Residues), allowing for a further increase by 27-34% of the carbonation rate. Then, for this specific application the natural and enhanced carbonation rates can be summed up, i.e. the potential total enhanced carbonation rate is 59-66%.

The process CO_2 emission due only to lime calcination (excluding fuel combustion) was assumed equal to 786 kg CO_2 per tonne of lime according to the BREF Document for Cement, Lime and Magnesium Oxide Manufacturing Industries published by the European Commission pursuant to Emissions Directive 2010/75/EU (Integrated Pollution Prevention and Control).

The potential amount of CO_2 reabsorbed through natural carbonation was estimated for conclusive and less conclusive applications. Conclusive applications, which represent 61% of the EuLA lime market in 2018, will reabsorb potentially 23% of the total process CO_2 emitted during calcination, while less conclusive applications, which represent 21% of the European lime market, will reabsorb potentially 10% of the total process CO_2 emitted during calcination. In total this leads to 33% of the calcination CO_2 emission being reabsorbed by conclusive and less conclusive applications (which account for 82% of the total European lime market).

Information about the carbonation time was found for all conclusive applications except for the aluminium industry. Carbonation in softening processes (drinking water), flue gas treatment and Precipitated Calcium Carbonate manufacturing (pulp and paper) occurs instantaneously, while an equation which links the rate of carbonation to the time was estimated for the remaining conclusive applications as summarized in Table 1.3. On the basis of these assumptions and according to the European lime market in 2018, 95% of the CO_2 which will be potentially reabsorbed through natural carbonation by conclusive applications will occur after one year from the use of lime.

Table 1.3. Equation which links the carbonation rate with time for construction materials and steel slags.

Application	**Equation**	**Comments**
Construction materials	$CR = MCR \cdot {(K\sqrt{t})}/{depth}$ where: *MCR* is the maximum natural carbonation rate; *K* is the carbonation constant; *t* is time (days); *depth*: is the application thickness that carbonates after 100 years.	Pure air lime mortars: *MCR*=92%; *K*=1 $mm/\sqrt{day}$; *depth*: 191 mm
		Mixed air lime mortars: *MCR*=92%; *K*=0.25 $mm/\sqrt{day}$; *depth*: 191 mm
		Hemp lime: *MCR*=55%; *K*=5.24 $mm/\sqrt{day}$; *depth*: 1001 mm
Steel slags	$CR = 0.0085 \cdot \sqrt{t}$ for the first 5 years $CR = 39\%$[1] after the first 5 years	*t* is expressed in days.

NOTE

[1] It is the minimum of the measured enhanced carbonation rate. It can be considered as a theoretical maximum natural carbonation rate reached after 5 years or more likely later. Note that typically the steel slags are stored in the open-air for 3-6 months only.

2 METHODOLOGY AND SCOPE OF THE WORK

The scope of the work is to assess the carbonation potential of lime in its different applications by reviewing the available literature on the topic. Carbonation is the reaction of lime with the CO_2 forming calcium carbonate ($CaCO_3$), thus removing CO_2 from the atmosphere and storing it permanently. The reaction is exothermic and therefore thermodynamically favourable, while calcination, i.e. the inverse reaction, requires energy. Through carbonation, lime can reabsorb a certain amount of the CO_2 previously emitted during calcination. The ratio between the amount of CO_2 absorbed during carbonation and the amount emitted during calcination (excluding fuel combustion emission) is the carbonation rate. In the applications where lime gets fully carbonated, the carbonation potential is 100% and the lime application can be considered carbon neutral with regards to non-combustion CO_2 emissions, also referred to as "process" emissions. In this work, the carbonation potential is assessed in natural conditions (i.e. under ambient carbon dioxide concentration) and in enhanced conditions (i.e. under enhanced carbon dioxide concentration and by optimising other parameters such as the temperature and the relative humidity). Enhanced carbonation conditions help to accelerate the process. The process routes for accelerating carbonation can be direct or indirect as shown in Figure 2.1. In the direct process, carbonation occurs in a single step, while in the indirect one the CaO is first extracted from the mineral matrix and subsequently carbonated (Pan et al., 2012).

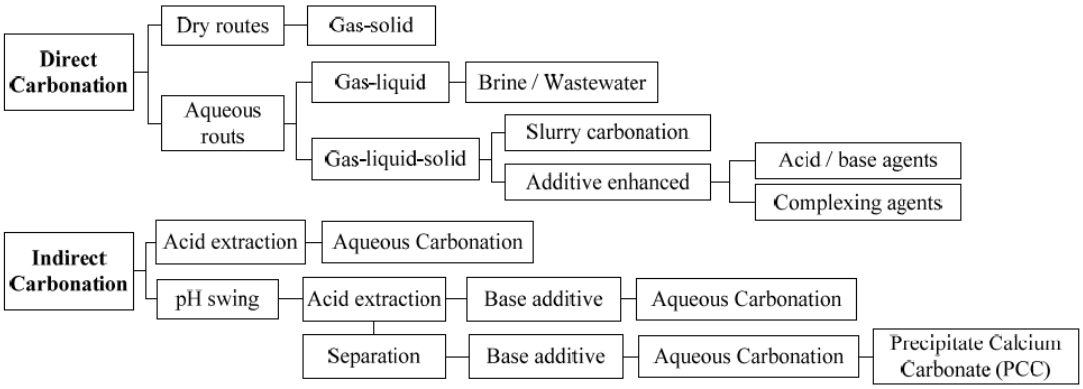


Figure 2.1. Various process routes of enhanced carbonation for CO_2 capture (Pan et al., 2012).

Upon assignment and clarification of the scope of work, Politecnico di Milano proposed to the EuLA Carbonation Ad-Hoc Task Force to work closely and in an iterative process through the different findings at application level.

For the duration of the project (January 2019 – June 2020) the following expert meetings were organized:

01.2019: Kick Off (KoM) expert meeting

03.2019: 2nd expert meeting

07.2019: 3rd expert meeting

10.2019: 4th expert meeting

03.2020: 5th and final expert meeting

The methodology developed by PoliMI was discussed during the KoM and refined during the various expert meetings, when necessary. Between the physical meetings, the exchange between PoliMI and experts was ensured via e-mails via the EuLA secretariat.

The iterative process between the consultant and the experts can be visualized in Figure 2.1. For some chapters, multiple iterations were necessary to capture all the literature but also to clarify the functionality of lime in the specific application.

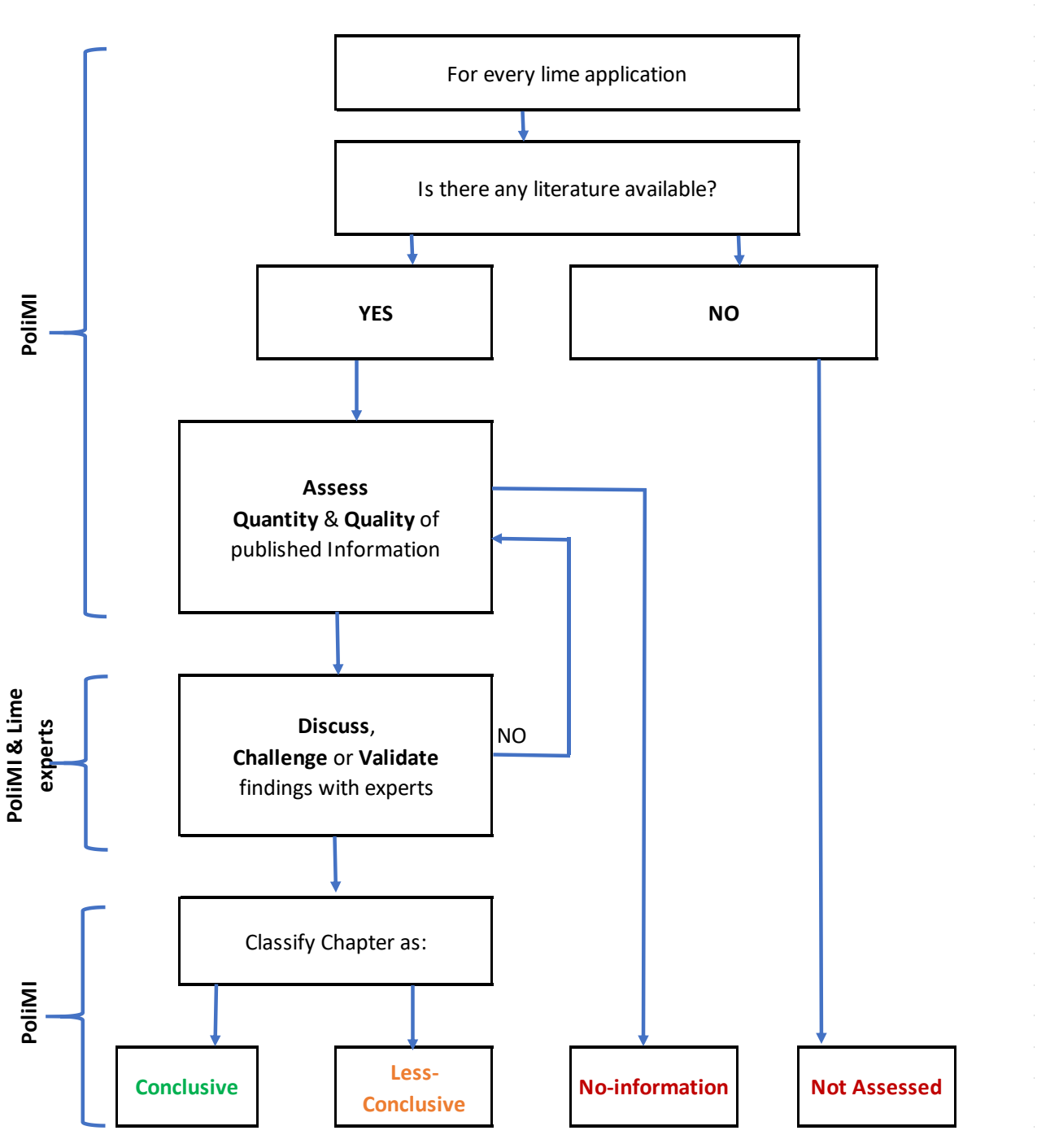


Figure. 2.1. Illustration of the workflow between PoliMI and the EuLA experts.

For the assessment of the different carbonation rates in various applications the following agreements were made:

Applications with conclusive scientific data, were defined those where the amount of literature published on carbonation allows for statistical treatment or the results presented are consistent throughout these publications/reports to establish the carbonation rate being natural or accelerated.

Applications with less conclusive scientific data, where the amount of literature published on carbonation is veryinsufficient to allow data comparability, thus the outcome is less conclusive to establish any carbonation rates (natural or accelerated).

Applications with no information available, where due to the low volume of lime in the application there are few studies on carbonation, and in particular no studies to estimate the carbonation rate.

Not assessed applications, where due to the low volume of lime in the application, there are no studies on carbonation. Thus, they are not covered in the scope of this literature review.

In Table 2.1, information about the literature assessed for each sub-application is reported. The colour indicates the robustness on the basis of the assessed literature for each sub-application.

Table 2.1. Information about literature assessed in this work for each sub-application. The colour indicates the robustness of the sub-application.

Lime application	Lime sub-application	Total assessed literature	Total relevant, reliable & adequate literature	Literature on Carbonation		Information source		Project maturity		
				NC	EC	EU	Non-EU	Lab scale	Pilot scale	Real test[1]
Iron and steel industry	Iron and steel slags	72	48	10	38	28	14	37	6	-
Construction materials	Sand lime bricks	14	1	1	-	1	-	-	1	-
	Light-weight lime concrete - Autoclaved aerated concrete	27	6	6	-	1	5	-	6	-
	Pure air lime mortars	1 literature review (100 pub.)	1 literature review (21 pub.)	21	-	-	-	9	-	4
	Mixed air lime mortars	1 literature review (90 pub.)	1 literature review (27 pub.)	27	-	-	-	-	-	-
	Hemp lime	15	9	9	1	8	1	4	-	6
Civil engineering	Soil stabilisation	20	6	1	1	2	1	1	2	-
	Asphalt pavements	7	-	-	-	-	-	-	-	-

Lime application	Lime sub-application	Total assessed literature	Total relevant, reliable & adequate literature	Literature on Carbonation		Information source		Project maturity		
				NC	EC	EU	Non-EU	Lab scale	Pilot scale	Real test[1]
Environmental protection	Drinking water	14	2	-	-	-	-	-	-	2
	Wastewater treatment	12	2	2	-	2	-	-	-	2
	Sludge treatment - dredging sediments	17	2	2	-	1	1	-	-	2
	Flue gas treatment	39	23	5	18	21	1	11	-	10
	Acid mine drainage	9	2	2	-	-	2	-	-	2
Agriculture	Soil neutralisation	12	-	-	-	-	-	-	-	-
	Increment of soil organic carbon	37	2	2	-	2	-	-	-	2
Chemical industry	Calcium carbide	6	-	-	-	-	-	-	-	-
Non-ferrous applications	Base and precious metals, lithium	71	-	-	-	-	-	-	-	-
Non-ferrous applications	TiO_2 production - Red gypsum	13	7	-	7	1	6	7	-	-
	Aluminium production - Red mud	41	26	1	11	1	11	10	-	2
Pulp and paper	Precipitated Calcium Carbonate (PCC)	52	13	1	-	1	-	-	-	1
All applications (total)		668	197	90	76	69	42	79	15	33

[1]Real test include: full-scale, field test, Life Cycle Assessment and BREF.

REFERENCES

Pan, S.-Y., Chang, E. E., Chiang, P.-C., 2012. *CO_2 Capture by Accelerated Carbonation of Alkaline Wastes: A Review on Its Principles and Applications*. Aerosol and Air Quality Research, 12, 770–791. DOI: 10.4209/aaqr.2012.06.0149

3. INTRODUCTION: LIME USE AND APPLICATIONS

Lime is used in a diverse range of applications. Table 3.1 provides an overview of the main applications and sub-applications where lime is being used.

Table 3.1. Lime applications and sub-applications.

Lime applications (Adapted from EuLA database)	**Lime sub-applications (Adapted from EuLA database)**
Iron & Steel industry	Iron & Steel industry
Construction Materials	Sand lime brick (Silica lime brick)
	Light-weight lime concrete
	Pure air lime mortars
	Mixed air lime mortars (90%)
	Hemp lime
	Other (paints, natural fibres ...)
Civil Engineering	Soil stabilisation
	Asphalt pavement
Environmental Protection	Drinking water
	Wastewater
	Sludge treatment
	Flue gas treatment
	Other (AMD, lake liming...)
Agriculture	Fertiliser
	Other (sanitation, aquafarming, ...)
Chemical Industry	Calcium carbide
	Soda
	Petrochemical
	Other (Salts, leather tanning, ...)
Other Industrial Consumers	Sugar
	Glass
	Non-ferrous metal industry without Aluminium
	Non-ferrous (Aluminium)
	Other
Pulp & Paper	Pulp and Paper

The EuLA 2018 market share among the sub-applications is reported in Figure 3.1.

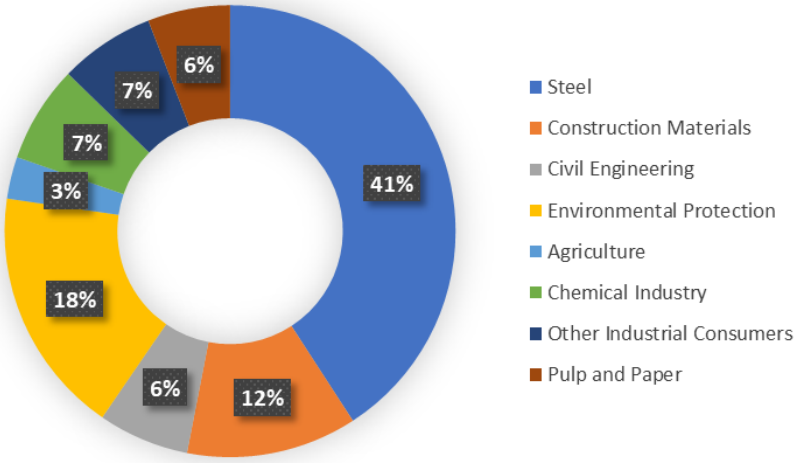


Figure 3.1. EuLA 2018 market share among the applications.

The upcoming application dedicated chapters will address each and any of the lime (sub)applications where information on carbonation was identified in the literature.

3.1 USE OF LIME IN IRON AND STEEL INDUSTRY

3.1.1 INTRODUCTION

Different types of slags are produced by the iron and steel industry. Their classification is based on the process from which they are originated. The "iron slags" are produced in the blast furnaces (BF) for pig iron production, whereas the generic term "steel slags" refers to all the slags produced by the processes for steel production. They included the "hot metal desulphurization slag" (defined as De-S slag), the "oxygen converter slag" (defined with the acronyms BOF, BOS or LD slag), the "arc furnace slag" (EAF slag) and the "secondary metallurgy slag" (from the Ladle Furnaces - LF - for the production of special steel or from the Argon Oxygen Decarburization - AOD - or Vacuum Oxygen Decarburization - VOD - processes for the production of the stainless steel - SS).

The composition and the volume of the slag depends on the iron or steelmaking process. On average, about 185 ± 5 kg of BF slag, 10-15 kg of De-S slag and 117 kg ± 5 kg of steel slag (BOF/EAF + secondary metallurgy slag) are produced per tonne of crude steel (US Geological Survey, 2018; Personal communication EuLa, 2019)

In technical terms, the slag can be considered an ionic solution of molten metal oxides and fluorides floating on the top of the liquid ferrous metal. The four major components forming the slag are oxides of metallic elements (Fe, Al, Si, Mn, Cr etc.) and of non-metallic elements (S and P), fluxes (CaO, CaO*MgO, CaF_2 etc.) and dissolved refractories (MgO, CaO*MgO, Al_2O_3).

The presence of Ca-compounds in the slag is the consequence of the use of quicklime (CaO) or limestone ($CaCO_3$) during the iron and steel making processes. Quicklime is used in the hot metal desulphurization process as well as in the BOF and EAF processes mainly as a fluxing agent to create a basic slag that can neutralise acid-forming elements, remove sulphur, phosphorous, silica and alumina inclusions and protect the refractories (Manocha and Ponchon, 2018). It is also used in a broad variety of secondary metallurgical processes for the removal of additional impurities and to prevent the reabsorption of impurities from the slag. In addition, quicklime can be used together with other materials, such as fluorspar, to form a synthetic slag, which is used as a flux to remove additional sulphur and phosphorus after the initial steel refining process. In the pig iron production process, on the contrary, quicklime is used in modest amount, mixed with limestone in a proportion of 1:6, mainly in the sintering process (Manocha and Ponchon, 2018).

Slag engineering is about finding the right balance between the refractory oxides (CaO and MgO) and the fluxing oxides (SiO_2, Al_2O_3, CaF_2, and iron oxide). The lime dissolution in the slag is a function of the lime quality (soft burnt lime dissolves much quicker), of the formation of high-melting di-calcium silicate, of the saturation point and the quantity of lime, of the temperature and of the process time (Manocha and Ponchon, 2018). Any unreactive lime, for either of these reasons, tends to leave undissolved lime in the slag. Such unreacted and unmelted CaO is called "free CaO" and is responsible of the slag high alkalinity.

When free CaO comes in contact with water it reacts forming $Ca(OH)_2$ and its volume duplicates. The presence of free CaO in the slag is thus deleterious in view of its recycling as construction material, because it can result in swelling and expansion phenomena leading to failure in confined construction applications. In order to avoid this problem, it is a good option to store the slag in open air so that the hydration reactions of CaO are completed before the slag is used.

After the collection from the furnace, the typical management of the slag consists in a period of storage in outside basins or in open yards for cooling and solidification. Here the slag is cooled naturally, or sometimes with water spray, and solidifies. After a certain period, the slag is crushed and classified to control the grain size and then subjected to metal separation to recover mixed-in metallic iron (JRC, 2013a). Then the slag can be further stored to promote hydration reactions (Horii et al., 2015).

During this storage period, CaO is hydrated into $Ca(OH)_2$, which quickly reacts with the atmospheric CO_2, producing $CaCO_3$. The process is referred to as "natural carbonation" or "natural ageing". Natural carbonation involves not only $Ca(OH)_2$, but also other hydraulically active phases (mainly calcium silicates and calcium aluminates) present in the matrix and resulting from the reaction of the quicklime (or limestone in the case of the BF slag) with the impurities in the furnace charge. The process begins with the rapid carbonation of the $Ca(OH)_2$ present in the fresh slag (if present); then, the Ca and/or Mg ions from silicates minerals dissolve and react with atmospheric CO_2 to generate solid carbonates, that precipitate on the outer surface of the particles. The overall exothermal dissolution-precipitation reaction can be written as (Quaghebeur et al., 2015):

$$Ca(OH)_2 + CO_2 \rightarrow CaCO_3 + H_2O$$

$$(Ca,Mg)_xSi_yO_{(x+2y)} + xCO_2 + H_2O \rightarrow x(Ca, Mg)CO_3 + ySiO_2 + H_2O$$

Iron and steel slag also contains MgO, which can potentially react with CO_2. However, MgO carbonation requires longer time and more sever conditions of temperature and pressure compared to CaO carbonation (Baciocchi et al., 2015; Pan et al., 2012). During natural ageing, therefore, MgO is hydrated to $Mg(OH)_2$, that is quite stable at ambient conditions and hardly reacts with CO_2.

The ageing process allows the improvement of the mechanical and geotechnical properties of the slag, reducing the content of free CaO and MgO, responsible of its high water absorption and expansion properties (Lekakh et al., 2008; Pan et al., 2012). In addition, slag carbonation results in a capture and permanent sequestration of the atmospheric CO_2 under the form of thermodynamically stable carbonate minerals.

The main limitation of the natural carbonation process is that it is extremely slow, so that the ageing period to which the slag is subjected to, usually 3-6 months (Lekakh et al., 2008; Motz and Geseiler, 2001), is often insufficient to complete the carbonation. A longer reaction period, of at least 9-12 months and up to 3 years, can be required to sufficiently reduce the level of free lime (Das et al., 2007; Wu et al., 2007). In some cases, carbonation reactions can still be observed after several years from the slag production, since gas diffusion through the matrix can be difficult (Gupta et al., 1994; Suer et al., 2009). Albrecht (2008) estimated that 2/3

of the free lime in steel slag reacts within the first 5 years, whereas carbonation of calcium silicates and calcium aluminates takes more than 5 years, reaching a final carbonation degree of only 1/3.

Forced carbonation of iron and steel slag is a method to reduce the time needed for natural ageing and increase the benefit of CO_2 sequestration. Slag carbonation can be accelerated by increasing the surface area of the particles and by optimizing CO_2 pressure, temperature, L/S ratio and other operating conditions (Costa et al., 2007; Haug et al., 2010; Chang et al., 2011).

Two are the main routes for accelerated carbonation:

- direct processes, in which carbonation occurs in a single process step. These processes can be divided into two types: gas-solid (dry) carbonation and wet carbonation, which operates with three phases (gas-liquid-solid). Wet carbonation can occur in the slurry-phase (L/S>1) or in aqueous solution (L/S<1). Drawbacks of the gas-solid process are the slow kinetics of carbonation chemistry and the significant energy input requirement (IPCC, 2005).
- indirect processes, in which alkaline earth metal is first extracted from the mineral matrix and subsequently carbonated, with precipitation of a pure calcium carbonate. Typical extracting agents are ammonium salts or acetic acid. The general problem of this process is that other elements, such as heavy metals, may also leach out during the extraction step, thus leading to impure carbonate precipitation.

By optimizing the operating conditions, it is possible to sequester higher amount of CO_2 in the slag, compared to the amount captured during natural ageing. In addition, the process provides a final material that is more stable than fresh slag and that can be used, for example, as mineral aggregate in concrete or cement production and as aggregate for road construction.

Regarding the recycling options of iron and steel slag, BF slag is largely used in civil engineering. Quickly granulated BF slag has latent hydraulic (pozzolanic) properties and can be used as alternative binder system-component for cements or for the production of geopolymers (i.e. binders activated by alkaline conditions) (Vlcek et al., 2013). Usually, after milling, it is added to Portland clinker or to concrete mixtures. Das et al. (2007) showed that about 50% of clinker can be replaced by granulated BF slags in cement production. The slow cooled BF slag, after demetallisation and milling/sieving operations, can be used as artificial dense aggregate, in asphalt mixtures, for hydraulic engineering or as a solidifying base (Vlcek et al., 2013). In 2016, almost all the BF slags produced in Europe were recycled, of which 81.4% was used in cement and concrete production and 20.9% for road construction (Euroslag, 2016). BF slag can be also used in agriculture for soil acidity correction due to its high content of Ca and the presence of Mg (National slag association).

Contrary to BF slag, recycling of steel slag is more limited. However, in 2016 about 77% of the steel slags produced in Europe were recycled (Euroslag, 2016). About 46% of the steel slag was used in road construction, 15.3% was re-used in the metallurgy sector, added in melting aggregates to partially replace the commercial lime (after crushing and screening to recover its steel content), 4.4% was used in cement and concrete production, 2.7% as fertilizer and 2.2% in hydraulic construction (Euroslag, 2016).

BOF slags are largely used in road construction and concrete or cement production. Due to their high strength and durability, they can be used as high quality aggregates for road construction (base and sub-base layers and asphaltic surface layer), provided that the content of free lime is lower than 7% in unbounded layers and 4% in asphaltic layers (Motz and Geiseler, 2001). In addition, ground into fine powder it can be used as cement additive and in concrete mixture (Tüfekci et al., 1997). However, its high iron content can minimize the hydraulic activity of blended cement (Belhadj et al., 2012).

EAF slag is usually used as aggregates and cementitious material in concrete, due to its high iron content resulting in a high resistance to erosion and fragmentation (Kuo et al., 2014).

LF slags have different mechanical properties compared to EAF and BOF slags and are not generally recovered in engineering applications (Pan et al., 2016). Recycling options for iron and steel slag are summarized in Table 3.1.1.

Table 3.1.1. Recycling options for iron and steel slags.

Type of slag	Utilisation	Notes	Reference
GGBF slag*	Cement production	Added to Portland clinker	Vlcek et al., 2013
	Cement production	Alternative binder system-component for cements. Application not included in the European Standard system	Vlcek et al., 2013
	Geopolymer production	Used as a binder activated in alkaline way. Application not included in the European Standard system. The slag must be doped with glass	Vlcek et al., 2013
ACBF slag*	Aggregates as a solidifying base, in asphalt mixture and for hydraulic engineering	The slag must be demetallised and have low content of free CaO and MgO	Vlcek et al., 2013
BF slag (independently of the type of cooling)	Recycled in the batch mixture in sintering plant and BF	Slag with high content of FeO, after demetallisation	Vlcek et al., 2013
	Recycled in the BF as fluxing agent	Slag with high content of CaO, MgO, Al_2O_3, after demetallisation	Vlcek et al., 2013
	Agriculture	As a source of lime and of minor nutrients in substitution of limestone/dolomite	National slag association; Volk et al., 1952
BOF/EAF slag	Recycled in the sintering furnace as fluxing agent	Slag with CaO content above 50%	Yi et al., 2012
	Cement/concrete production	Slag must be ground into fine powder to promote its cementitious properties	Tüfekci et al., 1997 Dippenaar, 2004
	Agriculture	As a source of CaO, SiO_2 and MgO and other minor nutrients in substitution of limestone/dolomite	Mäkelä et al., 2012; Wu et al., 2005
	Aggregates in road construction and for hydraulic engineering	Slag can be used in the sub-base layer and also in the asphaltic surface layers thanks to the high frictional and abrasion resistance. The content of CaO and MgO must be controlled (< 4-7% of free CaO). Another application can be for the construction of artificial reefs for seawood/coral breeding, due to the high content of $CaCO_3$	Yi et al., 2012; Motz and Geiseler, 2001; JFE, 2004 Dippenaar, 2004

* GGBF slag: ground granulated blast furnace slag; ACBF slag: air cooled blast furnace slag

3.1.2. LITERATURE ASSESSMENT FOR IRON AND STEEL SLAGS: MATERIAL AND METHODS

The literature review was carried out separately for the iron and the steelmaking slags, due to the differences between the two processes and the resulting different composition of the residues.

Iron slag

Concerning the iron slag, the literature review carried out to assess the amount of CO_2 that can be sequestered by the BF slag during its life cycle was based on 16 papers published in scientific journals, a US patent, two reports, two Best Available Techniques (BAT) Reference Documents, one on cement, lime and magnesium

oxide and one on iron and steel (Figure 3.1.1). The list of documents analysed for iron slag is reported in Table 3.1.2. For the most interesting papers, a summary was prepared (see Annex 1).

Apart from the BREF documents, two papers refer to natural ageing (Gupta et al., 1994 and Mayes et al., 2018), 9 documents focus on accelerated carbonation (Table 3.1.10), while the remaining ones were used to assess the iron slag mineral composition.

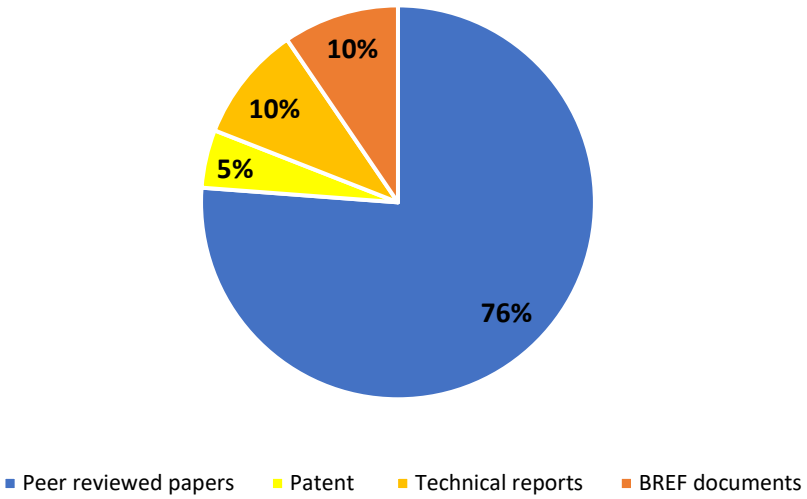


Figure 3.1.1. Sources used for the literature assessment on iron slag.

Table 3.1.2. List of the documents considered in the study for the iron slag.

Peer reviewed papers
Bang et al., 2016. *Leaching of metal ions from blast furnace slag by using aqua regia for CO_2 mineralization*. Energies 9(12), 996-1009
Chang et al., 2011a. *Performance evaluation for carbonation of steel-making slags in a slurry reactor*. Journal of Hazardous Materials 186(1), 558-564
Chang et al., 2011b. *CO_2 sequestration by carbonation of steelmaking slags in an autoclave reactor*. Journal of Hazardous Materials 195, 107-114
Cheng and Chiu et al., 2003. *Fire-resistant geopolymer produced by granulated blast furnace slag*. Minerals Engineering 16(3), 205-210
Chiang et al., 2014. *Towards zero-waste mineral carbon sequestration via two-way valorization of ironmaking slag*. Chemical Engineering Journal, 249, 260-269
Eloneva et al., 2008. *Fixation of CO_2 by carbonating calcium derived from blast furnace slag*. Energy 33(9), 1461-1467
Gupta et al., 1994. *Characterization of base and subbase iron and steel slag aggregates causing deposition of calcareous tufa in drains*. Transportation Research Record n.1434, published by Transportation Research Board
Hu et al., 2017. *Indirect mineral carbonation of blast furnace slag with $(NH_4)_2SO_4$ as a recyclable extractant*. Journal of Energy Chemistry 26(5), 927-935
Johnson, 2000. *Accelerated carbonation of waste calcium silicate materials*. SCI lecture papers series, 1-10
Kuwahara and Yamashita, 2013. *A new catalytic opportunity for waste materials: application of waste slag based catalyst in CO_2 fixation reaction*. Journal of CO_2 utilization 1, 50-59
Lee et al., 2016. *CO_2 sequestration technology through mineral carbonation: an extraction and carbonation of blast slag*. Journal of CO_2 utilization 16, 336-345
Mayes et al., 2018. *Atmospheric CO_2 sequestration in iron and steel slag: Consett, County Durham, United Kingdom*. Environmental Science and Technology 52(14), 7892-7900
Mun and Cho, 2013. *Mineral carbonation for carbon sequestration with industrial waste*. Energy Procedia, 37, 6999-7005
Proctor et al., 2000. *Physical and chemical characteristics of blast furnace, basic oxygen furnace and electric arc furnace steel industry slags*. Environmental Science and Technology 34(8), 1576-1582
Uliasz-Bochenczyk and Morkrzycki, 2017. *CO_2 mineral sequestration with the use of ground granulated blast furnace slag*. Mineral resources management 33(1), 111-124
Ukwattage et al., 2017. *Steel-making slag for mineral sequestration of carbon dioxide by accelerated carbonation*. Measurement 97, 15-22
Patent application publication
Ramme, 2008. *Carbon dioxide sequestration in foamed controlled low strength materials*. United States Patent Application Publication Publication Number: US2008/0245274 A1
Reports
National slag association. *Blast furnace slag as an agricultural liming material and source of minor plant nutrients*
Volk et al., 1952. *A comparison of blast furnace slag and limestone as a soil amendment*. Research Bulletin 708. Ohio agricultural experiment station. Wooster, Ohio
BREF documents
JRC, 2013a. *Best Available Techniques (BAT) Reference document for iron and steel production*
JRC, 2013b. *Best Available Techniques (BAT) Reference document for the production of cement, lime and magnesium oxide*

Steel slags

Considering the steel slags (which include the De-S slag), the literature review was based on 30 papers published in scientific journals, on the two Best Available Techniques (BAT) Reference Documents previously reported for iron slag, on a report by ENEA, the Italian National Agency for new technologies, energy and sustainable economic development, and on a master thesis (Figure 3.1.2). The list of the documents analysed

for this study is reported in Table 3.1.3. For the most interesting papers, a summary was prepared (see Annex 1).

Apart from the BREF documents, 7 papers focus on natural ageing (Gupta et al., 1994; Suer et al., 2009; Navarro et al., 2010; Horii et al., 2015; Yildirim et al., 2015; Rondi et al., 2016; Spanka et al., 2016), whereas the others focus on accelerated carbonation.

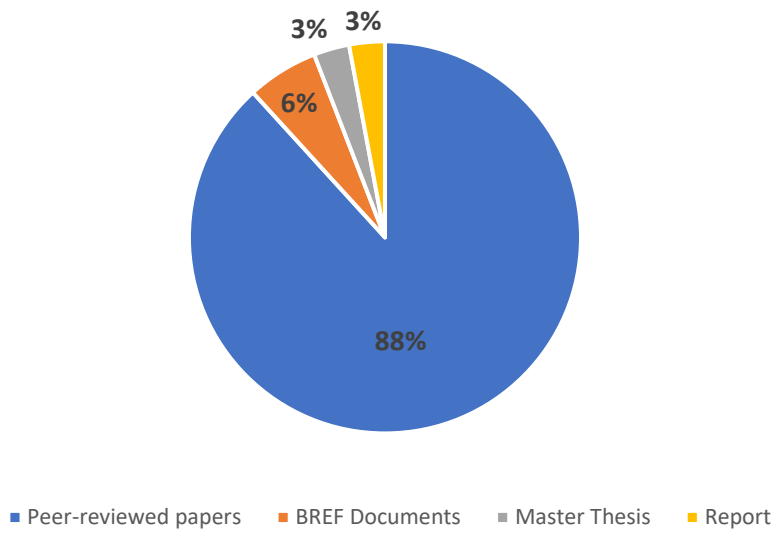


Figure 3.1.2. Sources used for the literature assessment on steel slag.

Table 3.1.3. List of the documents considered in the study for the steel slag literature review.

Peer reviewed papers
Baciocchi et al., 2015. *Thin-film versus slurry-phase carbonation of steel slag: CO_2 uptake and effects on mineralogy*. Journal of hazardous materials 283(11), 302-313
Baciocchi et al., 2016. *Accelerated carbonation of steel slags using CO_2 diluted sources: CO_2 uptakes and energy requirements*. Frontiers in Energy Research 3, article 56
Bonenfant et al., 2008. *CO_2 sequestration potential of steel slags at ambient pressure and temperature*. Ind. Eng. Chem. Res. 47(20), 7610-7616
Boone et al., 2014. *Monitoring of stainless-steel slag carbonation using X-ray computed microtomography*. Environmental Science and Technology 48(1), 674-680
Capobianco et al., 2014. *Carbonation of stainless steel slag in the context of in situ Brownfield remediation*. Mineral Engineering 59, 91-100

Table 3.1.3 (continued). List of the documents considered in the study for the steel slag literature review.

Chang, E.E., Pan, S.Y., Chen, Y.H., Tan, C.S. Chiang, P.C., 2012. *Accelerated Carbonation of Steelmaking Slags in a High-Gravity Rotating Packed Bed*. J. Hazard. Mater, 227–228, 97–106.

Dhoble and Ahmed, 2018. *Review on the innovative uses of steel slag for waste minimization*. Journal of Material Cycles and Waste Management 20(3), 1373-1382

Ghacham et al., 2016. *CO_2 sequestration by mineral carbonation of steel slags under ambient temperature: parameters influence, and optimization*. Environ Sci Pollut Res 23, 17635-17646.

Gupta et al., 1994. *Characterization of base and subbase iron and steel slag aggregates causing deposition of calcareous tufa in drains*. Transportation research record n. 1434, published by Transportation research board

Horii et al., 2015. *Overview of iron/steel slag application and development of new utilization technologies*. Nippon Steel & Sumitomo Metal Technological Report n. 109, July 2015

Huijgen and Comans., 2006. *Carbonation of steel slag for CO_2 sequestration: leaching of products and reaction mechanisms*. Environ. Sci. Technol. 40(8), 2790-2796

Huijgen et al., 2005. *Mineral CO_2 sequestration by steel slag carbonation*. Environmental Science and Technology 39(24), 9676-9682

Lekakh et al., 2008. *Kinetics of aqueous leaching and carbonization of steelmaking slag*. Metallurgical and Materials Transactions B 39(1), 125-134

Morone et al., 2014. *Valorization of steel slag by a combined carbonation and granulation treatment*. Minerals Engineering 59, 82-90

Motz and Geiseler, 2001. *Products of steel slags an opportunity to save natural resources*. Waste Management 21(3), 285-293

Navarro et al., 2010. *Physico-chemical characterization of steel slag. Study of its behaviour under simulated environmental conditions*. Environ. Sci. Technol. 44(14), 5383-5388

Pan et al., 2012. *CO_2 capture by accelerated carbonation of alkaline wastes: a review on its principles and applications*. Aerosol and air quality research 12(5), 770-791

Pan et al., 2013. *Ex situ CO_2 capture by carbonation of steelmaking slag coupled with metalworking wastewater in a rotating packed bed*. Environmental science and technology 47(7), 3308-3315

Pan et al., 2016. *Integrated and innovative steel slag utilization for iron reclamation, green material production and CO_2 fixation via accelerated carbonation*. Journal of Cleaner Production 137, 617-631

Pan et al., 2017. *CO_2 mineralization and utilization using steel slag for establishing a waste-to resources supply chain*. Scientific reports 7, Article Number 17227

Quaghebeur et al., 2010. *Carbstone: sustainable valorisation technology for fine grained steel slags and CO_2.* Refractories Worldforum 2(2), 75-79

Quaghebeur et al., 2015. *Accelerated carbonation of steel slag compacts: development of high-strength construction materials*. Frontiers in Energy Research 3, 1-12

Rondi et al, 2016. *Concrete with EAF steel slag as aggregate: a comprehensive technical and environmental characterization*. Composites Part B 90, 195-202

Santos et al., 2010. *Process intensification routes for mineral carbonation*. Proceeding of the third International Conference on accelerated Carbonation for Environmental and Materials Engineering ACEME10, Turku (Finland), Nov. 29-Dec. 1, 2010

Santos et al., 2013. *Accelerated mineral carbonation of stainless steel slags for CO_2 storage and waste valorization: effect of process parameters on geochemical properties*. International Journal of Greenhouse Gas Control 17, 32-45

Spanka, et al., 2016. *Influence of natural and accelerated carbonation of steel slags on their leaching behaviour*. Steel research international 87(6), 798-810

Suer et al., 2009. *Reproducing ten years of road ageing. Accelerated carbonation and leaching of EAF steel slag*. Science of the Total Environment 407(18), 5110-5118.

Table 3.1.3. (continued). List of the documents considered in the study for the steel slag literature review.

Yildirim and Prezzi, 2015. *Geotechnical properties of fresh and aged basic oxygen furnace steel slag*. J. Mater. Civ. Eng. 27(12), 1-11 Yu and Wang, 2011. *Study on characteristics of steel slag for CO_2 capture*. Energy Fuels 25(11), 5483-5492 Zingaretti et al., 2013. *Assessment of accelerated carbonation processes for CO_2 storage using alkaline industrial residue*s. Industrial and Engineering Chemistry Research 53(22), 9311-9324
Report Baciocchi et al., 2010. *Studio sulle potenzialità della carbonatazione di minerali e residui industriali per lo stoccaggio di anidride carbonica prodotta da impianti di piccola/media taglia*. Report RdS/2010/48 for ENEA
Master thesis Thuy, 2013. *Lab-scale feasibility of in-situ carbonation of alkaline industrial wastes*. Master thesis, Utrecht University (The Netherlands)
BREF documents JRC, 2013a. *Best Available Techniques (BAT) Reference document for iron and steel production* JRC, 2013b. *Best Available Techniques (BAT) Reference document for the production of cement, lime and magnesium oxide*

3.1.3 SLAG COMPOSITION

Iron slag

The chemical and mineralogical characterization of the slag is of fundamental importance to understand its tendency to carbonate.

The chemical composition of the iron slag mainly depends on the composition of the gangue accompanying the iron ore (Uliasz-Bochenczyk et al., 2017) and on the dosage of fluxing agents. The main constituents of the iron slag are in general Si, Ca, Mg, and Al. Focusing only on the elements of interest for CO_2 sequestration, the average content of the Ca compounds, expressed as CaO, amounts to about 40% of the weight of the slag and that of the Mg compounds (as MgO) to 9.9%. The typical composition of an iron slag is reported in Table 3.1.4.

The mineralogy significantly differs on the basis of the slag cooling technique. Iron slag can, in fact, be classified as granulated slag or air-cooled slag. The granulated slag is the result of a rapid cooling process using water, whereas air-cooled slag is produced by slow cooling under ambient atmosphere. Based on the analyses reported by Lee et al. (2016), the air-cooled slag has a crystalline phase, whereas the granulated slag is mainly amorphous, with the crystalline phases that amount for less than 50% of the weight of the slag. Generally, in both types of slag, Ca and Mg are found in silicate or ferrous compounds, such as srebrodolskite ($Ca_2Fe_2O_5$), larnite (Ca_2SiO_4), kirschsteinite ($CaFeSiO_4$), arkemanite ($Ca_2MgSi_2O_7$), or in the carbonate form, as calcite (Gupta et al., 1994; Lee et al., 2016; Hu et al., 2017). Among the analysed papers, only Ramme (2008) reports the presence of free lime in the iron slag (about 10% of the total Ca, expressed as CaO).

Table 3.1.4. Chemical composition of the iron slag. Elaboration of the data reported in the documents listed in Table 3.1.2.

Chemical composition (%)	Total Ca compounds as CaO	Total Mg compounds as MgO
Minimum-average-maximum	31.5-40.2-54.2 *46 cases*	3.34-9.9-14.9 *43 cases*

Steel slag

The main constituents of the steel slags are in general Ca, Fe, Si and Mg. Compared to iron slag, steel slags are usually richer in Ca and poorer in Si (Vlcek et al., 2013).

The typical content of Ca and Mg in steel slag, as well as its mineral composition, is reported in Table 3.1.5. Values come from the literature review of the documents listed in Table 3.1.3. In order to simplify the data analysis, slags were classified into 7 groups:

- De-S slag: slag produced by the desulphurization process of the hot metal;
- BOF slag: slag produced during the basic oxygen steelmaking process;
- EAF slag: slag produced in the EAF;
- Secondary metallurgy slag: the slag produced in the LF;
- BOF + LF slag: aggregated data were provided for the mix of slag extracted from the BOF and the LF furnace;
- EAF + LF slag: aggregated data were provided for the mix of slag extracted from the EAF and the LF furnace;
- SS metallurgy slag: slag produced during the SS making process. This group includes the slag produced in EAF furnaces dedicated to SS, as well as the slag produced in the AOD furnaces.

The data were statistically analysed by using the SPSS Statistics 25 software to understand if the distribution of total Ca and Mg compounds and free lime is the same for the different types of slag. The non-parametric Kruskal-Wallis test was used due to the non-normal distribution of data and the small number of cases[1]. This test can only determine the overall differences (if any) among the types of slag. The Mann-Whitney U-test was used to determine the difference (if any) between pairs of slag types for each parameter.

Concerning the total content of Ca and Mg compounds, the test result suggests that there is not any statistically significant difference among the different types of slag. On average, the total content of Ca, expressed as CaO, results equal to about 42.3% and that of Mg, expressed as MgO, is about 6.9%.

Considering the particle mineralogy, the most abundant mineral phases present in the fresh slag are portlandite ($Ca(OH)_2$), Ca-(Fe)-silicates, like larnite (Ca_2SiO_4), Ca-Fe-oxides, like srebrodolskite ($Ca_2Fe_2O_5$), Ca-Mg-silicates, like merwinite ($Ca_3Mg(SiO_4)_2$) and bredigite ($Ca_7Mg(Si_2O_7)$), Mg-Fe-oxides, magnesite ($MgCO_3$), dolomite ($CaMg(CO_3)_2$), amorphous SiO_2 and wuestite (FeO), free MgO and $Mg(OH)_2$ (Quaghebeur et al., 2015; Dhoble and Ahmed, 2018). Sometimes, calcite ($CaCO_3$) is also detected when fresh slags are analysed in laboratory, indicating that carbonation reactions can start very quickly during the storage in the steelworks.

Based on the data collected from the documents listed in Table 3.1.3, the average content of free lime (free CaO + $Ca(OH)_2$, expressed as CaO) is equal to 7% of the weight of the slag, with a maximum value of 21%. Most of the free lime is present as $Ca(OH)_2$, since CaO is quickly hydrated when comes in contact with water.

[1] The Kruskal Wallis test is used to determine if the rank totals for all the considered parameters are different for all experimental groups. In this study a significant level of 0.05 was assumed.

However, in this case, it is not correct to assume the same free lime content for all the types of slag. Based on the results of the Kruskall-Wallis test (significant level of 0.05) and of the Mann-Whitney U-test[2], the distribution of the free lime content in the BOF is significantly different to that in EAF or SS slag. On average, BOF slag contains more free lime compared to EAF and SS slag (about 7% compared to about 1% of the weight of the slag). No statistically significant difference was found between the other types of slag.

The average content of $CaCO_3$ is 4.3%.

Table 3.1.5. Chemical composition and mineralogy of different types of steel slag (min-average-max). Elaboration of the data reported in the documents listed in Table 3.1.3.

Chemical composition (% w)		**De-S slag**	**BOF slag**	**EAF slag**	**Secondary metallurgy slag**	**(BOF+LF) slag**	**(EAF+LF) slag**	**SS metallurgy slag**
Chemical composition	Total Ca compounds as CaO	43-46-49 *2 cases*	29.4-41.2-60 *31 cases*	18.2-40.2-60 *19 cases*	29.7-43.7-62.7 *15 cases*	44.3 *1 case*	15-41-68 *4 cases*	22.8- 47.7-61 *18 cases*
	Total Mg compounds as MgO	1-3-5 *2 cases*	0.01-6.5-15 *31 cases*	1.3-6.4-15 *21 cases*	1-10-21.5 *15 cases*	4 *1 case*	0.5-10.6-25 *4 cases*	2.7-6.4-11 *15 cases*
Mineralogy	Free lime (CaO + $Ca(OH)_2$ as CaO)	n.a.	0-7.3-21.2 *23 cases*	0.1-0.76-3 *7 cases*	2.5-10.8-19 *2 cases*	n.a.	n.a.	0-1.1-2.7 *5 cases*
	Free CaO	n.a.	0-3.8-10 *10 cases*	n.a.	n.a.	n.a.	n.a.	0-0.25-0.6 *4 cases*
	$Ca(OH)_2$	n.a.	0-9.4-28 *10 cases*	n.a.	n.a.	n.a.	n.a.	0-0.58-1.4 *4 cases*
	Free MgO	n.a.	0-3.5-7.9 *4 cases*	n.a.	n.a.	n.a.	n.a.	7.4-9.1-10.7 *3 cases*
	$Mg(OH)_2$	n.a.	0-5.7-17 *5 cases*	n.a.	n.a.	n.a.	n.a.	0-0.38-1.5 *3 cases*
	$CaCO_3$	n.a.	0.9-5.1-8.4 *6 cases*	0.1-2.8-3.5 *5 cases*	n.a.	n.a.	n.a.	0-2.8-9 *8 cases*

[2] The Mann Whitney U test was performed only on BOF, EAF, SS and secondary metallurgy slags, since content on free lime in BOF+LF and EAF+LF slags was not available. The significant level of the tests was thus equal to 0.05/4=0.0125.

3.1.4. POTENTIAL CARBONATION RATE IN IRON AND STEEL SLAG

Iron slag

The maximum theoretical CO_2 sequestration can be calculated considering the total Ca content in the iron slag. Assuming a 40.2% average content of total Ca compounds (expressed as CaO) in the iron slag, the maximum CO_2 uptake results equal to 316 gCO_2/kg slag.

It is worth pointing out that this figure widely overestimates the actual CO_2 uptake of the iron slag in natural conditions since, as previously reported, in the iron slag Ca is generally bounded in low reactive compounds.

Steel slag

As for the iron slag, the maximum theoretical CO_2 sequestration can be calculated considering the total Ca content in the steel slag. Assuming a 42.3% average content of total Ca compounds (expressed as CaO) in the steel slag, the maximum CO_2 uptake results equal to 332 gCO_2/kg slag. The corresponding value for each type of steel slag is reported in Table 3.1.6.

Table 3.1.6. Maximum theoretical CO_2 uptake based on the Ca content in the steel slag (see Table 3.1.5).

Maximum theoretical CO_2 uptake	**De-S slag**	**BOF slag**	**EAF slag**	**Secondary metallurgy slag**	**(BOF+LF) slag**	**(EAF+ LF) slag**	**SS metallurgy slag**
gCO_2/kg slag	361	324	316	345	348	322	345

However, generally, not all the Ca compounds react with CO_2. As previously illustrated, free CaO and $Ca(OH)_2$ react very fast, but Ca silicates require more time to dissolve in solution and react with CO_2. Those Ca silicates in the amorphous phase, as well as $CaCO_3$ and $CaSO_4$, don't react at all. For this purpose, Huijgen and Comans (2006) classified Ca compounds into three fractions, based on their tendency to dissolve in solution at different ambient conditions and thus to react with CO_2:

I) Ca easily leachable in moderate environment conditions (ambient temperature and modest CO_2 pressure). It mainly consists of $Ca(OH)_2$ (or CaO) and a part of Ca-(Fe)-silicates;
II) Ca-(Fe)-silicates that require high temperature and pressure to dissolve into solution;
III) Ca compounds that are insoluble in water.

Referring to their specific tests on BOF slag, fraction I amounted to 30% of the total Ca in the slag, whereas fraction II to about 32%.

The acid neutralization capacity (ANC) measure can, thus, be used to estimate the theoretical CO_2 uptake of a slag at ambient temperature and pressure. This value refers only to the fraction of Ca available for leaching at 25°C and so will give a much lower value than the theoretical value based on total Ca.

Based on the data about the acid neutralization capacity of BOF, EAF and secondary metallurgy slags reported by Huijgen et al. (2005) and Bonenfant et al. (2008), the sequestration capacity of steel slag at 25°C results equal to about 60-90 gCO_2/kg for BOF or EAF slag and 120 gCO_2/kg for secondary metallurgy slag. For the

same slag samples, maximum CO_2 uptake considering total Ca content results equal to about 250 gCO_2/kg of BOF or EAF slag and 450 gCO_2/kg of secondary metallurgy slag. These results suggest that most of the Ca compounds are insoluble at ambient temperature and pressure and cannot thus react with CO_2 to produce $CaCO_3$.

3.1.5. NATURAL CARBONATION OF IRON AND STEEL SLAG

Iron slag

Among the papers reported in Table 3.1.2, only two investigate natural carbonation of iron slag during its storage (Gupta et al., 1994 and Mayes et al., 2018).

Gupta et al. (1994) analysed aged air-cooled BF slag sampled from a stockpile exposed to the atmosphere for more than 6 months. The slag did not contain carbonates, suggesting that no carbonation reactions took place during storage. Ca was present only in Mg-Al-Fe-silicate compounds, which present a low reactivity with CO_2 in natural conditions.

Mayes et al. (2018) investigated the CO_2 sequestration by a > 20 million tons legacy slag deposit in north England (Consett, County Durham) where slags have been stockpiled for about 100 years. However, iron and steel slag were mixed together and it was thus impossible to separate the contribution of the two materials of slag to the amount of CO_2 overall captured by the deposit. In any case, the authors estimated that less than 1% of the maximum carbon-capture potential of the deposit has been achieved, due to the limited intake of atmospheric CO_2 into the heap.

The carbonation of iron slag under ambient atmosphere was investigated, also, by Ramme (2008). However, in this case, the authors focused on the CO_2 uptake during the curing of a foamed mixture, generated by mixing ground granulated BF slag with water and a foam generator, to produce a Controlled Low-Strength Material (CLSM). The authors found that the carbonation reactions only occurred in the outer layers of the specimens. After 182 days, only the first 3 cm of the specimens were carbonated, despite the high permeability of the material, which should favour the penetration of the CO_2. The analysis of the carbonated portion showed that about 36 gCO_2 were sequestered per kg of carbonated material, corresponding to about 3.12 gCO_2 per kg of foamed mixture.

Steel slag

Rondi et al. (2016) analysed fresh and aged EAF steel slag and found that after 3-4 months of natural ageing the content of calcium carbonate in the slag increased from 0.1% to 4.3%, corresponding to a CO_2 uptake of 19.3 gCO_2/kg slag. A greater CO_2 uptake was measured by Spanka et al. (2016) for a longer ageing period. They found that BOF slags subjected to natural ageing for 72 weeks were able to sequester up to 53 gCO_2/kg slag. The same authors measured a CO_2 uptake of 100 g per kg of EAF slag from high alloy stainless steel production (EAF SS) and of 34 gCO_2 per kg of EAF slag from carbon steel production (EAF C) after 48 weeks

of natural ageing. The low carbonation degree of EAF C slag compared to BOF and EAF SS slag can be explained by its different free CaO content. EAF SS and BOF slags used in the experiment contained 2.7% and 5.2% of free lime, respectively, whereas EAF C slag did not contain free lime. Carbonation of EAF C slag, thus, involved other Ca compounds, such as calcium silicates, that require more time to dissolve in solution and to be converted to $CaCO_3$.

Yildirim et al. (2015) analysed BOF steel slag and found that after one year of natural ageing in an open pit, free lime content in the slag decreased from 14.5% to 4.5%, corresponding to a CO_2 uptake of 82 gCO_2/kg slag. One year of ageing was insufficient to completely carbonate the slag, as a portion of free lime still remained in the slag. In addition, free MgO was found in aged slag after more than 17 months of monitoring. MgO hydrates at a very slow rate and it was not carbonated during the one-year storage in an open pit.

A CO_2 uptake of 87 gCO_2/kg slag was measured by Gupta et al. (1994) for BOF slag aged for more than 6 months. Free lime in fresh slag samples ranged between 1-10%, whereas after ageing it was equal to about 0.7%. Ageing was not sufficient to completely remove free lime, because it can be partially encapsulated by silicates which prevent its hydration and carbonation. In addition, the authors found that the carbonation process mainly reacted with the external layers of the slag stockpile and free lime content increased with the stockpile depth.

Data regarding the CO_2 uptake during natural ageing of steel slag are summarized in Table 3.1.7. CO_2 uptake during slag storage in an open pit, thus, ranges between 19.3 and 100 gCO_2/kg slag, depending on the ageing period and the content of free lime in the slag, with an average value of 62 gCO_2/kg slag. In order to achieve a good CO_2 sequestration, an ageing period of about 1 year must be secured. In addition, it is necessary to guarantee that the whole material comes in contact with air and thus with CO_2: huge piles with low porosity should be avoided, since the inner part of material will remain uncarbonated even after months of storage.

This last aspect is very important if we want to quantify the amount of CO_2 sequestered during the use of the slag in civil engineering as secondary aggregates. For example, Suer et al. (2009) analysed samples from a ten-years old asphalt road with EAF steel slag to assess the presence of ageing processes. They found that slag from the pavement edge showed traces of carbonation, whereas the road centre material was nearly identical to fresh slag.

Table 3.1.7. CO_2 uptake during natural ageing of steel slag.

Reference	Type of slag	CO_2 uptake (gCO_2/kg slag)	Age of the slag
Rondi et al., 2016	EAF (< 31.5 mm)	19.3	4 months
Spanka et al., 2016	BOF (< 11 mm)	53	72 weeks
	EAF (< 11 mm)	34	48 weeks
	SS (< 11 mm)	100	48 weeks
Yildirim et al., 2015	BOF (< 16 mm)	82	1 year
Gupta et al., 1994	BOF	87	6 months

The same environmental conditions of temperature and pressure of outdoor natural ageing were reproduced in the laboratory by Navarro et al. (2010) and Spanka et al. (2016). Data are reported in Table 3.1.8.

Navarro et al. (2010) exposed a sample of BOF and secondary metallurgy slags to air current and measured a CO_2 uptake of 45 gCO_2/kg slag after only 1 week. The main difference compared to the studies previously reported about outdoor natural ageing was the material particle size. The data about CO_2 uptake for slag aged in an open pit refer to a particle size of 10-30 mm, whereas Navarro et al. ground the slags to about 100 μm. Grinding the material increases the surface exposed to CO_2 and this was demonstrated to potentially improve the carbonation reactions (Quaghebeur et al., 2015; Huijgen et al., 2005). The authors repeated the test by using water vapour saturated air. CO_2 uptake increased to 49 gCO_2/kg slag after 1 week and 82 gCO_2/kg slag after 2 months. The presence of water favoured the kinetics of the process because the dissolved CO_2 reacts easily in an aqueous medium with the slag mineral phases to form carbonate species. This suggests the importance to spray the slag stored in open air with water, during natural ageing.

In addition to the tests of outdoor natural ageing previously reported, Spanka et al. (2016) exposed BOF and EAF slag from carbon steel production and from SS production to carbonation in the laboratory at environmental conditions of temperature and CO_2 pressure. Maximum carbonation was achieved after 12 weeks, corresponding to 37 gCO_2/kg for BOF slag, 9 gCO_2/kg slag for EAF C and 51 gCO_2/kg for EAF SS. In this case the particle size of the slag was the same both for outdoor and laboratory tests and, in fact, BOF and EAF SS slag showed more or less the same CO_2 uptake after 12 weeks both under natural climatic conditions and in the laboratory. The different behaviour of EAF C slag, which showed a lower CO_2 uptake under natural climatic conditions compared to the laboratory, can be explained by its low content of free lime.

Table 3.1.8. CO_2 uptake during laboratory experiment reproducing natural ageing of steel slag.

Reference	Type of slag	CO_2 uptake (gCO_2/kg slag)	Test duration	Note
Navarro et al., 2010	BOF+LF (< 100 μm)	45	1 week	Slag exposed to air current
	BOF+LF (< 100 μm)	49	1 week	Slag exposed to vapour saturated air current
	BOF+LF (< 100 μm)	82	8 weeks	
Spanka et al., 2016	BOF (< 11 mm)	37	12 weeks	Test carried out at a controlled humidity of 75%
	EAF (< 11 mm)	9	12 weeks	
	SS (< 11 mm)	51	12 weeks	

Data reported in Table 3.1.7 and 3.1.8 were statistically analysed to assess if the different types of slag have a different carbonation potential and to identify eventual correlations of the CO_2 uptake with the process parameters (i.e.: size dimension of the slag, ageing duration, content of total Ca compounds and free lime in the slag).

The Kruskal Wallis test (significant level of 0.05) showed that there isn't any statistically significant difference among the CO_2 uptake observed for the different types of slag. This means that the same value of sequestered CO_2 can be adopted for all the types of slag.

The correlation analysis[3] of the data (Table 3.1.9) shows a significant positive correlation of the CO_2 uptake with the content of total CaO and free lime in the slag, as it was expected. No significant correlation was found with the particle size and the duration of the ageing process, probably due to the fact that the tests performed on ground slag (Navarro et al., 2010) had a much shorter duration compared to the other tests, resulting in comparable CO_2 uptake.

Table 3.1.9. Pearson correlation coefficient of the data reported in Table 3.1.7 and in Table 3.1.8.

		CO2 uptake	particle size	test duration	total CaO content	free lime content
CO2 uptake	Correlazione di Pearson	1	-,302	,324	,607*	,584*
	Sign. (a una coda)		,183	,152	,018	,049
	N	12	11	12	12	9
particle size	Correlazione di Pearson	-,302	1	,308	-,608*	-,098
	Sign. (a una coda)	,183		,179	,024	,409
	N	11	11	11	11	8
test duration	Correlazione di Pearson	,324	,308	1	,019	,411
	Sign. (a una coda)	,152	,179		,477	,136
	N	12	11	12	12	9
total CaO content	Correlazione di Pearson	,607*	-,608*	,019	1	,523
	Sign. (a una coda)	,018	,024	,477		,074
	N	12	11	12	12	9
free lime content	Correlazione di Pearson	,584*	-,098	,411	,523	1
	Sign. (a una coda)	,049	,409	,136	,074	
	N	9	8	9	9	9

3.1.6. ACCELERATED CARBONATION POTENTIAL OF IRON AND STEEL SLAG

Iron slag

Accelerated carbonation has been proposed by several authors to promote carbon sequestration by iron slag, as well as to produce a marketable precipitated calcium carbonate (PCC) in the case of indirect carbonation processes. As previously reported, there are two main routes for accelerated carbonation: direct processes and indirect processes. Both routes will be investigated in this chapter. Compared to other alkaline materials, in fact, iron slag carbonates with more difficulty, mainly due to the fact that Ca is usually not present as CaO or $Ca(OH)_2$, but only in low reactive compounds (as previously reported in Chapter 3.1.3 - iron slag). In order to promote the carbonation process, some authors suggest using the indirect route, first extracting the Ca from

[3] Pearson correlation coefficient one-tailed, with significant level of 0.05.

the solid matrix by means of a solvent and, then, carbonating the Ca ions with an external CO_2 source (Eloneva et al., 2008).

Table 3.1.10 summarises the CO_2 uptake and the relative operating conditions for each of the tests considered in this document. Among the investigated papers, 4 report the results of direct carbonation processes and 5 focus on indirect carbonation. All these experiences refer to experimental assessment at the laboratory scale aimed at evaluating the best conditions of temperature, pressure, liquid/solid (L/S) ratio, size dimension etc. to promote carbonation and eventually PCC production. Information regarding industrial scale plants treating iron slag by accelerated carbonation was not found.

Table 3.1.10. Summary of the data used in the study for accelerated carbonation of iron slag.

Reference	**Type of slag***	**CO_2 uptake** (gCO_2/kg slag)	**Operating conditions**
		Direct carbonation	
Uliasz-Bochenczyk and Mokrzycki, 2017	GGBF (not ground)	42.76	22°C, 0.1 MPa, 100% CO_2, in dry conditions, 720 h
Johnson, 2000	GGBF (ground)	30	22°C, 0.3 MPa, 100% CO_2, in wet conditions (L/S not specified), 24 h
Chang et al. 2011a	BHC (<44 μm)	210	70°C, 0.1 MPa, 100% CO_2, L/S=10, 1 h
Chang et al. 2011b	BHC (<44 μm)	283.45	160°C, 4.8 MPa, 100% CO_2, L/S=10, 12 h
Chang et al. 2011b	BHC (<44 μm)	238.63	100°C, 4.8 MPa, 100% CO_2, L/S=10, 1 h
Chang et al. 2011b	BHC (<44 μm)	245.69	160°C, 9 MPa, 100% CO_2, L/S=10, 1 h
		Indirect carbonation	
Mun and Cho, 2013	BF (<74 μm)	90	Extraction with 0.1 M acetic acid at 350°C, L/S=10, 1 h Carbonation at 22°C, 0.1 MPa, 100% CO_2, L/S=10, 1 h
Hu et al., 2017	GGBF (D_{50}=50.43 μm)	316	Extraction with 3 M $(NH_4)_2SO_4$ at 80°C, L/S=4, 1 h Carbonation at 40-55°C, 0.1 MPa, with a solution of NH_4HCO_3 or $(NH_4)_2CO_3$, 1 h
Chiang et al., 2014	GGBF (D_{50}=138 μm)	66.97	Extraction with 0.5 M acetic acid at 30°C, L/S=7, 1 h Carbonation at 90°C, 0.6 MPa, 100% CO_2, L/S= 7, 1 h
Chiang et al., 2014	GGBF (D_{50}=138 μm)	278.33	Extraction with 2 M acetic acid at 30°C, L/S=7, 1 h Carbonation at 90°C, 0.6 MPa, 100% CO_2, L/S=7, 1 h

Eloneva et al., 2008	GGBF (D_{50}=500 μm)	227.28	Extraction with 3.68 M acetic acid at 70°C, L/S=20, 2 h Carbonation at 30°C, 0.1 MPa, 100% CO_2, L/S=20, 2 h
Lee et al., 2016	GGBF (< 74 μm)	123.16	Extraction with 2M NH_4NO_3 at 30°C, L/S=10, 1 h Carbonation at 22°C, 0.1 MPa, 98% CO_2, L/S=10, 1 h
Lee et al., 2016	GGBF (< 74 μm)	124.54	Extraction with 1M NH_4NO_3 at 30°C, L/S=10, 30 min Carbonation at 22°C, 0.1 MPa, 98% CO_2, L/S=10, 1 h
Lee et al., 2016	GGBF (< 74 μm)	122.93	Extraction with 2M NH_4Cl at 30°C, L/S=10, 1 h Carbonation at 22°C, 0.1 MPa, 98% CO_2, L/S=10, 1 h
Lee et al., 2016	GGBF (< 74 μm)	122.74	Extraction with 2M CH_3COONH_4 at 30°C, L/S=10, 1 h Carbonation at 22°C, 0.1 MPa, 98% CO_2, L/S=10, 1 h
Lee et al., 2016	GGBF (< 74 μm)	85.93	Extraction with 2M $(NH_4)_2SO_4$ at 30°C, L/S=10, 1 h Carbonation at 22°C, 0.1 MPa, 98% CO_2, L/S=10, 1 h

*GGBF=ground granulated blast furnace slag; BHC=blended hydraulic slag cement.

Focusing on direct carbonation tests, those carried out by Uliasz-Bochenczyk and Mokrzycki (2017) and by Johnson (2000) suggest that iron slag can sequester about 30-43 gCO_2/kg slag, when the carbonation process is carried out in controlled laboratory conditions. Uliasz-Bochenczyk and Mokrzycki carbonated ground granulated BF slag in dry conditions, just wetting the slag on the surface, without grinding it. The carbonation process was carried out in a closed chamber with pure CO_2 for 28 days. The process imitated the natural carbonation process that can happen during slag storage, with the only difference of subjecting the slag to a 100% CO_2 atmosphere. Johnson (2000) carbonated milled ground granulated BF slag in a water suspension and at modest pressure, by using a 100% CO_2 gas flow. The carbonation process lasted 24 hours. Despite the different conditions at which the tests were carried out (dry vs. wet, non-ground slag vs. ground slag), both authors observed that only 9-12% of the carbon sequestration potential based on the slag Ca content was actually achieved. Johnson suggested that the low carbonation degree of the BF slag is due to the absence of portlandite, one of the major reactants for carbonation, and to competing effects resulting from the low rate of hydration, which give an early opportunity for the intake of CO_2. In order to allow slag hydration, the glassy structure of the ground granulated BF slag must break and this happens only under alkaline conditions. Therefore, the absence of alkaline conditions and/or the slow kinetics of reactions with the slag may hinder the accelerated carbonation of this material (Johnson, 2000). In addition, the modest conditions of temperature and pressure at which the tests were carried may have conditioned the achieved results.

Much higher CO_2 uptakes were observed by Chang et al. (2011a and 2011b). However, their results refer to samples of a blended hydraulic slag cement (BHC) containing 90% of BF slag and 10% of Portland cement. The total content of Ca as CaO in the BHC was higher than the average value observed in the iron slag (53-54% vs. 40%). Furthermore, the authors observed the presence of free lime in the samples. It was not specified if the higher content of CaO and the presence of free lime was due to the Portland cement or to the specific composition of the BF slag used to produce the BHC. The tests were carried out in slurry conditions, at high temperature, both at atmospheric pressure and at high pressure in an autoclave. The BHC samples were ground and the carbonation was carried out with injection of pure CO_2 for 1-12 hours. The authors achieved a CO_2 uptake of 210-284 gCO_2/kg, depending on the operating conditions, corresponding to 49-68% of the potential carbon sequestration capacity of the BHC based on its Ca content. However, due to the different type of material, it is impossible to compare these results with those referred to the sole BF slag.

For the indirect carbonation process, an average CO_2 uptake of about 156 gCO_2/kg slag was observed, ranging from 90 to 316 gCO_2/kg slag depending on the operating conditions.

In indirect carbonation, the critical step is Ca extraction that must be performed in order to maximize Ca leaching from the slag and contextually minimizing the leaching of undesirable elements, such as Al, Fe, Mn and Si. This last aspect is particularly important when the main objective of the process is the production of a marketable PCC and, possibly, of other products (for example, zeolite as proposed by Chiang et al. (2014) or Al_2O_3 and Mg precipitate as proposed by Hu et al. (2017)). The choice of the type of solvent used for the extraction, as well as of its dosage and of the operating temperature and pressure are, thus, of primary importance to obtain a leachate solution rich in Ca and of acceptable purity. Several types of solvent have been proposed in the scientific literature. The most used are acetic acid, ammonium salts ($(NH_4)_2SO_4$, NH_4NO_3, NH_4Cl, CH_3COONH_4) and aqua regia. The dosage must be defined case by case in order to maximize Ca leaching and Ca selectivity. Increasing the solvent loading promotes Ca leaching but also the undesirable extraction of other elements, such as Al (Chiang et al., 2014). Usually, ambient or modest temperature and pressure are used in the extraction process. However, Hu et al. (2017) proposed operating at high temperature (300-350°C) to improve Ca and Mg leaching from the silicates. Obviously, this also improves the leaching of other elements, such as Al that must be removed before the carbonation step by using gaseous NH_3. On general, a contact time of 1-2 hours is sufficient to achieve a good efficiency of Ca extraction.

NaOH or $NaHCO_3$ are usually added before the carbonation step, to promote $CaCO_3$ precipitation. In acidic conditions, Ca cannot react with CO_2. It is, thus, necessary to increase the pH of the solution in order to favour $CaCO_3$ precipitation (Eloneva et al., 2008). Carrying out the carbonation step at modest pressure and temperature seems to be the best solution (Chiang et al., 2014). Working at high temperature and pressure weakly influences Ca precipitation, whereas it strongly promotes Mg precipitation that should be avoided if the aim of the process is also the production of a high-quality PCC (Chiang et al., 2014). The last point to be considered is the contact between Ca and carbon. Carbonation can be performed by injecting a CO_2 flow in

the Ca-rich solution (gas-liquid reaction) or by using a solution of $(NH_4)_2CO_3$ produced from the dissolution of the gaseous CO_2 in an ammonia solution (liquid-liquid reaction) (Chiang et al., 2014; Hu et al., 2017).

The statistical analysis of the data reported in Table 3.1.9 relatively to the indirect process does not show any statistically significant correlation between the CO_2 uptake and the other parameters. This can be explained by the fact that only the best results achieved during the experimentations are usually published. The CO_2 uptake corresponding to worst operating conditions is often not available. This limits the possibility to find a correlation between the CO_2 uptake and the solvent dosage or the operating temperature.

It is, finally, worth pointing out that all the tests considered here were carried out on ground granulated BF slag. Only Lee et al. (2016) reported the results of some tests on air-cooled BF slag. However, at the same operating conditions, the Ca extraction efficiency from the air-cooled BF slag resulted in only 11-17%, whereas that from the ground granulated BF slag was equal to 49-52%.

Based on the data previously reported, it is thus possible to state that the indirect carbonation of the iron slag is a complex process especially when aimed at the production of a marketable PCC. Controlling the process parameters at the different steps (T, P, chemicals concentration at the extraction and at the carbonation steps) is necessary in order to improve the selective precipitation of Ca. The best operating conditions must be defined on the basis of a compromise between the amount of CO_2 that can be sequestered, and thus the amount of the precipitate $CaCO_3$, and the purity of the precipitate. Increasing the CO_2 uptake means increasing the impurity in the precipitate and this results in a non-marketable PCC (Chiang et al., 2014). Up to now, indirect carbonation of iron slag is a process that still needs some improvement (Elenova et al., 2008). Despite this, the indirect process allows more CO_2 to be captured compared to the direct route. The different performance of the two carbonation routes was statistically confirmed by applying the Mann-Whitney U-test.

Steel slag

Accelerated carbonation has been proposed by several authors to improve the quality of the steel slag in view of its recycling as a secondary material, as well as for CO_2 capture and storage. The interesting aspect of this practice is the possibility to operate with industrial flue gases, capturing their CO_2 prior of the emission in the atmosphere.

Currently, however, all the experiences reported in the scientific literature refer to experimental assessment at the laboratory scale aimed at evaluating the best conditions of temperature, pressure, liquid/solid (L/S) ratio, size dimension etc. to promote carbonation. Information regarding industrial scale plants treating steel slag by accelerated carbonation was not found.

As previously reported, there are two main routes for accelerated carbonation: direct processes and indirect processes. Contrary to BF slag, steel slag contains a non-negligible amount of free lime that ensures that high carbonation level can be achieved thought direct carbonation processes, without having to apply the indirect route. For this reason, in this chapter, only direct processes will be considered.

Among the analysed documents, 14 papers report experiences of accelerated carbonation performed in slurry phase (L/S > 1), 10 papers of accelerated carbonation performed in aqueous solution (L/S < 1) and 5 papers refer to tests of accelerated carbonation performed without the addition of water. In addition, 3 papers reporting the results of accelerated carbonation tests performed in column were found. Due to the peculiarity of column tests, they were considered as a separate class, regardless of the L/S ratio adopted in the test.

The environmental conditions at which the tests were carried out change significantly from one author to another. Pressure and temperature ranged from natural climatic conditions to a maximum of 3 MPa and 200°C, respectively. The tests were performed with ambient air, CO_2 enriched air in order to simulate industrial flue gases containing from 10 to 40% of CO_2, or with a 100% CO_2 gas. For accelerated carbonation in the slurry phase, the adopted L/S ratio ranged from 3 to 62.5 l/kg, whereas the tests in aqueous solution were performed with a L/S of 0.12-0.5 l/kg. Slag was usually ground below 1 mm, often below 250 μm, with the exception of the test on granulated material carried out by Morone et al. (2014), that refers to slag ground at 10 mm, and the tests carried out by Spanka et al. (2016) on slag of particle size below 11 mm. Test duration was very variable, from a few minutes to a few hours, with the exception of the tests carried out by Spanka et al. (2016) that lasted 12 weeks.

Due to the broad variety of conditions at which the tests were carried out, they were classified into different groups:

I) accelerated carbonation tests in slurry phase, at harsh conditions of temperature and pressure, with 100% CO_2 gas ($P \geq 0.6$ MPa & $T \geq 50$°C);

II) accelerated carbonation tests in slurry phase, at harsh conditions of temperature and pressure, with CO_2 enriched flue gas ($P \geq 1$MPa & $T \geq 50$°C, $CO_2 < 100\%$);

III) accelerated carbonation tests in slurry phase, at modest or ambient conditions of temperature and pressure, with 100% CO_2 gas ($P \leq 0.6$ MPa & $T \leq 60$°C);

IV) accelerated carbonation tests in slurry phase, at modest or ambient conditions of temperature and pressure, with CO_2 enriched flue gas ($P \leq 1$MPa & $T \leq 50$°C & $CO_2 < 100\%$);

V) accelerated carbonation tests in aqueous phase, at harsh conditions of temperature and pressure, with 100% CO_2 gas ($P \geq 0.9$MPa & $T \geq 50$°C);

VI) accelerated carbonation tests in aqueous phase, at harsh conditions of temperature and pressure, with CO_2 enriched gas ($P \geq 0.7$MPa & $T \geq 50$°C & $CO_2 < 100\%$);

VII) accelerated carbonation tests in aqueous phase, at modest or ambient conditions of temperature and pressure, with 100% CO_2 gas ($P \leq 0.3$MPa & $T \leq 50$°C);

VIII) accelerated carbonation tests in aqueous phase, at modest or ambient conditions of temperature and pressure, with CO_2 enriched gas ($P = 0.1$ MPa & $T <= 50$ °C & $CO_2 < 100\%$);

IX) accelerated carbonation tests in dry conditions, at harsh conditions of temperature and pressure, with 100% CO_2 gas ($P = 2$MPa & $T \geq 80$°C);

X) accelerated carbonation tests in dry conditions, at ambient conditions of temperature and pressure, with 100% CO_2 (P=0.1 MPa & ambient T);
XI) accelerated carbonation tests in dry conditions, at modest or ambient conditions of temperature and pressure, with CO_2 enriched gas (P=0.1 MPa & T≤50°C & CO_2< 100%);
XII) carbonation column tests, at ambient conditions of temperature and pressure, with 100% CO_2 (P=0.1 MPa & ambient T);
XIII) carbonation column tests, at modest or ambient conditions of temperature and pressure, with CO_2 enriched gas (P=0.1 MPa & T<90°C & CO_2 < 100%).

Table 3.1.11 summarises the CO_2 uptake and the relative operating conditions for each of the tests considered in this document, whereas in Table 3.1.12 the average CO_2 uptake for the 13 test categories previously identified is reported.

The majority of the tests were performed on EAF, BOF and SS slag. Only two tests were performed on secondary metallurgy slag and none on De-S slag. The data analysis was carried out without distinction among the different types of slag, in order to maintain a sufficiently high number of cases for each of the identified groups for further statistical tests.

Table 3.11. Summary of all the data used in the study for accelerated carbonation of steel slag.

Reference	**Type of slag**	**CO_2 uptake** (gCO_2/kg slag)	**Operating conditions**
		Category I	
Baciocchi et al., 2016	BOF (< 150 μm)	325	100°C, 1 MPa, 100% CO_2, L/S=5, 24 h
Baciocchi et al., 2016	BOF (< 150 μm)	403	100°C, 1 MPa, 100% CO_2, L/S=5, 24 h
Baciocchi et al., 2010	BOF	150	100°C, 1.9 MPa, 100% CO_2, L/S=10, 4 h
Huijgen et al., 2005	BOF (< 38 μm)	184	100°C, 1.9 MPa, 100% CO_2, L/S=10, 30 min
Baciocchi et al., 2015	EAF (< 150 μm)	280	100°C, 1 MPa, 100% CO_2, L/S=5, 24 h
Baciocchi et al., 2015	BOF (< 150 μm)	403	100°C, 1 MPa, 100% CO_2, L/S=6, 24 h
Zingaretti et al., 2013	BOF (< 150 μm)	105	200°C, 1 MPa, 100%CO_2, L/S= 10, 30 min
Zingaretti et al., 2013	BOF (< 150 μm)	255	100°C, 1 MPa, 100%CO_2, L/S= 5, 30 min
Zingaretti et al., 2013	EAF (< 150 μm)	40	50°C, 1.9 MPa, 100%CO_2, L/S= 10, 1 h
Zingaretti et al., 2013	EAF (< 150 μm)	210	100°C, 1 MPa, 100%CO_2, L/S= 5, 30 min
Huijgen and Comans, 2006	BOF (< 38 μm)	154	150°C, 2 MPa, 100% CO_2, L/S= 10, 30 min
Huijgen and Comans, 2006	BOF (< 38 μm)	210	200°C, 3 MPa, 100% CO_2, L/S= 3, 1 h
Santos et al., 2013	SS (< 46 μm)	169	180°C, 0.6 MPa, 100% CO_2, L/S=16, 1 h
Santos et al., 2013	SS (< 46 μm)	227	90°C, 1.5 MPa, 100% CO_2, L/S=16, 1 h
Santos et al., 2013	SS (< 46 μm)	211	90°C, 0.6 MPa, 100% CO_2, L/S=16, 2 h
Santos et al., 2013	SS (< 46 μm)	132	90°C, 0.6 MPa, 100% CO_2, L/S=20, 1 h
Santos et al., 2013	SS (< 46 μm)	264	90°C, 1.5 MPa, 100% CO_2, L/S=62.5, 1 h
Santos et al., 2013	SS (< 39.3 μm)	208	180°C, 0.6 MPa, 100% CO_2, L/S=16, 1 h
Santos et al., 2013	SS (< 39.3 μm)	291	90°C, 0.9 MPa, 100% CO_2, L/S=16, 1 h
Santos et al., 2013	SS (< 39.3 μm)	270	90°C, 0.6 MPa, 100% CO_2, L/S=16, 2 h

Santos et al., 2013	SS (< 39.3 μm)	166	90°C, 0.6 MPa, 100% CO_2, L/S=20, 1 h
Santos et al., 2013	SS (< 39.3 μm)	312	90°C, 3 MPa, 100% CO_2, L/S=60, 1 h
		Category II	
Baciocchi et al., 2016	BOF (< 150 μm)	80	100°C, 1 MPa, 10% CO_2, L/S=5, 24 h
Baciocchi et al., 2016	BOF (< 150 μm)	81	100°C, 1 MPa, 10% CO_2, L/S=5, 24 h
Baciocchi et al., 2016	BOF (< 150 μm)	211	100°C, 1 MPa, 40% CO_2, L/S=5, 24 h
Baciocchi et al., 2016	BOF (< 150 μm)	292	100°C, 1 MPa, 40% CO_2, L/S=5, 24 h
		Category III	
Pan et al., 2013	BOF (< 62 μm)	81.3	25°C, 0.1 MPa, 100% CO_2, L/S=20, 1 min
Huijgen and Comans, 2006	BOF (< 38 μm)	76	30°C, 0.2 MPa, 100% CO_2, L/S=10, 5 min
Chang et al., 2012	BOF (< 62 μm)	289	60°C, 0.1 MPa, 100% CO_2, L/S=20, 30 min
Pan et al., 2017	EAF (< 15 μm)	380	50°C, unknown P, 100% CO_2, L/S=25, 40 min
Lekakh et al., 2008	EAF (< 150-250 μm)	60	Ambient T and P, 100% CO_2, L/S=8.3, 70 h
Lekakh et al., 2008	Secondary metallurgy (45-75 μm)	49	Ambient T and P, 100% CO_2, L/S=8.3, 70 h
Santos et al., 2013	SS (< 46 μm)	158	30°C, 0,6 MPa, 100% CO_2, L/S=16, 1 h
Santos et al., 2013	SS (< 39.3 μm)	182	30°C, 0.6 MPa, 100% CO_2, L/S=16, 1 h

Table 3.11 (continued). Summary of all the data used in the study for accelerated carbonation of steel slag.

Reference	Type of slag	CO_2 uptake (gCO_2/kg slag)	Operating conditions
	Category IV		
Bonenfant et al., 2008	EAF (38-106 μm)	17.4	20°C, 0.1 MPa, 15% CO_2, L/S=10, 24 h
Bonenfant et al., 2008	LS (38-106 μm)	247	20°C, 0.1 MPa, 15% CO_2, L/S=10, 40 h
Ghacham et al., 2016	EAF (< 24 μm)	52	Ambient T, 1.1MPa, 18% CO_2, L/S=10, 10 min
Pan et al., 2017	EAF (< 15 μm)	250	50°C, unknown P, 30% CO_2, L/S=25, 40 min
Santos et al., 2010	SS (< 29.7 μm)	123	Unknown T, 0.1 MPa, 20% CO_2, L/S=50, 35 min
	Category V		
Baciocchi et al., 2016	BOF (< 150 μm)	178	T=50°C, P= 1 MPa, 100% CO_2, L/S=0.3, 24 h
Baciocchi et al., 2016	BOF (< 150 μm)	202	T= 50°C, P= 1 MPa, 100% CO_2, L/S=0.3, 24 h
Baciocchi et al., 2015	EAF (< 150 μm)	176	T= 50°C, P= 1 MPa, 100% CO_2, L/S=0.3, 24 h
Baciocchi et al., 2015	BOF (< 150 μm)	209	T= 50°C, P= 1 MPa, 100% CO_2, L/S=0.3, 24 h
Zingaretti et al., 2013	BOF (< 126 μm)	125	T= 50°C, P= 0.9 MPa, 100% CO_2, L/S=0.3, 1 h
Baciocchi et al., 2010 (via Zingaretti et al., 2013)	SS	201	T= 50°C, P= 1 MPa, 100% CO_2, L/S=0.4, 1 h
Thuy, 2013	SS (<177 μm)	145	T= 50°C, P= 1 MPa, 100% CO_2, L/S=0.4, 24 h
Thuy, 2013	SS (177-840 μm)	74	T= 50°C, P= 1 MPa, 100% CO_2, L/S=0.4, 24 h
Thuy, 2013	SS (177-840 μm)	65	T= 50°C, P= 1 MPa, 100% CO_2, L/S=0.4, 8 h
Capobianco et al., 2014	SS (< 177 μm)	120	T= 50°C, P= 1 MPa, 100% CO_2, L/S=0.4, 4 h
Capobianco et al., 2014	SS (< 177 μm)	130	T= 50°C, P= 1 MPa, 100% CO_2, L/S=0.4, 8 h
Capobianco et al., 2014	SS (177-840 μm)	60	T= 50°C, P= 1 MPa, 100% CO_2, L/S=0.4, 4 h
Capobianco et al., 2014	SS (177-840 μm)	74	T= 50°C, P= 1 MPa, 100% CO_2, L/S=0.4, 24 h

Category VI			
Baciocchi et al., 2016	BOF (< 150 μm)	129	T=50°C, P= 0.7-1 MPa, 40% CO_2, L/S=0.3, 24 h
Baciocchi et al., 2016	BOF (< 150 μm)	195	T= 50°C, P= 0.7-1 MPa, 40% CO_2, L/S=0.3, 24 h
Category VII			
Baciocchi et al., 2010 (via Zingaretti et al., 2013)	EAF (< 126 μm)	149	T=50°C, P= 0.3 MPa, 100% CO_2, L/S=0.3, 1 h
Baciocchi et al., 2010 (via Zingaretti et al., 2013)	EAF (< 126 μm)	180	T=50°C, P= 0.3 MPa, 100% CO_2, L/S=0.3, 24 h
Baciocchi et al., 2010 (via Zingaretti et al., 2013)	SS	215	T=50°C, P= 0.3 MPa, 100% CO_2, L/S=0.4, 1 h
Baciocchi et al., 2010	BOF	108	T=50°C, P= 0.3 MPa, 100% CO_2, L/S=0.4, 2 h
Baciocchi et al., 2009 (via Pan et al., 2012)	SS	130	T=50°C, P= 0.3 MPa, 100% CO_2, L/S=0.4, 2 h
Zingaretti et al., 2013	BOF (< 126 μm)	81	T=50°C, P= 0.1 MPa, 100% CO_2, L/S=0.3, 1 h
Baciocchi et al., 2010 (via Zingaretti et al., 2013)	EAF (< 150 μm)	90	T=50°C, P= 0.1 MPa, 100% CO_2, L/S=0.4, 1 h
Morone et al., 2014	BOF (< 10 mm)	140	Ambient T and P, 100% CO_2, L/S=0.12, 1.5 h
Capobianco et al., 2014	SS (< 177 μm)	52	Ambient T and P, 100% CO_2, L/S=0.2, 4 h

Table 3.11 (continued). Summary of all the data used in the study for accelerated carbonation of steel slag.

Reference	Type of slag	CO_2 uptake (gCO_2/kg slag)	Operating conditions
		Category VIII	
Santos et al., 2010	SS (< 38.7 μm)	50	50°C, 0.1 MPa, 20% CO_2, L/S=0.5, 6h
Santos et al., 2010	SS (< 38.7 μm)	65	50°C, 0.1 MPa, 20% CO_2, L/S=0.2, 6 h
Santos et al., 2010	SS (< 38.7 μm)	90	30°C, 0.1 MPa, 20% CO_2, L/S=0.2, 6 h
Santos et al., 2010	SS (< 19.3 μm)	60	50°C, 0.1 MPa, 20% CO_2, L/S=0.2, 24 h
Santos et al., 2010	SS (< 38.7 μm)	20	50°C, 0.1 MPa, 20% CO_2, L/S=0.2, 24 h
Santos et al., 2010	SS (< 38.7 μm)	90	50°C, 0.1 MPa, 20% CO_2, L/S=0.5, 24h
Santos et al., 2010	SS (< 25.3 μm)	160	30°C, 0.1 MPa, 20% CO_2, L/S=0.5, 7 days
Santos et al., 2013	SS (< 46 μm)	13.7	30°C, 0.1 MPa, 20% CO_2, L/S=0.33, 3 h
Santos et al., 2013	SS (< 46 μm)	60	30°C, 0.1 MPa, 20% CO_2, L/S=0.33, 26 h
Santos et al., 2013	SS (< 46 μm)	100	30°C, 0.1 MPa, 20% CO_2, L/S=0.33, 94 h
Santos et al., 2013	SS (< 46 μm)	128	30°C, 0.1 MPa, 20% CO_2, L/S=0.33, 144 h
Santos et al., 2013	SS (< 39.3 μm)	25	30°C, 0.1 MPa, 20% CO_2, L/S=0.33, 3 h
Santos et al., 2013	SS (< 39.3 μm)	43	30°C, 0.1 MPa, 20% CO_2, L/S=0.33, 26 h
Santos et al., 2013	SS (< 39.3 μm)	146	30°C, 0.1 MPa, 20% CO_2, L/S=0.33, 94 h
Santos et al., 2013	SS (< 39.3 μm)	192	30°C, 0.1 MPa, 20% CO_2, L/S=0.33, 144 h
Morone et al., 2014	BOF (< 10 mm)	60	Ambient T and P, ambient air, L/S=0.12, 1 h
		Category IX	
Quaghebeur et al., 2015	SS (original size < 125 μm)	150	T=140°C, P=2MPa, 100%CO_2, compacted slag, 16 h
Quaghebeur et al., 2010	SS (original size < 1 mm)	177	T=140°C, P=2MPa, 100%CO_2, compacted slag, 16 h
Quaghebeur et al., 2015	BOF (original size < 125 μm)	120	T= 140°C, P=2MPa, 100%CO_2, compacted slag, 16 h
Quaghebeur et al., 2010	SS (original size < 1 mm)	188	T= 140°C, P=2MPa, 100%CO_2, compacted slag, 16 h
Boone et al., 2014	SS (original size < 500 μm)	59	T= 80°C, P=2MPa, 100%CO_2, compacted slag, 8 h
		Category X	
Spanka et al., 2016	BOF	46	Ambient T and P, 100% CO_2, 12 weeks
Spanka et al., 2016	EAF	41	Ambient T and P, 100% CO_2, 12 weeks
Spanka et al., 2016	SS	93	Ambient T and P, 100% CO_2, 12 weeks
		Category XI	
Spanka et al., 2016	BOF	37	Ambient T and P, 30% CO_2, 12 weeks

Spanka et al., 2016	EAF	38	Ambient T and P, 30% CO_2, 12 weeks
Spanka et al., 2016	SS	53	Ambient T and P, 30% CO_2, 12 weeks
Santos et al., 2010	SS (< 38.7 μm)	30	50°C, 0.1 MPa, 20% CO_2, 6 h
		Category XII	
Thuy, 2013	SS (177-840 μm)	57	T=22°C, P=0.1 MPa, 100% CO_2, L/S=0.2, 8 h
Thuy, 2013	SS (177-840 μm)	52	T=22°C, P=0.1 MPa, 100% CO_2, L/S=0.2, 8 h
Capobianco et al., 2014	SS (177-840 μm)	55	T=22°C, P=0.1 MPa, 100% CO_2, L/S=0.2, 4 h

Table 3.11 (continued). Summary of all the data used in the study for accelerated carbonation of steel slag.

Reference	Type of slag	CO_2 uptake (gCO_2/kg slag)	Operating conditions
Category XIII			
Van Zomeren et al., 2011	BOF (< 2.5 mm)	3	90°C, 0.1 MPa, 20% CO_2, L/S=0.4, 75 h
Van Zomeren et al., 2011	BOF (< 2.5 mm)	6	90°C, 0.1 MPa, 20% CO_2, L/S=1, 100 h
Van Zomeren et al., 2011	BOF (< 2.5 mm)	2.2	20°C, 0.1 MPa, 20% CO_2, L/S=1, 24 h
Van Zomeren et al., 2011	BOF (< 2.5 mm)	1.2	20°C, 0.1 MPa, 20% CO_2, L/S=0.4, 24 h
Van Zomeren et al., 2011	BOF (< 2.5 mm)	9	90°C, 0.1 MPa, 20% CO_2, L/S=0.4, 75 h
Van Zomeren et al., 2011	BOF (< 2.5 mm)	15	90°C, 0.1 MPa, 20% CO_2, L/S=1, 75 h

Table 3.12. Min-max and average CO_2 uptake for each of the test categories and corresponding operating conditions.

Test category	**CO_2 uptake (gCO_2/kg slag)**		
	Minimum	**Average**	**Maximum**
I *22 cases*	40 *(EAF slag < 150 μm; 50°C; 1.9MPa; L/S=10; 1 h)*	226	403 *(BOF slag < 150 μm; 100°C; 1MPa; L/S=5; 24 h)*
II *4 cases*	80 *(BOF slag < 150 μm; 100°C; 1MPa; 10%CO_2; L/S=5; 24 h)*	166	292 *(BOF slag < 150 μm; 100°C,, 1MPa; 40%CO_2; L/S=5; 24 h)*
III *8 cases*	49 *(LF slag 45-75 μm; ambient T and P; L/S=8.3; 70 h)*	159.5	380 *(EAF slag < 15 μm; 50°C; unknown P; L/S=25; 40 min)*
IV *5 cases*	17 *(EAF slag 30-106 μm; 20°C; 0.1MPa;15% CO_2; L/S=10; 24 h)*	138	250 *(EAF slag < 15 μm; 50°C; unknown P; 30% CO_2; L/S=25; 40 min)*
V *13 cases*	60 *(SS slag < 177 μm; 50°C, 1MPa; L/S=0.4; 4 h)*	135	209 *(BOF slag < 150 μm; 50°C, 1MPa; L/S=0.3; 24 h)*
VI *2 cases*	129 *(BOF slag < 150 μm; 50°C; 0.7-1 MPa; 40% CO_2; L/S=0.3; 24 h)*	162	195 *(BOF slag < 150 μm; 50°C; 0.7-1 MPa; 40% CO_2; L/S=0.3; 24 h)*
VII *9 cases*	52 *(SS slag < 177 μm; ambient T and P; L/S=0.2; 4 h)*	127	215 *(SS slag; 50°C; 0.3 MPa; L/S=0.4; 1 h)*

VIII *16 cases*	13.7 *(SS slag < 46 μm; 30°C; ambient P; 20% CO_2; L/S=0.33; 3 h)*	81	192 *(SS slag < 39.3 μm; 30°C; ambient P; 20% CO_2; L/S=0.33; 144 h)*
IX *5 cases*	59 *(compacted SS slag; 80°C; 2MPa;* *8 h)*	139	188 *(compacted SS slag; 140°C; 2MPa; 16 h)*
X *3 cases*	41 *(EAF slag; ambient T and P; 12 weeks)*	60	93 *(SS slag; ambient T and P; 12 weeks)*
XI *4 cases*	30 *(SS slag < 38.7 μm; 50°C; ambient P; 20% CO_2; 6 h)*	39.5	53 *(SS slag; ambient T and P; 30% CO_2; 12 weeks)*
XII *3 cases*	52 *(SS slag 177-840 μm; ambient T and P; L/S= 0.2; 8 h)*	55	57 *(SS slag 177-840 μm; ambient T and P; L/S= 0.2; 8 h)*
XIII *6 cases*	1.2 *(BOF slag < 2.5 mm; ambient T and P; 20% CO_2; L/S=0.4; 24 h)*	6	15 *(BOF slag < 2.5 mm; 90°C; ambient P; 20% CO_2; L/S=1; 75 h)*

The higher CO_2 uptakes were achieved when the slag was carbonated at high temperature and pressure, with a 100% CO_2 gas in a slurry phase. In this case, the average CO_2 uptake is about 226 gCO_2/kg slag. In general, the slurry phase condition results in higher carbonation yields compared to the aqueous phase, as reported by Baciocchi et al. (2015 and 2016). Average CO_2 uptake achieved in slurry phase tests (categories I-IV) ranged from 138 to 226 gCO_2/kg of slag, depending on the operating conditions, whereas the corresponding range for the tests in aqueous solutions (categories V-VIII) is 81-162 gCO_2/kg slag. As suggested by Santos et al. (2013), the slurry phase condition probably promotes the dissolution of reactive metals from the solid phase, as well as prevents the coating effect exerted by the precipitated carbonate product into the unreacted core of the slag particles.

For the tests carried out in dry phase (categories IX-XI), the average CO_2 uptake ranges between 39 and 139 gCO_2/kg slag, depending on the operating conditions. However, it is worth pointing out that the tests classified in category IX show some peculiarities: the material was subjected to carbonation after compaction in blocks, whereas results of carbonation tests generally refer to loose material. In addition, the tests were carried out in very harsh temperature and pressure conditions. When the carbonation was performed on free material and at ambient conditions of temperature and pressure (categories X and XI), the lack of water addition resulted in a lower CO_2 uptake compared to that achieved in the aqueous and slurry phase.

The CO_2 captured during carbonation column tests (categories XII-XIII) is modest, regardless of the applied L/S ratio, due both to the modest temperature and pressure conditions at which these tests were carried out and to the worst distribution of CO_2 inside the material (Capobianco et al., 2014).

The increase of the L/S ratio plays a positive role in aqueous solution carbonation, because it enhances Ca and CO_2 dissolution (Baciocchi et al., 2010), whereas in the slurry phase tests it is better to adopt L/S of about 5-10 (Huijgen et al., 2005; Ghacham et al., 2016), which results in a high ionic strength and, consequently, high solubility of Ca (Huijgen et al., 2005). For ratios below the optimal, the slurry does not mix well in the reactor, causing poor mass transfer, whereas for ratios above the optimal, the excess liquid in the slurry leads to a lower ionic strength (Georgakopoulos et al., 2016). For column carbonation tests, the carbonation rate is usually faster when the test is carried out under water saturated conditions (van Zomeren et al., 2011). Under unsaturated conditions, the variation of the L/S ratio does not significantly affect the CO_2 uptake (Capobianco et al., 2014).

Temperature plays a double role in the carbonation processes that are carried out in three phases: at high temperature, leaching of Ca from the matrix is likely to proceed faster, but the solubility of CO_2 in the solution decreases. For this reason, several authors observed that the CO_2 uptake increases with the temperature up to a certain value and then the conversion rate decreases for a further temperature increase. Huijgen et al. (2005) found a maximum temperature value of about 200°C, above which the CO_2 uptake decreases, whereas for Baciocchi et al. (2010) this value is about 100°C and for Pan et al. (2017) is between 50 and 55°C. The discrepancy among these authors' findings might be related to the different conditions at which the carbonation tests were carried out, as well as to the different mineralogy of the slag. In fact, the effects of the temperature on the CO_2 uptake is also related to the mineral composition of the slag, as found by Quaghebeur et al. (2015). They observed that increasing the temperature promotes CO_2 uptake in samples rich of Ca-Mg silicates, whereas reduces carbonation in samples containing mainly $Ca(OH)_2$.

The double role of the temperature is more evident when the carbonation is carried out in the slurry phase. For tests in aqueous phase, Baciocchi et al. (2010) found that increasing the temperature is always beneficial, since it promotes silicates dissolution.

CO_2 pressure plays a more important role when carbonation is carried out in the slurry phase, compared to aqueous phase, especially when high temperatures are applied. Increasing CO_2 pressure promotes CO_2 dissolution (Quaghebeur et al., 2015; Baciocchi et al.; 2016, Ghacham et al., 2016), as well as that of Ca (Ghacham et al., 2016). At temperature below the optimal, the effect of the CO_2 pressure on the conversion extent is negligible, because the limiting factor of carbonation is Ca leaching (Georgakopoulos et al., 2016). However, different experiences are also reported in the scientific literature. For example, Yu and Wang (2011) found that at high temperature, carbonation rate increases with lower CO_2 concentration in the flue gas, probably due to the presence of Fe, Mn and Al compounds in the slag that have a catalytic effect.

Another important parameter that influences CO_2 uptake is the particle size. Several authors found that milling and grinding is a necessary step to enhanced slag carbonation (Huijgen et al., 2015; Lekakh et al., 2008). Quaghebeur et al. (2015) observed a complete conversion of the free lime only in particles below 125 μm. Similar values were proposed by Costa (2009).

For reaction time, free lime and $Ca(OH)_2$ react very fast with CO_2, as well as the calcium silicates that are relatively easily leachable, whereas the other Ca compounds can require longer time, depending on the temperature and pressure at which carbonation is carried out (Huijgen et al., 2005). In general, a reaction time of at least 30 minutes is required in order to achieve a good conversion rate (Ghacham et al., 2016).

The previously illustrated relationships between the CO_2 uptake and the main process parameters are confirmed by the statistical analysis of the data reported in Table 3.1.11.

The Pearson correlation matrix, reported in Table 3.1.13, shows a positive linear correlation of the CO_2 uptake with the main operating parameters at which the test is carried out (temperature, pressure, CO_2 concentration in the gas and L/S ratio) and the content of free lime in the slag. A negative correlation was, on the contrary, found with the tests duration and the slag particle size, whereas no linear correlation was found with the total content of calcium compounds. This means that, on average, CO_2 sequestration is improved by working at high temperature and CO_2 partial pressure, in the presence of water and with ground slag. For test duration, the negative correlation can be explained by the fact that in the majority of the analysed tests, long carbonation periods are associated with modest temperature and pressure values, as well as low concentration of CO_2 in the gas, resulting in modest CO_2 uptake. Concerning the slag composition, the most important parameter is the presence of free lime, rather than that of total Ca compounds since, as previously reported, the carbonation process mainly involves free lime and portlandite.

Table 3.1.13. Pearson correlation matrix.

		test duration	CO2 uptake	particle size	T	P	CO2 concentration	L/S	tot CaO content	free lime content
test duration	Correlazione di Pearson	1	-,230*	,858**	-,261**	-,232*	-,069	-,153	,154	-,023
	Sign. (a due code)		,021	,000	,009	,021	,494	,128	,191	,877
	N	100	100	91	99	98	100	100	74	48
CO2 uptake	Correlazione di Pearson	-,230*	1	-,298**	,397**	,453**	,417**	,409**	,019	,306*
	Sign. (a due code)	,021		,004	,000	,000	,000	,000	,874	,035
	N	100	100	91	99	98	100	100	74	48
particle size	Correlazione di Pearson	,858**	-,298**	1	-,294**	-,287**	-,098	-,218*	-,341**	-,008
	Sign. (a due code)	,000	,004		,005	,006	,357	,038	,004	,957
	N	91	91	91	90	89	91	91	69	46
T	Correlazione di Pearson	-,261**	,397**	-,294**	1	,641**	,294**	,227*	-,213	,171
	Sign. (a due code)	,009	,000	,005		,000	,003	,024	,071	,250
	N	99	99	90	99	97	99	99	73	47
P	Correlazione di Pearson	-,232*	,453**	-,287**	,641**	1	,452**	,276**	-,289*	,343*
	Sign. (a due code)	,021	,000	,006	,000		,000	,006	,014	,017
	N	98	98	89	97	98	98	98	72	48
CO2 concentration	Correlazione di Pearson	-,069	,417**	-,098	,294**	,452**	1	,166	-,176	,094
	Sign. (a due code)	,494	,000	,357	,003	,000		,100	,134	,524
	N	100	100	91	99	98	100	100	74	48
L/S	Correlazione di Pearson	-,153	,409**	-,218*	,227*	,276**	,166	1	,168	-,198
	Sign. (a due code)	,128	,000	,038	,024	,006	,100		,152	,178
	N	100	100	91	99	98	100	100	74	48
tot CaO content	Correlazione di Pearson	,154	,019	-,341**	-,213	-,289*	-,176	,168	1	-,809**
	Sign. (a due code)	,191	,874	,004	,071	,014	,134	,152		,000
	N	74	74	69	73	72	74	74	74	42
free lime content	Correlazione di Pearson	-,023	,306*	-,008	,171	,343*	,094	-,198	-,809**	1
	Sign. (a due code)	,877	,035	,957	,250	,017	,524	,178	,000	
	N	48	48	46	47	48	48	48	42	48

*. La correlazione è significativa a livello 0,05 (a due code).

**. La correlazione è significativa a livello 0,01 (a due code).

A Principal Component Analysis (PCA)[4] on the data was also carried out, with the aim of finding possible correlations among the different parameters affecting carbonation, by means of reducing the number of truly independent variables. Two principal components were extracted, the first one explaining about 45% of the total variance of the model and the second one an additional 29%. Overall, more than 74% of the variance of each variable is explained by the model, with the exception of the temperature, for which the communality value is 50%.

The component matrix is reported in Table 3.1.14. The first component represents the slag characteristics (CaO content, free lime content, particle size), whereas the second component represents the test operating conditions (T, P, CO_2 concentration, L/S, test duration), as well as the CO_2 uptake. As shown in the component plot (Figure 3.1.3), the CO_2 uptake is more related to the operating conditions (T, P, CO_2 concentration, L/S) than to the slag characteristics.

[4] The analysis was carried out adopting the Varimax model for the component rotation with Kaiser normalization.

Table 3.1.14. Rotated component matrix.

	Component	
	1	2
Type_slag	-,959	-,065
CO2 uptake	,353	,735
particle size	,975	,064
T	,181	,684
P	,348	,776
CO2 concentration	,016	,867
L/S	-,270	,851
total CaO content	-,951	-,167
free lime content	,906	,042
test duration	,022	-,517

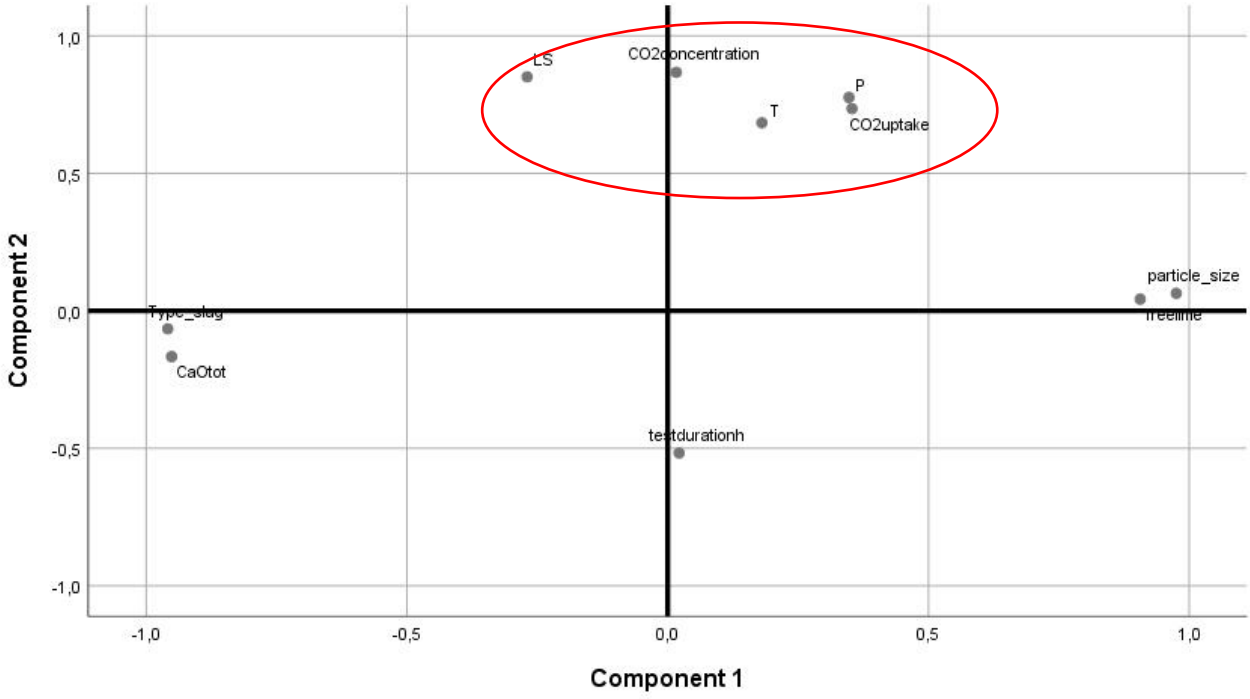


Figure 3.1.3. Component plot of the PCA analysis carried out on the data reported in Table 3.1.10.

3.1.7. DISCUSSION AND CONCLUSIONS

Iron slag as a possible sink for CO_2 sequestration

Based on the findings reported in the previous chapters, natural carbonation of iron slag during storage can be considered negligible. The main reason is the absence of portlandite in its structure. Ca and Mg are, in fact, usually present in the form of silicates or in other low reactive compounds.

In order to promote CO_2 sequestration, iron slag must be subjected to accelerated carbonation processes.

According to the scientific literature analysed in this work, the average CO_2 uptake achievable in direct carbonation processes is about 30-43 gCO_2/kg slag. This amount can be increased up to 156 gCO_2/kg slag on average, by previously extracting Ca from the solid matrix and then carbonating the Ca ions in the solution.

However, none of the analysed papers specifies if lime or limestone was used in the iron production process that generated the slag. Thus, it is not possible to assess if the CaO involved in the carbonation reactions comes from the addition of lime or of limestone and in which proportion. A rough estimation can be done by attributing the sequestered CO_2 to the lime or to the limestone proportionally to their consumption in the process. A further clarification must be done: when limestone is used in the process, it decarbonizes liberating CO_2 (440 g CO_2/kg $CaCO_3$). Even if a part of this CO_2 is later on captured by the CaO in the slag, the balance for the limestone results in a net emission of CO_2.

By considering the following assumptions:

- an average production of 244 kg of iron slag per tonne of crude steel[5];
- a specific lime addition per tonne of liquid steel of about 9.5 kg in the sintering process and 4.4 kg in the BF[6];
- 9% of the fluxing agents overall used in the iron production (sintering + BF) is lime and 91% limestone[7];

it results an average CO_2 uptake per tonne of lime added to the iron production process equal to 57.5 kg for the direct route and to 246.7 kg for the indirect one.

Considering also that the production of 1 tonne of lime releases in the atmosphere 786 kg of CO_2 (only from the calcination process, excluding the fuel consumption), it results that, on average, 7% of the CO_2 emitted during the calcination process for lime production can be captured if the slag is subjected to direct accelerated carbonation processes. This amount increases to 31.4% if the indirect route is used.

[5] The specific production of iron slag was calculated by considering that, in 2016, the production of BF slag in Europe amounted to 24.6 million of tons (Euroslag, 2016) and that of crude steel (from the BOF integrated route) to 100.86 million of tons (Eurofer, 2018).

[6] Lime addition in the sintering process was calculated on the basis of the data reported in the BREF Document for iron and steel production (2013): 10.2 kg lime/t sinter; 1.088 t sinter/t hot metal and 788-931 kg hot metal/t liquid steel. Similar values are reported by Manocha and Ponchon (2018).
Lime addition in the BF was calculated by considering that 20% of the fluxing agents (limestone/lime) used in the European BFs is lime and 80% is limestone, as suggested by EuLa experts, and the average overall dosage of limestone/lime in the BF is 25.7 kg/t hot metal (BREF, 2013).

[7] The percentage was calculated by considering the dosage of lime previously reported in the text and a specific limestone addition per tonne of liquid steel of about 122.6 kg in the sintering process and 17.7 kg in the BF. Limestone addition in the sintering process was calculated on the basis of the data reported in the BREF Document for iron and steel production (2013): 131.1 kg limestone/t sinter; 1088 kg sinter/t hot metal and 788-931 kg hot metal/t liquid steel.
Limestone addition in the BF was calculated by considering that 80% of the fluxing agents (limestone/lime) used in the European BFs consists in limestone, as suggested by EuLa experts, and the average overall dosage of limestone/lime in the BF is 25.7 kg/t hot metal (BREF, 2013).

Steel slag as a possible sink for CO_2 sequestration

Currently, after the collection from the furnace, the steel slag is stocked in piles and exposed to ambient conditions, with the principal aim to cool it down and to reduce its content of free lime. During the storage, Ca compounds in the matrix react with the atmospheric CO_2, resulting in the permanent sequestration of the CO_2 under the form of thermodynamically stable carbonate minerals.

Based on the scientific literature analysed in this work, CO_2 uptake during slag storage is on average equal to 62 gCO_2 per kg of slag, ranging from 19 to 100. These values refer to BOF and EAF slag and to an ageing period of 16-72 weeks, during which the slag is simply stored outside, without undergoing any particular treatment.

By considering the following assumptions:

- an average production of 106 kg of slag per tonne of crude steel for the BOF steelmaking route and of 92 kg of slag for the EAF steelmaking route (slag from the EAF furnace both for CS and SS + slag from the secondary metallurgy), as reported in Table 3.1.15;
- a specific lime addition of 30-67 kg per tonne of liquid steel for the BOF steelmaking route and of 25-60 kg for the EAF steelmaking route, including the lime addition in the downstream secondary metallurgy processes, as reported in the BREF Documents for iron and steel production (2013) and in Manocha and Ponchon (2018);

it results an average CO_2 uptake per tonne of lime added to the steelmaking process equal to about 137 kg for both the BOF and the EAF route.

Table 3.1.15. Specific production of slag per tonne of crude steel. Elaboration of the data reported by Euroslag for steel slag productions and by Eurofer for the production of crude steel (Euroslag, 2016; Eurofer, 2018).

Process	**Slag production in EU in 2016 (million tonnes)**	**Crude steel production in EU28 in 2016 (million tonnes)**	**Total slag in BOF/EAF steelmaking route (kg/t CS*)**
BOF	10.4	97.7	106.6
EAF CS*	4.5	64.4	92
EAF SS	1.3		
Special secondary metallurgy	2.0		

*CS=crude steel

Considering that the production of 1 tonne of lime releases in the atmosphere 786 kg of CO_2 (only from the calcination process, excluding the fuel consumption), it results that, on average, 17.5% of the CO_2 emitted during the calcination process is later on captured by the steel slag during its storage.

It must be underlined that this result is affected by a great uncertainty, related first of all to the steel slag carbonation process and then to the operating conditions adopted for steel production (specific amount of lime added to the process and specific production of slag).

Focusing only on the carbonation process, the actual CO_2 uptake achieved during ageing is highly variable, being affected by the slag composition and mineralogy and by the way the slag is stored (big or small piles, water spray etc.). If we assume the lower CO_2 uptake reported in the analysed literature, 19 gCO_2/kg, only 5.4% of the CO_2 emitted during the lime production process is captured during the steel slag carbonation process. Whereas, if we assume the maximum CO_2 uptake reported in the analysed literature for natural steel slag ageing (equal to 100 gCO_2/kg), about 28% of the CO_2 emitted during lime production process is then captured by the same lime that remains unreacted in the steel slag.

The results are summarized in Table 3.1.16.

Table 3.1.16. Percentage of CO_2 emitted during the lime production process that is captured by the lime in the steel slag during natural ageing.

CO_2 uptake	19.5 gCO_2/kg slag	62.5 gCO_2/kg slag	100 gCO_2/kg slag
% of captured CO_2	5.4	17.5	27.9

The amount of CO_2 sequestered by the slag can be increased by optimizing the ageing process. Operating at high temperature and pressure on a ground slag allows for an increase in its carbonation degree and, furthermore, the carbonation rate. Currently, industrial scale plants for accelerated carbonation of the steel slag are not operating yet. However, focusing on slurry phase carbonation, that seems to be the most promising route, and considering a carbonation time of not more than 1-2 hours, as suggested by Baciocchi et al. (2016) for full scale application, an average CO_2 uptake of about 200 gCO_2/kg slag[8] and 140 gCO_2/kg[9] can be achieved when a 100% CO_2 and a diluted gas flow are used, respectively.

Following the same procedure previously illustrated for natural ageing, if accelerated carbonation was implemented at full scale, it would allow to capture about 39-56% of the CO_2 emitted by the calcination process for lime production.

Recommendation on research need in iron and steel slag

The literature review carried out on iron and steel slag shows a general lack of data regarding natural ageing of the slag during storage, especially for iron slag. The authors suggest carrying out some analyses of iron and

[8] Average of the CO_2 uptake values reported in the literature for accelerated slurry phase carbonation with a 100% CO_2 gas and obtained for a reaction time below 2 hours (Table 3.1.11).

[9] Average of the CO_2 uptake values reported in the literature for accelerated slurry phase carbonation with industrial flue gases and obtained for a reaction time below 2 hours (Table 3.1.11).

steel slag of differing ages in order to assess the amount of CO_2 that can be actually sequestered by these materials and to better understand the time evolution of the carbonation process in outdoor ambient conditions.

In recent years a lot of effort has been focused on accelerated carbonation processes. Results of the laboratory tests seem very promising: both iron and steel slag can be used as a feedstock material for CO_2 sequestration. A strong push towards upscaling such processes to the industrial scale is then highly encouraged.

REFERENCES

Baciocchi, R., Costa, G., Zingaretti, D., Cazzotti, M., Werner, M., Polettini, A., Pomi, R., Falasca, M., 2010. *Studio sulle potenzialità della carbonatazione di minerali e residui industriali per lo stoccaggio di anidride carbonica prodotta da impianti di piccola/media taglia*. Report ENEA-Ministero dello Sviluppo Economico Ricerca di Sistema Elettrico

Baciocchi, R., Costa, G., Di Gianfilippo, M., Polettini, A., Pomi, R., Stramazzo, A., 2015. *Thin-film versus slurry-phase carbonation of steel slag: CO_2 uptake and effects on mineralogy*. Journal of Hazardous Materials 283, 302-313. DOI: https://doi.org/10.1016/j.jhazmat.2014.09.016

Baciocchi, R., Costa, G., Polettini, A., Pomi, R., Stramazzo, A., Zingaretti, D., 2016. *Accelerated carbonation of steel slags using CO_2 diluted sources: CO_2 uptakes and energy requirements*. Frontiers in Energy Research 3(56), 1-10. DOI: 10.3389/fenrg.2015.00056

Bang, J.H., Lee, S.W., Jeon, C., Park, S., Song, K., Jo, W.J., Chae, S., 2016. *Leaching of metal ions from blast furnace slag by using aqua regia for CO_2 mineralization*. Energies 9(12), 996-1008. DOI: 10.3390/en9120996

Belhadj, E., Diliberto, C., Lecomte, A., 2012. *Characterization and activation of basic oxygen furnace slag*. Cement and Concrete Composites 34, (1), 34-40. DOI: https://doi.org/10.1016/j.cemconcomp.2011.08.012

Bonenfant, D., Kharoune, L., Sauvé, S., Hausler, R., Níquette, P., Mimeault, M., Kharoune, M., 2008. *CO_2 sequestration potential of steel slags at ambient pressure and temperature*. Ind. Eng. Chem. Res. 47(20), 7610-7616. DOI: https://doi.org/10.1021/ie701721j

Boone, M.A., Nielsen, P., De Kock, T., Boone, M.N., Quaghebeur, M., Cnudde, V., 2014. *Monitoring of stainless-steel slag carbonation using X-ray computed microtomography*. Environmental Science and Technology 48(1), 674-680. dx.doi.org/10.1021/es402767q

Capobianco, O., Costa, G., Thuy, L., Magliocco, E., Hartog, N., Baciocchi, R., 2014. *Carbonation of stainless steel slag in the context of in situ Brownfield remediation*. Minerals Engineering 59, 91-100. DOI: https://doi.org/10.1016/j.mineng.2013.11.005

Chang, E.E., Chen, C.H., Chen Y.H., Pan, S.Y., Chiang, P.C., 2011a. *Performance evaluation for carbonation of steel-making slags in a slurry reactor*. Journal of Hazardous Materials 186(1), 558-564. DOI: 10.1016/j.jhazmat.2010.11.038

Chang, E.E., Pan, S.Y., Chen, Y.H., Chu, H.W., Wang C.F., Chiang, P.C., 2011b. *CO_2 sequestration by carbonation of steelmaking slags in an autoclave reactor*. J. Hazard. Mater. 195, 107-114. DOI: https://doi.org/10.1016/j.jhazmat.2011.08.006

Chang, E.E., Pan, S.Y., Chen, Y.H., Tan, C.S., Chiang, P.C., 2012. *Accelerated Carbonation of Steelmaking Slags in a High-Gravity Rotating Packed Bed*. J. Hazard. Mater, 227–228, 97–106. DOI: https://doi.org/10.1016/j.jhazmat.2012.05.021

Cheng, T.W. and Chiu, J.P., 2003. *Fire-resistant geopolymer produced by granulated blast furnace slag*. Minerals Engineering 16(3), 205-210. DOI: https://doi.org/10.1016/S0892-6875(03)00008-6

Chiang, Y.W., Santos, R.M., Elsen, J., Meesschaert, B., Martens, J.A., Van Gerven, T, 2014. *Towards zero-waste mineral carbon sequestration via two-way valorization of ironmaking slag*. Chemical Engineering Journal, 249, 260-269. DOI: http//dx.doi.org/10.1016/j.cej.2014.03.104

Costa, G., Baciocchi, R., Polettini, A., Pomi, R., Hills, C.D., Carey, P.J., 2007. *Current status and prespectives of accelerated carbonation processes on municipal waste combustion residues*. Environ. Monit. Assess. 135(1-3), 55-75. DOI: https://doi.org/10.1007/s10661-007-9704-4

Costa, G., 2009. *Accelerated carbonation of minerals and industrial residues for carbon dioxide storage*. Università degli Studi di Roma (via Pan et al., 2012)

Das, B., Prakash, S., Reddy, P.S.R., Misra, V.N., 2012. *An overview of utilization of slag and sludge from steel industries*. Resour. Conserv. Recycl. 50(1), 40-57. DOI: https://doi.org/10.1016/j.resconrec.2006.05.008

Dippenaar, R., 2004. *Industrial uses of slag. The use and re-use of iron and steelmaking slags*. VII International Conference on molten slags fluxes and salts. The South African Institute of Mining and Metallurgy

Dhoble, Y.N., and Ahmed, S., 2018. *Review on the innovative uses of steel slag for waste minimization*. Journal of Material Cycles and Waste Management 20(3), 1373-1382. DOI: https://doi.org/10.1007/s10163-018-0711-z

Eloneva, S., Teir, S., Salminen, J., Fogelholm, C.J., Zevenhoven, R., 2008. *Fixation of CO_2 by carbonating calcium derived from blast furnace slag*. Energy 33(9), 1461-1467. DOI: https://doi.org/10.1016/j.energy.2008.05.003

Eurofer, 2018. *European steel in Figures, 2018*. http://www.eurofer.org/News%26Events/News/European%20Steel%20in%20Figures%202018.fhtml (latest access April 2019)

Euroslag, 2016. *Statistics, 2016*. https://www.euroslag.com/products/statistics/statistics-2016/ (latest access April 2019)

Georgakopoulos, E., Santos, R.M., Chiang, Y.W., Manovic, V., 2016. *Influence of process parameters on carbonation rate and conversion of steelmaking slags. Introduction of the "carbonation weathering rate"*. Greenhouse Gases: Science and Technology 6(4), 470-491. DOI: https://doi.org/10.1002/ghg.1608

Ghacham, A.B., Pasquier, L.C., Cecchi, E., Blais, J.F., Mercier, G., 2016. *CO_2 sequestration by mineral carbonation of steel slags under ambient temperature: parameters influence, and optimization*. Environ Sci Pollut Res 23, 17635-17646. DOI : 10.1007/s11356-016-6926-4

Gupta, J.D., Kneller, W.A., Tamarisa, R., Skrypczak-Jankun, E., 1994. *Characterization of base and subbase iron and steel slag aggregates causing deposition of calcareous tufa in drains*. Transportation research record n. 1434, published by Transportation research board

Haug, T.A., Kleiv, R.A., Mutz, I.A., 2010. *Investigating dissolution of mechanically activated olivine for carbonation purpose*. Appl. Geochem. 25(10), 1547-1563. DOI: https://doi.org/10.1016/j.apgeochem.2010.08.005

Horii, K., Kato, T., Sughara, K., Tsutsumi, N., Kitano, Y., 2015. *Overview of iron/steel slag application and development of new utilization technologies*. Nippon Steel & Sumitomo Metal Technical Report n.109, July 2015. Available online: https://www.nipponsteel.com/en/tech/report/nssmc/pdf/109-03.pdf

Hu, J., Liu, W., Wang, L., Liu, Q., Chen, F., Yue, H., Liang, B., Lü, L., Wang, Y., Zhang, G., Li, C., 2017. *Indirect mineral carbonation of blast furnace slag with $(NH_4)_2SO_4$ as a recyclable extractant*. Journal of Energy Chemistry 26(5), 927-935. DOI: https://doi.org/10.1016/j.jechem.2017.06.009

Huijgen, W.J.J., Comans, R.N.J., Witkamp, G.J., 2005. *Mineral CO_2 sequestration by steel slag carbonation*. Environmental Science and Technology 39(24), 9676-9682. DOI: https://doi.org/10.1021/es050795f

Huijgen, W.J.J., and Comans, R.N.J., 2006. *Carbonation of steel slag for CO_2 sequestration: leaching of products and reaction mechanisms*. Environ. Sci. Technolog. 40(8), 2790-2796. DOI: https://doi.org/10.1021/es052534b

IPCC, 2005. *IPCC special report on carbon dioxide capture and storage*. Available online: https://www.ipcc.ch/site/assets/uploads/2018/03/srccs_wholereport-1.pdf

JFE, 2004. *Environmental report for JFE Holding Inc. and LFE Steel Corporation*. JFE: Tokyo, 2004 (via Yi et al., 2012)

Johnson, D.C., 2000. *Accelerated carbonation of waste calcium silicate materials*. SCI lecture papers series, 1-10

JRC, 2013a. *Best Available Techniques (BAT) Reference document for iron and steel production*. Available online: https://eippcb.jrc.ec.europa.eu/reference/BREF/IS_Adopted_03_2012.pdf

JRC, 2013b. *Best Available Techniques (BAT) Reference document for the production of cement, lime and magnesium oxide*. Available online: https://ec.europa.eu/jrc/en/publication/reference-reports/best-available-techniques-bat-reference-document-production-cement-lime-and-magnesium-oxide

Kuo, W.T., Shu, C.Y., Han, Y.W., 2014. *Electric arc furnace oxidizing slag mortar with volume stability for rapid detection*. Construction Building Materials 53, 635-641. DOI: https://doi.org/10.1016/j.conbuildmat.2013.12.023

Kuwahara, Y. and Yamashita, H., 2013. *A new catalytic opportunity for waste materials: application of waste slag-based catalyst in CO_2 fixation reaction*. Journal of CO_2 utilization 1, 50-59. DOI: https://doi.org/10.1016/j.jcou.2013.03.001

Lee, S., Kim, J.W., Chae, S., Bang, J.H., Lee, S.W., 2016. *CO_2 sequestration technology through mineral carbonation: an extraction and carbonation of blast slag*. Journal of CO_2 utilization 16, 336-345. DOI: https://doi.org/10.1016/j.jcou.2016.09.003

Lekakh, S.N., Rawlins, C.H., Robertson, D.G.C., Richards, V.L., Peaslee, K.D., 2008. *Kinetics of aqueous leaching and carbonization of steelmaking slag*. Metallurgical and material transactions B 39(1), 125-134. DOI: 10.1007/s11663-007-9112-8

Mäkelä, M., Watkins, G., Pöykiö, R., Nurmesniemi, H., Dahl, O., 2012. *Utilization of steel, pulp and paper industry solid residues in forest soil amendment: relevant physicochemical properties and heavy metal availability*. Journal of Hazardous Materials 207-208, 21-27. DOI: https://doi.org/10.1016/j.jhazmat.2011.02.015

Manocha, S. and Ponchon, F., 2018. *Management of lime in steel*. Metals 8, 686-702. DOI: 10.3390/met8090686

Mayes, W.M., Riley, A.L., Gomes, H.I., Brabham, P., Hamlyn, J., Pullin, H., Renforth, P., 2018. *Atmospheric CO_2 sequestration in iron and steel slag: Consett, County Durham, United Kingdom*. Environmental Science and Technology 52(14), 7892-7900. DOI: https://doi.org/10.1021/acs.est.8b01883

Morone, M., Costa, G., Polettini, A., Pomi, R., Baciocchi, R., 2014. *Valorization of steel slag by a combined carbonation and granulation treatment*. Minerals Engineering 59, 82-90. DOI: https://doi.org/10.1016/j.mineng.2013.08.009

Motz, H., and Geiseler, J., 2001. *Products of steel slags an opportunity to save natural resources*. Waste Management 21(3), 285-293. DOI: https://doi.org/10.1016/S0956-053X(00)00102-1

Mun, M. and Cho, H., 2013. *Mineral carbonation for carbon sequestration with industrial waste*. Energy Procedia 37, 6999-7005. DOI: https://doi.org/10.1016/j.egypro.2013.06.633

National slag association. *Blast furnace slag as an agricultural liming material and source of minor plant nutrients*. Available online:

http://www.nationalslag.org/sites/nationalslag/files/documents/nsa_185-5_bf_slag_as_agricultural_liming_material.pdf (latest access in April 2019)

Navarro, C., Díaz, M., Villa-García, M.A., 2010. *Physico-chemical characterization of steel slag. Study of its behaviour under simulated environmental conditions*. Environ. Sci. Technol. 44, 5383-5388. DOI: 10.1021/es100690b

Pan, S.Y., Chang, E.E., Chiang, P.C., 2012. *CO_2 capture by accelerated carbonation of alkaline wastes: a review on its principles and applications*. Aerosol and air quality research 12(5), 770-791. DOI: 10.4209/aaqr.2012.06.0149

Pan, S.Y., Chiang, P.C., Chen, Y.H., Tan, C.S., Chang, E.E., 2013. *Ex situ CO_2 capture by carbonation of steelmaking slag coupled with metalworking wastewater in a rotating packed bed*. Environmental Science and Technology 47(7), 3308-3315. DOI: https://doi.org/10.1021/es304975y

Pan, S.Y., Adhikari, R., Chen, Y.H., Li, P., Chiang, P.C., 2016. *Integrated and innovative steel slag utilization for iron reclamation, green material production and CO_2 fixation via accelerated carbonation*. Journal of Cleaner Production 137, 617-631. DOI: https://doi.org/10.1016/j.jclepro.2016.07.112

Pan, S.Y., Chung, T.C., Ho, C.C., Hou, C.J., Chen, Y.H., Chiang, P.C., 2017. *CO_2 mineralization and utilization using steel slag for establishing a waste-to resources supply chain*. Scientific reports 7(17227), 1-11. DOI : 10.1038/s41598-017-17648-9

Proctor, D.M., Fehling, K.A., Shay, E.C., Wittenborn, J.L., Green, J.J., Avent, C., Bigham, R.D., Connoly, M., Lee, B., Shepker, T.O., Zak, M.A., 2000. *Physical and chemical characteristics of blast furnace, basic oxygen furnace and electric arc furnace steel industry slags*. Environmental Science and Technology 34, 1576-1582. DOI: https://doi.org/10.1021/es9906002

Quaghebeur, M., Nielsen, P., Laenen, B., Nguyen, E., van Mechelen, D., 2010. *Carbstone: sustainable valorisation technology for fine grained steel slags and CO_2*. Refractories worldforum 2(2), 75-79. Available online: https://www.refractories-worldforum.com/paper?article_id=100038

Quaghebeur, M., Nielsen, P., Horckmans, L., van Mechelen, D., 2015. *Accelerated carbonation of steel slag compacts: development of high-strength construction materials*. Frontiers in Energy Research 3, 1-12. DOI: https://doi.org/10.3389/fenrg.2015.00052

Ramme, B.W., 2008. *Carbon dioxide sequestration in foamed controlled low strength materials*. United States Patent Application Publication Pub.No.: US2008/0245274 A1. Available online: http://www.freepatentsonline.com/20080245274.pdf

Rondi, L., Bregoli, G,, Sorlini, S., Cominoli, L., Collivignarelli, C., 2016. *Concrete with EAF steel slag as aggregate: a comprehensive technical and environmental characterization*. Composites Part B: Engineering 90, 195-202. DOI: https://doi.org/10.1016/j.compositesb.2015.12.022

Santos, R., Francois, D., Vandelvelde, E., Mertens, G., Elsen, J., Van Gerven, T., 2010. *Process intensification routes for mineral carbonation*. Proceedings of the third International Conference on accelerated Carbonation for Environmental and Materials Engineering ACEME10, Turku (Finland), Nov. 29-Dec. 1, 2010

Santos, R.M., Van Bouwel, J., Vandevelve, E., Mertens, G., Elsen, J., Van Gerven, T., 2013. *Accelerated mineral carbonation of stainless steel slags for CO_2 storage and waste valorisation: effects of process parameters on geochemical properties*. Int. J. Greenhouse Gas Control 17, 32-45. DOI: http://dx.doi.org/10.1016/j.ijggc.2013.04.004

Spanka, M., Mansfeldt, T., Bialucha, R., 2016. *Influence of natural and accelerated carbonation of steel slags on their leaching behaviour*. Steel research international 87(6), 798-810. DOI: https://doi.org/10.1002/srin.201500370

Suer, P., Lindqvist, J.E., Arm, M., Frogner-Kockum, P., 2009. *Reproducing ten years of road ageing. Accelerated carbonation and leaching of EAF steel slag*. Science of the Total Environment 407(18), 5110-5118. DOI: https://doi.org/10.1016/j.scitotenv.2009.05.039

Thuy, L.A.D., 2013. *Lab-scale feasibility of in-situ carbonation of alkaline industrial wastes*. Master thesis, Faculty of Geosciences, Utrecht University (The Netherlands).

Tüfekci, M., Demirbas, A., Genc, H., 1997. *Evaluation of steel furnace slags as cement additives*. Refereed paper, Cement and Concrete Research 27(11), 1713-1717. DOI: https://doi.org/10.1016/S0008-8846(97)00158-0

Uliasz-Bochenczyk, A. and Mokrzycki, E., 2017. *CO_2 mineral sequestration with the use of ground granulated blast furnace slag*. Mineral resources management 33(1), 111-124. DOI: 10.1515/gospo-2017-0008

Ukwattage, N.I., Ranjith, P.G., Li, X., 2017. *Steel-making slag for mineral sequestration of carbon dioxide by accelerated carbonation*. Measurement 97, 15-22. DOI: https://doi.org/10.1016/j.measurement.2016.10.057

Van Zomeren, A., van der Laan, S.R., Kobesen, H.B.A., Huiigen, W.J.J., Comans, R.N.J., 2011. *Changes in mineralogical and leaching properties of converter steel slag resulting from accelerated carbonation at low CO_2 pressure*. Waste Management 31, 2236-2244. DOI: 10.1016/j.wasman.2011.05.022

Vlcek, J., Tomkova, V., Ovcacikova, H., Ovcacik, F., Topinkova, M., Matejka, V., 2013. *Slags from steel production: properties and their utilization*. Metalurgija 52(3), 329-333.

Volk, G.W., Harding, R.B., Evans, C.E., 1952. *A comparison of blast furnace slag and limestone as a soil amendment*. Research Bulletin 708. Ohio agricultural experiment station. Wooster, Ohio

Wu, Z.H., Zou, Z.S., Wang, C.Z., 2005. *Application of converter slags in agriculture*. Multipurpose Util Min Resour 6, 25-28

Wu, S., Xue, Y., Ye, Q., Chen, Y., 2007. *Utilization of steel slag as aggregates for stone mastic asphalt (SMA) mixtures*. Build Environ 42(7), 2580-2585. DOI: https://doi.org/10.1016/j.buildenv.2006.06.008

Yi, H., Xu, G., Cheng, H., Wang, J., Wan, Y., Chen, H., 2012. *An overview of utilization of steel slag*. Procedia environmental sciences 16, 791-801. DOI: 10.1016/j.proenv.2012.10.108

Yildirim, I.Z., and Prezzi, M., 2015. *Geotechnical properties of fresh and aged basic oxygen furnace steel slag*. J. Mater. Civ. Eng 27(12), 1-11. Available online:

https://ascelibrary.org/doi/10.1061/%28ASCE%29MT.1943-5533.0001310

Yu, J. and Wang, K., 2011. *Study on characteristics of steel slag for CO_2 capture*. Energy Fuels 25(11), 5483-5492. DOI: https://doi.org/10.1021/ef2004255

Zingaretti, D., Costa, G., Baciocchi, R., 2013. *Assessment of accelerated carbonation processes for CO_2 storage using alkaline industrial residues*. Ind. Eng. Chem. Res. 53(22), 9311-9324. DOI: https://doi.org/10.1021/ie403692h

3.2 USE OF LIME IN CONSTRUCTION MATERIALS

3.2.1 USE OF LIME IN SAND LIME BRICK

3.2.1.1 INTRODUCTION

Sand Lime Bricks (SLB_S), also known as calcium silicate bricks, are a relative young building material consisting only of sand, lime, and water. Inert and stable pigments may be added to influence the final colour of the brick, e.g. iron oxide for red and brown bricks, chromium oxide for green units, ochre for yellow bricks (Ingham, 2013 and Anupoju, 2019). Worldwide, more than 30 billion calcium silicate bricks are produced annually, mainly in Europe (e.g., Germany, Poland, Holland, and Czech Republic), Asia (e.g., India and China), Australia, and Mexico (The Athena Sustainable Materials Institute, 1998).

The manufacturing process, discovered and patented by the researcher William Michealis in 1881, consists of three main steps (Figure 3.2.1.1):

- preparation, proportioning, and mixing of the raw materials;
- moulding under high pressure;
- autoclaving.

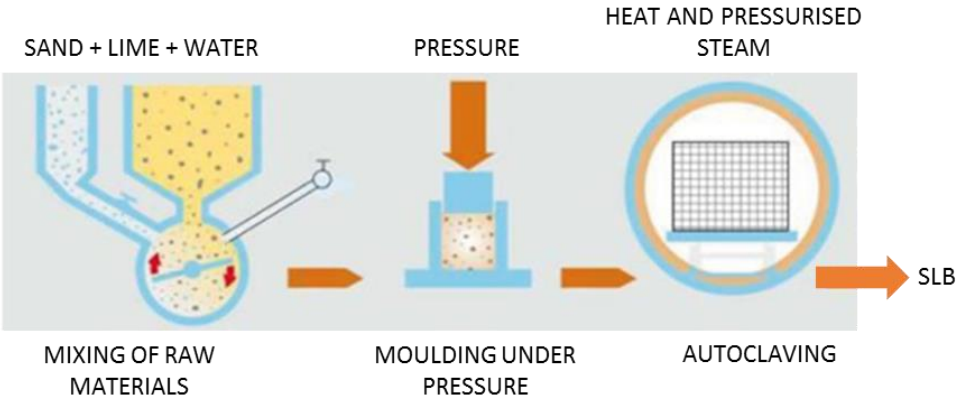


Figure 3.2.1.1. Main steps of sand lime brick production (Elaboration from Lieblang et al., 2017).

The first step is very important in determining the quality and the properties of the final brick. Sand is the main constituent of the solid mixture, while lime generally represents only 5-10% by weight. As an example, the German Federal Association of Sand Lime Brick Industry recommends a ratio between sand and lime equal to 12:1 (Bundesverband Kalksandstein Industrie e.V., 2018).

The sand essentially determines the properties of calcium silicate bricks, in particular the bulk density that is important for the sound insulation and the strength. Silicate minerals and crushed flints are mainly used (in the last case units are called flint-lime bricks). Regarding lime, according to the DIN EN 459 related to building lime, quicklime should be used with an average CaO content ranging from 81% to 95%. Lime should be perfectly hydrated before bricks are pressed. Otherwise, it will expand during the steam treatment and it will produce internal strains which are frequently sufficient to disrupt the brick (Lieblang et al., 2017; Sahu et al., 2017).

A 3-9% of water by mass (with reference to the solid mixture) is added, in order to prevent the crumbling of the material after the pressing step. Water should contain an amount of soluble salts and/or organic matter lower than 0.25% (The Athena Institute, 1998; Institut Bauen und Umwelt e.V., 2016; Anupoju, 2019).
The mixture of lime and sand is then pressed into the form of a brick, generally through a bi-directional hydraulic press, with the following functions:

- to give the brick its final size and shape;
- to bring sand and lime into very intimate contact, thus facilitating their chemical combination;
- to reduce the proportion of voids in the brick.

In the final stage, bricks are placed in an autoclave, where they are exposed to the synergistic effect of elevated temperature (about 200°C) and saturated steam at adequate pressure (approximately 16 bars), for 6-12 hours. This curing causes a chemical reaction between the lime and part of the sand (generally 15% by weight) to form calcium silicate hydrate, the binder that holds the rest of sand together (85% of the sand acts as inert filler). The most significant product of the autoclaving is tobermorite (Warren, 1917; Sahu et al., 2017).
In recent years, the use of fly ash in partial substitution of sand for the production of non-fired bricks was experimented. In fact, the presence of reactive silica and alumina makes fly ash suitable for the development of cementitious compounds when mixed with lime and water. The reaction between fly ash and lime can be accelerated either by curing the mixture at elevated temperature or by adding a small percentage of gypsum (Gourav et al., 2018). Cicek et al. (2007), for example, successfully investigated the use of fly ash from coal fired thermal power plants in Turkey in the production of bricks, finding that the optimum raw materials composition was: 68% fly ash, 20% sand, and 12% hydrated lime. The autoclaving process should be performed at 1.5 MPa for 6 hours. Always in relation to the use of industrial waste, Cao et al. (2015) analysed the production of carbonated steel slag-lime bricks in China by a steam curing process. Also copper tailings can be used to produce autoclaved sand-lime bricks, but their proportion in the brick batch must not exceed 50% by mass (Fang et al., 2011).
About this last topic, we underline that the use of industrial waste in the SLBs preparation is not performed and is very poorly studied in the European countries like Germany, where natural raw materials are available in great quantity and there is no dependence on imports (Lieblang et al., 2017).

3.2.1.2 LITERATURE ASSESSMENT FOR THE USE OF LIME IN SLB$_S$: MATERIALS AND METHODS

The published literature on the lime carbonation process in SLBs application is very scarce, at least as far as documents written in German or in English are considered. The German research (mainly performed by the Association Forschungsvereinigung Kalk-Sand e.V.) have been significantly involved in the testing of SLBs masonry units for over 50 years, but only one of the papers (Eden et al., 1995) effectively reports a value of actual CO_2 uptake by the building material. A literature source from the United Kingdom mentions the progressive process of carbonation of the brick during its service life, but without giving other relevant indications. Regarding contexts outside Europe, no literature was found about the carbonation of SLB$_S$, while

one paper reported the CO_2 sequestration efficiency of carbonated lime-steel slag bricks (Cao et al., 2015). The complete list of useful documents on the topic is reported in Table 3.2.1.1.

Table 3.2.1.1. List useful documents considered in the literature review about the use of lime in SLBs application.

1. Cao et al., 2015. *The properties of the carbonated brick made of steel slag-slaked lime mixture*. Journal of Wuhan University of Technology-Mater. Sci.Ed., 30(2), 250-255. DOI: https://doi.org/10.1007/s11595-015-1134-5
2. Eden et al., 1995.*Ökobilanz für den Baustoff Kalksandstein und Kalksand stein-Wandkonstruktionen*. (Life Cycle Assessment of Calcium Silicate Mansory Units). Research report n°82, Forschungsvereiningung Kalk-Sand eV, Hannover, November 1995.
3. Ingham, 2013. *Geomaterials under the microscope. Chapter 6, Concrete products, Calcium silicate units (pages 121-127).* Academic Press, Handcover ISBN 9780124072305. Available online: https://www.sciencedirect.com/topics/engineering/calcium-silicate
4. Heckroodt, 2002. *Guide to the deterioration and failure of building materials. Chapter 3: Calcium silicate masonry (page 66)*. Institution of Civil Engineers. DOI: https://doi.org/10.1680/gttdafofbm.31722.0003

3.2.1.3 POTENTIAL CARBONATION RATE IN SLB_S

During the service life of SLB_S, the lime in the brick gradually reacts with CO_2 from the atmosphere to form calcium carbonate. In this way, old bricks tend to be partially or fully carbonated with the binder including, or composed of, finely crystalline calcium carbonate. Bricks slowly gain in strength and hardness and finally resemble natural calcareous sandstone (Heckroodt, 2002/Ingham, 2013).

The only quantification of the carbonation potential for SLB_S available in the literature was performed by Eden et al. (1995) in relation to the German context. The authors reported an average CO_2 uptake equal to 20 kg of CO_2 per 1 ton of SLB_S along their service life (the testing duration is not reported). According to the amount of lime in the same bricks (85 kg CaO/t SLB), the value corresponds to 235 g CO_2/kg CaO. Considering that the production of 1 tonne of lime releases in the atmosphere 786 kg of CO_2 (only from the calcination process, excluding the fuel consumption) it results that, on average, 30% of the CO_2 emitted from the calcination process can be captured by SLB_S during their service life.

As regards non-fired bricks partially composed of industrial waste, Cao et al. (2015) evaluated the CO_2 sequestration efficiency of carbonated steel slag-lime bricks in China. Samples of brick were prepared at the lab-scale starting from a mixture of: 67% river sand, 28% steel slag from the BaoSteel Company in China (12% SiO_2, 41% CaO, 10% MgO, 17% Fe_2O_3 content) and 5% slaked lime as a by-product of the soda production (72% purity). A solid/water ratio equal to 6:1 was considered. Moulded bricks were cured at 50°C for 24 hours and then carbonated with a flux containing 20% of CO_2 by volume (60 ± 1% of relative humidity, 20±5°C of temperature). Authors quantified that each ton of brick can absorb 64 kg of CO_2. It should be stressed that this carbon sequestration cannot be all attributed to the lime because of the presence of free lime in the steel slag. Moreover, at the moment, this indication results of poor importance for the European countries like Germany, where no industrial waste or secondary material are used, due to the large availability of natural sand and limestone.

3.2.1.4 CONCLUSIONS AND RECOMMENDATION ON FUTURE RESEARCH NEED FOR SLBs

The literature review carried out about SLB_S application shows a general lack of data regarding the carbonation potential during the service life of bricks. The only indication is related to the German context and corresponds to a CO_2 uptake of about 235 kg per 1 ton of used lime, equal to 30% of the emission in the production stage of CaO. The value refers to the year 1995 and the testing time is not reported.

The future research should necessary perform analyses on sand lime bricks of different age in terms of service life in order to check the reported value and to better understand the time evolution of the carbonation process in outdoor ambient conditions.

REFERENCES

Anupoju, S., 2019. *Calcium silicate bricks or sand lime bricks for masonry construction*. The Constructor Civil Engineering Home. Available online: https://theconstructor.org/building/calcium-silicate-bricks-masonry-construction/17256/

Bundesverband kalksandstein industrie e.V., 2018. *Kalksandstein Planungshandbuch. Planung, Konstruktion, Ausführung*. Available online: https://www.kalksandstein.de/bv_ksi/binaries/content/59667/file_planungshandbuch_auflage7_gesch_de.pdf

Cao, W., Yang, Q.J., 2015. *The properties of the carbonated brick made of steel slag-slaked lime mixture*. Journal of Wuhan University of Technology-Mater. Sci.Ed., 30(2), 250-255. DOI: https://doi.org/10.1007/s11595-015-1134-5

Cicek, T., Tanriverdi, M., 2007. *Lime based steam autoclaved fly ash bricks*. Construction and Building Materials, 21(6), 1295-1300. DOI: 10.1016/j.conbuildmat.2006.01.005

Eden, W., Kaczmarek, T., Meyer, G., Waltermann, G., Steiger, P., 1995.*Ökobilanz für den Baustoff Kalksandstein und Kalksand stein-Wandkonstruktionen. (Life Cycle Assessment of Calcium Silicate Mansory Units)*. Research report n°82, Forschungsvereiningung Kalk-Sand eV, Hannover, November 1995

Fang, Y., Gu, Y., Kang, Q., Wen, Q., Dai, P., 2011. *Utilization of copper tailings for autoclaved sand-lime brick*. Construction and Building Materials, 25(2), 867-872.
DOI: https://doi.org/10.1016/j.conbuildmat.2010.06.100

Gourav, K., Venkatarama Reddy, B.V., 2018. *Bond Development in Burnt Clay and Fly Ash-Lime-Gypsum Brick Masonry*. Journal of Materials in Civil Engineering 30(9), 1-10. DOI: https://doi.org/10.1061/(ASCE)MT.1943-5533.0002412

Heckroodt, R.O., 2002. *Guide to the deterioration and failure of building materials. Chapter 3: Deterioration of masonry* (page 66). Institution of Civil Engineers. DOI: https://doi.org/10.1680/gttdafofbm.31722.0003

Ingham, J.P., 2013. *Geomaterials under the microscope. Chapter 6, Concrete products, Calcium silicate units* (pages 121-127). Academic Press, Handcover ISBN 9780124072305. Available online: https://www.sciencedirect.com/topics/engineering/calcium-silicate

Institut Bauen und Umwelt e.V., 2016. *Environmental Product Declaration of calcium silicate masonry units*. Available online: https://www.kalksandstein.de/bv_ksi/binaries/content/86126/file_europaeische_umwelt_produktdeklaration_englisch_21.12.2016_de.pdf

Lieblang, P., Konrad, D., Vogdt, F.U., Schäfers, M., Eden, W., 2017. *Resource efficiency of calcium silicate units (Ressourceneffizienz des Kalksandsteins)*. Mauerwerk 21(1), 3-8. DOI: 10.1002/dama.201700716

Sahu, M.K., Singh L., 2017. *Critical review on types of bricks type 6: calcium silicate bricks*. International Journal of Mechanical and Production Engineering, 5(11), 58-60. Available online: http://www.iraj.in/journal/journal_file/journal_pdf/2-416-151549647258-60.pdf

The Athena, Sustainable Materials Institute, 1998. *Life Cycle Analysis of Brick and Mortar Products*. Prepared by Venta G.J., Venta Glaser & Associates, Ottawa Canada. Available online: https://calculatelca.com/wp-content/themes/athenasmisoftware/images/LCA%20Reports/Brick_And_Mortar_Products.pdf

Warren, E.E., 1917. *Manufacture and properties of sand-lime brick*. Technologic Papers of the Bureau of Standards n°85, Department of Commerce. Available online: https://nvlpubs.nist.gov/nistpubs/nbstechnologic/nbstechnologicpaperT85.pdf

3.2.2 USE OF LIME IN LIGHT-WEIGHT LIME CONCRETE - AUTOCLAVED AERATED CONCRETE

3.2.2.1 INTRODUCTION

Autoclaved Aerated Concrete (AAC), also known as aerated cellular concrete, is an inorganic highly porous building material belonging to the category of the lightweight concrete. According to the European technical specifications for masonry units (EN 771-4:2011), a wide range of densities (300-1000 kg/m^3) for AAC can be produced in many shapes and forms (walls, roof panels, blocks, and lintels) for several applications such as structural, partition, and insulation purposes. The material offers good acoustic and thermal insulation, as well as fire and termite resistance. AAC is a popular building material in Europe since more than 60 years. The European Autoclaved Aerated Concrete Association (EAACA) reports a yearly production of around 15 million m^3 from more than 100 facilities in 18 countries (EAACA, 2019). Poland is the largest producer with about 30% market share by volume (Zapotoczna-Sytek, 2018).

AAC is typically manufactured from the following raw materials:

- fine sand with a minimum SiO_2 content of 85%, mainly in the crystallized form of quartz;
- cement (generally of Portland type) used as a binding material;
- ground burnt lime, acting as a binding agent, contributing to the mixture expansion and providing energy for the strengthening process in the initial setting (such energy derives from the exothermal reaction of CaO hydration). Traditionally, low reactive quicklime (hard-burnt lime) is used for AAC production, due to its slow and regular heat release during the mixture expansion and setting. However, hard-burnt lime is energetically costly and induces higher CO_2 emissions. For these reasons, in the recent years there is a growing trend towards the use of softer lime, which can also help to improve the plant productivity (Peter et al., 2018; Tungulin et al., 2018);
- gypsum, generally in the natural form of anhydrite, added to improve the quality of the final concrete (i.e., higher compressive strength and formation of well-crystallised tobermorite for a structure with a low shrinkage behaviour) and to control the setting times, since gypsum delays the slaking speed of lime. This is accomplished by a controlled heat development with a positive effect on the expansion and the stiffening behaviour (Chucholowski et al., 2018);
- aluminium powder or paste, used as a pore-forming agent.

In the typical European AAC formulations (examples are reported in Table 3.2.2.1), the content of the binder (cement plus lime) increases with decreasing density and the final AAC is classified as cement or lime active depending on the predominance of the type of used binder. Recently, the partial substitution of the virgin raw materials (sand, lime and/or cement) with industrial wastes rich in SiO_2 and CaO has been tested to reduce resources consumption and to lower the production costs. For example, in Poland, siliceous fly ash from the combustion of coal in conventional boilers are commonly used up to 70% of the components in AAC formulation, substituting natural sand and cement (Łagosz et al., 2011). In addition, the use of fluidized coal fly ashes has been investigated in the laboratory and at the semi-technical scale. Fluidized ashes can be used to produce AAC up to 40% in relation to the total ash content in the formulation. Their composition allows to

reduce the lime content by 10-20% and the gypsum request by 60% or even up to 100% (Łaskawiec et al., 2011).

Also the total substitution of sand with lead-zinc tailings (Wang et al., 2017) or coal bottom ash (Kurama et al., 2009) and the total replacement of lime with skarn-type copper tailings and blast furnace slag (Huang et al., 2012) were tested at the lab scale.

Table 3.2.2.1. Examples of typical European AAC formulations in terms of raw materials (Lesueur et al., 2011).

	P2 quality - 0.35	P2 quality - 0.4	P2 quality - 0.55
Target density (kg/m^3)	300-350	350-400	500-550
Target compressive strength (MPa)	> 2	> 2	> 4
Quartz sand (% on the solid mixture)	50% wt	55% wt	59% wt
Cement (% on the solid mixture)	28% wt	25% wt	18% wt
Lime (% on the solid mixture)	17% wt	15% wt	19% wt
Anhydrite (% on the solid mixture)	5% wt	5% wt	4% wt
Aluminium paste (% added to the solid)	0.22% wt	0.16% wt	0.08% wt
Ratio between water and solid	0.68	0.65	0.65

The manufacturing of AAC (Figure 3.2.2.1) starts with grinding the sand to the required fineness in a wet ball mill, where a sand slurry is produced. The other raw materials (lime, cement, and gypsum) are then automatically weighed and dosed into a mixer along with water, the expanding agent, and the sand slurry. After mixing, the slurry is poured into metal moulds in which the expanding agent (aluminium) reacts with lime (Reaction [3.2.2.1]) causing the formation of microscopic, finely dispersed bubbles in the fresh mixture and an increase of the volume (such expansion may be twice the original volume). The produced hydrogen foams out of the material and is substituted by air, which is a denser gas.

$$2Al + 3\ Ca(OH)_2 + 6H_2O \rightarrow 3CaO \cdot Al_2O_3 \cdot 6H_2O + 3H_2 \qquad [3.2.2.1]$$

Within few hours (typically 2.5-4), the initial hydration of cementitious compounds gives AAC sufficient strength to hold its shape and support its own weight, but the material is still soft. After cutting into the required size, the AAC is cured under hydrothermal conditions in an autoclave at around 180°C-190°C under saturated pressure (up to 2 MPa) for 5-15 hours (Klingner, 2008; Ekaputri et al., 2013; Masa Group, 2019; MHE International LLC, 2019).

From a mineralogical point of view, AAC consists primarily of 1.1 nm tobermorite (a well-crystallized calcium-silicate-hydrate-phase, with the chemical formula $5CaO \cdot 6SiO_2 \cdot 5H_2O$), X-ray amorphous C-S-H, non-reacted quartz, and gypsum. 65-90% of the volume of the hardened AAC consists in pores, 25-70% of which being air pores (diameter higher than 50 nm) and the remaining being micro-pores characterized by a good ability in capillary moisture transport (pore diameter lower than 2nm; Schober et al., 2011). The quality of the phase formation of tobermorite (in terms of crystal formation) should be examined and regularly checked by X-ray diffraction, in order to avoid AAC damaging (Figure 3.2.2.2).

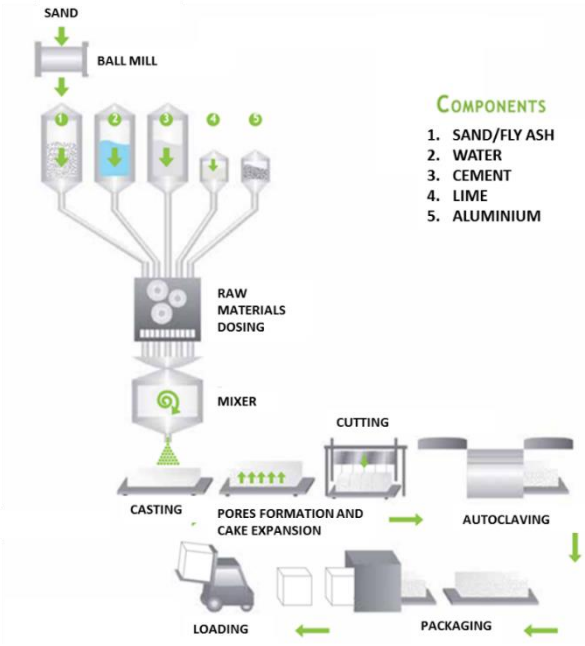


Figure 3.2.2.1. Main stages in the manufacturing of AAC (Image source: http://ualind.com/products/koncrete-aac-blocks/koncrete-manufacturing/).

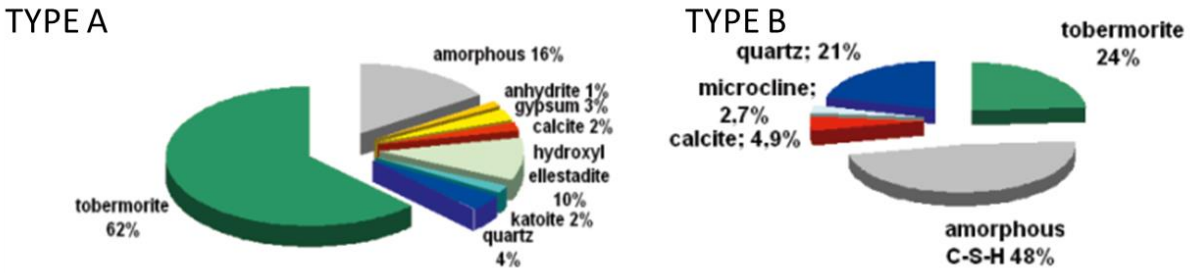


Figure 3.2.2.2. Mineralogical composition of autoclaved aerated concrete (PP2, density of 350 kg/m^3) with a good phase distribution (type A) and with a poor phase distribution (type B). Image source: Straube and Schoch (2014).

3.2.2.2 LITERATURE ASSESSMENT FOR THE USE OF LIME IN AAC: MATERIALS AND METHOD

The published literature on the AAC carbonation potential in the European context is quite scarce. In Germany, many companies have performed carbonation tests on AAC samples but only few information has been published so far (EuLA personal communication). Moreover, most of the results are related to artificial carbonation (carbonation under accelerated conditions, with CO_2 concentration ranging from 1-5%), which is not considered an appropriate method for the determination of the long-term behaviour of AAC under normal atmospheric conditions. In fact, the changes in the AAC micro-level structure are quite different between accelerated conditions and the normal ones; moreover, the ambient conditions of the test, especially the relative humidity, play a significant role on the results (Haas, 2005).

According to such premises, this literature assessment considered:

- the few peer reviewed papers related to AAC carbonation under natural conditions in the European context (papers 1-7-8 in Table 3.2.2.2);
- the published papers 2-6 in Table 3.2.2.2 related to a comprehensive Japanese research performed by Matsushita et al. (years 2000-2004) about the carbonation process of in-service AAC panels removed from buildings.

The complete list of the analysed documents is reported in Table 3.2.2.2.

Table 3.2.2.2. List of the documents considered in the literature review about the use of lime in AAC production.

Peer reviewed papers

1. Haas, 2005. *Carbonation of AAC*. 4th International Conference about autoclaved aerated concrete; innovation and developments, Taylor and Francis Group, London, ISBN. 0415383560
2. Matsushita et al., 2000a. *Carbonation degree of autoclaved aerated concrete*. Cement and Concrete Research 30(11), 1741-1745. DOI: https://doi.org/10.1016/S0008-8846(00)00424-5
3. Matsushita et al., 2000b. *Carbonation degree as durability criteria for autoclaved aerated concrete*. Special Publication about the 5th CANMET/ACI International conference on durability of concrete, 192, 1123-1134
4. Matsushita et al., 2004a. *Microstructure changes in autoclaved aerated concrete during carbonation under working and accelerated conditions*. Journal of Advanced Concrete Technology 2(1), 121-129. DOI: https://doi.org/10.3151/jact.2.121
5. Matsushita et al., 2004b. *Calcium silicate structure and carbonation shrinkage of a tobermorite-based material*. Cement and Concrete Research 34(7), 1251-1257. DOI: https://doi.org/10.1016/j.cemconres.2003.12.016
6. Matsushita et al., 2004c. *Carbonation Resistance of Water-Repellent Autoclaved Aerated Concrete*. Journal of the Society of Inorganic Materials 11(311), 219-233. DOI: https://doi.org/10.11451/mukimate2000.11.219
7. Straube et al., 2014. *The durability of autoclaved aerated concrete*. Mauerwerk, European Journal of Masonry 18 (3-4), 239-245. DOI: https://doi.org/10.1002/dama.201400630
8. Winkels et al., 2018. *Carbonation of autoclaved aerated concrete containing fly ash*. Ce/papers, Special issue: ICAAC - 6th International Conference on Autoclaved Aerated Concrete 2(4), 47-51. DOI: https://doi.org/10.1002/cepa.880

3.2.2.3 CARBONATION DEGREE OF AAC

In the carbonation process of AAC, tobermorite 11Å, the main structural mineral, chemically reacts with the atmospheric CO_2 in the presence of moisture and is decomposed into calcium carbonate polymorphic forms (calcite and vaterite) and silica gel (Matsushita et al., 2000a):

$$5CaO \cdot 6SiO_2 \cdot 5H_2O + 5CO_2 \rightarrow 5CaCO_3 + 6SiO_2 + 5H_2O \qquad [3.2.2.2]$$

In natural conditions, the carbonation is a very long process (the typical CO_2 concentration in the atmosphere ranges from 0.03 to 0.08%) and the consequences become noticeable over a period of years. Besides CO_2 concentration, the ambient conditions play also an important role in the process, since the carbonation is enhanced by the increase of the relative humidity in the air (Łaskawiec and Woyciechowski, 2018; Winkels et al., 2018).

Matsushita et al. (2000a and 2004a) have evaluated the carbonation progress of AAC under operating conditions in Japan. Panels aged from 5 to 33 years in the typical Japanese climate (0.03% volume of CO_2, 25-95% of relative humidity, and temperature ranging from 0°C to 35°C) were removed from several buildings and analysed for the carbonation process. The degree of carbonation was calculated according to the following formula:

$$D_C\ (\%) = (C\text{-}C_0) / (C_{MAX}\text{-}C_0) \qquad [3.2.2.3]$$

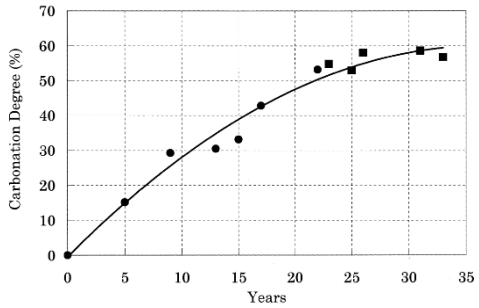
where:

C = amount of carbon dioxide combined as $CaCO_3$ in the analysed sample measured by a TG-DTA (ThermoGravimetry/Differential Thermal Analysis)[10];

C_0 = amount of carbon dioxide combined as $CaCO_3$ in the AAC before its operational life;

C_{MAX} = theoretical amount of carbon dioxide which can be stoichiometrically combined with the total amount of calcium oxide (24.9% by weight) in the sample to form $CaCO_3$.

According to [3.2.2.3], the AAC degree of carbonation increases with years of exposure and saturates to 60% approximately after 30 years (Figure 3.2.2.3). This means that 60% of the CaO content in the concrete is effectively converted into calcium carbonate by absorbing atmospheric CO_2 during the operational life. However, it should be stressed that the carbonation process in AAC cannot be completely associated to lime, considering the presence of lime in the Portland cement.



Operation year	CaO (% w_t)	Combined CO_2 (% w_t)			D_C (%)
		C	C_0	C_{MAX}	
0	24.9	0.91	0.91	19.56	0
5	26.7	3.95	0.91	20.98	15%
15	29.7	8.34	0.91	23.34	33%
25	24.2	10.49	0.91	19.01	53%
33	24.9	11.50	0.91	19.56	57%

Figure 3.2.2.3 Carbonation degree of AAC Japanese panels in different service years and corresponding parameters of calculation (Elaboration from Matsushita et al., 2000a and 2004a).

In the same research, the authors found that at a degree of carbonation below 20%, the double-chain silicate anion structure of the tobermorite is well maintained. From a carbonation degree of 25%, the tobermorite structure starts decomposing, reaching a carbonation shrinkage of 0.1%-0.25%, respectively for a 50-60% degree of carbonation (Matsushita et al., 2004b). In these conditions, analysed AAC panels showed degradation in span-deflection ratio, compressive strength, and drying shrinkage. A 50% degree of carbonation can be thus considered as the limit value for the durability of in-service AAC: when this value is reached, AAC may be deteriorated (Matsushita et al., 2000b). Another indication was that water-repellent AAC based on the addition of silicone-oil resulted to have twice carbonation resistance compared to normal AAC (Figure 3.2.2.4). Similarly, acrylic resin-finished AAC panels are 1.5 times more resistant against carbonation than the non-finished-ones (Matsushita et al., 2000b and 2004c).

[10] The TG-DTA method measures the amount of combined carbon dioxide in the material as the heating weight loss from 600°C to 800°C, corresponding to the decomposition of calcium carbonate. In this analysis, the amount of magnesium carbonate and of the carbon dioxide absorbed on the surface and dissolved into water is not included in the measure.

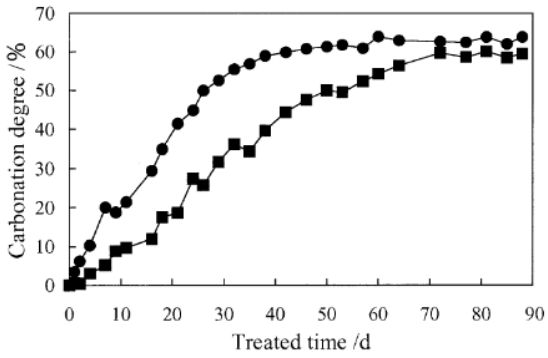


Fig. 2 Carbonation degree as a function of treated time.
● : Normal AAC
■ : Water-repellent AAC

Figure 3.2.2.4. Carbonation degree as a function of time for normal and water-repellent AAC. Samples were carbonated under the following conditions: 3% CO_2 vol., temperature of 20°C, relative humidity of 90% (Matsushita et al., 2004c).

For the German context, a number of research activities on AAC have been carried out in order to better assess the long-term durability of AAC constructed masonry units. Some preliminary indications about the carbonation potential of the material can be derived. During the 4th International Conference on AAC, Haas (2005) summarized the results of a long-term investigation about the carbonation behaviour of the well mineralized AAC. The author reported a 6% degree of carbonation after a period of 10 years of service life in normal climate conditions (Figure 3.2.2.5). However, unlike the work performed by Matsushita et al., the formula used for calculating the parameter is not explicitly reported in the available document. If the value of 6% is referred to the maximum CO_2 uptake, the value would be significantly lower than that reported in the Japanese research for the same period of service life (30% according to Figure 3.2.2.3); on the contrary, if the value is relative to the total mass of AAC, it will be comparable.

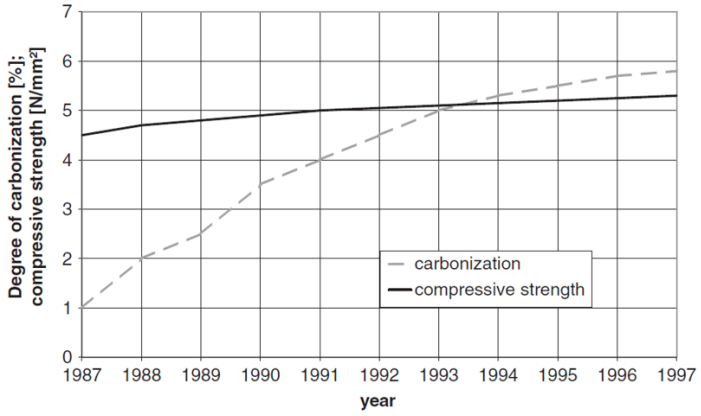


Figure 3.2.2.5. Evolution of the carbonation degree of well mineralized AAC as a function of time in normal climate conditions (Haas, 2005).

On the same topic, during the 6th International Conference on AAC, some authors studied the evolution of AAC phase composition over the time through X-Ray Diffraction (XRD) analysis. The results generally show

a progressive increase in the content of calcite, due to the decomposition of tobermorite, calcium silicate hydrate, and calcium aluminate hydrate in presence of CO_2 under normal climate conditions.

For example, Straube and Schoch (2014) studied the evolution of the mineral phase of AAC samples (quality P2 with density of 350 kg/m^3) stored for 2.5 years in a natural but rain-protected environment. AAC with good phase distribution (62% content of tobermorite) and poor phase distribution (24% tobermorite content) were analysed (Figure 3.2.2.2). Considering AAC blocks with a good phase distribution (type A in Figure 3.2.2.6), the XRD analysis showed a progressive reduction of the tobermorite content (from 62% w_t to 42% w_t) in favour of the carbonate phase (from 2% w_t to 35% w_t).

In a similar study, Winkels et al. (2018) evaluated the structural transformation of two different AAC products with the same density (about 450 kg/m^3), respectively based on quartz sand and fly ash. Samples of AAC extracted from the surface of buildings were stored for 1.5 years in normal climate conditions of 20°C and 65% relative humidity. The carbonation rate of AAC was then investigated in terms of ratio between the content of tobermorite and carbonates (Table 3.2.2.3). Analyses reveal that AAC products based on fly ash have a relative quick carbonation behaviour: after 1.5 years the ratio tobermorite to carbonates is reduced by 59%, with a final content of tobermorite lower than that of carbonates.

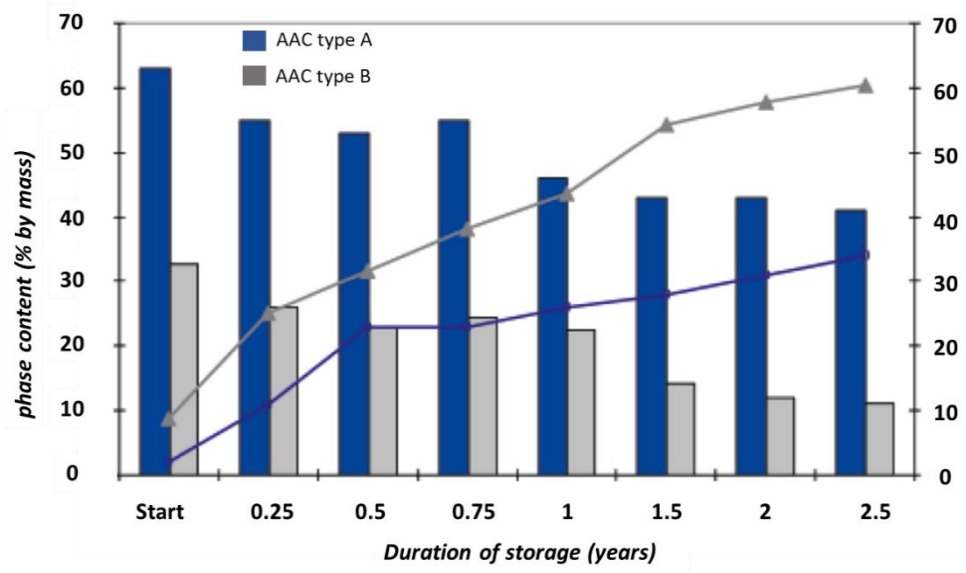


Figure 3.2.2.6. Changes in phase content of AAC to varying of the time storage in natural, rain protected ambient; column - tobermorite content; line carbonate phase (Straube et al., 2014). Legend: AAC type A - good phase distribution (62% tobermorite) and AAC type B - poor phase distribution (24% tobermorite).

Table 3.2.2.3. Ratio between the content of tobermorite and the content of calcium carbonate polymorphs before and after natural carbonation for 540 days (Winkels et al., 2018).

Type of sample	**Ratio tobermorite - carbonates content**		
	Beginning	**After 540 days**	**Δ (%)**
Sample based on quartz extracted from the building surface	6.2	3.9	-37%
Sample based on fly ash extracted from the building surface	1.7	0.7	-59%

Looking at the wider potential contribution of AAC with respect to climate change, it worth mentioning that AAC waste after useful life can be used as an active biofilter material for the reduction of the methane emission from landfills. Indeed, AAC fragments are a good substrate for the growth of Aerobic Methane Oxidizing Bacteria due to their high porosity, which provides protection and allows for a good exchange of oxygen and water. A large-scale experiment on a landfill site in Bremen showed good microbial activity, after a period of adaptation, without the decomposition of the AAC biofilter (Kuever et al., 2018).

3.2.2.4 RECOMMENDATION OF RESEARCH NEEDS IN AAC

For the European context, there is a general lack of literature data regarding the natural carbonation of lime in AAC during its service life. In Germany, many companies have performed dedicated tests but little information has been published so far, mainly in the context of the periodical International Conference about AAC.

An exhaustive research on this topic was performed by Matsushita et al. (2000-2005) in relation to AAC panels removed from Japanese buildings after being exposed to natural climatic conditions for 5-33 years. Under these conditions, the carbonation degree of AAC, calculated in relation to the maximum theoretical CO_2 uptake based on the CaO content, resulted equal to 60% after 30 years.

Making use of this value, the following aspects should be kept in mind:

- the reported carbonation potential cannot be exclusively attributed to lime, because of the presence of CaO in the Portland cement;
- the value can be used in the European contexts with climate conditions similar to Japan, since the process of carbonation is significantly affected by the ambient conditions of exposure;
- the value is derived for AAC panels of the producer Sumitomo Metal Mining Siporex Co, Ltd and are characterized by the following chemical composition: 25% CaO; 50% SiO_2; 2.6% Al_2O_3 and 2% Fe_2O_3 in terms of major components.

The publication of the already available quantitative data about the AAC carbonation process should be promoted in the European context, especially for Poland and Germany, that are the main producers of this building material. Moreover, new analyses on the topic should be performed, by using the same approach of Matsushita et al. for the determination of the carbonation degree. In this way, results can be compared. Fly ash AAC should be included in the investigation, due to their relative quick carbonation behaviour established by preliminary tests (e.g., Winkels et al., 2018).

REFERENCES

Chucholowski, C., Holger, M., Thienel, K-C., 2018. *Improving the recyclability, environmental compatibility, and CO_2 balance of autoclaved aerated concrete by replacing sulfate carrier and cement with calcined clays*. Ce/papers - special issue: ICAAC - 6th International Conference on Autoclaved Aerated Concrete, 2(4), 503-512. DOI: https://doi.org/10.1002/cepa.846

Ekaputri, J.J., Triwulan, T., Brahmantyo, D., Farid, R., Nasir, S., 2013. *Optimisation of pressure and curing time in producing autoclaved aerated concrete*. Proceeding the 6th Civil Engineering Conference in Asia Region: Embracing the Future through Sustainability, Jakarta, Indonesia, Volume, TS4C50-TS4C56. DOI: 10.13140/2.1.2505.6964

European Autoclaved Aerated Concrete Association, 2019: https://www.eaaca.org/

European Committee for Standardization - CEN, 2011. *Specification for masonry units-Part 4: autoclaved aerated concrete masonry units*. EN 771-4:2011

Haas M., 2005. *Carbonation of AAC*. International Conference about autoclaved aerated concrete; innovation and developments, Taylor and Francis Group, London, ISBN. 0415383560

Huang, X., Ni, W., Cui, W., Wang, Z., Zhu, L., 2012. *Preparation of autoclaved aerated concrete using copper tailings and blast furnace slag*. Construction and Building Materials 27(1), 1-5. DOI: 10.1016/j.conbuildmat.2011.08.034

Klingner R.E., 2008. *Using Autoclaved Aerated Concrete Correctly*. MASONRY Magazine: https://www.masonrymagazine.com/blog/2008/06/01/using-autoclaved-aerated-concrete-correctly/

Kuever, J., Remesch, M., Rabenstein, A., Bukowski, G., Kurkowski, H., Eden, W., 2018. *Removal of the greenhouse gas methane by using autoclaved aerated concrete as matrix for colonization of methane-oxidizing bacteria*. Ce/papers - special issue: ICAAC - 6th International Conference on Autoclaved Aerated Concrete, 2(4), 471-475. DOI: https://doi.org/10.1002/cepa.832

Kurama, H., Tpocu, İ.B., Karakurt, C., 2009. *Properties of the autoclaved aerated concrete produced from coal bottom ash.* Journal of Materials Processing Technology 209 (2), 767-773. DOI: https://doi.org/10.1016/j.jmatprotec.2008.02.044

Łagosz, A., Szymański, P., Walczak, P., 2011. *Influence of fly ash properties on properties of autoclaved aerated concrete*. 5th International Conference on Autoclaved Aerated Concrete "Securing a sustainable future", Bydgoszcz, Poland, 14-17 September 2011. Available online: https://www.researchgate.net/publication/260164131_Influence_of_the_fly_ash_properties_on_properties_of_autoclaved_aerated_concrete

Łaskawiec, K., Gebarowski, P., Zapotoczna-Sytek, G., Malolepszy, J., 2011. *Fly ashes of new generation as a raw material to the production of autoclaved aerated concrete (AAC)*. 5th International Conference on Autoclaved Aerated Concrete "Securing a sustainable future", Bydgoszcz, Poland, 14-17 September 2011. Available online: http://www.gbv.de/dms/tib-ub-hannover/723846030.pdf

Łaskawiec, K. and Woyciechowski, P., 2018. *Effect of carbonation on the performance of autoclaved aerated concrete*. Ce/papers - special issue: ICAAC - 6th International Conference on Autoclaved Aerated Concrete, 2(4): 37-41. DOI: 10.1002/cepa.885

Lesueur, D., Mücke, F., Oeinck, H., Peter, U., Pust, Ch., Verhelst, F., 2011. *Impact of quicklime reactivity and origin on Autoclaved Aerated Concrete production*. 5th International Conference on Autoclaved Aerated Concrete "Securing a sustainable future", Bydgoszcz, Poland, 14-17 September 2011. Available online: https://www.ttu.ee/public/e/eneli-liisma/Liisma2018/5-mezhdunarodnaya-konferentsiya-po-avtoklavnomu-gazobetonu-sbornik-dokladov-2011-_pol_.pdf

Masa Group, 2019. *Autoclaved Aerated Concrete Production*. https://www.masa-group.com/en/products/aac-production/

Matsushita, F., Aono, Y., Shibata, S., 2000a. *Carbonation degree of autoclaved aerated concrete*. Cement and Concrete Research 30(11), 1741-1745. DOI: https://doi.org/10.1016/S0008-8846(00)00424-5

Matsushita, F. and Shibata, S., 2000b. *Carbonation degree as durability criteria for autoclaved aerated concrete*. Special Publication about the 5th CANMET/ACI International conference on durability of concrete, 192, 1123-1134

Matsushita, F., Aono, Y., Shibata, S., 2004a. *Microstructure changes in autoclaved aerated concrete during carbonation under working and accelerated conditions*. Journal of Advanced Concrete Technology 2(1), 121-129. Available online: https://www.jstage.jst.go.jp/article/jact/2/1/2_1_121/_pdf/-char/en

Matsushita, F., Aono, Y., Shibata, S., 2004b. *Calcium silicate structure and carbonation shrinkage of a tobermorite-based material*. Cement and Concrete Research 34(7), 1251-1257. DOI: https://doi.org/10.1016/j.cemconres.2003.12.016

Matsushita, F., Aono, Y., Shibata, S., 2004c. *Carbonation Resistance of Water-Repellent Autoclaved Aerated Concrete*. Journal of the Society of Inorganic Materials 11(311), 219-233. DOI: https://doi.org/10.11451/mukimate2000.11.219

MHE International LLC, 2019. *Autoclaved Aerated Concrete - Production and Manufacturing Process.* https://www.mhe-international.com/mhe-aac-consultant/production-manufacturing-process/

Peter, U., Nowak, P., Oeinck, H., Spicker, V., Pust, C., 2018. *Investigation of the strength development of autoclaved aerated concrete*. Ce/papers - special issue: ICAAC - 6th International Conference on Autoclaved Aerated Concrete, 2(4), 557-563. DOI: https://doi.org/10.1002/cepa.874

Schober, G., 2011. *Porosity in autoclaved aerated concrete (AAC): a review on pore structure, types of porosity, measurement methods and effects of porosity on properties*. 5th International Conference on Autoclaved Aerated Concrete "Securing a sustainable future", Bydgoszcz, Poland, 14-17 September 2011. Available online: https://www.ttu.ee/public/e/eneli-liisma/Liisma2018/5-mezhdunarodnaya-konferentsiya-po-avtoklavnomu-gazobetonu-sbornik-dokladov-2011-_pol_.pdf

Straube, B. and Schoch, T., 2014. *The durability of autoclaved aerated concrete*. Mauerwerk, European Journal of Masonry 18(3-4), 239-245. DOI: https://doi.org/10.1002/dama.201400630

Tungulin, D., Behrenberg, B., Lutter, J., Wallmeier, W., 2018. *Quicklime with defined reaction time window for aerated autoclaved concrete production*. Ce/papers - special issue: ICAAC - 6th International Conference on Autoclaved Aerated Concrete, 2(4), 223-229. DOI: https://doi.org/10.1002/cepa.853

Wang, C., Liu, Z., Li, J., Jiao, S., Zhang, Y., 2017. *Study on preparation of autoclaved aerated concrete using lead-zinc tailings*. Chemical Engineering Transactions, 62, 931-936. DOI: 10.3303/CET1762156

Winkels, B., Nebel, H., Raupach, M., 2018. *Carbonation of autoclaved aerated concrete containing fly ash*. Ce/papers - special issue: ICAAC - 6th International Conference on Autoclaved Aerated Concrete, 2(4), 47-51. DOI: https://doi.org/10.1002/cepa.880

Zapotoczna-Sytek, G., 2018. *Durability of autoclaved aerated concrete based on Polish experience.* Ce/papers - special issue: ICAAC - 6th International Conference on Autoclaved Aerated Concrete, 2(4), 53-62. DOI: https://doi.org/10.1002/cepa.850

3.2.3 USE OF LIME IN MORTARS

Lime products are one of the oldest “industrial” type products known to mankind and have been used in constructions for thousands of years. To produce lime, limestone, chalk or marble rock (essentially calcium carbonate) is heated to around 1000°C. At these temperatures, it chemically dissociates into calcium oxide and carbon dioxide. Calcium oxide is known as quicklime or burnt lime and is highly reactive.

In most building material applications, including mortars, renders and plasters, the quicklime is reacted with water to form calcium hydroxide, known as hydrated lime or slaked lime. Hydrated lime has been used as a binder in mortars, renders and plasters for millennia. It hardens slowly by reacting with carbon dioxide in the atmosphere to form back into calcium carbonate, a reaction known as carbonation. Lime which does this is known as “air lime” because it reacts only with air.

The process by which limestone becomes quicklime, then hydrated lime, then limestone again is known as the lime cycle.

There are some deposits of limestone where the rock has a proportion of certain other minerals, mainly silica. When heated to form quicklime, some compounds are formed which are a combination of calcium and silica (calcium silicates). When this type of quicklime is made into hydrated lime form, the resulting material can be used to make mortars, renders and plasters which “set” in only a few hours by reaction of the calcium silicates with water in the mix (“hydraulic” reaction). This type of lime is known as “natural hydraulic lime”.

Natural hydraulic lime also has a high content of calcium hydroxide (typically 50%), and so over time it also hardens by reaction with atmospheric carbon dioxide (carbonation).

Deposits from which natural hydraulic lime can be produced are found in limited quantities and the overall volumes produced are small compared to air lime.

Today it is common to incorporate a strongly hydraulic manufactured binder such as Portland cement into mortar mixes. This provides a rapid gain of early strength, allowing fast construction progress, but it also can lead to a brittle and crack- prone material which cannot accommodate minor movements and results in poor durability. Lime (normally hydrated lime) is included in these mixtures to provide better long-term durability and overall performance of the masonry.

Cement/lime mortars are known in much of Europe as mixed air lime mortars. The table below illustrates some typical mortar formulations for Europe.

Table 3.2.3.1. Typical mortar formulations found in Europe (EESAC, 2014).

Table 1: Composition of the mortars considered in the present study

Type of mortar	Volumetric composition of the mortar			Additives
	Cement	Hydrated lime	Sand	
A	0	1	3	No
B	1	0.5	4.5	No
C	1	0	5	Yes
D	1	0	3	Yes
E	1	1	6	Yes
F	1	2	9	Yes
G	1	3	10	Yes

The literature reviews carried out by EESAC analyzed the carbonation rate of two types of mortars: pure air lime-based mortars (EESAC, 2013) and mixed air lime mortars, that are a mixture of air lime and hydraulic binder (EESAC 2014). Comprehensively, 190 publications were found researching in different bibliographical datasets for both types of mortars. After a pre-selection and check of the found studies, 21 publications were considered reliable and adequate for air lime mortars and 27 publications for mixed air lime mortars.

From the literature reviews, it results that during the lifetime of the air lime mortars the slaked lime ($Ca(OH)_2$) carbonates, i.e. it reacts with atmospheric CO_2 forming calcium carbonate ($CaCO_3$). In the reviewed studies, the carbonation depth is measured with the phenolphthalein method while the carbonation level, i.e. the percentage of initial slaked lime that carbonates, is measured by means of thermogravimetric analysis. The first method consists in spraying on mortar samples a phenolphthalein[11] solution, that is a pH indicator. In this way, two areas are distinguishable: the uncarbonated area and the carbonated area, characterized by pH higher than 8.2 and lower than 8.2, respectively, since carbonation causes a pH reduction. The boundary which separates the two areas is called carbonation front, which moves over the time from the surface to the inner part of the construction product. The distance between the surface and the carbonation front is called carbonation depth, whose evolution in time can be described by Fick's law [Equation 3.2.3.1]:

$$d = K\sqrt{t} \qquad \text{[Equation 3.2.3.1]}$$

where d is the carbonation depth (mm); K is the carbonation coefficient or the carbonation rate ($mm/year^{1/2}$) and t is the time of exposure to CO_2 (years). From EESAC literature review, it results that K value is about 1 $mm/(day)^{1/2}$ in the case of mortars natural carbonation. Assuming a time period of 100 years, the carbonation depth is equal to 190 mm according to [Equation 3.2.3.1] with K=1 $mm/(day)^{1/2}$. Furthermore, through thermogravimetric analysis, it results that in the carbonated area, i.e. from the surface to the carbonation front, 80-92% of the initial slaked lime is carbonated, while in the uncarbonated area, i.e. ahead of the carbonation front, the carbonation level is in the range of 10-20%. As a result, pure air lime mortars application with

[11] Phenolphthalein is a chemical compound used as pH indicator which changes colour at a pH of 8.2. It is red when pH is higher than 8.2, colourless if below 8.2.

thickness lower than 190 mm can be considered 80-92% carbonated after 100 years (EESAC, 2013). In the case of mixed air lime mortars consisting of air lime and Ordinary Portland Cement (OPC), that is the most commonly used hydraulic binder, the substitution of 20% of the binder amount with cement is sufficient to decrease the porosity and consequently the diffusivity of CO_2 in the mortars' pores. Thus, the carbonation rate decreases. Since K of OPC is about 0.25 mm/(day)$^{1/2}$, i.e. 4 times lower than air lime mortars partially due to the decrease in pore size, it was estimated that partial substitution of air lime with hydraulic binder causes a reduction of carbonation rates by a factor of 2 to 5 compared to pure air lime mortars (EESAC, 2014).

Despotou et al. (2016) have also investigated which factors affected lime based mortars carbonation in addition to the thickness and the composition of the walls, i.e. the temperature and the water content. The temperature rise lowers the carbonation process, while the amount of water in the pores is pivotal because pore water is needed for dissolution of calcium hydroxide and CO_2, but at the same time high water content hinders the CO_2 diffusion.

Based on carbonation rate found by EESAC studies, Schlegel and Shtiza evaluated, using the Life Cycle Assessment methodology (ISO 14040 – 14044), the environmental footprint of mortars, renders and plasters with different lime content (2014) and of different types of mortars (2016). In the first study, 17 formulations of mortars, renders and plasters were compared assessing the potential environmental impacts with the "cradle-to-gate" approach. The main results of the study regarding mortars and renders was that the differences between products with low and high lime contents were no relevant, while regarding plasters, the lime-based plasters have the lowest environmental impact in three indicators (i.e. primary energy consumption, abiotic depletion and water eutrophication) whereas the gypsum-based plasters have the lowest environmental footprint in the remaining indicators. Furthermore, the carbon footprint of mortars lowers if the carbonation of hydrated lime in the first years of the mortar use phase is considered (Schlegel and Shtiza, 2014). On the other hand, the study published in 2016 compared seven types of mortars as indicated in Table 3.2.3.1. One tonne of mortar was considered as the functional unit and the system boundaries included from the raw materials production to the use phase. The results indicated that mortar made only of hydrated lime without cement (Type A) has the lowest impact in the following indicators: acidification potential, eutrophication potential and global warming potential, due especially to the high amount of CO_2 sequestrated over a life span of 100 years (Schlegel and Shtiza, 2016).

In conclusion, the carbonation of mortars is a well-known process and a wide scientific literature on the topic is available as shown by the literature review carried by EESAC. The carbonation rate of pure air lime mortars is 80-92% after 100 years in application with lower than 190 mm, while the carbonation rate of mixed air lime mortars lowers due to the porosity decrease caused by cement addition in mortars mix.

REFERENCES

Despotou, E., Shtiza, A., Schlegel, T., Verhelst, F., 2016. *Literature study on the rate and mechanism of carbonation of lime in mortars.* In: Mauerwerk European Journal of Masonryf, 20 (2016), 2, 124-137. DOI: 10.1002/dama.201500674

EESAC, 2013. *An estimation of the carbonation degree of air-lime based mortars based on a bibliographic review.*

EESAC, 2014. *An estimation of the carbonation degree of mortars consisting of a combination of air lime and hydraulic binder based on a bibliographic review.*

Schlegel, T., Shtiza, A., 2014. *Environmental footprint study of mortars, renders and plasters formulations with no, low or high hydrated lime content*. In: 9th International Masonry Conference 2014 in Guimarães, Portugal, 7-9 July 2014.

Schlegel, T., Shtiza, A., 2016. *Lime carbonation, environmental footprint of seven mortars placed on the European market*. In: Modena, da Porto and Valluzzi (Eds) Brick and Block Masonry – Trends, Innovations and Challenges. CRC Press. ISBN 978-1-138-02999-6

3.2.4 USE OF LIME IN HEMP LIME

3.2.4.1 INTRODUCTION

Hemp lime construction material was originally developed in France in substitution of wattle and daub infill in timber frame buildings. Then, the interest in hemp lime materials has grown in the construction sector because of its good thermal insulation performance and low carbon footprint. The components of hemp lime are hemp shiv, which is the chopped woody core of the stalks of the hemp plant (*Cannabis sativa*), air lime binder with pozzolanic cementitious or hydraulic lime additives and in some cases surfactants (Shea et al., 2012). Air lime binder is hydrated lime which is pure calcium hydroxide ($Ca(OH)_2$). Hydrated lime is obtained from lime or calcium oxide by adding water during the slaking process. Binders based on hydrated lime are the results of experimental works on different binders, that showed how the pure hydraulic binders like hydraulic lime or cement are unable to hydrate completely, leaving a poorly bound, powdery core in the hemp lime walls because the shiv competes strongly with the binder for the available water (Lawrence, 2015).

The proportion of binder used in the mix influences the mechanical performance and the density that will affect the thermal resistance of the hemp lime, one of its important properties. The thermal conductivity of hemp fibres is around 0.037–0.042 W/m/K, which is comparable with conventional insulation materials such as rock wool (0.033–0.046 W/m/K) (Lawrence, 2015). In addition to low density with associated low thermal conductivity, another property of hemp lime construction material is its porous structure, which allows it to dampen variations in environmental heat and humidity. Furthermore, hemp shiv is more resistant to biological decay and requires lower levels of fertilisation and irrigation compared to other crops used for bio-based building materials. Moreover, hemp shiv is a renewable resource and offers the opportunity of being recycled at end of life (Lawrence et al., 2012).

The amount of CO_2 sequestered in hemp lime material is larger than the greenhouse gas (GHG) emissions generated during transport, construction and manufacturing processes of the building material both excluding (Arrigoni et al., 2017; Ip and Miller, 2012) and including (Boutin et al., 2006; Prétot et al., 2014) the end of life phase in the life cycle assessment. Boutin (2006) and Prétot (2014) assumed that the material is landfilled and does not decompose. Consequently, only the greenhouse gas emissions for the transport to the landfill are taken into account in the life cycle assessments. Thus, according to these assumptions hemp lime construction material has a “negative” carbon footprint. In fact, carbon is stored in the construction material thanks to two different process: the photosynthesis and the carbonation. The former occurs during hemp growth, when CO_2 is absorbed from the atmosphere by the plant. It is estimated that each kg of hemp shiv sequesters 2.1 kg of CO_2 (Boutin et al., 2006). In addition to photosynthesis, $Ca(OH)_2$ in the binder absorbs CO_2 from the

atmosphere to form calcium carbonate ($CaCO_3$) according to the carbonation reaction [Reaction 3.2.4.1].

$Ca(OH)_2 + CO_2 \rightarrow CaCO_3$ [Reaction 3.2.4.1]

Therefore, during the lifetime of the construction material, the lime binder re-absorbs a certain amount of CO_2 that was originally emitted during the production of hydrated lime. Furthermore, hemp lime material allows to indirectly reduce the CO_2 emissions in the use phase of the material because its low thermal conductivity allows to save energy for ventilation and conditioning (Lawrence et al., 2012).

Carbonation with binder hydration affects also the compressive strength of hemp lime concrete contributing to a strength gain at later ages (Walker et al., 2014). Walker et al. (2014) assessed binder composition which in turn affects mechanical properties and durability of hemp lime concretes. Six different binder mixes were analysed, including commonly used ones and lime-based mixes with pozzolanic additives such as Ground Granulated Blast-furnace Slag (GGBS) and metakaolin which is a calcined kaolin clay lime. The studied binder mixes are reported in Table 3.2.4.1. In this study, the microstructure of samples with different binder composition is assessed through a Scanning Electron Microscope (SEM) analysis. After six months, the hemp interface in lime-pozzolan binders is largely carbonated, while commercial binder showed abundant hydrates instead of builder's binder that was characterized by a lower amount of hydrates.

Table 3.2.4.1. Composition of hemp concretes analysed by Walker et al. (2014).

Binder name given by the authors	Binder composition (% by weight)	Binder:hemp:water ratio (by weight)		
		Binder	Hemp	Water
Builder's mix	70% calcium lime (CL90s), 20% hydraulic lime (NHL3.5), 10% Portland cement (CEM I)	2	1	3.1
Commercial mix for hemp lime application	100% commercial binder (lime-based binder with hydraulic addition)	2	1	2.9
GGBS	70%, calcium lime, 30% GGBS	2	1	3.1
GGBS+Water Retainer (WR)	70%, calcium lime, 30% GGBS, 0.5% methyl cellulose	2	1	3.1
Metakaolin	80% calcium lime, 20% Metakaolin	2	1	3.3
Metakaolin+WR	80% calcium lime, 20% Metakaolin, 0.5% methyl cellulose	2	1	3.1

3.2.4.2 LITERATURE ASSESSMENT FOR THE USE OF LIME IN HEMP CONSTRUCTION MATERIALS: MATERIAL AND METHODS

Different studies available in the literature have analysed the carbonation of lime binder in hemp-based construction material. Nine studies were found, that are listed in Table 3.2.4.2. Six of them (Arrigoni et al., 2017; Boutin et al., 2006; Ip and Miller, 2012; Lecompte et al., 2017; Prétot et al.,

2014; Sinka et al., 2018) evaluated the carbon footprint of hemp lime material through the Life Cycle Assessment (LCA) methodology. One of those six studies (Arrigoni et al., 2017), together with the study by Jami and Kumar (2017) estimated the carbonation rate of lime binder through X-Ray Diffractometric analysis, while only the study by Chabannes et al. (2015) carried out a thermogravimetric analysis under natural and accelerated carbonation conditions. Only one study (Hirst et al., 2014) measured the carbonation depth at different ages and assumed an equation which links carbonation depth to time. Thus, four out of nine are experimental studies.

Table 3.2.4.2. List of consulted documents for the literature review about the use of lime in hemp construction materials.

Peer-reviewed papers

1. Arrigoni, A., Pelosato, R., Melià, P., Ruggieri, G., Sabbadini, S., Dotelli, G., 2017. *Life cycle assessment of natural building materials: the role of carbonation, mixture components and transport in the environmental impacts of hempcrete blocks.* Journal of Cleaner Production 149: 1051-1061. DOI: http://dx.doi.org/10.1016/j.jclepro.2017.02.161
2. Boutin, M.-P., Flamin, C., Quinton, S., Gosse, G., Lille, I., 2006. *Etude des caractéristiques environnementales du chanvre par l'analyse de son cycle de vie.* Paris, Ministère de l'agriculture et de la pêche.
3. Chabannes, M., Garcia-Diaz, E., Clerc, L., Bénézet, J.-C., 2015. *Studying the hardening and mechanical performances of rice husk and hemp-based building materials cured under natural and accelerated carbonation.* In: Construction and Building Materials, 94, 105-115. DOI: http://dx.doi.org/10.1016/j.conbuildmat.2015.06.032
4. Ip, K. and Miller, A., 2012. *Life cycle greenhouse gas emissions of hemp-lime wall constructions in the UK.* Resources, Conservation and Recycling, 69, 1-9. DOI: https://doi.org/10.1016/j.resconrec.2012.09.001
5. Jami, T., and Kumar, S. (2017). *Assessment of carbon sequestration of hemp concrete*. International Conference on Advances in Construction Materials and Systems, Chennai, India. Available online: https://www.researchgate.net/publication/320058537_Assessment_of_Carbon_Sequestration_of_Hemp_Concrete
6. Prétot, S., Collet, F., Garnier, C., 2014. *Life cycle assessment of a hemp concrete wall: impact of thickness and coating*. Building and Environment, 72, 223-231. DOI: https://doi.org/10.1016/j.buildenv.2013.11.010
7. Sinka, M., Van den Heede, P., De Belie, N, Bajare, D., Sahmenko, G., Korjakins, A., 2018. *Comparative life cycle assessment of magnesium binders as an alternative for hemp concrete*. In: Resources, Conservation & Recyling, 133, 288-299. DOI: https://doi.org/10.1016/j.resconrec.2018.02.024
8. Hirst, E. A. J., Walker, P., Paine, K. A., Yates, T., 2012. *Characteristics of low-density hemp-lime building materials*. In: Proceedings of Institution of Civil Engineers: Construction Materials, 165, 1, 15-23. DOI: https://doi.org/10.1680/coma.1000021

Meeting proceedings or seminars

9. Lecompte, T., Levasseur, A., Maxime, D., 2017. *Lime and hemp concrete LCA: a dynamic approach of GHG emissions and capture*. In: 2nd International Conference on Bio-based Building Materials & 1st Conference on ECOlogical valorisation og GRAnular and Fibrous materials, June 21st-23th 2017, Clermont-Ferrand, France.

3.2.4.3 POTENTIAL CARBONATION RATE OF LIME IN HEMP CONSTRUCTION MATERIALS

Carbonation in hemp lime building materials occurs like in other building materials. At first, the atmospheric CO_2 diffuses inside the material pores and dissolves in water in the pores, forming carbonic acid H_2CO_3. Then, the carbonic acid dissociates in bicarbonate (HCO_3^-) and carbonate (CO_3^{2-}) ions that form $CaCO_3$ reacting with the Ca^{2+} ions released by the dissolution of $Ca(OH)_2$, contained in the binder, in the pore water. All processes involved in the carbonation can be synthetized in Reaction 3.2.4.1, reported in section 3.2.4.1 (Chabannes et al., 2015). Since carbonation is related

to the content of calcium hydroxide ($Ca(OH)_2$) in the binder, and it depends on its composition, all such parameters are reported in Table 3.2.4.5. The carbonation rate was calculated as the ratio between the carbonated $Ca(OH)_2$ and the initial $Ca(OH)_2$ content of the binder, assuming that all $Ca(OH)_2$ in the binder is available for carbonation.

Experts of lime binder producers estimated that 249 kg CO_2 are absorbed for each metric tonne of lime binder, as reported in the study by Boutin et al. (2006). They evaluated with the LCA methodology the impact on climate change of hemp–lime construction material. The study was commissioned by the French Ministry of Agriculture and considered 1 m^2 of load bearing wall as a functional unit, with lime binder and hemp shives ratio equal to 2:1. The binder composition is 75% hydrated lime, 15% hydraulic binder and 10% pozzolanic binder. Thus, the calcium hydroxide content of the binder is 750 kg/t of binder, assuming that hydrated lime is 100% $Ca(OH)_2$. Furthermore, assuming that only hydrated lime carbonates, the carbonation rate is 56%, i.e. more than half of the hydrated lime is carbonated after 100 years.

Carbonation rate of $Ca(OH)_2$ in hydrated lime was assumed equal to 100% by Ip and Miller (2012) and Prétot et al. (2014) studies. Thus, the hydrated lime CO_2 uptake over the building material lifetime is equal to the entire amount of CO_2 emitted during lime production. Prétot et al. (2014) made a further assumption that also calcium hydroxide in hydraulic lime fully carbonates. Based on Prétot et al. study, Sinka et al. (2018) LCA made the same assumptions. A lower carbonation rate was assumed by Lecompte et al. (2017), based on thermogravimetric analysis results on carbonation of non-hydraulic lime mortars (Lawrence, 2006), i.e. 85% instead of 100%.

Arrigoni et al. (2017) carried out a LCA study considering two types of binders and measured through X-Ray Diffractometric (XRD) the $CaCO_3$ formed in hemp lime samples after 8 months. The composition of the first binder analysed is 80% “dolomitic lime” and 20% cement, while the second binder is composed only of “dolomitic lime”. It was assumed that calcium hydroxide in “dolomitic lime” fully carbonates (the $Ca(OH)_2$ content of “dolomitic lime” is 50%), while cement carbonation was assumed 75% of the calcium in cement. As a result, the maximum CO_2 uptake per metric tonne of binder is 325 kgCO_2 and 297 kgCO_2, respectively for mixed binder and pure “dolomitic lime” binder. These values are compared with the amount of calcium carbonate measured through XRD analysis. Samples of the hemp lime bricks with the two different types of binders were analysed. The content of $Ca(OH)_2$ and $CaCO_3$ were measured at regular time intervals from hemp lime bricks production up to 8 months (30, 75, 110, 150 and 240 days). Samples at different depths (0-2, 2-4, 4-6, 6-8 and 8-10 cm) were extracted, crushed and sieved in order to separate hemp shives from the binder. Only one face of the blocks was exposed to air. After 8 months, no carbonation was detected at the inner depths and the total amount of CO_2 captured was 7 kg and 12 kg per metric tonne of

binder. Thus, carbonation rate is 3.7% and 2.4% respectively for mixed binder and pure "dolomitic lime" binder. Given these low values, the assumption of a complete carbonation seems unrealistic.
Jami and Kumar (2017) also evaluated through XRD analysis the CO_2 uptake. The samples were hemp lime cubes with a 7 cm side. Each cube was made of 118 g of binder which is composed of $Ca(OH)_2$ by 90%. Thus, the maximum CO_2 uptake is 70 g CO_2 per cube if only $Ca(OH)_2$ carbonates, calculated as follows:

$$70gCO_2 = 0.90 \times 118g\ Ca(OH)_2 \times M_wCO_2 / M_w\ Ca(OH)_2 \qquad \text{[Equation 3.2.4.1]}$$

where M_w indicates the molecular weight.
After 28 days, the total CO_2 uptake is 14 g CO_2 per cube, i.e. the carbonation rate is 20%. This estimation of the carbonation rate is much higher than the one found by Arrigoni et al. This difference can be partially explained by the different composition of the binders analysed by the two studies and by the fact that the faces exposed to air are five in Jami and Kumar study while it is only one in Arrigoni et al. study.
The study by Chabannes et al. (2015) evaluated the carbonation rate through Thermo-Gravimetric Analysis (TGA) of concrete based on two different biogenic materials, i.e. rice husks and hemp. In addition to the carbonation rate, hardening and mechanical properties were assessed under natural and accelerated carbonation conditions. Cylindrical samples of Lime Hemp Concrete (LHC) with a diameter of 11 cm and a height of 22 cm were produced. Binder to hemp weight ratio was 2:1, while the water to binder weight ratio was 1.5:1. Lime binder contains equal amounts of hydrated lime and hydraulic lime whose $Ca(OH)_2$ content was respectively 85% and 45%, as shown in Table 3.2.4.3. Once the cylindrical specimens were demoulded after 24 hours, they were cured under two different natural conditions for 10 months and accelerated carbonation conditions. The former natural condition was called Indoor Standard Condition (ISC), i.e. in a climate-controlled room at 20°C and 50% relative humidity, while the latter one was called Outdoor exposed Condition (OC) under shelter. In OC, the temperature ranged from 0°C up to 30°C and the relative humidity from 45% up to 75%. Accelerated Carbonation Curing (ACC) was preceded by an initial conditioning which consisted in storing the specimens during 40 days in the climate-controlled room at 20°C and 50% relative humidity. Then, the CO_2 curing was carried out in a glass enclosure fed by CO_2 for one month. In the glass enclosure, the room temperature was 20±2°C and the relative humidity was fixed at 65±5%. At first, a partial vacuum was created in the enclosure with a vacuum pump in order to reach an absolute pressure equal to 0.50±0.05 bar. CO_2 was then injected until the absolute pressure reached the atmospheric, i.e. 1 bar. Thus, the concentration of CO_2 was maintained at 50%v/v. The enclosure was refilled 42 times by CO_2. After the curing time, the samples were powdered and sieved (80 μm mesh

size) before TGA (Thermogravimetric analyser STA 409 Cell, Netzsch). Thermal degradation was conducted from 25°C up to 950°C at 10 °C min^{-1} under air atmosphere. During TGA, the weight loss of samples occurred in three ranges of temperature. The first temperature range is between 100°C and 400°C and the weight loss was considered due to the loss of water from C–S–H hydrates, while between 400°C and 500°C the weight loss was considered due to water loss caused by the dehydroxylation of $Ca(OH)_2$. Lastly, between 600°C and 900°C the weight loss was assumed due to the release of CO_2 by $CaCO_3$. It was called loss of CO_2 (LCO_2) and measured as %. Starting from LCO_2, $CaCO_3$ was calculated according to the following equation:

$$CaCO_3(\%) = LCO_2(\%) \times M_wCaCO_3 / M_wCO_2 \quad \text{[Equation 3.2.4.2]}$$

with M_WCaCO_3 and M_WCO_2 indicating the molar masses of $CaCO_3$ and CO_2.
The resulting $CaCO_3$ content is reported in the second column of table 3.2.4.4. Higher $CaCO_3$ content is observed in OC than in ISC because it is characterized by better RH conditions which enhanced the dissolution of CO_2 in the pores.

Since the initial $CaCO_3$ content in binder is 10%, the amount of $Ca(OH)_2$ which is carbonated can be calculated with the following equation:

$$\text{Carbonated } Ca(OH)_2 \text{ (kg/t)} = (CaCO_3(\%) - 10\%) \times 1000 \text{ kg/t} \times M_wCa(OH)_2 / M_wCaCO_3$$

[Equation 3.2.4.3]
Once the amount of carbonated $Ca(OH)_2$ was obtained (results in the third column of Table 3.2.4.4), the carbonation rate can be evaluated as the ratio between the calculated carbonated $Ca(OH)_2$ and the initial $Ca(OH)_2$ in the binder which is 65% (see table 3.2.4.3). Thus, the carbonation rate in accelerated conditions is 65.2%, while in natural conditions it is 33.7% and 54.5% respectively for indoor and outdoor sheltered condition. These rates are higher than those found in the study by Arrigoni et al. (2017). One of the reasons could be the different composition of the binder with higher content of $Ca(OH)_2$ available for carbonation in the samples analysed by Chabannes, but also in this study the rate of carbonation is lower than 100%.

Results of the literature on carbonation hemp lime construction material are compiled in Table 3.2.4.5.

Table 3.2.4.3. Main mineralogical components of hydrated lime and hydraulic lime in Chabannes et al. (2015) study.

Material	%$Ca(OH)_2$	%C_2S	%$CaCO_3$
Hydrated lime	85	-	10
Hydraulic lime	45	30	10
50/50 wt.%	65	15	10

Table 3.2.4.4. $CaCO_3$ content measured through thermogravimetric analysis; amount of carbonated $Ca(OH)_2$; Rate of carbonation (Chabannes et al., 2015).

Curing condition	$CaCO_3$ measured	kg carbonated $Ca(OH)_2$ /t binder	Carbonation rate
ISC (10 months)	39.6%	219	33.7%
OC (10 months)	57.9%	354	54.5%
ACC (40 days + 1 month)	67.3%	424	65.2%

Table 3.2.4.5. Binder CO_2 uptake and carbonation rate of hemp lime constructions according to binder composition.

Reference	Type of study	Geographical context	Type of construction	Composition	Binder composition	Binder CO_2 uptake	Carbonation rate of lime	Carbonation time	Notes
Boutin et al. (2006)	LCA study	France	Load-bearing wall (density of 330 kg/m^3 and U-value[12] of 0.42 W/m^2/K) Construction method: spraying Lifespan: 100 years	Binder: 54.5 kg/m^2 Hemp: 24.8 kg/ m^2 Water: 37.2 kg/m^2 Timber frame: 5.5 kg/ m^2	75% hydrated lime, 15% hydraulic lime, 10% pozzolanic material	249 kgCO_2 /t binder	56% (provided experts)	100 years	Binder uptake provided by experts of lime binder producer. Carbonation rate estimated assuming carbonation of only hydrated lime that is 100% $Ca(OH)_2$
Ip and Miller (2012)	LCA study	United Kingdom	Non-load-bearing wall (density 275 kg/m^3 and U-value 0.19 W/m^2/K) Lime-hemp mixture is poured into the timber shuttering and manually tamped Lifespan: 100 years	Binder: 50 kg/m2 Hemp: 30 kg/m2 Water: 75 kg/m2 Timber frame: 4.6 kg/ m^2	75% hydrated lime, 15% hydraulic lime, 10% pozzolanic material	453 kgCO_2 /t binder	100% (assumed)	100 years	Each t of binder contains 577 kgCaO. Emission of 786 gCO_2/kgCaO from the chemical reaction: $CaCO_3 \rightarrow CaO + CO_2$
Prétot et al. (2014)	LCA study	France	Load-bearing wall (U-value 0.36 W/m^2/K) Construction method: spraying Lifespan: 100 years	Binder: 45 kg/ m^2 Hemp: 20.4 kg/m^2 Water: 67 kg/ m^2 Timber frame: 20 kg/ m^2	75% hydrated lime, 15% hydraulic lime, 10% pozzolanic material	462 kgCO_2 /t binder	100% (assumed)	100 years	Binder CO_2 uptake assumptions: $Ca(OH)_2$ in hydrated lime and hydraulic lime full carbonates (100%). Hydraulic lime $Ca(OH)_2$ content: 60%.
Chabannes et al. (2015)	Experimental study	France	Cylindrical samples of Lime Hemp Concrete (diameter 11 cm and height 22 cm) Binder to hemp weight ratio = 2:1	Binder: 285 kg/m^3 Hemp: 142.5 kg/ m^3 Water: 427.5 kg/ m^3	50% hydraulic lime, 50% hydrated lime (binder composition details in Table 3.2.4.3)	ISC 130 kgCO_2 /t binder*	33.7% (measured)	10 months	Natural carbonation – Indoor Standard Condition (ISC) Temperature: 20°C Relative humidity: 50%
						OC 210 kgCO_2 /t binder*	54.5% (measured)	10 months	Natural carbonation – Outdoor exposed Condition (OC) Temperature: 0°C-30°C Relative humidity: 45%-75%
						ACC 252 kgCO_2 /t binder*	65.2% (measured)	40 days (initial curing) + 1 month (ACC)	Accelerated Carbonation Condition Temperature: 20±2°C Relative humidity: 65±5% [CO2]: 50%v/v

[12] The U-value is also called overall heat transfer coefficient. The lower is the U-value, the better is the thermal performance of the wall.

* Binder CO_2 uptake estimated from the Thermogravimetric analysis results. It is calculated multiplying carbonated $Ca(OH)_2$ (third column of table 3.10.3) by ratio among the molecular weight of CO_2 and that of $Ca(OH)_2$.

Reference	Type of study	Geographical context	Type of construction	Composition	Binder composition	Binder CO_2 uptake	Carbonation rate of lime	Carbonation time	Notes
Lecompte et al. (2016)	LCA study	France	Wall with U-value 0.085 $W/m^2/K$ Construction method: cast into shutter	Binder: 167 kg m^3 Hemp: 100 kg/m^3 Water: 250 kg/ m^3	75% hydrated lime 15% hydraulic lime 10% pozzolanic material	464 $kgCO_2$ /t binder	85% (assumed)	70 years	Carbonation rate assumed by literature[13]
Arrigoni et al. (2017)	Experimental and LCA study	Italy	Non-load-bearing wall (density of 330 kg/m^3 and U-value of 0.27 $W/m^2/K$) Construction method: blocks	Hempcrete block composition: Binder: 44.5 kg/m^2 Hemp: 31.4 kg/m^2 Water: 58.6 kg/m^2	*Case A* 80% dolomitic lime 20% cement	12 kg CO_2 /t binder (measured) 325 kg CO_2 /t binder (full carbonation)	3.7% (measured) 100% (assumed)	240 days	Binder CO_2 uptake: 75% of CaO in cement carbonates and 100% of $Ca(OH)_2$ in dolomitic lime carbonates. Dolomitic lime $Ca(OH)_2$ content: 50%. Measurement through X-Ray Diffractometric (XRD) analysis (only one blocks face exposed to air)
					Case B 100% dolomitic lime	7 kg CO_2 /t binder (measured) 297 kg CO_2 /t binder (full carbonation)	2.4% (measured) 100% (assumed)	240 days	
Jami and Kumar (2017)	Experimental study	India	Analysis on a cube of 343 cm^3 with dry density of 567.05 kg/m^3 (after 28 days)	Binder to Hemp weight ratio = 2.15 Water to Binder weight ratio = 1.3	100% Hydrated lime (with 90% of $Ca(OH)_2$ content)	14 kg CO_2 /t binder (measured) 70 kg CO_2 /t binder (assumed)	20% (measured)	28 days	Samples under ambient condition Measurement through XRD analysis
Sinka et al. (2018)	LCA study	Latvia	Load bearing wall with timber frame (U-value 0.18 $W/m^2/K$, compressive strength 0.5 MPa, thickness 541 mm)	Binder: 125.6 kg/m^2 Hemp: 308 kg/m^2 Water: 302 kg/m^2	70% hydrated lime 20% hydraulic binder 10% pozzolanic material	487 $kgCO_2$ /t binder	100% (assumed)	100 years	Binder CO_2 uptake considering: 594 gCO_2/kg hydrated lime and 356 gCO_2/kg hydraulic lime (Prétot et al., 2014). Carbonation rate assumed by Prétot et al. (2014).

[13] Lawrence, R.M.H., Mays, T.J., Walker, P., D'Alaya, D., 2006. *Determination of carbonation profiles in non-hydraulic lime mortars using thermogravimetric analysis*. In: Thermochemica acta, 444, 179-189.

3.2.4.4 Carbonation depth over time

Hirst et al. (2012) measured at different ages up to 91 days the carbonation depth, i.e. the depth behind which lime is carbonated. Three different binders (THB-A, THB-B and BC) were used for producing the specimens. THB-B was the commercial binder composed mainly of CL90 air lime with the addition of hydraulic components and other additives to improve porosity and consistence. THB-A is the same binder of THB-B blended with components for reducing setting time and making it more suitable for use in colder temperatures. BC was a binder based on natural hydraulic lime. The proportion of binder, hemp and water is different in order to produce a mix with different density as reported in the first two columns of Table 3.2.4.6. Specimen were cast in cylindrical cardboard moulds with diameter of 100 mm and height of 200 mm at temperature of 20±1°C and relative humidity (RH) of 60±5% for one week. Then, the specimens were demoulded and cured in a conditioning room at 20°C and 60% RH for up to 91 days. At selected ages, samples were removed from the conditioning room and split in half and the exposed face sprayed with an ethyl alcohol phenolphthalein solution. Phenolphthalein is a pH indicator which is pink when the pH is higher than 9, otherwise it is colourless. Since hemp lime material shows a more irregular carbonation boundary than one of lime mortars due to its porosity and the relatively large size of hemp shivs, the carbonation depth was measured from eight equally spaced points around the cross-section of each specimen and then the mean of the measurements was calculated. Based on the measurements, the authors assumed that the carbonation depth (d) is proportional to the square root of time as for mortars and cement materials. The assumed equation which links the carbonation depth to the time is the following:

$$d = K\sqrt{t} \qquad \text{[Equation 3.2.4.4]}$$

where K is the carbonation constant (mm/day$^{1/2}$) and t is the time expressed in days. The estimated K ranges from 3.7 to 8.4, as reported in Table 3.2.4.6.

For all specimens except THB-A at a density of 220 kg/m^3, the correlation was good (R^2>0.9), i.e. the Equation 3.2.4.4 explains well the relationship among carbonation depth and time. Furthermore, the specimens are fully carbonated after 91 days, i.e. the carbonation depth is higher than half of the specimens' diameter (50 mm). It results that carbonation of hemp lime begins at early age and it is slower at higher mix density.

Table 3.2.4.6. Carbonation constant for different binders and different mix density due to different binder:hemp:water ratio.

Binder	Binder:hemp:water ratio (by weight)			Mix density (kg/m^3)	Carbonation constant K ($mm/day^{1/2}$)
	Binder	Hemp	Water		
THB-A	1	1	1	220	8.4
	1.5	1	2	275	6.7
	2	1	3	330	3.7
THB-B	1.5	1	2	275	5.8
BC	1.5	1	2	275	5.5

3.2.4.5 CONCLUSIONS

With the exclusion of the rate found by Arrigoni et al., that is very different from the other ones probably due to the different binder composition, the measured carbonation rate in natural conditions ranges from 20% to 54.5% after 28 days and 10 months, respectively. Since construction material lifespan is on the order of the years, the higher value should be considered. Furthermore, the upper value measured under natural condition is similar to the one provided by the lime binder producers experts, i.e. 56%. The experimental works on carbonation of hemp lime construction materials showed that the assumption of achieving full carbonation seems overestimated, and a carbonation rate lower than 100% should then be considered. On this matter, a higher carbonation rate (65.2%) can be reached under accelerated carbonation conditions.

About carbonation time, Hirst et al. (2012) found that carbonation depth is proportional to the square root of time like for mortars. Furthermore, the carbonation begins at early age and it is lower at higher hemp lime mix density, but after 91 days all cylindrical samples with diameter of 50 mm were fully carbonated.

Based on the results of these studies, it can be assumed that around 55% of the lime used in hemp lime material carbonates after 91 days at application thickness lower than 50 mm.

It is expected that further studies will analyse the carbonation depth over time also in real cases since there is a growing interest in construction materials with low carbon footprint, that can also be used for storing CO_2 temporary or permanently (Ashraf, 2016).

REFERENCES

Arrigoni, A., Pelosato, R., Melià, P., Ruggieri, G., Sabbadini, S., Dotelli, G., 2017. *Life cycle assessment of natural building materials: the role of carbonation, mixture components and transport in the environmental impacts of hempcrete blocks.* Journal of Cleaner Production 149: 1051-1061. DOI: http://dx.doi.org/10.1016/j.jclepro.2017.02.161

Ashraf, 2016. *Carbonation of cement-based materials: Challenges and opportunities.* In: Construction and Building Materials, 120, 558-570. DOI: 10.1016/j.conbuildmat.2016.05.080

Boutin, M.-P., Flamin, C., Quinton, S., Gosse, G., Lille, I., 2006. *Etude des caractéristiques environnementales du chanvre par l'analyse de son cycle de vie.* Paris, Ministère de l'agriculture et de la pêche.

Chabannes, M., Garcia-Diaz, E., Clerc, L., Bénézet, J.-C., 2015. *Studying the hardening and mechanical performances of rice husk and hemp-based building materials cured under natural and accelerated carbonation.* In: Construction and Building Materials, 94, 105-115. DOI: http://dx.doi.org/10.1016/j.conbuildmat.2015.06.032

Hirst, E. A. J., Walker, P., Paine, K. A., Yates, T., 2012. *Characteristics of low-density hemp-lime building materials.* In: Proceedings of Institution of Civil Engineers: Construction Materials, 165, 1, 15-23. DOI: https://doi.org/10.1680/coma.1000021

Ip, K. and Miller, A., 2012. *Life cycle greenhouse gas emissions of hemp-lime wall constructions in the UK.* Resources, Conservation and Recycling, 69, 1-9. DOI: https://doi.org/10.1016/j.resconrec.2012.09.001

Jami, T., and Kumar, S. (2017). *Assessment of carbon sequestration of hemp concrete*. International Conference on Advances in Construction Materials and Systems, Chennai, India. Available online: https://www.researchgate.net/publication/320058537_Assessment_of_Carbon_Sequestration_of_Hemp_Concrete

Lawrence, M., Fodde, E., Paine, K., Walker, P., 2012. *Hygrothermal performance of an experimental hemp-lime building*. In: Key Engineering Materials, 517, 413-421. DOI: https://doi.org/10.4028/www.scientific.net/KEM.517.413

Lawrence, M., 2015. *Reducing the environmental impact of construction using renewable materials*. In: Journal of Renewable Materials, 3 (3), 163-174. DOI: https://doi.org/10.7569/JRM.2015.634105

Lawrence, R.M.H., Mays, T.J., Walker, P., D'Alaya, D., 2006. *Determination of carbonation profiles in non-hydraulic lime mortars using thermogravimetric analysis*. In: Thermochemica acta, 444, 179-189.

Lecompte, T., Levasseur, A., Maxime, D., 2017. *Lime and hemp concrete LCA: a dynamic approach of GHG emissions and capture*. In: 2nd International Conference on Bio-based Building Materials & 1st Conference on ECOlogical valorisation og GRAnular and Fibrous materials, June 21st-23th 2017, Clermont-Ferrand, France.

Prétot, S., Collet, F., Garnier, C., 2014. *Life cycle assessment of a hemp concrete wall: impact of thickness and coating*. Building and Environment, 72, 223-231. DOI: https://doi.org/10.1016/j.buildenv.2013.11.010

Sinka, M., Van den Heede, P., De Belie, N, Bajare, D., Sahmenko, G., Korjakins, A., 2018. *Comparative life cycle assessment of magnesium binders as an alternative for hemp concrete*. In: Resources, Conservation & Recyling, 133, 288-299. DOI: https://doi.org/10.1016/j.resconrec.2018.02.024

Shea, A., Lawrence, M., Walker, P., 2012. *Hygrothermal performance of an experimental hemp-lime building.* In Construction and Building Materials, 36, 270-275. DOI: http://dx.doi.org/10.1016/j.conbuildmat.2012.04.123

Walker, R., Pavia, S., Mitchell, R., 2014. *Mechanical properties and durability of hemp-lime concretes.* In: Construction and Building Materials, 61, 340-348. DOI: http://dx.doi.org/10.1016/j.conbuildmat.2014.02.065

3.2.5 USE OF LIME IN OTHER CONSTRUCTION MATERIALS

Lime is also used in other construction materials' sub-applications such as paints and natural fibres. The carbonation in these sub-applications was not assessed due to the lack of publications/reports on carbonation.

3.3 USE OF LIME IN CIVIL ENGINEERING

3.3.1 USE OF LIME IN SOIL STABILISATION

3.3.1.1 INTRODUCTION

The availability of natural high-quality soil to be used as a construction material is more and more limited due to environmental and economic reasons; moreover, soils are non-renewable resources and therefore they should be recycled as much as possible (Di Sante et al., 2015).

The chemical stabilisation of fine grained soils, that implies blending with a stabilizer (typically lime, cement fly ash or bitumen), is a well-established and low cost technique used to improve the engineering properties such as compaction efficiency, immediate bearing capacity, trafficability, water sensitivity, shear resistance, stiffness (resistance to deformation), and wear resistance (durability; Ashraf et al., 2018). Following this process, treated soils can be used in many geotechnical and geoenvironmental applications like creation of sub-bases and subgrades for road and airport structures, backfill for bridge abutments and retaining walls, embankments construction, canal lining or slope protection (Bell, 1989).

Among the different soil additives used to improve the engineering properties, lime is the well-established chemical stabilizer used primarily for clay soils. When lime is added to the soil, the following three basic reactions occur, causing immediate and long-term changes:

- drying of wet soil. If quicklime is used, it will chemically react with water and release heat (65.2 kJ/mol), according to reaction [3.3.1.1]. As a consequence, the soil is dried twice because part of its water content will participate in this reaction and because the heat generated by the exothermal reaction will evaporate additional moisture. The hydrated lime produced will subsequently react with clay particles, causing additional drying due to the reduction of soil's moisture holding capacity. When hydrated lime is used, drying occurs only due to this last mechanism (Firoozi et al., 2017).

  $$CaO + H_2O \rightarrow Ca(OH)_2 + \text{heat} \qquad [3.3.1.1]$$

  Moreover, the soil water content is further decreased during mixing operation, particularly in hot and windy atmospheric conditions.

- Short-term modification reactions. Modification reactions are rapid (they generally happen within 24-72 hours from the mixing) and occur primarily from the cation exchange between calcium divalent ions in the lime and monovalent ions (such as Na^+ and K^+) at the negative charge sites on the surface of clay particles (the number of exchange sites increases with pH). The cation exchange leads to a substantial contraction of the diffused double layer (adsorbed water layer) thickness around the clay particles. In this way, soil becomes less susceptible to volume changes with the addition of water. In addition, the reduction in thickness transforms the structure of clay particles from a flat, parallel structure to a more random edge-to-face orientation (flocculation) and forms weak bonds at the edge-surface interfaces of the clay particles (agglomeration; Figure 3.3.1.1). As a result, a reduction in soil plasticity, an improvement in texture (from a plastic clay to a friable material, granular in appearance) and an increase in shear strength is obtained after

compaction (Prusinski and Bhattacharja, 1999; Rogers and Glendinning, 2000; Cherian and Arnepalli, 2015; Di Sante et al., 2015).

- Long-term pozzolanic reactions. The release of OH^- ions from lime dissolution causes a progressive increase of the pH up to 12.4. The highly alkaline pH conditions increase the solubility and reactivity of silica and alumina ions present in the soil clay particles. Pozzolanic reactions [Reactions 3.3.1.2 and 3.3.1.3] then occur between calcium ions and the silica and alumina dissolved from the lattices of clay minerals. New cementitious compounds, i.e. calcium silicate hydrate and aluminate hydrate gels are formed; they recombine with time in a rigid matrix leading to increased soil strength and durability. Pozzolanic reactions take place slowly on the order of weeks or years and are promoted by high lime dosage, extended curing times and elevated temperatures. The lime content must be capable of maintaining a high pH environment for a long period. Indeed, without the formation of adequate networks of cementitious compound, the system may be susceptible to detrimental leaching of calcium, which results in decreased pH, disruption of pozzolanic action, and reverting back the soil toward its original unstabilised state (Prusinski and Bhattacharja, 1999; Rogers and Glendinning, 2000; Cherian and Arnepalli, 2015; Di Sante et al., 2015)

$$Ca^{2+} + 2OH^- + \text{soluble clay silica} \rightarrow \text{calcium silicate hydrate} \quad [3.3.1.2]$$

$$Ca^{2+} + 2OH^- + \text{soluble clay alumina} \rightarrow \text{calcium aluminate hydrate} \quad [3.3.1.3]$$

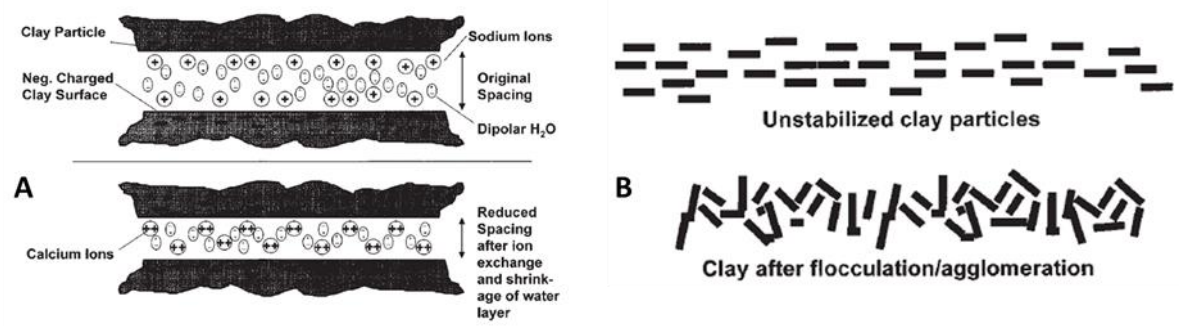


Figure 3.3.1.1. Lime-soil modification: cation exchange (Figure A) and flocculation-agglomeration process (Figure B). Source: Prusinski and Bhattacharja, 1999.

The typical amount of lime required for soil stabilization in US is indicated between 2% and 8% by weight of the dry soil (Jacobson et al., 2003; National Lime Association, 2004; Jha and Sivapullaiah, 2018).[14] In the past, some authors have developed different empirical formulations and protocols to determine the exact lime requirement for stabilization targets. Most of methods proposed to calculate, as a rule of thumb, the minimum lime addition based on the clay percentage of soil. For example, Ingles and Metcalf (1972) suggested dosing 1% of lime (by weight of dry soil) for each 10% of clay in the soil. Also the protocol established by Eades and Grim (1966) is frequently used and it is based on the calculation of the Initial Consumption of Lime (ICL), i.e.

[14] The dosage can be lower (1% – 1.5%) in the case of soil improvement.

the minimum quantity of lime the soil needs to reach a pH of 12.40 within one hour and that ensures an increase in compressive strength.

Quicklime and hydrated lime are both suitable chemical forms for soil stabilization. Quicklime is the most commonly used reactant in Europe, also due to the following advantages (Makusa, 2013):

- higher available free lime content per unit mass (the reactant is more cost effective);
- higher density, which implies less requirement of storage space and less generation of dust;
- better performance at drying out due to the release of heat from the exothermic hydration reaction.

The better performances of quicklime were also recently proved by the research performed by Amadi and Okeiyi (2017). At 10% dosage[15], compared to hydrated lime, quicklime caused the soil to have plasticity 1.4 times lower and resulted in swell values about 2.2 times lower. Advantages of quicklime were also detected in terms of durability of mixtures and unconfined compressive strength. According to such results, the use of $Ca(OH)_2$ is restricted to the stabilization of soils with high clay content and intermediate water content where its main advantage is raising the plastic limit of the clayey soil.

3.3.1.2 LITERATURE ASSESSMENT FOR THE USE OF LIME IN SOIL STABILISATION: MATERIAL AND METHODS

Some studies about lime carbonation in the soil stabilisation technique are available in the existing literature (see Table 3.3.1.1 for the complete list). Most of the listed studies assessed the actual consequences of carbonation on soil mechanical properties and found adequate techniques of curbing the phenomenon, especially in areas characterized by hot-dry climates.

To the authors' knowledge, only three studies (Eades et al., 1962; Deneele et al., 2013; Haas and Ritter, 2018) reported a measure of the potential carbonation of lime added to the soil, i.e. the percentage of lime converted into calcium carbonate.

[15] Though this high dosage is applied in experimental conditions, it is not common in the reality.

Table 3.3.1.1. List of consulted documents for the literature review about the use of lime in soil stabilisation application.

Peer-reviewed papers

9. Haas et al., 2018. *Soil improvement with quicklime - long-time behaviour and carbonation*. Road Materials and Pavement Design, 20(8), 1941-1951. DOI: https://doi.org/10.1080/14680629.2018.1474793
10. Jawad et al., 2014. *Soil stabilization using lime: advantages, disadvantages and proposing a potential alternative*. Research Journal of Applied Sciences, Engineering and Technology, 8(4): 510-520. DOI: 10.19026/rjaset.8.1000

Meeting proceedings or seminars

11. Bagonza et al., 1987. *Carbonation of stabilized soil-cement and soil-lime mixtures*. In: Proceedings of Seminar H, PTRC Transport and Planning Summer Annual Meeting, University of Bath, 7-11 September 1987. London: PTRC Education and Research Services, 29-48
12. Deneele et al., 2013. *La carbonatation d'un sol traite a la chaux-approche experimentale (The carbonation of a lime-treated soil-experimental approach)*. Conference TerDOUEST 2013 Seminar, at Marne-la-Vallée
13. Eades et al., 1962. *Formation of new minerals with lime stabilization as proven by field experiments in Virginia*. In: Lime Stabilization mix design, properties, and process, 41st annual meeting of Highway Research Board, 8-12 January 1962. Available online: http://onlinepubs.trb.org/Onlinepubs/hrbbulletin/335/335.pdf
14. Paige-Green, 2011. *Considerations for ensuring the durability of chemically stabilized road materials*. Proceedings of the Institution of Civil Engineers-Ground Improvement, 164(4): 245-252. DOI: 10.1680/grim.900044

3.3.1.3 FUNDAMENTALS OF CARBONATION OF LIME IN SOIL STABILISATION

In addition to short-term modification reactions and pozzolanic reactions, the carbonation of lime is a potential reaction during lime stabilization of soils, especially in hot-dry climates where the control of curing is difficult. In the existing literature on the topic, the carbonation is indicated as deleterious (Paige-Green, 2011; Jawad et al., 2014) due to the following reasons:

- the calcium carbonate has weak bonding and its formation consumes lime, affecting negatively the pozzolanic reactions;
- the carbonation reaction causes a significant increase in volume. If the expansive forces generated by expansion exceed the tensile strength of the soil, cracking, weakening and/or pulverization of the stabilized material will occur;
- if the pH of the material decreases below 10 as a result of carbonation, the calcium silicate hydrate products become unstable and decompose. Thus, the strength of the soil may decrease with time and become insufficient to provide the required structural properties.

In relation to carbonation, Bagonza et al. (1987) examined the influence of temperature, humidity, and CO_2 concentration on the carbonation in natural conditions. Stabilised soils exposed to higher temperature (40°C) showed an important loss of strength due to the loss of water in the pores, which increases the amount of air voids and thus the level of carbon dioxide that can penetrate the soil. Always in relation to the water content, experimentations in South Africa have shown that carbonation is most detrimental at a relative humidity of 40%-70% and thus the stabilized material must be kept in a moist condition for at least 7 days. Placing a moist layer of material on the completely stabilised layer has been shown to be one of the most effective techniques for reducing moisture changes and encouraging proper cementation (Paige-Green, 2011).

3.3.1.4 POTENTIAL CARBONATION RATE OF LIME IN SOIL STABILISATION

In some analysed studies on the topic (e.g., Bagonza et al., 1987 and Deneele et al., 2013), the entity of the carbonation phenomenon in the lime-stabilised soils was measured by using the phenolphthalein indicator solution, originally implemented to assess the carbonation on concrete samples. Phenolphthalein ($C_{20}H_{14}O_4$) is an organic compound widely used as pH indicator, i.e. a substance that changes colour depending on the pH of the material on which it is applied (its turning point is at 9). When the surface of the sample appears bright red, the pH is greater than 9 and the soil is in the stability range of the CSH-type cementitious compounds; otherwise, if no colour change is evident, carbonation has probably taken place (the calcium carbonate has a pH between 8 and 8.5). Deneele et al. (2013), for example, measured the carbonation extent in lime-stabilised soil samples exposed to natural conditions by spraying the solution of phenolphthalein and measuring the carbonation penetration from the outside to the centre of the sample. Results showed a carbonation rate of 0.7 mm per day for 2% lime treatment and of 0.35 mm per day in case of 5% lime addition. According to such experimentation, the diffusion of CO_2 within the sample seems to be more effective with a lower dosage of lime.

Apart from the measurement of carbonation penetration, some authors also reported the degree of carbonation of lime expressed as percentage referred to the overall added amount (Table 3.3.1.2). Haas and Ritter (2018) assessed a 37% carbonation degree in the European context with a detailed field research. The analysis was based on soil samples collected in 2013 from an embankment built for a motorway in southeast Germany in 1979 (34 years before). Before the construction, quicklime was added to the soil in a total volume of 2.5% by weight to increase its mechanical properties, since the soil was composed of a layer of sift silts and deeper of clay sediments. In 2013, soil samples were drilled from the embankment and their content of total lime, available lime, and carbonates[16] was measured according to test methods defined in EN 459-2 (2010). The main result of the study in terms of carbonation was that, after 34 years, 37% of the quicklime added was carbonated, 47% was involved in pozzolanic reactions while the remaining 16% was still available for chemical reactions. The findings of Haas et al. (2018) confirmed the earlier carbonation datum obtained by Eades et al. (1962) in a previous field research on lime-stabilised clay soils[17] located in another geographical context (Virginia, USA) and treated with another chemical formulation of lime ($Ca(OH)_2$). Analyses showed that samples from soils treated with 5% of lime contained 2.5% of $CaCO_3$ (1.85% of hydrated lime). According to the reported value, the carbonation degree of the added lime corresponded to 37%.

Finally, Deneele et al. (2013) studied the evolution of the carbonation of silty soil samples[18] specifically treated with 5% of quicklime in laboratory and then the curing occurs under three different conditions. The first one is a classic curing for soil treatment studies in laboratory, i.e. the samples are sealed in cellophane film and stored in laboratory at 25±3°C. In this condition, around 30% of the added quicklime is carbonated after a

[16] The calcium carbonate content was established by determining the CO_2 content of the sample.
[17] The three analysed soils were composed of different clay minerals.
[18] The size fraction lower than 80 μm represented 99.4% of the material.

short period of time (90 days). In the second curing condition, the samples are exposed to natural conditions in a rain-protected environment (average temperature of 12°C-18°C and average relative humidity of 61-68%) for a short period of time (90 days). Results showed a 70% average carbonation degree. In an accelerated carbonation chamber occurs the last curing (10% of CO_2, average temperature of 30±5°C and average relative humidity of 70±5%). Under accelerated carbonation, the carbonation degree results 80% after 3 days of curing. However, differently to the previous studies of Haas and Ritter (2018) and Eades et al. (1962), this study was performed on samples purposely created at the lab-scale and not collected from the field some years after the lime treatment for earthworks.

Table 3.3.1.2. Summary of the literature documents reporting a carbonation degree for lime-stabilised soils in the existing literature.

Reference	Haas and Ritter (2018)	Eades et al. (1962)	Deneele et al. (2013)		
Geographical context	Southeast Germany	Virginia (USA)	Marche-les-Dames (Belgium)		
Type of work	Field research	Field research	Lab-scale study		
Type of soil	Soft silts and then water-bearing layers of sand and Upper Tertiary clay sediments with deposits of coal	1 SOIL: deeply weathered micaceous schist, which seldom offers a clay horizon 2 SOIL: deeply weathered granite which has resulted in micaceous silty clay 3 SOIL: heavy clay	Soil A1 group: - Plasticity index equal to 5 - 99.4% of material lower than 80µm		
Amount and type of lime	2.5% CaO on dry weight	3-5% $Ca(OH)_2$ on dry weight	2-5% CaO on dry weight		
Carbonation degree	37%	37% for 5% lime	30% for 5% lime	70% for 5% lime	80% for 5% lime
Test duration	34 years	3-4 years	90 days	90 days	3 days
Carbonation conditions	Natural conditions	Natural conditions	Classic curing (sealed in cellophane film)	Natural conditions (rain-protected environment)	Accelerated carbonation

3.3.1.5 CONCLUSIONS AND RECOMMENDATION ON FUTURE RESEARCH NEEDED FOR SOIL STABILISATION

According to the performed assessment, the existing literature on the topic is quite scarce. For the European context, only one field research is available (Haas et al., 2018) which reported an average carbonation degree equal to 37%, 34 years after the lime application. Results are valid for a lime dosage of 2.5% (quicklime) and the German climate conditions.

The results obtained are site-specific because the amount of quicklime added and the reactions occurred depend on soil characteristics (e.g., content of clay, particle size, different minerals of clay) and climate conditions. For this reason, further field analyses on different soils and different climate conditions following a common methodology are necessary within the European context in order to consolidate the first results. In particular, analyses in hot-dry climates areas should be considered a matter of priority, since carbonation is promoted in these conditions.

REFERENCES

Amadi, A.A. and Okeiyi A., 2017. *Use of quick and hydrated lime in stabilization of lateritic soil: comparative analysis of laboratory data*. International Journal of Geo-Engineering, 8(3), 1-13. DOI: 10.1186/s40703-017-0041-3

Ashraf, M.A., Hossen, M.A., Ali, M.A., Chakaraborty, B.P., 2018. *Stabilisation of soil by mixing with different percentages of lime*. Proceedings of the 4th International Conference on Civil Engineering for Sustainable Development, 9-11 February 2018, Khulna, Bangladesh. Available online: https://www.researchgate.net/publication/323880919_Stabilization_of_soil_by_mixing_with_different_percentages_of_lime

Bagonza, S., Peete, J.M., Newill, D., Freer-Hewish, R., 1987. *Carbonation of stabilized soil-cement and soil-lime mixtures*. In: Proceedings of Seminar H, PTRC Transport and Planning Summer Annual Meeting, University of Bath, 7-11 September 1987. London: PTRC Education and Research Services, 29-48. Available online: https://assets.publishing.service.gov.uk/media/5cdbefe2ed915d5c54bcba2c/1_515_PA1187_1987.pdf

Bell, F.G., 1989. *Lime stabilization of clay soils*. Bulletin of the International Association of Engineering Geology, 39(1), 67-74. DOI: https://doi.org/10.1007/BF02592537

Cherian, C. and Arnepalli, D.N., 2015. *A critical appraisal of the role of clay mineralogy in lime stabilization*. International Journal of Geosynthetics and Ground Engineering, 1(8), 1-20. DOI: 10.1007/s40891-015-0009-3

Deneele, D., Nael, J., Dony, A., Colin, J., Herrier, G., Lesueur, D., 2013. *La carbonatation d'un sol traite a la chaux-approche experimentale (The carbonation of a lime-treated soil-experimental approach)*. Conference TerDOUEST 2013 Seminar, at Marne-la-Vallèe. Available online: https://www.researchgate.net/publication/315114454_THE_CARBONATION_OF_A_LIME-TREATED_SOIL_-_EXPERIMENTAL_APPROACH

Di Sante, M., Fratalocchi, E., Mazzieri, F., Brianzoni, V., 2015. *Influence of delayed compaction on the compressibility and hydraulic conductivity of soil-lime mixtures*. Engineering Geology, 185: 131-138. DOI: https://doi.org/10.1016/j.enggeo.2014.12.005

Eades, J.L., Nichols, F.P., Grim R.E., 1962. *Formation of new minerals with lime stabilization as proven by field experiments in Virginia*. In: Lime Stabilization mix design, properties, and process, 41st annual

meeting of Highway Research Board, 8-12 January 1962. Available online: http://onlinepubs.trb.org/Onlinepubs/hrbbulletin/335/335.pdf

Eades, J.L. and Grim, R.E., 1966. *A quick test to determine lime requirements for lime stabilization*. Highway Research Record, 139, 61-72. Available online: http://onlinepubs.trb.org/Onlinepubs/hrr/1966/139/139-005.pdf

Firoozi, A.A., Olgun, C.G., Firoozi, A.A., Baghini, M.S., 2017. *Fundamentals of soil stabilization*. International Journal of Geo-Engineering, 8(26), 1-16. DOI: https://doi.org/10.1186/s40703-017-0064-9

Haas, S. and Ritter, H.J., 2018. *Soil improvement with quicklime - long-time behaviour and carbonation*. Road Materials and Pavement Design, 20(8), 1941-1951. DOI: https://doi.org/10.1080/14680629.2018.1474793

Ingles, O.G. and Metcalf, J.B., 1972. *Soil stabilization principles and practice*. Transport and Road Research Laboratory, Volume 11, 374 pages

Jacobson, J.R., Filz, G.M., Mitchell, J.K., 2003. *Factors affecting strength gain in lime-cement columns and development of a laboratory testing procedure.* Contract Research sponsored by Virginia Transportation Research Council, Final Contract Report. Available online: http://www.virginiadot.org/vtrc/main/online_reports/pdf/03-cr16.pdf

Jawad, I.T., Taha, M.R., Majeed, Z.H., Khan, T.A., 2014. *Soil stabilization using lime: advantages, disadvantages and proposing a potential alternative*. Research Journal of Applied Sciences, Engineering and Technology, 8(4), 510-520. DOI: 10.19026/rjaset.8.1000

Jha, A.K. and Sivapullaiah P.V., 2018. *Lime stabilization of soil: a physico-chemical and micro-mechanistic perspective*. Indian Geotechnical Journal, 1-9. DOI: https://doi.org/10.1007/s40098-019-00371-9

Makusa, G.P., 2013. *State of the art review, Soil stabilization methods and materials*. Department of Civil, Environmental and Natural resources engineering, Division of Mining and Geotechnical Engineering, Luleå University of Technology. Available online: https://www.diva-portal.org/smash/get/diva2:997144/FULLTEXT01.pdf

National Lime Association, 2004. *Lime-treated soil construction manual, lime stabilization & lime modification*. Bulletin 326, available online: https://www.graymont.com/sites/default/files/pdf/tech_paper/lime_treated_soil_construction_manual.pdf

Paige-Green, P., 2011. *Considerations for ensuring the durability of chemically stabilized road materials*. Proceedings of the Institution of Civil Engineers - Ground Improvement, 164(4): 245-252, doi: 10.1680/grim.900044

Prusinski, J.R. and Bhattacharja, S., 1999. *Effectiveness of Portland cement and lime in stabilizing clay soils*. Journal of the Transportation Research Board, 1652 (1), 215-227. DOI: https://doi.org/10.3141/1652-28

Rogers, C.D.F. and Glendinning, S., 2000. *Lime requirement for stabilization*. Journal of the Transportation Research Board, 1721 (1), 9-18. DOI: https://journals.sagepub.com/doi/pdf/10.3141/1721-02

3.3.2 USE OF LIME IN ASPHALT PAVEMENTS

Hydrated lime is used as additive in asphalt pavement due to its proven beneficial effects on durability of the road construction. This is because hydrated lime improves the resistance to chemical ageing, moisture damage and frost, and enhances the mechanical properties such as modulus, strength, rutting resistance, fatigue and thermal cracking (EuLA, 2010).

In order to produce hydrated lime, which is mainly calcium hydroxide ($Ca(OH)_2$), water is added to quicklime, i.e. calcium oxide (CaO). Quicklime, in turn, is the product of the calcination process during which limestone, made of calcium carbonate ($CaCO_3$), is heated up to 900°C in dedicated kilns and CO_2 is released into the atmosphere (EuLA, 2010).

The use of hydrated lime as additive in Hot Mix Asphalts (HMA) found great interest in the USA thanks to its favourable effect on the resistance to moisture damages and to frost that affected particularly the asphalt produced during the 1970s. In this period, the asphalt quality decreased as a consequence of the poor quality of the bitumen due to the petroleum crisis of 1973 and hydrated lime demonstrated to be an effective additive to tackle this issue. In the following years, the multiple benefits of hydrated lime as additive were studied. Thus, Little et al. (2006) and the European Lime Association (EuLA, 2010) reviewed the literature on benefits of hydrated lime as additive in HMA.

EuLA (2010) concluded that the effectiveness of hydrated lime is the result of four effects, two on the aggregate and two on the bitumen. One of the modifications on the aggregate is surface precipitation of calcium ions which favours the bitumen-aggregate adhesion, while the other one is clay flocculation which makes the clayey particles adhering to the aggregate surface and consequently inhibiting their detrimental effect on the mixture. Moreover, hydrated lime which is alkaline neutralizes the acidic moieties of the bitumen, counteracting the effect of the "bad" adhesion promoters which are originally present inside the bitumen. The results of the neutralization are the formation of water-insoluble calcium salts, the slowdown of the age hardening kinetics and the enhancement of the moisture resistance. Finally, the physical effect on the bitumen is the high porosity of hydrated lime which explains its stiffening effect above room temperature stronger than the one exhibited by mineral fillers. Further research is still needed on the temperature dependence of the stiffening effect of hydrated lime on the bitumen (EuLA, 2010; Lesueur et al., 2013).

Because of the above-mentioned properties, hydrated lime influences the durability of asphalt mixtures. In USA, field measurements showed that the addition of hydrated lime at the rate of 1-1.5% in the mixture (based on dry aggregate) increases the durability by 2 to 10 years, i.e. by 20 to 50%. Meanwhile, the French Northern motorway company, Sanef, observed that the asphalt durability is longer by 20-25%. As a result, hydrated lime use in asphalt mixtures has grown in most European countries, e.g. 70% of the highways in the Netherlands are treated with hydrated lime (EuLA, 2010).

The Life Cycle Assessment (LCA) study by Schlegel et al. (2013) evaluated the environmental benefits given by the increased durability. In the study, a road made of HMA treated with hydrated lime is compared with a road without hydrated lime addition. The functional unit is a road located in France with a length of 1 km and a width of 3.5 m, with a functional life of 50 years. The modelling approach is from cradle-to-grave, i.e. from the raw materials supply throughout the use phase until the end of life of the functional unit. Being a comparative LCA, the study did not consider the abrasion of the tyres, the fuel consumption and the related emissions of the vehicles using the road because they are assumed the same in both cases. Then, it was assumed that the HMA durability with hydrated lime was increased by 25%. Thus, the road maintenance of HMA with hydrated lime occurred every 12.5 years instead of 10 years that were assumed for the case of the HMA road without hydrated lime addition. The result of the study is that the hydrated lime addition and the consequent increase of the asphalt durability allow to save 43% of the total primary energy consumption and 23% of the greenhouse gas emission in the entire life cycle of the road in comparison with the case of the HMA road without hydrated lime treatment (Schlegel et al., 2013).

Both in Europe and in USA, there is a strong consensus on 1-1.5% hydrated lime content in HMA, but the way to dose hydrated lime in the mix in Europe is different from the one applied in USA. The two methods used in Europe are both the addition of the hydrated lime to the asphalt mix as pure hydrated lime at the asphalt plant, i.e. separately from the other fillers, or as a mixed filler (EuLA, 2010; AENOR, 2019). The former way consists in storing lime in a specific silo with direct access to the mixer at the asphalt plant which can be discontinuous or continuous. In discontinuous plants, the hydrated lime is weighted with the mineral filler in the same device and a screw conveyor connects the hydrated lime silo to the existing system. In a continuous plant, a rotary vane feeder dispenses hydrated lime that is injected into the drum through a screw conveyor typically at a distance of 1 meter before the binder injection point. Differently from the previous method, the hydrated lime can be added as a mixed filler using the same silo for mineral filler at the asphalt plant. In this case, the hydrated lime is mixed with the filler before the asphalt plant and it is supplied to the asphalt plant as mixed filler. The mixed filler is a standard product in Europe subdivided in the categories reported in Table 3.3.2.1 in compliance with the specifications for aggregates in asphalt mixtures defined by EN 13043 (EuLA, 2010; AENOR, 2019).

Table 3.3.2.1 Mixed filler categories as described in EN 13043 (EuLA, 2010; AENOR, 2019).

Category	Calcium hydroxide content (% by weight)
Ka_{25}	≥ 25
Ka_{20}	≥ 20
Ka_{10}	≥ 10
$Ka_{declared}$	<10
Ka_{NR}	No Requirement

In USA, the methods for adding hydrated lime are various and different from the European ones (AENOR, 2019). The most common is the addition of the hydrated lime in dry form to the wet aggregate using a pugmill. Another method consists in the treatment of the aggregates with the hydrated lime slurry instead of dry hydrated lime and, after the stockpile of the lime-treated aggregates for a marination period that ranges from 24-48 hours to more than 40 days, the marinated aggregates are supplied to the asphalt plant. Through the marination, clayey aggregates are better treated, and the quality control is simplified because the hydrated lime content can be measured directly on the stockpiled material (EuLA, 2010). Although this method requires space and the equipment for making the lime slurry and for metering the slurry onto the aggregates which makes this method expensive (Epps et al., 2013). Since carbonated lime is unable to react with HMA or fines, one of the drawbacks of the marination is the recarbonation of the hydrated lime, i.e. the formation of carbonated lime ($CaCO_3$) due to the reaction of hydrated lime with the atmospheric CO_2. For this reason, a specific marination period is recommended in several States, e.g. in Nevada no longer than 45 days (EuLA, 2010).

The study by Graves (1992), that is reported in the literature review by Little et al. and in the proceeding of the meeting on Moisture Sensitivity of Asphalt Pavements (Epps et al., 2003) assessed the carbonation rate of hydrated lime in stockpiled lime-treated aggregates. The percentage of uncarbonated hydrated lime was measured, referred to the initial content at different depths for an exposure time up to 180 days, as shown in Figure 3.3.2.1. After 180 days, hydrated lime is fully carbonated in the first two inches and partially carbonated at deeper levels. Thus, assuming that the hydrated lime content is equal at the different depths and the maximum depth was 5 inches, it results that at least 40% of hydrated lime was fully carbonated. Since the hydrated lime is still present in the first inch of the marinated aggregates until 60 days that is less than the typical marination period, natural carbonation of the hydrated lime added to stockpiled aggregates was demonstrated not to be a problem (Epps et al., 2003; Little et al., 2006).

As a conclusion, it results from the literature review carried out that no specific information about carbonation of hydrated lime use in Hot Mix Asphalts in Europe is available.

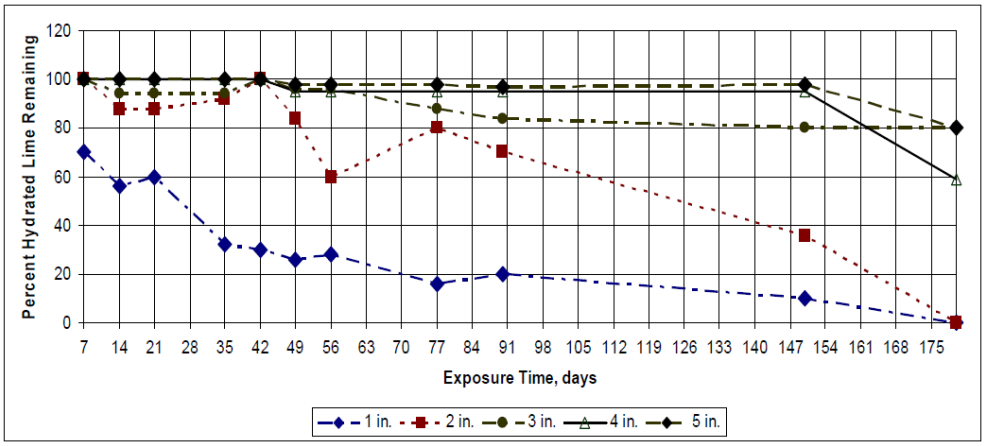


Figure 3.3.2.1. Effect of exposure time and stockpile carbonation on the active $Ca(OH)_2$ remaining from Graves (1992) study, as reported in Little et al. (2006).

REFERENCES

AENOR (Asociación Española de Normalización y Certificación), 2019. *PNE-UNE 41260-1 IN:2019 Materials for road pavements. Bituminous mixes. Part 1: Use of hydrated lime as a filler mineral powder*.

Epps, J., Berger, E., Anagnos, J. N., 2003. *Topic 4 – Treatments*. In: Moisture Sensitivity of Asphalt Pavements A NATIONAL SEMINAR, February 4 - 6 2003, San Diego, California. DOI: 10.17226/21957

EuLA, 2010. *Hydrated lime: a proven additive for durable asphalt pavements. Critical literature review.* Report to the European Lime Association / Asphalt Task Force.

Graves, R. E., 1992. *Lime in Sand for Hot Mix Asphalt - Test Project Summary.* In: Internal Memorandum, Chemical Lime Group.

Lesueur, D., Joëlle, P., Ritter, H.-J., 2013. *The mechanisms of hydrated lime modification of asphalt mixtures: a state-of-the-art review.* In: Road Materials and Pavement Design, 14, 1, 1-16. DOI: 10.1080/14680629.2012.743669

Little, D. N., Epps, J. A., Sebaaly, P. E., 2006. *The benefits of hydrated lime in Hot Mix Asphalt.* Prepared for the National Lime Association.

Schlegel, T., Puiatti, D., Ritter, H.-J., Lesueur, D., Denayer, C., Shtiza, A., 2016. *The limits of partial life cycle assessment studies in road construction practices: A case study on the use of hydrated lime in Hot Mix Asphalt.* In: Transportation Research Part D, 48, 141-160. DOI: 10.1016/j.trd.2016.08.005

3.4 USE OF LIME IN ENVIRONMENTAL PROTECTION

3.4.1 USE OF LIME IN DRINKING WATER TREATMENT

3.4.1.1. INTRODUCTION

Lime is used in the treatment of all types of water, both drinking water and wastewater, municipal and industrial, to improve the chemical and/or mineral characteristics and to remove specific pollutants before the water is transferred to a purification plant, discharged into a surface water body or used for domestic and industrial purposes. Main applications in this sector are, but not limited to, the followings:

- softening: hard water is softened by using lime and, if necessary, soda by precipitating the dissolved calcium and magnesium as insoluble calcium carbonate and magnesium hydroxide, respectively;
- pH adjustment: lime is widely used, mainly in the form of milk of lime, in the adjustment of pH especially in larger plants, since it is cheaper than other chemicals such as sodium hydroxide and sodium carbonate. Limestone and dolomite are cheaper but they are seldom used due to: 1) slower reaction rate; 2) fouling phenomena if the water is high in sulphates or humic acids (Metcalf & Eddy Inc., 2013);
- acid neutralisation: lime is a strong base and has a high neutralising capacity for inorganic acids contained in water (sulphuric, hydrochloric, hydrofluoric, nitric, etc.), that will react with lime to form salts;
- metals removal by chemical precipitation in the form of insoluble hydroxides or carbonates, as a function of the pH value (Table 3.4.1.1). Lime and limestone are the most commonly employed precipitant agents due to their availability and low cost. Other advantages include the simplicity of the process, the inexpensive equipment requirement, and the convenient and safe operation (Barakat, 2011);
- removal of fluoride, phosphate, sulphate and nitrogen: the removal of these compounds is based on their precipitation in the form of calcium salts with low solubility. A dedicated explanation for each compound is reported in Table 3.4.1.2, but it is important to note that these are obsolete processes applied to very specific treatment situations;
- alkalinity adjustment: lime is generally added together with iron and aluminium coagulants to avoid depletion of the alkali reserve and keep a neutral pH (the coagulants consume alkalinity and lower the pH). The Ca^{2+} ions can also have a function of coagulant, though with a low efficiency.

In municipal wastewater treatment, lime can perform other tasks, i.e. sanitation of screenings residues, reduction of BOD and COD content in primary sedimentation and mitigation of bulking phenomena.

This chapter is dedicated to the carbonation potential of lime in the softening process. The lime carbonation in the neutralisation of acidic water or during coagulation is dealt in the Chapter 3.2 (use of lime in the biosolids application).

Table 3.4.1.1. Optimum pH range for the precipitation of the various metal ions, with the relative approximate concentration (Carmeuse, 2019).

Type of metal	Optimum precipitation pH	Approximate concentration at optimum pH (mg/l)
Fe^{3+}	7-8.5	< 0.3
Al^{3+}	5.5-8	< 0.03
Cr^{3+}	9.5	0.3
Cu^{2+}/Cu^{3+}	7.5	0.07
Fe^{2+}	> 10	High
Pb^{2+}	10-10.3	0.03
Ni^{2+}	9.8-10.2	0.1
Cd^{2+}	10.5	0.1
Zn^{2+}	10.5-11.0	0.01
Mn^{2+}	9.5	< 0.01

Table 3.4.1.2. Indications about the use of lime for the removal of fluoride and nutrients from water.

Compound	Indications
Fluoride	Generally, lime is used as a calcium source that reduces fluoride concentration down to 10-20 mg/L. Adsorption then follows as a simple, robust, low cost post-treatment to decrease the level of fluoride ions below the discharge limits (Melidis, 2015)
Phosphate	At a pH higher than 10, at ambient temperature, calcium ions react with phosphate to precipitate as hydroxylapatite ($Ca_{10}(PO_4)_6(OH)_2$. The reaction takes place after the reaction of lime with the natural alkalinity of water (softening process) and so the dosage of the reactant depends on the initial water alkalinity. Levels of 2-3 mg/L can be reached, but the effluent must be re-carbonated before the biological treatment or before the discharge into the receiving water body (Metcalf & Eddy Inc., 2013)
Nitrogen	In an ammonia stripping treatment, lime is generally added to wastewater until pH reaches 10.8-11.5, converting ammonium hydroxide ions to ammonia gas ($NH_4^+ + OH^- \rightarrow H_2O + NH_3$). The method is used for the treatment of highly concentrated wastewaters such as landfill leachate, supernatants from anaerobic digestion or specific flows of the petrochemical industry. The treatment, however, releases ammonia in the air, with potential odour and toxicity issues (Capodaglio et al., 2015)

Details about the softening process of water

The water softening process, patented by Professor Thomas Clark in 1841, aims to reduce raw water hardness, alkalinity, and silica to avoid undesirable effects of scaling. The water is treated with lime or a combination of lime and soda ash. These chemicals react with the hardness and alkalinity in the water to form insoluble compounds that precipitate and are removed by sedimentation and, usually, filtration.

Lime will remove the temporary hardness (hardness that may be reduced in concentration simply by heating), i.e. calcium and magnesium bicarbonates. According to the chemistry of the process (Al-Mutaz, 1999), slaked lime reacts with dissolved carbon dioxide at first and the reaction is completed at a pH equal to 8.3 [Reaction 3.4.1.1]. Then, the carbonate hardness caused by calcium and magnesium bicarbonates is precipitated as calcium carbonate [Reaction 3.4.1.2] and magnesium hydroxide. As regards magnesium, magnesium bicarbonate is firstly converted to magnesium carbonate at a pH of 9.4 [Reaction 3.4.1.3]. Since magnesium

carbonate is soluble, an excess of lime (usually 1.25 meq/L) can optionally be added to convert it into $Mg(OH)_2$, at a pH greater than 9, generally equal to 10.6 [Reaction 3.4.1.4].

$$Ca(OH)_2 + CO_2 \rightarrow CaCO_3\downarrow + H_2O \quad [3.4.1.1]$$

$$Ca(OH)_2 + Ca(HCO_3)_2 \rightarrow 2CaCO_3\downarrow + 2H_2O \quad [3.4.1.2]$$

$$Ca(OH)_2 + Mg(HCO_3)_2 \rightarrow MgCO_3 + CaCO_3\downarrow + 2H_2O \quad [3.4.1.3]$$

$$MgCO_3 + Ca(OH)_2 \rightarrow CaCO_3\downarrow + Mg(OH)_2\downarrow \quad [3.4.1.4]$$

The overall amount of lime required (meq/L) is calculated as: CO_2 (meq/L) + carbonate hardness (meq/L) + magnesium ion (meq/L) + excess of lime (generally 1.25 meq/L).

When the removal of the permanent hardness (noncarbonated hardness caused by magnesium sulphate and chloride) is also desired, the soda-lime process is used [Reactions 3.4.1.5-3.4.1.8].

$$MgCl_2 + Ca(OH)_2 \rightarrow Mg(OH)_2\downarrow + CaCl_2 \quad [3.4.1.5]$$

$$CaCl_2 + Na_2CO_3 \rightarrow CaCO_3\downarrow + 2NaCl \quad [3.4.1.6]$$

$$MgSO_4 + Ca(OH)_2 \rightarrow Mg(OH)_2\downarrow + CaSO_4 \quad [3.4.1.7]$$

$$CaSO_4 + Na_2CO_3 \rightarrow CaCO_3\downarrow + Na_2SO_4 \quad [3.4.1.8]$$

The process can be performed at ambient temperature (cold lime treatment) or at a temperature between 49-60°C (warm lime softening), because the solubility of calcium and magnesium is reduced by increasing temperature. The warm process is generally used to prepare the feed to a demineralization system. In this case, the ionic loading on the demineralizer is reduced and thus its capital and operating costs.

When a very good silica reduction is necessary, the hot softening process (108-116°C) can be applied. The silica reduction is performed through its adsorption on the magnesium hydroxide. If the fed water does not contain enough Mg to reduce silica to the desired level, dolime can be added without any increase of the concentration of dissolved solids. This scheme of treatment requires CO_2 gas stripping.

Predicted analyses of a typical raw water treated by various lime and lime-soda softening processes are presented in Table 3.4.1.3. It can be noticed that it is not possible to remove all the hardness from the water because of the little solubility of calcium carbonate and magnesium hydroxide. In order to accelerate the process, coagulants and flocculating agents can be added. An alternative is adding inert fine particles in water, such as sand or previously precipitated $CaCO_3$ so that they can act as nucleation centers and hence reduce drastically the reaction time. A good example in this regard is the pellet reactor (van Dijk and Wilms, 1991), which consists of a large cylindrical vessel (Figure 3.4.1.1), partially filled with a suitable seed material, generally filter sand. Water is fed from the bottom, at such a velocity (50-120 m/h) that the sand bed is fluidized. Milk of lime is also added and is mixed with the incoming water due to the turbulence caused by the water injection. Calcium carbonate precipitates on the sand particles, while softened water flows outward from the top. The larger and heavier pellets accumulate at the base of the reactor where they can be periodically removed and replaced.

Table 3.4.1.3. Typical characteristics of raw water and effluents from a lime or lime-soda softening process (Suez Water Technology & Solutions, 2019).

Parameter	Raw water	Lime softening (cold)	Lime-soda softening (cold)	Lime-soda softening (hot)
Total hardness (as $CaCO_3$) ppm	250	145	81	20
Ca hardness (as $CaCO_3$) ppm	150	85	35	15
Mg hardness (as $CaCO_3$) ppm	100	60	46	5
SiO_2 (as SiO_2) ppm	20	19	18	1-2
pH	7.5	10.3	10.6	10.5

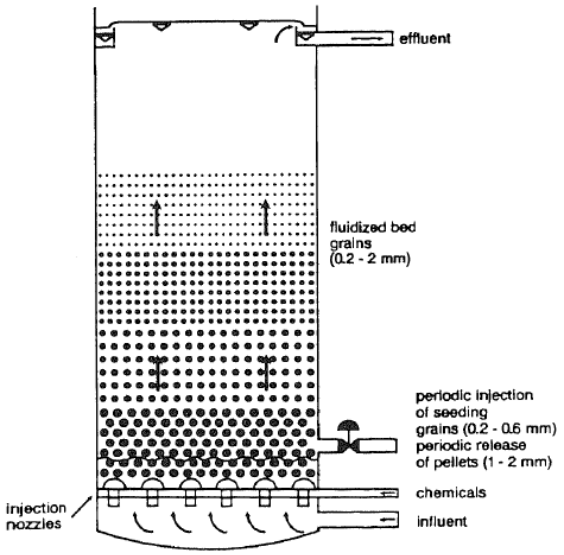


Figure 3.4.1.1. Basics of pellet reactor for lime softening (adapted from van Dijk and Wilms, 1991).

This process generates a residue that is a dense, stable and biologically inert material with a high pH, typically greater 10.5, due to the high alkalinity. This sludge settles to a solids content ranging from 2% to 15% and the Ca:Mg ratio is indicative of its ability to thicken and dewater. When this ratio is equal to five or higher, a solid content of 50-60% can be reached by dewatering; on the contrary, a high presence of magnesium (Ca:Mg < 2) leads to difficulties in handling and dewatering (Wiley, 1981/EPA, 2011).

Lime sludge is typically disposed in surface lagoons, landfilled or used to fill borrow pits and strip mines area. In recent years, possible ways of reuse have been studied. One promising application is to use the material as a Ca-rich soil conditioner in agriculture. According to Van Leeuwen et al. (2011), other feasible routes include the recovery of sludge in the cement production, in the wet or dry scrubbing for SOx control in power plants, in the wastewater neutralization and as filling material for road construction mixed with fly ash. Moreover, Korchuganova et al. (2018) investigated the possibility to use the sludge for the production of calcium nitrate

for industrial purposes, after its purification from iron and organic matter residues (according to the quality standards, the iron content in the product should be lower than 0.05%).

3.4.1.2. LITERATURE ASSESSMENT FOR THE USE OF LIME IN THE WATER SOFTENING PROCESS: MATERIALS AND METHOD

To the authors' knowledge, the scientific literature on lime carbonation in the softening process is almost absent. Most of the scientific literature focuses on the technology (description and related improvements like for example in van Dijk and Wilms, 1991) and on the process sludge (characteristics and ways of recovery alternative to the disposal). The only document dealing with lime carbonation is the work of Scholz et al. (1997), which reports balances of mass, energy, and carbon dioxide for different lime applications (exhaust gases desulphurization, use for building materials, and water softening). The article from Scholz et al. considers all CO_2 emissions (from process and fuel consumption) in its calculations. For the purpose of this literature review, the carbonation data were calculated for the process emissions only. The BREF document related to the common wastewater and waste gas treatment/management systems was also consulted, but no significant information was derived.

3.4.1.3. NATURAL CARBONATION OF LIME IN THE SOFTENING PROCESS

Scholz et al. (1997) reported the specific balance for the softening process, according to the following hypotheses: 1) use of lime only and not of lime-soda; 2) presence of calcium bicarbonate only, in terms of temporary hardness. Under these assumptions, authors assumed a 100% carbonation rate of the hydrated lime, according to Reaction [3.4.1.2]:

$$\mathbf{Ca(OH)_2} + \mathbf{Ca(HCO_3)_2} \rightarrow 2CaCO_3\downarrow + 2H_2O \qquad [3.4.1.2]$$

In particular, 1 mole of lime is used for the treatment of 1 mole of $Ca(HCO_3)_2$, indirectly uptaking the mole of carbon dioxide from the atmosphere used in the process of formation of hardness [Reactions 3.4.1.9 and 3.4.1.10].

$$\mathbf{CO_2}\ (\text{from air}) + H_2O \rightarrow H_2CO_3\ (\text{carbonic acid}) \qquad [3.4.1.9]$$

$$H_2CO_3\ (\text{carbonic acid}) + CaCO_3\ (\text{from rocks erosion}) \rightarrow \mathbf{Ca(HCO_3)_2} \qquad [3.4.1.10]$$

The complete carbonation of lime during the treatment is indirectly confirmed by Wiley (1981). The author says that "*the presence of CaO or $Ca(OH)_2$ in the sludge is an indication of poor slaking or dissolving of the lime and this is problematic due to the increase of the reagent costs, the increase of the sludge quantity, and the problems of its dewaterability. In this situation, corrective actions should be undertaken to eliminate these*

problems", implying that with better handling the CaO or $Ca(OH)_2$ is normally absent and therefore fully carbonated.

According to these indications, it can be assumed that under ideal conditions the amount of CO_2 emitted during the production of lime from limestone is all reabsorbed during softening process.

REFERENCES

Al-Mutaz, I.S. and Al-Yousef S.O.A., 1999. *Lime recovery from Riyadh Water Treatment Plants*. Proceedings of the 4th Gulf Water Conference, Bahrain, February, 13-18, 1999. Available online: https://www.researchgate.net/publication/278620957_Lime_Recovery_from_Riyadh_Water_Treatment_Plants

Barakat, M.A., 2011. *New trends in removing heavy metals from industrial wastewater*. Arabian Journal of Chemistry, 4(4), 361-377. DOI: https://doi.org/10.1016/j.arabjc.2010.07.019

Capodaglio, A.G., Hlavínek, P., Raboni, M., 2015. *Physico-chemical technologies for nitrogen removal from wastewaters: a review*. Ambiente & Água 10(3), 481-498. DOI: 10.4136/ambi-agua.1618

Carmeuse, 2019. *The use of lime in water treatment*. http://www.carmeuse.com/waste-water-treatment

EPA - Unites States Environmental Protection Agency, 2011. *Drinking water treatment plant residuals management technical report. Summary of residuals generation, treatment, and disposal at large community water systems*. September 2011, EPA 820-R-11-003

European Commission, Joint Research Centre, 2016. Best available techniques (BAT) reference document for common wastewater and waste gas treatment/management systems in the chemical sector. JRC science for policy report. Available online:
https://eippcb.jrc.ec.europa.eu/reference/BREF/CWW_Bref_2016_published.pdf

Korchuganova, O., Afonina, I., Prygorodov, P., Mokhonko, V., Kanarova, K., 2018. *Utilization of lime-softening sludge to obtain calcium nitrate*. Eastern-European Journal of Enterprise Technologies, 4(94), 46-53. DOI: 10.15587/1729-4061.2018.141007

Melidis, P., 2015. *Fluoride removal from aluminium finishing wastewater by hydroxyapatite*. Environmental Processes, 2(1), 205-213. DOI: https://doi.org/10.1007/s40710-014-0056-0

Metcalf & Eddy Inc., 2013. *Wastewater Engineering: treatment and resource recovery*. Edited by McGraw-Hill Education, Fifth edition, pages 1498-1502. ISBN: 9780073401188

Scholz, R., Jeschar, R., Jennes, R., Fuchs, W., 1997. *Umweltgesichtspunkte bei der Herstellung und Anwendung von Kalkprodukten, Teil 3*. Zement, Kalk, Gips International, 50(11), 632-644. Available online: https://www.tib.eu/de/suchen/id/tema%3ATEMAU98030018586/Umweltgesichtspunkte-bei-der-Herstellung-und-Anwendung/

Suez Water Technologies & Solutions, 2019. *Handbook of Industrial Water Treatment., Chapter 7: precipitation softening.* Available online: https://www.suezwatertechnologies.com/handbook/handbook-industrial-water-treatment

van Dijk, J.C. and Wilms, D.A., 1991. *Water treatment without waste material - fundamentals and state of the art of pellet softening*. J Water SRT - Aqua, 40(5): 263-280.

Van Leeuwen, J., White, D.J., Baker, R.J., Jones, C., 2011. *Reuse of water treatment residuals from lime softening, Part I: Applications for the reuse of lime sludge from water softening*. Land Contamination & Reclamation, 18(4), 393-415. DOI: 10.2462/09670513.1012

Wiley, 1981. *Lime softening sludge treatment and disposal*. American Water Works Association, 73(11), 600-608. Preview available online: https://www.jstor.org/stable/41270613?seq=1#page_scan_tab_contents

3.4.2 USE OF LIME IN WASTEWATER TREATMENT PLANT - BIOSOLIDS AND INDUSTRIAL SLUDGE APPLICATIONS

This chapter is related to the use of lime in the treatment of biosolids and industrial sludge i.e., dredging sediments and mining sludge from acid mine drainage.

3.4.2.1 TREATMENT OF BIOSOLIDS

Introduction

Sewage sludge is defined as any solid, semisolid or liquid organic residue from the municipal wastewater treatment. Over 10 million tons of Dry Matter (DM) are annually generated in the European countries and the total production is expected to increase in the following years, due to the constant rise in the number of households connected to sewers and to the increasingly stringent quality standards (Lyberatos et al., 2011; European Commission, 2019). Sewage sludges are also defined as biosolids, including some animal by-products that can be treated in the same way. Due to the chemical-physical processes involved in the wastewater treatment, biosolids tend to concentrate heavy metals, poorly biodegradable trace organic compounds as well as potentially pathogenic organisms. On the other hand, biosolids are also rich in nutrients such as nitrogen and phosphorous and contain organic matter that is useful when soils are depleted or subject to erosion (European Commission, 2019).

Lime is widely used in the treatment of biosolids with the following goals: 1) biosolids conditioning to improve their dehydration efficiency; 2) sanitation against pathogenic agents that can be harmful for the human health and the environment; 3) reduction of odours and of insects attraction; 4) increment of the total solids content and concurrent reduction of the ratio between volatile solids and total solids; 5) precipitation of some heavy metals in the biosolids, thereby reducing their solubility and mobility. Depending on the process, lime can be added in the form of hydrated lime or in the form of quicklime. The treatment can be performed either before or after the sludge dewatering unit. Pre-treatment is typically part of a sludge conditioning before dehydration (Metcalf & Eddy, 2013).

The biosolids treatment with lime generally originates a product suitable to be used in the agriculture as organic soil conditioner, with liming and also fertilising properties. Regarding the liming effects, Willet et al. (1986) verified that the calcium carbonate in the sludge increases the soil pH more effectively than agricultural lime, probably because of the finer particle size. After the application of lime-treated sludge, a yield improvement is obtained with a higher intake of CO_2 by plants and crops.

Literature assessment about the use of lime in biosolids treatment: material and methods

The literature review about the CO_2 sequestration from the lime treatment of biosolids was based on:

- papers published in the scientific literature by the federal association of the German lime industry;
- a report published by the French agency of the environment and energy management (ADEME) related to the characteristics (amount, quality, and agronomic value) of limed biosolids from wastewater treatment plants in France;

- the proceedings of the workshop on "Problems about sludge", organized by the Joint Research Centre (Stresa, Italy, 1999);
- two books on wastewater treatment.

The BREF document on common wastewater and waste gas treatment was also consulted, but no additional information was derived. The complete list of documents is reported in Table 3.4.2.1.

Table 3.4.2.1. List of the documents considered in the review about the use of lime in biosolids treatment.

Scientific papers
Neuschäfer et al., 1991. *Deponierfähigkeit von Klärschlämmen - Erfordernisse an die Vor - und Nachbehandlung der Schlämme* (Landfill capacity of sewage sludge. Requirements of pre and post-treatment of sludge). Abwassertechnik, Heft 2, S33-36. Available online: https://www.kalk.de/service/publikationen/fachpublikationen/klaerschlamm/
Bever et al., 1989. *Mineralogische und chemische Untersuchen an Klärschlamm-Kalk-und Klärschlamm-Kalk-Ton Mischungen* (Mineralogical and chemical analysis of limed sewage sludge and of limed sewage sludge and clay mixtures). Abwassertechnik, Heft 3, S31-35. Available online: https://www.kalk.de/service/publikationen/fachpublikationen/klaerschlamm/
Witte et al., 2000. *Senkung des Schlammindex durch gezielte Steuerung der Kalkdosierung am Biespiel der Kläranlage Wathlingen* (Reduction of the sludge index through control of the lime dosage at the wastewater treatment plant in Wathlingen). Wasser und Abfall, Heft 1-2, S52-57
Reports and workshop proceedings
ADEME, 2001. *Les boues chaulées des stations d'épuration municipales - production, qualité et valuer agronomique* (Limed sludge from municipal wastewater treatment plants - production, quality and agronomic value). ISBN: 9782868175601
Andreadakis, 2000. *Workshop on problems around sludge - Session 1: sludge treatments and their effects on pathogens; Treatment and disinfection of sludge using quicklime*. 18-19 November 1999, Stresa, Italy. Available online: https://ec.europa.eu/environment/archives/waste/sludge/problems.htm
Books
Bonomo, 2008. *Trattamenti delle acque reflue* (wastewater treatment). Edited by McGraw-Hill Education, pages 536-537 and 584-585. **ISBN:** 9788838665189
Metcalf & Eddy|AECOM, 2013. *Wastewater Engineering: treatment and resource recovery*. Edited by McGraw-Hill Education, Fifth edition, pages 1498-1502. ISBN: 9780073401188
BREF document
Joint Research Centre, 2016. *Best Available Techniques (BAT) Reference Document for common wastewater and waste gas treatment/management systems in the chemical sector*.

Literature assessment for the use of lime in biosolids: involved chemical reactions

The addition of lime to biosolids involves a series of chemical reactions that modify their final chemical composition. The main reactions, simplified for illustrative purposes, are indicated from Reaction [3.4.2.1] to [3.4.2.3] (Neuschäfer et al., 1991/Metcalf & Eddy, 2013).

$$CaO + H_2O \rightarrow Ca(OH)_2$$

Carbon dioxide: $Ca(OH)_2 + 2CO_2 \rightarrow Ca(HCO_3)_2$ [3.4.2.1]

$$Ca(OH)_2 + Ca(HCO_3)_2 \rightarrow 2CaCO_3 + 2H_2O$$

Phosphorus: $3Ca(OH)_2 + 2\ MePO_4 \rightarrow Ca_3(PO_4)_2 + 2Me(OH)_3$ [3.4.2.2]

Fats: $Fat + Ca(OH)_2 \rightarrow$ glycerol + fatty acids [3.4.2.3]

As shown in the Reaction [3.4.2.1], a part of the dosed lime reacts with the CO_2 generated from the biological activity in the biosolids or with the atmospheric CO_2. Generally, the reaction with the atmospheric CO_2 is minimized by the plant operators with proper biosolids storage (low surface area and low temperatures; Andreadakis, 2000). The following sections report the main collected data about the typical lime dosage and its carbonation rate in the treated biosolids for both a pre and post-stabilization.

Literature assessment about the use of lime in biosolids: pre-treatment

The treatment of biosolids with lime before a dewatering unit is generally applied for combining the sludge stabilisation and conditioning. Although lime has only slight dehydration effects on colloids, it is commonly used in conjunction with ferric iron salts, in order to:

- provide pH control to maintain it in the optimal range for the coagulation and flocculation (the ferric salts react with the bicarbonate alkalinity, thus reducing pH);
- odour reduction and disinfection;
- production of $CaCO_3$ from the Reaction [3.4.2.1] that provides a granular structure to biosolids, thus increasing porosity and reducing compressibility.

Lime can be used either in the form of hydrated lime or as burnt lime. When using burnt lime, the reagent is generally slurried with water prior to adding it to biosolids or can be used in powdered form when the lime has delayed reactivity properties (Hanzl et al., 2010). The lime conditioning is typically performed before a screw press or a pressure-type filter press, while it is less used with centrifuges because in some cases there are problems of abrasive wear and scaling problems. In case of a milk-of-lime dosage, the typical dosage in terms of $Ca(OH)_2$ ranges from 15% on the DM (11% CaO equivalent) for raw primary biosolids to 30% on the DM (23% CaO equivalent) for activated sludge (ADEME, 2001/Bonomo, 2008/Metcalf & Eddy, 2013). For example, the report of ADEME (2001) indicates an average dosage of 29% on the DM for hydrated lime (22% CaO equivalent), as a result of 44 analyses in French wastewater treatment plants (Table 3.4.2.2). If a powder product based on a delayed reactivity of lime is used, the total lime consumption can be reduced up to 30%, with a reduction of the total sludge volume, a saving of iron chloride (between 10-30%), and an increase of the filtering efficiency by up to 25% (Hanzl et al., 2010).

Table 3.4.2.2. Lime average dosage, final content of DM, and final pH for biosolids conditioned with lime (ADEME, 2001).

Process	Number of analyses	Average dosage of lime (% on the dry matter)	Final dry matter (%)	Final pH
Conditioning	44	29 ± 13 as $Ca(OH)_2$	34 ± 6	11.5

Regarding the carbonation potential of lime, Neuschäfer et al. (1991) reported the results of three analyses on biosolids samples previously subjected to a conditioning process with ferric chloride and burnt lime followed by dehydration (Figure 3.4.2.1). The total content of lime in the treated biosolids resulted 28.5% on the average, expressed as CaO on the dry biosolids. About 49% of the total lime (13.9% of the dry biosolids) was bound in

the form of calcium carbonate according to the Reaction [3.4.2.1], 33% of the total lime (9.4% on the DM of biosolids) resulted precipitated as calcium phosphate (Reaction [3.4.2.2]), while the remaining 18% of the total lime (5% of the dry sludge) resulted still free or in minor amount "*bound (unknown)*". According to these data, the calculated CO_2 uptake from lime is about 110 g/kg dry biosolids (385 g/kg of used CaO). The study does not indicate the period of time elapsed between the lime dosage and the performed analyses.

Also Bever et al. (1989) evaluated the carbonation process of lime added to biosolids in a conditioning step followed by dehydration. Periodical analyses on biosolids were performed from the moment of lime dosage up to 1.5 years, by simulating the landfill disposal[19] through a semi-technical scale model at the University Bundeswehr in Munich. Over the time, a progressive increase of the lime chemically bound as $CaCO_3$ was observed (from 10.5% CaO on the DM at the beginning up to 16.9% after 1.5 years), with a contextual reduction of the soluble lime (from 14.6% CaO on the dry weight at the beginning up to 6.9% after 1.5 years; Table 3.4.2.3).

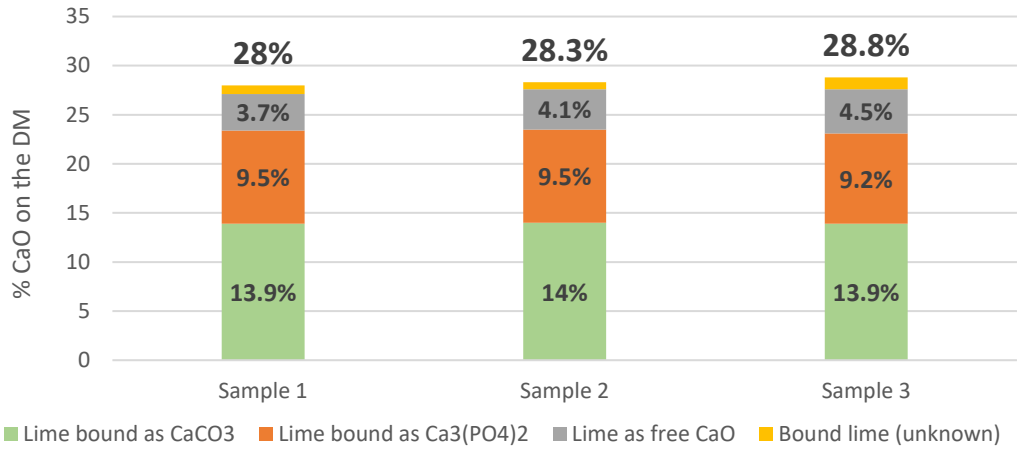


Figure 3.4.2.1. Total amount of lime and relative chemical repartitioning in samples of biosolids after a ferric chloride-burnt lime conditioning followed by dehydration (elaboration from Neuschäfer et al., 1991).

Table 3.4.2.3. Evolution of the CaO "bound as $CaCO_3$" content and "soluble CaO" content in biosolids conditioned with $FeCl_3$ and $Ca(OH)_2$, dehydrated with a chamber filter press, and disposed in landifill (elaboration from Bever et al., 1989).

Process	Just after the treatment	1 month	3 months	1 year	1.5 years
CaO bound as $CaCO_3$ (% on DM)	10.5	11.1	11.3	12.9	16.2
Soluble CaO (% on DM)	14.6	12.1	9.4	6.9	6.9
Sum (% on DM)	25.1	23.2	20.7	19.8	23.1
% of CaO converted to $CaCO_3$	42%	48%	55%	65%	70%

[19] Please note that the simulation of the landfill disposal is beyond the boundaries of this study mainly focused on the use phase. Most important indications and results of the document are reported anyway.

Literature assessment about the use of lime in biosolids: post-treatment

In the post-treatment process (at the end of the sludge treatment line), lime is added to increase the pH value up to 12 or higher, with the benefits exposed in the introduction Section. In this case, quicklime (CaO) is generally used, to take benefits from pH, temperature increase and chemical binding of the water by CaO hydration. Quicklime and sludge are mixed in a pugmill, a paddle mixer, or a screw conveyor. An adequate mixing is very important to ensure the contact between the reagent and the smaller particles of biosolids, thus avoiding pockets of putrescible material.

In this treatment, a CaO dosage of 20-40% on the DM is recommended to assure a stable pH at 12.5 for a period over 3 months (Andreadakis, 2000/Bonomo, 2008/Metcalf & Eddy, 2013). For example, the report by ADEME (2001) indicates an average burnt lime dosage of 21% on the DM after a dehydration process with centrifuges (34 case studies) and of 33% after a dehydration process with belt filter presses (69 case studies; see Table 3.4.2.4). A lower dose implies a certain microbial activity, the production of CO_2 and a consequent drop of the pH in all the material within a few weeks.

Table 3.4.2.4. Lime dosage, final content of dry matter and final pH of biosolids after a post-stabilisation (ADEME, 2001).

Process	Number of analyses	Average dosage of lime (% on the dry sludge)	Final dry matter (%)	Final pH
Stabilisation after a centrifuge	34	21 ± 8 as CaO	27± 5	12
Stabilisation after a belt filter press	69	33 ± 21 as CaO	26± 5	12

Witte et al. (2000) deeply analysed the post stabilisation of biosolids with lime in the wastewater treatment plant of Wathlingen, Lower Saxony (Figure 3.4.2.2 reports the relative process layout). The surplus sludge produced from the clarifier after the biological treatment is destined to a centrifugation process and then mixed with burnt lime. In the year 1997, the use of hydrated lime in the aerobic reactor of nitrification was implemented, in order to improve the characteristics of the recirculated activated sludge and of the surplus sludge.

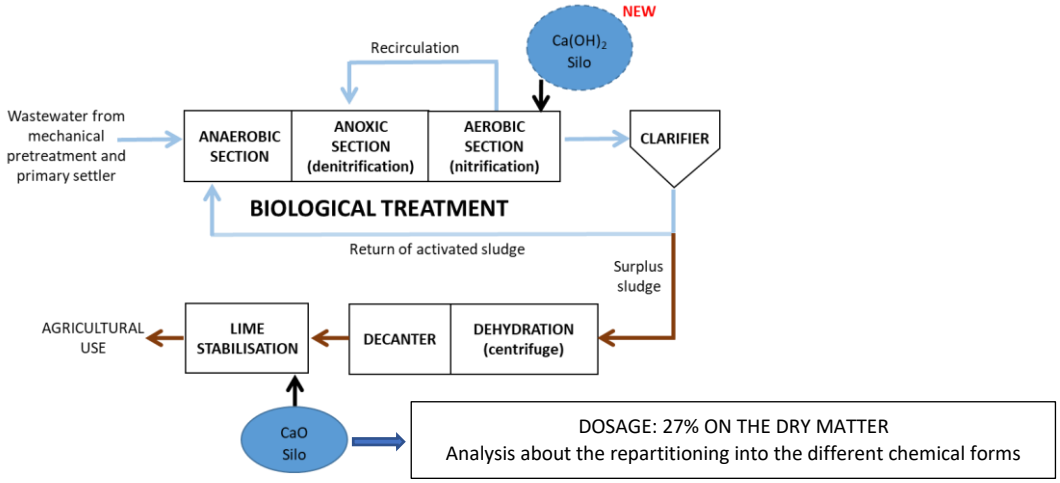


Figure 3.4.2.2. Flow diagram of the wastewater treatment plant in Wathlingen, with a focus on the biological section (elaboration from Witte et al., 2000)**.**

Among the different experimental tests performed to optimize the plant configuration, an analysis on the chemical partitioning of the dosed CaO in the lime stabilisation process is reported (Table 3.4.2.5). The total added CaO corresponds to 26.7% of the dry sludge. About 43% of this lime (11.6% on the DM of biosolids) was converted to calcium carbonate according to the Reaction [3.4.2.1], 36% of the input lime (9.6% on the DM) was bound as calcium silicate, while the remaining 21% of the input lime (5.5% on the DM) resulted still free. According to these data, the calculated CO_2 uptake from lime is about 91 g/kg dry biosolids (340 g/kg of dosed CaO). No indication about the period of time elapsed between the lime dosage and the performed analysis is given in the document.

Table 3.4.2.5. Chemical partitioning of the CaO dosed in the post-stabilisation process of the surplus sludge in the wastewater treatment plant of Wathlingen (elaboration from Witte et al., 2000).

	% CaO on the DM of biosolids
Lime bound as $CaCO_3$	11.6%
Lime bound as calcium silicate	9.6%
Lime - free CaO	5.5%
Total amount of CaO	26.7%

Always in relation to a post-stabilisation treatment, Bever et al. (1989) have studied the evolution of the carbonation process of CaO added to biosolids after a dehydration step with belt filter press. Periodical analyses were performed from the moment of the dosage up to 1.5 years, by simulating the landfill disposal through a semi-technical scale model at the University Bundeswehr in Munich. Over the time, a progressive increase of the lime chemically bound as $CaCO_3$ was observed (from 7.4% on the dry weight at the beginning up to 13.4% after 1.5 years), with a contextual reduction of the soluble lime (from 26.4% on the dry weight at the beginning up to 19.7% after 1.5 years; Table 3.4.2.6).

Table 3.4.2.6. Evolution of the content of CaO "bound as $CaCO_3$" and "soluble CaO" in biosolids treated with burnt lime after a dehydration process with belt filter press (elaboration from Bever et al., 1989).

Process	Just after the treatment	1 month	3 months	1 year	1.5 years
CaO bound as $CaCO_3$ (% on DM)	7.4	9.0	11.2	12.7	13.4
Soluble CaO (% on DM)	26.4	25.2	19.8	19.1	19.7
Sum (% on DM)	33.8	34.2	31.0	31.8	33.1
% of CaO converted to $CaCO_3$	22%	26%	36%	40%	40%

Conclusions and future research need

Based on the very few data reported in the previous sections, a certain amount of the CO_2 derived from the biological activity or from the atmosphere effectively reacts with the lime dosed during a pre or post-stabilisation process of biosolids. In particular, a CO_2 uptake of 340-385 kg CO_2 per 1 tonne of lime was derived, corresponding to 43-49% of the CO_2 emitted during the calcination process in lime production (the production of 1 tonne of lime releases in the atmosphere 786 kg of CO_2, excluding the energy consumption).

However, this range of CO_2 uptake can be only considered a preliminary indication and it is not representative of the current European context. This is because it derives only from two literature sources, related to analyses performed about 30 years ago, in wastewater treatment plants of one country (Germany).

For this reason, authors suggest to carry out some more analyses on biosolids samples in different time intervals after the lime dosage in order to assess the amount of CO_2 that can be actually sequestered by this material and to better understand the time evolution of the carbonation process in ambient conditions (preliminary indications from the existing literature reveal a progressive increment of the carbonation process in the time). In these analyses, the influence of the final destination of the material (i.e., landfill, incineration or agricultural use) should be also investigated.

REFERENCES

ADEME, 2001. *Les boues chaulées des stations d'épuration municipales - production, qualité et valuer agronomique* (Limed sludge from municipal wastewater treatment plants - production, quality and agronomic value). ISBN: 9782868175601

Andreadakis, A.D., 2000. *Workshop on problems around sludge - Session 1: sludge treatments and their effects on pathogens; Treatment and disinfection of sludge using quicklime*. 18-19 November 1999, Stresa, Italy. Available online: https://ec.europa.eu/environment/archives/waste/sludge/problems.htm

Bever, J., Peschen, N., Retzlaff, C., 1989. *Mineralogische und chemische Untersuchen an Klärschlamm-Kalk-und Klärschlamm-Kalk-Ton Mischungen* (Mineralogical and chemical analysis of limed sewage sludge and of limed sewage sludge and clay mixtures). Abwassertechnik, Heft 3, S31-35. Available online:

https://www.kalk.de/service/publikationen/fachpublikationen/klaerschlamm/

Bonomo, L., 2008. *Trattamenti delle acque reflue* (wastewater treatment). Editor McGraw-Hill Education, 536-537 and 584-585. **ISBN:** 9788838665189

European Commission, 2019. Website: https://ec.europa.eu/environment/waste/sludge/

Hanzl, P., Ponchon, F., Van Meyel, J.P., 2010. *Sludge treatment with delayed reactivity lime-effective solution for new EU member States*. Conference Proceeding of the 2th European Conference on Sludge Management, Budapest, 9-10 September 2010

Joint Research Centre - Brinkmann, T., Santonja, G.G., Yükseler, H., Roudier, S., Sancho, L.D., 2016. *Best Available Techniques (BAT) Reference Document for common waste water and waste gas treatment/management systems in the chemical sector*. *Industrial Emissions Directive 2010/75/EU*. DOI: 10.2791/37535

Lyberatos, G., Sklyvaniotis, M., Angelakis, A., 2011. *Sewage biosolids management in EU countries: challenges and prospective*. Fresenius Environmental Bulletin 20(9), 2489-2495. Available online: https://www.researchgate.net/publication/236274617_Sewage_biosolids_management_in_EU_countries_Challenges_and_prospective

Metcalf & Eddy|AECOM, 2013. Wastewater Engineering: treatment and resource recovery. Edited by McGraw-Hill Education, Fifth edition, pages 1498-1502. ISBN: 9780073401188

Neuschäfer, Peschen, Schmidit, 1991. *Deponierfähigkeit von Klärschlämmen - Erfordernisse an die Vor - und Nachbehandlung der Schlämme* (Landfill capacity of sewage sludge. Requirements of pre and post-treatment of sludge). Abwassertechnik, Heft 2, S33-36. Available online:

https://www.kalk.de/service/publikationen/fachpublikationen/klaerschlamm/

Willet, I.R., Jakobsen, P., Malafant, K.W.J., 1986. *Fertilizer and liming value of lime-treated sewage sludge*. Fertilizer Research 8(3), 313-328. DOI: https://doi.org/10.1007/BF01048634

Witte, H., Strunkheide, J., Priebe, L., 2000. *Senkung des Schlammindex durch gezielte Steuerung der Kalkdosierung am Biespiel der Kläranlage Wathlingen* (Reduction of the sludge index through control of the lime dosage at the wastewater treatment plant in Wathlingen). Wasser und Abfall, Heft 1-2, S52-57

3.4.3 USE OF LIME IN SLUDGE TREATMENT - DREDGING SEDIMENTS TREATMENTS

Introduction

The handling and management of dredged sediments is an important environmental issue. In Europe, about 200 million cubic meters of sediments are dredged annually, over half of which are contaminated and expensive to dispose of (PIANC, 2010; Table 3.4.3.1). The dredged materials can range from very fine sediments to sands and gravels. The fine sediments are generally associated to high water content, low shear strength, high compressibility and the presence of organic contaminants (e.g., PAHs, PBCs, TBT) and heavy metals in particular lead, chromium, zinc, mercury, cadmium, and copper (Agostini et al., 2007/Makusa, 2015).

Table 3.4.3.1 Average annual production of dredged sediments in the European countries (million cubic meters).

Country	Sea	Inland	Sum
Belgium/Flanders	5	9.2	14.2
Denmark	4.5		4.5
France	50	6	56
Germany	41	5	46
Italy	4		4
Netherlands	19	9	28
Portugal	4		4
Spain	8.5		8.5
Sweden	1.4	0.1	1.5
UK	30	0.7	30.7

Until the early 90's, sea dumping, disposal in a proper landfill and capping were the most common practices of sediments management. However, the dumping ban, the high taxes associated to land disposal, the scarcity of landfills, and the constant demand for dredging operations have increased the attention to beneficial uses of fine sediments in the civil engineering sector after a proper treatment (i.e., thermal treatment, bio-remediation, stabilisation and solidification by hydraulic binders, and washing; Zuliani et al., 2016/Amar et al., 2018).

The Stabilization/Solidification (S/S) treatment is defined as a reclamation technology that involves mixing sediments with pozzolanic binders, typically lime, Portland cement, and fly ash. This technology converts contaminants (especially heavy metals) into less soluble, mobile or toxic forms (stabilisation step) and entraps the waste into a monolithic solid structure (solidification). Lime can be used alone or in a mixture with cement or other binders, generally in percentage ranging from 2-10% by dry weight (Federico et al., 2015). Just as an example, Russo et al. (2015) successfully experimented a lime stabilisation process on marine sediments (3% of quicklime on the dry weight), for their reuse as construction material for docks. Similarly, Yoobanpot et al. (2018) investigated the reuse of sediments as pavement material after a stabilisation process, indicating 6% of hydrated lime by dry weight as the optimal content of the binder.

Literature assessment about the use of lime in the treatment of sediments

To the authors' knowledge, very little information about the use of lime and its carbonation potential in the S/S treatment of sediments is available in the scientific literature. The complete list of consulted documents is reported in Table 3.4.3.2.

Table 3.4.3.2. List of the documents considered in the review about the use of lime in the S/S treatment.

Scientific papers
Du et al., 2016. *Effect of carbonation on leachability, strength and microstructural characteristics of KMP binder stabilized Zn and Pb contaminated soils*. Chemosphere 144, 1033-1042. DOI: https://doi.org/10.1016/j.chemosphere.2015.09.082
Firoozi et al., 2017. *Fundamentals of soil stabilisation*. International Journal of Geo-Engineering 8 (26), 1-16. DOI: https://doi.org/10.1186/s40703-017-0064-9
Guha et al., 2006. *Leaching of mercury from carbonated and non-carbonated cement-solidified dredged sediment*s. Soil and Sediment Contamination 15 (6), 621-635. DOI: 10.1080/15320380600959131
Haas et al., 2018. *Soil improvement with quicklime - long-time behaviour and carbonation*. Road Materials and Pavement Design. DOI: https://doi.org/10.1080/14680629.2018.1474793
Jawad et al., 2014. *Soil stabilization using lime: advantages, disadvantages and proposing potential alternative*. Research Journal of Applied Sciences, Engineering and Technology 8(4), 510-520. DOI: 10.19026/rjaset.8.1000
Tarabadkar, 2009. *Accelerated carbonation of contaminated sediments and its application*. Master of Science in Civil Engineering, University of New Hampshire. https://pdfs.semanticscholar.org/5940/89c1f70063f906b3a0aaea24e94112b49f5d.pdf?_ga=2.245001221.1867771113.1565794463-1586852716.1565794463
Meeting Proceedings
Eades et al., 1962. *Formation of new minerals with lime stabilization as proven by field experiments in Virginia*. In: Lime Stabilization mix design, properties, and process, 41st annual meeting of Highway Research Board, 8-12 January 1962. Available online: http://onlinepubs.trb.org/Onlinepubs/hrbbulletin/335/335.pdf
Website
Carmeuse website: http://www.carmeuse-waterandwaste.com/application-solutions/sediment-treatment-reuse

Potential carbonation rate of lime in the traditional S/S treatment of sediments

In a S/S treatment with lime used as hydraulic binder, two types of reactions between lime and sediments happen: 1) short-term reactions, occurring in a few hours or days, i.e., hydration, cation exchange, and flocculation/agglomeration; 2) long-term pozzolanic reaction (several months or years). The drying of the wet material and the increase in its workability is attributed to the immediate reactions, whereas the increase in strength and durability is associated with the long-term treatment.

At the beginning, if quicklime is used, it immediately hydrates and releases heat. Sediments are thus dried, both because water participates in the hydration reaction and because the heat generated can evaporate additional moisture. The produced hydrated lime dissociates into Ca^{2+} and OH^- and reacts with clay particles, causing additional drying due to the reduction of the moisture holding capacity. If hydrated lime is used instead of quicklime, drying occurs only through the reduction of the water holding capacity. After the initial mixing, the calcium ions (Ca^{2+}) from the binder migrate to the surface of the clay particles and displace bound water and other cations. As a consequence, sediments become friable, granular, easier to work, and compact. Moreover, the plasticity index decreases, as does the tendency to swell and shrink. This process, which is

called “flocculation and agglomeration,” generally occurs in a matter of hours. In this period, also the carbonation reaction can occur between part of the free lime and CO_2.

Over the time, the pH of the mixture increases, causing the reduction in solubility of heavy metals. When the pH value exceeds 12.4, silica and alumina bound to the minerals become soluble and react with the calcium ions from the lime to form Calcium-Silicate-Hydrates (CSH) and Calcium-Aluminate-Hydrates (CAH), cementitious products similar to those formed in the Portland cement (Reactions [3.4.3.1] and [3.4.3.2]).

$$Ca^{2+} + 2(OH)^- + SiO_2 \text{ (soluble)} \rightarrow CSH \quad [3.4.3.1]$$

$$Ca^{2+} + 2(OH)^- + Al_2O_3 \text{ (soluble)} \rightarrow CAH \quad [3.4.3.2]$$

In this way, the mixture is transformed from a sandy, granular material to a hard, relatively impermeable layer with a significant load bearing capacity (Jawad et al., 2014/Firoozi et al., 2017/Carmeuse, 2019).

To the authors’ knowledge, a quantitative evaluation about the carbonation potential of the lime used in a S/S treatment of sediments is not available at the moment. However, some preliminary indications can be derived from the same treatment applied to soils, keeping in mind that the main differences in terms of composition (i.e., content of water and organic matter) and of natural ambient (freshwater, marine water or air) may lead to a slightly different behaviour in the carbonation process.

Two scientific researchers were dedicated to experimentally verify the formation of calcium carbonate as a new mineral in a solidified lime-soil mixture and to quantify its amount in the long-term period (Table 3.4.3.3). In detail, Haas and Ritter (2018) examined samples of an embankment of silty soil treated with CaO in occasion of the construction of a motorway in Germany. After 34 years, 37% of the input quicklime was converted to $CaCO_3$ due to the carbonation reaction. Also an earlier research performed by Eades et al. (1962) has assessed the presence of calcium carbonate in soil samples previously treated with hydrated lime: about 35% of the input lime was carbonated after 3 years.

Table 3.4.3.3. Summary of the literature papers related to the carbonation potential of lime in a traditional S/S treatment of soil.

Reference	Haas and Ritter (2018)	Eades et al. (1962)
Type of work	Experimental assessment at the full scale	Experimental assessment at the full scale
Goal and scope	Analysis on an embankment in southeast Germany. The embankment was built in 1979 from excavated silty soil during the construction of the motorway A3 Regensburg-Passau. The soil was treated with quicklime (2.5% w/w) to improve the earthwork structure and to give long-term stability	In the years 1956-1957 subgrade soils on three projects in Virginia were stabilized with hydrated lime. The projects, located approximately 150 miles apart, were constructed on three different soil types. The three projects were sampled during 1960 in order to study the effects of the addition of the hydrated lime
Main results	Samples were tested using methods for compressive strength and chemical analysis. After 34 years, the results showed compressive strengths up to 6 MPa, with 37% of the quicklime being used in carbonation and 47% in pozzolanic reactions. 16% of the CaO is still free	- after 3 years, the X-ray diffraction analysis revealed the formation of new minerals, i.e. calcium silicate-hydrates and calcium carbonate - samples treated with 5% lime contained about 2.5% of calcium carbonate

Potential carbonation rate of lime in the S/S treatment under accelerated carbonation

Heavy metals may interfere with the hydration reaction of cement in a S/S treatment of sediments. To overcome this problem, a variation of the traditional S/S technology based on the accelerated carbonation has been recently tested in the scientific literature. The supply of a CO_2-rich gas during the mixing process with the binder can activate the reaction of unhydrated cement, increases the early strength of the mixture, neutralizes its alkaline nature (the pH generally falls by three units, from 11 to 8), reduces the solubility of certain heavy metals, and improves the mechanical characteristics.

The new technique has been successfully experimented also for the treatment of sediments (e.g, Guha et al., 2004/ Tarabadkar, 2009), using Portland cement as a binder, alone or mixed with lime and powdered activated carbon.

According to Du et al. (2016), the carbonation reaction mainly involves the conversion of the major hydration products, ie., portlandite ($Ca(OH)_2$) and Calcium Silicate Hydrate to calcium carbonate as expressed in the Reactions [3.4.3.3-4]. In addition, long-term attack by carbonic acid can decompose the C–S–H gels into calcium carbonate, acid-insoluble silica gel and water (Reaction [3.4.3.5]).

$$Ca^{2+} + 2(OH)^- + 2CO_2\ (aq) \rightarrow CaCO_3 + H_2O \qquad [3.4.3.3]$$

$$x\ CaO \cdot SiO_2 \cdot nH_2O \rightarrow (x\text{-}y)\ CaO \cdot SiO_2 \cdot nH_2O + y\ Ca(OH)_2 \qquad [3.4.3.4]$$

$$CSH + HCO_3^- \rightarrow CaCO_3 + SiO_2\ (gel) + H_2O \qquad [3.4.3.5]$$

A detailed quantification of the CO_2 uptake by a solidification/stabilisation process under accelerated carbonation has been performed for the Portland cement used alone as binder. Tarabadkar (2009) studied the application of the S/S treatment to a mixture of mildly contaminated sediments (65%) from the tidal estuary of the Great Bay (New Hampshire), of Portland Cement (25%), and water (10%). Under these conditions, an effective CO_2 uptake of 5.2% (expressed on the total weight of the mixture) was measured. This value corresponds to about 27% of the theoretical CO_2 uptake (18.99%). In relation to the combination of PC and lime instead, Guha et al. (2004) assessed that an increasing dose of lime in the mixture results in higher CO_2 uptake, probably due to more availability of portlandite for carbonation (Table 3.4.3.4). However, a comparison of the carbonation index between the use of PC alone or in combination with lime is not reported.

Table 3.4.3.4. Mixture composition for the treatment of S/S under accelerated carbonation of Medway estuarine sediments and related carbonation index (elaboration from Guha et al., 2004).

	Sample A	**Sample B**
Composition of the mixture (w/w)	Lime: 5%	Lime: 10%
	PC: 10%	PC: 10%
	Moisture: 38%	Moisture: 35%
	Sediment: 47%	Sediment: 45%
Carbonation index espressed as: % $CaCO_3$ (carbonated sample) - $CaCO_3$ (non-carbonated sample)	2.4%	4.2%

Conclusions and future research needs

The literature review about the use of lime in the solidification/stabilisation treatment of sediments does not allow to assess the carbonation potential in the traditional process and in the new treatment based on accelerated carbonation. Research on this topic should be thus promoted.

REFERENCES

Agostini, F., Skoczylas, F., Lafhaj, Z., 2007. *About a possible valorisation in cementitious materials of polluted sediments after treatment*. Cement and Concrete Composites 29(4), 270-278. DOI: https://doi.org/10.1016/j.cemconcomp.2006.11.012

Amar, M., Benzerzour, M., Safhi, A.E.M., Abriak, N.E., 2018. *Durability of a cementitious matrix based on treated sediments.* Cases studies in Construction Materials 8, 258-276. DOI: https://doi.org/10.1016/j.cscm.2018.01.007

Bertos, M.F., Simons, S.J.R., Hills, C.D., Carey, P.J, 2004. *A review of accelerated carbonation technology in the treatment of cement-based materials and sequestration of CO_2*. Journal of Hazardous Material 112(3), 193-205. DOI: 10.1016/j.jhazmat.2004.04.019

Chen, Q., Ke, Y., Zhang, L., Tyrer, M., Hills, C.D., Xue, G., 2009. *Application of accelerated carbonation with a combination of Na_2CO_3 and CO_2 in cement-based solidification/stabilization of heavy metal-bearing sediment*. Journal of Hazardous Materials, 166(1), 421-427. DOI: https://doi.org/10.1016/j.jhazmat.2008.11.067

Du, Y-J., Wei M-L., Reddy, K.R., Wu H-L., 2016. *Effect of carbonation on leachability, strength and microstructural characteristics of KMP binder stabilized Zn and Pb contaminated soils*. Chemosphere 144, 1033-1042. DOI: https://doi.org/10.1016/j.chemosphere.2015.09.082

Eades, J.L., Nichols Jr, F.P., Grim, R.E., 1962. *Formation of new minerals with lime stabilization as proven by field experiments in Virginia*. In: Lime Stabilization mix design, properties, and process, 41st annual meeting of Highway Research Board, 8-12 January 1962. Available online: http://onlinepubs.trb.org/Onlinepubs/hrbbulletin/335/335.pdf

Federico, A., Vitone, C., Murianni, A., 2015. *On the mechanical behaviour of dredged submarine clayey sediments stabilized with lime or cement*. Canadian Geotechnical Journal, 52(12), 2030-2040. DOI: https://doi.org/10.1139/cgj-2015-0086

Firoozi, A.A., Olgun, G.C., Firoozi, A.A., Baghini, M.S, 2017. *Fundamentals of soil stabilisation*. International Journal of Geo-Engineering 8 (26), 1-16. DOI: https://doi.org/10.1186/s40703-017-0064-9

Guha, B., Hills, C.D., Carey, P.J., MacLeod, C.L., 2006. *Leaching of mercury from carbonated and non-carbonated cement-solidified dredged sediments*. Soil and Sediment Contamination 15(6), 621-635. DOI: 10.1080/15320380600959131

Haas, S. and Ritter. H.J., 2018. *Soil improvement with quicklime - long-time behaviour and carbonation*. Road Materials and Pavement Design. DOI: https://doi.org/10.1080/14680629.2018.1474793

Jawad, I.T., Taha, M.R., Majeed, Z.H., Khan, T.A., 2014. Soil stabilization using lime: advantages, disadvantages and proposing potential alternative. Research Journal of Applied Sciences, Engineering and Technology 8(4), 510-520. DOI: 10.19026/rjaset.8.1000

Makusa, G.P., 2015. *Stabilization-Solidification of High Water Content Dredged Sediments. Strength, Compressibility and Durability Evaluations.* Doctoral Thesis, Division of Mining and Geotechnical Engineering, Luleå University of Technology, Sweden. Available online: https://www.diva-portal.org/smash/get/diva2:990295/FULLTEXT01.pdf

PIANC, 2010. *Dredging and the Environment - international guidance for best practice*. PIANC 125th Anniversary Celebration in ASIA, Nayoga JAPAN, 12-14 September 2010. Oral presentation available online: http://pianc-jp.org/en/news/images/II-1%20Mr.%20Kothe%20%28Presentation%29.pdf

Russo, G., Deneele, D., Croce, P., Modoni, G., 2015. *Lime treatment procedures for the reuse of dredged marine sediments*. Coastal and Maritime Mediterranean Conference, Edition 3, Ferrara, Italia, 177-182. DOI: 10.5150/cmcm.2015.035

Tarabadkar, K., 2009. *Accelerated carbonation of contaminated sediments and its application*. Master of Science in Civil Engineering, University of New Hampshire. Available online: https://pdfs.semanticscholar.org/5940/89c1f70063f906b3a0aaea24e94112b49f5d.pdf?_ga=2.245001221.1867771113.1565794463-1586852716.1565794463

Yoobanpot, N., Pitthaya, J., Krissakorn, K., Pornkasem, J., Suksun, H., 2018. Reuse of dredged sediments as pavement materials by cement dust and lime treatment. Geomechanics and Engineering 15(4), 1005-1016. DOI: https://doi.org/10.12989/gae.2018.15.4.1005

Zuliani, T., Mladenovič, A., Ščančar, J., Milačič, R., 2016. *Chemical characterisation of dredged sediments in relation to their potential use in civil engineering*. Environmental Monitoring and Assessment, 188 (234), 1-12. DOI: https://doi.org/10.1007/s10661-016-5239-x

3.4.4 USE OF LIME IN THE FLUE GAS CLEANING SYSTEMS

3.4.4.1. INTRODUCTION

Flue gas generated from combustion plants, in particular coal-fired power plants and waste incineration facilities contain significant amount of acid gases (HCl, SOx, HF). The raw gas at the outlet of the combustion chamber of municipal solid waste (MSW) incinerators contains a range of 300-2000 mg/m_n^3 of HCl and 200-1000 mg/m_n^3 of SO_2 (Zhang et al., 2019; Antonioni et al., 2014; Quina et al., 2011), whereas up to 600-6500 mg/m_n^3 of SO_2 are usually found in the flue gas of coal-fired power plants (Nygaard et al., 2004; Chang et al., 2003; EU, 2017), depending on the sulphur and chlorine content in the waste and in the coal.

Acid gases removal can be performed by using different alkaline agents, such as lime, limestone, soda or sodium bicarbonate.

A preliminary abatement of the acid gases can be performed directly inside the furnace, by adding sorbents directly in the combustion chamber. This is a very common practice in coal power plants and in solid waste incinerators equipped with a fluidised bed combustor, but it can be performed also in grate furnaces. The main alkaline reagents used in this case are limestone, dolomia or hydrated lime (EU, 2018). This technique alone is not sufficient to meet the required SO_2 and HCl emission limits; however, it is a useful pre-treatment to decrease the concentration of acid gases in the raw gas and, thus, the subsequent use of sorbents along the flue gas treatment line.

In the flue gas cleaning (FGC) system, the removal of the acid gases can be performed in a wet, dry or semi-dry way (EU, 2017; EU, 2018):

- wet processes: the flue gas is put in contact with water or a water solution containing an alkaline agent, such as NaOH or a micronized limestone slurry. NaOH is mainly used in waste incineration, whereas limestone is largely used for the flue gas desulphurization (FGD) in coal power plants, where it represents 82% of the installed wet FGD capacity worldwide (Benko and Mizsey, 2007). Eventually, milk of lime can be used in substitution of limestone (EU, 2018). Usually the process is carried out in two steps: in the first one, HCl and HF are removed by using only water at a very acidic pH. In the second step, SO_2 is removed at a pH close to neutrality or slightly alkaline, thanks to the injection of NaOH or limestone in the water solution. In coal power plants, where the main acid gas is SO_2 and limestone is usually used for its neutralization, the residue consists in calcium sulphate (gypsum), which is usually recovered and sold, in order to reduce the overall operating costs of the plant;
- semi-dry processes: the sorption agent is added to the flue gas flow in an aqueous solution or suspension, typically as milk of lime or as a lime slurry solution. The water will evaporate inside the flue gas, and then the reaction products are dry and are separated in a conventional dedusting unit, typically a fabric filter;
- dry processes: the dry sorption agent, hydrated lime or sodium bicarbonate, is injected in the flue gas flow as a very fine powder. The reaction products are dry and are separated in the downstream dedusting stage.

The aim of this study is to quantify the potential CO_2 uptake associated with the use of lime in FGC systems. Therefore, the evaluation focuses on the dry and semi-dry neutralization processes that use lime or milk of lime, as usually happens in waste incineration plants. On the contrary, limestone or soda are the preferred neutralization agents in wet systems.

Focusing on lime as neutralization agent, the main chemical reactions involved in the removal of the acid gases are reported from Reaction [3.4.4.1] to Reaction [3.4.4.6] (Chin et al., 2005a):

$Ca(OH)_2 + 2HCl(g) \rightarrow CaCl_2 + 2H_2O(g)$ [3.4.4.1]

$Ca(OH)_2 + HCl(g) \rightarrow Ca(OH)Cl + H_2O(g)$ [3.4.4.2]

$Ca(OH)_2 + SO_2(g) \rightarrow CaSO_3*1/2H_2O + 1/2H_2O(g)$ [3.4.4.3]

$Ca(OH)_2 + SO_2(g) + 1/2O_2 \rightarrow CaSO_4 + H_2O(g)$ [3.4.4.4]

$CaSO_3*1/2H_2O + 1/2O_2(g) + 3/2H_2O(g) \rightarrow CaSO_4 + 1/2H_2O$ [3.4.4.5]

$CaSO_3*1/2H_2O + 2HCl(g) \rightarrow CaCl_2 + SO_2(g) + 3/2H_2O(g)$ [3.4.4.6]

where:

- Reaction [3.4.4.2] has a stronger tendency to occur in full-scale application compared to Reaction [3.4.4.1] (Chin et al., 2005a);
- for what concerns SO_2, in the presence of excess O_2 or H_2O, $CaSO_4$ can be formed either directly ([3.4.4.4]) or with $CaSO_3*1/2H_2O$ as an intermediate ([3.4.4.5]);
- $CaSO_3*1/2H_2O$ can, then, react with HCl to form $CaCl_2$, as reported in Reaction [3.4.4.6].

Lime can also react with CO_2 in the flue gas (usually in concentration of 10-12% vol.), following reaction [3.4.4.7]. However, the $CaCO_3$ that is formed can subsequently react with HCl and SO_2, releasing back the CO_2 previously sequestered (Reactions [3.4.4.8] - [3.4.4.10]) (Chin et al., 2005a; Ho et al., 1996; Tan et al., 2014).

$Ca(OH)_2 + CO_2(g) \rightarrow CaCO_3 + H_2O(g)$ [3.4.4.7]

$CaCO_3 + HCl(g) \rightarrow Ca(OH)Cl + CO_2(g)$ [3.4.4.8]

$CaCO_3 + 2HCl(g) \rightarrow CaCl_2 + CO_2(g) + H_2O(g)$ [3.4.4.9]

$CaCO_3 + SO_2(g) + 1/2O_2(g) \rightarrow CaSO_4 + CO_2(g)$ [3.4.4.10]

The thermodynamic and the kinetic of these reactions suggest that the lime used for acid gas neutralization can actually sequester some CO_2. However, the quantification of this uptake is difficult. A detailed analysis is reported in Chapter 3.4.4.3.

Usually a large excess of sorbent is used compared to the stoichiometric amount for neutralization, due to the short contact time between the sorbent and the pollutant gas, typically in the range of a few seconds (Chin et al., 2005a), and to the kinetic limits of the reactions. In semi-dry applications, about 7-10 kg of quicklime per

tonne of waste are used, corresponding to a stoichiometric ratio of 1.4-2.5; whereas in dry application the average feeding of hydrated lime is 10-20 kg/t waste in terms of CaO equivalent, corresponding to a stoichiometric ratio of 1.5-2.5 (EU, 2018).

Lime conversion rate is usually very modest. In dry and semi dry neutralization processes, the conversion rate can be as low as 10% (Chin et al., 2005a; Ho et al., 1999; Tan et al., 2014). The low value is due to the phenomenon of pore-clogging in lime particles where the formation of a layer of product on the surface of the sorbent acts as a barrier for further reaction (Yan et al., 2003; Stein et al., 2002). As a results, the solid residues generated by the process, which are often separated from the flue gas together with the fly ash generated by the combustion process and take the name of air pollution control residues (APCR), contain high amount of free lime available for carbonation (Jiang et al., 2013; Costa et al., 2007).

Accelerated carbonation of these residues has been largely proposed as a technology to improve their chemical stability and their leaching behaviour, before their final disposal or recycling (Costa et al., 2007). APCR are, in fact, enriched of micro-pollutants that are transferred from the flue gas to the solid residues during combustion. This phenomenon is amplified when activated carbon is injected together with lime in the neutralization process. Furthermore, accelerated carbonation of these residues allows for a contextual CO_2 sequestration and, for this reason, it is considered more interesting than other treatment technologies, such as solidification and/or chemical stabilization (Costa et al., 2007). Another interesting aspect is the fact that these residues are generated directly at a CO_2 point source emission. Thus, the incineration flue gases can be directly used for carbonation, with the aim of capturing their content of CO_2 (Costa et al., 2007; Jiang et al., 2013).

Carbonation of APCR can also occur naturally, as a result of weathering processes that occur during their temporary storage, utilization or final disposal when they come in contact with the atmospheric CO_2 (Jiang et al., 2013). However, this process is usually slow and only becomes significant over the long-term (Jiang et al., 2013). For this reason, natural carbonation of APCR is not considered of any interest by the scientific community, which has focused on the accelerated process.

3.4.4.2. LITERATURE ASSESSMENT ON THE USE OF LIME IN FGC SYSTEMS: MATERIALS AND METHODS

The literature review carried out to assess the amount of CO_2 that can be sequestered when lime is used for acid gas neutralization was based on 22 papers published in scientific journals, one website, one conference presentation available online and the BREF documents for large combustion plants and for waste incineration (Figure 3.4.4.1).

Excluding the BREF documents, 5 sources focus on the kinetic of the acid gases neutralization process and on the influence of the CO_2 in the raw gas on the removal efficiency of SOx and HCl, showing that lime reacts also with CO_2. The other documents focus on accelerated carbonation of APCR at the laboratory scale (14 sources) and at the full-scale (5 sources). No data were found about natural carbonation of APCR.

The list of the analysed documents is reported in Table 3.4.4.1. For the most interesting documents, a summary was prepared (see Annex IV).

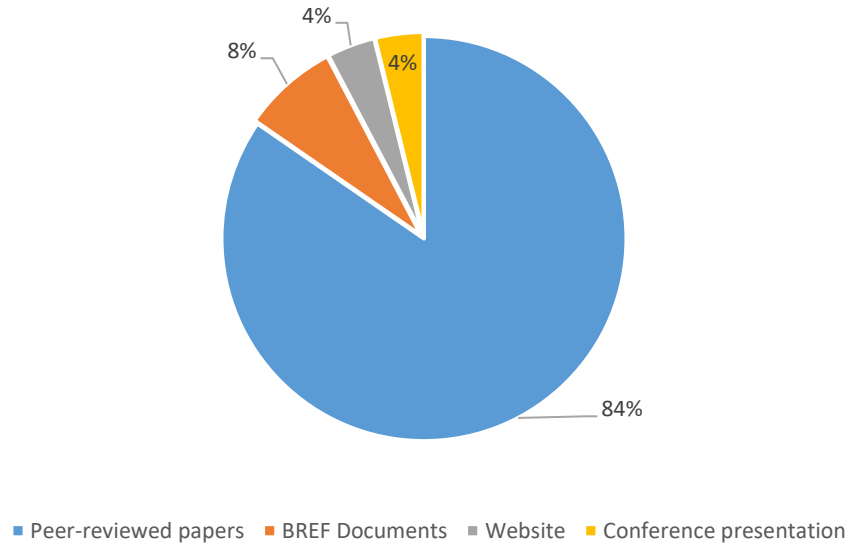


Figure 3.4.4.1. Sources used for the literature assessment on the use of lime in FGC systems.

Table 3.4.4.1. List of the documents considered in the study about the use of lime in FGC system.

Peer reviewed papers
Araizi, et al., 2016. *Enhancement of accelerated carbonation of alkaline waste residues by ultrasound*. Waste Management 50, 121-129.
Baciocchi et al., 2006. *CO_2 sequestration by direct gas-solid carbonation of air pollution control (APC) residues*. Energy Fuels 20(5), 1933-1940
Baciocchi et al.., 2009a. *The effects of accelerated carbonation on CO_2 uptake and metal release from incineration APC residues*. Waste Management 29(12), 2994-3003
Baciocchi et al., 2009b. *Comparison of different reaction routes for carbonation of APC residues*. Energy Procedia 1(1), 4851-4858
Bodénan and Deniard, 2003. *Characterization of flue gas cleaning residues from European solid waste incinerators: assessment of various Ca-based sorbent processes*. Chemosphere 51(5), 335-347
Bogush et al., 2015. *Element composition and mineralogical characterisation of air pollution control residue from UK energy-from-waste facilities*. Waste Management 36, 119-129
Cappai et al., 2012. *Application of accelerated carbonation on MSW combustion APC residues for metal immobilization and CO_2 sequestration*. Journal of Hazardous Materials 207-208, 159-164
Chin et al., 2005a. *Study of the reaction of lime with HCl under simulated flue gas conditions using X-ray diffraction characterization and thermodynamic prediction*. Ind. Eng. Chem. Res. 44(23), 8730-8738
Chin et al., 2005b. *Hydrated lime reaction with HCl under simulated flue gas conditions*. Ind. Eng. Chem. Res. 44(10), 3742-3748
De Boom and Degrez., 2012. *Belgian MSWI fly ashes and APC residues: a characterisation study*. Waste Management 32(6), 1163-1170
Ecke et al., 2002. *Treatment-oriented characterization of dry scrubber residue from municipal solid waste incineration*. Journal of Material Cycles and Waste Management 4(2), 117-126
Fernández Bertos et al., 2004. *Investigation of accelerated carbonation for the stabilisation of MSW incinerator ashes and the sequestration of CO_2*. Green Chemistry 6, 428-436
Gunning et al., 2009. *Production of lightweight aggregate from industrial waste and carbon dioxide*. Waste Management 29(10), 2722-2728
Gunning et al., 2013. *Commercial application of accelerated carbonation: Looking back at the first year 2013*. Conference Proceedings of ACEME, 2013, 185-192

Gunning and Hills, 2014. *Carbon negative: first commercial application of accelerated carbonation technology*. 7th International Scientific Conference: Science and Higher Education in Function of Sustainable Development, 3-4 October 2014, Uzice, Serbia

Ho et al., 1996. *Influence of CO_2 and O_2 on the reaction of $Ca(OH)_2$ under spray-drying flue gas desulfurization conditions*. Ind. Eng. Chem. Res. 35(11), 3915-3919

Jiang et al., 2013. *Influence of SO_2 in incineration flue gas on the sequestration of CO_2 by municipal solid waste incinerator fly ash*. Journal of Environmental Sciences 25(4), 735-740

Karlsson et al., 1981. *Adsorption of hydrochloric acid on solid slaked lime for flue gas clean up*. Journal of the Air Pollution Control Association 31(11), 1177-1180

Li et al., 2007. *Accelerated carbonation of municipal solid waste incineration fly ashes*. Waste Management 27(9), 1200-1206

Prigiobbe et al., 2009. *Gas-solid carbonation kinetics of air pollution control residues for CO_2 storage*. Chemical Engineering Journal 148(2-3), 270-278

Sun et al., 2008. *Kinetic study of accelerated carbonation of municipal solid waste incinerator air pollution control residues for sequestration of flue gas CO_2*. Energy & Environmental Science 1(3), 370-377

Tan et al., 2014. *Laboratory study on high-temperature adsorption of HCl by dry-injection of $Ca(OH)_2$ in a dual-layer granular bed filter*. Frontiers of Environmental Science & Engineering 8(6), 863-870

BREF documents

EU, 2017. *Best Available Techniques (BAT) Reference Document for Large Combustion Plants*

EU, 2018. *Best Available Techniques (BAT) Reference Document for Waste Incineration*

Website

O.C.O Technology Ldt, 2019. Company website: https://oco.co.uk/about-us/

Conference presentation

Carey, 2018. *Developing an innovative and profitable process that combines waste CO_2 and thermal residues, to create a carbon negative aggregate for construction and lock CO_2 in for good within our built environment*. Available online: http://nas-sites.org/dels/files/2018/02/1-5-CAREY-Carbon8-Systems-NAS.pdf

3.4.4.3. POTENTIAL CO_2 SEQUESTRATION IN THE FLUE GAS CLEANING SYSTEMS

Flue gases from waste incineration and coal combustion contain about 10-12% of CO_2 that can interfere with the neutralization reactions between lime and the acid gases (HCl and SOx). The influence of CO_2 on the lime conversion rate has been studied by several authors at a laboratory scale, under controlled conditions (Karlsson et al., 1981; Ho et al., 1996; Chin et al., 2005a and 2005b; Tan et al., 2014). Different ranges of temperature and gas composition have been investigated, as reported in Table 3.4.4.2. However, the results are quite similar.

Table 3.4.4.2. Influence of the CO_2 concentration on the acid gas neutralization efficiency in waste incineration and coal power plants: operating conditions of the tests reported in the analysed literature.

Reference	Investigated process	Operating conditions of the test
Karlsson et al., 1981	Dry adsorption of HCl, in a fixed bed reactor	Composition of the synthetic gas: CO_2 concentration = 0-8% HCl concentration = 630 ppm SO_2 concentration = 0 ppm O_2 concentration = 0% Relative humidity = 0-10% T = 150-400°C Time frame = 600-1200 min
Ho et al., 1996	Dry flue gas desulfurization process	Composition of the synthetic gas: CO_2 concentration = 3.2-12.6% SO_2 concentration = 1000 ppm HCl concentration = 0 ppm O_2 concentration = 0-5.4% Relative humidity = 50-70% T = 60-70°C Time frame = 60 min
Chin et al., 2005a Chin et al., 2005b	Dry neutralization process	Composition of the synthetic gas: CO_2 concentration = 10% HCl concentration = 540 ppm SO_2 concentration = 1000 ppm O_2 concentration = 9% Relative humidity = 10% T = 200°C Time frame = 800 min
Tan et al., 2014	High temperature dry adsorption of HCl in a granular bed filter	Composition of the synthetic gas: CO_2 concentration = 10% HCl concentration = 1000 ppm SO_2 concentration = 0 ppm O_2 concentration = 10% Relative humidity = unknown T = 500-700°C Time frame = 120 min

Lime reacts simultaneously with SO_2, HCl and CO_2 to form $CaCO_3$, Ca(OH)Cl and $CaSO_3*1/2H_2O$ or $CaSO_4*1/2H_2O$. The process is quite complex, due to the competition among the different species for reacting with lime, or with the neutralisation salts when the unreacted lime core cannot be reached anymore by the gas species. In the first minutes, the presence of CO_2 in the flue gas will increase the lime conversion rate compared to a system where only HCl and SO_2 are present. However, after 10-20 minutes, lime ceases to react due to the formation of an impervious product layer that does not allow the gas diffusion inside the lime particles. At this point, SO_2 and HCl start to react with $CaCO_3$ previously formed, until it is completely converted to $CaSO_3$/$CaSO_4$, Ca(OH)Cl and $CaCl_2$, releasing the CO_2 previously captured. The process can require some hours to complete (Ho et al., 1996; Chin et al., 2005a; Chin et al., 2005b). Although the initial conversion rate of lime is greater in the presence of CO_2, the final value, at the equilibrium conditions, is lower (Ho et al., 1996; Chin et al., 2005b). For example, Tan et al. (2014) report a Ca utilization efficiency of 74.4% without CO_2 and of 36.8% in presence of CO_2, for a molar ratio Ca/Cl of 2.5 and a temperature of 600°C. Chin et al. (2005b) report a Ca conversion of almost 100% when the synthetic gas contains only HCl (at a concentration

of 540 ppm), of about 60% when also SO_2 is present (at a concentration of 1000 ppm) and between 45 and 55% when both SO_2 and CO_2 (at a concentration of 10%) are present. This can be explained by the fact that both $CaCO_3$ and $CaSO_4$ have a higher propensity to cause pore blockage of the lime sorbent compared to Ca(OH)Cl (Chin et al., 2005b). The negative effect of the CO_2 on the Ca conversion rate seems to be higher with increasing operation temperature (Karlsson et al., 1981; Bodenan and Deniard, 2003).

In full scale plants, however, the contact time between the lime and the flue gas is typically of just a few seconds. Thus, what happens in the time interval between 10 min and one hour (typically investigated in the documents of Table 3.4.4.2) is of little interest for the present investigation. Considering the kinetic proposed by Ho et al. (1996) for the carbonation and sulphation process of $Ca(OH)_2$ in the presence of SO_2 and CO_2, which is described by Equations [3.4.4.11] and [3.4.4.12], it is evident that, in the first seconds, the carbonation reaction prevails on the sulphation one. Chin et al. (2005b) report that the HCl reaction rate with $Ca(OH)_2$ is even lower compared to that of SO_2 and CO_2 in the first minutes. This means that, in full-scale plants, lime reacts preferably with CO_2 and only in a second step with SO_2 and HCl.

$$X_c = \frac{1}{k_2}[1 - \exp(-k_1 k_2 t) \quad [3.4.4.11]$$

$$X_s = \frac{1}{k_2} * ln\,(1 + k_1 k_2 t) \quad [3.4.4.12]$$

where Xc and Xs are the molar fractions of $CaCO_3$ and $CaSO_3$*1/2H_2O in the sample and k_1 and k_2 are the kinetic constants.

The amount of CO_2 that reacts with lime in the FGC systems can be estimated from the content of inorganic carbon (i.e., the carbon in the form of carbonate or bicarbonate) found in the APCR.

Inorganic carbon in fresh APCR can have three origins:

a) from the CO_2 in the incineration flue gas that reacts with the injected lime, as previously described;
b) from the CO_2 in the atmosphere that reacts with the Ca compounds in the APCR after their sampling (only if the APCR are not opportunely stored before analyses in order to isolate them from the atmosphere);
c) from the inorganic carbon in the incinerated waste (if the fly ashes generated by the combustion process are not separated in a previous filtration step).

Considering that the inorganic carbon in MSW mainly derives from the presence of stones or inert materials, and it is usually very modest, and that only about 0.1% of the total carbon in the waste is transferred to the APCR (Belevi and Moench, 2000), we can assume that contribution c) is negligible. Natural carbonation of APCR is a long process, thus contribution b) can be also considered negligible. As suggested by Bodenan and Deniard (2003), the content of inorganic carbon in APCR is, therefore, an indication of the amount of CO_2 that is trapped by lime in the FGC system.

From the data in Table 3.4.4.3, we can thus assume that about 84 gCO_2 are trapped in 1 kg of APCR, as a consequence of the lime carbonation process taking place in the flue gas treatment line.

Table 3.4.4.3. Content of inorganic carbon in APCR (elaboration of the data reported in Bodenan and Deniard, 2003; Fernandez-Bertos et al., 2004; Baciocchi et al., 2006; Baciocchi et al., 2009a).

Type of flue gas control system	Inorganic carbon (%)
Single filtration unit	2.0 [1.2-5.5] *Data from 11 tests*
Double filtration unit	3.0 [1.3-3.8] *Data from 5 tests*
Average[20]	2.3

3.4.4.4. CO_2 SEQUESTRATION BY APCR

APCR composition

The major elements found in APCR are Ca, Cl, Si, Al, Na, K, S, Mg, Fe, and O. Their composition is strictly dependent on the sorbent used in the neutralization process, whether it is lime or sodium bicarbonate. Considering only lime-derived APCR, Ca and Cl compounds constitute up to 75-95% w/w APCR (Costa et al., 2007). The average content of Ca and its mineralogy speciation is reported in Table 3.4.4.4. Data are reported separately for plants having a single or a double filtration step, in order to assess if the Ca content is different when the residues contain or not the fly ash[21]. The statistical analysis[22] of the data suggest that there is not a significant difference between the two types of residues for what concerns their Ca content. Thus, the average content of Ca compounds in APCR can be assumed equal to 42.4% on weight expressed in terms equivalent CaO. Calcium is mainly present as free lime (lime and portlandite) or as anhydrite ($CaSO_4$) and CaClOH. The presence of unreacted $Ca(OH)_2$ is due to the excess dosage of sorbent in the flues gas treatment line, because of the low neutralization efficiency as discussed in Chapter 3.4.4.1. It is interesting to notice that regardless of the type of flue gas treatment process (dry, semi-dry or wet), the filtration mode, and the characteristics of the Ca-based sorbent, $Ca(OH)_2$ does not react completely with HCl. Thus, CaClOH is usually found in APCR, whereas $CaCl_2$ is generally not detected (Bodenan and Deniard, 2003).

Some $CaCO_3$, in the form of calcite, vaterite or aragonite (Li et al., 2007; Sun et al., 2008; Bogush et al., 2015) can be present in the APCR, mainly as the result of carbonation processes taking place in the FGC system, where lime can react with the CO_2 in the flue gas, as reported in Chapter 3.4.4.3.

[20] Based on the Kruskal-Wallis tests, the distribution of the content of inorganic carbon in the samples "single filtration unit" and "double filtration unit" is the same. Therefore, the average content of inorganic carbon in APCR can be assumed equal to 2.3% on weight, regardless of the FGC system configuration.

[21] The neutralization products from acid gases removal are usually separated together with the fly ash produced by the combustion process, since most of the incineration plants are equipped with a single filtration unit. When the plant is equipped with two filtration steps, the first one allows for the removal of most of the fly ash, whereas the second step is dedicated to the separation of the neutralization salts and of the residual fly ash.

[22] The non-parametric Kruskal-Wallis test was used due to the non-normal distribution of data and the small number of cases.

Table 3.4.4.4. Chemical composition and mineralogy of APCR (minimum-average-maximum). Elaboration of the data reported in: Baciocchi et al., 2006 and 2009a/Bodénan et al. 2003/Bogush et al., 2015/Cappai et al., 2012/De Boom et al., 2012/Ecke et al., 2002/Fernández et al., 2004/Jiang et al., 2013/Sun et al., 2008.

Type of residues	**Chemical composition**	**Mineralogy**			
	total Ca compounds as CaO (%)	Free lime ($Ca(OH)_2$ + CaO) as CaO (%)	$CaCO_3$ as CaO (%)	$CaSO_4$ as CaO (%)	CaClOH as CaO (%)
Single filtration unit	14.3-41.7-77.0 *25 cases*	10.7-30.6-47.8 *4 cases*	6.0-7.3-10.1 *5 cases*	0-2.1-5.3 *4 cases*	8.8-12.9-16.2 *4 cases*
Double filtration unit	38.8-45.7-54.5 *5 cases*	11.4 *1 case*	7.1-10.4-13.7 *2 cases*	0-1.1-2.2 *2 cases*	11.4-12.9-14.4 2 *cases*
Average	42.4	26.8	8.2	1.8	12.9

Potential carbonation rate in APCR

The presence of Ca reacting compounds, such as $Ca(OH)_2$ and CaClOH, makes APCR a potential CO_2 sequestering material (Baciocchi et al., 2006a,b; Fernández et al., 2004; Li et al., 2007).

The maximum theoretical amount of CO_2 that can be sequestered by APCR as a consequence of their content of Ca can be calculated on the basis of their composition. Assuming a 42.4% average content of Ca compounds (Table 3.4.4.4), the maximum CO_2 sequestration potential results equal to about 333 gCO_2 per kg of APCR.

However, not all the Ca compounds will react with CO_2. The analysis of carbonated APCR reveals that the principal compounds interested by the carbonation reactions are free lime and CaClOH. Several authors report that both free lime and Ca(OH)Cl disappear after carbonation, whereas the content of calcite/vaterite increases, based on the Reactions [7], [13] and [14] (Li et al., 2007; Wang et al., 2010):

$$2CaClOH \rightarrow CaO*CaCl_2 + H_2O \quad [13]$$

$$CaO*CaCl_2 + CO_2 \rightarrow CaCl_2 + CaCO_3 \quad [14]$$

On the contrary, $CaSO_4$ seems not reacting with CO_2, at least in natural conditions. $CaSO_4$ was, in fact, found in 5-years aged APCR sampled from a landfill in Sweden (Ecke et al., 2002). By considering Ca speciation and, thus, assuming a 26.8% average content of free lime and a 12.9% average content of CaCl(OH), as reported in Table 3.4.4.4, the CO_2 sequestration potential results equal to about 261 gCO_2 per kg of APCR.

Accelerated carbonation of APCR

Accelerated carbonation has been proposed by several authors to improve the chemical stability and the leaching behaviour of APCR, before their final disposal or recycling, as well as for CO_2 capture and storage (Baciocchi et al., 2006; Fernández-Bertos, 2004). The interesting aspect of this practice is the possibility to operate directly with the incineration flue gas, capturing CO_2 prior of its emission in the atmosphere (Baciocchi et al., 2009b).

Usually, the direct carbonation route is applied to APCR, because of their high content of soluble Ca (Costa et al., 2007). From a theoretical point of view, two different types of treatment can be performed:

- aqueous carbonation, where water is added to the APCR in order to achieve a liquid/solid ratio (L/S) of about 0.2-0.6. Slurry-phase carbonation (L/S >1) is usually not considered viable, due to the high soluble salts content of APCR (Costa et al., 2007);
- gas-solid carbonation if the process is carried out in dry conditions, without adding water to the APCR.

Currently, most of the experiences reported in the scientific literature refer to experimental assessment at the laboratory scale aimed at evaluating the best conditions of temperature, pressure, liquid/solid (L/S) ratio, size dimension etc. to promote carbonation. An accelerated carbonation process at the industrial scale was recently applied in the United Kingdom by the company Carbon8 Aggregates Limited.

Among the application at the lab-scale, 7 papers report experiences of accelerated carbonation performed in aqueous phase and 5 papers of accelerated carbonation performed in dry phase. Only two papers (Cappai et al., 2012; Araizi et al., 2016) report the results of accelerated carbonation tests performed in wet condition (L/S >1). Table 3.4.4.5 reports a summary of all tests and the relative operating conditions is reported. Due to the broad variety of conditions at which the tests were carried out, they were classified into different groups:

I) accelerated carbonation tests in aqueous phase, at modest or ambient conditions of temperature and pressure, with 100% CO_2 gas ($P \leq 0.3$ MPa and $T \leq 50°C$);

II) accelerated carbonation tests in aqueous phase, at modest or ambient conditions of temperature and pressure, with CO_2 enriched flue gas ($P \leq 0.3$ MPa, $T \leq 80°C$, $CO_2 < 100\%$);

III) accelerated carbonation tests in aqueous phase, at high pressure, with 100% CO_2 gas ($P \geq 1$ MPa and $T \geq 30°C$);

IV) accelerated carbonation tests in wet phase, at ambient conditions of temperature and pressure, with 100% CO_2 gas;

V) accelerated carbonation tests in dry phase, at modest or ambient conditions of temperature and pressure, with 100% CO_2 gas ($P \leq 0.3$ MPa and $T \leq 30°C$);

VI) accelerated carbonation tests in dry phase, at modest or ambient conditions of temperature and pressure, with CO_2 enriched flue gas ($P \leq 0.3$ MPa and $T \leq 30°C$; $CO_2 < 100\%$);

VII) accelerated carbonation tests in dry phase, at high temperature, with 100% CO_2 gas (P= 0.1 MPa & $T \geq 200°C$);

VIII) accelerated carbonation tests in dry phase, at high temperature, with CO_2 enriched flue gas ($P \leq 0.3$ MPa and $T \geq 350°C$; $CO_2 < 100\%$).

On average, aqueous-based experiments are carried out at modest temperature, eventually increasing the pressure at a maximum value of 1 MPa. On the contrary, dry-based experiments are often carried out at high temperature and atmospheric pressure. The duration of the tests is very variable, from a few seconds to some days.

Table 3.4.4.5. Summary of all the data used in the study. All the tests were carried out on APCR sampled from plants equipped with a single filtration unit.

Reference	Particle size	CO_2 uptake (gCO_2/kg APCR)	Operating conditions
		Category I	
Fernández-Bertos et al., 2004	< 212 μm	21.8	Ambient T and P, 100% CO_2, L/S=0.2, 24 h
Araizi et al., 2016	< 295μm	92	Ambient T and P, 100% CO_2, L/S=0.2, 1 h
Araizi et al., 2016	< 295μm	133	Ambient T and P, 100% CO_2, L/S=0.4, 1 h
Araizi et al., 2016	< 295μm	125	Ambient T and P, 100% CO_2, L/S=0.6, 1 h
Araizi et al., 2016	< 295μm	68	Ambient T and P, 100% CO_2, L/S=0.8, 1 h
Baciocchi et., 2009a	10-40 μm	155	30°C, 0.3 MPa, 100% CO_2, L/S=0.02, 4 h
Baciocchi et., 2009a	10-40 μm	229	30°C, 0.3 MPa, 100% CO_2, L/S=0.1, 4 h
Baciocchi et., 2009a	10-40 μm	240	30°C, 0.3 MPa, 100% CO_2, L/S=0.2, 4 h
Baciocchi et., 2009a	10-40 μm	80	30°C, 0.3 MPa, 100% CO_2, L/S=0.02, 1 h
Baciocchi et., 2009a	10-40 μm	240	50°C, 0.3 MPa, 100% CO_2, L/S=0.02, 1 h
Baciocchi et al., 2009b	10-40 μm	250	30°C, 0.3 MPa, 100% CO_2, L/S=0.2, 10 min
Sun et al., 2008	< 300 μm	75	20°C, 0.3 MPa, 100% CO_2, L/S=0.3, 150 min
Li et al., 2007	< 300 μm	90	Ambient T, 0.3 MPa, 100% CO_2, L/S=0.1, 3 h
Li et al., 2007	< 300 μm	110	Ambient T, 0.3 MPa, 100% CO_2, L/S=0.2, 3 h
Li et al., 2007	< 300 μm	110	Ambient T, 0.3 MPa, 100% CO_2, L/S=0.3, 3 h
Li et al., 2007	< 300 μm	100	Ambient T, 0.3 MPa, 100% CO_2, L/S=0.4, 3 h
Li et al., 2007	< 300 μm	75	Ambient T, 0.3 MPa, 100% CO_2, L/S=0.5, 3 h
Li et al., 2007	< 300 μm	40	Ambient T, 0.3 MPa, 100% CO_2, L/S=0.6, 3 h
Li et al., 2007	< 300 μm	30	Ambient T, 0.3 MPa, 100% CO_2, L/S=0.8, 3 h
		Category II	
Ecke et al., 2002	unknown	44.6	Ambient T and P, 25% CO_2, L/S=0.25, 10 days
Sun et al., 2008	< 300 μm	120	20°C, 0.3 MPa, 20% CO_2, L/S=0.3, 150 min
Sun et al., 2008	< 300 μm	100	20°C, 0.3 MPa, 40% CO_2, L/S=0.3, 150 min
Sun et al., 2008	< 300 μm	87	20°C, 0.3 MPa, 60% CO_2, L/S=0.3, 150 min
Sun et al., 2008	< 300 μm	80	20°C, 0.3 MPa, 80% CO_2, L/S=0.3, 150 min
Sun et al., 2008	< 300 μm	108	20°C, 0.3 MPa, 20% CO_2, L/S=0.2, 150 min
Sun et al., 2008	< 300 μm	110	20°C, 0.3 MPa, 20% CO_2, L/S=0.4, 150 min
Sun et al., 2008	< 300 μm	90	20°C, 0.3 MPa, 20% CO_2, L/S=0.5, 150 min
Sun et al., 2008	< 300 μm	90	10°C, 0.3 MPa, 20% CO_2, L/S=0.3, 150 min
Sun et al., 2008	< 300 μm	120	30°C, 0.3 MPa, 20% CO_2, L/S=0.3, 150 min
Sun et al., 2008	< 300 μm	118	40°C, 0.3 MPa, 20% CO_2, L/S=0.3, 150 min
Sun et al., 2008	< 300 μm	70	80°C, 0.3 MPa, 20% CO_2, L/S=0.3, 150 min

Reference	**Particle size**	**CO_2 uptake** (gCO_2/kg APCR)	**Operating conditions**
		Category III	
Baciocchi et., 2009a	10-40 μm	140	30°C, 1 MPa, 100% CO_2, L/S=0.02, 5 h
Baciocchi et., 2009a	10-40 μm	270	30°C, 1 MPa, 100% CO_2, L/S=0.02, 25 h
		Category IV	
Cappai et al., 2012	unknown	200	Ambient T and P, 100% CO_2, L/S=2.5, 3 h
Araizi et al., 2016	< 295μm	18	Ambient T and P, 100% CO_2, L/S=5, 1 h
Araizi et al., 2016	< 295μm	43	Ambient T and P, 100% CO_2, L/S=10, 1 h
Araizi et al., 2016	< 295μm	40	Ambient T and P, 100% CO_2, L/S=25, 1 h
Araizi et al., 2016	< 295μm	60	Ambient T and P, 100% CO_2, L/S=50, 1 h
Araizi et al., 2016	< 295μm	90	Ambient T and P, 100% CO_2, L/S=100, 1 h
		Category V	
Baciocchi et., 2009a	10-40 μm	86	30°C, 0.3 MPa, 100% CO_2, L/S=0, 4 h
Jiang et al., 2012	< 74 μm	87	Ambient T and P, 100% CO_2, L/S=0, 9 min
		Category VI	
Jiang et al., 2013	< 74 μm	41	Ambient T and P, 12% CO_2, L/S=0, 100 min
Jiang et al., 2013	< 74 μm	17	Ambient T and P, 12% CO_2 and 1000 ppm SO_2, L/S=0, 75 min
		Category VII	
Baciocchi et al., 2006	10-40 μm	40	200°C; ambient P; 100% CO_2; L/S=0; 6 h
Baciocchi et al., 2006	10-40 μm	50	300°C; ambient P; 100% CO_2; L/S=0; 6 h
Baciocchi et al., 2006	10-40 μm	120	400°C; ambient P; 100% CO_2; L/S=0; 6 h
Baciocchi et al., 2006	10-40 μm	120	500°C; ambient P; 100% CO_2; L/S=0; 6 h
		Category VIII	
Baciocchi et al., 2009b	10-40 μm	250	400°C; 0.3 MPa; 10% CO_2; L/S= 0; 2 min
Prigiobbe et al., 2009	10-40 μm	177	350°C; ambient P; 10% CO_2; L/S=0; 2 h
Prigiobbe et al., 2009	10-40 μm	183	350°C; ambient P; 10% CO_2; L/S=0; 2 h
Prigiobbe et al., 2009	10-40 μm	159	350°C; ambient P; 22% CO_2; L/S=0; 2 h
Prigiobbe et al., 2009	10-40 μm	182	350°C; ambient P; 50% CO_2; L/S=0; 2 h
Prigiobbe et al., 2009	10-40 μm	166	350°C; ambient P; 50% CO_2; L/S=0; 2 h
Prigiobbe et al., 2009	10-40 μm	216	400°C; ambient P; 10% CO_2; L/S=0; 2 h
Prigiobbe et al., 2009	10-40 μm	201	400°C; ambient P; 22% CO_2; L/S=0; 2 h
Prigiobbe et al., 2009	10-40 μm	206	400°C; ambient P; 50% CO_2; L/S=0; 2 h
Prigiobbe et al., 2009	10-40 μm	233	450°C; ambient P; 10% CO_2; L/S=0; 2 h
Prigiobbe et al., 2009	10-40 μm	218	450°C; ambient P; 10% CO_2; L/S=0; 2 h

Prigiobbe et al., 2009	10-40 μm	210	450°C; ambient P; 22% CO_2; L/S=0; 2 h
Prigiobbe et al., 2009	10-40 μm	200	450°C; ambient P; 22% CO_2; L/S=0; 2 h
Prigiobbe et al., 2009	10-40 μm	202	450°C; ambient P; 50% CO_2; L/S=0; 2 h
Prigiobbe et al., 2009	10-40 μm	196	450°C; ambient P; 50% CO_2; L/S=0; 2 h
Prigiobbe et al., 2009	10-40 μm	225	500°C; ambient P; 10% CO_2; L/S=0; 2 h
Prigiobbe et al., 2009	10-40 μm	222	500°C; ambient P; 10% CO_2; L/S=0; 2 h
Prigiobbe et al., 2009	10-40 μm	229	500°C; ambient P; 22% CO_2; L/S=0; 2 h
Prigiobbe et al., 2009	10-40 μm	204	500°C; ambient P; 22% CO_2; L/S=0; 2 h
Prigiobbe et al., 2009	10-40 μm	205	500°C; ambient P; 50% CO_2; L/S=0; 2 h

The average CO_2 uptake for the eight test categories previously identified is reported in Table 3.4.4.6. Based on the test of Kruskall-Wallis, the distribution of the amount of CO_2 captured by the APCR is statistically different for the eight groups. This means that the process parameters (dry or aqueous route, T, P, CO_2 concentration etc.) have an actual influence on the results. The process route (i.e. dry or aqueous) is important but it is not the main parameter affecting the entity of the CO_2 uptake. By choosing the proper operating temperature, pressure and CO_2 concentration, it is possible to achieve similar CO_2 uptake operating both in dry and aqueous conditions (Baciocchi et al., 2009b). For example, an average CO_2 uptake of 205 gCO_2/kg APCR can be obtained by operating in aqueous conditions, at 1 MPa of total pressure and with a pure CO_2 gas (test category III). A similar result can be also obtained in dry conditions, by operating at high temperature (about 350-400°C) with a gas containing about 10-20% of CO_2 (test category VIII).

Table 3.4.4.6. minimum, average and maximum CO_2 uptake for each of the tests categories and corresponding operating conditions.

Test category	CO_2 uptake (gCO_2/kg APCR)		
	Minimum	**Average**	**Maximum**
I 19 cases	22 *(d<212 μm; ambient T and P; 100% CO_2; L/S=0.2; 1 h)*	119	250 *(d=10-40μm; 30°C, 0.3MPa; 100% CO_2; L/S=0.2; 10 min)*
II 12 cases	45 *(d unknown; ambient T and P; 25% CO_2; L/S=0.25; 10 days)*	95	120 *(d < 300 μm; 20-30°C, 0.3MPa; 20% CO_2; L/S=0.3; 150 min)*
III 2 cases	140 *(d=10-40 μm; 30°C; 1 MPa; 100% CO_2; L/S=0.02; 5 h)*	205	270 *(d=10-40 μm; 30°C; 1 MPa; 100% CO_2; L/S=0.02; 25 h)*
IV 6 cases	*18* *(d<295 μm; ambient T and P; 100% CO_2; L/S=5; 1 h)*	75	*200* *(d unknown; ambient T and P; L/S=2.5; 3 h)*
V 2 cases	86 *(d=10-40 μm; 30°C, 0.3 MPa; 100% CO_2; L/S=0; 4 h)*	86.5	87 *(d<74 μm; ambient T and P; L/S=0; 100% CO_2; 9 min)*
VI 2 cases	17 *(d<74 μm; ambient T and P; 12% CO_2; L/S=0; 100 min)*	29	41 *(d<74 μm; ambient T and P; 12% CO_2 + 1000 ppm SO_2; L/S=0; 90 min)*
VII 4 cases	40 *(d=10-40 μm; 200°C; ambient P; 100% CO_2; L/S=0; 6 h)*	82.5	120 *(d=10-40 μm; 500°C; ambient P; 100% CO_2; L/S=0; 6 h)*
VIII 20 cases	159 *(d=10-40 μm; 350°C; ambient P; 22% CO_2; L/S=0; 2 h)*	204	250 *(d=10-40 μm; 400°C; 0.3 MPa; 10% CO_2; L/S=0; 2 min)*

As shown by the Principal Component Analysis (PCA) in Figure 3.4.4.2[23], the principal parameter affecting the CO_2 uptake is the content of Ca in the APCR, as also suggested by Baciocchi et al. (2009b). Among the process parameters, the most relevant are the temperature, the particle size and the L/S ratio (directly correlated with the process route). The CO_2 pressure plays a secondary role, as well as the test duration, which is usually sufficiently long to achieve the equilibrium conditions.

In more detail:

- the temperature plays a double role on the carbonation reactions: high temperatures initially enhance the kinetics of the process, by increasing the Ca^{2+} dissolution from the solid matrix. However, the CO_2 solubility/diffusion through the layer of the reaction products decreases at high temperature, resulting in a reduction of the final conversion value (Fernández-Bertos et al., 2004). This last aspect is more evident for aqueous-based carbonation processes that, for this reason, are usually performed at ambient or modest

[23] Two principal components were extracted, the first one explaining about 52% of the total variance of the model and the second one an additional 37%. Overall, more than 50% of the variance of each variable is explained by the model, with the exception of the CO2 concentration in the gas, for which the communality value is only 22%.

temperature. In particular, Baciocchi et al. (2009) observed that the temperature has a greater influence when the L/S ratio is below the optimal value, otherwise its influence on the CO_2 uptake is negligible. The best operating temperature were found to be around 20 and 30°C (Sun et al., 2008). On the contrary, in gas-solid carbonation, the process must be carried out at a temperature above 350°C, otherwise the kinetics are too slow to proceed. In a temperature range of 400-500°C, the influence of the temperature variation on the final CO_2 uptake is negligible (Prigiobbe et al., 2009);

- in aqueous carbonation, L/S ratios of 0.2-0.3 are usually adopted. Too low L/S ratios result in modest CO_2 uptake, because a certain amount of water is needed for the solubilisation of CO_2 and Ca ions. However, when the L/S ratio is above the optimal value, the CO_2 uptake decreases due to a higher resistance toward CO_2 diffusion through the increasing intergranular water film thickness (Baciocchi et al., 2009a; Sun et al., 2008);
- the influence of the CO_2 partial presrazisure is quite modest. Many authors observed that the final CO_2 uptake is not influenced by the CO_2 pressure at which the carbonation is carried out if the other parameters (T and L/S) are within the optimal range, because, in this case, the process is controlled by Ca ions dissolution rather than by CO_2 diffusion (Prigiobbe et al., 2009; Baciocchi et al., 2009a and b). However, different results are reported in other scientific sources. For example, Sun et al. (2008) observed that, whereas the carbonation kinetic is positively influenced by the CO_2 partial pressure, the final CO_2 uptake increases up to a certain value of the CO_2 pressure and then decreases[24]. The authors suggested that, when the CO_2 pressure is high, larger $CaCO_3$ crystals form, which are more likely to block the pores, making further carbonation more difficult. On the contrary, Jiang et al. (2013) observed that both the final CO_2 uptake and the reaction kinetics are positively influenced by the CO_2 pressure.

Another parameter that can influence the CO_2 uptake is the presence of SOx in the CO_2 enriched gas. This aspect can be interesting if one wants to directly use the incinerator flue gas as a source of CO_2. Based on the authors' knowledge, this aspect was investigated only by Jiang et al. (2013). They observed that the presence of SOx in the CO_2 enriched gas decreases the amount of CO_2 sequestered by the APCR. SOx inhibits CO_2 sequestration, because it clogs the pores of the residue, thus reducing its ability to sequester CO_2.

Regarding the application of the technology at the industrial scale, the society Carbon8 Aggregates Limited (C8A), a spin-out company from the Greenwich University, was founded in the year 2010 with the licence to treat the APCR thought the patented process Accelerated Carbonation Technology (ACT) to manufacture lightweight aggregates. In the year 2012, the first-full scale commercial plant was realised at Brandon (Suffolk) and then a second and a third production facilities were made operational at Avonmouth (near Bristol) in the year 2016 and in Leeds in the year 2018.

The patented process has multiple treatment stages. Firstly, the APCR are mixed and stabilised with carbon dioxide. Fillers, other carbonable waste (e.g., biomass ash and cement bypass dust) and binders (like Portland

[24] The best operating condition was found to be: 0.3 MPa of total pressure and a CO_2 concentration of 20%.

cement) can be added. According to the patent indications (WIPO patent Application Number WO/201608268; Hills and Carey, 2017), the operative conditions of the treatment are: L/S ratio equal to 0.25, ambient T, ambient or modest P (< 2 bar), 100% CO_2 or CO_2 enriched gas (50% CO_2 as minimum content), treatment duration: 10-20 minutes.

The material is then agglomerated in a pelletizing unit with the aim to increase the grains size by mechanical agitation in a revolving drum. Finally, the aggregate is stored in a curing chamber for about 3 days to harden under a flow of dry CO_2. The carbon dioxide helps to overcome the detrimental effect of the saturated pore network caused by the agglomeration (Gunning et al., 2009, 2013, 2014/O.C.O. Technology Ltd, 2019). The resulting lightweight aggregate, called M-LS aggregate (Manufactured-Limestone aggregate), was classified as an End of Waste material by the UK Environment Agency, i.e. it is a distinct and marketable product that can be used in exactly the same way as virgin aggregates, with no worse environmental impacts. In particular, regarding the environmental aspect, the M-LS aggregate is classified as carbon-negative because the quantity of CO_2 captured in the process is greater than the equivalent CO_2 emissions generated during the manufacture (the overall balance in terms of climate change is equal to -44 kgCO_2 equivalent per 1 ton of produced aggregate; Carey et al., 2015). Pellets of the aggregate are grey, sub-rounded and are supplied in particle grading generally ranging from 2-20 mm. The material has various applications but it is principally used in the production of building blocks. For example, the British Company Lignacite Ltd (the UK's largest independent concrete block manufacturer) uses sand and gravel combined with the M-LS aggregate (up to 55% of the final volume) to build the Carbon Buster block (Lignacite Ltd, 2013).

From the few available information about the CO_2 used in the process, the most recent available source reports a 7-10% consumption on the APCR weight, that is enough to stabilise the product at reduced costs (Carey, 2018). This range is in accordance with CO_2 uptake values obtained at the lab-scale in similar conditions by Araizi et al. (92 g/kg APCR), Li et al. (110 g/kg APCR) and Sun et al. (80-90 g/kg APCR; See Table 3.4.4.5).

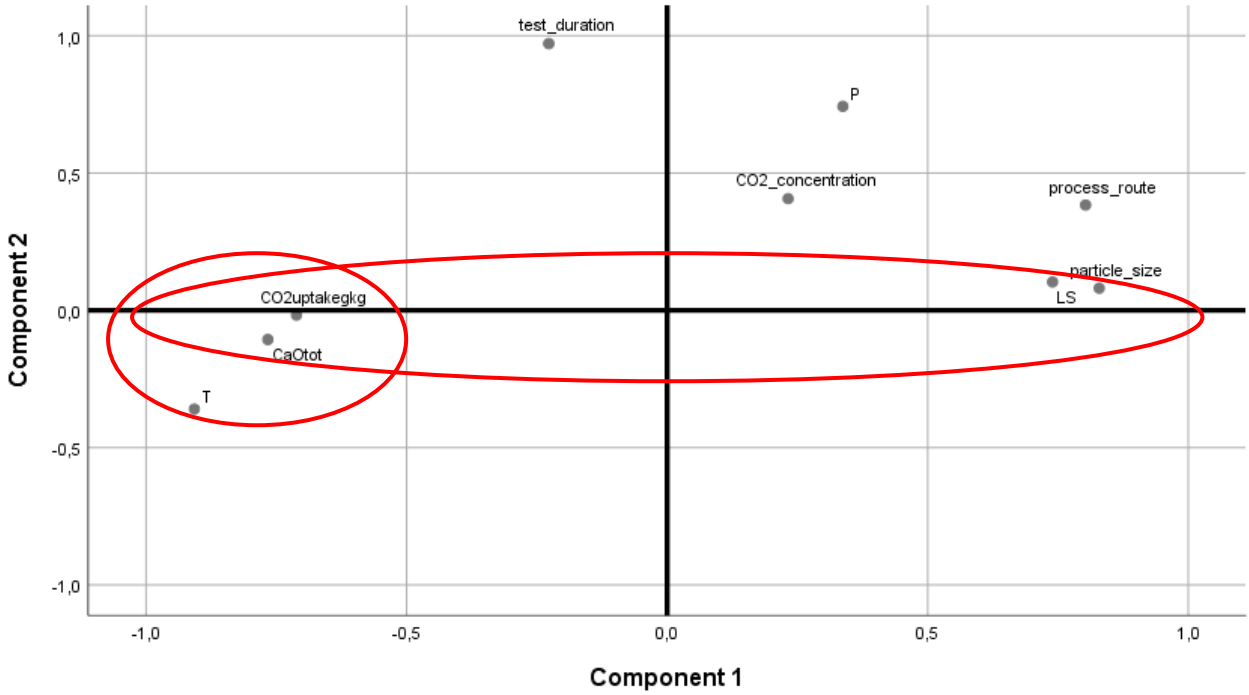


Figure 3.4.4.2. Component plot of the Principal Component Analysis (PCA) carried out on the data reported in Table 3.4.4.5.

3.4.4.5 DISCUSSION AND CONCLUSIONS

CO_2 sequestration as a consequence of the use of lime in FGC systems

Based on what reported in the Chapter 3.4.4.3, a certain amount of CO_2 in the flue gas will react with the lime dosed in the FGC systems, thus reducing its emission into the atmosphere.

Focusing of waste incineration, where lime is one of the main sorbents used for acid gas removal, and by assuming:

- an average CO_2 uptake of 84 g/kg of APCR;
- a production of 30-60 kg APCR/t incinerated waste (EU, 2018);
- a dosage of 10-20 kg CaO/t incinerated waste (EU, 2018);

it results an average CO_2 uptake of about 250 kgCO_2 per tonne of lime added to the FGC system.

Considering also that the production of 1 tonne of lime releases in the atmosphere 786 kg of CO_2 (only from the calcination process, excluding the energy consumption), it results that, on average, 32% of the CO_2 emitted during the calcination process for lime production can be captured in the FGC system as a consequence of the lime dosage for acid gas removal.

Furthermore, a non-negligible amount of unreacted lime remains in the APCR and can be exploited for CO_2 sequestration. Natural carbonation of APCR has not been investigated in the scientific literature, however many publications are available about accelerated carbonation at lab-scale and at the industrial scale (experience in the United Kingdom).

Based on the tests at the lab-scale, the average CO_2 uptake achievable in accelerated carbonation processes range is about 30-200 gCO_2/kg APCR, depending on the operating conditions. At the full scale UK experience the same uptake ranges from 70-90 gCO_2/kg APCR.

Considering the lab-scale tests, this means that an extra amount of CO_2, equal to about 90-600 kg per tonne of lime used in the FGC system, can be theoretically sequestered if the APCR are carbonated in controlled conditions. This value corresponds to 11-76% of the CO_2 emitted during the calcination process for lime production. In the unique full-scale experience about 210-270 kg CO_2 per ton of used lime are sequestered, corresponding to 27%-34% of the CO_2 emitted during lime production.

Thus, overall, about 40-100% of the CO_2 emitted during the calcination process for lime production could be theoretically absorbed by the lime dosed in the FGC system (59%-66% in the analysed industrial experience), directly when lime reacts with the CO_2 in the flue gas and indirectly if the APCR are subjected to accelerated carbonation processes.

Recommendation on research needs in FGC system

The literature review carried out on APCR shows a general lack of data regarding natural ageing of these residues during storage before treatment or during final disposal. The authors suggest to carry out some analyses of APCR of different age in order to assess the amount of CO_2 that can be actually sequestered by this material and to better understand the time evolution of the carbonation process in outdoor ambient conditions.

On the contrary, in recent years many efforts have been directed towards accelerated carbonation processes. Results of the laboratory tests seem very promising: APCR can be used as a feedstock material for CO_2 sequestration, furthermore improving their leaching and environmental behaviour before disposal. However, research activity is still at the laboratory scale and there is still a long road ahead for full scale implementation of the accelerated carbonation process of APCR.

REFERENCES

Araizi, P.K., Hills, C.D., Maries, A., Gunning, P.J., Wray, D.S., 2016. *Enhancement of accelerated carbonation of alkaline waste residues by ultrasound*. Waste Management 50, 121-129. DOI: http://dx.doi.org/10.1016/j.wasman.2016.01.006

Antonioni, G., Guglielmi, D., Cozzani, V., Stramigioli, C., Corrente, D., 2014. *Modelling and simulation of an existing MSWI flue gas two-stage dry treatment*. 92(3), 242-250. DOI: 10.1016/j.psep.2013.02.005

Baciocchi, R., Polettini, A., Pomi, R., Prigiobbe, V., Von Zedwitz, V.N., Steinfeld, A., 2006. *CO_2 sequestration by direct gas-solid carbonation of air pollution control (APC) residues*. Energy Fuels 20(5), 1933-1940. DOI: https://doi.org/10.1021/ef060135b

Baciocchi, R., Costa, G., Di Bartolomeo, E., Polettini, A., Pomi, R., 2009a. *The effect of accelerated carbonation on CO2 uptake and metal release from incineration APC residues*. Waste Management 29(12), 2994-3003. DOI: https://doi.org/10.1016/j.wasman.2009.07.012

Baciocchi, R., Costa, G., Polettini, A., Pomi, R., Prigiobbe, V., 2009b. *Comparison of different reaction routes for carbonation of APC residues*. Energy Procedia 1 (1), 4851-4858. DOI: https://doi.org/10.1016/j.egypro.2009.02.313

Belevi, H., Moench, H., 2000. *Factors determining the element behaviour in municipal solid waste* incinerators. 1. Field studies. Environ. Sci. Technol. 34(12), 2501-2506. DOI: https://pubs.acs.org/doi/abs/10.1021/es991078m

Benkő, T., Mizsey, P., 2007. *Comparison of flue gas desulphurization processes based on life cycle assessment*. Chemical Engineering 51(2), 19-27. DOI: https://doi.org/10.3311/pp.ch.2007-2.04

Bodénan, F., Deniard, P., 2003. *Characterization of flue gas cleaning residues from European solid waste incinerators: assessment of various Ca-based sorbent processes*. Chemosphere 51(5), 335-347. DOI: https://doi.org/10.1016/S0045-6535(02)00838-X

Bogush, A., Stegemann, J.A., Wood, I., Roy, A., 2015. *Element composition and mineralogical characterisation of air pollution control residue from UK energy-from-waste facilities*. Waste Management 36, 119-129. DOI: https://doi.org/10.1016/j.wasman.2014.11.017

Carey, P.J., Hills, C.D., Gunning, P.J., 2015. *Concrete: innovation and its practical application. The world's first commercially available carbon negative aggregate and its uses*. 43th annual convention of the Institute of Concrete Technology, 26 March 2015. Available online: http://www.ukqaa.org.uk/wp-content/uploads/2015/07/Carbon8-submission-for-EN-13055-v2.pdf

Carey, P.J., 2018. *Developing an innovative and profitable process that combines waste CO_2 and thermal residues, to create a carbon negative aggregate for construction and lock CO2in for good within our built environment*. Available online: http://nas-sites.org/dels/files/2018/02/1-5-CAREY-Carbon8-Systems-NAS.pdf

Cappai, G., Cara, S., Muntoni, A., Piredda, M., 2012. *Application of accelerated carbonation on MSW combustion APC residues for metal immobilization and CO_2 sequestration*. Journal of Hazardous Materials 207-208, 159-164. DOI: 10.1016/j.jhazmat.2011.04.013

Chang, J.S., Urashima, K., Tong, Y.X., Liu, W.P., Wei, H.Y., Yang, F.M., Liu, X.J., 2003. *Simultaneous removal of NOx and SO_2 from coal boiler flue gases by DC corona discharge ammonia radical shower system: pilot plant tests*. Journal of Electrostatics 57 (3-4), 313-323. DOI: 10.1016/S0304-3886(02)00168-7

Chin, T., Yan, R., Tee Liang, D., 2005a. *Study of the reaction of lime with HCl under simulated flue gas conditions using x-ray diffraction characterization and thermodynamic prediction*. Ind. Eng. Chem. Res. 44(23), 8730-8738. DOI: https://doi.org/10.1021/ie058021v

Chin, T., Yan, R., Tee Liang, D., Tay, J.H., 2005b. *Hydrated lime reaction with HCl under simulated flue gas conditions*. Ind. Eng. Chem. Res. 44(10), 3742-3748. DOI: https://doi.org/10.1021/ie040206z

Costa, G., Baciocchi, R., Polettini, A., Pomi, R., Hills, C.D., Carey, P.J., 2007. *Current status and perspectives of accelerated carbonation processes on municipal waste combustion residues*. Environ. Monit. Assess., 135(1-3), 55-75. DOI: 10.1007/s10661-007-9704-4

De Boom, A., Degrez, M., 2012. *Belgian MSWI fly ashes and APC residues: a characterisation study*. Waste Management 32(6), 1163-1170. DOI: https://doi.org/10.1016/j.wasman.2011.12.017

Ecke, H., Menad, N., Lagerkvist, A., 2002. *Treatment-oriented characterization of dry scrubber residue from municipal solid waste incineration*. Journal of Material Cycles and Waste Management 4(2), 117-126. DOI: https://doi.org/10.1007/s10163-001-0063-x

EU, 2017. *Best Available Techniques (BAT) Reference Document for Large Combustion Plants*

EU, 2018. *Best Available Techniques (BAT) Reference Document for Waste Incineration*

Fernández Bertos, M., Li, X., Simons, S.J.R., Hills, C.D., Carey, P.J., 2004. *Investigation of accelerated carbonation for the stabilisation of MSW incinerator ashes and the sequestration of CO_2*. Green Chemistry 6, 428-436. DOI: 10.1039/b401872a

Gunning, P.J., Hills, C.D., Carey, P.J., 2009. *Production of lightweight aggregate from industrial waste and carbon dioxide*. Waste Management 29, 2722-2728. DOI: 10.1016/j.wasman.2009.05.021

Gunning, P., Hills, C.D., Carey, P.J., 2013. *Commercial application of accelerated carbonation: Looking back at the first year 2013*. Conference Proceedings of ACEME, 2013, pages 185-192. Abstract of the paper available online: https://gala.gre.ac.uk/id/eprint/13577/

Gunning, P., Hills, C.D., 2014. *Carbon negative: first commercial application of accelerated carbonation technology*. 7th International Scientific Conference: Science and Higher Education in Function of Sustainable Development, 3-4 October 2014, Uzice, Serbia. Available online: https://pdfs.semanticscholar.org/0f3d/5fdc40eba9b1780f323b4b2b94d6a267eb9d.pdf

Hills, C.D. and Carey, P.J. (2017). *WIPO patent Application Number WO/201608268: Improved production of aggregates*. Available online: https://patentscope.wipo.int/search/en/detail.jsf?docId=GB205861767&tab=NATIONALBIBLIO&_cid=P10-K1J5T9-46220-1

Ho, C.S., Shih, S.M, Lee, C.D., 1996. *Influence of CO_2 and O_2 on the reaction of $Ca(OH)_2$ under spray-drying flue gas desulfurization conditions*. Ind. Eng. Chem. Res. 35(11), 3915-3919. DOI: https://doi.org/10.1021/ie9600506

Jiang, J., Tian, S., Zhang, C., 2013. *Influence of SO_2 in incineration flue gas on the sequestration of CO_2 by municipal solid waste incinerator fly ash*. Journal of Environmental Sciences 25(4), 735-740. DOI: https://doi.org/10.1016/S1001-0742(12)60142-9

Karlsson, H.T., Klingspor, J., Bjerle, I., 1981. *Adsorption of hydrochloric acid on solid slaked lime for flue gas clean up*. Journal of the Air Pollution Control Association 31(11), 1177-1180. DOI: https://doi.org/10.1080/00022470.1981.10465343

Li, X., Fernández Bertos, M., Hills, C.D., Carey, P.J., Simon S., 2007. *Accelerated carbonation of municipal solid waste incineration fly ashes*. Waste Management 27(9), 1200-1206. DOI: https://doi.org/10.1016/j.wasman.2006.06.011

Lignacite Ltd, 2013. *Carbon Buster Commodity Blocks*. Available online: http://www.ukqaa.org.uk/wp-content/uploads/2015/07/Carbon8-submission-for-EN-13055-v2.pdf

Nygaard, H.G., Kiil, S., Johnsson, J.E., Jensen, J.N., Hansen, J., Fogh, F., Dam-Johansen, K., 2004. *Full-scale measurements of SO_2 gas phase concentrations and slurry compositions in a wet gas desulphurisation spray absorber*. Fuel 83(9), 1151-1164. DOI: https://doi.org/10.1016/j.fuel.2003.12.007

O.C.O Technology Ldt, 2019. Company website: https://oco.co.uk/about-us/

Prigiobbe, V., Polettini, A., Baciocchi, R., 2009. *Gas-solid carbonation kinetics of Air Pollution Control residues for CO_2 storage*. Chemical Engineering Journal 148(2-3), 270-278. DOI: https://doi.org/10.1016/j.cej.2008.08.031

Quina, M.J., Bordabo J.C.M., Quinta-.Ferreira, R.M., 2011. *Air pollution control in municipal solid waste incinerators*. In The impact of air pollution on health, economy, environment and agricultural sources. Edited by Khallaf M.K., published by IntechOpen, 2011. ISBN 978-953-307-528-0, pages 331-359

Stein, J., Kind, M., Schlünder, E.U., 2002. *The influence of HCl on SO_2 absorption in the spray dry scrubbing process*. Chemical Engineering Journal 86(1-2), 17-23. DOI: https://doi.org/10.1016/S1385-8947(01)00267-4

Sun, J., Fernandez Bertos, M., Simons, S.J.R., 2008. *Kinetic study of accelerated carbonation of municipal solid waste incinerator air pollution control residues for sequestration of flue gas CO_2*. Energy Environ. Sci. 1, 370-377

Tan, J., Yang, G., Mao, J., Dai, H., 2014. *Laboratory study on high-temperature adsorption of HCl by dry-injection of $Ca(OH)_2$ in a dual-layer granular bed filter*. Front. Environ. Sci. Eng. 8(6), 863-870. DOI : https://doi.org/10.1007/s11783-013-0618-9

Wang, L., Jin, Y., Nie, Y., 2010. *Investigation of accelerated and natural carbonation of MSWI fly ash with a high content of Ca*. Journal of Hazardous Materials 174(1-3), 334-343. DOI: https://doi.org/10.1016/j.jhazmat.2009.09.055

Yan, R., Chin, T., Liang, D.T., Laursen, K., Ong, W.Y., Yao, K., Tay, J.H., 2003. *Kinetic study of hydrated lime reaction with HCl*. Environ. Sci. Technol. 37(11), 2556-2562. DOI: https://doi.org/10.1021/es020902v

Zhang, H., Yu, S., Shao, L., He, P., 2019. *Estimating source strengths of HCl and SO_2 emissions in the flue gas from waste incineration*. Journal of Environmental Sciences 75, 370-377. DOI: https://doi.org/10.1016/j.jes.2018.05.019

3.4.5 USE OF LIME IN OTHER ENVIRONMENTAL PROTECTION APPLICATION

3.4.5.1 TREATMENT OF SLUDGE FROM ACID MINE DRAINAGE (AMD)

Introduction: the problem of AMD and lime treatment process

Acid Mine Drainage (AMD), also known as Acid Rock Drainage, is one of the major environmental problems faced by the mining and mineral industries worldwide. It derives from the exposure of sulphide ores and minerals to water and oxygen. Once the ore is exposed, sulphate and heavy metals such as iron, copper, lead, nickel, manganese, cadmium, aluminium, and zinc are released into water. AMD has generally a low pH (about 2-3), high salinity, and high heavy metals content (Moodley et al., 2018).

In the chemistry of the phenomenon, there are four main reactions [3.4.5.1-4] associated with the formation of AMD and they are expressed in terms of pyrite, since it is the most common mined sulphide mineral. AMD is formed starting from the exposure of pyrite to oxygen and water, resulting in hydrogen ions release (release of acidity), sulphate ions, and ferrous iron. Ferrous iron is oxidized to ferric iron (Reaction [3.4.5.2]). Ferric iron can then either precipitate as $Fe(OH)_3$, a red-orange precipitate seen in water affected by acid rock drainage (Reaction [3.4.5.3]), or it can react directly with pyrite to produce more ferrous iron and further acidity, as shown in Reaction [3.4.5.4]. Oxidizing bacteria generally accelerate the rates of the involved chemical reactions (Kaur et al., 2018/Moodley et al., 2018).

$$2FeS_2\,(s) + 7O_2 + 2H_2O \rightarrow 2Fe^{2+} + 4SO_4^{2-} + 4H^+ \qquad [3.4.5.1]$$

$$2Fe^{2+} + 1/2\,O_2 + 2H^+ \rightarrow 2Fe^{3+} + H_2O \qquad [3.4.5.2]$$

$$2Fe^{3+} + 6H_2O \rightarrow 2Fe(OH)_3\,(s) + 6H^+ \qquad [3.4.5.3]$$

$$14Fe^{3+} + FeS_2\,(s) + 8H_2O \rightarrow 2SO_4^{2-} + 15Fe^{2+} + 16H^+ \qquad [3.4.5.4]$$

AMD initially forms in the groundwater of an active mine, but the rate of generation is kept to a minimum through the use of pumps. When the mine is shut down, the production can rapidly increase if the pumping operations cease and the groundwater level rises.

In Europe, several active and abandoned mine sites are affected by AMD. For example, the Ria de Huelva in South-western Spain is one of the most heavily metal-contaminated estuaries in the world, as a result of AMD derived from the Iberian Pyrite Belt, an area of more than 4800 ha, with around 90 mines (most of them abandoned) and 200 million m^3 of mining waste as a legacy (Basallote et al., 2019). In Germany, there are more than 100 acid lakes with a pH < 4 as a consequence of piryte oxidation (Sahoo et al., 2013). In Southern France, sulfidic tailings from Carnoulès mining activity have generated acid water (pH=2.73–3.37) containing high dissolved concentrations of arsenic (1-3.5 mmol/l) and iron (20-40mmol/l; Casiot et al., 2003).

The common treatment method of AMD streams typically involves alkali addition in order to raise the pH to between 6 and 9 (in case of high concentration of manganese, a pH equal to 10.5 is required). In this pH range, the concentration of dissolved metals generally decreases due to the formation of insoluble metal hydroxides and oxy-hydroxides. A partial sulphate removal through the precipitation of gypsum is also obtained, though

with a low efficiency. Lime is the most widely used alkali applied in the remediation treatment, mainly due to its relative low cost and availability. The treatment generates voluminous sludge (generally 10% of the volume of the treated water), with a quite low solid content and difficulty in the settling operations (Kaur et al., 2018). In the conventional treatment with lime (Figure 3.4.5a), the AMD is neutralised in a mix tank with controlled addition of lime to obtain the desired pH. The slurry is then contacted to a flocculant and fed to a clarifier for the solid/liquid separation. The sludge is collected from the bottom of the clarifier and pumped to a dehydration unit to increase its density prior disposal. The High-Density Sludge (HDS) process has recently substituted the standard configuration at the industrial scale (Figure 3.4.5b). Instead of contacting lime directly with the polluted water, the HDS system contacts the recycled sludge from the clarifier with lime. The mixture then flows to the rapid mix tank and then to the precipitation reactor. Mechanical aeration is often performed in this latter reactor with the aim to promote the oxidation of reduced metals such as Fe^{2+} and Mn^{2+} to Fe^{3+} and Mn^{4+} so that they can quickly convert into oxide and hydroxide precipitates. The fact that lime and the recycled particles of sludge are combined forces the precipitation reactions to occur on the surface of the existing particles, thereby increasing their size and density. The slurry then is contacted to a flocculant and fed to the clarifier. Main advantages of the HDS configuration are:

- increase of the solid content of the sludge with a better handling of the disposal: a typical HDS plant produces a sludge with a dry content up to 70% compared to 40% in the conventional treatment;
- improvement of the lime efficiency: with the recirculation of the sludge, the HDS process allows solids more time to fully react with lime. This, of course, implies full utilization of all the chemical within the process, decreasing the excess of lime dosage;
- less problems of gypsum scaling on the reactor walls and conduits to the clarifier: if the AMD contains high sulphate concentrations, gypsum scaling can occur following the addition of Ca from lime. By recycling sludge, the precipitation of gypsum occurs on the surface of existing particles rather than on the reactor walls (Aubè et al., 2003/Coulton et al., 2004).

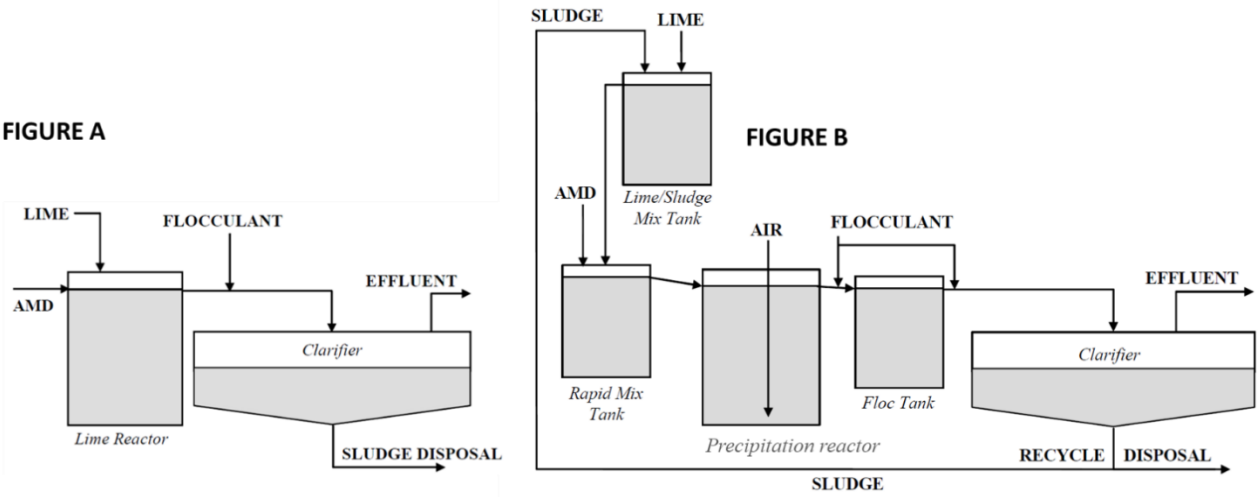


Figure 3.4.5. Main steps of the neutralization process of AMD with lime: conventional process (Figure A) and High-Density Sludge Process (Figure B).

A further possible option is the combination of a limestone-lime treatment, in order to take economical advantage and to improve the sludge properties (the use of limestone generates higher density sludge, with better settling properties).

In this case, a two-step process is required. First, the AMD is treated with limestone to a pH of 4.0 to 4.5, the range where limestone is most effective. The stream then passes to a second reactor where lime is applied to raise the pH range to the desired level (Heviánková et al., 2013).

Literature assessment about the use of lime in AMD treatment: material and methods

The literature review in this chapter is dedicated to the evaluation of the carbonation process of lime used in the treatment of AMD streams, due to the reaction with carbon dioxide already dissolved in the AMD stream itself or with the atmospheric CO_2 dissolved during the treatment. The focus is to verify the possible presence of calcite in the process sludge. The list of the few available documents on the theme is reported in Table 3.4.5.1.

Table 3.4.5.1. List of the documents considered in the review about the presence of calcite in the process sludge of the AMD treatment.

Scientific paper Jageman et al., 1987. *The use of pre-aeration to reduce the cost of neutralizing acid mine drainage*. Proceedings America Society of Mining and Reclamation, 131-135. Available online: https://www.asmr.us/Portals/0/Documents/Conference-Proceedings/1988-Volume-1/0131-Jageman.pdf
Website Industry treatment solution for AMD (WesTech). http://www.westech-inc.com/en-usa/industry-solutions/mineral-overview/acid-mine-drainage (Last Access: September, 2019)

Literature assessment about the use of lime in AMD treatment: sludge characteristics and calcite content

According to the existing literature, acid mine drainage from an underground mine may contain bicarbonate ions and carbonic acid due to the passage of the stream on limestone and the subsequent neutralization of the products of pyrite oxidation, as reported in the Reactions [3.4.5.5] and [3.4.5.6].

$$H_2SO_4 + 2CaCO_3 \rightarrow Ca^{2+} + SO_4^{2-} + Ca(HCO_3)_2 \quad [3.4.5.5]$$

$$H_2SO_4 + Ca(HCO_3)_2 \rightarrow Ca^{2+} + SO_4^{2-} + 2H_2CO_3 \quad [3.4.5.6]$$

If these compounds react with the lime added during the treatment, they form sparingly soluble calcium carbonate according to the Reactions [3.4.5.7] and [3.4.5.8] (Jageman et al., 1987).

$$H_2CO_3 + Ca(OH)_2 \rightarrow CaCO_3 + 2H_2O \quad [3.4.5.7]$$

$$2HCO_3^- + Ca(OH)_2 + Ca^{2+} \rightarrow 2CaCO_3 + 2H_2O \quad [3.4.5.8]$$

However, from the very few information collected, it seems that in the full-scale treatment plants the occurrence of these reactions is generally avoided/reduced through a step of AMD de-carbonation before the lime neutralisation. In this step, the dissolved carbonates in the AMD stream are stripped as gaseous CO_2 through mechanical aeration. In this way, a reduction of the lime request as well as of the sludge amount is obtained (Jageman et al., 1987/WesTech website, 2019).

Conclusions and future research needs

Based on the few collected data from the reviewed papers, it can be derived a negligible presence of calcite in the process sludge from the treatment of an acid mine drainage stream with lime, thus excluding any possible/measurable effect on its carbonation potential.

REFERENCES

Aubé, B. and Zinck, J., 2003. *Lime treatment of acid mine drainage in Canada*. Brazil-Canada Seminar on Mine Rehabilitation, Florianópolis, Brazil, 1-3 December. Available online: https://www.researchgate.net/publication/237648554_Lime_Treatment_of_Acid_Mine_Drainage_in_Canada

Basallote, M.D., Cánovas, C.R., Pérez-López, R., Olías M., Macías, F., Nieto, J.M, 2019. *Metal partitioning and pH-buffering during mixing processes in an estuary strongly affected by acid mine drainage -The Ria de Huelva estuary (SW Spain)*. Conference Paper: Proceedings IMWA 2019 Conference - Mine Water: Technological and Ecological Challenges: 409-415, Perm (Russia). Available online: https://www.imwa.info/imwaconferencesandcongresses/proceedings/306-proceedings-2019.html

Casiot, C., Morin, G., Juillot, F., Bruneel, O., Personné, J-C., Leblanc, M., Duquesne, K., Bonnefoy, V., Elbez-Poulichet, F., 2003. *Bacterial immobilization and oxidation of arsenic in acid mine drainage (Carnoulès creek, France)*. Water Research 37(12), 2929-2936. DOI:10.1016/S0043-1354(03)00080-0

Coulton, R., Bullen, C., Williams, C., Williams, K., 2004. *The formation of high density sludge from minewater with low iron concentrations*. Proceedings of Mine Water Process, Policy and Progress, Newcastle upon Tyne, UK, pages 145-153

Heviánková, S., Bestová, I., Kyncl, M., Šimková, L., Zechnen, M., 2013. *Calcium carbonate as an agent in acid mine water neutralisation*. Inzynieria Mineralna 14(2), 159-166. Available online: http://www.potopk.com.pl/Full_text/2013_full/2013_2_29.pdf

Jageman, T.C., Yokley, R.A., Heunisch, G.W., 1987. *The use of pre-aeration to reduce the cost of neutralizing acid mine drainage*. Proceedings America Society of Mining and Reclamation, 131-135. Available online: https://www.asmr.us/Portals/0/Documents/Conference-Proceedings/1988-Volume-1/0131-Jageman.pdf

Kaur, G., Couperthwaite, S.J., Hatton-Jones, B.W., Millar, G.J., 2018. *Alternative neutralisation materials for acid mine drainage treatment*. Journal of Water Process Engineering 22, 46-58. DOI: https://doi.org/10.1016/j.jwpe.2018.01.004

Moodley, I., Sheridan, C.M., Kappelmeyer, U., Akcil, A., 2018. *Environmentally sustainable acid mine drainage remediation: Research developments with a focus on waste/by-products*. Minerals Engineering 126, 207-220. DOI: http://dx.doi.org/10.1016/j.mineng.2017.08.008

Sahoo, P.K., Kim, K., Equeenuddin, S.M., Powell, M.A., 2013. *Current Approaches for mitigating acid mine drainage*. Reviews of environmental contamination and toxicology, 226, 1-32. DOI: 10.1007/978-1-4614-6898-1_1

3.4.5.2 OTHER ENVIRONMENTAL PROTECTION APPLICATIONS

In addition to acid mine drainage, lime is applied in other environmental protection applications e.g. lake liming in order to counteract acidity. As an example, in the lake Orta in Northern Italy a total of 10,900 t of pure calcium carbonate were dissolved during one year, following a drastic decrease in the pH occurred due to uncontrolled industrial discharge. This had allowed the complete neutralisation of the water mass, bringing the pH back to its original levels (Calderoni and Tartari, 2000).

A possible future lime application is ocean liming, that is a carbon dioxide removal process consisting in the addition of alkaline materials, e.g. calcium oxide or calcium hydroxide, for increasing ocean alkalinity (Lenton et al., 2018; Renforth et al., 2013). As a result, CO_2 is removed from the atmosphere and uptaken by the ocean, while at the same time ocean acidification is counteracted. Around 1.4-1.7 moles of CO_2 is stored in the form of bicarbonates (HCO_3^-) in the ocean per mole of added Ca^{2+} (Renforth and Henderson, 2017). Further studies on this process are currently in progress, for example in the framework of the Desarc-Maresanus project by Politecnico di Milano and CMCC (https://www.desarc-maresanus.net/en_gb/), especially focused on the alkalinisation of the Mediterranean Sea with calcium hydroxide in order to achieve net Negative Emissions of CO_2 (Caserini et al., 2019).

REFERENCES

Calderoni, A., Tartari, G.A., 2000. *Evolution of the water chemistry of Lake Orta after liming.* J. Limnol., 60 (Suppl. 1): 69-78

Caserini, S., Barreto, B., Lanfredi, C., Cappello, G., Ross Morrey, D., Grosso, M., 2019. *Affordable CO_2 negative emission through hydrogen from biomass, ocean liming, and CO_2 storage*. Mitigation and Adaptation Strategies for Global Change, 24,1231-1248. DOI 10.1007/s11027-018-9835-7

Lenton, A., Matear, R. J., Keller, D. P., Scott, V., Vaughan, N. E., 2018. *Assessing carbon dioxide removal through global and regional ocean alkalinization under high and low emission pathways*. Earth System Dynamics, 9, 339-357. DOI: 10.5194/esd-9-339-2018

Renforth, P., Henderson, G., 2017. *Assessing ocean alkalinity for carbon sequestration.* Reviews of Geophysics, 55, 3, 636-674. DOI: 10.1002/2016RG000533

Renforth, P., Jenkins, B. G., Kruger, T., 2013. *Engineering challenges of ocean liming*. Energy, 60, 442-452. DOI: 10.1016/j.energy.2013.08.006

3.5 USE OF LIME IN AGRICULTURE APPLICATIONS

3.5.1 USE OF LIME IN FERTILISERS

3.5.1.1 INTRODUCTION

The problem of soil acidification

Currently, approximately 30% (3,950 million ha) of the world's ice-free land area is composed of acid soils, defined as soils with a pH < 5.5 in their surface layers (Von Uexküll et al., 1995). Soil acidification is a slow natural process and part of normal weathering, but it can be accelerated by intensive agriculture practices (i.e. use of ammonium-based fertilisers or urea, legumes cultivation, farm products removal) and industrial or mining activities (acid deposition). At pH lower than 5, soil acidification affects the soil fertility and the yield of many crops mainly due to the increased presence of toxic elements (such as soluble forms of Al and Mn) and to the deficiency of essential nutrients (phosphorus, calcium, magnesium, and molybdenum; Blume et al., 2009). Historically, liming is the most common practice adopted to neutralize the soil acidity. Liming affects three aspects of soil properties (Brady, 1969):

- CHEMICAL PROPERTIES. The increase of soil pH to a suitable value involves several chemical changes, such as the reduction of aluminium and manganese in their soluble toxic forms, the availability of nutrients (N, P, and K) for the plants, the increase of the exchangeable calcium and magnesium base cations, and the insolubilization of some undesirable substances like heavy metals to avoid intake by the plant.
- PHYSICAL PROPERTIES. Lime adds calcium to the soils, which gives a better structure and allows improved air and water retention and flow. It also enhances root settlement and plant growth.
- BIOLOGICAL PROPERTIES. Liming is known to have impacts on both the abundance and community composition of almost all types of soil organisms including bacteria, fungi, archaea, pathogens, nematodes, and earthworms (Table 3.5.1.1). This aspect has an influence on the mineralization of the organic matter, on the elimination of certain organic intermediate products, which might be toxic for plants, and on the transformation processes of the nitrogen in soil.

Table 3.5.1.1. Main impacts of liming on soil biota and associated biological processes (Holland et al., 2018).

Type of organism	Organism change	Associated processes
Bacteria	↑ Abundance Composition change	↑ Decomposition rates Influence on nitrogen cycling and chitinase activity
Details on Rhizobia	Composition change	Improved nodulation and increased N fixation
Fungi	↓ Abundance	↓ aggregate stability ↑ incorporation of carbon into fungal structures
Details on arbuscular mycorrhizal (AM) fungi	↑ AM fungal spore production Changes in AM fungal community composition	Absence of indications
Pathogens	↓ Abundance	↓ Disease
Archea	Shift in composition towards ammonia-oxidizing archea	Absence of indications
Earthworms	↑ Abundance (especially anecic)	↑ Decomposition rates and soil aggregation

Types of liming materials

A liming material shall be a CE marked fertilising product aimed at correcting soil acidity, which then improves physical, chemical, and biological soil properties, containing oxides, hydroxides, carbonates, or silicates of the nutrients calcium (Ca) or magnesium (Mg). Currently, the category of the liming materials accounts for 2.25% (EUR 500 million annually) of the fertiliser market value in Europe (EC, 2016).

Table 3.5.1.2 reports a list of the most common liming materials with their value of Calcium Carbonate Equivalent (CCE). The CCE is a measure of the acid-neutralizing capacity of a liming material compared to pure calcium carbonate, used as the reference compound (CCE equal to 100%). A liming material with a CCE bigger than 100% (e.g., burnt lime and hydrated lime) has a greater capacity to neutralize the soil acidity than pure calcium carbonate; on the contrary, when the value of CCE is lower than 100%, a larger quantity is needed to obtain the same neutralizing effect. In the following, the characteristics of the most used liming materials are reported.

Table 3.5.1.2. Main liming materials, chemical formula, and value of CCE (as adapted from Mullins et al., 2009).

Liming material	Chemical formula	Typical CCE (%)	Main characteristics
Calcium carbonate	$CaCO_3$ (pure)	100	Reference compound
Calcitic limestone (generally referred as agricultural limestone)	$CaCO_3$	80-100	- Slow dissolution → slow-acting agent - Importance of fineness → coarse particles can even not be reactive and never dissolve in soil - easy handling and cheap
Dolomitic limestone	$CaCO_3$-$MgCO_3$	95-108	- Slightly more expensive and less reactive than $CaCO_3$ - Supply of magnesium
Quick lime	CaO	150-179	- Fast-acting agent - Highest neutralising value - Care must be taken during the handling, storage and in the application (possible formation of flakes/granules)
Hydrated lime	$Ca(OH)_2$	120-136	- Fast-acting agent - High neutralizing value
Marl	$CaCO_3$	70-90	- Natural, chalky material - Found in beds as an unconsolidated mixture of materials composed of calcium carbonate, shell fragments, and impurities (mainly sand, silt, and clay)
Ground Oyster Shells	$CaCO_3$	90-100	Hard tissue consisting of calcium carbonate and organic matrices
Wood ash	Ca, Mg and K oxides	40-50	- Ash from wood burning containing oxides and hydroxides of calcium, magnesium, potassium, and sodium with effect on soil acidity

CALCITIC and DOLOMITIC LIMESTONE are commonly used as liming materials because of their low price and more easy handling compared to the alternative products. Since carbonates dissolve very slowly, the fineness of these materials plays an important role in the neutralization of the pH. According to the reference European regulation (EC, 2013), a standard limestone (calcitic or dolomitic type) should meet the following criteria of fineness by wet sieving:

- at least 97% to pass through a 3.15 mm sieve;
- at least 80% to pass through a 1 mm sieve;
- at least 50% to pass through a 0.5 mm sieve.

Dolomitic limestone is slightly more expensive than calcitic and generally reacts more slowly; however, it has the advantage of supplying magnesium.

BURNT LIME is a powdery material that shows the highest neutralizing value among the available products (Table 3.5.1.2) and reacts with the soil much more rapidly than the carbonate forms do. For this reason, it is used when an immediate reaction with the soil is required. Drawbacks of this product include high cost and special attention during the handling, storage and the application. Indeed, after the application, the immediate absorption of water causes the material to form flakes or granules that may harden and become insoluble

because of the formation of $CaCO_3$ on their surface. Only by very thorough mixing with the soil, this problem can be prevented.

HYDRATED LIME is similar to burnt lime in terms of powdery nature, high CCE, and speed of action, but it is easier to handle. This material generally presents a higher cost per mass of sold product compared to limestone or quicklime. However, the selection of a specific liming material from an economical point of view should be based on its price expressed per mass of CCE, by accounting for its neutralizing capacity (Brady, 1969; Havlin et al., 2013).

Consumption of agricultural lime in Europe

The application of lime is performed during available access to the field usually before seeding or animal grazing, i.e. in the early spring or in the fall season when rain, snow, and cycles of freezing and thawing can help lime break down and begin to work. The best advice is to incorporate the product in the ground to bring the best action and to prevent it from recarbonation (in case of use of CaO) or runoff with rain. After a first "major" liming, it is recommended to continue the following years (preservation liming) in order to maintain the optimum pH level reached by the first treatment. Common lime requirements are in the order of some tons per hectare (0.3 - 3 t/ha) every 2-3 years, but the proper dosage depends on the combination of different parameters, such as:

- the initial soil pH and the desired level to be reached/maintained. Depending on the type of soil and on the relative content of the organic matter, the optimum pH level for crop land is 4.5-7.5, while for a permanent grassland it is slightly lower (see Table B.1 and B.2 from CEN 2006 technical specification);
- the soil's buffering capacity, i.e. its ability to resist changes in pH. The buffering capacity of the soil depends on many factors including the texture and the amount of clay and organic matter. All other conditions being equal, a soil with a high level of clay and organic matter can require two or three times the amount of lime compared to a sandy soil with a low organic matter content;
- the soil crop;
- the quality of the liming material, i.e. its chemical composition (neutralizing value), its moisture content, and its fineness.

In the northern European countries, characterized by a predominant presence of acid soils and forests, liming is performed at a relatively high rate (about 2-10 t/ha), every 4-5 years, mainly in the form of calcitic or dolomitic limestone (Biasi et al., 2008). For example, in the United Kingdom, in the year 2015, about 19% of the arable soils and 21% of grasslands showed a pH lower than 6.0 and 5.5, respectively (PAAG, 2015). Almost 60% of the applied liming material was ground limestone with an average application rate of 4 t/ha (DEFRA, 2016). In Germany, a dosage of 3 t/ha of dolomite with a repetition every 3-5 years is recommended (Eichinger et al., 2012).

The use of burnt or hydrated lime in Europe is typical in southern countries like Italy, Spain, and France (EuLA personal communication; Mijangos et al., 2010). Unicalce S.p.A., for example, indicates for Italy a predominant use of CaO as liming material (70% of the current market), suggesting an average dosage of 1 t/ha, sufficient to raise the pH level of the soil by one point. For a more accurate amount, a specific calculator

can be used by entering the type of crop, and data about soil clay content, soil organic matter content, and the measured pH (Unicalce S.p.A., 2019).

3.5.1.2 LIMING, CARBON SEQUESTRATION, AND CLIMATE CHANGE

At least two potential pathways of CO_2 uptake from lime application have been suggested in the scientific literature:

- the potential CO_2 uptake during the neutralization of acidity in the soil;
- the possible long-term increment of the Soil Organic Carbon (SOC) stock in the mineral layer, due to the higher plants yield (higher C_{org} inputs) and the improvement of the soil structure.

Another potential effect related to liming and climate change is the possible mitigation of the nitrification-induced N_2O emission from the agricultural lands.

Potential CO_2 uptake during soil neutralization

Both limestone and lime are used for agriculture applications, but action mode and equilibriums are not the same.

Limestone ($CaCO_3$)

The Tier 1 approach of the IPCC Guidelines for National Greenhouse Gas Inventories (IPCC, 2006) calculates agricultural limestone CO_2 emissions as 100% of the total content of carbon. However, this assumption is challenged by some authors (e.g., West and McBride, 2005/Hamilton et al., 2007), showing that the CO_2 emissions depend on the rate of dissolution of the carbonate mineral and whether such dissolution is driven by the carbonic acid or by other strong acids such as HNO_3.
In a moderate acid soil (pH 5-6.5) or a neutral soil, most of the dissolution of limestone can be ascribed to the carbonic acid weathering, according to the Reaction [1].

$$CaCO_3 + H_2O + CO_2 \rightarrow Ca^{2+} + 2\ HCO_3^- \quad [1]$$

The resulting bicarbonate ($2HCO_3^-$) may remain in the soil or may leach, potentially following the hydrologic flow down rivers and into the oceans.
The portion of bicarbonate remaining into the soil can react with available H^+ to form carbonic acid (H_2CO_3). H_2CO_3 is in equilibrium with soil CO_2, hence, reaction to carbonic acid yields CO_2 that is released to the atmosphere. This latter equilibrium is as follows (Reaction [2]):

$$H_2CO_3 \leftrightarrow CO_2 + H_2O \quad [2]$$

Thus, if the bicarbonate remains into the soil no net emission of CO_2 is generated as a net effect of the chemical Reactions [1] and [2]. The fate of bicarbonate that leaches is more uncertain. West and McBride (2005), for example, assumed that most of the leached bicarbonate reaches the ocean where it is partially precipitated back to $CaCO_3$ by calcite-precipitating organisms, with the emission of CO_2 (0.6 moles per mole of $CaCO_3$). The

United States Department of Agriculture (2014), on the contrary, assumed that all the leached bicarbonate is sequestered for decades to centuries.

In an acid soil, part of the applied $CaCO_3$ can come in contact with strong acids such as HNO_3. When in contact with acidity (H^+), $CaCO_3$ will decompose and release CO_2:

$$CaCO_3 + 2\ H^+ \rightarrow Ca^{2+} + H_2O + CO_2 \quad [3]$$

Table 3.5.1.3 reports the emission factors proposed in the exiting literature for the agriculture limestone application.

Quicklime (CaO) or hydrated lime ($Ca(OH)_2$)

When burnt lime is applied to the soil, it rapidly reacts with water producing hydrated lime in the form of a fine powder:

$CaO + H_2O \rightarrow Ca(OH)_2$ (only in case of a CaO liming material application)

Despite its quite low solubility, calcium hydroxide completely dissociates as Ca^{2+} and $2OH^-$ in the acid soil, since it is a strong base. The hydroxyde ion (OH^-) then reacts with the active acidity, i.e. free hydrogen ions (H^+) in the soil solution and with the other free cations, especially Al^{3+}, to form water and insoluble compounds like $Al(OH)_3$. Due to these reactions, the hydrogen ions (potential acidity) and cations absorbed on the soil colloids are released into the soil solution to maintain the chemical equilibrium and are neutralized in their turn:

$$2H\text{-soil} + Ca^{2+} + 2(OH)^- \rightarrow Ca\text{-soil} + 2H_2O \quad [4]$$

$$2\ Al\text{-soil} + 3Ca^{2+} + 6(OH)^- \rightarrow 3Ca\text{-soil} + 2Al(OH)_3 \quad [5]$$

Dissolved lime can also neutralize the carbon dioxide available in the form of carbonic acid (H_2CO_3):

$$Ca^{2+} + 2(OH)^- + H_2CO_3 \rightarrow CaCO_3\downarrow + 2H_2O \quad [6]$$

$$Ca^{2+} + 2(OH)^- + 2H_2CO_3 \rightarrow Ca(HCO_3)_2 + 2H_2O \quad [7]$$

The resulting calcium bicarbonate [Reaction 7] may be leached down the soil profile and possibly transported to rivers and oceans in the long-term (sequestration from decades to centuries) or can remain in the soil where it is expected to release CO_2 into the atmosphere, though with a slow kinetic.

To the authors' knowledge, the way in which lime reacts and moves within the soil system has not been yet particularly investigated in the scientific literature, also because this process depends on many parameters such as:

- the soil pH and it's buffering capacity;
- the temperature and moisture content;
- the mineralogy and chemical composition of the porous matrix;
- the precipitation and infiltration rate;
- the intensity of the nitrification process, that is facilitated by an intensive use of nitrogen fertilizers. The resulting strong nitric acid (HNO_3) can react with the dissolved lime/produced carbonates according to the following reactions:

$$Ca^{2+} + 2(OH)^- + 2HNO_3 \rightarrow Ca^{2+} + 2NO^{3-} + 2H_2O \quad [8]$$

$$CaCO_3 + 2HNO_3 \rightarrow Ca^{2+} + 2NO^{3-} + H_2O + CO_2 \quad [9]$$

- the type of crops/plants in the analysed area.

In the future, the effects of burnt/hydrated lime neutralization into the soil can be studied by adopting a geochemical modelling approach coupled with laboratory tests. The research could be articulated in two main steps:

- *step 1 - analysis in batch conditions*. The objective of this step is to study the interaction between lime and soil at the equilibrium, according to the variation of the following parameters: 1) dosage of lime; 2) mineralogy and chemical composition of the soil porous matrix; 3) moisture content and temperature; 4) soil pH and buffering capacity;
- *step 2 - 1D transport model*. The objective of this step is to model lime reactions and movement into the system considering the processes of infiltration, leaching, and the other phenomena influencing the fate of the dosed lime (e.g., nitrification and biological activity).

Input data can be derived from the literature or from laboratory and field-dedicated tests.

Table 3.5.1.3. CO_2 net emission or sink during soil neutralisation with limestone reported in the scientific literature.

Literature Source	Geographical site	Comments and conclusions
Guidelines for National Greenhouse Gas Inventories (IPCC, 2006)	Global factor → To be used when a country-specific emission factor lacks	100% of the mass of C is emitted as CO_2 - CALCITIC LIMESTONE: 120 g C/kg limestone (440 g CO_2) - DOLOMITIC LIMESTONE: 130 g C/kg dolomite (478 g CO_2)
Australian Government - Ministry of the Environment and Energy (2018a)	Australia - Methodology for the calculation of the Carbon Credits Units due to the management of a land in a way that increases the soil organic carbon or reduce the CO_2 emission (The Carbon Credits - Carbon Farming Initiative, Act 2011 [1])	
Bernoux et al. (2003) and Cerri (2010)	Brazil - first estimation of CO_2 fluxes from the liming practice of agricultural soils in the period 1990-2000	
Tongwane et al. (2016)	South Africa - national GHG profile produced from the cultivation of field crops	

West and McBride (2005)	Study performed in the Mississippi River Basin, where the vast majority of lime in the U.S.A. is applied	Only 49% of the mass of C is emitted as CO_2 - CALCITIC LIMESTONE: 59 g C/kg limestone (216 g CO_2) - DOLOMITIC LIMESTONE: 64 g C/kg dolomite (235 g CO_2) Main hypotheses of the calculation (calcitic limestone): - 38% of limestone is dissolved by strong acids (Reaction [3]) → + 167 gCO_2/kg $CaCO_3$ - 62% of limestone is dissolved by carbonic acid (Reaction [1]) → - 273 gCO_2/kg $CaCO_3$ -50% of the resulting bicarbonate remains into the soil, is converted into carbonic acid and CO_2 is then released (Reaction [2]) → + 273 gCO_2/kg $CaCO_3$ - 50% of the resulting bicarbonate leaches through the soil and then is transported into the ocean. Here 60% of it precipitated as $CaCO_3$ with the emission of CO_2→ 49 gCO_2/kg $CaCO_3$
Cai et al. (2014)	U.S.A. - CO_2 emission factor from agricultural limestone in the GREET_1 2014 model [2]	Authors assumed an emission factor from agricultural liming equal to 216 g CO_2/kg $CaCO_3$, the value calculated by West and McBride (2005). This factor is considered reasonable for the United States, because limestone is generally applied in the Mississippi River Basin (where the study of West and McBride was performed) or in areas will similar soils and rainfall regimes
USEPA (2019)	U.S.A. - Inventory of U.S. Greenhouse Gas Emissions and Sinks 1990-2017	
Hamilton et al. (2007)	U.S.A. - Authors collected hydrochemical samples from soils and streams draining watersheds of different land use and cover, mostly within southwestern Michigan	- Samples of soil solutions indicated that limestone can act as either a source or a sink for CO_2. However, infiltrating waters, drainage waters and streams draining agricultural watersheds tended to indicate a net CO_2 uptake (25-50% of the carbon limestone content); - When nitrate concentrations increased in infiltrating waters, limestone switched from a net CO_2 sink to a source → a more efficient use of N fertilizers is recommended
United States Department of Agriculture - USDA (2014)	U.S.A. - Report of USDA for the quantification of GHG fluxes in agriculture and forestry	Liming implies a net C sink in the soil equal to 40 g C/kg $CaCO_3$ (-147 gCO_2/kg $CaCO_3$) Main hypotheses of the calculation (calcitic limestone): - 1/3 of limestone is dissolved by strong acids (Reaction [3]) → + 147 gCO_2/kg $CaCO_3$ - 2/3 of limestone is dissolved by carbonic acid (Reaction [1]). The resulting bicarbonate leaches and it is sequestered for decades to centuries → - 293 gCO_2/kg $CaCO_3$

Cho et al. (2019)	Two years-field study on a moderately acidic upland soil, cropped with maize in South Korea. A periodical liming with limestone was performed (2 t/ha)	About 33% of the mass of C in the applied limestone (143 g CO_2/kg $CaCO_3$) is emitted as CO_2 The value derives from: 1) a direct measure of the emitted C by the agricultural upland (94 g CO_2/kg limestone); 2) the emission factor from the oceans proposed by West and McBride, 2005 (49 g CO_2/kg limestone)
Biasi et al. (2008)	Two years-field experiment on a peatland cultivated with a bioenergy crop in eastern Finland. Periodical liming with dolomitic limestone was performed at a rate of 780 g/m^2	15.2% of the applied dolomite (15.4 gCO_2-C/m^2) was released as CO_2 from the managed peatland. All the emission occurred in the first year.

[1] In the year 2011, the Australian Parliament passed The Carbon Credits (Carbon Farming Initiative) Act 2011. This Act enables landholders and farmers to have the opportunity to earn Australian Carbon Credit Units by managing their land in a way that could increase the storage of soil organic carbon or can avoid or reduce the CO_2 emission in the atmosphere. In this context, in the year 2018, a methodology for the determination of the carbon credits was purposed. Through this methodology, landholders should measure the soil carbon stocks at the selected site before implementing the new management project and at regular intervals during the project to estimate the relative carbon sequestration. Emissions from other sources that may change as a result of the project such as emissions from livestock, tillage events and application of lime or synthetic fertilizers must be included into the abatement calculation (Australian Minister for the Environment and Energy, 2018a and 2018b).

[2] The GREET Model is a one-of-a-kind analytical tool that simulates the energy use and emissions output of various vehicle and fuel combinations. This model is sponsored by the U.S. Department of Energy's (DOE), Office of Energy Efficiency and Renewable Energy (https://greet.es.anl.gov/).

Effect of liming on Soil Organic Carbon (SOC) stocks

Soil is a large reservoir of organic carbon. The global SOC storage in the upper 1-m layer of soil has been estimated at about 1500 Gt, equal to 60% of the total carbon in the terrestrial ecosystem (Lal et al., 2004). In the last 150 years, human activities have led to a depletion of SOC levels, mainly due to soil tillage, accelerated erosion, leaching, and plant and crop residues removal or burning. This depletion has created a soil carbon sink capacity, that now represents an opportunity to increase the carbon storage (Lal et al., 2009). In particular, for the European context, 50% of the arable soil is classified as low in soil carbon and more than 10 million ha are subjected to strong erosion. For this reason, the European Commission recently funded the specific Focus Group on "*Moving from source to sink in arable farming*" with the aim of identifying agricultural practices that can enhance carbon storage in the long term (reduced tillage techniques and precision farming, crop rotations, cover crops, intercropping, organic and fertiliser amendments from local sources, regulating irrigation water use). The Focus Group composed of farmers, researchers and advisers discussed success and failure factors for the adoption of these practices, and their transferability to different conditions. They also identified knowledge gaps and research needs (eip-agri, 2019). Recently, also the Joint Research Centre published a study on the same theme (Lugato et al., 2018 from JRC). In the research, a biogeochemistry model was applied on 8,000 soil sampling locations in the European Union to quantify the net CO_2 equivalent fluxes associated to C-mitigating agricultural practices. Results show that significant CO_2 mitigation can be achieved in the first twenty years by any soil carbon management scheme. However, particular attention should be paid on practices introducing additional N to the soil (e.g., N-fixing cover crops) that can potentially turn the agroecosystems from a GHG sink source to a net GHG in the long term due to the increased N_2O emissions over the time.

Regarding the agricultural use of lime, the influence of liming on SOC sequestration has been studied in recent years (Goulding et al., 2016). In general terms, the net effect of liming can be the result of three main processes (Figure 3.5.1.1):

1) INCREASE OF BIOLOGICAL ACTIVITY AND MINERALIZATION OF THE ORGANIC MATTER. In the short-term, liming increases the soil microbial activity, thus favouring the soil respiration rate and the mineralization of the organic matter, with CO_2 release into the atmosphere;
2) IMPROVEMENT OF SOIL AGGREGATION AND STRUCTURAL STABILITY. Positive effects of liming on the soil structure can be ascribed to the flocculating and cementing actions of the calcium ions and of the newly precipitated Al-hydroxy polymers. In particular, the high Ca^{2+} concentration can result in the compression of the double layer between clay particles, thereby decreasing the repulsive force between them. Moreover, increased microbial activity can favour aggregate stability, since biomass produces extracellular gelatinous polysaccharides that act as binding agents in the soil (Haynes et al., 1998). These improvements and the strengthening of the soil structure limit the biodegradation of SOC within soil aggregates;
3) INCREASE OF PLANT PRODUCTIVITY. In the long-term, periodical liming increases the plant yields and thus the return of the organic matter into the soil in the form of dying roots and decaying crop residues.

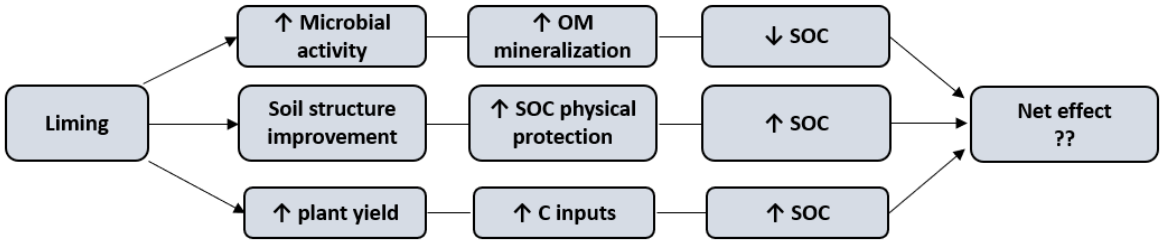


Figure 3.5.1.1. Potential effects of liming on SOC (Paradelo et al., 2015).

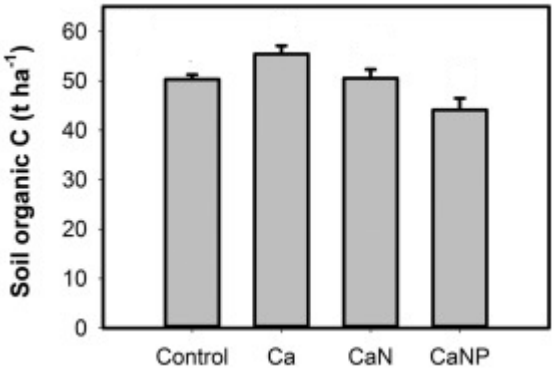
The net effect of these counteracting but interactive processes on SOC levels is not well understood yet.
A dozen cases of field-based measurements associated to a quantitative evaluation of the liming impacts on SOC stocks around Europe were found in the scientific literature (See the Appendix B). In each field-experiment, limed and un-limed soil plots from humus and mineral layers were accurately compared in terms of either Organic Carbon Content - TOC (g C/kg soil) or SOC stocks, i.e. the amount of organic C in a fixed layer of the soil per unit area (Lefèvre et al., 2017):

$$SOC\ \left(\frac{tC}{ha}\right) = TOC\ \left(\frac{gC}{kg_{fine\ soil}}\right) \times BD\left(\frac{kg_{soil}}{m^3}\right) \times layer\ depth\ (m) \times FE\ \left(\frac{kg_{fine\ soil}}{kg_{soil}}\right) \times \left(\frac{10{,}000\ m^2}{1\ ha}\right) \qquad [10]$$

Where:
TOC = total organic carbon content in the fine soil (< 2mm). In a soil free of carbonates, the total C represents also the organic carbon; otherwise, TOC is calculated as the difference between the total carbon and the mineral carbon;
BD = bulk density of the analysed sample (dry weight of a known volume of soil);
FE = relative contribution of the coarse fragment-free soil (fragments < 2mm) to the total soil mass.

Only in three analysed case studies (Table 3.5.1.4), limed plots received a periodical application of burnt lime (Mijangos et al., 2010/Paradelo et al., 2015) or hydrated lime (Sochorová et al., 2016); in the other studies the use of limestone (dolomitic or calcitic type) was predominant. The study by Mjangos et al. (2010) was related to a short time span, i.e. the sampling was made only six months after liming, while the other two studies evaluated the effects in the long-term, after seven decades (Sochorová et al., 2016) or eight decades (Paradelo et al., 2015).
In the shorter field study (Mijangos et al., 2010), no significant variation of the organic carbon content in the analysed mountain grasslands was detected, as this parameter is known to change very slowly over time and, therefore, at least 5-10 years may be required to see a possible change. On the contrary, the long-term studies showed that a regular liming corresponds to higher SOC stocks in the soil, though with an increment that is very variable. In Sochorová et al. (2016) the average difference in the SOC stocks between limed and control plots was equal to 5 tC/ha in the analysed period (about 77 kgC/ha every year), while in Paradelo et al. (2015) the same parameter was only 1.1 kgC/ha/year (Table 3.5.1.4).
This huge difference can be related to the land use. In the first study, related to a grassland area, the higher effects of liming can be attributed to the increased productivity of plants and so to the increased return of organic matter into the soil. In the second study, focused on a bare fallow area, no plant growth has been allowed for 80 years and so only the effect associated with the improvement of the soil structure was seen.

The study performed by Sochorová et al. (2016) also underlined that the positive liming-induced effects on SOC may be significantly reduced when the lime is added together with mineral N/P fertilizers (Figure 3.5.1.2).



LEGEND (Dosage reported in kg/ha/year)

Control: unfertilized plot

Ca: Lime as $Ca(OH)_2$ - 715 Ca

CaN: 100N, 752 Ca

CaNP: 100N, 35 P, 936 Ca. P fertiliser is applied in the form of Ca_3PO_4

Figure 3.5.1.2. SOC stocks in the topsoil (0-10 cm) of a grassland in the Eifel Mountains (western Germany) as affected by the management treatments. The Figure is from Sochorová et al. (2016).

Current available literature is not sufficient to predict the net effect of burnt/hydrated lime on SOC stocks under different conditions. The number of analysed studies on the topic (3 papers) is still insufficient and only related to grasslands and a bare fallow area. The future research should consider the following aspects:

- additional data on SOC stocks in limed/un-limed corresponding samples should be collected through field experiments around Europe, considering a wider range of land use and soil types. In particular, there is a lack of data about $CaO/Ca(OH)_2$ liming effects on forest soils and croplands. In relation to this aspect, Paradelo et al. (2015) underlined that SOC data may be already available (the determination of this parameter is routinely performed in most laboratories) but they were not yet published, simply because it is not considered of primary importance;
- SOC stocks variation should be investigated on a long-term time span (i.e. decades), since at least 10 years are required to detect the effect of the changed management practice on the soil organic carbon levels (eip-agri, 2019);
- comparison of results among the different studies should be facilitated, by: 1) providing detailed data in terms of soil characteristics, land use, experimental design, sampling procedures, type and amount of liming, time span (see Table 3.5.1.4 and Table C.1, as an example); 2) by following the reference protocol for the assessment of SOC stocks proposed by the European Union (Stolbovov et al., 2007) In particular, some published studies report only the measure of the TOC parameter, giving a partial overview of the SOC change into the soil (Paradelo et al., 2016). It is thefore important to measure the soil bulk density in limed and control plots (the parameter could have been reduced by liming; Chan et al., 2007) and then to calculate the corresponding SOC stocks according to the Formula 10 (See page 11);
- the interaction between liming effects on SOC and other contextual management practices, such as fertilisation, should be better investigated. Sochorova et al. (2016), indeed, showed that the positive liming-induced effects on SOC stocks may be significantly reduced when lime is added together with inorganic fertilisers.

Table 3.5.1.4. List of liming field experiments with burnt or hydrated lime: field characteristics, way of sampling, liming dosage, and impacts on TOC/SOC stocks. All the scientific papers are related to the European context.

Literature source	Geographical site	Type of soil and land use	Investigated soil horizon	Liming application		TOC or SOC stocks		Main comments and conclusions
				Type of product	Amount (t/ha)	Limed plot	Un-limed plot	
Study 1 Mijangos et al. (2010)	Arraba area (Basque country, Spain)	Typic Dystrudept Calcareous grassland	0-10 cm depth	Burnt lime (92% CaO)	2.43 t/ha Sampling six months after the application	58 g/kg	52 g/kg	1) Liming did not result in any significant change in OC content 2) OC content in soil changes very slowly over the time → about 5-10 years are required to see possible significant changes
	Kurtzegan area (Basque country, Spain)	Aeric Humaquept Siliceous grassland				169 g/kg	186 g/kg	
Study 2 Sochorová et al. (2016)	Eifel Mountains (Western Germany)	Pseudogley soil Nardetum grassland	0-10 cm depth	$Ca(OH)_2$	Scenario only lime: 715 kg Ca/ha/year (sampling taken after 70 years)	55.5 tC/ha	50.1 tC/ha	1) Positive liming-induced effects on SOC stocks. Advantages were significantly reduced when lime is applied together with the inorganic fertilizers 2) Agricultural fertilization aimed at the maximization of the production partly or fully negates the C sequestration potential in a grassland ecosystem
					Scenario combination of lime and N/P mineral fertilizers: 100 kg N/ha/year 35 kg P/ha/year 936 kg Ca/ha/year[1]	44.0 tC/ha	50.1 tC/ha	
Study 3 Paradelo et al. (2015)	Versailles (France)	Luvisol soil Bare fallow	0-20 cm	CaO	1 t/ha Sampling after 80 years	1.5 t/ha	1.41 t/ha	1) Limed plots showed slightly higher SOC stocks than un-limed plots. In limed plots the aggregate stability was higher and the macrostructure better developed 2) The C protected by the gain in structure due to liming corresponded to a small gain in SOC stock

[1] The P mineral fertilizer is applied in the form of Ca_3PO_4 and was not counterbalanced by reducing the lime input in the same treatment.

Effect of liming on N_2O emissions

Looking at the more general problem of climate change, liming has been shown to affect the nitrification-induced N_2O emission from agricultural lands and forests. For example, in Germany, Brumme and Beese (1992) observed a reduction of N_2O emission in limed plots of a beech forest from 5.6 to 1.5 kg N_2O-N/ha/year, 5 years after liming. Similar indications were derived by Borken and Brumme (1997), who observed that a periodical superficial liming of acidic forest soils resulted in a reduction of the N_2O emission by 9-62% on average. In both cases, the liming material was dolomitic limestone.

More recently, Hénault et al. (2019) confirmed the role of liming in decreasing N_2O emissions during some experiments at the field scale carried out in France on acidic soils. The abatement of N_2O emissions was obtained in the range 26-66%, following a rapid increase in the soil pH. The average potential abatement of N_2O emissions due to liming was estimated at 49%, but the authors recommend that the deployment of this solution should be based on site-specific assessment.

However, some studies on the same topic have assessed an increase of N_2O emission from limed soils, justified by the fact the liming can increase the availability of soil nitrate, which is a substrate for N_2O formation through denitrification. For example, the application of CaO to black fertilized soils (Mollisol)[25] in China generated a cumulative N_2O emission that was 1.6 - 4 times higher than the reference situation (Han et al., 2011; see Table 3.5.1.5). Further research on this topic is therefore necessary. Timing of liming and nitrogen application has to be also taken into account.

Table 3.5.1.5. Cumulative N_2O-N emission from a black soil in China, in different fertilisation conditions (Han et al., 2011). Soil samples (soil moisture equal to 60%) were incubated at 25°C for 144 hours.

Geographical Site	**Type of soil and land use**	**Investigated soil horizon**	**Type of fertilisation**	**Cumulative N_2O emission (144 hours incubation)**	
				Limed	**Un-limed**
Heilongjiang Province (China)	Black soil (Mollisol) Loess clay	0-20 cm depth	Fertilisation with ammonium	576 µg N/kg	362 µg N/kg
			Fertilisation with nitrate	1669 µg N/kg	421 µg N/kg
			No fertilisation	53 µg N/kg	69 µg N/kg

[25] Mollisol is generally defined as a soil with a thick dark surface horizon (mollic epipedon) rich in organic matter. This soil develops on grasslands, a vegetation that has extensive fibrous root systems and it is typically saturated with basic cations (Ca^{2+}, Mg^{2+}, Na^{+}, and K^{+}).

3.5.1.3 CONCLUSIONS AND RECOMMENDATION ON RESEARCH NEEDS IN AGRICULTURE

In the current scientific literature, two potential pathways of CO_2 uptake from agricultural lime/limestone application have been suggested:

- the potential CO_2 uptake during the neutralization of acidity in the soil;
- the possible long-term increase of the Soil Organic Carbon (SOC) stocks in the mineral layer.

Regarding the effect of liming during neutralization, the existing literature focuses on the application of limestone ($CaCO_3$), mainly in contexts outside Europe (e.g., USA, Australia, and Brazil).
The IPCC Guidelines report a CO_2 emission factor equal to 100% of the total carbon in the limestone. However, this assumption is challenged by some authors (e.g., West and McBride, 2005/Hamilton et al., 2007), showing that the CO_2 emission/uptake depends on the rate of dissolution of the carbonate mineral and whether such dissolution is driven by the carbonic acid (with a sequestration of CO_2 from the atmosphere) or by other strong acids such as HNO_3 (release of CO_2).
In the future, the effects of burnt/hydrated lime neutralization into the soil should be deeply studied in the European context, by adopting a geochemical modelling approach coupled with laboratory tests.

Concerning the effect of liming on the soil organic carbon, the current scientific literature is not sufficient to give strong conclusions about the topic. In some cases, an increment of the SOC stocks or TOC was detected, probably caused by a higher C_{org} input into the limed soil for the increased yield productivity. On the other side, reductions have also been reported, probably in connection with the increased mineralisation process. In the future, additional data should be collected through field experiments around Europe, by considering the following aspects:

- inclusion of a wide range of land uses, soil types, and liming reagents (currently there are very few studies for burnt and hydrated lime);
- analysis of the unpublished SOC data from past in situ experiments in Europe. The determination of this parameter is routinely performed in laboratories, but results are not always published, maybe because not considered of primary importance;
- investigation on a long-term time span (i.e. decades), since at least 10 years are required to detect the effect of liming on the soil organic carbon levels;
- comparison of the results among the different field studies, by promoting the use of a reference protocol and guidelines for the assessment of SOC stocks;
- better investigation of the interaction between liming effects and other contextual management practices, such as the fertilisation.

REFERENCES

Australian Minister for the Environment and Energy, Josh Frydenberg, 2018a. *Explanatory statement - Carbon Credits (Carbon Farming Initiative - Measurement of Soil Carbon Sequestration in Agricultural Systems) Methodology Determination 2018 (Including the Supplement Document)*. Document of 25/01/2018. Available online: https://www.legislation.gov.au/Details/F2018L00089

Australian Minister for the Environment and Energy, Josh Frydenberg, 2018b. *Explanatory statement - Carbon Credits (Carbon Farming Initiative - Measurement of Soil Carbon Sequestration in Agricultural Systems) Methodology Determination 2018*. Authorised Version registered to F2018L0089 in 07/02/2018.

Available online: https://www.legislation.gov.au/Details/F2018L00089/Explanatory%20Statement/Text

Bernoux, M., Volkoff, B., Carvalho, M., Cerri, C.C., 2003. *CO_2 emissions from liming of agricultural soils in Brazil*. Global Biogeochemical Cycles 17(2), 1-4. DOI: 10.1029/2001GB001848

Biasi, C., Lind, S.E., Pekkarinen, N.M., Huttunen, J.T., Shurpali, N.J., Hyvönen, N.P., Repo, M.E., Martikainen, P.J., 2008. *Direct experimental evidence for the contribution of lime to CO_2 release from managed peat soil*. Soil Biology & Biochemistry 40 (10), 2660-2669. DOI: 10.1016/j.soilbio.2008.07.011

Blume, H-P., Brümmer, G.W., Horn, R., Scheffer, F., Kandeler, E., Knabner, IK, Kretzschmar, R., Stahr, K., Wilke, B-M., 2009. *Scheffer/Schachtschabel: Lehrbuch der Bodenkunde*. Spektrum Akademischer Verlag. ISBN: 9783827422514

Borken, W. and Brumme, R., 1997. *Liming practice in temperate forest ecosystems and the effects on CO_2, N_2O and CH_4 fluxes*. Soil Use and Management 13 (s4), 251-257. DOI: https://doi.org/10.1111/j.1475-2743.1997.tb00596.x

Brady, N.C., 1969. *Chapter 15: lime and its soil-plant relationships*. In: the nature and properties of soils, 7th edition. MCMILLAN CO. ISBN-10: 0023165200

Brumme, R., and Beese, F., 1992. *Effects of liming and nitrogen fertilization on emissions of CO_2 and N_2O from a temperate forest*. Journal of geophysical research 97 (D12), 12851-12858. DOI: https://doi.org/10.1029/92JD01217

Cai, H., Wang, M., Han, J., 2014. *Update of the CO_2 emission factor from agricultural liming*. GREET Publications, Argonne National Laboratory. Available online: https://greet.es.anl.gov/publications

CEN - European Committee for Standardization, 2006. *Liming materials - Determination of the lime requirement - Guidelines, principles, and parameters*. Management Centre: rue de Stassart, 36 Brussels.

Cerri, C.C., 2010. *Management practices for greenhouse gas emission reduction and carbon removal in brazilian agriculture, livestock, and forestry*. Centro de Energia Nuclear na Agricultura - CENA/USP. Available online: http://www.fbds.org.br/fbds/IMG/pdf/doc-410.pdf

Chan, K.Y., Conyers, M.K., Scott, B., 2007. *Improved structural stability of an acidic hardsetting soil attributable to lime application.* Communications in soil science and plant analysis 38 (15), 2163-2175. DOI: 10.1080/00103620701549108

Cho, S.R., Jeong, S.T., Kim, G.Y., Lee, J.G., Lee, G.J., Kim, P.J., Kim, G.W, 2019. *Evaluation of the carbon dioxide (CO_2) emission factor from lime applied in temperate upland soil*. Geoderma 337, 742-748. DOI: https://doi.org/10.1016/j.geoderma.2018.10.007

Department for Environment, Food & Rural Affairs - DEFRA, 2016. *The British survey of fertiliser practice - fertiliser use on farm crops for crop year 2015*. ISBN 978-0-99297-351-3. Available online: https://assets.publishing.service.gov.uk/government/uploads/system/uploads/attachment_data/file/516111/fertiliseruse-report2015-14apr16.pdf

EC - European Commission, 2013. *Commission Regulation (EU) No 463/2013 of 17 May 2013 amending Regulation (EC) No 2003/2003 of the European Parliament and of the Council relating to fertilisers for the purposes of adapting Annexes I, II and IV thereto to technical progress*. Official Journal of the European Union L134, pp: 1-14. Available online: https://eur-lex.europa.eu/legal-content/EN/TXT/?uri=CELEX:32013R0463

EC - European Commission, 2016. *Circular Economy Package - Proposal for a regulation of the European Parliament and of the Council laying down rules on the making available on the market of CE marked*

fertilising products and amending Regulations (EC) No 1069/2009 and (EC) No 1107/2009. SWD (2016) 65 final, Brussels, 17.03.2016. Available online:

https://ec.europa.eu/transparency/regdoc/rep/10102/2016/EN/SWD-2016-64-F1-EN-MAIN-PART-1.PDF

Eichinger, M.M. and Eckmüllner, O., 2012. *60 Jahre Waldbodenkalkung im Habsburg-Lothringen'schen Gut Persenbeug. Eine ökonomische und ökologische Auswertung (60 years forest soil liming in Habsuburg Lorreine Gut Persenbeug. An economic and ecological evaluation).* Performed by Höhere Lehranstalt für Umwelt und Wirtschaft des Zisterzienserstiftes Zwettl. Available online:

http://cms.hluwyspertal.ac.at/hluwweb/images/Downloads/Umweltlabor/20120606_finale_waldkalkungsbroschuere.pdf

eip-agri - agriculture & innovation, 2019. *Focus Group Moving from source to sink in arable farming. Final report June 2019*. Focus Group funded by the European Commission.

Available online: https://ec.europa.eu/eip/agriculture/en/publications/eip-agri-focus-group-moving-source-sink-arable

Fornara, D.A., Steinbeiss, S., McNamara, N.P., Gleixner, G., Oakley, S., Poulton, P.R., Macdonald, A.J., Bardgett, R.D, 2011. *Increases in soil organic carbon sequestration can reduce the global warming potential of long-term liming to permanent grassland*. Global Change Biology 17 (5), 1925-1934. DOI: 10.1111/j.1365-2486.2010.02328.x

Goulding, K.W.T., 2016. *Soil acidification and the importance of liming agricultural soils with particular reference to the United Kingdom*. Soil Use Management 32 (3), 390-399. DOI: 10.1111/sum.12270

Grieve, I.C., Davidson, D.A., Bruneau, P.M.C., 2005. *Effects of liming on void space and aggregation in an upland grassland soil.* Geoderma 125 (1-2), 39-48. DOI: https://doi.org/10.1016/j.geoderma.2004.06.004

Hamilton, S.K., Kurzman, A.L., Arango, C., Jin, L., Robertson, G.P., 2007. *Evidence for carbon sequestration by agricultural liming*. Global biogeochemical cycles (21) 2, 1-12. DOI: https://doi.org/10.1029/2006GB002738

Han, Z., Zhang, X., Qiao, Y., Wang, L., 2011. *Alkaline ameliorants increase nitrous oxide emission from acidified black soil in northeastern China.* Journal of Environmental Sciences 23 (Supplement), S45-S48. DOI: https://doi.org/10.1016/S1001-0742(11)61075-9

Havlin, J.L., Tisdale, S.L., Nelson, W.L., Beaton, J.D, 2013. *Soil fertility and Fertilizers: an introduction to nutrient management*, 8th edition. Publisher: Pearson, ISBN-10**:** 9780135033739

Haynes, R.J. and Naidu, R., 1998. *Influence of lime, fertilizer and manure applications on soil organic matter content and soil physical conditions: a review*. Nutrient Cycling in Agroecosystems 51, 123-137. DOI: https://link.springer.com/content/pdf/10.1023%2FA%3A1009738307837.pdf

Hénault, C., Bourennane, H., Ayzac, A. et al. Management of soil pH promotes nitrous oxide reduction and thus mitigates soil emissions of this greenhouse gas. Sci Rep 9, 20182 (2019). https://doi.org/10.1038/s41598-019-56694-3

Holland, J.E., Bennett, A.E., Newton, A.C., White, P.J., McKenzie, B.M., George, T.S., Pakeman, R.J., Bailey, J.S., Fornara, D.A., Hayes, R.C., 2018. *Liming impacts on soils, crops and biodiversity in the UK: A review*. Science of the Total Environment 610-611, 316-332. DOI: https://doi.org/10.1016/j.scitotenv.2017.08.020

Intergovernmental Panel on Climate Change, 2006. Chapter 11: *N_2O emissions from managed soils and CO_2 emissions from lime and urea application.* In: IPCC Guidelines for National Greenhouse Gas Inventories. Available online:

https://www.ipcc-nggip.iges.or.jp/public/2006gl/pdf/4_Volume4/V4_11_Ch11_N2O&CO2.pdf

Lal, R., 2004. *Soil carbon sequestration impacts on global climate change and food security*. Science 304 (5677), 1623-1627. DOI: 10.1126/science.1097396

Lal, R., 2009. *Sequestering atmospheric carbon dioxide*. Critical reviews in Plant Science 28(3), 90-96. DOI: https://www.tandfonline.com/doi/pdf/10.1080/07352680902782711?needAccess=true

Lefèvre, C., Fatma, R., Viridiana, A., Liesl, W., 2017. *Soil organic carbon, the hidden potential. Food and* Agriculture Organization of the United Nations, Rome (Italy). ISBN 978-92-5-109681-9

Lugato, E., Leip, A., Jones, A., 2018. *Mitigation potential of soil carbon management overestimated by neglecting N_2O emissions*. Nature Climate Change 8(3), 219-223. DOI: 10.1038/s41558-018-0087-z

Mijangos, I., Albizu, I., Epelde, L., Amezaga, I., Mendarte, S., Garbisu, C., 2010. *Effects of liming on soil properties and plant performance of temperate mountainous grasslands.* Journal of Environmental Management 91 (10), 2066-2074. DOI: 10.1016/j.jenvman.2010.05.011

Mullins, G.L., Alley, M.M., Wysor, W.G., Phillips, S.B., 2009. *Sources of lime for acid soils in Virginia*. Publication 452-510, produced by Communications and Marketing, College of Agriculture and Life Sciences, Virginia Polytechnic Institute and State University. Available online: https://www.researchgate.net/publication/242590369_Sources_of_Lime_for_Acid_Soils_in_Virginia

Nilsson, S.I., Andersson, S., Valeur, I., Persson, T., Bergholm, J., Wirén, A., 2001. *Influence of dolomite lime on leaching and storage of C, N, and S in a Spodosol under Norway spruce (Picea abies (L.) Karst.)*. Forest Ecology and Management 146 (1-3), 55-73. DOI: 10.1016/S0378-1127(00)00452-7

Paradelo, R., Virto, I., Chenu, C., 2015. *Net effect of liming on soil organic carbon stocks: a review*. Agriculture, Ecosystems & Environment 202, 98-107. DOI: https://doi.org/10.1016/j.agee.2015.01.005

Persson, T., Rudebeck, A., Wirén, A., 1995. *Pools and fluxes of carbon and nitrogen in 40-year-old forest liming experiments in Southern Sweden*. Water, Air, and Soil Pollution, 85(2), 901-906. DOI: https://doi.org/10.1007/BF00476944

Poulton, P.R., Pye, E., Hargreaves, P.R., Jenkinson, D.S., 2003. *Accumulation of carbon and nitrogen by old arable land reverting to woodland*. Global Change Biology 9 (6), 942-955. DOI: https://doi.org/10.1046/j.1365-2486.2003.00633.x

Professional Agricultural Analysis Group - PAAG, 2015. *Collection of data from routine soil analysis in the UK*. Available online: http://www.nutrientmanagement.org/

Šimek, M., Hopkins, D.W., Kalčík, J., Picek, T., Šantrůčková, H., Staňa, J., Trávník, K., 1999. *Biological and chemical properties of arable soils affected by long-term organic and inorganic fertilizer applications*. Biology and Fertility of Soils 29 (3), 300-308. DOI: https://doi.org/10.1007/s003740050556

Sochorová, L., Jansa, J., Verbruggen, E., Hejcman, M., Schellberg, J., Kiers, E.T., Johnson, N.C., 2016. *Long-term agricultural management maximizing hay production can significantly reduce belowground C storage*. Agriculture, Ecosystems & Environment 220, 104-114. DOI: https://doi.org/10.1016/j.agee.2015.12.026

Šrámek, V., Fadrhonsová, V., Vortelová, L., Lomský, B., 2012. *Development of chemical soil properties in the western Ore Mts. (Czech Republic) 10 years after liming*. Journal of Forest Science 58 (2): 57-66. DOI: 10.17221/72/2011-JFS

Stolbovoy, V., Montanarella, L., Filippi, N., Selvaradjou, S-K, Panagos, P., Gallego, J., 2005. *Soil sampling protocol to certify the changes of organic carbon stock in mineral soils of European Union*. European Commission-JRC.

Available online: http://publications.jrc.ec.europa.eu/repository/bitstream/JRC32323/EUR21576.pdf

Unicalce S.p.A., 2019. *Calculation tool for liming requirement*. Available online: https://www.unicalce.it/en/calculation-tool/

Tongwane, M., Mdlambuzi, T., Moeletsi, M., Tsubo, M., Mliswa, V., Grootboom, L., 2016. *Greenhouse gas emissions from different crop production and management practices in South Africa*. Environmental Development, 19(90), 23-35. DOI: https://doi.org/10.1016/j.envdev.2016.06.004

United States Department of Agriculture - USDA, 2014. *Quantifying Greenhouse Gas Fluxes in Agriculture and Forestry: Methods for Entity-Scale inventory*. USDA Technical Bulletin 1939. Available online: https://www.usda.gov/oce/climate_change/Quantifying_GHG/USDATB1939_07072014.pdf

United States Environmental Protection Agency – USEPA, 2019. *Inventory of U.S. Greenhouse Gas Emissions and Sinks* 1990-2017. Available online: https://www.epa.gov/sites/production/files/2019-04/documents/us-ghg-inventory-2019-main-text.pdf

Von Uexküll, H.R. and Mutert, E., 1995. *Global extent, development and economic impact of acid soil*. Plant and Soil 171 (1), 1-15. Available online: https://www.jstor.org/stable/42947399

Wellbrock, N., Bolte, A., Flessa, H., 2016. *Dynamik und räumliche Muster forstlicher Standorte in Deutschland: Ergebnisse der Boden-zustandserhebung im Wald 2006 bis 2008*. Braunschweig: Johann Heinrich von Thünen-Institut, Thünen Report 43. DOI: 10.3220/REP1473930232000

West, T.O., McBride, A.C., 2005. *The contribution of agricultural lime to carbon dioxide emissions in the United States: dissolution, transport, and net emissions***.** Agriculture, Ecosystems and Environment 108 (2), 145-154. DOI: https://doi.org/10.1016/j.agee.2005.01.002

3.5.2 USE OF LIME IN OTHER AGRICULTURE APPLICATIONS

In addition to the applications mentioned in the previous chapter, lime is also used in agriculture as biocide for destroying harmful organisms. Information about carbonation of lime as biocide was not available in the literature.

3.6 USE OF LIME IN THE CHEMICAL INDUSTRY

3.6.1 USE OF LIME IN CALCIUM CARBIDE

Calcium carbide (CaC_2) is mainly used in the production of Acetylene (C_2H_2), where lime (CaO) is first reduced by reacting with a source of carbon, e.g. petroleum coke, according to Reaction 3.6.1. Then, calcium carbide reacts with water producing gaseous acetylene and liquid calcium hydroxide ($Ca(OH)_2$) as indicated in Reaction 3.6.2 (IPCC, 2006).

$$CaO + 3C \rightarrow CaC_2 + CO \qquad \text{[Reaction 3.6.1]}$$

$$CaC_2 + 2H_2O \rightarrow C_2H_2 + Ca(OH)_2 \qquad \text{[Reaction 3.6.2]}$$

Since excess water is supplied to the reaction, the by-product of acetylene is a suspension of calcium hydroxide in water that is called carbide lime or also carbide lime slurry. The suspension obtained is settled in tanks in order to recover water, that is recycled in the process, and more concentrated carbide lime with 25-30% of dry matter. Additional water can be removed through press-filtering, reaching 50% of dry matter in carbide lime. Globally, the amount of carbide lime produced is around 500 thousand metric tons per year (EIGA, 2017).

The dry matter of carbide lime slurry is composed mostly of calcium hydroxide (85-95%) with minor parts of calcium carbonate (1–10%), unreacted carbon and silicates (1–3%). Furthermore, carbide lime can contain metals (Mg, Br, Sr, Cd, Cu, Pb, Fe, Mn, Ni and Zn). For this reason and its basic pH (higher than 12), carbide lime should be managed with care. However, carbide lime is not considered as a waste, since its properties are quite similar to hydrated lime produced from limestone. Thus, carbide lime finds applications in agriculture and other sectors that are summarized in Table 3.6.1. Therefore, carbide lime use in substitution of hydrated lime gives environmental benefits because it avoids the hydrated lime production and the related impacts (Cardoso et al., 2009).

Table 3.6.1. Sectors where carbide lime is used according to its $Ca(OH)_2$ content, expressed as percentage on wet matter (EIGA, 2017).

Carbide lime slurry containing 25-30% of $Ca(OH)_2$	Carbide lime slurry containing 50% of $Ca(OH)_2$
• In sugar plants for cleaning beet juice (to flocculate the impurities) or washing the beets or in the plant's water treatment or facilitating cake pressing. • For surface treatment in plants that use acid baths and phosphate baths. • In wastewater treatment. • In smoke treatment	• In liming soil to correct pH. • In road construction work for soil stabilization.

Another use of carbide lime slurry is for producing Precipitated Calcium Carbonate (PCC) which should meet high purity requirement for its utilization, e.g. as artificial pigment in paper production

or as drug carriers in pharmaceutics (Jimoh et al., 2016). Jimoh et al. studied the characteristics and crystal morphology of PCC obtained from carbide lime under different condition of temperature, CO_2 flow rate, total dissolved solid and carbide lime concentration. The result of the study is that under reaction conditions of 2M carbide lime concentration, final pH of 6.98, reaction time of 90 minutes and CO_2 flowrate of 452.30 mL/min, the purity of PCC was 99%, then meeting the end user requirement.

Altiner (2019) studied the use of carbide lime for PCC production as a way for sequestrating CO_2 from flue gas and storing it in calcium carbonate under accelerated carbonation condition, while Morales-Flórez et al. (2015) studied the natural carbonation process of calcium oxide obtained through heating carbide lime as CO_2 mineral sequestration process. Altiner (2019) found that the ratio of CO_2 converted into solid carbonate phase was in the range of 31–95% when bubbling into the slurry a mixture of CO_2/N_2 flow rate of 0.75 L min^{-1} with CO_2 concentration of 16.30%. The highest conversion ratio of CO_2 into $CaCO_3$ was obtained at specific experimental condition of reaction temperature (80°C), stirring speed (300 rpm), solid-to liquid ratio (1.5% by weight), and amount of Na-oleate (2% by weight of obtained $CaCO_3$). Meanwhile, Morales-Flórez et al. analysed the natural carbonation of samples made of calcium oxide that was produced by heating the carbide lime slurry at two different temperatures, i.e. 600°C and 800°C. Then, the increase of the samples mass due to natural carbonation was measured up to 4000h. The samples weight increased up to 1.7 times compared to their initial one. This value is around 95% of 1.79 that is the ratio of the molecular weights of calcium carbonate (100 g/mol) and calcium oxide (56 g/mol). Thus, all samples reached 95% carbonation rate, but samples pre-heated at 600°C carbonated faster than samples pre-heated at 800°C, i.e. respectively after around 500 hours and 800 hours, as shown by Figure 3.6.1. The difference is due to the lower particle size of the samples pre-heated at 600°C and consequently to their higher active area surface.

In conclusion, the carbonation of lime used in calcium carbide depends on the actual use of the carbide lime, that is the by-product of the main application of calcium carbide, i.e. the acetylene production.

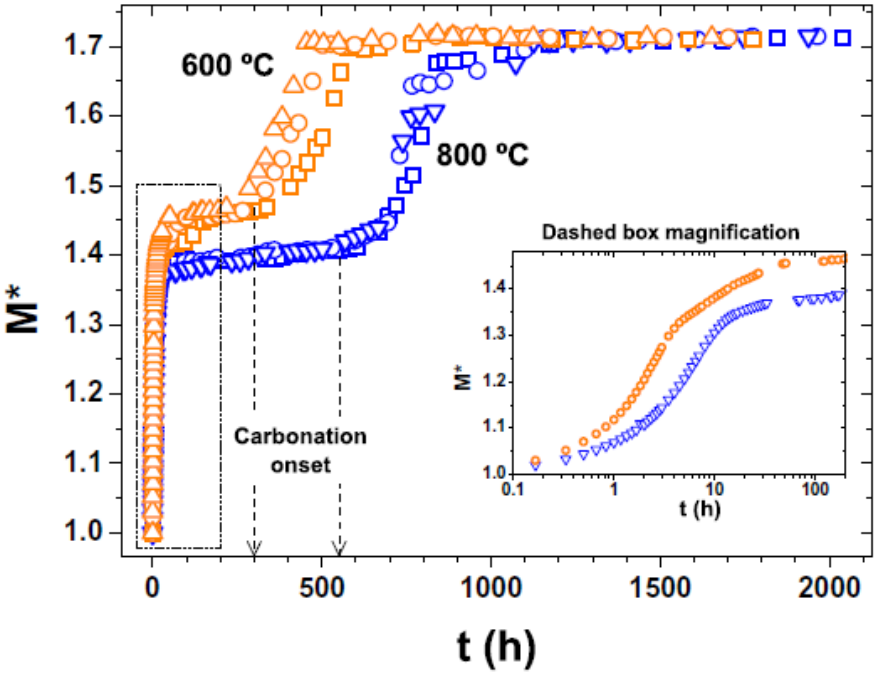


Figure 3.6.1. Increase of the normalized mass of the two samples pre-heated at 600°C and 800°C, respectively coloured in orange and in blue. Inset magnifies first 200 h of weathering (Morales-Flórez et al., 2015).

REFERENCES

Altiner, M., 2019. *Use of Taguchi approach for synthesis of calcite particles from calcium carbide slag for CO_2 fixation by accelerated mineral carbonation.* In: Arabian Journal of Chemistry, 12, 531-540. DOI: 10.1016/j.arabjc.2018.02.015

Cardoso, F. A., Fernandes, H. C., Pileggi, R. G., Cincotto, M. A., John, V. M., 2009. *Carbide lime and industrial hydrated lime characterization.* In: Powder Technology, 195, 143-149. DOI: 10.1016/j.powtec.2009.05.017

European Industrial Gases Association AISBL (EIGA), 2017. *Guide to carbide lime applications.* DOC 143/17.

IPCC, 2006. *IPCC Guidelines for National Greenhouse Gas Inventories. Volume 3: Industrial Processes and Product Use. Chapter 3: Chemical Industry Emissions.*

Jimoh, O. A., Mahmed, N., Okoye, P. U., Ariffin, K. S., 2016. *Utilization of milk of lime (MOL) originated from carbide lime waste and operating parameters optimization study for potential precipitated calcium carbonate (PCC) production.* In: Environmental Earth Science, 75, 1251. DOI: 10.1007/s12665-016-6053-z

Morales-Flórez, V., Santos, A., Romero-Hermida, I., Esquivias, L., 2015. *Hydration and carbonation reactions of calcium oxide by weathering: Kinetics and changes in the nanostructure.* In: Chemical Engineering Journal, 265, 194-200. DOI: 10.1016/j.cej.2014.12.062

3.6.2 USE OF LIME IN OTHER CHEMICAL INDUSTRY APPLICATIONS

In addition to calcium carbide, lime is used in other chemical industry sub-applications such as soda production and petrochemical industry. Information about the lime carbonation in these sub-applications was not available in the literature.

3.7 USE OF LIME IN OTHER INDUSTRIAL CONSUMERS

3.7.1. USE OF LIME IN THE NON-FERROUS METALLURGY

GENERALITIES ON BASE METALS PRODUCTION

Base metals include cadmium, copper, lead, nickel, tin and zinc. They are often found jointly, as complex ores, in the same mineral deposit. In this case, they can be separated during the mineral processing phase by selective floatation. When this is not possible, they are separated at the smelter, like for cadmium (EU, 2009).

Cadmium is, in fact, always associated with other metals, such as zinc, lead or copper, since there are no cadmium mines that directly produce a Cd concentrate. Then, it must be recovered at the smelter.

Copper is mostly found in nature associated with sulphur. It is mainly extracted from low-grade ores containing copper sulphide. The process includes the mining and the concentration of copper sulphide minerals, followed by smelting and electrolytic refining to produce a pure copper cathode.

Lead is mainly found in sulphide ores or in complex ores associated with zinc and a small amount of silver and copper. A lead concentrate is obtained by floatation and, then, the metal is recovered by smelting of the concentrate.

Nickel can be recovered from laterites deposits, where it is found as nickeliferous limonite ((Fe, Ni)O(OH)) and garnierite (a hydrous nickel silicate), or from magmatic sulphide deposits, where the principal ore mineral is pentlandite ($(Ni,Fe)_9S_8$) (EU, 2009). It can be recovered by hydrometallurgical or pyrometallurgical processes.

Zinc is usually found as sphalerite (ZnS) and it is recovered from the mine concentrate by leaching and electrowinning.

One of the main residues of base metal metallurgy are the tailings generated by the mining and concentration operations. Base metals tailings are quite similar to each other and consist in the pulverized rock, mainly sulphides and carbonates, that remains after the valuable metal-bearing minerals have been extracted from the ore. They usually are in the form of a slurry with 20-40% of solids by weight and are managed in ponds. As the tailings become compact and dry, grass and other vegetation is planted to stabilize the environment (EU, 2009).

If not managed properly, the tailings storage can be responsible for the environmental pollution of the surrounding areas, due to the release of metals and acids (Benvenuti et al., 1997; Yukselen, 2002; Gokcekus et al., 2003). The main issue about base metal mining tailings is, in fact, their Acid Mine Drainage (AMD) potential. The sulphide in tailings can, in fact, oxidise when entering into contact with water or air, generating an acidic leachate. This affects the physical stability of the tailings pond/dam and the chemical stability of the tailings themselves (EU 2009). However, if the content of buffering carbonates (depending on the original ore composition) is sufficiently high (for example 20-80%), no AMD is expected to occur during tailings storage (EU, 2009).

The next chapters focus on the most relevant base metals: copper, nickel, zinc and lead. The carbonation potential of the metallurgy slags and of the tailings generated by their production processes will be investigated.

3.7.1.1. COPPER PRODUCTION

Introduction

Primary copper can be produced by pyrometallurgical or hydrometallurgical processes.

Worldwide, approximately 20% of primary copper is produced by the direct leaching of ores (hydrometallurgical route). The hydrometallurgical route is applied to oxidic or mixed oxidic/sulphidic ores, without precious metals. The material is crushed and then leached with sulphuric acid. The liquor is concentrated by solvent extraction. Copper in the organic solution is stripped by sulphuric acid and the stripped solution is sent to the electro-winning stage. Lime or limestone can be used for various precipitation steps, as indicated by Dreisinger et al. (2006), who report a $CaCO_3$ and CaO consumption of 0-4.11 and 0-0.32 tonne per tonne of produced copper, respectively, depending of the applied process. However, information about the characteristics of the residues produced by the hydrometallurgical processes and their content of calcium compounds was not found.

The remaining 80% of copper is produced by pyrometallurgical processes. Pyrometallurgical route involves different steps, depending on the concentrate used. Usually sulphidic concentrates are used, which consist of complex/iron sulphides and are produced by flotation from ore that contain 0.2-2% of copper in the form of sulphide minerals (EU, 2017).

In this case, the involved stages are (EU, 2017):

- crushing and flotation of the mineral material to produce the copper concentrate. Copper tailings are produced at this stage;
- roasting and smelting of the concentrate to produce a melt that can be separated into a matte (consisting mainly in copper sulphide CuS and Cu_2S with some iron sulphide or iron oxide) and a slag rich in iron and silica. A fluxing agent that contains silica and, eventually, lime or limestone, is usually added to the melt to promote the formation of slag. The main reaction involved in this stage is the oxidation of the chalcopyrite ($CuFeS_2$) to FeO and CuS [Reaction 3.7.1.1]. After that, FeO reacts with the silica, producing the slag [Reaction 3.7.1.2]. Besides FeO, it is possible to find also FeS, which is removed with the slag [3.7.1.3].

$$2CuFeS_{2(s)} + 3O_{2(g)} \rightarrow 2FeO_{(s)} + 2CuS_{(s)} + 2\ SO_{2(g)} \quad [3.7.1.1]$$

$$FeO_{(s)} + SiO_{2(s)} \rightarrow FeO{*}SiO_{2(l)} \quad [3.7.1.2]$$

$$2FeS_{(l)} + 3O_2 + 2SiO_{2(l)} \rightarrow 2FeO{*}SiO_{2(l)} + 2\ SO_{2(g)} \quad [3.7.1.3]$$

Two smelting processes are generally used: bath smelting and flash smelting. The main difference is the degree of oxygen enrichment, which is higher in the flash process in order to produce an autothermal or nearly autothermal operation. For copper concentrates which have high silica but low iron contents (i.e., concentrates that have chalcocite (Cu_2S) and bornite (Cu_5FeS_4) as primary minerals and small amounts of pyrite and chalcopyrite), the so-called “direct to blister” smelting process is preferred (Somerville et al., 2016).

- converting of the matte. This phase includes two stages. In the first one, air/oxygen is blown through the matte to promote iron oxidation [Reaction 3.7.1.4]. Flux agents are added to promote the formation of a slag and remove iron [Reaction 3.7.1.5]. In the second stage, the copper sulphide is oxidised to blister copper (98.5% of Cu) [Reactions 3.7.1.6 and 7].

$$2FeS + 3O_2 \rightarrow 2FeO + 2SO_2 \quad [3.7.1.4]$$

$$2FeO + 2SiO_2 \rightarrow 2FeSiO_3 \quad [3.7.1.5]$$

$$Cu_2S + O_2 \rightarrow 2Cu + SO_2 \quad [3.7.1.6]$$

$$CuS + O_2 \rightarrow Cu + SO_2 \quad [3.7.1.7]$$

- fire refining of the blister copper. It consists of an oxidation stage, performed by blowing air into the molten metal to oxidise impurities and to remove final traces of sulphur, followed by a reduction stage, in which a reducing agent (natural gas, propane or ammonia) is added to partially remove the oxygen that is dissolved in the liquid copper. The metal resulting from this process is cast into anodes, with a 99% purity grade;
- electrolytic refining. Anode copper is electrorefined to produce a cathode copper with a quality at least equal or better than the grade A quality standard of the London Metal Exchange. The process is carried out in an electrolytic cell where a cast copper anode and a cathode are placed in a solution of copper sulphate and sulphuric acid. The copper ions dissolve from the impure anode, pass into the solution, and finally deposit on the cathode [Reactions 3.7.1.8 and 9]. Cathode sheets are usually dipped in lime water to protect them from sulphur in the "melting down" process.

$$\text{anode: } Cu_{(s)} \rightarrow Cu^{2+}_{(aq)} + 2e^- \quad [3.7.1.8]$$

$$\text{cathode: } Cu^{2+}_{(aq)} + 2e^- \rightarrow Cu_{(s)} \quad [3.7.1.9]$$

Secondary copper is produced by pyrometallurgical processes. The process is similar to that used for primary production. Which stages are actually used mainly depends on the copper content of the secondary raw materials (EU, 2017). The process is carried out in reducing conditions. Iron (in the form of iron copper or normal iron scraps), carbon (in the form of coke or natural gas) and fluxing agents are added to reduce the metal oxides.

As emerged from the previous description, lime is added at different stages of the copper production process:

- during the milling operation of the ore minerals and during flotation to optimize copper recovery. The aim is to provide alkaline conditions that enable the collector to make ore particles surface very hydrophobic, enabling their flotation. At the same times, flotation of pyrite (FeS_2) is depressed, since lime reacts with pyrite producing $CaSO_4$ and $Fe(OH)_3$. This makes pyrite particles surface very hydrophilic and inhibits their flotation (EU, 2009 and EU, 2017);
- during the smelting and the converting processes to promote the removal of impurities (such as magnesia and alumina) and decrease the dissolved copper content in the slag (Sommerville et al., 2016). Lime can

also suppress the stability of solid olivine and its precipitation from the molten slag, thus enabling the smelting of high MgO raw materials (Taskinen, 2011). In addition, it gives stability to the slag structure (Gorai et al., 2003). Lime can be substituted by the cheaper limestone, as reported both in the BREF Document for Non-Ferrous Metals Industries (EU, 2017) and in Somerville et al. (2016);

- during the electrorefining process to protect the cathode.

For what concerns the amount of lime or limestone added to the process, the BREF Document for Non-Ferrous Metals Industries (EU, 2017) reports a limestone addition of 27-38 kg per tonne of copper cathodes for the secondary copper production process. Taskinen (2010 and 2011) suggests the addition of 5-15% of lime to the iron silicate system in "direct to blister" smelting processes in order to expand the molten slag range to include the stability range of blister copper containing less than 1% sulphur. Norgate and Rankin (2000) report an addition of 26 kg of limestone per tonne of concentrate fed to the smelter.

The amount of lime added to the milling and flotation stages is not reported in the literature, as observed also by other authors (Bruckard et al., 2011).

Focusing on the residues management, copper tailings are produced in the form of a slurry or a paste and are usually stacked in storage areas, consisting in a pond or constructed using earth dams (Ahmari et al., 2015). As previously said in the introduction, copper tailings must be managed properly, in order to avoid problems of acid leaching from the pond.

An average production of 128 tons of solid copper tailings per ton of produced copper is reported by Gordon (2002), whereas Bridge (2000) reports a value of 196.5 tons of liquid and solid copper tailings per ton of produced copper.

Due to their mechanical properties, several authors report the possibility to use copper tailings as a construction material mixed with cement or lime (Ahmari et al., 2015), for example as a raw material in the production of tiles, bricks, concrete and mortars (Marghussian et al., 1999; Zhao et al., 2009; Fang et al., 2011; Onuaguluchi and Eren, 2012a; Gupta et al., 2017). However, for the moment, copper tailings are mainly landfilled in tailing storage areas or used for mine backfilling.

The slags produced from primary smelting and converting stages are rich in copper and are, usually, treated by pyrometallurgical processes in order to recover their content of Cu and, eventually, of other metals. Usually they are fed to electric furnaces where they react with carbon in the form of coke or with the electrodes themselves and produce an inert slag. Alternatively, converter slag can be recirculated in the smelting furnace. Similarly, other slags rich in copper, such as the refining slags, are usually recirculated to a prior process stage, mostly to the converting stage or, in secondary production, to the smelting stage (EU, 2017).

An alternative option for the treatment of the slags is to crush and mill the cooled slags and then deliver them to a flotation process in order to recover some concentrate rich in copper which can be returned to the smelter. Other processes, less used, are the carbothermic reduction of the slag to recover copper and cobalt, and the pyro-hydrometallurgical process to recover copper, cobalt and magnet grade iron oxide (Gorai et al., 2003). In the carbothermic process, after the treatment, iron, which is the major component of the slag, remains in the

form of oxide (Fe_2O_3), as a residue of not much commercial value, which then requires disposal. The addition of lime allows for a partial recovery of the iron (Yucel et al., 1999; Premchand et al., 2000). The pyro-hydrometallurgical process consists in the reduction of the slag with coke in arc furnaces, followed by the leaching with H_2S of the liquid alloy rich in Fe resulting from the pyrometallurgical treatment (Acma et al., 1997).

The inert slags after the treatment for Cu recovery, or more in general all the slags containing < 0.8% of Cu, are discarded as waste or used as secondary materials with properties similar to those of natural basalt or obsidian (Gorai et al., 2003.) Copper slag has, in fact, excellent mechanical properties and can be used in substitution of natural aggregates in road and embankment construction, as filling material, abrasive material or as ballast, in the production of concrete, cement, bricks and tiles (EU, 2017; Gorai et al., 2003; Shi et al., 2008; Al-Jabri et al., 2011). Due to the high content of Fe, it can be used as iron adjustment material during the cement clinker production (Huang, 2001). The presence of CaO gives pozzolanic properties to the copper slags (Deja and Malolepszy, 1986), especially under the activation of NaOH (Shi and Qian, 2000; Ahmari et al., 2015). This allows to use the slags as partial or full replacement for Portlandite cement in concrete or as a cement raw material (Gorai et al., 2003). However, in practice, slag use is limited to mine filling or as an aggregate in hot mix asphalt pavements (Collins and Ciesielski, 1994), in order to avoid the risk of possible release of heavy metals from the slag (Kalinkin et al., 2012).

The amount of slags produced depends on the concentrates composition and on the considered production stage. In direct-to-blister smelting process, the average slag production amounts to about 1.4-1.6 t/t of produced copper (Sommerville et al., 2016). Gorai et al. (2003) reported an average production of slag from the smelting and the converting stages of 2.2 t/t copper; 2.2-3 tons of copper slag per tonne of produced copper is also reported by Sharma and Khan (2017).

Literature assessment on copper tailings and slags: material and methods

The literature assessment was focused only on the pyrometallurgical route to produce copper, since, based on the authors knowledge, data about the content of Ca compounds in the residues of the hydrometallurgical route were not available.

In any case, the scientific literature on copper tailings and copper slags carbonation is almost absent. Thus, the literature review focuses mainly on the characterization of these residues in terms of Ca content and mineralogy. The only data regarding carbonation are related to the depth of carbonation measured on concrete specimens containing copper slags and/or copper tailings.

Overall, 13 papers published in scientific journals, one conference paper and the BREF Documents for the non-ferrous metals industries (EU, 2017) and for the management of tailings and waste-rock in mining activities (EU, 2009) were considered, as reported in Table 3.7.1.1. Among these documents, only 4 reported data about the depth of carbonation of concrete specimens containing copper tailings or slags (Moura et al., 2007; Shi et al., 2008; Gupta et al., 2017; Sharma and Khan, 2017).

Table 3.7.1.1. List of the documents considered in the study for the review about copper slags and tailings.

Peer reviewed papers
Ahmari et al., 2015. *Alkali activation of copper mine tailings and low-calcium flash-furnace copper smelter slag*. J. Mater. Civ. Eng. 27, 04012193
Al-Jabri et al., 2011. *Effect of copper slag as a fine aggregate on the properties of cement mortars and concrete*. Constrution and Building Materials 25, 933-938
Brindha and Nagan, 2011. *Durability studies on copper slag admixed concrete*. Asian Journal of Civil Engineering 12, 563-578
Fang et al., 2011. *Utilization of copper tailing for autoclaved sand-lime brick*. Construction and Building Materials 25, 867-872
Gorai et al., 2003. *Characteristics and utilization of copper slag*. *A review*. Resources, Conservation and Recycling 39, 299-313
Gupta et al., 2017. *Utilization of copper tailings in developing sustainable and durable concrete*. J. Mater. Civ. Eng 29, 04016274
Khanzadi and Behnood, 2009. *Mechanical properties of high-strenght concrete incorporating copper slag as coarse aggregate*. Construction and Building Materials 23, 2183-2188
Moura et al., 2007. *Copper slag waste as a supplementary cementing material to concrete*. J. Mater.Sci 42, 2226-2230
Onuaguluchi and Eren, 2012a. *Recycling of copper tailings as an additive in cement mortars*. Construction and Building Materials 37, 723-727
Potysz et al., 2016. *Characterization and pH-dependent leaching behaviour of historical and modern copper slags*. Journal of geochemical exploration 160, 1-15
Sharma and Khan, 2017. *Durability assessment of self compacting concrete incorporating copper slag as fine aggregates*. Construction and building materials 155, 617-629
Shi et al., 2008. *Utilization of copper slag in cement and concrete*. Resources, Conservation and Recycling 52, 1115-1120
Thomas et al., 2013. *Strength and durability characteristics of copper tailing concrete*. Construction and Building Materials 48, 894-900
Conference paper
Somerville et al., 2016. *Fluxing strategies for the direct to blister smelting of high silica and low iron copper concentrates*. Proceedings of the 10th International Conference on Molten Slags, Fluxes and Salts (Molten16)
BREF documents
EU, 2009. BREF Document for Management of Tailings and Waste-Rock in Mining Activities
EU, 2017. BREF Document for the Non-Ferrous Metals Industries

Copper tailings and slags composition

Copper tailings

The chemical composition of copper tailings is reported in Table 3.7.1.2. The main constituent is silica, about 49% on weight of the residue. Ca compounds amount, on average, to about 11.6%, expressed as CaO. However, CaO content in the tailings can be very variable, from less than 1% to about 30%. Its amount firstly depends on the presence of carbonates in the ore and only secondly on the addition of lime/limestone during the milling operations and during flotation.

Considering their mineralogy, copper tailings are mainly crystalline materials, consisting of quartz (SiO_2), albite ($NaAlSi_3O_8$), sanidite ($(K_{0.831}N_{0.169})(AlSi_3O_8)$), gypsum ($CaSO_4$) and andradite ($Ca_3*Fe_2^{3+}*Si_3O_{12}$) (Ahmari et al., 2015; Fang et al., 2011). Gypsum is produced as a consequence of the reaction between the lime added during the flotation process and the pyrite in the ore.

The presence of a sufficient amount of Ca in the copper tailings, especially in the form of carbonates, is very important to maintain a neutral pH in the tailing pond/dam and avoid situations closed to AMD. Usually, in fact, mining tailings are characterized by pH values around or below 7 (Hansen et al., 2007; Das and Maiti, 2009; Karam et al., 2009; Yin et al., 2011).

Table 3.7.1.2. Chemical composition of copper tailings (min-average-max value). Elaboration of the data reported in the documents listed in Table 3.7.1.1.

Total Ca as CaO (%)	**Total Mg as MgO (%)**	**Cu (%)**	**SiO_2 (%)**	**Fe (%)**
0.16-11.6-29.2 *7 cases*	0.49-3.1-6.9 *7 cases*	0.04-0.20-0.26 *6 cases*	11.2-49.6-75 *8 cases*	0.5-5.6-29.8 *8 cases*

Copper slags

As previously illustrated, different pyrometallurgical technologies can be used for copper production, applying different type of furnaces, smelting temperatures and additives. Considering also the differences in the initial input material, it is evident that slags produced form different pyrometallurgical processes may have different chemical and phase composition (Potysz et al., 2016).

Generally, copper slags can be classified as air-cooled or granulated slag. Air-cooled slags are produced by slow cooling under ambient atmosphere, whereas the granulated slags are the result of a rapid cooling process using water. Air-cooled slag has a black colour and a crystalline structure, whereas granulated slag has an amorphous structure and is more porous, with a lower specific gravity and higher absorption capacity than air-cooled slag (Gorai et al., 2003; Potysz et al., 2016).

On average, silicate amorphous glass is the main constituent of copper slags (Potysz et al., 2016). The main mineral phases are fayalite (Fe_2SiO_4), magnetite (Fe_3O_4) and pyroxene ($Ca(Fe,Mg)(SiO_3)_2$) (Kiyak et al., 1999; Ahmari et al., 2015)). Ca is mainly present in silicate compounds (Potysz et al., 2016).

The chemical composition of copper slags is reported in Table 3.7.1.3. A distinction was made between the inert slags resulting from the treatment for Cu recovery and those produced at specific stages of the pyrometallurgical process, collected before being sent to Cu recovery treatment. On average, the main constituents are silica and Fe. The main difference between the different types of slags is the content of Cu, which is obviously lower in the inert slag resulting from the treatment for Cu recovery. For what concerns the Ca content (expressed as CaO), it is very variable, from less than 1% to about 20% of the weight of the slags, with an average value of about 6%. No statistically significant difference among the different types of slags[26] was, however, observed.

[26] Test of Kruskal-Wallis.

Table 3.7.1.3. Chemical composition of copper slags (min-average-max value). Elaboration of the data reported in the documents listed in Table 3.7.1.1.

Type of slags		Total Ca as CaO (%)	Total Mg as MgO (%)	Cu (%)	SiO_2 (%)	Fe (%)
Inert slag after Cu recovery		0.15-5.35-20.90 *20 cases*	0.75-2.13-5.73 *16 cases*	0.26-0.83-2.1 *19 cases*	24.7-30.8-41 *22 cases*	5.7-19-43 *22 cases*
Slag from a specific furnace, prior to slag treatment for Cu recovery	Copper slag from direct to blister smelting	1.2-6.01-15.00 *3 cases*	1.20-1.56-2.00 *3 cases*	3.35-5.46-7.75 *3 cases*	33.0-38.7-43.6 *3 cases*	16.9-23.9-30.6 *3 cases*
	Copper slag from flash furnace	n.a.	n.a.	1.0-1.75-2.5 *2 cases*	30-31.5-33 *2 cases*	38 *1 case*
	Copper slag from Pierce-Smith converter	n.a.	n.a.	3-4-5 2 cases	25 *1 case*	40-42.5-45 *2 cases*
	Copper slag from shaft furnace	17.6 *1 case*	6.3 *1 case*	1.09 *1 case*	44.9 *1 case*	3.7 *1 case*

Potential carbonation rate in copper tailings and slags

The maximum theoretical amount of CO_2 that can be sequestered by the copper residues (tailings and slags) as a consequence of their content of Ca can be calculated on the basis of their composition.

Assuming an 11.6% average content of CaO in the copper tailings and a 6% average content in the copper slags, as reported in Tables 3.7.1.2 and 3.7.1.3, the maximum CO_2 sequestration potential results equal to about 91 gCO_2 per kg of copper tailings and 47 gCO_2 per kg of copper slags.

However, these figures are absolutely theoretical. Generally, not all the Ca compounds will react with CO_2. Free lime and portlandite react very fast, but Ca silicates require more time to dissolve in solution and react with CO_2 and some of them, which are in the amorphous phase, do not react at all. Considering that most of the Ca in copper slags is found in the form of silicates, a much lower CO_2 uptake is expected in natural environmental conditions. Furthermore, both lime and limestone can be added during the pyrometallurgical process, the latter being responsible of a net CO_2 emission due to its calcination in the furnace.

For what concerns copper tailings, their Ca content is not necessarily the consequence of the addition of lime or limestone during the process, but it mainly comes from the mineral. Furthermore, considering that tailings' pH is usually below the neutrality, it is expected that no carbonation reactions occur during storage.

Carbonation of concrete specimens containing copper slags and/or copper tailings

Copper slags and tailings can be used in substitution of natural aggregates in the production of concrete mixture. Several authors (for example, Khanzadi and Behnood, 2009; Onuaguluchi and Eren, 2012b; Thomas et al., 2013) reported the results of mechanical and chemical tests carried out on concrete specimens containing copper slags/tailings, in order to assess their compressive strength, electrical resistivity, the resistance to sulphate attack, the sorptivity, etc.. In some cases, also the results of accelerated carbonation tests performed on these specimens are reported, in terms of depth of the carbonation front (Moura et al., 2007; Hwang and

Laiw, 1989; Aynao and Sakata, 2000; Gupta et al., 2017; Sharma and Khan, 2017). However, no data were found about the amount of CO_2 that can be sequestered by these residues.

Sharma and Khan (2017) used granulated copper slags to replace 0 to 100% of natural sand in a concrete mixture of Portland cement, fly ashes, coarse aggregate minerals, sand, water and a superplasticizer based on polycarboxylic ethers. The accelerated carbonation tests were carried out on 28 days cured prism specimens of 100mmx100mmx500mm, which were exposed for 4-8-12-16 weeks to a CO_2 enriched atmosphere (4% of CO_2). The results showed that the use of copper slag in concrete production reduces the carbonation depth. With 0% copper slag, a carbonation depth of 21.3, 25.54, 31.5 and 37.8 mm was observed after 4,8,12 and 16 weeks of CO_2 exposure, respectively. With 100% substitution of the sand with copper slag, carbonation depth values were 15.4, 19.3, 22.9, 26.7 mm. This was explained by the authors with the high content of ferrous oxide in the copper slag, which increases the pH of pore solution and makes concrete matrix to be alkaline in nature.

Moura et al. (2007) tested some concrete specimens containing ground copper slags in a quantity equal to 29% of the weight of the cement. Accelerated carbonation tests were carried out in a controlled chamber under a 5% CO_2 atmosphere for 180-240 days. After 240 days, copper slag concrete showed a decrease in the advancing of the carbonation front of 80% for a water/cement ratio of 0.5 and of 35.7% for a water/cement ratio of 0.6 compared to the control specimens without addition of copper slags. The authors suggested that copper slag concrete has a lower diffusivity of CO_2 because of the denser structure of the hardened copper slag cement paste when compared to ordinary Portland cement.

Similar results were reported by Hwang and Laiw (1989) and Aynao and Sakata (2000), when copper slag are used in concrete production.

Gupta et al. (2017) used copper tailings in partial substitution of natural fine aggregates in concrete. The concrete specimens, with a substitution ratio copper tailings/sand of 0-80%, were carbonated for 12 weeks in a controlled chamber under a 5% CO_2 enriched atmosphere. Contrary to the experiences previously reported, the depth of carbonation was found to increase with increasing replacement of copper tailings. The depth increased from 15 mm (with 0% of copper tailings in the specimen), to 16 mm (with 10% of copper tailings), to 25 mm (with 50% of copper tailings) and to 33 mm (with 80% of copper tailings). This was explained by the authors with the minor difference in the particle size of copper tailings compared to natural sand.

Although the different authors provide different explanations to the variation of the depth of carbonation when copper slags/tailings are used in concrete production, no one concludes that the reason can be the different Ca content of the copper residues compared to natural sand. This suggests that the Ca in the slags/tailings can hardly react with the atmospheric CO_2.

Discussion and conclusions

Based on the present survey, scientific literature about carbonation of copper tailings and copper slags is absent. For what concerns copper slags, this can be explained by the fact that they do not contain Ca in a form available for carbonation, for example portlandite. Most of the Ca in the copper slag is bounded in low reactive

silicate compounds and, in fact, copper slag is widely used in several civil engineering applications in substitution of natural aggregates, without giving problems of expansions that are sometimes observed with other waste (such as iron slags or waste incineration bottom ash) as a consequence of their content of free lime. It is, thus, possible to conclude that carbonation of copper slag is negligible, both during storage and when it is recycled in civil engineering applications.

For what concerns copper tailings, they are usually stored in dam/pond sites. The stored residue has a pH value around or below 7, where carbonation reactions cannot occur.

3.7.1.2. NICKEL PRODUCTION

Introduction

Worldwide, about 60% of nickel comes from sulphide deposits, where it is found in the form of pentandlite, and 40% from laterite deposits, where it is in the form of limonite or saprolite.

The production of nickel from laterite ores is more expensive because, unlike sulphide ores, they cannot be upgraded or concentrated by flotation or gravity prior to processing (Norgate and Jahanshahi, 2011). This means that almost the entire amount of mined minerals must be processed. Once the mineral is extracted, three main routes are available for nickel production (EU, 2017; Norgate and Jahanshahi, 2011), depending on the characteristics of the ore:

- the combined pyrometallurgical/hydrometallurgical process route with ammonia-based extracting agents was developed for laterite ores in the 1920s. The minerals are roasted and then leached with an ammonia/ammonium carbonate solution. The main problem is that much of the cobalt is lost in the leached residue as a consequence of the roasting operation (Parkinson, 1999). For this reason, it is no longer used for the processing of the limonite ore, which is usually rich of cobalt;
- the hydrometallurgical process route with sulphuric acid as extracting agent is mainly used for limonite ores where nickel and cobalt are bounded within goethite or clays. It consists in the leaching of the minerals with sulphuric acid in autoclaves at high temperature (230-260°C) and high pressure (up to 43 bar). The resulting solution is purified by direct solvent extraction or electrowinning, or by indirect methods such as precipitation. In the precipitation method, a mixed nickel and cobalt sulphide is produced using hydrogen sulphide gas. The precipitate is, then, leached under oxidative conditions (i.e. with high O_2 partial pressure) and cobalt is removed by solvent extraction followed by hydrogen reduction. The raffinate from cobalt extraction is treated by hydrogen reduction, briquetting and sintering to produce nickel briquettes. This process, cannot be used for saprolite ores, because they contain magnesia that would consume too much acid;
- the pyrometallurgical process route to produce ferro-nickel is mainly used for silica and magnesia-rich saprolite ores. The minerals are calcined in a rotary kill and then are smelted with a source of carbon in an electric arc furnace to separate the nickel/iron-containing phase from the silica-magnesia slag. A final refining step is necessary, to remove impurities like sulphur, silicon, and phosphorous.

For what concerns the sulphidic ores, nickel-bearing sulphidic minerals are usually concentrated by flotation and then nickel is recovered by pyrometallurgical processes, like for copper. Nickel concentrates are smelted under oxidising conditions to remove iron sulphide and other impurities and to produce a nickel matte. The matte is treated to reject iron and recover nickel, copper, cobalt and precious metals. It can be treated pyrometallurgically, but hydrometallurgical processes are more commonly used. The possible treatments include electrorefining, leaching, reduction and precipitation (EU, 2017):

- leaching can be carried out at ambient pressure or in autoclave, by using chloride, sulphate or ammonia solutions and oxygen or chlorine gases as an oxidant. For example, the matte obtained from low-grade laterite ore is usually subjected to high pressure acid leaching with sulphuric acid, like for the oxidic ore. Impurities, like copper and iron, precipitate as a cake and are removed. Nickel is recovered from the purified solutions by electrowinning or by hydrogen reduction. Alternatively, ammonia and ammonium sulphate can be added to the solution to produce a nickel powder;
- in the carbonyl process, nickel carbonyl is formed by the reaction of the nickel matte with CO at low temperature and pressure. Nickel carbonyl is volatile and it is refined by separation from the solid impurities and thermal decomposition;
- nickel matte with low copper content can be cast into anodes that are dissolved in a diaphragm electrolytic cell using a chloride/sulphate electrolyte. The electrolyte from the anode compartment is purified and circulated through the cathode bag.

Limestone is extensively used for the ore preparation, whereas lime is usually preferred in the leaching stage to promote selective precipitation of impurities and other metals. However, the use of limestone in the leaching process is also documented in the literature. For example, Norgate and Rankin (2000) report an addition of 3 tonnes of limestone per tonne of produced Ni in the pressure acid leaching process of laterite ore. Kerfoot et al. (2002) suggest the use of limestone and lime to promote iron precipitation as $Fe(OH)_3$ in an alternative hydrometallurgical process for the recovery of Ni and Co from sulphidic flotation concentrates though atmospheric pressure chlorine leaching under acidic conditions, followed by an oxidative acid pressure leaching and the final recovery of nickel by an electrowinning step. When lime and/or limestone are used in hydrometallurgical processes that use sulphuric acid, the neutralization process of the acid results in the precipitation of gypsum.

Limestone or lime are also used as a fluxing agent in the pyrometallurgical process route. No data about their dosage were found in the literature.

For what concerns the generation of residues, tailings are produced during the milling operations and the flotation of sulphidic ore minerals, as well as during the leaching operation of laterite ores. These residues are usually stored in impoundments, like for the other base metals tailings. The risk of AMD is particularly high for the tailings derived from the milling and concentration operation of sulphidic ores minerals.

For what concerns the residues produced by the leaching activities on laterite ore, they mainly consist in the precipitate formed during the leaching stages. The amount depends on the quality of the raw materials and on

the efficiency of the precipitation step. The main residues of the hydrometallurgical process route usually consist in iron residues, in the form of jarosite or goethite (EU, 2017). Usually, these tailings are landfilled. However, they can still contain significant amount of metals. Thus, treatment of the tailings could enhance the recovery of valuable metals by reducing the soluble losses and thereby also reducing the environmental impacts (Zainol and Nicol, 2009).

Solid residues are also produced by the pyrometallurgical processes, in the form of slag. The slags produced in the single furnaces are usually treated for metals recovery in electric arc furnaces. The process is called slag cleaning. The resulting slag usually contains a very low concentration of leachable metals and it is suitable for use in construction (EU, 2017). The BREF Document for Non-Ferrous Metals Industries (EU, 2017) reports that about 5 t of slags are produced per tonne of nickel matte at the converting stage. More in general, the slags produced by the pyrometallurgical route amount to 4-16 times the weight of the produced metal (EU, 2017; Warner et al., 2006).

Nickel slag can be used in substitution of natural aggregate in road construction, in the production of hot-mix asphalt aggregate, concrete and blended cement (Wang and Thompson, 2011). It can be also used in industrial blast cleaning as ultra blast (Samnur et al., 2016). However, compared to steel slag, the possible recycling options are more limited, due to its poorer pozzolanic performance and its higher Mg content, which may induce volume expansion problems (Choi and Choi, 2015). For this reason, a great amount of nickel slag is disposed in landfill sites (Yang et al., 2017).

Literature assessment on nickel tailings and slags: material and methods

The scientific literature on nickel tailings and nickel slags carbonation is quite poor. Thus, the literature review focuses mainly on the characterization of these residues in terms of Ca content and mineralogy.

Overall, 9 papers published in scientific journals, 4 conference papers, one patent document and the BREF Documents for the non-ferrous metals industries (EU, 2017) and for the management of tailings and waste-rock in mining activities (EU, 2009) were considered, as reported in Table 3.7.1.4. Among these documents, only 6 report the possibility to use nickel slag and tailings for CO_2 sequestration, however they all agree that their carbonation potential is mainly related to the content of Mg compounds.

Table 3.7.1.4. List of the documents considered in the study for the review about nickel tailings and slags.

Peer reviewed papers
Assima et al., 2014. *Impact of temperature and oxygen availability on the dynamics of ambient CO_2 mineral sequestration by nickel mining residues*. Chemical Engineering Journal 240, 394-403
Bodénan et al., 2014. *Ex situ mineral carbonation for CO2 mitigation: Evaluation of mining waste resources, aqueous carbonation processability and life cycle assessment (Carmex project)*. Minerals Engineering 59, 52-63
Choi and Choi, 2015. *Alkali-silica reactivity of cementitious materials using ferro-nickel slag fine aggregates produced in different cooling conditio*ns. Construction and Building Materials 99, 279-287
Coto et al., 2008. *Cobalt and nickel recoveries from laterite tailings by organic and inorganic bio-acids*. Hydrometallurgy 94, 18-22
Hernández et al., 2007. *Recovery of metals from Cuban nickel tailings by leaching with organic acids followed by precipitation and magnetic separation*. Journal of Hazardous Materials B139, 25-30
Kalinkin et al., 2012.*Geopolymerization behavior of Cu-Ni slag mechanically activated in air and in CO_2 atmosphere*. International Journal of Mineral Processing 112-113, 101-106
Mu et al., 2010. *Leaching of magnesium from desiliconization slag of nickel laterite ores by carbonation process*. Trans. Nonferrous Met. Soc. China 20, s87-s91
Samnur et al., 2016. *Study on physical-chemical properties of furnace-nickel-slag powder for geopolymer application*. Jurnal Pendidkan Fisika Indonesia 12, 177-182
Yang et al., 2017. *Geopolymer with improved thermal stability by incorporating high-magnesium nickel slag*. Construction and Building Materials 155, 475-484
Patent document
Kerfoot et al., 2002. *Hydrometallurgical process for the recovery of nickel and cobalt values from a sulfidic flotation concentrate*. Patent no. US 6428604 B1
Conference papers
Beaudoin et al., 2017. *Passive mineral carbonation of Mg-rich mine wastes by atmospheric CO_2*. Energy Procedia 114, 6083-6086
Chae et al., 2014. *Mineral carbonation with ferrous nickel slag*. Proceedings of the 4th International Conference on Environmental Pollution and Remediation. Prague, 11-13 August, 2014
Norgate and Rankin, 2000. *Life cycle assessment of copper and nickel production*. Proceeding of the Minprex Conference, 11-13- September 2000 Melbourne, 133-138
Siegrist et al., 2017. *Analysis of the potential for negative CO_2 emission mine sites through bacteria-mediated carbon mineralization: evidence from Australia*. Energy Procedia 114, 6124-6132
BREF documents
EU, 2009. *BREF Document for Management of Tailings and Waste-Rock in Mining Activities*
EU, 2017. *BREF Document for the Non-Ferrous Metals Industries*

Nickel tailings and slags composition

Nickel tailings

With the name of nickel tailings, we usually mean both the residues generating by the milling and the flotation operations of sulphidic ore minerals and the precipitates generating during the leaching operations of laterite ore minerals. Often the two types of residues are deposited in the same impoundment, sometimes with other residues from different mining activities.

Tailings from sulphide ores mainly consist in pyrrhotite ($Fe_{(1-x)}S$), which can be oxidised during storage promoting the precipitation of amorphous or crystalline ferric hydroxide (ferrihydrite, goethite) and basic ferric sulphate mineral phases (such as jarosite $KFe_3(SO_4)_2(OH)_6$), as well as gypsum (Johnson et al., 2000). In mafic

and ultramafic ores, a non-negligible amount of Mg is also observed (Siegrist et al., 2017). $CaCO_3$ can be present in the tailings in small amounts, on the basis of the ore composition and as a consequence of the addition of lime/limestone during the milling operations (Johnston et al., 2000). Its presence, along with that of $FeCO_3$ and $Al(OH)_3$, is very important in acting against AMD, thanks to its pH-buffering properties. The pH of this residues is, in any case, usually below 7, with value of 2-3 in the surface layers of the impoundment (Johnson et al., 2000). Quantitative data about Ca content in the tailings from sulphide ores were not available. For what concerns the tailings produced by the hydrometallurgical treatment of laterite ores, they mainly consist in magnetite, quartz, fayalite ($(Fe,Mg)_2SiO_4$), donathite ($(Fe,Mg)(Cr,Fe)_2O_4$), trevorite ($NiFe_2O_4$), fosterite (Mg_2SiO_4), crysolite ($(Fe,Mg)_2SiO_4$) and lizardite ($Mg_3[Si_{2-x}O_5](OH)_{4-4x}$) and brucite ($Mg(OH)_2$) (Hernández et al., 2007; Coto et al., 2008; Assima et al., 2014). Laterite ores are formed on ultramafic rocks and are, thus, particular rich in MgO. Hernández et al. (2007) and Coto et al. (2008) reported a similar composition for the tailings produced by the combined pyrometallurgical/hydrometallurgical treatment of laterite ores with ammonia/ammonium carbonate solution as extracting agent. On average, they contain 24% of Mg compounds, expressed as MgO and 14% of silica (Table 3.7.1.5). Only one datum about the Ca content in the nickel tailings was found, equal to 0.1% as CaO (Assima et al., 2014).

Table 3.7.1.5. Chemical composition of nickel tailings from laterite ores (min-average-max value). Elaboration of the data reported in the documents listed in Table 3.7.1.4.

Total Ca as CaO (%)	**Total Mg as MgO (%)**	**SiO_2 (%)**
0.1 *1 case*	7.8-24.2-40.5 *3 cases*	5.9-14.8-32.3 *3 cases*

Nickel slags

Nickel slags are usually produced in the pyrometallurgical processes for the treatment of sulphidic ores. Their average chemical composition is reported in Table 3.7.1.6. The main constituents are silica and magnesium. The content of Ca, expressed as CaO, is modest, with an average value of 3.5%.

For what concerns the mineralogy, some differences are observed between air-cooled and water-cooled slags. In any case, the main mineral phases are enstatite ($MgSiO_3$), forstetite (Mg_2SiO_4), diopsite ($CaMgSi_2O_6$), silica, iron oxide and in minor amount silimanite ($Al_2(SiO_4)O$) and calcium peroxide (CaO_2) (Samnur et al., 2016; Choi and Choi, 2015)

Table 3.7.1.6. Chemical composition of nickel slags (min-average-max value). Elaboration of the data reported in the documents listed in Table 3.7.1.4.

Total Ca as CaO (%)	Total Mg as MgO (%)	SiO_2 (%)
0-3.49-10.95 *9 cases*	11.92-25.69-32.17 *6 cases*	30-45.30-62.80 *10 cases*

Potential carbonation rate in nickel tailings and slags

The maximum theoretical amount of CO_2 that can be sequestered by the nickel residues (tailings and slags) due to their content of Ca can be calculated on the basis of their chemical composition.

For what concerns the nickel tailings, no data about their actual content of Ca is available. Based on the information reported in the documents listed in Table 3.7.1.5, Ca content in the tailings is negligible. Thus, its contribution to any eventual carbonation process interesting nickel tailings can be considered null.

For what concerns the slags, the maximum CO_2 sequestration potential results equal to about 27 gCO_2 per kg of nickel slags, on the basis of the average calcium content reported in Table 3.7.1.6. However, generally, not all the Ca compounds react with CO_2. Free lime and portlandite react very fast, but Ca silicates require more time to dissolve in solution and react with CO_2 and some of them, which are in the amorphous phase, do not react at all. Considering that most of the Ca in nickel slags is found in the form of silicates, a much lower CO_2 uptake is expected under natural environmental conditions.

Natural and accelerated carbonation of nickel tailings and slags

Natural carbonation of nickel tailings from mafic and ultramafic ores has been reported by several authors (for example, Beaudoin et al., 2017), due to their high content of Mg. Several studies have also been published about accelerated carbonation of Mg-rich tailings (Assima et al., 2014; Siegrist et al., 2017). However, the carbonation process of nickel tailings will not be further investigated in this context, since it involves only the Mg compounds and not the Ca ones.

Similar results were found for nickel slags. Chae et al. (2014) and Bodénan et al. (2014) investigated the possibility to exploit nickel slag for carbon dioxide sequestration. However, both sources agree that the carbonation potential of this residue is the consequence of its high content of Mg and not of Ca.

The only indication that the Ca compounds in the slags can contribute to the CO_2 sequestration was found in Kalinkin et al. (2012). The authors investigated the possibility to use Cu-Ni granulated slag to synthesize a geopolymer. The slags were mechanical activated, before reacting with a sodium silicate solution. Mechanical activation was carried out both in ambient air and in a pure CO_2 atmosphere, by grinding the slag for 10 minutes in a centrifugal planetary mill. During the milling operation, about 1 g of CO_2 per kg of slag was sequestered when the activation was carried out in ambient air, and about 8 g in CO_2 atmosphere. CO_2 was sequestered in the forms of $MgCO_3$, $FeCO_3$, $CaCO_3$, and $CaMg(CO_3)_2$. In any case, the amount of CO_2 sequestered by the slag was absolutely modest, almost negligible in ambient air and not completely attributable to the Ca compounds.

Discussion and conclusions

Based on the little information reported in the scientific literature, it is possible to conclude that carbonation processes affecting nickel tailings and slags are mainly related to their content of magnesium. Ca content in nickel slags is very modest and in a chemical form poorly available for carbonation. Its content in the tailings is almost null.

Furthermore, as both lime and limestone can be added during the hydrometallurgical/pyrometallurgical processes, and in the hydrometallurgical process limestone is more used compared to lime, it is expected that the addition of these reagents in the nickel production results in a net emission of CO_2, rather than a CO_2 sequestration.

3.7.1.3. ZINC AND LEAD PRODUCTION

Introduction

The carbonation potential of the residues produced by Pb and Zn metallurgy will be investigated in the same chapter, since Pb and Zn ores are often mixed and thus their residues (tailings and slags) will be managed in the same dumps/impoundments.

Lead production

Lead is mainly produced by pyrometallurgical processes. Primary lead production from lead ores and concentrates can be carried out by sintering/smelting in a blast furnace (named Imperial Smelting Furnace) or by direct smelting. Currently, only one Imperial Smelting Furnace is operating in Europe, whereas it is still used in non-EU countries (EU, 2017).

In direct smelting, the sintering stage is not carried out separately. Several processes can be used for the direct smelting of lead concentrates: the Ausmelt/ISASMELT, the Kaldo, the QLS and the integrated Kivcet processes are the most common. Secondary materials, such as some lead-acid battery scrap fractions (paste or grids), can be added to the concentrate, together with smelting additives and fluxes (EU, 2017).

Secondary lead production is used to recover lead-acid batteries. Other secondary materials can be fed to the plant, such as lead-containing dross, ashes, matte, residues and slags.

Two main processes can be used for the recovery of lead from automotive batteries (EU, 2017):

- blast furnace recycling process, where the batteries are first of all drained of acids and then the polypropylene (PP) plastic fraction can be separated. Drained batteries are then mixed with coke, fluxes and other lead scraps and fed into the furnace. An antimony lead bullion is produced, along with a silica-based slag and a lead-iron matte can be recovered in a primary lead smelter;
- mechanical battery separation process followed by smelting: batteries are drained of acids, broken and separated into metallic compounds, lead oxide-sulphate paste ($PbSO_4$, PbO and PbO_2), PP, non-recyclable plastics, rubber and dilute sulphuric acid by means of screens, wet classifiers and filters. The lead oxide-sulphate paste is then recovered in a smelting process. Different types of furnaces can be used: blast furnaces, rotary furnaces, reverberatory furnaces and electric furnaces. Paste desulphurization prior to smelting can reduce the quantity of the slag.

Like in all pyrometallurgical processes, fluxes are needed to promote the slag formation. Usually limestone is used, together with silica (Penpolcharoen, 2005). However, other fluxes can be used, such as Na_2CO_3 (EU, 2017). No quantitative data about the addition of limestone or other fluxes in the process were found.

Lead can also be recovered from other residues than batteries, as well as from the residues and the flue-dusts from copper smelting.

In any case, crude lead produced in primary or secondary production may contain impurities and other metals, such as copper, silver, and antimony that must be removed by electrolytic refining or pyrometallurgical refining. Electrolytic refining is very expensive and currently not practiced in the EU. The pyrometallurgical refining process includes a first "softening" step, where Cu, Sn, Sb, As and Bi are removed, and a desilverization step, where Ag is removed. Cu is removed by precipitation as S was added to the bullion. Sn, Sb and As are removed by oxidation. Ag is recovered using the Parkes process, which consists in the addition of Zn to precipitate an Ag-Zn intermetallic compound which is then sent to further treatment. Bi is recovered by addition of Ca and Mg; the resulting intermetallic compound is sent to further treatment. Zn is recovered by vacuum distillation. Finally, the residual oxides are eliminated from the Pb after leaching in NaOH (de Andrade Lima and Bernandez, 2011).

Zinc production

Zinc is usually found as sphalerite (ZnS), but it can be extracted also from oxide, silicate or carbonate minerals. In any case, the concentrate is obtained by grinding and flotation of the Zn-bearing minerals (EU, 2009).

After that, Zn can be recovered from the concentrate by pyrometallurgical or hydrometallurgical processes, which are also known as Imperial Smelting Furnace distillation process and roast-leach-electrowinning process, respectively.

The pyrometallurgical method for primary zinc production is no longer in use in Europe. Only one Imperial Smelting Furnace is still operating in Poland (EU, 2017). However, this process is largely used in non-EU countries and, in Europe, it is mainly used for secondary zinc production. Approx. 30% of the total EU zinc production comes, in fact, from secondary sources, such as end-of-life products (sheet, brass, die-cast parts), galvanising residues and recycled products from zinc-containing residues (such as the Waelz oxide recovered from the dust of the electric arc furnace for steel production) (EU, 2017).

In the pyrometallurgical process, primary (i.e. the Zn concentrate) and secondary raw materials can be mixed together to prepare the charge. Usually limestone and sand are added to the sinter plant as fluxing agents. In the sinter plant, metal sulphides are oxidised. The charge materials prepared in the sinter plant are fed to the Imperial Smelting Furnace where liquid lead is separated in the sedimentation tank, the slag-forming components are smelted and separated from the charge and the zinc evaporates and is separated in the gas stream flow with CO, CO_2 and N_2. The gas leaves the charge-heating zone of the furnace and enters into the condenser where it dissolves in liquid lead. In the homogeneous zinc-lead alloy, which is produced at the condenser, there is a coexistence of liquid phases, one rich in zinc and one rich in lead. The upper zinc-rich layer is separated and goes through the flux agent tank, through the liquidation tank, where excess lead is

separated from zinc, and finally is sent to the rectification process. This consists in the purification of the zinc by reflux distillation in columns.

The hydrometallurgical route is used for extracting zinc from zinc sulphide, oxide, carbonate or silicate concentrates and also from some secondary materials such as Waelz oxide. This route accounts for 90% of the total world zinc production. The process is complex and includes the flowing steps (EU, 2017):

- roasting: zinc sulphide concentrate is roasted in closed fluidised bed roasters to produce zinc oxide and sulphur dioxide. Up to 25% of secondary zinc oxide material (such as the Waelz oxide) can be added as a coolant to the roaster feed material;
- calcine processing: the zinc oxide (calcine) is cooled down in a rotary or in a fluidised bed cooler and then is ground to about 50 μm;
- leaching: calcine is leached in different steps by using a gradually increasing strength of hot sulphuric acid. Zinc is extracted from the calcine with an efficiency of 70-95% and concentrated in the liquor, with other metals such as Cu, Cd, Co and Ni, whereas iron is removed by precipitation. As zinc ores usually contain high amount of Fe, the process results in a large production of residues in the form of jarosite, goethote and haematite. Alternatively, ZnS ores can be directly leached without being oxidised in a roasting furnace. The leaching must be performed at high temperature with the injection of oxygen. The process is more expensive but faster;
- purification: the purification of the zinc-bearing liquor can be carried out by using zinc powder, to reduce and precipitate metallic impurities [Reaction 3.7.1.10], or by solvent extraction, to extract a pure $ZnSO_4$ solution. The latter process is mainly used to treat secondary zinc materials, such as Waelz oxide;

$$Me^{2+} + Zn^0 \rightarrow Me^0 + Zn^{2+}, \text{ where } Me^{2+} = \text{Cu, Cd, Co, Ni, Tl or Pb} \qquad [3.7.1.10]$$

- electrolysis: the purified solution is fed to a cell house where zinc is electrowon using lead anodes and aluminium cathodes. Zinc is deposited at the cathode and oxygen is formed at the anode. Zinc is recovered from the cathode by stripping.

As previously reported, Waelz oxide can be used as input material to the hydrometallurgical process. Waelz oxide is a zinc-rich intermediate product produced from residues, such as the dust from electric arc steelmaking furnaces (EAF dust), in Waelz kilns or slag fuming furnaces (EU, 2017).

The process consists in the recovery of zinc and lead from the residues by reducing, volatilising and oxidizing zinc and lead again. The EAF dust is fed to the Waelz furnace along with other zinc-rich materials, coke breeze and lime or silica, depending if the process is run in basic or acid conditions. The reducing atmosphere of the solid bed promotes the reduction of zinc and lead, which volatilise into the gas. Zinc vapours are sucked by an exhaust chimney and subsequently oxidize when they come in contact with air, producing the Waelz oxide. The Waelz oxide is separated from the gas stream by an electrostatic precipitator or a fabric filter. It can be briquetted or sintered and sent to a pyrometallurgical zinc plant or it can be washed with water and sodium carbon, in a neutral or alkaline environment, to remove chlorides, fluorine, sodium and potassium and then

sent to a roast-leach-electrowinning plant, at the roasting or directly at the leaching step (EU, 2017; Palamini et al., 2018). Alkaline operation is usually preferred, to guarantee a longer duration of the refractory (Mombelli et al., 2015). In this case, the average addition of lime in the Waelz process is 0.21 t/t dry product (EU, 2017).

Management of lead and zinc residues

The upgrading and the concentration of Pb and Zn ores through grinding and flotation generate Zn and Pb tailings, in the form of a slurry with 20-45% solid content (Bascetin and Tuylu, 2017). The tailings composition depends on the mineralogy of the gangue minerals. They can consist mainly in carbonates or in silicates, with usually high concentration of sulphides (Khalil et al., 2019). Lime or limestone can be used in the flotation process to adjust the pulp's pH, enriching the tailings of Ca compounds (EU, 2009; Bascetin and Tuylu, 2017). These residues are usually discharged in dams as mud. No data about the amount of tailings produced per tonne of concentrate were found.

Both primary and secondary lead production processes result in the production of a residual slag. Secondary lead slags amount to about 13-25% of the weight of the lead produced (EU, 2017). For what concerns primary lead slags, Kreusch et al. (2007) and de Andreade Lima and Bernandez (2011) reported a production of 100-350 kg of slag per ton of metallic lead produced. A much higher production, of 1 ton of slag per ton of metal generated, is reported by Sobanska et al. (2000) referring to the lead smelting plant of Noyatelles-Godault in France.

The slags produced by Zn pyrometallurgical route or by the Waelz kiln process amount to about 10-70% of the weight of the metal produced, depending on the quality of the concentrate (EU, 2017).

Although mechanical properties of Zn and Pb slags would make them suitable to be used as a construction materials (EU, 2017)[27], they can contain high concentration of potentially toxic metals that can be leached into soils when the slags are stored or used in civil unbounded applications (Parsons et al., 2001; Ettler et al., 2003; Piatak and Seal, 2010; Barna et al., 2004). For example, secondary lead slag can contain antimony, which can cause emission of stiobane when the slag is stored in dump (EU, 2017), whereas primary lead slag usually contains high concentration of Pb. The slags produced by Zn pyrometallurgical route or by the Waelz kiln process are usually disposed in landfill since they are classified as hazardous waste (Mombelli et al., 2015), with the exception of Spain, where Zn slag can be recycled as construction material (Busé et al., 2014).

For this reason, different studies have been performed in the recent years aimed at reducing the environmental impact of the slag through additional thermal, chemical or thermo-chemical treatments during or after the deslagging process (Mombelli et al., 2015; Forrester, 2006), with the final goal of recycling the slags rather than disposing them in landfill. For example, for what concerns primary Pb slag, the QSL and the Kivcet furnaces usually incorporate an integral reduction zone to reduce the Pb content of the slag below an acceptable

[27] Zn and Pb slags were used in the past as construction materials in several countries, such as Poland and Brazil (Tyszka et al., 2014; Lima and Bernandez, 2011)

level. The Kaldo furnace uses an adjacent slag fuming furnace, whereas the Ausmelt/ISASMELT furnace may be operated in a two-stage operation, with one furnace or with two parallel furnaces, in order to treat the primary slag inside the process. The resulting slag has a very low concentration of leachable metals and can, thus, be used as secondary raw materials in construction (EU, 2017). Another example regards the Waelz plant in Pontenossa (Italy), that has recently implemented a thermal treatment of its Waelz slags that consists in its smelting, along with acidic fluxes and reducing agents, in order to recover the residual non-ferrous metals still present in the slags, such as Zn, Pb and Cd (Palamini et al., 2018). These metals are reduced during the process and evaporate, and subsequently are condensed from the gaseous stream in the same way as the Waelz oxide, having also approximately the same chemical composition. The slags produced by the process are actually inert and can be recycled in unbounded applications (Palamini et al., 2018). Alternatively, the slags can be recovered in bounded applications. For example, Mao et al. (2019) propose to add Pb-Zn smelting slags in supported alkali-activated slag cementitious materials, made up with blast furnace slags.

For what concerns the hydrometallurgy route for Zn production, the main residue comes from the leaching process and consists in iron-based solids (goethite, jarosite or haematite). Their amount depends on the composition of the concentrate. Usually, they are partially used as raw materials in internal or external processes and the rest of the residue is landfilled in isolated areas or ponds (EU, 2017). To reduce their environmental impacts, associated to the possible leaching of metals, they can be neutralized or treated with sulphide (EU, 2017).
Leaching residues with high amounts of Zn or Pb can be recycled in the Imperial Smelting Furnace process, as Zn-Fe concentrate, or in a lead smelter, as $PbSO_4$ concentrate. Alternatively, they can be recycled in Waelz kilns (EU, 2017).

Literature assessment on lead and zinc tailings and slags: material and methods

The scientific literature on lead and zinc tailings and slags carbonation is almost absent. Thus, the literature review focuses mainly on the characterization of these residues in terms of Ca content and mineralogy.
Overall, 20 papers published in scientific journals, one conference paper, one patent and the BREF Documents for the non-ferrous metals industries (EU, 2017) and for the management of tailings and waste-rock in mining activities (EU, 2009) were considered, as reported in Table 3.7.1.6.

Table 3.7.1.6. List of the documents considered in the study for the review about the lead and zinc production.

Peer reviewed papers
Barna et al., 2004. *Leaching assessment of road materials containing primary lead and zinc slags*. Waste management 24, 945-955
Coya et al., 2000. *Ecotoxicity assessment of slag generated in the process of recycling lead from waste batteries*. Resources, Conservation and Recycling 29, 291-300
Ettler et al., 2001. *Primary phases and natural weathering of old lead-zinc pyrometallurgical slag from Pribram, Czech Republic*. The Canadian Mineralogist 39, 873-888
Ettler et al., 2004. *Leaching of lead metallurgical slag in citric solutions. Implications for disposal and weathering in soil environments*. Chemosphere 57, 567-577
De Andrade Lima and Bernandez, 2011. *Characterization of the lead smelter slag in Santo Amaro, Bahia, Brazil*. Journal of Hazardous Materials 189, 692-699
Ogundiran et al., 2013. *Immobilisation of lead smelting slag within spent aluminate-fly ash based geopolymers*. Journal of Hazardous Materials 248-249, 29-36
Onisei et al., 2012. *Synthesis of inorganic polymers using fly ash and primary lead slag*. Journal of Hazardous Materials 205-206, 101-110
Penpolcharoen, 2005. *Utilization of secondary slag as construction material*. Cement and Concrete Research 35, 1050-1055
Seignez et al., 2007. *Effect of Pb-rich and Fe-rich entities during alteration of a partially vitrified metallurgical waste*. Journal of Hazardous Materials 149, 418-431
Seignez et al., 2006. *Weathering of metallurgical slag heaps: multi-experimental approach of the chemical behaviors of lead and zinc*. WIT Transaction on Ecology and the Environment 92, 31-40
Seignez et al., 2008. *Leaching of lead metallurgical slag and pollutant mobility far from equilibrium conditions*. Applied Geochemistry 23, 3699-3711
Sobanska et al., 2000. *Alteration in soils of slag particles resulting from lead smelting*. C.D. Acad. Sci. Paris, Sciences del la Terre et des planetes 331, 271-278
Piatak and Seal, 2010. *Mineralogy and the release of trace elements from slag from the Hegeler Zinc smelter, Illinois (USA)*. Applied Geochemistry 25, 302-320
Mao et al., 2019. *The solidification of lead-zinc smelting slag through bentonite supported alkali-activated slag cementitious material*. International Journal of Environmental Research and Public Health 16, 1121
Vanaecker et al., 2014. *Behavior of Zn-bearing phases in base metal slag from France and Poland: a mineralogical approach for environmental purposes*. Journal of Geochemical Exploration 136, 1-13
Nouairi et al., 2018. *Study on Zn-Pb ore tailings and their potential in cement technology*. Journal of African Earth Sciences 139, 165-172
Othmani et al., 2015. *The flotation tailings of the former Pb-Zn mine of Touiref (NW Tunisia): mineralogy, mine drainage prediction, base-metal speciation assessment and geochemical modeling*. Environ. Sci. Pollut. Res. 22, 2877-2890
Bascetin and Tuylu, 2018. *Application of Pb-Zn tailings for surface paste disposal: geotechnical and geochemical observations*. International Journal of mining, reclamation end environment 32, 312-326
Khalil et al., 2019. *Pb-Zn mine tailings reprocessing using centrifugal dense media separation*. Minerals Engineering 131, 28-37
Tyszka et al., 2014. *Extensive weathering of zinc smelting slag in a heap in upper Silesia (Poland): potential environmental risks posed by mechanical disturbance of slag deposits*. Applied Geochemistry 40, 70-81
Patent document
Forrester, 2006. *Method for stabilization of lead smelter slag and matte*. US Patent n. US 7,121,995 B2
Conference paper
Palamini et al., 2018. The Waelz process: state of the art and innovation to decrease the environmental impact. Proceedings of the 4th European Conference on Clean Technologies in the Steel Industry, Bergamo 28-29 November 2018
BREF documents
EU, 2017. BREF Document for the Non-Ferrous Metals Industries.
EU, 2009. BREF Document for Management of Tailings and Waste-Rock in Mining Activities.

Lead and zinc tailings and slags composition

Lead and zinc tailings

The chemical composition of Pb-Zn tailing is reported in Table 3.7.1.7. The content of Ca can vary significantly, from 2% of the weight of the residue to more than 50%. This difference mainly depends on the type of gangue minerals in the Pb-Zn deposit. Usually zinc and lead are extracted from sulphide ore, but the gangue minerals can consist in carbonates or silicates (Khalil et al., 2019). For example, Khalil et al. (2019) analysed two different tailings produced at two mine sites. In both sites, Pb and Zn were developed from sulphide minerals. However, the rest of the gangue minerals had a different composition. Where the dominant minerals were carbonates (Dolomite), the content of Ca and Mg compounds in the tailings amounted to more than 40% of the weight of the residue, whereas where the dominant minerals consisted in silicates, SiO_2 was the main component of the tailings and Ca content was about 2%.

Furthermore, lime or limestone are usually added during the milling and flotation operations, thus increasing the Ca content of the tailings. On average, Ca compounds, expressed as CaO, amount to about 25% of the weight of the tailings.

Considering tailings mineralogy, the main crystalline phases are quartz, galena (PbS), calcite, dolomite, kaolinite ($Al_2Si_2O_5(OH)_4$), pyrite (FeS_2), gypsum, albite ($NaAlSi_2O_8$) (Nauairi et al., 2018; Othmani et al., 2015; Khalil et al., 2019). Other phases that have been observed in historical tailings are actinolite ($Ca_2(Mg_{4.5-2.5}Fe^{2+}_{0.5-2.5})Si_8O_{22}(OH)_2$), chlorite ($(Mg,Fe)_3(Si,Al)_4O_{10}(OH)_2*(Mg,Fe)_3(OH)_6$), epidote ($Ca_2Al_2Fe(SiO_4)(Si_2O_7)O(OH)$), pyrrhotite ($Fe_{1-x}S$) and saponite ($(Ca/2,Na)_{0.3}(Mg,Fe^{2+})_3(Si,Al)_4O_{10}(OH)_2*4(H_2O)$, sphalerite (ZnS), ankerite ($Ca(Fe,Mg,Mn)CO_3$) and siderite ($FeCO_3$) (Babel et a., 2018; Othmani et al., 2015). Cerussite ($PbCO_3$), gypsum, Fe-oxides, anglesite ($PbSO_4$) are usually secondary minerals, produced as a consequence of the weathering process affecting the tailings during their storage (Othmani et al., 2015).

Calcite can be present in high amount. Babel et al. (2018) observed up to 11.5% of calcite in historical Zn tailings. Much higher values, up to 87%, was observed by Othmani et al. (2015) in over 50 years old Tunisian Pb-Zn tailings. The authors analysed both oxidised and non-oxidised tailings (collected from the unoxidised zone of the dump, at a depth of more than 6 m). No significant difference was observed between the two types of samples, suggesting that calcite content was not the consequence of a carbonation process but was mainly related to the ore composition and eventually to the addition of limestone during flotation. The elevate content of Ca ensures acid neutralization capacity (ANC) to the tailings, useful to avoid AMD problems (Othmani et al., 2015).

Table 3.7.1.7. Chemical composition of Pb-Zn tailings (min-average-max value). Elaboration of the data reported in the documents listed in Table 3.7.1.6.

Total Ca as CaO (%)	Total Mg as MgO (%)	SiO_2 (%)
2.0-25.5-54.6 *6 cases*	0.5-5.2-17.3 *6 cases*	5.6-29.8-68.4 *5 cases*

Lead and zinc slag

The chemical composition of lead and zinc slags is reported in Table 3.7.1.8. Slag composition and its mineralogy depend on the concentrate compositions, on the type of pyrometallurgical process and on the slag cooling methods (with air or with water). Therefore, some little differences in the slag composition and mineralogy are usually observed between Pb and Zn slag, as well as between air and water cooled slag from the same precipitate. However, considering the overall Ca content in the slags, the same value can be assumed for both lead and zinc slags, as suggested by the statistical test of Kruskal-Wallis. Thus, on average, Ca compounds, expressed as CaO, amount to about 13.5% of the weight of the slags, ranging from less than 1% to more than 40%.

Table 3.7.1.8. Chemical composition of Pb-Zn slags (min-average-max value). Elaboration of the data reported in the documents listed in Table 3.7.1.6.

Type of slags	Total Ca as CaO (%)	Total Mg as MgO (%)	SiO_2 (%)
Zn smelting slag	0.2-11.4-30.2 *14 cases*	0.6-1.6-7.5 1*2 cases*	2.0-37.0-57.1 *14 cases*
Waelz slag	23.2 *1 case*	5.2 *1 case*	6.7 *1 case*
Pb smelting slag (primary and secondary production)	1.0-15.5-42.0 *10 cases*	0.2-2.9-7.5 8 *cases*	4.0-29.6-54.6 *10 cases*
Pb-Zn smelting slag	12.5 *1 case*	3.3 *1 case*	3.1 *1 case*

For what concerns the mineralogical composition, a greater variability is observed among the different types of slags (Piatak and Seal, 2010). However, on average, the principal phases that can be found in the slags are: feldspar (mainly plagioclase $CaAl_2Si_2O_8$-$NaAlSi_3O_8$), pyroxene, olivine, glass and spinel (gahnite $ZnAl_2O4$, hercynite $FeAl_2O_4$, magnetite Fe_2O_4) and secondary goethite (FeOOH), hematite (Fe_2O_3) and gypsum (Piatak and Seal, 2010; Warchulski and Szopa, 2014; Vanaecker et al., 2014). Other primary phases that can be observed in Zn and Pb slags are mullite ($Al_6Si_2O_{13}$), willemite (Zn_2SiO_4), hardystonite ($Ca_2ZnSi_2O_7$), gahnite, zincite (ZnO), tridymite (SiO_2), melitites ($Ca_2ZnSi_2O_7$), franklinite (Zn, Mn^{2+},Fe^{2+})(Fe^{3+},Mn^{3+})$_2O_4$), pyrrhotite ($Fe_{1-x}S$), chalcopyrite ($CuFeS_2$) and copper sulphide. Zn sulphates, Zn carbonates, ion (hydroxides), together with gypsum, are observed in the filling discontinuities, as a consequence of the weathering reactions. In lead slags, kirchsteinite ($CaFeSiO_4$), litharge (PbO) and drop of metallic Pb can also be observed (Ettler et al., 2001; de Andrade Lima and Bernandez, 2011; Onisei et al., 2012).

The presence of a small amount of calcite was reported by Sobanska et al. (2016) and by Tyszka et al. (2014) in historical Zn and Pb slags.

Potential carbonation rate in lead and zinc tailings and slags

The maximum theoretical amount of CO_2 that can be sequestered by the lead and zinc residues (tailings and slags) due their content of Ca can be calculated on the basis of their chemical composition.

Assuming a 25.5% average content of CaO in the Pb/Zn tailings and a 13.5% average content in the Pb/Zn slags, as reported in Tables 3.7.1.7 and 3.7.1.8, the maximum CO_2 sequestration potential results equal to about 200 gCO_2 per kg of tailing and 105 gCO_2 per kg of slag.

However, these figures are absolutely theoretical.

For what concerns the tailings, in fact, we can assume that no carbonation reactions will affect this residue. The reasons are various: first of all, Ca compounds in Pb-Zn tailings mainly consist in calcite or silicate compounds, which are usually not available for carbonation reactions. The presence of free lime is not reported in the literature, even when lime is used in the flotation process. Furthermore, Pb-Zn tailings contain high content of sulphide minerals that can be potentially oxidised when in contact with air, producing acids. As shown by Wong et al. (1998), when lime is used in the flotation process, fresh tailings have a pH above or around 7. However, this value significantly decreases in old tailings due to oxidation reactions of the sulphide minerals, especially pyrite. In such a pH condition, carbonation reactions cannot occur. On the contrary, CO_2 can be released in the atmosphere as a consequence of the neutralization of sulphate ions by the tailings alkalinity, as shown in [11] (Othmani et al., 2015).

$$CaCO_3\,(s) + 2H^+ + SO_4^{2-} + 2H_2O \leftrightarrows CaSO_4{*}2H_2O\,(s) + H_2CO_3 \qquad [11]$$

For what concerns the slags, since Ca in lead and zinc slags is usually present in the form of silicates or calcite, thus as low- or non-reactive phases, a much lower CO_2 uptake is expected under natural environmental conditions.

Natural carbonation of lead and zinc slags

As previously reported, data about natural carbonation of lead and zinc slags were not found. However, based on the indications reported in some papers, it is possible to infer that a slight carbonation of the slag can happen, but it does not necessarily interest the Ca compounds.

Vanaecker et al. (2014) observed the presence of secondary phases that are the consequence of carbonation processes happened in historical Zn slag. However, these reactions seem to interest more the Zn ions released in acidic local conditions by zincite and other Zn compounds than the Ca ions. Ca ions, released by the dissolution of melilite and hardystonite, react with sulphate ions, precipitating as gypsum.

Calcite precipitation was, on the contrary, observed by Sobanska et al. (2016) on the surface of Fe-rich phases of pyrometallurgical 10 year old slags from a Pb-Zn smelter plant in the North of France, where the slags from the Imperial smelting Furnace and those from the Lead Blast Furnace were stored together in the same area. The presence of calcite was also observed by Tyszka et al. (2014) in a historical slag deposit of Zn smelting slag in Poland. However, the two dominant secondary phases are gypsum and hematite, suggesting that Ca preferably reacts with sulphates, precipitating as gypsum.

Ettler et al. (2004) investigated the leaching behaviour of lead smelter slags in acidic conditions, with the aim of understanding the weathering process of slag in soil environment. In one out of two samples, they observed

the precipitation of carbonates as cerrusite ($PbCO_3$) and calcite, as a consequence of the fixation of the dissolved atmospheric CO_2. The precipitation of cerrusite and hydrocerrusite precipitation was also observed by Seignez et al. (2007). The authors suggested that the source of CO_3^{2-} can be both slag alteration or the dissolution of the atmospheric CO_2 in the pore water.

Discussion and conclusions

Like for the other base metals residues, based on our knowledge, scientific literature about carbonation of lead and zinc tailings and slags is almost absent.

For what concerns the pyrometallurgical slags, based on the little information reported in the scientific literature, it is possible to assess that carbonation processes interesting these residues are really modest and mainly related to local release of Zn and Pb ions. Ca in the slags usually reacts with sulphate ions, precipitating as gypsum. In order to verify such a conclusion, we suggest to carry out some analyses on fresh and old lead and zinc slags to assess the presence of carbonation reactions and eventually to subject the slags to accelerated carbonation tests.

For what concerns lead and zinc tailings, they are usually stored in dam/pond sites. The stored residue is characterized by a pH value around or below 7, depending on its content of alkaline compounds (mainly calcite). In such a condition of pH, carbonation reactions cannot occur.

3.7.1.4. USE OF LIME IN PRECIOUS METALS PRODUCTION - GOLD PRODUCTION

Introduction

Gold is usually found in its native form in exogenetic (formed at the earth's surface) or endogenetic (formed within the earth) ores. Otherwise, it can be found in combination with tellurium, as calaverite ($AuTe_2$) and sylvanite ($AuAgTe_4$). Other sources of gold are jewellery, sweeps, dental scraps and some by-products obtained from the processing of other non-ferrous metals, such as the anode slimes from copper production and the leach residues from lead and zinc production (EU, 2017).

For what concerns primary gold production, the mining and the applied mineral processing techniques depend on the nature of the ore deposit. Exogenetic gold mainly consist in alluvial gold, that is elemental gold, often in very fine particles, found in riverbeds and floodplains. Otherwise, it can be found as oxidized ore bodies that have formed under a process called secondary enrichment. Endogenetic gold ores include vein and lode deposits of elemental gold in quartzite or mixture of quartzite and various iron sulphide minerals.

Alluvial deposits are usually concentrated by gravity techniques. Oxide ore deposits are frequently of such a low grade that extensive mineral processing cannot be economically justified. In this case, they are just shattered by explosives and piles into heaps for extraction by cyanidation. Endogenetic deposits contain gold that is highly disseminated within a base metal sulphide mineral. These deposits are mined, crushed and ground and then concentrated by gravity separation to recover coarse particles of native gold and then subjected to froth flotation to concentrate the sulphide mineral fraction containing gold.

Different methods can be used to recover gold from the concentrate/mined minerals (Wong and Arum, 2009). The principal two are:

- fine particulate gold can be recovered by amalgamation. The fine mineral particles are put in contact with fresh mercury. Gold dissolves in mercury forming an alloy called amalgam. Then the amalgam is heated and mercury is separated by distillation;
- cyanidation is the most commonly used leaching process for gold extraction. The ore, after mining and eventually concentration, is comminuted and mixed with water to form a slurry. The slurry is combined with a solution of sodium, potassium or calcium cyanide. Slaked lime or soda are usually added to ensure that the pH is maintained above 8 during the entire process, in order to prevent the formation of the toxic hydrogen cyanide (Breuer et al., 2010). Air, or pure oxygen, is thus injected into the slurry (additional mixing can be required). Metallic gold is oxidized and dissolved in an alkaline cyanide solution according to the so-called Elsner Reaction [3.7.1.12]. When gold dissolution is complete, the gold-bearing solution is separated from the solids.

$$4Au + 8CN^- + 2H_2O + O_2 \rightarrow 4Au(CN)_2^- + 4OH^- \qquad [3.7.1.12]$$

In case of low-grade ores, heap leaching is practiced. In this case, the heaps obtained by the mining activities are sprayed with a diluted solution of sodium cyanide which percolates down through the pile ore, dissolving the gold.

Granular activated carbon can be added to the slurry during or after gold solubilisation. The dissolved gold is absorbed on the carbon, which can be separated by screening. Gold is then leached from the carbon by a strong solution of NaOH and it is recovered from the solution by electrowinning or by the Merrill-Crowe process. In the latter process, the gold-bearing solution is deoxygenated and passed through a filter-press where the gold is displaced from the solution by reduction with zinc metal powder.

In the case of ores rich in sulphide minerals, a roasting process is usually required before cyanidation, in order to oxidise sulphides minerals, which would consume the cyanide reagent before it can dissolve gold.

The gold extracted by amalgamation or cyanidation must be refined, as it contains a lot of impurities, such as Zn, Cu, Si, and Fe. Two principal methods can be used (EU, 2017):

- Miller process, where the impure gold is melted at about 1000°C and gaseous chlorine is blown into the liquid. The impurities present in gold react with gaseous chlorine and are separated from the molten gold, which, at this temperature, is the only metal present that does not react to form stable molten or volatile chloride. The process is operated to produce either 98% gold, which is cast into anodes for electrorefining, or 99.5% gold, which is cast into bullion bars;
- Wohwill process, where the impure gold, or the anodes from the Miller process, are refined by electrolysis. A purity of 99.99% can be achieved.

As previously reported, gold can be also recovered from various scraps and from by-products of the metallurgy of other base metals.

Gold can be recovered from copper anode slimes by a multistep pyrometallurgical process (EU, 2017; Chen et al., 2015). First of all, the slimes are roasted with sulphuric acid or oxygen for the removal of Se and Cu. Then the roasted product is smelted with coke and some fluxing agents (silica, lime, and sodium carbonate) to produce a fluid slag, which collects most of the impurities, such as the residual Cu, Se, Sb, Bi, Te, and Ni. Gold, silver and a small amount of impurities (a part of the Cu and Se) remain with the Pb-Au-Ag alloy, which is named Doré metal. Doré metal usually contains 25-99.55% of silver and 0-99% of gold and it is refined by oxidation at 900-1200°C. Finally, the Au-Ag alloy is treated in electrolytic cells. Silver is recovered at the cathode, whereas gold and platinum group metals (PGM) are concentrated in slimes and then recovered by electrolytic refining.

Hydrometallurgical and solvent extraction processes are also used for the recovery of precious metals from anode slimes. Gold is recovered by leaching the slimes with hot hydrochloric acid and chlorine gas or with sulphuric acid and some oxidants (EU, 2017; Chen et al., 2015).

As previously reported, lime is often used in the cyanidation process to control the pH of the slurry. Furthermore, it can result in the coagulation of fine-grain minerals, enhancing the permeability of the pore pile, when heap leaching is performed, and improving the contact between the minerals and the CN^-. Lime is also able to fix arsenic in the ores, by converting it into $Ca_3(AsSO_3)_2$ (Fu et al., 2015). Data about the average lime consumption in the cyanidation process were not found.

The main residues produced by the gold production industry are slags in pyrometallugical processes and tails streams containing high concentration of cyanide in the cyanidation process.

Slags are usually recirculated in the furnace or recovered in lead production plants.
Cyanide tailings must be detoxified before being stored in dedicated ponds. Two main processes are available: the INCO-licensed process and the Caro's acid process (Hewitt et al., 2012). Both processes oxidise the cyanide to cyanate, which is less toxic and can then react to form carbonated and ammonia [Reactions 3.7.1.13 and 3.7.1.14].

$CN^- + O \rightarrow OCN^-$ [3.7.1.13]

$OCN^- + 2H_2O \rightarrow HCO_3^- + NH_3$ [3.7.1.14]

The Caro's process uses H_2SO_5 acid, whereas the INCO process uses a SO_2/air detoxification circuit to convert cyanide to cyanate. This process blows compressed air through the tailings while adding sodium metabisulfite, which releases SO_2. Lime is used to maintain the pH at around 8.5.
If the gold mine is contaminated by arsenic, this can be found in the tailings in the form of arsenite and arsenate, as a consequence of the oxidation of the arsenopyrite during cyanidation. In this case, arsenic must be removed from the tailings before discharge into the tailings facility (Hamberg, 2014). The preferred method is the co-precipitation of As with ferric ions during the INCO process. Addition of lime, with the consequent precipitation of gypsum, can enhance the effect of co-precipitation of As with Fe-hydrates, removing sulphate ions from the solution [3.7.1.15]. In fact, the stability of As-bearing Fe-hydrates decreases in a sulphate media, since sulphate ions compete with arsenate for adsorption on Fe(III)-precipitate sites (Riveros et al., 2001). Furthermore, lime (or limestone) is usually used to treat mine tailings to promote the precipitation of sulphate compounds as gypsum and, thus, to limit the long term liabilities associated with the natural generation of acid mine drainage (Fleming et al., 2010).

$2H_3AsO_4 + Fe_2(SO_4)_3 + 3Ca(OH)_2 \rightarrow 2FeAsO_4(s) + 3CaSO_4(s) + 6H_2O$ [3.7.1.15]

Literature assessment on gold cyanidation tailings: material and methods

The literature review reported in this chapter focuses only of gold cyanidation tailings, since no information about the other residues produced by the gold metallurgy was found. In any case, the scientific literature on gold cyanidation tailings characterization and carbonation is almost absent.
Overall, 3 papers published in scientific journals, one PhD thesis and the BREF Documents for the non-ferrous metals industries (EU, 2017) and for the management of tailings and waste-rock in mining activities (EU, 2009) were considered, as reported in Table 3.7.1.9.

Table 3.7.1.9. List of the documents considered in the study for the review about the gold cyanidation tailings.

Peer reviewed papers Hasan et al., 2018. *Potential of soil, sludge and sediment for mineral carbonation process in Selinsing gold mine, Malaysia*. Minerals 8, 257-271 Paktunc et al., 2004. *Speciation and characterization of arsenic in gold ores and cyanidation tailings using X-ray absorption spectroscopy*. Geochimica et Cosmochimica Acta 68,5, 969-983 Zagury et al., 2004. *Characterization and availability of cyanide in solid mine tailings from gold extraction plants*. Science of the Total Environment 320, 211-224
PhD Thesis Hamberg, 2014. *Characterization and solidification of Arsenic-rich cyanided tailings*. Lulea University of Technology
BREF documents EU, 2009. *BREF Document for Management of Tailings and Waste-Rock in Mining Activities* EU, 2017. *BREF Document for the Non-Ferrous Metals Industries*

Composition of gold cyanidation tailings

Chemical composition of gold cyanidation tailings is reported in Table 3.7.1.10. The results show a wide variability in the tailings composition due to the different mineralogy of the ore deposit. Ca concentration, expressed as CaO, ranges from 1 to about 17.5%, with an average value of 6%.

Regarding the tailings mineralogy, the main phases usually observed are: quartz, kaolinite ($Al_2Si_2O_5(OH)_4$), goethite ($FeO(OH)$), chlorite-serpentine ($(Mg,Al)_6(Si,Al)_4O_{10}(OH)_8$), illite ($(K,H_3O)(Al,Mg,Fe)_2(Si,Al)_4O_{19}[(OH)_2,(H_2O)]$), pyroxene ($(Ca,Na,Fe,Mg)(Cr, Al, Fe, Mg, Co)(Si,Al)_2O_6$), amphibole, talc ($Mg_3Si_4O_{10}(OH)_2$), wallostonite ($CaSiO_3$), muscovite ($KAl_2(Si_3Al)_{10}(OH,F)_2$) and plagioclase feldspar ($NaAlSi_3O_8$-$CaAl_2Si_2O_8$) (Hasan et al., 2018; Paktunc et al., 2004). Ca is present in complex silicates compounds, as calcite, magnesite and gypsum, the last one formed during the treatment process of the cyanidation effluents as a consequence of the addition of lime (Hamber, 2014; Paktunc et al., 2004). The prevalence of Ca-Mg compounds or Fe compounds depends on the nature of the ore deposit and has evident consequences on the AMD potential of the tailings pond.

Table 3.7.1.10. Chemical composition of gold cyanidation tailings (min-average-max value). Elaboration of the data reported in the documents listed in Table 3.7.1.9.

Total Ca as CaO (%)	Total Mg as MgO (%)	SiO_2 (%)	Total Fe as FeO (%)
1.3-6.0-17.5 13 cases	0-1.2-3.2 *15 cases*	7.5-27.8-64.7 *9* cases	1.4-12.5-30.7 *15 cases*

Potential carbonation rate in gold cyanidation tailings

A rough estimation of the maximum amount of CO_2 that can be sequestered by the gold cyanidation tailings as a consequence of their content of Ca compounds can be based on their chemical composition (Table 3.7.1.10), and results equal, on average, to about 47 gCO_2/kg gold tailings. However, this value is absolutely theoretical. Ca is mainly present in the form of silicates, calcite or gypsum, depending on the ore composition and on the detoxification process to which the tailings are subjected. These compounds are characterized by a

low reactivity and, thus, a much lower amount of CO_2 is expected to be sequestered under natural environmental condition, despite the alkaline pH of the tailings, which can promote the carbonation process.
Depending on the ore composition and on the detoxification process used for the tailings treatment, the concentration of Ca in the tailings could be negligible and more Mg could be present. In this case, the main phases potentially involved in the carbonation process are Mg silicates and Fe-oxides, such as chlorite-serpentine, sepiolite and stipnomelane, as reported by Hasan et al. (2018).

Natural and accelerated carbonation of gold cyanidation tailings

Based on the survey, the natural or accelerated carbonation of gold cyanidation tailings has not been studied in the scientific literature. The only paper reporting the presence of carbonation processes in gold cyanidation tailings deposits is the one by Zagury et al. (2004). The authors analysed fresh and aged gold tailings stored in two gold mining sites in Canada and observed that, over time, the pH of the tailings gradually decreased (from 10.5 to about 7 in 6 years) due to neutralization of the alkaline environment during rainwater infiltration and because of the CO_2 uptake. However, they did not investigate which chemical compounds were actually interested by the carbonation reactions.

Discussion and conclusions

The scientific literature about gold cyanidation tailings carbonation is almost absent. Based on the few data about tailings chemical and mineralogy composition, it is not expected that a great amount of CO_2 will be sequestered during the tailings storage, as a consequence of their content of Ca.
In any case, we suggest to carry out some analyses of gold cyanidation tailings of different age in order to quantify their content of Ca, its mineral phases and to assess if the atmospheric CO_2 is actually sequestered by this material under natural environmental conditions or if the decrease of the pH value observed by Zaguri et al. (2004) in old tailings is due to other reasons.

3.7.1.5. PLATINUM GROUP METALS (PGMs) PRODUCTION

Introduction

Platinum Group Metals (PGMs) include platinum, palladium, rhodium, ruthenium, iridium, and osmium. The principal raw materials are concentrates produced from ores, mattes and slimes from nickel and copper production. Secondary materials, such as spent chemicals and automotive exhaust catalysts and electronic and electrical equipment waste, are also significant sources (EU, 2017).
For what concerns the primary production, PGMs are usually found in nature associated with other metals, such as nickel, copper, and gold (EU, 2017; Mpinga et al., 2015). The ore is mined and then crushed and milled in fine particles, usually below 30 μm, to liberate the valuable minerals. Then PGM-bearing particles are separated by froth flotation (or mill-float-mill-float open circuit in the case of chromite rich ore). The produced concentrate is smelted in electric furnaces and the matte containing the valuable metals is treated in converters to remove iron and sulphur. Limestone is usually added as a fluxing agent during smelting and

conversion (Jones, 2005). Then, the base metals Ni, Co, and Cu are separated from the matte by hydrometallurgical processes, consisting in leaching operations. The resulting slime contains 10-50% of precious metals (Cole and Joe Ferron, 2002) and is refined to a high level of purity by using a combination of solvent extraction, distillation, and ion-exchange techniques.

An alternative route is the hydrometallurgical treatment of the concentrate from the flotation process. Several processes are available, depending on the characteristics of the ore. Usually, lime or limestone are added during the process to control the pH and promote selective separation of the different metals (Mpinga et al., 2015).

For what concerns the secondary production, PGM-containing materials are smelted to form a metal matte or dissolved to bring the PGMs into a solution. The matte or the leachate solution are then refined to recover the individual metals.

The principal source of secondary PGMs are the automotive catalysts. In the pyrometallurgical route, the spent catalyst is mixed with fluxes, collector (Cu, Ni, Pb or Fe) and reductant and sent to smelting. The resulting PGMs-collector alloy is further treated. In the hydrometallurgical route, spent catalysts are roasted and then subjected to leaching processes, where HCl, NaOH, H_2SO_4 or chemical solvents are used as extracting agents (Panda et al., 2018).

The processes involved in PGMs production result in the production of several waste materials that can still contain significant amount of metals (slags and tailings). These residues are usually treated by hydrometallurgical processes to recover residual metals and reduce their hazardousness. One of the possible options is the cyanidation process, like for gold. In this case, high amount of alkaline materials (such as lime or limestone) are added to maintain the pH above 9 (Mpinga et al., 2015).

Converter slags can be also treated by pyrometallurgical processes in order to reduce their content of metals (Jones, 2005). Quantitative data about lime dosage during the processes and residues production were not found in the available literature.

Literature assessment on PGMs tailings: material and methods

The literature review reported in this chapter focuses only of PGM tailings from the mine and flotation activities, since no information about the other residues produced by the PGMs metallurgy was found. In any case, even the scientific literature on PGMs tailings characterization and carbonation is almost absent.

Overall, 3 papers published in scientific journals, one conference paper and the BREF Documents for the non-ferrous metals industries (EU, 2017) and for the management of tailings and waste-rock in mining activities (EU, 2009) were considered, as reported in Table 3.7.1.11.

Table 3.7.1.11. List of the documents considered in the study for the review about PGMs tailings.

Peer reviewed papers Meyer et al., 2014. *Mineral carbonation of PGM mine tailings for CO_2 storage in South Africa: a case study*. Minerals Engineering 59, 45-51 Ncongwane et al., 2018. *Assessment of the potential carbon footprint of engineered processes for the mineral carbonation of PGM tailings*. International Journal of Greenhouse Gas Control 77, 70-81 Vogeli et al., 2011. *Investigation of the potential for mineral carbonation of PGM tailings in South Africa*. Minerals Engineering 24, 1348-1356
Conference paper Amponsah-Dacosta and Reid, 2014. *Mineralogical characterization of selected South African Mine tailings for the purpose of mineral carbonation*. Proceedings of the Annual International Mine Water association Conference- An Interdisciplinary Response to Mine Water Challenges. Xuzhou, China
BREF documents EU, 2009. *BREF Document for Management of Tailings and Waste-Rock in Mining Activities* EU, 2017. *BREF Document for the Non-Ferrous Metals Industries*

Composition of PGMs tailings

The average chemical composition of PGM tailings is reported in Table 3.7.1.12. Ca compounds, expressed as CaO, amount to about 5.8% of the weight of the residue.

For what concerns the mineral composition, PGM tailings are mainly composed of silicates and oxides, but sulphides, such as pyrite and pyrrhotite, may also be present in small amount (Vogeli et al., 2011; Amponsah-Dacota and Reid, 2014), depending on the ore composition. On average, the main mineral phases are orthopyroxene (manly enstantite $Mg_2Si_2O_6$), plagioclase (anorthite $CaAl_2Si_2O_8$) and the alteration minerals talc and serpentine ($2Mg_3Si_2O_5(OH)_4$) (Vogeli et al., 2011).

Table 3.7.1.12. Chemical composition of PGM tailings (min-average-max value). Elaboration of the data reported in the documents listed in Table 3.7.1.11.

Total Ca as CaO (%)	**Total Mg as MgO (%)**	**SiO_2 (%)**	**Total Fe as FeO (%)**
2.4-5.8-8.7 *7 cases*	13.3-16.9-21.9 *7 cases*	16.0-40.9-49.9 *7 cases*	4.0-11.1-18.4 *7 cases*

Potential carbonation rate in PGM tailings

A rough estimation of the maximum amount of CO_2 that can be sequestered by the PGM tailings as a consequence of their content of Ca compounds can be based on their chemical composition (Table 3.7.1.12), and resulted equal to about 45 gCO_2/kg PGM tailings.

A similar result was found by Vogeli et al. (2011). They calculated the potential CO_2 sequestration of PGM tailings on the base of their mineral composition. Based on their evaluation, about 80% of the minerals in PGM tailings are potentially suitable for CO_2 uptake, sequestering the gas as $CaCO_3$, $MgCO_3$, and $FeCO_3$. Considering the sole contribution of the Ca compounds, the maximum theoretical CO_2 sequestration results equal to about 28-59 gCO_2/ kg of residue, depending on the tailings composition.

These figures are only theoretical. Although the fine particle size of the tailings and their alkaline pH are favourable elements for carbonation, the chemical reactivity of the Ca compounds usually detected in PGM tailings is low (Vogeli et al., 2011). Thus, a lower amount of CO_2 is expected to be sequestered under ambient conditions. Furthermore, the concentration of Ca in the tailings is not only the consequence of lime/limestone addition during the flotation process, but it is mainly related to the gangue minerals composition.

Accelerated carbonation of PGM tailings

The possibility to use PGM tailings in accelerated carbonation process to sequester CO_2 was investigated by Ncongwane et al. (2018) and Meyer et al. (2014). However, the authors did not provide quantitative data.

Ncongwane et al. (2018) analysed different technologies to use PGM tailings for CO_2 sequestration. However, the study focuses only on Mg conversion, since the main mineral phase that can be potentially involved in carbonation reactions is enstatite pyroxene, a Mg silicate of low reactivity. An effective conversion was observed only in indirect accelerated carbonation processes, where chemical agents are used to extract Mg from the tailings and carbonation is carried out in a second step.

The carbonation of Ca compounds is, on the contrary, reported in Meyer et al. (2014). They carried out some accelerated carbonation tests on South Africa PGM tailings, by using the two-step pH swing method. Different chemicals were tested to extract Ca, Mg, and Fe from the solid residue, as well as different conditions of temperature and pressure. The leaching step resulted in an extraction efficiency of the Ca ion included between 12 and 30%, depending on the operating conditions. After the carbonation step, only 29.9% of the Ca in the tailings was converted and precipitated as ankerite ($(Ca(Mg,Fe)(CO_3)_2$), dolomite ($CaMg(CO_3)_2$) and gaylussite ($Na_2Ca(CO_3)_2*5H_2O$). However, considering that Ca content in the analysed tailings accounted for only 5 and 8% of the weight of the residues, it is evident that the overall contribution of Ca to the carbonation process was modest.

Discussion and conclusions

Based on the previous results and considering the low reactivity of Ca and Mg compounds present in the PGM tailings (Ncongwane et al., 2018; Meyer et al., 2014), it can be stated that PGM tailings will unlikely carbonate under natural environmental conditions.

3.7.1.6. USE OF LIME IN LITHIUM PRODUCTION

Introduction

Lithium can be produced from raw materials or it can be recovered from spent batteries.

Regarding primary production, lithium can be extracted from ores/minerals by roasting followed by leaching, or it can be extracted from brines by evaporation and precipitation (Garrett, 2004). Currently, lithium production from brine is nearly two times than that from minerals (Choubey et al., 2016).

The principal minerals from which lithium is extracted are spodumene ($LiAlSi_2O_6$), petalite ($LiAlSi_4O_{10}$) and lepidolite ($LiKAl_2F_2Si_3O_9$). It can be also recovered from clay minerals, such as hectorite ($Na_{0.3}(Mg,Li)_3Si_4O_{10}(F,OH)_2$) (Meshram et al., 2014). The complex ores are first enriched to concentrate the lithium bearing minerals by size reduction, froth flotation and magnetic separation (Choubey et al., 2016). Then, two main routes are available for its recovery from the concentrate:

- the alkaline route, where the mineral reacts with limestone or a mixture of calcium sulphate and CaO or $Ca(OH)_2$ at high temperature to convert silicate to soluble lithium aluminate, from which LiOH or Li_2CO_3 are obtained (Meshram et al., 2014). Several processes are available. For example, lithium concentrate obtained by the flotation of spodumene ores is usually pulverized, mixed with limestone or lime, and calcined at 825-1050°C (see for example reaction [3.7.1.16] when limestone is used). Usually, a 5-10% addition of lime/limestone is sufficient (Kroll et al., 1953). The calcined mass is cooled and finely pulverized and lithium is extracted by leaching at high temperature and pressure, using water in the presence of CO_2 or a water solution of sodium chloride, sodium sulphate, sodium or calcium nitrate or calcium chloride, or a mixture of such salts. Lithium is recovered as carbonate (Kroll et al., 1953; Choubey et al., 2016).

$$Li_2O*Al_2O_3*4SiO_2\,(s) + CaCO_3 \rightarrow Li_2O(s) + CaO*Al_2O_3*4SiO_2\,(s) + CO_2\,(g) \qquad [3.7.1.16]$$

  Lepidolite concentrate is pre-roasted at 860°C under water steam atmosphere for defluorination and then is leached in a lime-milk autoclave at 150°C, in order to precipitate impurities of Al and Fe and the Ca and the Mg content of the lithium-bearing solution. Finally, Li_2CO_3 is precipitated by adding Na_2CO_3 (Yan et al., 2012a).

  Lithium recovery from zinnwaldite ore ($LiF*KF*FeO*Al_2O_3*3SiO_2$) can be performed by roasting with $CaCO_3*LiCO_3$ followed by CO_2 bubbling or solvent extraction (Jandova et al., 2010) or by roasting with limestone, gypsum and sodium sulphate or with gypsum and $Ca(OH)_2$, followed by water leaching with injection of CO_2 and precipitation (Siame and Pascoe, 2010; Kondas and Jandova, 2006). A mass ratio of concentrate/$CaSO_4$/$Ca(OH)_2$ of 6/4.2/2 is reported by Choubey et al. (2016).

- the acid route, where the concentrates are digested with H_2SO_4 or roasted with the addition of Na_2SO_4 and/or K_2SO_4 in order to dissolve Li_2SO_4 in the aqueous system. Lime is added to purify the Li-bearing solution by increasing the pH first to 5.5-6.5 and then to 11-13 and promoting the precipitation of the Al and Fe impurities and of Ca and Mg in the solution as metal hydroxide and gypsum. Yan et al. (2012b)

report the addition of 10% of CaO with respect to the mass of the lepidolite concentrate. Finally, lithium is recovered by precipitation by adding Na_2CO_3 to the solution [3.7.1.17], or by hydrolyzing $LiSO_4$ as $LiHCO_3$ and then bubbling CO_2 through the solution (Yan et al., 2012b; Choubey et al., 2016). This route is mainly used for lepidolite, amblygolite ($2LiF*Al_2O_3*P_2O_5$) and zinnwaldite minerals (Kondas and Jandova, 2006). Spudomene concentrate must be thermally treated before digestion, to convert α to β-spudomene, which can be attacked by acid, following reaction [3.7.1.18] (Choubey et al., 2016).

$$Li_2SO_4 + Na_2CO_3 \rightarrow Li_2CO_3 + Na_2SO_4 \quad [3.7.1.17]$$

$$LiAlSi_2O_6 + H_2SO_4 \rightarrow Li_2SO_4 + Al_2O_3SiO_2 + H_2O \quad [3.7.1.18]$$

A less common method is the chlorination process in which the ore is roasted in the presence of chlorine gas or HCl at 880-1100°C (Meshram et al., 2014). A similar process was proposed by Vyas et al. (1975), by using $CaCO_3$ and $CaCl_2$.

For what concerns lithium recovery from brines[28], this is first concentrated by solar evaporation. Then, magnesium is removed from the brine by precipitation as a consequence of the addition of $Ca(OH)_2$ to increase the pH above 11. At this point, lithium carbonate can be added to the Ca-Li salt solution to remove Ca, which precipitates as $CaCO_3$, that can be used for the production of the lime milk used in the previous step. Otherwise, $CaCl_2$ can be added to the solution. In this case, Ca will precipitate as gypsum. Finally, Na_2CO_3 is added to the Li salt solution in order to recover the lithium carbonate (Mashram et al., 2014; Choubey et al., 2016). The purity of the technical-grade of the recovered Li_2CO_3 can be upgraded to electrochemical-grade by adding $Ca(OH)_2$ to produce LiOH by vacuum crystallization and then treating the LiOH with a HCl solution to recrystallize high purity LiCl. By bubbling CO_2, LiCl is precipitated as Li_2CO_3 (Reactions [3.7.1.19] and [3.7.1.20]) (Choubey et al., 2016).

$$Li_2CO_3 + Ca(OH)_2 \rightarrow 2LiOH + CaCO_3 \quad [3.7.1.19]$$

$$LiOH + HCl \rightarrow LiCl + H_2O \quad [3.7.1.20]$$

If the brine contains boron, it must be removed in the first stage of the process by solvent extraction using a fatty alcohol. Then, the concentrate is subjected to the 3-stages precipitation previously described, where $Ca(OH)_2$, $CaCl_2$ and Na_2CO_3 are used to remove Mg and Ca and precipitate Li as Li_2CO_3 (Choubey et al., 2016). The use of CaO instead of $Ca(OH)_2$ to precipitate magnesium gives better filtration properties and improves lithium yield (Boryta et al., 2011). Usually lime is added in excess of a Ca/Mg mole ratio of 3, or by adjusting the pH above 11 (Boryta et al., 2011).

[28] Brine sources include lithium found in salt-water deposits (lakes, salars, oilfield brines and geothermal brines) (Meshram et al., 2014).

Regarding the secondary production of lithium, spent batteries are usually treated by pyrometallurgical processes. However, in this case, lithium is not recovered (Meshram et al., 2014). In order to recover lithium, alternative processes, mainly based on hydrometallurgical techniques and electrolysis, are used. Addition of lime in these processes is documented only in Koichi et al. (2012), referring to the proposal of a new technology. For this reason, these processes will be not further analyzed in this document.

The main residues of the lithium production process are the tailings from the beneficiation process and the slags resulting from the leaching activities of the sintered/calcined concentrates.
Lithium ore beneficiation does not involve the addition of lime and, thus, the produced tailings are not of interest for the present study.
Lithium slags are classified into slag of alkali process and slag of acid process (Yiren et al., 2019). The first is produced from leaching, purification and separation of lithium hydroxide production by sintering of the concentrate with limestone or lime. The latter refers to the residue produced by leaching the concentrate with H_2SO_4, before the introduction of Na_2CO_3 to precipitate lithium as Li_2CO_3. In this process, a significant amount of lime (or limestone) is added to neutralize the excess of H_2SO_4 and adjust the pH for removing impurities (Yiren et al., 2019).
Referring to the slag from the acid lithium production process, its production amounts to about 8-10 tonnes per tonne of lithium carbonate (He et al., 2017; Qiu et al., 2016).
Currently, lithium slags are mainly disposed in dedicated ponds. However, their composition and mechanical properties make them suitable for use as supplementary cementitious material (He et al., 2017; Tan et al., 2015; He et al., 2018) or to produce new materials, such as synthetic zeolite (Chen et al., 2012).

Literature assessment on lithium slag: material and methods

The literature review reported in this chapter focuses only on lithium slag from the alkaline or acid production process from minerals, since no information about the residues produced by the lithium production process from brines was found. In any case, even the scientific literature on lithium slag characterization and carbonation is almost absent.
Overall, 10 papers published in scientific journals, one conference paper and the two patents were considered, as reported in Table 3.7.1.13. Among these documents, only 8 report quantitative data about the chemical composition of lithium slags and only one refers to the carbonation on this residue when it is used for concrete production.

Table 3.7.1.13. List of the documents considered in the study for the review about lithium slag.

Peer reviewed papers
Chen, et al., 2012. *Synthesis and characterization of zeolite X from lithium slag*. Applied Clay Science 59-60, 148-151
Choubey et al., 2016. *Advance review on the exploitation of the prominent energy-storage element: Lithium. Part I: from mineral and brine resources*. Minerals Engineering 89, 119-137
He et al., 2017. *Mechanical properties, drying shrinkage, and creep of concrete containing lithium slag*. Construction and Building Materials 147, 296-304
He et al., 2018. *Microstructure of ultra high performance concrete containing lithium slag*. Journal of Hazardous Materials 353, 35-43
Lin et al., 2015. *Synthesis and adsorption property of zeolite FAU/LTA from lithium slag with utilization of mother liquid*. Chinese Journal of Chemical Engineering 23, 1768-1773
Meshram et al., 2014. *Extraction of lithium from primary and secondary sources by pre-treatment, leaching and separation: a comprehensive review*. Hydrometallurgy 150, 192-208
Tan et al., 2015. *Utilization of lithium slag as an admixture in blended cements: physico-mechanical and hydration characteristics*. Journal of Wuhan University of Technology-Mater. Sci. Ed. 30(1), 129-1233
Yan et al., 2012a. *A novel process for extracting lithium from lepidolite*. Hydrometallurgy 121-124, 54-59
Yan et al., 2012b. *Extraction of lithium from lepidolite by sulfation roasting and water leaching.* International Journal of Mineral Processing 110-111, 1-5
Yiren et al., 2019. *Micro-morphology and phase composition of lithium slag from lithium carbonate production by sulphuric acid process*. Construction and Building Materials 203, 304-313
Conference paper
Luo et al., 2017. *Influence of lithium slag from lepidolite on the durability of concrete*. Proceedings of the 3rd International Conference on Energy Materials and Environment Engineering. IOP Conf, Series: Earth and Environmental Science 61 012151
Patent documents
Boryta et al., 2011. *Production of lithium compounds directly from lithium containing brines*. Unites States Patent US 8,057,764,B2
Kroll, A.V., 1953. *Method of recovering lithium compounds from lithium minerals*. United States Patent US 2,662,809

Composition of lithium slag

The average chemical composition of lithium slag is reported in Table 3.7.1.14.

Considering the overall Ca content, the same value can be assumed for the slags deriving from both acid and alkaline lithium production process, as suggested by the statistical test of Kruskal-Wallis. Thus, on average Ca compounds amount to about 8.4% of the weight of the slag (expressed as CaO), ranging from less than 1% to about 27%. The different content of CaO is mainly the consequence of the different dosage of lime or limestone in the precipitation process (Yiren et al., 2019).

For what concerns the mineral composition, the main phases found in lithium slag are quartz, gypsum, calcite, pyrophyllite ($Al_2Si_4O_{10}(OH)_2$) and amorphous SiO_2 and Al_2O_3. Small amount of spodumene, kaolinite and lithium carbonate can also be detected, depending of the ore composition (Yiren et al., 2019). Compared to cement, lithium slag results richer in SiO_2 and poorer in CaO, having a composition similar to that of fly ash. Due to a certain pozzolanic reactivity because of the high content of active silicon dioxide and aluminium oxide, it can be used as supplementary cementitious material (He et al., 2017).

Focusing on Ca, in the slag from the acid production process it is mainly found in the form of gypsum, as the consequence of the reaction of $CaCO_3/Ca(OH)_2$ with the excess H_2SO_4 in the leaching process. Sometimes,

little amount of $Ca(OH)_2$ can also be found (Yiren et al., 2019). On the contrary, for what concerns the slag from the alkaline production process, significant amounts of free lime can be found, as reported in Yan et al. (2012b).

Table 3.7.1.14. Chemical composition of lithium slag (min-average-max value). Elaboration of the data reported in the documents listed in Table 3.7.1.13.

Type of slag	Total Ca as CaO (%)	SiO_2 (%)	Total Mg as MgO (%)
From sulphuric process of spodumene	0.2-6.6-14.0 *7 cases*	47.7-58.6-71.7 *7 cases*	0.16-0.35-0.54 *6 cases*
From lime-milk process of lepidolite	2.0-14.6-27.2 *2 cases*	47.6 *1 case*	0.12 *1 case*

Potential carbonation rate in lithium slag

A rough estimation of the maximum amount of CO_2 that can be sequestered by the lithium slags as a consequence of their content of Ca compounds can be based on their chemical composition (Table 3.4.c.14), and resulted equal to about 66 gCO_2/kg slag.

However, this figure is only theoretical. The actual CO_2 that can be sequestered by lithium slag depends on the Ca speciation, that is on the percentage of Ca found as free lime, calcite or gypsum. To a first approximation, we can consider that only free lime will react with the atmospheric CO_2 during slag storage. Based on the little literature available on the topic, some free lime can be found in the slag, however quantitative data have not been found. Thus, it is not possible to give a more realistic quantification of the potential CO_2 uptake of this residue. We can only suggest that, probably, the slag from the alkaline production process is more prone to capture CO_2 than the slag from the acid production process, since it usually contains more free lime.

Carbonation of concrete specimens containing lithium slag

Lithium slag can be used in the production of concrete or blended cements in partial substitution of the cement. Several authors (for example, Tan et al., 2015; He et al., 2017; Luo et al., 2017) report the results of mechanical and chemical tests carried out on concrete specimens containing lithium slags, in order to assess their compressive strength, electrical resistivity, the resistance to sulphate attack, the sorptivity, etc.. Luo et al. (2017) also report the results of accelerated carbonation tests performed on these specimens, in terms of depth of the carbonation front. Based on their analyses, the carbonation depth grows with increasing the amount of lithium slag in the specimen, as a consequence of its content of gypsum. Gypsum in lithium slag works as a sulphate activator, promoting the hydration reaction between the $Ca(OH)_2$ in the cement and active silica and alumina to produce more hydrated calcium silicate (C-S-H) and hydrated calcium aluminate compounds (Tan et al., 2015). Thus, the alkalinity of the concrete decreases and, as a consequence, also its resistance to carbonation. However, it is worth specifying that, in this case, the growth of the carbonation depth does not mean that a greater amount of CO_2 reacts with the alkalinity in the concrete and is sequestered. The variation in the carbonation depth is, in fact, the consequence of a change in the mineralogy of the concrete mixture and, thus, of its reactivity with the atmospheric CO_2.

Discussion and conclusions

Based on the little literature available on lithium production residues, it is not possible to exclude that lithium slags can potentially sequester some CO_2. In fact, they contain some free lime that can potentially react with the atmospheric CO_2 during their storage. However, quantitative data about calcium speciation were not found. Thus, the authors suggest to perform more analyses on lithium slags, to assess their content of Ca compounds and their mineralogy. In any case, it is not expected that a great amount of CO_2 can be sequestered by the lithium slags, due to the modest content of Ca reported in the literature (8% on average on the weight of the slags). Furthermore, both lime and limestone can be used in the calcination/sintering process. In the case of limestone, CO_2 is released during the thermal treatment, as a consequence of its calcination.

For what concerns the lithium production from brines, no literature was found about the residues of this process. However, by considering the typical layout of this process, we can deduce that the lime, added to promote Mg removal, precipitates as calcium and magnesium salts that can be recycled in the process or used in other chemical applications. Thus, it is not expected that these residues can be involved in any carbonation reactions.

Finally, for what concerns the CO_2 directly used in the lithium production processes, it is generally bubbled in the system to promote Li_2CO_3 precipitation or it is used for the improvement of its purity. In any case, it is injected downstream the precipitation stages aimed at the removal of the impurities and of the Ca and Mg content of the Li-bearing solution. Thus, it is not expected that this CO_2 will react with the lime.

REFERENCES

Acma, E., Sesigur, H., Addemir, O., Tekin, A., 1997. *Processing of Küre (Turkey) copper slag for the recovery of copper and cobalt and the production of gamma Fe_2O_3*. Trans. Indian. Inst. Met. 50, 147-151 (via Gorai et al., 2003)

Ahmari, S., Parameswaran, K., Zhang, L., 2015. *Alkali activation of copper mine tailings and low-calcium flash-furnace copper smelter slag*. J. Mater.Civ. Eng. 27(6), 04012193

Al-Jabri, K.S., Al-Saidy, A.H., Taha, R., 2011. *Effect of copper slag as a fine aggregate on the properties of cement mortars and concrete*. Construction and Building Materials 25(2), 933-938. DOI: https://doi.org/10.1016/j.conbuildmat.2010.06.090

Amponsah-Dacosta, M., Reid, D.L., 2014. *Mineralogical characterization of selected South African Mine tailings for the purpose of mineral carbonation*. Proceedings of the Annual International Mine Water association Conference-An Interdisciplinary Response to Mine Water Challenges. Xuzhou, China. Available online: https://www.imwa.info/docs/imwa_2014/IMWA2014_Amponsah-Dacosta_686.pdf

Assima, G.P., Larachi, F., Molson, J., Beaudoin, G., 2014. *Impact of temperature and oxygen availability on the dynamics of ambient CO_2 mineral sequestration by nickel mining residues*. Chemical Engineering Journal 240, 394-403. DOI: https://doi.org/10.1016/j.cej.2013.12.010

Ayano, T. and Sakata, K., 2000. *Durability of concrete with copper slag fine aggregate*. Proceeding of the fifth CANMET/ACI International Conference on durability concrete, SP 192, 141-158 (via Shi et al., 2008)

Barna, R., Moskowicz, P., Gervais, C., 2004. *Leaching assessment of road materials containing primary lead and zinc slags*. Waste management 24(9), 945-955. DOI: 10.1016/j.wasman.2004.07.014

Bascetin, A., Tuylu, S., 2017. *Application of Pb-Zn tailings for surface paste disposal: geotechnical and geochemical observations*. International Journal of Mining, Reclamation and Environment 32(5), 312-326. DOI: https://doi.org/10.1080/17480930.2017.1282411

Beaudoin, G., Nowamooz, A., Assima, G.P., et al., 2017. *Passive mineral carbonation of Mg-rich mine wastes by atmospheric CO_2*. Energy Procedia 114, 6083-6086. DOI: https://doi.org/10.1016/j.egypro.2017.03.1745

Benvenuti, M., Mascaro, I., Corsini, F., Lattanzi, P., Parrini, P., Tanelli. G., 1997. *Mine waste dumps and heavy metal pollution in abandoned mining district of Boccheggiano (Southern Tuscany, Italy)*. Environ. Geol. 30(3-4), 238-243. DOI: https://doi.org/10.1007/s002540050152

Bodénan, F., Bourgeois, F., Petiot, C., Augé, T., Bonfils, B., Julcour-Lebigue, C., Guyot, F., Boukary, A., Tremosa, J., Lassin, A., Gaucher, E.C., Chiquet, P., 2014. *Ex situ mineral carbonation for CO_2 mitigation: Evaluation of mining waste resources, aqueous carbonation processability and life cycle assessment (Carmex project)*. Minerals Engineering 59, 52-63. DOI: https://doi.org/10.1016/j.mineng.2014.01.011

Boryta, D.A., Kullberg, T.F., Thurston, A.M., 2011. *Production of lithium compounds directly from lithium containing brines*. Unites States Patent US 7449161B2. Available online: https://patents.google.com/patent/US7449161B2/en

Breuer, P., Sutcliffe, C., Meakin, R., 2010. *Comparison of industrial cyanide destruction processes.* Proceedings of the XXV International Mineral Processing congress, Brisbane, Australia, 6-10 September 2010

Bridge, B., 2000. *The social regulation of resource access and environmental impact: production, nature and contradiction in the US copper industry*. Geoforum 31(2), 237-256. DOI: https://doi.org/10.1016/S0016-7185(99)00046-9

Brindha, D. and Nagan, S., 2011. *Durability studies on copper slag admixed concrete*. Asian Journal of Civil Engineering 12(5), 563-578

Bruckard, W.J., Sparrow, G.J., Woodcock, J.T., 2011. *A review of the effects of the grinding environment on the flotation of copper sulphides*. International Journal of Mineral processing 100(1-2), 1-13. DOI: https://doi.org/10.1016/j.minpro.2011.04.001

Busè, R., Mombelli, D., Mapelli, C., 2014. *Recupero dei metalli dalle polveri di aspirazione dei forni: processo Waelz* (In Italian). La metallurgia italiana 5, 19-27. Available online: https://docplayer.it/10729346-Recupero-dei-metalli-dalle-polveri-di-aspirazione-dei-forni-processo-waelz.html

Chae, S., Jang, Y., Jun, C., Lee, S., Bang, J., Song, K., Cho, H., Lee, M., 2014. *Mineral carbonation with ferrous nickel slag*. Proceedings of the 4th International Conference on Environmental Pollution and Remediation. Prague, 11-13 August 2014. Available online: https://avestia.com/ICEPR2014_Proceedings/papers/85.pdf

Chen, D., Hu, X., Shi, L., Cui, Q., Wang, H., Yao, H., 2012. *Synthesis and characterization of zeolite X from lithium slag*. Applied Clay Science 59-60, 148-151. DOI: https://doi.org/10.1016/j.clay.2012.02.017

Chen, A., Peng, Z., Hwang, J.Y., Ma, Y., Liu, X., Chen, X., 2015. *Recovery of silver and gold from copper anode slimes*. JOM 67(2), 493-502. DOI: https://doi.org/10.1007/s11837-014-1114-9

Choi, Y.C. and Choi, S., 2015. *Alkali-silica reactivity of cementitious materials using ferro-nickel slag fine aggregates produced in different cooling conditions*. Construction and Building Materials 99, 279-287. DOI: https://doi.org/10.1016/j.conbuildmat.2015.09.039

Choubey, P.K., Kim, M.S., Srivastava, R.R., Lee, J.C., Lee, J.Y., 2016. *Advance review on the exploitation of the prominent energy-storage element: Lithium. Part I: from mineral and brine resources*. Minerals Engineering 89, 119-137. DOI: https://doi.org/10.1016/j.mineng.2016.01.010

Cole, S. and Joe Ferron, C., 2002. *A review of the beneficiation and extractive metallurgy of the Platinum Group Elements, highlighting recent process innovation*. SGS Mineral Services Technical paper 2002-3. Available online: https://www.sgsgroup.com.bd/-/media/global/documents/technical-documents/sgs-technical-papers/sgs-min-tp2002-03-beneficiation-and-extractive-metallurgy-of-pge.pdf

Collins, R.J. and Ciesielski, S.K., 1994. *Recycling and use of waste materials and by-products in highway construction*. National Cooperative Highway Research Programme, Synthesis of highway practice 199. Transportation Research Board, Washington.

Coto, O., Galizia, F., Hernández, I., Marrero, J., Donati, E., 2008. *Cobalt and nickel recoveries from laterite tailings by organic and inorganic bio-acids*. Hydrometallurgy 94(1-4), 18-22. DOI: https://doi.org/10.1016/j.hydromet.2008.05.017

Coya, B., Maranon, E., Sastre, H., 2000. *Ecotoxicity assessment of slag generated in the process of recycling lead from waste batteries*. Resources, Conservation and Recycling 29(4), 291-300. DOI: https://doi.org/10.1016/S0921-3449(00)00054-9

Das, M. and Maiti, S.K., 2008. *Comparison between availability of heavy metals in dry and wetland tailing of an abandoned copper tailing pond*. Environ. Monit. Assess. 137(1-3), 343-350. DOI: https://doi.org/10.1007/s10661-007-9769-0

De Andrade Lima, L.R.P., Bernandez, L.A., 2011. *Characterization of the lead smelter slag in Santo Amaro, Bahia, Brazil*. Journal of Hazardous Materials 189(3), 692-699. DOI: 10.1016/j.jhazmat.2011.02.091

Deja, J. and Malolepszy, J., 1994. *Long-term resistance of alkali activated slag mortars to chloride solution*. Proceedings if the third CANMET/ACI International Conference of durability of concrete, 657-671 (via Shi et al., 2008)

Dreisinger, D., 2006. *Copper leaching from primary sulphides: options for biological and chemical extraction of copper*. Hydrometallurgy 83(1-4), 10-20. DOI: https://doi.org/10.1016/j.hydromet.2006.03.032

Ettler, V., Legendre, O., Bodénan, F., Touray, J.C., 2001. *Primary phases and natural weathering of old lead-zinc pyrometallurgical slag from Pribram, Czech Republic*. The Canadian Mineralogist 39(3), 873-888. DOI: https://doi.org/10.2113/gscanmin.39.3.873

Ettler, V., Piantone, P., Touray, J.C., 2003. *Mineralogical control on inorganic contaminant mobility in leachate from lead-zinc metallurgical slag: experimental approach and long-term assessment*. Mineral. Mag. 67(6), 1269-1283. DOI: https://doi.org/10.1180/0026461036760164

Ettler, V., Komárková, M., Jehlicka, J., Coufal, P., Hradil, D., Machovic, V., Delorme, F., 2004. *Leaching of lead metallurgical slag in citric solutions. Implications for disposal and weathering in soil environments*. Chemosphere 57(7), 567-577. DOI: 10.1016/j.chemosphere.2004.07.022

EU, 2009. *Best Available Techniques (BAT) Reference Document for Management of Tailings and Waste-Rock in Mining Activities*. Available online: https://eippcb.jrc.ec.europa.eu/reference/BREF/mmr_adopted_0109.pdf

EU, 2017. *Best Available Techniques (BAT) Reference Document for the Non-Ferrous Metals Industries*. Available online: https://eippcb.jrc.ec.europa.eu/reference/nfm.html

Fang, Y., Gu, Y., Kang, Q., Wen, Q., Dai, P., 2011. *Utilization of copper tailing for autoclaved sand-lime brick*. Construction and Building Materials 25(2), 867-872. DOI: https://doi.org/10.1016/j.conbuildmat.2010.06.100

Forrester, K.E., 2006. *Method for stabilization of lead smelter slag and matte*. US Patent n. 7,121,995B2. Available online: https://patents.google.com/patent/US7121995

Fu, K., Chen, S., Wang, Z., Xiao, J., Luo, D., 2015. *Lime-assisted cyanide leaching of refractory gold ores from Ajialongwa mine*. Proceedings of the 11th International Congress for Applied Mineralogy (ICAM), 107-113. DOI: https://doi.org/10.1007/978-3-319-13948-7_12

Garrett, D.E., 2004. *Handbook of lithium and natural calcium chloride: their deposits, processing, uses and properties*. 1st edition, Elsevier, Amsterdam, The Netherlands

Gokcekus, H., Kabdasli, S., Kabdasli, I., Turker, U., Tunay, O., Olmez, T., 2003. *Pollution of coastal region impacted by acid mine drainage in Morphou Bay, Northern Cyprus*. J. Environ. Sci. Health. 38(8), 1445-1457. DOI: https://doi.org/10.1081/ESE-120021469

Gorai, B., Jana, R.K., Premchand, 2003. *Characteristics and utilization of copper slag. A review*. Resources, Conservation and Recycling 39(4), 299-313. DOI: https://doi.org/10.1016/S0921-3449(02)00171-4

Gordon, R.B., 2002. *Production residues in copper technological cycles*. Resour. Conserv. Recycl. 36(2), 87-106. DOI: https://doi.org/10.1016/S0921-3449(02)00019-8

Gupta, R.C., Mehra, P., Thomas, B.S., 2017. *Utilization of copper tailing in developing sustainable and durable concrete*. J. Mater. Civ. Eng. 29(5), 04016274. DOI: https://ascelibrary.org/doi/10.1061/%28ASCE%29MT.1943-5533.0001813

Hamberg, R., 2014. *Characterization and solidification of Arsenic-rich cyanided tailings*. PhD Thesis, Luleå University of Technology

Hansen, H.K., Rojo, A., Ottossen, L.M., 2007. *Electrokinetic remediation of copper mine tailings: implementing bipolar electrodes*. Electrochimica Acta 52(10), 3355-3359. DOI: https://doi.org/10.1016/j.electacta.2006.02.069

Hasan, S.N.M.S, Kusin, F.M., Jusop, S., Yusuff, F.M., 2018. *Potential of soil, sludge and sediment for mineral carbonation process in Selinsing gold mine, Malaysia*. Minerals 8, 257-271. DOI: https://doi.org/10.3390/min8060257

He, Z.H., Li, L.Y., Du, S.G., 2017. *Mechanical properties, drying shrinkage, and creep of concrete containing lithium slag*. Construction and Building Materials 147, 296-304. DOI: https://doi.org/10.1016/j.conbuildmat.2017.04.166

He, Z.H., Du, S.G., Chen. D., 2018. *Microstructure of ultra high performance concrete containing lithium slag*. Journal of Hazardous Materials 353, 35-43. DOI: https://doi.org/10.1016/j.jhazmat.2018.03.063

Hernández, C.M.F., Banza, A.N., Gock, E., 2007. *Recovery of metals from Cuban nickel tailings by leaching with organic acids followed by precipitation and magnetic separation*. Journal of Hazardous Materials B139 (1-2), 25-30. DOI: https://doi.org/10.1016/j.jhazmat.2006.03.074

Hewitt, D., Breuer, P., Jeffery, C., 2012. *Cyanide detoxification of cyanidation tails and processes streams*. https://publications.csiro.au/rpr/download?pid=csiro:EP123765&dsid=DS3 (latest access 7-6-2019)

Huang, K., 2001. *Use of copper slag in cement production*. Sichan Cement 4, 25-27 (via Shi et al., 2008)

Hwang, C.L. and Laiw, J.C., 1989. *Properties of concrete using copper slag as a substitute for fine aggregate*. Proceeding of the 3rd International Conference on fly ash, silica fume, slag and natural pozzolans in concrete. SP 114-82, 1677-1695

Jandová, J., Dvořák, P., Vu, H.N., 2010. *Processing of zinnwaldite waste to obtain Li_2CO_3*. Hydrometallurgy 103(1-4), 12-18. DOI: https://doi.org/10.1016/j.hydromet.2010.02.010

Johnson, R.H., Blowes, D.W., Robertson, W.D., Jambor, J.L., 2000. *The hydrogeochemistry of the nickel Rim mine tailings impoundment, Sudbury, Ontario*. Journal of Contaminant Hydrology 41(1-2), 49-80. DOI: https://doi.org/10.1016/S0169-7722(99)00068-6Get

Jones, R.T., 2005. *An overview of Southern African PGM smelting*. Proceedings of the 44th annual Conference of Metallurgists, Calgary, Alberta, Canada, 21-24 August 2005, 147-178. Available online: https://www.mintek.co.za/Pyromet/Files/2005JonesPGMsmelting.pdf

Kalinkin, A.M., Kumar, S., Gurevich, B.I., Alex, T.C., Kalinkina, E.V., Tyukavkina, V.V., Kalinnikov, V.T., Kumar, R., 2012. *Geopolymerization behavior of Cu-Ni slag mechanically activated in air and in CO_2 atmosphere*. International Journal of Mineral Processing 112-113, 101-106. DOI: https://doi.org/10.1016/j.minpro.2012.05.001

Karam, A., Khiari, L., Jaouich, A., 2009. *Influence on tailing pH on the sorption of copper by sulphide mine tailing*. Journal of Arid Land Studies 19, 233-236. DOI: https://pdfs.semanticscholar.org/4554/9ac384a4112ecfcb199e6da72a1addab748f.pdf

Kerfoot, D.G.E., Krause, E., Love, B.J., Singhal, A., 2002. *Hydrometallurgical process for the recovery of nickel and cobalt values from a sulfidic flotation concentrate*. Patent no. US 6428604 B1. Available online: https://www.lens.org/lens/patent/100-251-960-219-790

Khalil, A., Argane, R., Benzaazoua, M., Bouzahzah, H., Taha, Y., Hakkou, R., 2019. *Pb-Zn mine tailings reprocessing using centrifugal dense media separation*. Minerals Engineering, 131, 28-37. DOI: https://doi.org/10.1016/j.mineng.2018.10.023

Khanzadi, M. and Behnood, A., 2009. *Mechanical properties of high-strength concrete incorporating copper slag as coarse aggregate*. Construction and Building Materials 23(6), 2183-2188. DOI: https://doi.org/10.1016/j.conbuildmat.2008.12.005

Kiyak, B., Özer, A., Altunğdan, S.H., Erdem, M., Tümen, F., 1999. *Cr(VI) reduction in aqueous solution by using copper smelter slag*. Waste Manage 19(5), 333-338. DOI: https://doi.org/10.1016/S0956-053X(99)00141-5

Koichi, Y., Koji, O., Akira, A., Tsuri, M., 2012. *Separation and recovery of valuables from used lithium ion batteries*. Japan Patent, JP 2012229481A (via Hu et al., 2017)

Kondas, J. and Jandova, J., 2006. *Lithium extraction from zinnwaldite waste after gravity dressing of Sn-W ores*. Acta Metall. Slovaca 12, 192-202.

Kreusch, M.A., Ponte, M.J.J.S., Ponte, H.A., Kaminari, N.M.S., Marino, C.E.B., Mymrin, V., 2007. *Technological improvements in automotive battery recycling*. Resour. Conserv. Recycl. 52(2), 368-380. DOI: https://doi.org/10.1016/j.resconrec.2007.05.004

Kroll, A.V., 1953. *Method of recovering lithium compounds from lithium minerals*. United States Patent US 2,662,809.

Lin, G., Zhuang, Q., Cui, Q., Wang, H., Yao, H., 2015. *Synthesis and adsorption property of zeolite FAU/LTA from lithium slag with utilization of mother liquid*. Chinese Journal of Chemical Engineering 23(11), 1768-1773. DOI: https://doi.org/10.1016/j.cjche.2015.10.001

Luo, Q., Huang, S., Zhou, Y., Li, J., Peng, W., Wen, Y., 2017. *Influence of lithium slag from lepidolite on the durability of concrete*. Proceedings of the 3rd International Conference om Energy Materials and Environmental Engineering. IOP Conf, Series: Earth and Environmental Science 61 012151. Available online: https://www.researchgate.net/publication/316347227_Influence_of_lithium_slag_from_lepidolite_on_the_durability_of_concrete

Mao, Y., Muhammad, F., Yu, L., Xia, M., Huang, X., Jiao, B., Shiau, Y.C., Li, D., 2019. *The solidification of lead-zinc smelting slag through bentonite supported alkali-activated slag cementitious material*. International Journal of Environmental Research and Public Health 16(7), 1121. DOI: 10.3390/ijerph16071121

Marghussian, V.K. and Maghsoodipoor, A., 1999. *Fabrication of unglazed floor tiles containing Iranian copper slags*. Ceramics International 25(7), 617-622. DOI: https://doi.org/10.1016/S0272-8842(98)00075-3

Meshram, P., Pandey, B.D., Mankhand, T.R., 2014. *Extraction of lithium from primary and secondary sources by pre-treatment, leaching and separation: a comprehensive review*. Hydrometallurgy 150, 192-208. DOI: https://www.sciencedirect.com/science/article/pii/S0304386X14002278

Meyer, N.A., Vögeli, J.U., Becker, M., Broadhurst, J.L., Reid, D.L., Franzidis, J.P., 2014. *Mineral carbonation of PGM mine tailings for CO_2 storage in South Africa: a case study*. Minerals engineering 59, 45-51. DOI: https://doi.org/10.1016/j.mineng.2013.10.014

Mombelli, D., Mapelli, C., Barella, S., Gruttadauria, A., Di Landro, U., 2015. *Laboratory investigation of Waelz slag stabilization*. Process Safety and Environmental Protection 94, 227-238. DOI: https://doi.org/10.1016/j.psep.2014.06.015

Moura, W.A., Goncalves, J.P., Lima, M.B.L., 2007. *Copper slag waste as a supplementary cementing material to concrete*. J. Mater. Sci. 42(7), 2226-2230. DOI: https://doi.org/10.1007/s10853-006-0997-4

Mpinga, C.N., Eksteen, J.J., Aldrich, C., Dyer, L., 2015. *Direct leach approaches to Platinum Group Metal (PGM) ores and concentrates: a review*. Minerals Engineering 78, 93-113. DOI: https://doi.org/10.1016/j.mineng.2015.04.015

Mu, W.N., Zhai, Y.C., Liu, Y., 2010. *Leaching of magnesium from desiliconization slag of nickel laterite ores by carbonation process*. Trans. Nonferrous Met. Soc. China 20 (Supplement 1), s87-s91. DOI: https://doi.org/10.1016/S1003-6326(10)60018-0

Ncongwane, M.S., Broadhurst, J.L., Petersen, J., 2018. *Assessment of the potential carbon footprint of engineered processes for the mineral carbonation of PGM tailings*. International Journal of Greenhouse Gas Control 77, 70-81. DOI: https://doi.org/10.1016/j.ijggc.2018.07.019

Norgate, T. and Rankin, W., 2000. *Life cycle assessment of copper and nickel production*. Proceeding of the Minprex Conference, 11-13- September 2000 Melbourne, 133-138

Norgate, T. and Jahanshahi, S., 2011. *Assessing the energy and greenhouse gas footprints of nickel laterite processing*. Mineral Engineering, 24, 698-707. DOI: 10.1016/j.mineng.2010.10.002

Nouairi, J., Hajjaji, W., Costa, S.C., Senff, L., Patinha, C., Ferreira da Silva, E., Labrincha, J.A., Rocha, F., Medhioub, M., 2018. *Study on Zn-Pb ore tailings and their potential in cement technology*. Journal of African Earth Sciences 139, 165-172. DOI: https://doi.org/10.1016/j.jafrearsci.2017.11.004

Ogundiran, M.B., Nugteren, H.W., Witkamp, G.J., 2013. *Immobilisation of lead smelting slag within spent aluminate-fly ash based geopolymers*. Journal of Hazardous Materials 248-249, 29-36. DOI: https://doi.org/10.1016/j.jhazmat.2012.12.040

Onisei, S., Pontikes, Y., Van Gerven, T., Angelopoulos, G.N., Velea, T., Predica, V, Moldovan, P., 2012. *Synthesis of inorganic polymers using fly ash and primary lead slag*. Journal of Hazardous Materials 205-206, 101-110. DOI: https://doi.org/10.1016/j.jhazmat.2011.12.039

Onuaguluchi, O., Eren, Ö., 2012a. *Recycling of copper tailings as an additive in cement mortars*. Construction and Building Materials 37, 723-727. DOI: https://doi.org/10.1016/j.conbuildmat.2012.08.009

Onuaguluchi, O. and Eren, Ö., 2012b. *Cement mixture containing copper tailings as an additive: durability properties*. Materials Research 15(6), 1029-1036. DOI: http://dx.doi.org/10.1590/S1516-14392012005000129

Othmani, M.A., Souissi, F., Bouzahzah, H., Bussière, B., da Silva, E.F., Benzaazoua, M., 2015. *The flotation tailings of the former Pb-Zn mine of Touiref (NW Tunisia): mineralogy, mine drainage prediction, base-metal speciation assessment and geochemical modeling*. Environ. Sci. Pollut. Res. 22(4), 2877-2890. DOI: https://www.ncbi.nlm.nih.gov/pubmed/25220771

Paktunc, D., Foster, A., Heald, S., Laflamme, G., 2004. *Speciation and characterization of arsenic in gold ores and cyanidation tailings using X-ray absorption spectroscopy*. Geochimica et Cosmochimica Acta 68(5), 969-983. DOI: https://doi.org/10.1016/j.gca.2003.07.013

Palamini, C., Mapelli, C., Barella, S., Mombelli, D., 2018. *The Waelz process: state of the art and innovation to decrease the environmental impact*. Proceedings of the 4th European Conference on Clean Technologies in the Steel Industry, Bergamo, 28-29 November 2018

Panda, R., Jha, M.K., Pathak, D.D., 2018. *Commercial processes for the extraction of Platinum Group Metals (PGMs)*. In book: Rare metal technology. DOI: 10.1007/978-3-319-72350-1_11

Parkinson, G., 1999. *Leaching metal…for all it's worth*. Chemical Engineering, 28-31 November (via Norgate and Jahanshahi, 2011)

Parsons, M.B., Bird, D.K., Einaudi, M.T., Alpers, C.N., 2001. *Geochemical and mineralogical controls on trace element release from the Penn Mine base-metal slag dump, California*. Applied Geochemistry 16(14), 1567-1593. DOI: https://pubs.er.usgs.gov/publication/70022965

Penpolcharoen, M., 2005. *Utilization of secondary lead slag as construction material*. Cement and Concrete Research 35(6), 1050-1055. DOI: https://doi.org/10.1016/j.cemconres.2004.11.001

Piatak, N.M. and Seal II, R.R., 2010. *Mineralogy and the release of trace elements from slag from the Hegeler Zinc smelter, Illinois (USA)*. Applied Geochemistry 25(2), 302-320. DOI: https://doi.org/10.1016/j.apgeochem.2009.12.001

Potysz, A., Kierczak, J., Fuchs, Y., Grybos, M., Guibaud, G., Lens, P.N.L., van Hullebusch, E.D., 2016. *Characterization and pH-dependent leaching behaviour of historical and modern copper slags*. Journal of Geochemical Exploration 160, 1-15. DOI: https://doi.org/10.1016/j.gexplo.2015.09.017

Premchand et al., 2000. *Characterisation and utilisation of copper slag of Sterlite Industries India Ldt*. Report submitted to SIIL Tuticorin, India: National Metallurgical Laboratory CSIR, October 2000 (via Gorai et al., 2003)

Qiu, Y., Wu, D., Yan, L., Zhou, Y., 2016. *Recycling of spodumene slag: preparation of green polymer composites*. RSC Adv. 6, 36942-36953. DOI: 10.1039/c6ra03119f

Riveros, P.A., Dutrizac, J.E., Spencer, P., 2001. *Arsenic disposal practices in the metallurgical industry*. Canadian Metallurgical Quarterly 40(4), 395-420. DOI: https://doi.org/10.1179/cmq.2001.40.4.395

Samnur, S., Husain, H., Zulfi, A., Sujiono, E.H., 2016. *Study on physical-chemical properties of furnace-nickel-slag powder for geopolymer application*. Jurnal Pendidkan Fisika Indonesia 12(2), 177-182. DOI: https://journal.unnes.ac.id/nju/index.php/JPFI/article/view/4728

Seignez, N., Bulteel, D., Damidot, D., Gauthier, A., Potdevin, J.L., 2006. *Weathering of metallurgical slag heaps: multi-experimental approach of the chemical behaviours of lead and zinc*. WIT Transaction on Ecology and the Environment 92, 31-40. DOI: 10.2495/WM060041

Seignez, N., Gauthier, A., Bulteel, D., Buatier, M., Recourt, P., Damidot, D., Potdevin, J.L., 2007. *Effect of Pb-rich and Fe-rich entities during alteration of a partially vitrified metallurgical waste*. Journal of Hazardous Materials 149(2), 418-431. DOI: 10.1016/j.jhazmat.2007.04.007

Seignez, N., Gauthier, A., Bulteel, D., Daminot, D., Potdevin, J.L., 2008. *Leaching of lead metallurgical slags and pollutant mobility far from equilibrium conditions*. Applied Geochemistry 23, 3699-3711. DOI: 10.1016/j.apgeochem.2008.09.009

Siame, E. and Pascoe, R.D., 2011. *Extraction of lithium from micaceous waste from China clay production*. Miner. Eng. 24(14), 1595-1602. DOI: https://doi.org/10.1016/j.mineng.2011.08.013

Shan, C., Wang, J., Zheng, J., Yu, Y., 2012. Study on application of nickel slag in cement concrete. Bull. Chin. Ceram.Soc. 31, 1263-1268 (via Yang et al., 2017)

Sharma, R. and Khan, R.A., 2017. *Durability assessment of self compacting concrete incorporating copper slag as fine aggregates*. Construction and Building Materials 155, 617-629. DOI: https://doi.org/10.1016/j.conbuildmat.2017.08.074

Shi, C., Qian, J., 2000. *High performance cementing materials from industrial slags*. *A review*. Resources, Conservation and Recycling 29(3), 195-207. DOI: https://doi.org/10.1016/S0921-3449(99)00060-9

Shi, C., Meyer, C., Behnood, A., 2008. *Utilization of copper slag in cement and concrete*. Resources, Conservation and Recycling 52(10), 1115-1120. DOI: https://doi.org/10.1016/j.resconrec.2008.06.008

Siegrist, M., Southam, C., Bowman, G., Wilson, S.A., Southam, G., 2017. *Analysis of the potential for negative CO_2 emission mine sites through bacteria-mediated carbon mineralization: evidence from Australia*. Energy Procedia 114, 6124-6132. DOI: https://doi.org/10.1016/j.egypro.2017.03.1749

Sobanska, S., Ledésert, B., Deneele, D., Laboudigue, A., 2000. Alteration in soils of slag particles resulting from lead smelting. C.D. Acad. Sci. Paris, Sciences del la Terre et des planetes 331, 271-278

Somerville, M., Chen, C., Alvear, G.R.F., Nikolic, S., 2016. *Fluxing strategies for the direct to blister smelting of high silica and low iron copper concentrates*. Proceedings of the 10th International Conference on Molten Slags, Fluxes and Salts (Molten16), 667-675

Tan, H., Li, X., He, C., Ma, B., Bai, Y., Luo, Z., 2015. *Utilization of lithium slag as an admixture in blended cements: physico-mechanical and hydration characteristics*. Journal of Wuhan University of Technology-Mater. Sci. Ed. 30(1), 129-1233. DOI: https://doi.org/10.1007/s11595-015-1113-x

Taskinen, P., 2010. *Direct-to-blister smelting of copper concentrates: the fluxing chemistry*. Proceedings of the seethataman seminar, Material processing towards properties, Sigtuna (Sweden), 14-15 June 2010 (Via Taskinen, 2011)

Taskinen, P., 2011. *Direct-to-blister smelting of copper concentrates: the slag fluxing chemistry*. Mineral Processing and Extractive Metallurgy 120(4), 240-246. DOI: https://doi.org/10.1179/1743285511Y.0000000013

Thomas, B.S., Damare, A., Gupta, R.C., 2013. *Strength and durability characteristics of copper tailing concrete.* Construction and Building Materials 48, 894-900. DOI: https://doi.org/10.1016/j.conbuildmat.2013.07.075

Tyszka, R., Kierczak, J., Pietranik, A., ettler, V., Mihaljevic, M., 2014. Extensive weathering of zinc smelting slag in a heap in upper Silesia (Poland): potential environmental risks posed by mechanical disturbance of slag deposits. Applied Geochemistry 40, 70-81

Vanaecker, M., Courtin-Nomade, A., Bril, H., Laureyns, J., Lenain, J.F., 2014. Behavior of Zn-bearing phases in base metal slag from France and Poland: a mineralogical approach for environmental purposes. Journal of Geochemical Exploration 136, 1-13

Vogeli, J., Reid, D.L., Becker, M., Broadhurst, J., Franzidis, J.P., 2011. *Investigation of the potential for mineral carbonation of PGM tailings in South Africa*. Minerals Engineering 24(12), 1348-1356. DOI: https://doi.org/10.1016/j.mineng.2011.07.005

Vyas, M.H., Sanghavi, J.R., Seshadri, K., 1975. *Lithium extraction from Indian lepidolite ores*. Res. Ind. 20, 68-70

Wang, G. and Thompson, R., 2011. *Slag use in high-way construction. The philosophy and technology of its utilization*. International Journal of Pavement Research and Technology 4(2), 97-103. DOI: http://www.ijprt.org.tw/mailweb/files/sample/V4N2_97-103.pdf

Warner, A., Diaz, C., Dalvi, A., Mackey, P., Tarasov, A., 2006. *JOM word nonferrous smelter survey, part III: nickel: laterite*. Journal of Metals, 58(4), 11-20. DOI: https://doi.org/10.1007/s11837-006-0209-3

Wong, J.W.C., Ip, C.M., Wong, M.H., 1998. Acid-forming capacity of lead-zinc mine tailings and its implications for mine rehabilitation. Environmental Geochemistry and Health 20, 149-155

Wong, W.L.E., Arun, S.M., 2009. *Gold extraction and recovery process*. Internal report, M3TC, National University of Singapore. Available online: https://pdfs.semanticscholar.org/7559/67e38c3b788c9d41aaedec4f3d5ebd921855.pdf

Xiao, M.S., Wang, S.H., Zhang, Q.F., Zhang, J.W., 1997. Leaching mechanism of the spodumene sulphuric acid process. Rare Met. 1, 37-45 (via Yiren et al., 2019)

Yan, Q., Li, X., Yin., Z., Wang, Z., Guo, H., Peng, W., Hu, Q., 2012a. *A novel process for extracting lithium from lepidolite*. Hydrometallurgy 121-124, 54-59. DOI: https://doi.org/10.1016/j.hydromet.2012.04.006

Yan, Q., Li, X., Wang, Z., Wu, X., Wang, W., Wang, J., Guo, H., Hu, Q., Peng, W., 2012b. *Extraction of lithium from lepidolite by sulfation roasting and water leaching*. International Journal of Mineral Processing 110-111, 1-5. DOI: https://doi.org/10.1016/j.minpro.2012.03.005

Yang, T., Wu, Q., Zhu, H., Zhang, Z., 2017. *Geopolymer with improved thermal stability by incorporating high-magnesium nickel slag*. Construction and Building Materials 155, 475-484. DOI: https://doi.org/10.1016/j.conbuildmat.2017.08.081

Yin, G., Li, G., Wei, Z., Wan, L., Shui, G., Jing, X., 2011. *Stability analysis of a copper tailings dam via laboratory model tests: a Chinese case study*. Mineral Engineering 24(2), 122-130. DOI: https://doi.org/10.1016/j.mineng.2010.10.014

Yiren, W., Domgmin, W., Yong, C., Dapeng, Z., Ze, L., 2019. *Micro-morphology and phase composition of lithium slag from lithium carbonate production by sulphuric acid process*. Construction and Building Materials 203, 304-313. DOI: https://doi.org/10.1016/j.conbuildmat.2019.01.099

Yucel, O., Sahin, F.C., Sirin, B., Addemir, O., 1999. *A reduction study of copper slag in a DC arc furnace*. Scand. J. Metal. 28, 93-99 (via Gorai et al., 2003)

Yukselen, M.A., 2002.Characetrization of heavy metal contaminated soils in Northern Cyprus. Environ. Geol. 42, 503-597 (Via Onuaguluchi and Eren, 2012a)

Zagury, G.J., Oudjehani, K., Deschênes, L., 2004. *Characterization and availability of cyanide in solid mine tailings from gold extraction plants*. Science of the Total Environment 320(2-3), 211-224. DOI: https://doi.org/10.1016/j.scitotenv.2003.08.012

Zainol, Z. and Nicol, M.J., 2009. *Comparative study of chelating ion exchange resins for the recovery of nickel and cobalt from laterite leach tailings*. Hydrometallurgy 96(4), 283-287. DOI: https://doi.org/10.1016/j.hydromet.2008.11.005

Zhao, F., Zhao, J., Liu, H., 2009. *Autoclaved brick from low silicon tailings*. Constr. Build. Mater. 23(1), 538-541. DOI: https://doi.org/10.1016/j.conbuildmat.2007.10.013

3.7.2. USE OF LIME IN THE TREATMENT OF THE RED GYPSUM FROM TITANIUM DIOXIDE INDUSTRY

3.7.2.1 INTRODUCTION

Red gypsum is the principal waste produced by titanium dioxide manufacturing industry where ilmenite is used as a raw material.

Ilmenite (nominally $FeO{\cdot}TiO_2$ or $TiFeO_3$) is the main mineral, which constitutes titanium ore. It consists of 40-65% of TiO_2, with the rest being mainly ferrous and ferric oxides with some amount of other oxide impurities of chromium, manganese, vanadium, magnesium, aluminium, calcium, silicon and others, depending on its geological history (Barksdale, 1961). Titanium can also be found in nature as rutile, which is a richer form of TiO_2 (93-96% TiO_2) not generally found in deposits valid for commercial use and, finally, as leucoxene ($Fe_2O_3{\cdot}nTiO_2$), a natural alteration product of ilmenite, typically containing more than 65% of TiO_2 (Barksdale, 1961).

Titanium dioxide can be produced by two different processes: the sulphate process (about 40% of the worldwide TiO_2 production) using concentrate sulphuric acid, and the chloride process (about 60% of the worldwide TiO_2 production) using chlorine gas. The processes differ in their chemistry and raw material requirements.

Red gypsum is originated by the sulphate process. In this process, ilmenite is digested with concentrated sulphuric acid (98%). The general reactions are the following:

$$FeTiO_3 + 2H_2SO_4 \rightarrow TiOSO_4 + FeSO_4 + H_2O \quad [3.7.2.1]$$

$$TiOSO_4 + (n+1)H_2O \rightarrow TiO_2{*}nH_2O + H_2SO_4 \quad [3.7.2.2]$$

$$TiO_2{*}nH_2O \rightarrow TiO_2 + nH_2O \quad [3.7.2.3]$$

Ilmenite is digested in a solution of sulphuric acid at a temperature of about 100°C, dissolving as titanyl sulphate ($TiOSO_4$) and iron sulphate ($FeSO_4$) [Reaction 1]. The solution is then cooled to around 15°C and iron scraps are added to promote $FeSO_4$ crystallisation, which is removed by filtration. The titanium liquor is, then, heated again at around 110°C and subjected to hydrolysis. During this process, a precipitate of titanium dioxide hydrate is formed [Reaction 2]. The precipitate is separated from the solution of sulphuric acid by filtration and is washed with water to reduce its content of acid and heavy metals ions. Despite washing, the quality of the titanium dioxide hydrate is usually insufficient for a direct use in the production of the white pigment. Thus, annealing salts are usually added before calcination. During calcination, the titanium dioxide crystals grow to their final crystalline size and residual water and H_2SO_4 are removed [Reaction 3]. The dried titanium dioxide is sent to a finishing phase, where it can be milled and the particle surface can be coated with silica or alumina (Gazquez et al., 2014; Grzmil et al., 2008).

The sulphate process requires the use of very large quantities of sulphuric acid and produces a great amount of acid waste that needs to be treated. Its treatment consists in a neutralization process with addition of lime and/or limestone, that generates a residue called red gypsum, formed mainly of gypsum and iron hydroxides.

Usually, a two-step process is applied, in which both limestone and lime are used: limestone is used in the first step to neutralize the acidity linked with H_2SO_4, whereas lime is used in the second step to increase the pH to a final value of about 8, by reacting with $FeSO_4$ (Huntsman Tioxide, 2011):

$H_2SO_4 + CaCO_3 \rightarrow CaSO_4 + CO_2 + H_2O$ [3.7.2.4]

$FeSO_4 + Ca(OH)_2 \rightarrow Fe(OH)_2 + CaSO_4$ [3.7.2.5]

Based on a personal communication provided by EuLA, the molar ratio limestone/lime is approx. 5/1 (personal communication, 2019). The process is more efficient when compared with the use of only lime, but it is also more expensive (Gazquez et al., 2014).

Due to its high content of Ca, red gypsum can react with the atmospheric CO_2, undergoing carbonation reactions. Several authors proposed to use red gypsum as a feedstock for CO_2 sequestration by accelerated carbonation (Rahamani et al., 2014; Pérez-Moreno et al., 2015).

Two main routes have been proposed:

- direct processes, in which carbonation occurs in a single step. Red gypsum is mixed with water, with eventual addition of a base to promote $CaCO_3$ precipitation, and then put in contact with a CO_2 gas flow. Dissolution of $CaSO_4$ in the water solution and Ca carbonation occur simultaneously. During the process, also $FeSO_4$ reacts with CO_2 producing a precipitate of $FeCO_3$.
- indirect processes, in which $CaSO_4$ and $FeSO_4$ are first extracted from the mineral matrix to produce a Ca and Fe-rich solution and then, in a second step, Fe is precipitated and the Ca-rich solution is carbonated with precipitation of a pure calcium carbonate. Typical extracting agent is H_2SO_4, whereas to promote Fe and other impurities precipitation, usually NaOH or NH_4OH are used. The reactions involved in the process are (Perez-Moreno et al., 2015):

$CaSO_4*2H_2O + 2NaOH \rightarrow Ca(OH)_2 + Na_2SO_4 + 2H_2O$ [3.7.2.6]

$CaSO_4*2H_2O + 2NH_4OH \rightarrow Ca(OH)_2 + (NH_4)_2SO_4 + 2H_2O$ [3.7.2.7]

$CO_2 + H_2O \rightarrow H_2CO_3 \rightarrow 2H^+ + CO_3^{2-}$ [3.7.2.8]

$Ca(OH)_2 \rightarrow Ca^{2+} + 2OH^-$ [3.7.2.9]

$CO_3^{2-} + Ca^{2+} \rightarrow CaCO_3$ [3.7.2.10]

Red gypsum can be used as a solidifying agent for loose clay soils to make them stable (for highways, etc.) or, blended with organic fertiliser, for capping and landscaping activities of quarries, landfills, and contaminated sites. It can also be used in the cement industry and, in some European countries (such as Italy and UK), as a fertilizer in agriculture (EU, 2007).

3.7.2.2 LITERATURE ASSESSMENT FOR RED GYPSUM: MATERIALS AND METHODS

The scientific literature on red gypsum carbonation is very limited. Thus, the literature review carried out to assess the amount of CO_2 that can be sequestered by the red gypsum due to the use of lime in the neutralization process was based only on 9 papers published in scientific journals, on a report from a titanium industry and

on the Best Available Techniques (BAT) Reference Document for the manufacture of large volume inorganic chemicals, solids and other industry published in the year 2007 (Figure 3.7.2.1).

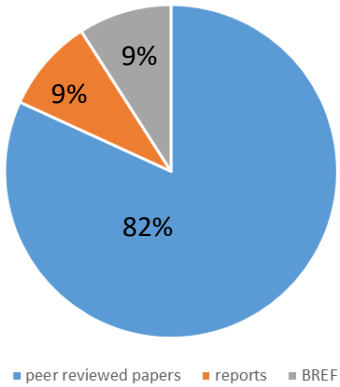


Figure 3.7.2.1. Sources used for the literature assessment on red gypsum.

All the analysed documents refer to accelerated carbonation tests performed at the laboratory scale. No data were found about natural carbonation of red gypsum during disposal or during its life cycle, when it is recycled as a construction material or as a fertilizer. Furthermore, all the experiences reported in the scientific literature refer to experimental assessment at the laboratory scale aimed at evaluating the best conditions of temperature, pressure, liquid/solid (L/S) ratio, size dimension etc. to promote carbonation. Information regarding industrial scale plants treating red gypsum by accelerated carbonation was not found.

Another limitation of the study is that most of the analysed papers (the ones published by Rahmani et al. and Azdarpour et al.) refer to the same sample of red gypsum, which was subjected to several accelerated carbonation tests, both direct and indirect, at different operating conditions. Thus, the representativeness of the collected data is limited. The list of the analysed documents is reported in Table 3.7.2.1.

Table 3.7.2.1. List of the documents considered in the study.

Peer reviewed papers
Azdarpour et al., 2014. *Direct carbonation of red gypsum to produce solid carbonates*. Fuel Processing Technology 126, 429-434
Azdarpour et al., 2015. *Mineral carbonation of red gypsum via pH-swing process: effect of CO_2 pressure on the efficiency and products characteristics*. Chemical engineering Journal 264, 425-436
Azdarpour et al., 2018. *CO_2 sequestration through direct aqueous mineral carbonation of red gypsum*. Petroleum 4(4), 398-407
Fauziah et al., 2011. *Co-application of red gypsum and sewage sludge on acidic tropical soils*. Communications in soil science and plant analysis 42(21), 2561-2571
Gázquez et al., 2014. *A review of the production cycle of titanium dioxide pigment*. Materials Sciences and Applications 5, 441-458
Pérez-Moreno et al., 2015. *CO_2 sequestration by indirect carbonation of artificial gypsum generated in the manufacture of titanium dioxide pigments*. Chemical Engineering Journal 262, 737-746
Rahmani et al., 2014a. *Calcite precipitation from by-product red gypsum in aqueous carbonation process*. RCS Advances 4, 45548-45557
Rahmani et al., 2014b. *Mineral carbonation of red gypsum for CO_2 sequestration*. Energy&Fuels 28, 5953-5958
Rahmani et al., 2016. *Kinetics analysis of CO_2 mineral carbonation using byproduct red gypsum*. Energy Fuels 30(9), 7460-7464
Reports
Huntsman Tioxide, 2011. *Relazione tecnica allegata alla richiesta di autorizzazione alla costruzione e gestione di un reattore sperimentale finalizzato alla verifica della fattibilità dell'uso dei gessi rossi provenienti dalla produzione di TiO_2 come materiale per la copertura definitiva di discariche di RS non pericolosi*
BREF documents
EU, 2007. *Reference document on Best Available Techniques for the Manufacture of Large volume inorganic chemicals, solids and other industry*

3.7.2.3. RED GYPSUM COMPOSITION

Red gypsum consists mainly of calcium sulphate and ferrous sulphate, with non-negligible amounts of TiO_2 (Azdarpour et al., 2018). If limestone is used for the neutralization of the acid waste, a small amount of $CaCO_3$ can be found in the red gypsum, as a consequence of its excess dosage. The high concentration of Ca in the mineral composition of red gypsum makes it a potential feedstock for CO_2 sequestration (Rahamani et al., 2014).

Based on the analysed documents, the average content of Ca, expressed as CaO, in the red gypsum is about 28% on weight, ranging from 22% to 32%. Ca is usually found as $CaSO_4$. Only one document reports the presence of $CaCO_3$ (about 4-6% of the weight of the red gypsum), as a consequence of the excessive use of limestone, together with lime, in the neutralization process (Huntsman Tioxide, 2011). The content of Fe, expressed as Fe_2O_3, results equal to 10% of the weight of the red gypsum on average, ranging from 3% to 29%. Data used in the study are summarized in Table 3.7.2.2.

Table 3.7.2.2. Chemical composition and mineralogy of red gypsum (min-average-max value). Elaboration of the data reported in the documents listed in Table 3.7.2.1.

Total Ca as CaO (%)	Total Fe as Fe_2O_3 (%)	$CaCO_3$ (%)
22.3-28.3-32.2 *8 cases*	3-10.4-28.9 *8 cases*	4-6 *1 case*

3.7.2.4. POTENTIAL CARBONATION RATE IN RED GYPSUM

The maximum theoretical amount of CO_2 that can be sequestered by the red gypsum as a consequence of the use of lime/limestone in the neutralization process of the acid waste can be calculated considering the total content of Ca in the red gypsum.

Assuming a 28.3% average content of CaO in the red gypsum (Table 3.7.2.2), CO_2 sequestration results equal to about 222 gCO_2 per kg of red gypsum. This value refers only to the CO_2 that can be sequestered as a consequence of its reaction with $CaSO_4$. Red gypsum contains also $FeSO_4$, which can react with CO_2, but since the focus of this study is on lime, the $FeSO_4$ contribution is not of interest and it was not calculated.

It is also worth pointing out that the value previously reported is valid when only lime is used for the neutralization of the acid waste. If limestone is also used, as usually happens, the CO_2 potential sequestration must be calculated from the total content of Ca reduced by the amount of Ca in the form of $CaCO_3$. In addition, when limestone is used in the neutralization process of the titanium acid waste, CO_2 is produced by the reaction of limestone with sulphuric acid, on the basis of the Reaction [4] (1 mol of CO_2 per mol of $CaCO_3$). This amount should be, thus, subtracted from the theoretical CO_2 potential sequestration of the red gypsum. Assuming that the molar ratio between limestone and lime used in the neutralization process is 5, as suggested by EuLa, about 185 gCO_2 are emitted during the neutralization process. Thus, the net potential CO_2 uptake, based on its CaO content, results equal to 37 gCO_2/kg red gypsum.

3.7.2.5. ACCELERATED CARBONATION POTENTIAL IN RED GYPSUM

The CO_2 uptake and the operating conditions for each of the tests considered in this document are summarised in Table 3.7.2.3. All the data refer to accelerated carbonation tests performed at the laboratory scale.

As previously explained, two are the main routes for accelerated carbonation: the direct process and the indirect one. Both processes are analysed in the scientific literature to exploit the red gypsum for CO_2 sequestration. Table 3.7.2.4 summarizes the data of Table 3.7.2.3, reporting the min-max and average CO_2 uptake obtained in direct and indirect carbonation processes.

The indirect process generally performs better than the direct one, allowing for a higher CO_2 uptake. An average CO_2 uptake of 134 gCO_2 per kg of red gypsum resulted from the literature analysis, ranging from 12.7 to 253 gCO_2/kg depending on the operating conditions at which the test is carried out. In addition, the indirect process results in the production of a precipitated calcium carbonate that, if sufficiently pure, can be sold as a product. At the expense of a greater complexity of the process, the indirect process allows for a complete exploitation of the red gypsum, which is used not only as a feedstock for CO_2 sequestration, but also as a raw material to produce a valuable product.

The direct process can be performed in water or in alkaline solution, with addition of ammonia. Adding ammonia can help to achieve higher carbonation rate and higher purity of the precipitated calcium carbonate (Azdarpour et al., 2014). Based on the data reported in Table 3.7.2.4, the average CO_2 uptake when the carbonation is carried out in aqueous solution results equal to 23 gCO_2/kg red gypsum, whereas when NH_4OH is added during the test, the CO_2 uptake increases on average to 56 gCO_2/kg red gypsum, with a maximum value of 104 gCO_2/kg red gypsum, when the carbonation is performed at high pressure (7MPa).

Table 3.7.2.3. CO_2 uptake and relative operative conditions at the lab-scale for seven literature sources.

Reference	**CO_2 uptake** (gCO_2/kg red gypsum)	**Operating conditions**
Azdarpour et al., 2014	32.1	Direct carbonation with addition of NH_4OH. Particle size=400-500 μm; P= 2 MPa; T=25°C; L/S=5; 100% CO_2; 60 min
	57.5	Direct carbonation with addition of NH_4OH. Particle size < 45 μm; P=2 MPa; T=25°C; L/S=5; 100% CO_2; 60 min
	7.9	Direct carbonation with addition of NH_4OH. Particle size=75-100 μm; P= 0.1 MPa; T=25°C; L/S=5; 100% CO_2; 60 min
	103.8	Direct carbonation with addition of NH_4OH. Particle size=75-1000μm; P= 7 MPa; T=25°C; L/S=5; 100% CO_2; 60 min
	54.0	Direct carbonation with addition of NH_4OH. Particle size=75-100 μm; P=2 MPa; T=25°C; L/S=5; 100%CO_2; 60 min
	71.1	Direct carbonation with addition of NH_4OH. Particle size= 75-100 μm; P= 2 MPa; T=200°C; L/S=5; 100% CO_2; 60 min
	66.5	Direct carbonation with addition of NH_4OH. Particle size= 75-100 μm; P= 2 MPa; T= 300°C; L/S=5; 100% CO_2; 60 min
Azadarpour et al., 2018	2.4	Direct aqueous carbonation. Particle size <45 μm; P=0.1 MPa; T=25°C; L/S=5; 100% CO_2; 60 min
	59.7	Direct aqueous carbonation. Particle size <45 μm; P=7 MPa; T=25°C; L/S=5; 100% CO_2; 60 min
	16.1	Direct aqueous carbonation. Particle size <45 μm; P=2 MPa; T=25°C; L/S=5; 100%CO_2; 60 min
	31.7	Direct aqueous carbonation. Particle size <45 μm; P=2 MPa; T=200°C; L/S=5; 100%CO_2; 60 min
	25.8	Direct aqueous carbonation. Particle size <45 μm; P=2 MPa; T=400°C; L/S=5; 100%CO_2; 60 min
	21.3	Direct aqueous carbonation. Particle size=300-500 μm; P=2 MPa; T=200°C; L/S=5; 100% CO_2; 60 min
	29.0	Direct aqueous carbonation. Particle size=45-100 μm; P=2 MPa; T=200°C; L/S=5; 100% CO_2; 60 min
	27.9	Direct aqueous carbonation. Particle size=100-212 μm; P=2 MPa; T=200°C; L/S=5; 100% CO_2; 60 min
	23.7	Direct aqueous carbonation. Particle size=212-300 μm; P=2 MPa; T= 200°C; L/S=5; 100% CO_2; 60 min
	0.0	Direct aqueous carbonation. Particle size <45 μm; P=2 MPa; T=25°C; L/S=5; 100% CO2; 5 min
	12.2	Direct aqueous carbonation. Particle size <45 μm; P=2 MPa; T=25°C; L/S=5; 100% CO_2; 30 min
	22.6	Direct aqueous carbonation. Particle size <45 μm; P= 2 MPa; T=25°C; L/S=5; 100% CO_2; 120 min

Table 3.7.2.3 (continued). CO_2 uptake and relative operative conditions at the lab-scale for seven literature sources.

Reference	CO_2 uptake (gCO_2/kg red gypsum)	Operating conditions
Rahmani et al., 2014a	62.0	Indirect carbonation with addition of H_2SO_4 and NH_4OH. Particle size<75 μm; P=6.4 MPa; T=25°C; L/S=10; 100% CO_2; 180 min; 400 rpm
	122.3	Indirect carbonation with addition of H_2SO_4 and NH_4OH. Particle size<75 μm; P=6.4 MPa; T=50°C; L/S=10; 100% CO_2; 180 min; 400 rpm
	125.4	Indirect carbonation with addition of H_2SO_4 and NH_4OH. Particle size<75 μm; P=6.4 MPa; T=60°C; L/S=10; 100% CO_2; 180 min; 400 rpm
	78.8	Indirect carbonation with addition of H_2SO_4 and NH_4OH. Particle size<75 μm; P=6.4 MPa; T=75°C; L/S=10; 100% CO_2; 180 min; 400 rpm
	110.0	Indirect carbonation with addition of H_2SO_4 and NH_4OH. Particle size<75 μm; P= 6.4 MPa; T= 60°C; L/S=30; 100%CO_2; 180 min; 400 rpm
	77.4	Indirect carbonation with addition of H_2SO_4 and NH_4OH. Particle size<75 μm; P= 6.4 MPa; T= 60°C; L/S=100; 100%CO_2; 180 min; 400 rpm
	94.2	Indirect carbonation with addition of H_2SO_4 and NH_4OH. Particle size<75 μm; P= 6.4 MPa; T= 60°C; L/S=200; 100%CO_2; 180 min; 400 rpm
	88.4	Indirect carbonation with addition of H_2SO_4 and NH_4OH. Particle size=75-125 μm; P=6.4 MPa; T=60°C; L/S=10; 100% CO_2; 180 min; 400 rpm
	55.4	Indirect carbonation with addition of H_2SO_4 and NH_4OH. Particle size= 125-200 μm; P=6.4 MPa; T=60°C; L/S=10; 100% CO_2; 180 min; 400 rpm
	37.8	Indirect carbonation with addition of H_2SO_4 and NH_4OH. Particle size>200 μm; P=6.4 MPa; T=60°C; L/S=10; 100% CO_2; 180 min; 400 rpm
	70.4	Indirect carbonation with addition of H_2SO_4 and NH_4OH. Particle size<75 μm; P=6.4 MPa; T=60°C; L/S=10; 100% CO_2; 180 min; 100 rpm
	94.2	Indirect carbonation with addition of H_2SO_4 and NH_4OH. Particle size<75 μm; P=6.4 MPa; T=60°C; L/S=10; 100% CO_2; 180 min; 200 rpm
	113.5	Indirect carbonation with addition of H_2SO_4 and NH_4OH. Particle size<75 μm; P=6.4 MPa; T=60°C; L/S=10; 100% CO_2; 180 min; 300 rpm
Pérez-Moreno et al., 2015	202.4	Indirect carbonation with addition of H_2SO_4 and NH_4OH. Unknown particle size; P= 0.1 MPa; T= 75°C; L/S=20; 100%CO_2; 60 min
	140.8	Indirect carbonation with addition of H_2SO_4 and NaOH. Unknown particle size; P= 0.1 MPa; T= 75°C; L/S=20; 100%CO_2; 60 min
Azdarpour et al., 2015	104.6	Indirect carbonation with addition of H_2SO_4 and NH_4OH. Particle size= 100-212 μm; P=1 MPa; T=25°C; L/S=2; 100% CO_2; 30 min
	253.0	Indirect carbonation with addition of H_2SO_4 and NH_4OH. Particle size= 100-212 μm; P=1 MPa; T=25°C; L/S=5; 100% CO_2; 30 min
	82.0	Indirect carbonation with addition of H_2SO_4 and NH_4OH. Particle size= 100-212 μm; P=1 MPa; T=25°C; L/S=5; 100% CO_2; 5 min
	136.6	Indirect carbonation with addition of H_2SO_4 and NH_4OH. Particle size= 100-212 μm; P=0.1 MPa; T=25°C; L/S=5; 100% CO_2; 30 min
Rahmani et al., 2016	253.0	Indirect carbonation with addition of H_2SO_4 and NH_4OH. Particle size= 100-212 μm; P=0.8 MPa; T=25°C; L/S=5; 100% CO_2; 30 min; 400 rpm
	250.0	Indirect carbonation with addition of H_2SO_4 and NH_4OH. Particle size <38 μm; P=0.1 MPa; T=60°C; L/S=10; 100% CO_2; 120 min; 400 rpm
	230.2	Indirect carbonation with addition of H_2SO_4 and NH_4OH. Particle size <38 μm; P=0.1 MPa; T=60°C; L/S=30; 100% CO_2; 120 min; 400 rpm
	189.8	Indirect carbonation with addition of H_2SO_4 and NH_4OH. Particle size <38 μm; P=0.1 MPa; T=60°C; L/S=100; 100% CO_2; 120 min; 400 rpm
	207.5	Indirect carbonation with addition of H_2SO_4 and NH_4OH. Particle size <38 μm; P=0.1 MPa; T=60°C; L/S=200; 100% CO_2; 120 min; 400 rpm

Table 3.7.2.3 (continued). CO_2 uptake and relative operative conditions at the lab-scale for seven literature sources.

Reference	**CO_2 uptake** (gCO_2/kg red gypsum)	**Operating conditions**
Rahmani et al., 2014b	250.0	Indirect carbonation with addition of H_2SO_4 and NH_4OH. Particle size <38 μm; P=6.4 MPa; T=unknown; L/S=10; 100% CO_2; 180 min; 400 rpm
	12.7	Indirect carbonation with addition of H_2SO_4 and NH_4OH. Particle size <38 μm; P=0.1 MPa; T=unknown; L/S=10; 100% CO_2; 180 min; 400 rpm
	38.0	Indirect carbonation with addition of H_2SO_4 and NH_4OH. Particle size <38 μm; P=1 MPa; T=unknown; L/S=10; 100% CO_2; 180 min; 400 rpm
	139.2	Indirect carbonation with addition of H_2SO_4 and NH_4OH. Particle size <38 μm; P=unknown; T=60°C; L/S=10; 100% CO_2; 15 min; 400 rpm
	172.0	Indirect carbonation with addition of H_2SO_4 and NH_4OH. Particle size <38 μm; P=unknown; T=60°C; L/S=10; 100% CO_2; 30 min; 400 rpm
	250	Indirect carbonation with addition of H_2SO_4 and NH_4OH. Particle size <38 μm; P=unknown; T=60°C; L/S=10; 100% CO_2; 180 min; 400 rpm

Table 3.7.2.4. Minimum-maximum and average CO_2 uptake for direct and indirect carbonation tests.

Type of test	**CO_2 uptake (gCO_2/kg red gypsum)**		
	Minimum	**Average**	**Maximum**
Aqueous direct carbonation test (*12 cases*)	0	22.7	59.7
Direct carbonation test with addition of NH_4OH (*7 cases*)	7.9	56.1	103.8
Indirect carbonation test (*31 cases*)	12.7	134.7	253

All the tests were performed using a pure CO_2 stream in slurry conditions (L/S > 2). Pressure ranged from the atmospheric value to 7 MPa and the temperature from ambient up to 400°C. The test duration ranged from 5 min to 3 hours. Red gypsum was usually sieved in different size classes to observe the influence of the particle size on the carbonation process.

The statistical analysis of the data (Table 3.7.2.5) shows a significant correlation between the CO_2 uptake and the type of test (direct carbonation in aqueous solution; direct carbonation with addition of NH_4OH; indirect carbonation). The operating conditions at which the test is carried out (T, P, reaction time, stirring rate etc.) have a lower influence, with the exception of the temperature. Thus, what really influences the carbonation yield is the fact that carbonation is carried out directly on the red gypsum or on the extracted Ca ions.

In addition, the statistical analysis shows a significant negative correlation between the CO_2 uptake and temperature. The influence of temperature on the carbonation process has been investigated by several authors. They found that the CO_2 uptake increases with the temperature up to a certain value and then the conversion rate decreases for a further temperature increase. In their tests of direct carbonation, Azdarpour et al. (2014) found that both carbonation efficiency and product purity increase with increasing temperature up to 200°C, then a further increment of the temperature results in a decrease of the carbonation efficiency and product purity. For Rahmani et al. (2014), who performed indirect carbonation tests, the optimal temperature is around 55-60°C. The difference between the two sources findings might be related to the different type of tests they referred to (direct vs. indirect): in direct carbonation tests, working at high temperature promotes Ca dissolution

from the matrix and ions precipitation, thus improving also the purity of the precipitated calcium carbonate. On the other hand, at high temperatures the CO_2 solubility is significantly reduced. In indirect processes, Ca is solubilised in a previous step[29], thus carrying out the carbonation at high temperatures has only negative effects. Even if the statistical analysis of the data did not show other significant correlations between the CO_2 uptake and the other process parameters, the scientific literature generally agrees that CO_2 uptake is in direct relationship with the CO_2 pressure (Rahamani et al., 2014b). Azdarpour et al. (2014) found that in direct processes, under atmospheric pressure, only Ca reacts with CO_2. Fe starts to react only at a CO_2 pressure of 0.5 MPa. Increasing the CO_2 pressure facilitates its dissolution in the slurry and enhances the carbonation kinetics.

In addition, the particle size seems to be a key parameter to maximize red gypsum carbonation (Azdarpour et al., 2014). Reducing particle size causes an increase in particle surface area, which results in enhanced reaction rates (Rahamani et al., 2014a).

Also the L/S ratio can influence the CO_2 uptake. Azdarpour et al. (2015) found that increasing the L/S ratio from 2 to 5 results in an improvement of the Ca carbonation but, with a further increase of the L/S ratio, the carbonation efficiency decreases, since the concentration of dissolved CO_2 decreases. A similar behaviour was observed by Rahamani et al. (2014a), with the only difference that they found a threshold value for the L/S ratio of 10 instead of 5.

Rahamani et al. (2014) also investigated the role of the stirring rate. The maximum carbonation rate was achieved for a stirring rate of 400 rpm. Up to 400 rpm, increasing the stirring rate promotes the CO_2 transfer due to rising disorder between the liquid and gas boundary. A further increase of the stirring rate has a reverse effect on Ca conversion, probably as a consequence of the reduction of the CO_2 concentration in the solution due to an excessive mechanical agitation (CO_2 out-gassing).

For reaction time, the carbonation rate is faster in the indirect process compared to the direct one. For example, Azdarpour et al. (2015) obtained a carbonation degree of more than 30% after only 5 minutes of reaction when they operated in two stages, whereas no signs of red gypsum carbonation were found after 5 minutes when they operated in a single stage (Azdarpour et al., 2018).

Finally, we want to point out that most of the data reported in Table 3.7.2.4 mainly refer to the same sample of red gypsum, from a titanium industry in Malaysia, which was subjected to several tests at different operating conditions. Thus, it is impossible to evaluate an eventual relationship between the CO_2 uptake and the red gypsum composition.

[29] A good control of the temperature during the dissolution step is necessary to guarantee that most of the Ca is dissolved in the solution and that Fe ions and other impurities precipitate.

Table 3.7.2.5. Correlation analysis of the data reported in Table 3.7.2.3.

		Type_test	CO2 uptake	particle size	L/S	P	T	test duration	CaO tot	stirring rate
Type_test	Correlazione di Pearson	1	,536**	-,151	,251	,216	-,300*	,478**	-,141	.c
	Sign. (a due code)		,000	,291	,070	,132	,033	,000	,315	,000
	N	53	53	51	53	50	51	53	53	26
CO2 uptake	Correlazione di Pearson	,536**	1	-,088	,223	-,132	-,288*	,042	-,200	,193
	Sign. (a due code)	,000		,539	,109	,363	,041	,763	,152	,346
	N	53	53	51	53	50	51	53	53	26
particle size	Correlazione di Pearson	-,151	-,088	1	-,177	-,117	,068	-,258	.c	,036
	Sign. (a due code)	,291	,539		,213	,427	,642	,068	,000	,863
	N	51	51	51	51	48	49	51	51	26
L/S	Correlazione di Pearson	,251	,223	-,177	1	,034	-,083	,258	-,004	,141
	Sign. (a due code)	,070	,109	,213		,816	,562	,062	,977	,493
	N	53	53	51	53	50	51	53	53	26
P	Correlazione di Pearson	,216	-,132	-,117	,034	1	-,131	,673**	,235	-,234
	Sign. (a due code)	,132	,363	,427	,816		,376	,000	,101	,282
	N	50	50	48	50	50	48	50	50	23
T	Correlazione di Pearson	-,300*	-,288*	,068	-,083	-,131	1	-,131	,010	-,090
	Sign. (a due code)	,033	,041	,642	,562	,376		,360	,944	,675
	N	51	51	49	51	48	51	51	51	24
test duration	Correlazione di Pearson	,478**	,042	-,258	,258	,673**	-,131	1	,130	-,176
	Sign. (a due code)	,000	,763	,068	,062	,000	,360		,352	,389
	N	53	53	51	53	50	51	53	53	26
CaO tot	Correlazione di Pearson	-,141	-,200	.c	-,004	,235	,010	,130	1	.c
	Sign. (a due code)	,315	,152	,000	,977	,101	,944	,352		,000
	N	53	53	51	53	50	51	53	53	26
stirring rate	Correlazione di Pearson	.c	,193	,036	,141	-,234	-,090	-,176	.c	1
	Sign. (a due code)	,000	,346	,863	,493	,282	,675	,389	,000	
	N	26	26	26	26	23	24	26	26	26

**. La correlazione è significativa a livello 0,01 (a due code).

*. La correlazione è significativa a livello 0,05 (a due code).

c. Calcolo impossibile da eseguire perché almeno una delle variabili è costante.

3.7.2.6. DISCUSSION AND CONCLUSIONS

Red gypsum as a possible sink for CO_2 sequestration

Red gypsum is the main waste produced by the titanium dioxide manufacturing industry where ilmenite is used as a raw material. It consists mainly of calcium sulphate and ferrous sulphate, with non-negligible amount of TiO_2 (Azdarpour et al., 2018).

Due to its high content of Ca, red gypsum is considered as a potential feedstock for CO_2 sequestration (Rahamani et al., 2014). Based on our knowledge, all the data reported in the literature refer to accelerated carbonation tests performed at a laboratory scale. Natural carbonation of red gypsum during its storage or when it is recycled as a construction material or as a fertilizer is not documented, as well as accelerated carbonation at the industrial scale.

Based on the analysed literature, when red gypsum is directly carbonated, the average CO_2 uptake results equal to 23-56 gCO_2/kg red gypsum whereas, when indirect accelerated carbonation is performed, 134 gCO_2 are sequestered per kg of red gypsum.

By assuming:

- an average content of CaO in the red gypsum of 28.3%, corresponding to a lime/limestone addition in the acid waste neutralization process of about 0.28 kgCaO per kg of produced red gypsum;

- a release in the atmosphere of about 786 kg of CO_2 per tonne of produced lime, only from the calcination process, excluding the fuel consumption;

it results that about 60% of the CO_2 emitted from the lime industry can be captured by the red gypsum if it is used as a feedstock for indirect accelerated carbonation. This amount decreases to 10-25% when direct carbonation is carried out (depending on whether NH_4OH is added or not during the process).

Such values refer to laboratory tests performed in controlled conditions. CO_2 uptake in natural environmental conditions, during the red gypsum life cycle, is expected to be lower.

Furthermore, the CO_2 sequestration during carbonation is the consequence of the presence of Ca in the red gypsum, regardless of whether lime or limestone is used in the acid waste neutralization process. In addition, the values previously reported refer only to the carbonation process, without taking into account the possible emission of CO_2 in the previous acid waste neutralization process due to the use of limestone. Since none of the papers reported in Table 3.7.2.1 report whether the neutralization process was performed with addition of lime and/or limestone and in which proportion, only an estimate of the net CO_2 uptake, derived from the CO_2 emitted during the acid neutralization process, can be done.

By assuming:

- a molar ratio between limestone and lime used in the neutralization process equal to 5, as suggested by EuLa;
- a release in the atmosphere of 440 kg of CO_2 per tonne of limestone used in the neutralization process;

it follows that, despite red gypsum can be used as a feedstock material to sequester CO_2, the acid waste management (neutralization process + carbonation of red gypsum) results in a net CO_2 emission. The amount of CO_2 emitted by the limestone as a consequence of the Reaction [4] is, in fact, more that the amount of CO_2 that can be captured by the red gypsum during the carbonation process. An average CO_2 emission of 51 gCO_2/ t red gypsum can be estinated when the indirect carbonation process is performed, increasing to about 163 g CO_2/t red gypsum when the direct route is applied.

<u>Recommendation on research needs on red gypsum</u>

The scientific literature on red gypsum carbonation is very limited. Based on the authors' knowledge, all the documents published in the scientific literature refer to accelerated carbonation tests performed at the laboratory scale. No data were found about natural carbonation of red gypsum during disposal or during its life cycle, when it is recycled as a construction material or as a fertilizer.

Another limitation of the present study is that most of the analysed papers refer to the same sample of red gypsum, which was subjected to several accelerated carbonation tests, both of direct and indirect type, at different operating conditions. Thus, the representativeness of the collected data is limited.

Furthermore, none of the documents report whether the Ca content in the red gypsum is the result of the use of lime and/or limestone in the acid waste neutralization process.

It is suggested that analyses of red gypsum from different titanium oxide production plants be carried out, in order to have a more representative database. Samples should be collected from red gypsum landfills ensuring materials of different age in order to assess the amount of CO_2 that can be actually sequestered by the red

gypsum in ambient conditions and to better understand the time evolution of the carbonation process. It will be essential to known the acid waste neutralization process generating the red gypsum, in particular if lime and/or limestone is used and in what proportion, in order to assess the actual net CO_2 sequestration/emission due to the overall waste acid management process.

REFERENCES

Azdarpour, A. Asadullah, M., Junin, R., Manan, M., Hamidi, H., Mohammadian, E., 2014. *Direct carbonation of red gypsum to produce solid carbonates*. Fuel Processing Technology 126, 429-434. DOI: https://doi.org/10.1016/j.fuproc.2014.05.028

Azdarpour, A., Asadullah, M., Mohammadian, E., Junin, R., Hamidi, H., Manan, M., Daud, A.R.M., 2015. *Mineral carbonation of red gypsum via pH-swing process: effect of CO2 pressure on the efficiency and products characteristics*. Chemical Engineering Journal 264, 425-436. DOI: https://doi.org/10.1016/j.cej.2014.11.125

Azdarpour, A., Karaei, M.A., Hamidi, H., Mohammadian, E., Honarvar, B., 2018. *CO_2 sequestration through direct aqueous mineral carbonation of red gypsum*. Petroleum 4(4), 398-407. DOI: https://doi.org/10.1016/j.petlm.2017.10.002

Barksdale, J., 1961. *Titanium, its occurrence, chemistry and technology*. 2nd edition, the Roland Press Company, New York (via Gazquez et al., 2014)

EU, 2007. *Reference document on Best Available Techniques for the Manufacture of Large volume inorganic chemicals-solids and other industry*. http://eippcb.jrc.ec.europa.eu/reference/BREF/lvic-s_bref_0907.pdf (latest access 11-3-2019)

Fauziah, C.I., Nur Hanani, M., Zauyah, S., Samsuri, A.W., Rosazlin, A., 2011. *Co-application of red gypsum and sewage sludge on acidic tropical soils*. Communications in soil science and plant analysis 42(21), 2561-2571. DOI: https://doi.org/10.1080/00103624.2011.61403

Gázquez, M.J., Bolívar, J.P., Garcia-Tenorio, R., Vaca, F., 2014. *A review of the production cycle of titanium dioxide pigment*. Materials Sciences and Applications 5, 441-458. DOI: http://dx.doi.org/10.4236/msa.2014.57048

Grzmil, B.U., Grela, D., Kic, B., 2008. *Hydrolysis of titanium sulphate compounds*. Chemicals papers 62(1), 18-25. DOI: 10.2478/s11696-007-0074-8

Huntsman Tioxide, 2011. *Relazione tecnica allegata alla richiesta di autorizzazione alla costruzione e gestione di un reattore sperimentale finalizzato alla verifica della fattibilità dell'uso dei gessi rossi provenienti dalla produzione di TiO_2 come materiale per la copertura definitiva di discariche di RS non pericolosi*. Available online (In Italian): http://www.lavoroambienteesalute.it/wp-content/uploads/2011/07/Relazione-Tecnica-Feb-2011.pdf (latest access 11-3-2019)

Pérez-Moreno, S.M., Gázquez, M.J., Bolívar, J.P., 2015. *CO_2 sequestration by indirect carbonation of artificial gypsum generated in the manufacture of titanium dioxide pigments*. Chemical Engineering Journal 262, 737-746. DOI: https://doi.org/10.1016/j.cej.2014.10.023

Rahmani, O., Tyrer, M., Junin, R., 2014a. *Calcite precipitation from by-product red gypsum in aqueous carbonation process*. RCS Advances 4, 45548-45557. DOI: 10.1039/c4ra05910g

Rahmani, O., Junin, R., Tyrer, M., Mohsin, R., 2014b. *Mineral carbonation of red gypsum for CO_2 sequestration*. Energy Fuels 28, 5953-5958. DOI: dx.doi.org/10.1021/ef501265z

Rahmani, O., Kadkhodaie, A., Highfield, J., 2016. *Kinetics analysis of CO_2 mineral carbonation using byproduct red gypsum*. Energy Fuels 30(9), 7460-7464. DOI: https://doi.org/10.1021/acs.energyfuels.6b00246

3.7.3. USE OF LIME IN THE ALUMINIUM PRODUCTION PROCESS

3.7.3.1. INTRODUCTION

Red mud is a side-product of the Bayer process, the principal means of refining bauxite ore for alumina extraction. In the Bayer process, bauxite is digested in a caustic liquor of Na and Ca-hydroxides. This process produces two output streams, liquor pregnant with alumina that is for alumina precipitation and a solid residue, called red mud, for disposal. This waste residue is a slurry, with a water content of about 50-70%.

Approximately, a range of 0.3-6.2 tonnes of red mud per tonne of alumina are produced in the Bayer process (EAA, 2014; Li et al., 2016; McConchie et al., 2005), more frequently between 0.7-2 t red mud/t alumina (EAA, 2014; Yadav et al., 2010).

Its chemical composition and mineralogy depends on the quality and nature of the bauxite ore and on the extraction conditions (Li et al., 2016). On average, the main constituents are Fe_2O_3, Al_2O_3, SiO_2, NaOH, CaO and TiO_2 (Collazo et al., 2006). The concentration of ferric oxide, which is responsible for the red colour, depends on the composition of bauxite, whereas the content of sodium and calcium compounds, as well as their speciation, are related to the process, in particular the amount of soda and lime added during the Bayer process and the pressure and the temperature at which the extraction is carried out. Moreover, red mud is often subjected to washing and filtration to recycle part of the caustic liquor through the plant (Bott et al., 2005; Colling and Jamieson, 2004).

Red mud is highly alkaline, with a pH generally above 13, depending on its content of sodium and calcium compounds (Santini et al., 2011).

Soda content varies between 0.1 and 12.3%, expressed as Na_2O (Bánvölgyi, 2015). The chemical form in which soda is present in the red mud depends on the type of digestion process (Bánvölgyi, 2015):

- at low temperature (140-150°C) only gibbsite is solubilised, whereas quartz remains un-attacked. The main sodium aluminium hydrosilicate products is, thus, sodalite ($3Na_2O*Al_2O_3*6SiO_2*Na_2SO_4$);
- at high temperature (240-250°C) boehmine and diaspore are also solubilised and quartz starts reacting. The preferred sodium aluminium hydrosilicate product becomes cancrinite ($Na_6Al_6Si_6O_{24}*2CaCO_3$), the rest is soldalite. Solubilisation of diaspore requires more severe conditions (T > 250-280°C and/or higher caustic concentration).

Lime is added to the digestion or in the pre-desilication step for different purposes (Bánvölgyi, 2015):

- to convert the caustic soluble P-compounds to insoluble Ca-phosphates;
- to convert Na-titanates to Ca-titanates;
- to convert Na-Al-hydrosilicates to Ca-Al-hydrosilicates;
- to enhance the conversion of the (alumo)-goethite into hematite;
- to enhance the digestion (solubilisation) of diaspore;
- to reduce the soda loss associated with sodalite formation (Smith, 2015).

Lime can be added as quicklime or slaked lime. Usually 0.5-1% CaO w/w of the bauxite weight is added to the low temperature digestion to convert P content to insoluble compounds. A minimum of 2% of CaO must

be added for the digestion of diaspore. It is important to limit the lime addition below 5% of the bauxite weight, in order to avoid decrease in the extraction yield of diasporic alumina (Whittington, 1996; Li et al., 2016).
When quicklime or slaked lime enter into contact with the Bayer liquor, they react with both aluminate and carbonate ions, producing calcite or tri-calcium aluminate (TCA, $3CaO{\cdot}Al_2O_3{\cdot}6H_2O$). Lime can also react with silica, by including it into the structure of TCA producing hydrogarnet (HG, $Ca_3AlFe{*}SiO_4{*}OH$). This reaction is more frequent when lime is added at the pre-desilication step when TCA forms. If added directly to digestion, its dissolution releases calcium ions that may be consumed by a variety of reactions and the formation of HG is less likely (Smith, 2015).

The management of red mud has changed substantially since the last 50 years. Before 1980s, the practice was to pump the tailings slurry, at a concentration of about 20% solids, into lagoons or ponds sometimes created in former bauxite mines or depleted quarries. It was also common practice for the tailings to be discharged into rivers, estuaries, or the sea via pipelines or barges; in other instances, the residue was shipped out to sea and disposed of in deep ocean trenches many kilometres offshore. All disposal in the sea, estuaries and rivers has now ended because it is forbidden (Power et al., 2011).
In the last decades, dry stacking has been increasingly adopted, because of residue storage space running out and because of increasing concern over wet storage. With this method, tailings are thickened until they reach a solid content of at least 48-55%, and then deposited in such a way that it consolidates and dries (EAA, 2014)
After deposition, liquor alkalinity is slowly diluted by the infiltration of rainwater; however, desorption of absorbed hydroxide and carbonate and dissolution of alkaline solid phases such as TCA and, at lower pH, sodalite, supplies liquor alkalinity until the reserve of alkaline species and solid are exhausted due to their reaction with the atmospheric CO_2.
Red mud slurry natural carbonation involves both pore water carbonation and solid phase reactions of TCA dissolution and calcite precipitation (Khaitan et al., 2009). The pore water carbonation occurs by the rapid absorption of atmospheric CO_2 that forms carbonic acid and neutralizes the excess base in the form of NaOH, $NaCO_3^-$ and $Al(OH)_4^-$ in the pore water. Initially, CO_2 converts pore water hydroxide alkalinity (derived from the NaOH remaining from the Bayer extraction of alumina) to carbonate alkalinity. Then, pore water carbonate alkalinity (CO_3^{2-}) is converted to bicarbonate alkalinity (HCO_3^-), which dominates at pH values lower than 10.3. These reactions reach the state of dynamic equilibrium unless the reaction products are removed from the solution. Carbonate ions can react with a range of divalent metal cations (typically Ca and Mg) to forms stable carbonate minerals (Si et al., 2013). Soluble Ca ions are usually present in the red mud in modest amount, mainly as a consequence of the dissolution of TCA. Dissolution products of TCA depend on the solution chemistry (Santini et al., 2011): without carbonate and bicarbonate present, TCA dissolves until chemical equilibrium prevails:

$$3CaO{*}Al_2O_3{*}6H_2O_{(s)} \leftrightarrow 3Ca^{2+}_{(aq)} + 2Al(OH)_4^-{}_{(aq)} + 4OH^-_{(aq)}$$

In the presence of sufficient carbonate, calcite and sodium aluminate are formed:

$3CaO*Al_2O_3*6H_2O_{(s)} + 2Na^+_{(aq)} + 3CO_3^{2-}{}_{(aq)} \rightarrow 3CaCO_{3\,(s)} + 2NaAl(OH)_{4\,(aq)} + 4(OH)^-{}_{(aq)}$

In the presence of sufficient bicarbonate, calcite and dawsonite or aluminium hydroxide are formed:

$3CaO*Al_2O_3*6H_2O_{(s)} + 8HCO_3^-{}_{(aq)} + 2Na^+_{(aq)} \leftrightarrow 2NaAl(OH)_2CO_{3\,(s)} + 3CaCO_{3\,(s)} + 3CO_3^{2-}{}_{(aq)} + 8H_2O$

$3CaO*Al_2O_3*6H_2O_{(s)} + 6HCO_3^-{}_{(aq)} \leftrightarrow 2Al(OH)_{3(s)} + 3CaCO_{3(s)} + 3CO_3^{2-}{}_{(aq)} + 6H_2O$

In addition to TCA, other Ca-bearing minerals can act as a source of Ca (Si et al., 2013):

$CaSiO_{4\,(s)} + 2H_2CO_{3\,(aq)} \rightarrow 2CaCO_{3\,(s)} + SiO_{2\,(s)} + 2H_2O$

$CaTiO_{3\,(s)} + H_2CO_{3\,(aq)} \rightarrow CaCO_{3\,(s)} + TiO_{2\,(s)} + H_2O$

However, such chemical reactions may be kinetically very slow under ambient conditions, making this carbonation pathway insignificant since, within a red mud storage facility, a given volume of red mud is usually only exposed to the atmosphere for a limited period of time before it is covered by a new layer of red mud. The carbonation reactions proceed until either the stocks of TCA are exhausted or calcium concentration increases so that the liquor is saturated with respect to TCA. In a freely draining system exposed to rainfall, calcium concentration in the liquor would be unlikely to achieve saturation with respect to TCA, and any TCA present will continue to dissolve and release hydroxide. Reserve alkalinity may maintain a leachate pH of 13 for more than 20 years in uncarbonated bauxite red mud deposits (Santini et al., 2011).

Due to the high pH, the disposal of red mud slurry can generate some problems:

1) costly maintenance of large red mud pond areas;
2) risk of caustic for all living organisms;
3) leakage of alkaline compounds into the ground water;
4) overflow of materials and dusting of dry surfaces interfering with nearby rehabilitation on plant life

(Enick et al., 2001; Brunori et al., 2005).

The first thing to do is, thus, to neutralize the mud, reducing its pH to < 10.5, where pH 7-9 is the desired end-point. Currently there are three main neutralization methods:

1) seawater neutralization: it is used by some coastal refineries and involves the addition of excess seawater to precipitate the soluble hydroxides and carbonates as insoluble hydroxides ($Mg_3(OH)_6$), carbonates ($CaCO_3$ and $MgCO_3$) and hydroxyl-carbonates ($Mg_6Al_2CO_3OH_{16}*4H_2O$, $CaAl_2CO_3OH_4*3H_2O$) (Menzies et al., 2004; Hanahan et al., 2004);
2) BaseconTM® neutralization: it is similar to seawater neutralization but uses artificial Ca and Mg rich brines > 20 times the concentration of seawater to improve efficiency and to allow variation of the Ca:Mg ratio to favour particular mineral precipitates (McConchie et al., 2005; Clark et al., 2005;

Bonenfant et al., 2008; Khaitan et al., 2009). The neutralized mud is called BauxsolTM® and it is classified as an environmental non-hazardous product in several countries;

3) CO_2 neutralization: red mud retains significant amount of soluble and solid-phase alkalinity. As shown before, natural carbonation of red mud during storage is extremely slow and the carbonation degree can be very modest even after 20 years. Carbonation can be accelerated by using industrial gas enriched of CO_2 or liquid CO_2 (Enick et al., 2001; Shi et al., 2000; Bonenfant et al., 2008; Khaitan et al., 2009) and/or by adding an external Ca source to promote carbonate precipitation (Si et al., 2013).

The addition of an external source of Ca can be very useful to improve red mud carbonation and permanently store CO_2.When in contact with a CO_2 source, the pH of red mud rapidly decreases, due to the reactions between CO_2 and the hydroxide component (Johston et al., 2010; Sahu et al., 2010):

$CO_{2\,(aq)} + OH^-_{\,(aq)} \rightarrow HCO_3^-{}_{(aq)}$

$OH^-_{\,(aq)} + HCO_3^-{}_{(aq)} \rightarrow H_2O + CO_3^{\,2-}{}_{(aq)}$

$H_2O + CO_{2\,(aq)} \rightarrow HCO_3^-{}_{(aq)} + H^+_{\,(aq)}$

$[Al(OH)_4]^-_{\,(aq)} + CO_{2\,(aq)} + Na^+_{\,(aq)} \rightarrow Al(OH)_{3\,(s)} + Na^+_{\,(aq)} + HCO_3^-{}_{(aq)}$

$2[Al(OH)_4]^-_{\,(aq)} + CO_{2\,(aq)} + 2Na^+_{\,(aq)} \rightarrow 2Al(OH)_{3\,(s)} + 2Na^+_{\,(aq)} + CO_3^{2-}{}_{(aq)} + H_2O$

However, rebounds occur when the CO_2 source is removed from the residue slurry, especially when the content of free lime is modest or null, because CO_2 is not permanently stored in stable precipitate forms such as calcite. The pH reduction following these reactions is, thus, only temporary. In bauxite residues, alkalinity is mainly stored in compounds such as hydrogrossular and sodalite, which have a buffer capacity between pH 11 and 8. Hence, at pH < 8, the decomposition of such compounds may take place, with the partial dissolution of Na and Ca. During the carbonation process, the carbonate and hydrogen carbonate ions may react with Na^+ ions present in solution to form Na_2CO_3 and/or $NaHCO_3$. However, these two compounds have a relatively high solubility in water. In the absence of continuous CO_2 gas injection, the concentration of HCO_3^-/CO_3^{2-} is reduced and, consequently, alkaline anions in the solution such as $Al(OH)_4^-$ and OH^- start buffering the pH of the slurry (Sahu et al., 2010) and CO_2 is released. In order to permanently capture the CO_2 in a stable precipitate form, such as calcite, an extra supply of Ca is thus needed (Rivera et al., 2017; Si et al., 2013). The Ca content and the supply of CO_2 are, thus, essential factors to induce the reactions. The initial Ca content varies depending on the original bauxite ore. As long as the CO_2 supply continues, the amount of Ca is regarded as the limiting factor and additional Ca is required to stimulate the reaction (Han et al., 2014). Enhancement of CO_2 sequestration by using red mud quick carbonation potential is easy: it only requires sufficient supply of divalent binding metals. Where soluble Ca and or Mg bearing substances, such as gypsum and concentrated brines, are used, CO_2 sequestration is improved.

Lime is, also, added to the red mud for soda and alumina recovery. The process is called causticisation or calcification-carbonation, depending on whether it is performed in a single stage or in two stages. In the two-stage process, the red mud is first treated with lime to transform the silicon phase (sodium aluminosilicates

hydrate $Na_2O*Al_2O_3*xSiO_2(6-2x)H_2O$ - SAS) into hydrogarnet (HG) and then, in the second step, HG is decomposed with CO_2 to recover alumina. Na_2O is recovered in the first step (Li et al., 2016). The lime addition is usually performed at high temperature: Li et al. (2016) found an optimal calcification temperature of 180°C and an optimal carbonation temperature of 80-120°C; Creswell and Milne (1984) proposed to perform the causticisation process at a temperature of 260°C. A similar temperature was used by Solymar et al. (1997) for the treatment of the red mud in a pilot plant in Hungary, achieving a good result for the soda recovery but a modest one for alumina. Lower temperatures, of about 90°C, were, on the contrary, used in full scale plants operating in Hungary from mid 1950s for about 25 years (Bánvölgyi, 2015). The theoretical lime consumption is 2 kg CaO/kg of recovered Na(OH), but in practice 3-4 kg CaO/kg NaOH is needed, probably due to the side reaction of formation of tricalcium aluminate hexahydrate (Bánvölgyi, 2015). The resulting red mud mainly contains $CaCO_3$ and Ca silicate and a negligible amount of soda and can be directly used for the production of cement (Li et al., 2016).

When the process is performed at a temperature of 1100-1400°C it is called a sintering process. The sintering process is carried out with the aim of reducing the chemically combined soda content of the red mud and requires the addition of lime (or limestone) and possibly of some amount of sodium carbonate. The SAS in the red mud is transformed to beta-dicalcium-silicate (C_2S), meanwhile water-soluble sodium aluminate and sodium ferrite are formed (Bánvölgyi, 2015). The sintering process was used in the past in China, USA and Kazakhstan (Bánvölgyi, 2015), however due to the high energy consumption of the process, and the consequent high cost, it is not used any more (Cooling, 2007).

Regarding the recycling options of the red muds, they can be used for the production of ceramics and bricks, in cement and concrete production or in pigment productions (JRC, 2018; Diane, 1997; Liu and Zhang, 2011). Due to the high content of iron, they can be used to produce iron sinter and pellets for ferrous metallurgy. Similarly, it is possible to extract aluminum oxide, chromium, vanadium, titanium oxide and rare earths metals (Paramguru et al., 2006).

Furthermore, red muds can be used to produce toned paper in the woodpulp and paper industry or to improve the soil structure and as a micro fertilizer and a neutralizer of pesticides in agriculture (Paramguru et al., 2006).

3.7.3.2. LITERATURE ASSESSMENT FOR RED MUD: MATERIALS AND METHODS

The literature review carried out to assess the amount of CO_2 that can be sequestered by red mud during its life cycle considered 20 peer-reviewed papers, 1 conference paper, 1 master thesis, 2 reports by the Alcoa Society and one by the European Aluminium Association and the Reference Document on Best Available Techniques for the Management of waste from extractive industries (Figure 3.7.3.1). The list of the documents analysed for this study is reported in Table 3.7.3.1. For the most interesting papers, a summary was prepared (see Annex II).

Among the examined peer-reviewed papers, only 11 out of 20 report quantitative data about red mud carbonation, of which one refers to the natural carbonation happening during red mud storage (Si et al., 2013),

while the others to accelerated laboratory tests. One reports indicates the data of a full-scale carbonation process carried out in the Kwinana Alcoa refinery in Australia.

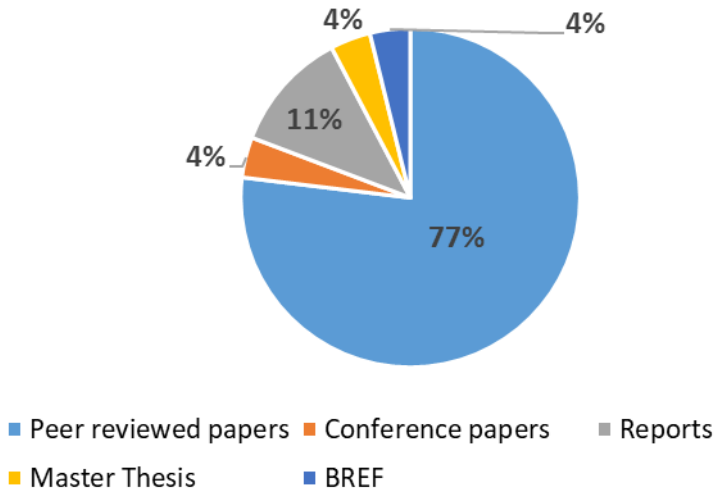


Figure 3.7.3.1. Sources used for the literature assessment on red mud.

Table 3.7.3.1. List of the documents considered in the study.

Peer reviewed papers

Bonenfant et al., 2008. *CO_2 sequestration by aqueous red mud carbonation at ambient pressure and temperature*. Ind. Eng. Chem. Res. 47(20), 7617-7622

Clark et al., 2015. *Comparison of several different neutralisations to a bauxite refinery residue: potential effectiveness environmental ameliorants*. Applied Geochemistry 56, 1-10

Diane, 1997. *Étude comparative des boues rouges de l'usine d'alumine de Friguia (Guinée) et des déchets de bauxite de la British Aluminium Company d'Awaso (Ghana)*. Bulletin des laboratoires des Ponts et Chaussées 211, 33-39

Dilmore et al., 2008. *Sequestration of CO_2 in mixtures of bauxite residue and saline wastewater*. Energy Fuels 22(1), 343-353

Han et al., 2017. *Bauxite residue neutralization with simultaneous mineral carbonation using atmospheric CO_2*. Journal of Hazardous Materials 326, 87-93

Johnston et al., 2010. *Alkaline conversion of bauxite refinery residues by neutralization*. Journal of Hazardous Materials 182(1-3), 710-715

Jones et al., 2006. *Carbon capture and the aluminium industry: preliminary studies*. Environ. Chem. 3(4), 297-303

Khaitan et al., 2009. *Mechanisms of neutralization of bauxite residue by carbon dioxide*. J. Environ. Eng. 135(6), 433-438

Kong et al., 2017. *Natural evolution of alkaline characteristics in bauxite residue*. Journal of cleaner production 143, 224-230

Li et al., 2016. *Calcification-carbonation method for red mud processing*. Journal of Hazardous Materials 316, 94-101

Liang et al., 2018. *Red mud carbonation using carbon dioxide: effects of carbonate and calcium ions in goethite surface properties and settling*. Journal of Colloid and Interface Science 517, 230-238

Liu et al., 2007. *Characterization of red mud derived from a combined Bayer process and bauxite calcination method*. Journal of Hazardous Materials 146(1-2), 255-261

Renforth et al., 2012. *Contaminant mobility and carbon sequestration downstream of the Ajka (Hungary) red mud spill: the effects of gypsum dosing*. Science of the Total Environment 421-422, 253-259

Rivera et al., 2017. *Neutralisation of bauxite residue by carbon dioxide prior to acidic leaching for metal recovery*. Minerals Engineering 112, 92-102

Sahu et al., 2010. *Neutralization of red mud using CO_2 sequestration cycle*. Journal of hazardous materials 179 (1-3), 28-34

Santini et al., 2011. *In situ neutralisation of uncarbonated bauxite residue mud by cross layer leaching with carbonated bauxite residue mud*. Journal of hazardous materials 194, 119-127

Shi et al., 2000. *Carbon dioxide sequestration via pH reduction of red mud using liquid CO_2.* ACS Div. Fuel Chem. 45, 703-705

Si et al., 2013. *Red mud as a carbon sink: variability, affecting factors and environmental significance*. Journal of Hazardous Materials 244-245, 54-59

Yadav et al., 2010. *Sequestration of carbon dioxide (CO_2) using red mud*. Journal of Hazardous Materials 176(1-3), 1044-1050

Yang and Xiao, 2008. *Development of unsintered construction materials from red mud wastes produced in the sintering alumina process*. Construction and Building Materials 22(12), 2299-2307

Conference papers

Bánvölgyi, 2015. *Opportunities within the alumina refineries to make bauxite residue easy to downstream use*. Bauxite residue valorisation and best practices conference, Leuven 5-7/10/2015

Reports

Alcoa World Alumina Australia, 2005. *Pinjarra Alumina refinery efficiency upgrade. Greenhouse Gas management plan 2005*

Alcoa, 2013. *Long-term residue management strategy. Kwinana 2013 Partial Report.*

EAA, 2014. *Bauxite residue management: best practice*

Master thesis

Grosso, 2012. *Tailing del processo Bayer: analisi dell'alcalinità e studio del processo industriale di filtropressatura al fine di ridurne l'impatto ambientale*. Alma mater studiorum-Università degli studi di Bologna.

BREF documents

JRC, 2018. *Reference Document in Best available Techniques for the Management of waste from extractive industries*

3.7.3.3. RED MUD COMPOSITION

Red mud chemical and mineralogical composition depends on the quality and nature of the bauxite ore and on the alumina extraction conditions (T, P, amount of soda and lime) (Li et al., 2016).

On average, the main constituents of red mud are Fe_2O_3 (18-60% on weight), Al_2O_3 (10-26%), SiO_2 (3-50%), Na_2O (2-12%), CaO (2-10%) and TiO_2 (trace-10%) (Collazo et al., 2006; JRC, 2018).

Focusing on CO_2 sequestration capacity of the red mud as a consequence of lime addition during the Bayer process, the element of interest is Ca.

Based on the data reported in the documents listed in Table 3.7.3.1, the total Ca content, expressed as CaO, ranges between 1.4% and 47% of the weight of the red mud, with an average value of 15.6%.

The highest values refer to Chinese red mud samples. In China, in fact, bauxite ore is usually characterized by a low grade of Al, then a substantial amount of lime must be added during the process. This method is called bauxite calcination. The average Ca content in Chinese red mud results equal to 28% of the weight of the residue, expressed in terms of CaO. A high concentration of lime, 43-47% in weight expressed as CaO, is also found in red mud treated for soda recovery, by applying the causticisation process.

When excluding Chinese red muds and red muds treated for soda recovery, the average Ca content results equal to about 6.7% in weight, expressed as CaO, as reported in Table 3.7.3.2.

Considering the mineralogy of the red mud (Table 3.7.3.2), Ca is mainly present in the form of calcite, calcium silicates and calcium alumino-silicates, TCA or in titanium compounds (perovskite $CaTiO_3$ and kassite $CaTi_2O_4(OH)_2$). Free lime was detected in only in samples of Chinese red mud and in modest amount (maximum 2.3% on weight).

Table 3.7.3.2. Chemical composition and mineralogy of red muds (minimum-average-maximum value). Elaboration of the data reported in the documents listed in Table 3.7.3.1.

Type of sample	Total Ca compounds, as CaO (%w)	Mineral composition (% w)				
		$CaCO_3$	TCA	Free lime	Ca silicates and Ca-Al-silicates	Perovskite and kassite
Red mud general	1.4-15.6-47 *30 cases*	1.3-17.4-46.8 *10 cases*	0-7.3-20 *6 cases*	0-0.3-2.3 *7 cases*	0-7.5-30 *4 cases*	0-9.3-19.6 *6 cases*
Chinese red mud	3.9-28.0-41.7 *9 cases*	32.8-42-46.8 *3 cases*	n.a.	0-0.8-2.3 *3 cases*	n.a.	10.2-14.6-19.6 *3 cases*
Red mud treated for soda recovery	43-45-47 *2 cases*	n.a.	n.a.	n.a.	n.a.	n.a.
Other red mud	1.4-6.7-14 *19 cases*	1.3-6.8-20 *7 cases*	0-7.3-20 *6 cases*	0 *4 cases*	0-7.5-30 4 cases	0-4-12 *3 cases*

3.7.3.4. POTENTIAL CARBONATION RATE IN RED MUD

The maximum theoretical CO_2 sequestration due to the use of lime in the Bayer process can be calculated considering the total Ca content in the red mud, excluding the eventual addition of other Ca sources to promote carbonation (for example, gypsum).

Assuming an average CaO content in the red mud of 15.6%, CO_2 uptake results equal to 123 gCO_2/kg red mud. This value increases up to 220 gCO_2/kg for the Chinese red mud, whose content of Ca resulted higher than the average. For a low Ca content, as found in the non-Chinese red mud and samples not treated for soda recovery, CO_2 uptake results modest, equal to about 53 gCO_2/kg red mud (Table 3.7.3.2).

These values represent the amount of CO_2 captured by the red mud if all the Ca compounds solubilize and react with the atmospheric CO_2. However, Ca solubility is very modest. Often less than 5% of the Ca dissolve in the liquor, as most of the Ca in the red mud is present in the form of silicates, alumina silicates and calcite (Rivera et al., 2017).

The main source of soluble Ca in the red mud is TCA (Santini et al., 2011), which can be detected in the red mud when lime is added in excess (Smith, 2015). The maximum theoretical CO_2 sequestration can thus be calculated on the basis of the TCA content, assuming that all the TCA dissolves to form $CaCO_3$, as proposed by Khaitan et al. (2009). Considering an average content of TCA equal to 7.3% by weight (Table 3.7.3.2), the amount of CO_2 potentially sequestered results equal to 12 gCO_2/kg red mud.

However, dissolution of Ca-bearing minerals typically presents in the red mud, including TCA, can be very slow (Han et al., 2017). The slow dissolution kinetic of these compounds can strongly limit the actual sequestration potential of the red mud during its storage, since only the surface material in the storage impoundment is exposed to the atmospheric CO_2 and usually the time elapsed between two subsequent storage operations is not sufficient to guarantee the complete dissolution of TCA (Khaitan et al., 2009).

A more reliable estimate of the amount of CO_2 potentially captured by the red mud can be, thus, based on the Acid Neutralizing Capacity (ANC) measured at pH 8.3 (pH of a $CaCO_3$ saturated solution in equilibrium with the atmospheric air), as reported by Bonenfant et al. (2008). They found a CO_2 sequestration capacity based on ANC equal to only 7 gCO_2/kg red mud, against a value of 56 gCO_2/kg based on the total Ca content. The difference between the two values was explained by the substantial insolubility of most of the Ca compounds at ambient temperature and pressure, that cannot thus react with CO_2 to produce $CaCO_3$.

Attention must be paid to the fact that the ANC of a red mud cannot be attributed completely to Ca compounds, unless otherwise specified (like in Bonenfant et al., 2008). Red mud neutralization behaviour is, in fact, associated not only with the dissolution of sodalite, TCA, $CaCO_3$ and other Ca compounds, but also with soluble free Na_2CO_3 and NaOH and with hydroxylis on the surface of iron oxides (Kong et al., 2017):

$Na_2CO_3 + 2H^+ \rightarrow 2Na^+ + H_2O + CO_2$ (pH > 8)

$NaOH + H^+ \rightarrow Na^+ + H_2O$ (pH > 8)

$FeO, Fe_2O_3\text{-}OH + H^+ \rightarrow FeO, Fe_2O_3 + H_2O$ (pH < 6)

$Na_6Al_6Si_6O_{24}*2NaOH + 8H^+ + 10H_2O \rightarrow 8Na^+ + 6H_2SiO_3 + 6Al(OH)_3$ (pH 6-8)

$Ca_3Al_2(OH)_{12} + 6H^+ \rightarrow 3Ca^{2+} + 2Al(OH)_3 + 6H_2O$ (pH 6-8)

$CaCO_3 + 2H^+ \rightarrow Ca^{2+} + H_2O + CO_2$ (pH 6-8)

Rapid-reacting ANC is, usually, related mainly to soluble NaOH and Na_2CO_3 (Liu et al., 2007; Si et al., 2013), whereas Ca compounds act as an alkali store and can provide alkaline compounds for more than 20 years (Kong et al., 2017).

Kong et al. (2017) reported the ANC of fresh and aged red mud calculated at a final pH equal to 7. The corresponding potential CO_2 sequestration results equal to 17.2 gCO_2/kg for the fresh red mud and 5.5 gCO_2/kg for the 20 years old red mud. The authors explained the higher ANC of fresh red mud compared to the old one with the partial removal of NaOH and Na_2CO_3 by leaching during rainfall and with the partial consumption of sodalite and TCA. Liu et al. (2007) reported the ANC of a Chinese red mud sample from a combined Bayer process and bauxite calcination method, compared to that of a Chinese red mud from a standard Bayer process. The higher addition of Ca in the combined process results in a higher ANC value. The theoretical CO_2 uptake (in any case not ascribable only to the Ca compounds) is thus equal to 220 gCO_2/kg for the red mud from the combined process and 110 gCO_2/kg for the standard red mud.

The same consideration can be done for the theoretical CO_2 uptake based on alkalinity reported by some authors[30]. For example, Si et al. (2013) reported the maximum carbon sequestration capacity of three red mud samples. They obtained a CO_2 uptake of about 200-220 gCO_2/kg from two of these samples and 56 gCO_2/kg for the other one, which was treated with seawater prior to disposal, reducing its content of soluble alkalis. However, most of this alkalinity was related to Na compounds, as soluble Ca concentrations in the three red mud samples was quite low. This explains the different CO_2 potential sequestration measured by Bonenfant et al. (2008) compared to that measured by the other authors. The value reported in Bonenfant et al. (2008) refers to the CO_2 sequestered only due to the presence of Ca alkalinity, whereas the values reported by the other authors refer to the total ANC/alkalinity, mostly related to the presence of NaOH.

3.7.3.5. NATURAL CARBONATION OF RED MUD

Data about the CO_2 actually sequestered by red muds during their storage are reported only by Si et al. (2013). The authors analysed three red mud samples: two from two Alumina refineries in China, where a combined sintering and Bayer process is used, and one from an Australian refinery, where the red mud is treated with seawater before disposal. The age of the samples is unknown, however red muds were collected from the surface of the disposal area of the three facilities, that means they are quite fresh samples. Based on the chemical analysis of the samples (carbon content), the authors calculated an amount of CO_2 sequestered by the red mud of about 85-151 gCO_2/kg red mud for the Chinese samples and 38 gCO_2/kg red mud for the Australian one. The mineralogical analysis showed that the carbonate minerals consisted of calcite, vaterite and monohydrocalcite, suggesting that the carbonates were primarily bound to Ca. The lower CO_2 uptake of the Australian red mud can be explained by its lower content of Ca compared to Chinese red mud (8.6% w/w of CaO for the Australian red mud; more than 25% w/w for the Chinese red mud). The ratio between the amount of sequestered CO_2 and the content of total Ca in the three samples of red mud is, in any case, comparable, indicating that more or less the same fraction of Ca compounds reacts with the atmospheric CO_2, probably the soluble fraction. Since most of the Ca is bound in silicate or titanium compounds or found as calcite, the concentration of soluble Ca is quite modest, limiting the further formation of any Ca carbonates. The actual amount of sequestered CO_2 was equal to about 40-68% of the potential CO_2 sequestration calculated on the basis of the total alkalinity (which includes other sources of alkalinity, in addition to Ca compounds). In order to enhance CO_2 sequestration by using all the water extractable alkalinity of the red mud (deriving mainly from NaOH), the authors suggested providing an external source of soluble Ca and Mg-bearing substances, such as gypsum and concentrate brines. This allows precipitating the soluble alkalinity, currently not completely used, as stable Ca or Mg carbonates.

[30] Both alkalinity and ANC measure the overall buffering capacity against acidification of a solution. The alkalinity is measured on a filtered solution, whereas the ANC is measured on a solution which contains particulate matters (not filtered solution).

The chemical and mineralogical analysis of aged red mud samples is reported by other authors, however without any information about the amount of sequestered CO_2.

Kaithan et al. (2009) analysed several samples collected at different depth from some impoundment cells of two facilities in Texas (USA). The magnitude of the pH lowering and of the TCA depletion depends on the age of the stored red mud. 30-35 years old red mud was neutralized to a pH of 9.5 up to a depth of about 90 cm, while 5 years old red mud had a pH of 10.4 at the surface and a pH of 12.1 at a depth of about 90 cm. This suggests that carbonation at ambient conditions of temperature and CO_2 pressure is a slow process, progressing at the time scale of decades.

Liu et al. (2007) analysed red mud samples collected from a red mud storage facility in China, where fresh, 5 years and 10 years old red muds are present. The pH of the red mud decreases with increasing storage time, from 11.58 for fresh red mud to 9.61 for 10 years old red mud. The acid neutralization capacity calculated over a period of about 2 years resulted equal to about 10 molH^+/kg for fresh red mud and slightly lower for the old red mud, probably due to partial removal of NaOH by leaching during rainfall events. In both fresh and aged samples, the rapid-reacting ANC accounted for less than 20% of the total ANC and was mostly related to soluble Na, since most of the Ca in the red mud is present in low-soluble compounds. Considering the mineralogy of the residue, some mineral phase (probably mainly calcite) undergoes crystallization with time after its disposal in the storage facility. Old red mud was thus more stable and less reactive than fresh red mud.

Similar results were found by Kong et al. (2017), who analysed several samples of red mud collected from a Chinese refinery. Samples included fresh as well as aged red mud (5-20 years old). The alkalinity decreased with increasing age of the red mud. The same behaviour was observed for the ANC, due to the partial removal of NaOH and Na_2CO_3 by leaching during rainfall and alkali compound transformation.

Yang and Xiao (2008) analysed red mud samples from the landfill site of a Chinese Aluminium plant. They found that TCA and dicalcium silicates in fresh red mud samples were transformed into calcite in 10 years old red mud, due to carbonation.

Han et al. (2017) simulated natural ageing of red mud by spreading 100 kg of residue in a 4 m^2 area and leaving it in contact with atmospheric CO_2 for almost 1 year. The pH stabilized after about 4 months to around 10, meaning that only pore water alkalinity was exhausted by the reaction with the atmospheric CO_2. In order to further reduce the pH value, the authors mixed the red mud with an external source of Ca ($CaCl_2$ or flue gas desulphurisation gypsum in a concentration of 1 mol/kg red mud). Thanks to the external source of Ca, alkalinity precipitated as $CaCO_3$, lowering the pH below 9.

Based on the experiences previously reported, it is possible to conclude that the carbonation potential is limited by the concentration of soluble Ca ions. When lime is added in excess during the Bayer process, as generally done in Chinese refineries, Ca content in the residue is sufficient to promote natural red mud carbonation during its storage. However, in general, Ca content in the red mud is modest, since alkalinity is mainly the consequence of the use of soda in the Bayer process, rather than of lime addition. In this case, CO_2 is absorbed by the pore water, consuming the alkalinity associated with Na compounds, but only a small fraction precipitates in the stable form of calcite. In addition, since Ca solubility can be very modest as most of the Ca

is present in the form of silicates or calcite, the carbonation process proceeds very slowly. Most of the time, carbonation reactions are not completed before a layer of fresh red mud is deposited above aged red mud in the storage pond, resulting in uncompleted carbonation of the red mud deposit.

3.7.3.6. ACCELERATED CARBONATION POTENTIAL IN RED MUD

Accelerated carbonation has been proposed by several authors to improve the quality of the red mud by reducing its pH and alkalinity, with the advantage of a contextual CO_2 capturing and storage. The interesting aspect of this practice is the possibility to operate with industrial flue gas, capturing the CO_2 in the flue gas prior to its emission in the atmosphere. In addition, the optimization of the process parameters (temperature, CO_2 partial pressure, L/S ratio) allows acceleration of the carbonation reactions.

Currently, only one experience of red mud carbonation in a full-scale plant is reported in the literature. The Alcoa Technology Delivery Group implemented a full-scale red mud carbonation in the Kwiniana refinery in west Australia in the year 2007. The plant uses liquid CO_2 produced by the nearby CSBP ammonia plant and was designed to treat all the residues produced by the refinery, sequestering about 70.000 tCO_2/year, or 35 gCO_2/kg red mud. The material resulting from the carbonation of red mud is commercialized with the name of Alkaloam® to be used in agriculture to improve phosphorous absorption. Also, the coarse residues (bauxite sand) produced by the refinery are carbonated, producing a material called red sand® commercialized as a general filling construction material, for example for road base construction (EAA, 2014; Alcoa World Alumina Australia, 2005). However, due to the high cost of the treatment, Alcoa has decided to give up the process. Accelerated carbonation of red mud will not be performed any more in the next years. Alcoa has decided to apply a new filtration method that will reduce the volume of the entrained liquor in the red mud, thereby promoting in-situ remediation via leaching and natural carbonation (Alcoa, 2013). The accelerated carbonation process and the new filtration system are, in fact, incompatible since, as demonstrated by Liang et al. (2018), CO_3^{2-} adsorption on the red mud particles can have adverse effects on the particles aggregation or flocculation and can decrease the settling velocity and deteriorate the clarity of supernatant.

Another experience of red mud carbonation at full-scale is reported by Renforth et al. (2012) regarding the emergency management of the Aika red mud spill in Hungary of the 4th October 2010. Carbonation of red mud was artificially promoted by dosing gypsum, as a source of Ca ions. The aim of the treatment was to promote calcium precipitation with consumption of alkalinity and reduction of the pH value, and thus to affect the mobility of contaminants downstream the spill. Based on the analysis of several samples collected from a series of stations across the 3,072 km^2 Marcal river system, it was demonstrated that gypsum addition actually resulted in the carbonation of the red mud by reaction with the atmospheric CO_2. On average, the addition of 860 g of gypsum per kg of red mud resulted in a CO_2 sequestration of 220 g.

Excluding these two experiences of full-scale carbonation, all the other data reported in the scientific literature refer to laboratory tests aimed at understanding the chemistry and the kinetic of red mud carbonation.

The tests considered in this study were summarised in Table 3.7.3.3. With the exception of the test carried out by Rivera et al. (2017) and Shi et al. (2000), all the tests were performed at ambient condition of temperature and at modest pressure, often with a 100% CO_2 gas or, in any case, with enriched CO_2 gases. Most of the tests were carried out in slurry phase (L/S of 5 or 10). Only the three tests reported by Yadav et al. (2010) were performed in aqueous phase, with an L/S ration of 0.3-0.5. The samples were put in contact with a CO_2 stream for at least 2 hours, up to 24 hours.

With the exclusion of the test reported in Jones et al. (2006), which can be considered an outlier[31], the resulting CO_2 uptake ranges from 5 mg/kg red mud to about 71 gCO_2/kg red mud, with an average value of 31 gCO_2/kg red mud. The lowest value refers to the test carried out by Johnston et al. (2010), whereas the highest value refers to the test carried out by Bonenfant et al. (2008) on the leachates and leached hydrated matrixes isolated by the red mud suspension after three subsequent leaching operations.

Most of the authors observed that the final CO_2 sequestration was modest because the majority of the injected CO_2 simply dissolves in the aqueous phase as H_2CO_3, reacting with the pore water alkalinity forming soluble carbonate or bicarbonate (mainly Na_2CO_3 and $NaHCO_3$), instead of precipitating as $CaCO_3$ (Jones et al., 2006; Han et al., 2017). The consequence was that, once the CO_2 injection ceased, the dissolved carbonate species gradually degassed and CO_2 moved towards the atmosphere. This is particularly true when Ca content in the red mud is modest and most of the alkalinity consists in Na species. CO_2 uptake can be improved by working with more than one carbonation cycle, by carbonating the filtrate, as suggested by Sahu et al. (2010) and Bonenfant et al (2008). However, especially when Ca content in the red mud is modest, CO_2 sequestration is mostly related to the content of NaOH in the liquor (Sahu et al., 2010; Rivera et al., 2017).

Based on the data reported in Table 3.7.3.3, CO_2 uptake seems to be influenced more by the red mud composition (Ca speciation) rather than by the operating conditions at which the test is carried out. For example, the high temperature and/or pressure used by Rivera et al. (2017) and Shi et al. (2010) did not result in higher CO_2 uptake compared to the average. The experiments carried out by Yadav et al. (2010) clearly demonstrated that the amount of CO_2 sequestered by the red mud is related to the red mud composition. The highest CO_2 uptake was obtained for the fraction richest in chantalite and cancrinite.

The statistical analysis of the data (Table 3.7.3.4) did not show any significant correlation among the CO_2 uptake and the other parameters, except for the test duration. Since Ca is mainly present in the form of silicates or alumina silicates, its dissolution in the aqueous phase is not immediate and can require long reaction time.

In order to improve CO_2 sequestration in a stable mineral phase, the addition of an external source of Ca or Mg has been proposed by several authors (Table 3.7.3.3). Johnston et al. (2010) and Clark et al. (2015)

[31] The CO_2 uptake reported in Jones et al. (2006) was excluded from the average because it does not consider the amount of CO_2 that degasses after the end of the experiment when the CO_2 injection ceases. The amount of CO_2 absorbed during the test (748 gCO_2/kg red mud), thus, highly overestimates the actual amount of CO_2 that can be sequestered by the red mud in a stable form (i.e. the total amount of CO_2 absorbed during the tests minus the amount of CO_2 that degasses after the end of the CO_2 injection). Most of the CO_2 was, in fact, absorbed in the slurry solution as H_2CO_3 or as bicarbonates (Jones et al., 2006).

combined CO_2 gas neutralization with the addition of bivalent cations such as $CaCl_2$ and $MgCl_2$. Without an external source of Ca, the amount of CO_2 permanently sequestered by the red mud was negligible (5 mg/kg red mud). With the addition of 26.3 gCa/kg red mud and 111.5 gMg/kg red mud, CO_2 uptake increased up to 17 gCO_2/kg red mud. The authors suggested that the addition of Ca and Mg precipitates the majority of soluble alkalinity, whereas the addition of the CO_2 only precipitates alumina-alkalinity. However, this sequestration capacity cannot be attributed to the lime used during the Bayer process.

Similar results were obtained by Han et al. (2017). The authors carried out some long-term neutralization batch experiments in which red mud was carbonated in a stirred reactor under atmospheric pressure for 55 days in a slurry phase. The pH decreased up to 9.3 during the tests, but without significant change in the carbon content, meaning that the pH drop was closely associated with the removal of the pore water alkalinity. Only when an external source of Ca was added, the pH decreased below 8 and the content of carbon in the samples increased, meaning that active carbonation reactions occurred. With $CaCl_2$ addition, a CO_2 uptake of 83 gCO_2/kg red mud was achieved.

Finally, Dilmore et al. (2008) carried out some carbonation tests on a mixture of red mud and oil and gas brine produced water. Red mud was used as a caustic source and brine as a source of Ca ions. With a mixture composition of 80% red mud and 20% brine, about 5 gCO_2 were sequestered by 1 kg of the mixture.

The previous experiences showed that when no Ca is added, calcite precipitation is regulated by the dissolution of the Ca-bearing minerals that are present in the red mud, that can be modest and very slow. When a Ca source is added, carbonation reactions are promoted and the carbonation rate becomes faster.

Table 3.7.3.3. Summary of the data available from the literature on accelerated carbonation that have been used in the study.

Reference	**CO_2 uptake** (gCO_2/kg RM)	**Operating conditions**	**Comments**
Without addition of external Ca sources			
Sahu et al., 2010	5.7	Particle size=0.1-160 μm; ambient T & P; 100% CO_2; L/S= 10; 5 hours	Absorption method based on more than one sequestration cycle. CO_2 was mainly sequestered in the form of Na_2CO_3, $NaHCO_3$ and H_2CO_3
	70.2	Particle size=0.1-160 μm; ambient T & P; 100% CO_2; L/S= 10; 3 carbonation cycles of 5 hours each	
Johnston et al., 2010 Clark et al., 2015	0.005	Particle size=unknown; T=unknown; P=0.7 MPa; 100% CO_2; L/S= 5; 25 min	CO_2 mainly sequestered as bicarbonates. Ca in the red mud mainly comes from the lime regeneration of hydroxides. Its dissolution in the liquor is modest
Rivera et al., 2017	10	Particle size=unknown; T=150°C; P=3MPa; 100% CO_2; L/S= 5; 2 hours	Most of the CO_2 sequestration is related to the dissolution of Na. Ca dissolution from the solid is modest
Yadav et al., 2010	53	Particle size= 30 μm; ambient T; P=0.35 MPa; 100% CO_2; L/S= 0.3; 3.5 hours	The tested red mud does not contain free NaOH. Carbonation is, thus, related to the presence of cancrinite, chantalite and sodium aluminosilicate mineral phases. CO_2 precipitates as $CaCO_3$
	35	Particle size= 50 μm; ambient T; P=0.35 MPa; 100% CO_2; L/S= 0.35; 3.5 hours	
	7	Particle size= 5 μm; ambient T; P=0.35 MPa; 100% CO_2; L/S= 0.5; 3.5 hours	
Bonenfant et al., 2008	41.5	Particle size=38-106 μm; ambient T & P; 15% CO_2; L/S= 10; 24 hours	Carbonation of leachates and leached-hydrated matrixes (after three successive leachings). About half of the total carbonation capacity of the fresh mud is consumed during the carbonation of the first leachate and is related to the NaOH content. The leached-hydrate matrixes conserve the other half of the carbonation potential of the fresh red mud, which is related both to NaOH and Ca compounds
	70.9	Particle size=38-106 μm; ambient T & P; 15% CO_2; L/S=10; carbonation tests of 3 leachates + 3 leached hydrated matrixes	
Shi et al., 2000	23	Particle size=unknown; ambient T; 10 MPa; liquid CO_2; L/S= 2-10; 4 hours	The authors don't give any indications of the chemical form in which the CO_2 is sequestered
Jones et al., 2006	748	Particle size=unknown; ambient T; 0.7 Mpa; 100% CO_2; L/S=15; 20 min	The paper does not take into account CO_2 rebound. All the CO_2 absorbed during the tests in the form of bicarbonates or H_2CO_3 was considered as sequestered. Alkalinity is not precipitated as carbonates in any great amount
With addition of external Ca sources			
Johnston et al., 2010 Clark et al., 2015	17	Particle size= unknown; T= unknown; P=0.7 MPa; 100% CO_2; L/S= 5; 25 min; addition of 26.3 g Ca/kg red mud and 111.5 g Mg/kg red mud	The presence of Ca and Mg from the brine promotes alkalinity precipitation as carbonates.

Table 3.7.3.3 (continued). Summary of the data available from the literature on accelerated carbonation that have been used in the study.

Reference	CO_2 uptake (gCO_2/kg RM)	Operating conditions	Comments
Dilmore et al., 2008	4.8*	Test on a liquid mixture of 80% red mud and 20% oil brine; ambient T; 0.689 MPa; 100% CO_2	The CO_2 is sequestered mainly as calcite, as a consequence of the carbonation of the Ca ions from the brine, and as Na-Al-CO_2 bearing minerals, as a consequence of the carbonation of the Na and Al ions from the red mud
Han et al., 2017	83	Particle size=unknown; ambient T & P; ambient air; L/S=31.5; 55 days; addition of 125 gCa/kg red mud as $CaCl_2$	The presence of Ca from $CaCl_2$ promotes alkalinity precipitation as carbonates. This was not observed without the addition of an external source of Ca. In that case, the CO_2 was absorbed in the pore water solution but did not precipitate

*per kg of mixture

Table 3.7.3.4. Correlation analysis of the data reported in Table 3.7.3.3.

		particle_size	duration	L/S	T °C	P	CO2 conc	CO2 uptake	CaO tot
particle_size	Correlazione di Pearson	1	,488	,929**	.b	-,931**	-,153	,215	1,000**
	Sign. (a due code)		,326	,007	,000	,007	,773	,683	.
	N	6	6	6	6	6	6	6	2
duration	Correlazione di Pearson	,488	1	,601	-,308	-,284	-,903**	,707*	,416
	Sign. (a due code)	,326		,066	,420	,427	,000	,022	,584
	N	6	10	10	9	10	10	10	4
L/S	Correlazione di Pearson	,929**	,601	1	-,095	,244	-,462	,245	,786
	Sign. (a due code)	,007	,066		,808	,496	,179	,496	,214
	N	6	10	10	9	10	10	10	4
T °C	Correlazione di Pearson	.b	-,308	-,095	1	,175	,192	-,370	,458
	Sign. (a due code)	,000	,420	,808		,653	,620	,328	,542
	N	6	9	9	9	9	9	9	4
P	Correlazione di Pearson	-,931**	-,284	,244	,175	1	,240	-,224	,383
	Sign. (a due code)	,007	,427	,496	,653		,504	,534	,617
	N	6	10	10	9	10	10	10	4
CO2 conc	Correlazione di Pearson	-,153	-,903**	-,462	,192	,240	1	-,485	-,461
	Sign. (a due code)	,773	,000	,179	,620	,504		,155	,539
	N	6	10	10	9	10	10	10	4
CO2 uptake	Correlazione di Pearson	,215	,707*	,245	-,370	-,224	-,485	1	-,351
	Sign. (a due code)	,683	,022	,496	,328	,534	,155		,649
	N	6	10	10	9	10	10	10	4
CaO tot	Correlazione di Pearson	1,000**	,416	,786	,458	,383	-,461	-,351	1
	Sign. (a due code)	.	,584	,214	,542	,617	,539	,649	
	N	2	4	4	4	4	4	4	4

3.7.3.7. DISCUSSION AND CONCLUSIONS

Red mud as a possible sink for CO_2 sequestration

Red mud management consists in its thickening to a high-density slurry (48-55% solids or higher) and then in its deposition in open pits in order to promote consolidation and drying.

Once in contact with the atmosphere, red mud alkalinity reacts with CO_2, resulting in a slow decrease of the pH value. Initially, CO_2 is rapidly absorbed in the liquor, where it forms carbonic acid and neutralizes the excess base in the form of NaOH, $NaCO_3^-$ and $Al(OH)_4^-$. Then, the carbonate ions react with soluble Ca ions to form stable carbonate minerals. However, soluble Ca ions are usually present in the red mud in modest amount, mainly as a consequence of the dissolution of TCA which, at ambient conditions, can require decades. Working at high CO_2 partial pressure, as happens in the accelerated carbonation process, does not seem to significantly improve red mud carbonation degree. CO_2 uptake during natural ageing reported by Si et al. (2013) is, in fact, comparable to the values achieved by other authors during accelerated carbonation tests in controlled environment.

Based on the data published in the literature, the amount of CO_2 that can be permanently sequestered by the red mud seems to be linked more to its Ca content and to the reaction time than to the temperature and the CO_2 partial pressure at which the carbonation process is carried out. The limiting factor of the carbonation process during red mud storage, with respect to that carried out in a stirring reactor, is the actual contact between the residue and the CO_2. Only the surface material in the storage impoundment is, in fact, exposed to the atmospheric CO_2 and usually the time elapsed between two subsequent storage operations is not sufficient to guarantee the complete carbonation of the red mud. It is, therefore, essential to store the red mud in such a way to guarantee a good contact with the atmosphere for a sufficient time.

For a red mud containing about 7-9% of Ca compound as CaO, the average CO_2 uptake results equals to about 32.5 gCO_2/kg, regardless of the process (natural ageing, full scale accelerated carbonation as carried out in the Kwiniana refinery in west Australia, and accelerated carbonation at a laboratory scale). When the content of Ca in the red mud is higher, as in the Chinese samples that contain about 26% of Ca as CaO or in red mud treated for soda recovery, CO_2 uptake of about 120 gCO_2/kg red mud can be observed. However, CO_2 sequestration cannot be attribute completely to the Ca in the red mud. Most of the CO_2 is sequestered as a consequence of the reactions with the pore alkalinity, in the form of NaOH, $NaCO_3^-$ and $Al(OH)_4^-$.

Then, by assuming:

- a production of 0.7-2 tonnes of red mud per tonne of alumina;
- an average CO_2 uptake of 32.5 gCO_2/kg for a red mud containing about 7% of CaO, corresponding to a lime addition during the Bayer process of about 49-140 kg per tonne of alumina;
- a release in the atmosphere of 786 kg of CO_2 per tonne of produced lime (only from the calcination process, excluding the fuel consumption);

it results that potentially 59% of the CO_2 emitted from the lime industry can be later captured by the red mud during its storage. Similar values are obtained for red mud containing more Ca. However, as previously illustrated, the CO_2 sequestration potential of the red mud is mainly due to its content of NaOH, especially

when the content of Ca is modest. Thus, it is not possible to attribute the CO_2 sequestration to the lime added during the Bayer process.

By assuming as CO_2 uptake the value calculated by Bonenfant et al. (2008) on the basis of the ANC, equal to 7 gCO_2 per kg of red mud, for a red mud containing 7.77% of CaO, it results that only 11.5% of CO_2 emitted by the lime industry can be potentially captured by the Ca in the red mud. It is then clear that the potential CO_2 sequestration by the sole Ca compounds in the red mud is much more limited than the value resulting by considering its total alkalinity.

Recommendation on research needs on red mud

As previously illustrated, data regarding natural carbonation of red mud are insufficient. In addition, it is difficult to estimate how much of the sequestered CO_2 can be attributed to the Ca compounds in the red mud and how much to the Na compounds.

Another aspect to investigate is the actual contact time of the external surface of red mud with the atmosphere during storage, which can be insufficient to guarantee the complete reaction of CO_2 with the red mud alkalinity, especially that from the Ca compounds. Dissolution of Ca-bearing minerals typically present in the red mud, including TCA, can be, in fact, very slow (Han et al., 2017).

It is, therefore, suggested carrying out some analyses of red mud of different age in order to assess the amount of CO_2 that can be actually sequestered by this material and to better understand the time evolution of the carbonation process in outdoor ambient conditions. Collecting a large database may, also, allow a statistical analysis of the data aimed at defining possible correlation between the CO_2 uptake and the content of CaO in the red mud.

REFERENCES

Alcoa, 2005. *Alcoa World Alumina Australia. Pinjarra Alumina refinery efficiency upgrade. Greenhouse Gas management plan 2005*. https://www.alcoa.com/australia/en/pdf/Greenhouse_Management_Plan_Final_Feb_07.pdf (latest access 28-2-2019)

Alcoa, 2013. *Long-term residue management strategy. Kwinana 2013 Partial Report*. https://www.alcoa.com/australia/en/pdf/kwinana_refinery_ltrms_report_2013PR.pdf (latest access 28-2-2019)

Bánvölgyi, G., 2015. *Opportunities within the alumina refineries to make bauxite residue easy to downstream use*. Bauxite residue valorisation and best practices conference, Leuven 5-7/10/2015. Available online: http://conference2015.redmud.org/wp-content/uploads/2015/10/Gy%C3%B6rgy-George-B%C3%81NV%C3%96LGYI-secure.pdf

Bonenfant, D., Kharoune, L., Sauvé, S., Hausler, R., Niquette, P., Mimeault, M., Kharoune, M., 2008. *CO_2 sequestration by aqueous red mud carbonation at ambient pressure and temperature*. Ind. Eng. Chem. Res. 47(20), 7617-7622. DOI: 10.1021/ie7017228

Bott, R., Langeloh, T., Hahn, J., 2005. *Re-usage of dry bauxite residue*. Proceedings of the 7th International Alumina Quality Workshop. AQW Ltd, Perth, Australia, 236-241 (via Clark et al., 2015)

Brunori, C., Cremisini, C., Massanisso, P., Pinto, V., Torricelli, L., 2005. *Reuse of a treated red bauxite waste: studies on environmental compatibility*. J. Hazard. Mater. 117(1), 55-63. DOI: 10.1016/j.jhazmat.2004.09.010

Clark, M.W., Johnston, M., Reichelt-Brushett, A., 2015. *Comparison of several different neutralisations to a bauxite refinery residue: potential effectiveness environmental ameliorants*. Applied Geochemistry 56, 1-21. DOI: 10.1016/j.apgeochem.2015.01.015

Collazo, A., Cristóbal, M.J., Nóvoa, X.R., Pena, G., Pérez, M.C., 2006. *Electrochemical impedance spectroscopy as a tool for studying steel corrosion inhibition in simulated concrete environments-red mud used as rebar corrosion inhibitor*. Journal of ASTM International 3(2), 1-10. DOI: https://doi.org/10.1520/JAI11785

Cooling, D.J., Jamieson, E., 2004. *Bauxite Residues - A High Volume Resource*. Paper of the Conference Green Processing, At Perth, Australia, Volume: 225-228

Cooling, D.J., 2007. Improving the sustainability of residue management practices. Alcoa World Alumina Australia. PASTE 2007, Proceedings of the 10th International Seminar on Paste and Thickened Tailings, Perth, Australia

Diane, M.S., 1997. *Étude comparative des boues rouges de l'usine d'alumine de Friguia (Guinée) et des déchets de bauxite de la British Aluminium Company d'Awaso (Ghana)*. Bulletin des laboratoires des Ponts et Chaussées 211, 33-39. Available online: https://www.ifsttar.fr/collections/BLPCpdfs/blpc__211_33-39.pdf

Dilmore, R., Lu, P., Allen, D., Soong, Y., Hedges, S., Fu, J.K., Dobbs, C.L., Degalbo, A., Zhu, C., 2008. *Sequestration of CO_2 in mixtures of bauxite residue and saline wastewater*. Energy Fuels 22(1),343-353. DOI: https://doi.org/10.1021/ef7003943

European Aluminium Association - EAA, 2014. *Bauxite residue management: best practice*. http://www.world-aluminium.org/media/filer_public/2014/09/03/bauxite_residue_management_-_best_practice.pdf (latest access 28-2-2019)

Enick, R.M., Beckman, E.J., Shi, C., Xu, J., Chordia, L., 2001. *Remediation of metal-bearing aqueous waste streams via direct carbonation*. Energy Fuels 15(2), 256-262. DOI: https://doi.org/10.1021/ef000245x

Grosso, A., 2012. *Tailing del processo Bayer: analisi dell'alcalinità e studio del processo industriale di filtropressatura al fine di ridurne l'impatto ambientale*. Alma mater studiorum-Università degli studi di Bologna, Corso di Studio in Chimica Industriale.

Han, Y.S., Ji, S., Lee, P.K., Oh, C., 2017. *Bauxite residue neutralization with simultaneous mineral carbonation using atmospheric CO_2*. Journal of Hazardous Materials 326, 87-93. DOI: 10.1016/j.jhazmat.2016.12.020

Hanahan, C., McConchie, D., Pohl, J., Creelman, R., Clark, M., Stocksiek, C., 2004. *Chemistry of seawater neutralization of bauxite refinery residues (red mud)*. Environ. Eng. Sci. 21(2), 125-138. DOI: https://doi.org/10.1089/109287504773087309

Johnston, M., Clark, M.W., McMahon, P., Ward, N., 2010. *Alkalinity conversion of bauxite refinery residues by neutralization*. Journal of Hazardous Materials 182(1-3), 710-715. DOI: 10.1016/j.jhazmat.2010.06.091

Jones, G., Joshi, G., Clark, M.W., McConchie, D.M., 2006. *Carbon capture and the aluminium industry: preliminary studies*. Environ. Chem. 3(4), 297-303. DOI: 10.1071/EN06018

JRC, 2018. *Reference Document in Best available Techniques for the Management of waste from extractive industries*

Khaitan, S., Dzombak, D.A., Lowry, G.V., 2009. *Mechanisms of neutralization of bauxite residue by carbon dioxide*. J. Environ. Eng. 135(6), 433-438. DOI: 10.1061/(ASCE)EE.1943-7870.0000010

Kong, X., Guo, Y., Xue, S., Hartley, W., Wu, C., Ye, Y., Cheng, Q., 2017. *Natural evolution of alkaline characteristics in bauxite residue*. Journal of cleaner production 143, 224-230. DOI: DOI: 10.1016/j.jclepro.2016.12.125

Li, R., Zhang, T., Liu, Y., Lv, G., Xie, L., 2016. *Calcification-carbonation method for red mud processing*. Journal of Hazardous Materials 316, 94-101. DOI: https://doi.org/10.1016/j.jhazmat.2016.04.072

Liang, G., Chen, W., Nguyen, A.V., Nguyen, T.A.H., 2018. *Red mud carbonation using carbon dioxide: effects of carbonate and calcium ions on goethite surface properties and settling*. Journal of Colloid and Interface Science 517, 230-238. DOI: 10.1016/j.jcis.2018.02.006

Liu, Y., Lin, C., Wu, Y., 2007. *Characterization of red mud derived from a combined Bayer process and bauxite calcination method*. Journal of Hazardous Materials 146 (1-2), 255-261. DOI: 10.1016/j.jhazmat.2006.12.015

Liu, X., and Zhang, N., 2011. *Utilization of red mud in cement production: a review*. Waste Management and Research 29(10), 1053-1063. DOI: 10.1177/0734242X11407653

McConchie, D.M., Clalrk, M.W., Davies-Mc Conchie, F.G., Zilstra, H., Faux, D., Ferguson, L., 2005. *Recent advances in the treatment and reuse of bauxite refinery residues (BauxsolTM)*. 7th International Alumina Quality Workshop. AQW Ldt, Perth, Australia, 66-68 (via Clark et al., 2015)

Menzies, N.W., Fulton, I,M., Morrel, W.J., 2004. *Seawater neutralization of alkaline bauxite residue and implications for revegetation*. J. Environ. Qual. 33(5), 1877-1884. DOI: 10.2134/jeq2004.1877

Paramguro, R.K., Rath, P.C., Misra, V.N., 2006. *Trends ion red mud utilization. A review*. Mineral Processing and Extractive Metallurgy Review 26(1), 1-29. DOI: https://doi.org/10.1080/08827500490477603

Power, G., Gräfe, M., Klauber, C., 2011. *Bauxite residue issues: I. Current management, disposal and storage practices*. Hydrometallurgy 108(1-2), 33–45. DOI: https://doi.org/10.1016/j.hydromet.2011.02.006

Renforth, P., Mayes, W.M., Jarvis, A.P., Burke, I.T., Manning, D.A.C., Gruiz, K., 2012. *Contaminant mobility and carbon sequestration downstream of the Ajka (Hungary) red mud spill: the effects of gypsum dosing*. Science of the Total Environment 421-422, 253-259. DOI: https://doi.org/10.1016/j.scitotenv.2012.01.046

Rivera, R.M., Ounoughene, G., Borra, C.R., Binnemans, K., 2017. *Neutralisation of bauxite residue by carbon dioxide prior to acidic leaching for metal recovery*. Minerals Engineering 112, 92-102. DOI: 10.1016/j.mineng.2017.07.011

Sahu, R.C., Patel, R.K., Ray, B.C., 2010. *Neutralization of red mud using CO_2 sequestration cycle*. Journal of hazardous materials 179(1-3), 28-34. DOI: 10.1016/j.jhazmat.2010.02.052

Santini, T.C., Hinz, C., Rate, A.W., Carter, C.M., Gilkes, R.J., 2011. *In situ neutralisation of uncarbonated bauxite residue mud by cross layer leaching with carbonated bauxite residue mud*. Journal of hazardous materials 194, 119-127. DOI: 10.1016/j.jhazmat.2011.07.090.

Shi, C., Xu, J., Beckman, E., Enick, R., 2000. *Carbon dioxide sequestration via pH reduction of red mud using liquid CO_2.* ACS Div. Fuel Chem. 45, 703-705

Si, C., Ma, Y., Lin, C., 2013. *Red mud as a carbon sink: variability, affecting factors and environmental significance*. Journal of Hazardous Materials 244-245, 54-59. DOI: http://dx.doi.org/10.1016/j.jhazmat.2012.11.024

Smith, P., 2015. *Reactions of lime under high temperature Bayer digestion conditions*. 10th International alumina quality Workshop, 19-23 April 2015. Perth, Western Australia

Solymar, K., Steiner, J., Zoldi, J., 1997. *Technical peculiarities and viability of hydrothermal treatment of red mud*. Proceeding of TMS Light Metals, 49-54

Whittington, B.I., 1996. *The chemistry of CaO and $Ca(OH)_2$ relating to the Bayer process*. Hydrometallurgy 43(1-2), 13-35. DOI: https://doi.org/10.1016/0304-386X(96)00009-6

Yadav, V.S., Prasad, M., Khan, J., Amritphale, S.S., Singh, M., Raju, C.B., 2010. *Sequestration of carbon dioxide (CO_2) using red mud*. Journal of Hazardous Materials 176(1-3), 1044-1050. DOI: https://doi.org/10.1016/j.jhazmat.2009.11.146

Yang, J., Xiao, B., 2008. *Development of unsintered construction materials from red mud wastes produced in the sintering alumina process*. Construction and Building Materials 22(12), 2299-2307. DOI: https://doi.org/10.1016/j.conbuildmat.2007.10.005

3.7.4 USE OF LIME IN OTHER INDUSTRIAL CONSUMERS APPLICATIONS

Lime is also used in sugar production, glass production and other processes, that were not assessed due to the lack of publications/reports on carbonation.

3.8. USE OF LIME IN THE PULP AND PAPER - PRECIPITATED CALCIUM CARBONATE (PCC) PRODUCTION

3.8.1 INTRODUCTION

Calcium carbonate minerals occur in three types of crystalline polymorphs: the most common and stable form is *calcite* (trigonal crystal system of Ca, C and O atoms), with different crystal shapes (scalenohedral, rhombohedral, cubic, prismatic). Less common is *aragonite*, which has a discrete or clustered needle orthorhombic crystal structure. The rarest and generally unstable crystal form is the *vaterite* calcium carbonate mineral (hexagonal crystal system). The formation of any of these polymorphs is strictly dependent on some parameters such as reaction temperature and pressure, saturation level and pH of the reactant solution during the carbonation process. Out of these crystal forms, only aragonite and calcite (mainly scalenohedral, prismatic and rhombohedral types) have major commercial applications and are produced on an industrial scale (Teir et al., 2005).

There are two sources of calcium carbonate: ground calcium carbonate (GCC), which is obtained from limestone deposits through a mechanical route, and precipitated calcium carbonate (PCC), also referred to as *synthetic* or *refined* calcium carbonate, which is produced by a chemical route combining carbon dioxide (CO_2) with lime (CaO) under controlled operating conditions.

PCC includes a wide range of high-purity crystalline materials. It is largely used as a coating pigment or filler in many industrial applications like paper (61%), paints (10%), plastics (10%), rubbers (11%), adhesives/sealants (2%) and others (6%), for a total annual market in Europe of roughly 2.1 million tonnes (data from IMA Europe, Schyvinck 2012). Depending on their use, PCC products must meet specific requirements in terms of purity, morphology, mean size and particle size distribution, specific surface area, brightness and so on. Table 3.8.1 shows a summary of the main properties of commercial PCC products used in the pulp and paper industry, derived from Sundermann (2016).

The main advantage of the chemical process lies in the better control over the purity and characteristics of the final PCC products that cannot be achieved through the mechanical process; the most challenging properties for PCC commercialisation are purity, morphology, and particle size (Sundermann, 2016). There are several PCC grades but the purity of commercial PCC is usually higher than 98-99% (Sundermann, 2016; Teir et al., 2005).

Each crystal type is suitable for a specific industrial application: for instance, calcite-PCC of nanometer size with rhombohedral morphology is highly effective for use as a coating in paper making (Jimoh et al., 2017). By regulating the operating conditions of the precipitation process (temperature, pressure, particle size, saturation and pH of reactant solution, gas flow rate, agitation speed, reaction time), in fact, different kinds of crystals can be obtained in terms of morphology (prismatic, rhombohedral, scalenohedral - shape) and particle size (from micrometer to nanometer sized) (Jimoh et al., 2017; Teir et al., 2016). An example is reported in Figure 3.8.1, showing the influence of gas flow rate and reactant concentration on the crystallization of calcite; low concentration of $Ca(OH)_2$ favours the formation of rhombohedral calcite crystals with particle size below

100 nm at ambient temperature and low gas flow rate (Jimoh et al., 2017); at higher concentration and gas flow rate, scalenohedral calcite can be obtained.

Table 3.8.1. Quality parameters of commercially available PCC products used in the pulp and paper industry, derived from Sundermann (2016).

Supplier	**Application**	**Morphology**	**Purity (% $CaCO_3$)**	**Brightness (dry)**	**Median size d_{50} (µm)**
SMI	Filler: increases paper whiteness, brightness and opacity	Scalenohedral calcite	98	98	1.3-2.2
SMI	Filler: improved paper runnability, porosity control	Prismatic calcite	97	97	0.7-2.2
SMI	Coating: paper surface coating where high brightness is desired	Prismatic calcite	n/a	n/a	0.6-2.2
SMI	Coating: gives high brightness and opacity increases not attainable with other PCC grades	Aragonite	n/a	n/a	0.4-0.6
Omya	Filler: gives high brightness, opacity and bulk in papermaking	Scalenohedral calcite	99	95	1.8
Schaefer Kalk	No grade specific uses; it is used in pulp and paper, plastics and pharmaceuticals industries	Scalenohedral calcite	99	93-99	1-3
		Scalenohedral calcite +aragonite (35%)	99	97-99	0.8
		Rhombohedral calcite	99	96-98	0.5
		Platelike calcite	96	97-99	1.1

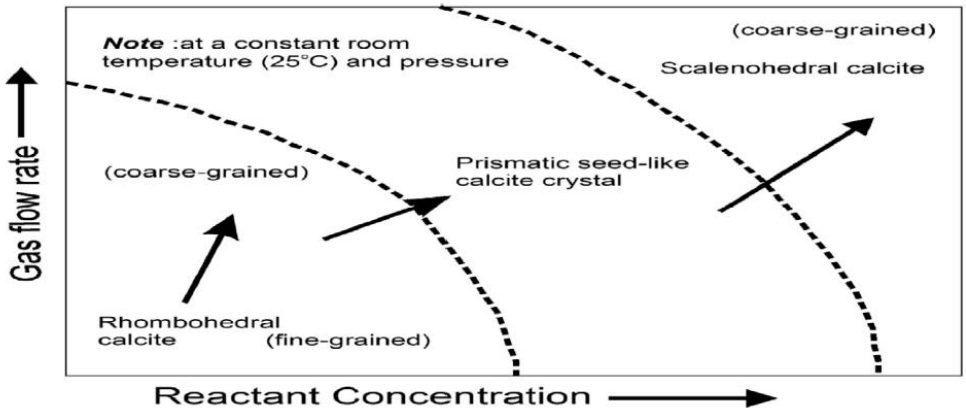


Figure 3.8.1. Crystallization hypothesis for PCC production in the liquid-gas system from $Ca(OH)_2$ suspension. Source: Jimoh et al. (2017).

Recently, aragonite is receiving increasing attention from a technical viewpoint due to its capability to improve the mechanical properties of plastic composites (e.g. tensile strength, impact resistance, flexural modulus, thermal properties) thanks to its intrinsic needle-like shape. Many research studies have been conducted to synthetize pure aragonite, but the formation mechanism is still not fully understood (Sudermann, 2016). According to Sudermann (2016), Li et al. (2014), Thriveni et al. (2013) and Ahn et al. (2005), the synthesis of pure aragonite PCC can be obtained at a high reaction temperature (>60-80°C), high initial pH of the solution

(> 9-10), short reaction time (< 2 h), low supersaturation level (Ca^{2+}/CO_3^{2-} in the range 2.2–6 Sudermann, 2016) and low gas flow rate. In contrast, Li et al. (2014) produced aragonite at room temperature (25°C) in $CaCl_2$ – NH_4Cl solution; they also found that increasing the carbonation temperature leads to a reduction in aragonite concentration.

Generally, the use of additives in the carbonation step can promote aragonite formation, but some problems for solvent reuse and PCC purification may be encountered. Among inorganic additives, magnesium containing compounds (e.g. $MgCl_2$) are found to favour aragonite as stated by Thriveni et al. (2013), while Ahn et al. (2005) obtain similar results by using Na_2CO_3; Lei et al. (2006) found that, at higher temperature (80°C), organic solvents such as glycol or glycerine can accelerate aragonite formation. Whereas according to the patented method n. EP2371766A1 (Pohl et al., 2011), the formation of aragonite crystals can be increased by using specific additives as strontium compounds and aragonite seed crystals.

Manufacturing processes for PCC

Different methods exist to chemically synthetize PCC with the prospect of achieving definite properties in terms of purity, morphology, particle size and distribution, as well as specific surface area.

In total, there were 12 producers of PCC in the EU-25 area in 2003 and 42 operating plants (European Commission, 2007); their location and capacity data are reported in Table 3.8.2.

Table 3.8.2. PCC production capacity, producers and location in EU-25 in 2003. Source: BREF on Large Volume Inorganic Chemicals - Solids and Others Industry (European Commission, 2007).

Producers	Country	Location	Capacity		Type of PCC
			kt per year	%	
	Finland	Imatra			Slurry
	Finland	Kemi			Slurry
	Finland	Kuusankosi			Slurry
	France	Etival Clairefontaine			Slurry
	Portugal	Setubal			Slurry
	Sweden	Nymölla			Slurry
	Sweden	Lessebo			Slurry
Producer A		**Subtotal**	**550**	**21.0**	
	Austria	Golling			Slurry
	Hungary	Szolnok			Slurry
	Netherlands	Moerdijk			Slurry
	Portugal	Fatima			Slurry
	Spain	Hernani			Slurry
Producer B		**Subtotal**	**555**	**21.2**	
	Austria	Wattens			Slurry
	Germany	Hahnstätten			Dry
	Germany	Neidenfels			Slurry
Producer C		**Subtotal**	**88**	**3.3**	
	Austria	Ebensee			Dry
	UK	Lostock			Dry
	France	Giraud			Dry
	France	Quimperlé			Slurry
	Germany	Rheinberg			Dry-slurry
	Italy	Angera			Dry
Producer D		**Subtotal**	**224**	**8.5**	
	Belgium	Hermalle sous Huy			Dry-slurry
	UK	Lifford			Dry
	Finland	Äänekoski			Slurry
	Finland	Anjalankoski			Slurry
	Finland	Lappeenranta			Slurry
	Finland	Tervakoski			Slurry
	France	Saillat			Slurry
	France	Docelles			Slurry
	France	Alizay			Slurry
	Germany	Schongau			Slurry
	Germany	Walsum			Slurry
	Poland	Kwidzyn			Slurry
	Portugal	Figueira da Foz			Slurry
	Slovakia	Ruzomberok			Slurry
Producer E		**Subtotal**	**1100**	**42.0**	
	Spain	Argelaguer			Dry
	Germany	Leuna			Dry
	France	Caffiers			Dry
	Poland	Janikowo			Dry
	Poland	Inowroclaw			Dry
	UK	Brassington			Dry
	Spain	Revilla de Camargo			Dry
Other Producers		**Subtotal**	**105**	**4.0**	
Total			**2622**	**100**	

Almost all commercially available PCC is currently manufactured by direct carbonation of hydrated lime with pure CO_2 or CO_2 containing gases (Personal communication EuLa, 2019; European Commission, 2007; Ahn et al., 2005; Jimoh et al., 2017; Teir et al., 2005). In this conventional PCC production, i.e. the so-called *carbonation process*, pure limestone (or lime slurry) is typically used as raw material as it is generally free of contaminants, with only 2% impurities made mostly of silica (more details about the process in Chapter 3.8.2). Other existing commercial methods for synthetizing PCC (Erdogan and Eken, 2017; Othman et al., 2017; Wardhani et al., 2018; Teir et al., 2005) include the calcium chloride process, the lime-soda process and the

CalciTech process. All of them use hydrated lime (or milk of lime) as the raw material but they differ in the layout, process equipment, and in the use of chemicals; these aspects, in turn, affect the impurities that are found in the final PCC products.

In the *calcium chloride process*, $CaCl_2$ reacts with Na_2CO_3 to form a calcium carbonate precipitate and a sodium chloride solution according to Reaction [3.8.1]:

$$CaCl_2 + Na_2CO_3 \rightarrow CaCO_3\downarrow + 2\ NaCl \qquad [3.8.1]$$

This process is the simplest, but it requires a low-cost source of calcium chloride in order to be economically convenient; therefore, it is usually carried out in a satellite facility close to a Solvay process soda ash plant (Teir et al., 2005). However, since the calcium carbonate precipitates in presence of sodium chloride [Reaction 3.8.1] and other impurities, the derived PCC may contain up to 0.10% NaCl (see Table 3.8.3) which is close to the upper limit for some applications (e.g. glass production), thus reducing its marketability. The inherent technical problem of salts inclusion (mainly sodium chloride and gypsum), together with the lower costs of the conventional carbonation process, has reduced the use of the Solvay-process calcium carbonate compared to the conventional PCC, being used as raw material for cement production or burned in a lime kiln to regenerate lime (Mattila and Zevenhoven, 2014; Steinhauser, 2008; Teir et al., 2016).

Table 3.8.3. Chemical composition of PCC products by process, expressed as % by weight (source: Teir et al., 2016).

	PCC (carbonation)	**PCC (Solvay)**
$CaCO_3$	98.36	98.62
$CaSO_4$	0.08	0.63
$MgCO_3$	0.7	0.21
Al_2O_3	0.09	0.01
Fe_2O_3	0.07	0.01
SiO_2	0.1	0.02
NaCl	-	0.10
% H_2O loss[(a)]	0.6	0.3
pH[(b)]	9.4	8.5

[(a)] At 110°C; [(b)] Saturated solution.

In the so-called *lime-soda process*, the hydrated lime is reacted with sodium carbonate (Na_2CO_3) to produce a sodium hydroxide solution from which the calcium carbonate is precipitated, as shown in Equation [3.8.2]:

$$Ca(OH)_2 + Na_2CO_3 \rightarrow\ CaCO_3\downarrow +\ 2NaOH \qquad [3.8.2]$$

This process is commonly used by alkali manufacturers, whose crucial objective is the recovery of sodium hydroxide, while the coarse PCC is obtained only as a by-product (Teir et al., 2005). For instance, NaOH is

used in the kraft pulping cycle in converting green liquor into white liquor. However, the PCC formed in this process is not suited as a paper filler due to its larger particle size. It is usually re-burned in kiln to recover lime, used in cement plants or disposed of as a waste (Islam and Quader, 2008).

The *CalciTech* process is a recently patented method (patent number US7378073/2008) for obtaining a form of PCC named as *Speciality Calcium Carbonate (SCC)* from by-products or waste materials containing lime or hydrated lime, such as carbide lime (i.e. the by-product of acetylene production). The CalciTech process, depicted in Figure 3.8.2, comprises dissolving the carbide lime into an aqueous solution of a polyhydroxy compound solution (sorbitol or other sugar alcohols due to their thermal stability) and optionally separating the insoluble impurities from the calcium ion solution by filtration. After separation of impurities, the Ca solution is treated with CO_2 as a precipitating agent to obtain calcium carbonate. By controlling the amount of CO_2 fed based on pH measurements, the properties of the precipitate can be tailored. Then, a combination of filter press and washing equipment is used to separate the solids from the sorbitol solution that can be reused in the dissolution step after adjusting its weight (from 26% to 29% according to the patent). This method is able to produce high purity PCC in the form of calcite with rhombic structure, small particle size, and narrow size distribution with an overall efficiency, in terms of PCC produced, between 98.3-99% of the theoretical value[32]. The process yield, i.e. the amount of PCC produced from 1 tonne of carbide lime (CL), resulted in the range 1.084-1.165 tPCC/tCL. As the amount of CO_2 sequestered per tonne of PCC is 440 $kgCO_2$/t PCC based on stoichiometry, the CO_2 uptake per tonne of carbide lime from the CalciTech process is in the range 469-509 $kgCO_2$/tCL.

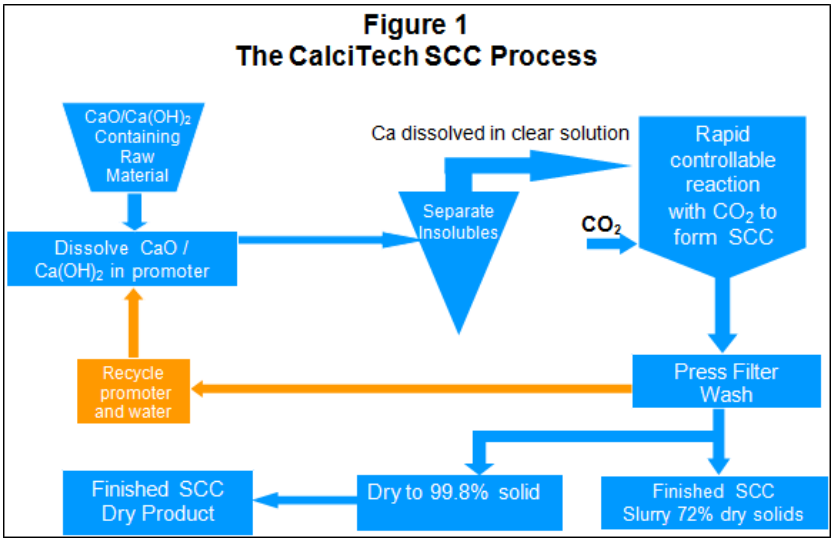


Figure 3.8.2. Flow diagram of the Calcitech process for the SCC manufacture from by-products or waste materials containing $CaO/Ca(OH)_2$.

[32] The theoretical yield is computed based on the content of $Ca(OH)_2$ in the carbide lime and the stoichiometric ratio between $CaCO_3$ and $Ca(OH)_2$ which is 1.351.

During the last 10-20 years, several studies have been carried out, at the laboratory and pilot scale, to test the applicability of different types of alkaline waste materials (steel slag, air pollution control residues, oil shale ash, waste concrete, cement kiln dust, and so on) for PCC production through indirect mineral carbonation as an alternative method to mitigate anthropogenic CO_2 emissions and store CO_2 in stable carbonates, while treating waste at the same time.

Based on such premises, the literature assessment related to the carbonation of lime was focused on the traditional carbonation process, based on which almost all commercially available PCC is currently manufactured (Chapter 3.8.2) and on the PCC production by indirect carbonation of alkaline waste, in particular iron and steel slags (Chapter 3.8.3). This last Chapter is based on the current outcomes related only on laboratory scale tests and pilot scale experiences.

3.8.2. PRODUCTION OF PCC BY THE TRADITIONAL CARBONATION PROCESS

Description of the process

The *carbonation process* (Figure 3.8.3) is currently the most applied and cost-efficient method for PCC production (European Commission, 2007; Mattila and Zevenhoven, 2014; Teir et al., 2005; Wardhani et al., 2018). In case of "*merchant*" PCC plants, i.e. those not linked to other plants supplying CO_2 (power plants, paper mills, soda ash plants), the raw material is pure limestone and the calcination step is included in the processing line. Otherwise, for "*satellite*" PCC plants, the exhaust CO_2 gases from the customer facilities are used while the raw material, i.e. lime (CaO) or hydrated lime ($Ca(OH)_2$), is provided by one or more suppliers. Considering the typical configuration of a PCC *merchant* plant, the mined rock is firstly crushed to the particle size needed for manufacturing (small stones or powder) and, then, eventually refined to separate some of the impurities (e.g., feldspar and siliceous minerals) before calcining. Calcination of limestone is carried out in lime kilns where heat is provided to decompose the rock into calcium oxide (CaO) and carbon dioxide (CO_2), as shown in Reaction [3.8.3]. Temperatures between 900 and 1100°C are typically adopted (JRC, 2013; Jimoh et al., 2017; Mattila and Zevenhoven, 2014; Wardhani et al., 2018). The off-gas from the calciners, mostly containing CO_2 and water vapour, can be captured and usually purified for reuse in the PCC production step. A scrubbing unit for cleaning up the flue-gases is often incorporated in the case of satellite PCC plants, since the purity of CO_2 strongly affects the quality of final PCC products.

Calcination: $CaCO_3 + \text{Heat} \rightarrow CaO + CO_2 \uparrow$ [3.8.3]

Formation of a hydroxide: $CaO + H_2O \rightarrow Ca(OH)_2$ [3.8.4]

Carbonation/ Precipitation: $Ca(OH)_2 + CO_2 \rightarrow CaCO_3 \downarrow + H_2O$ [3.8.5]

The resulting CaO is then hydrolysed into distilled water to form a slurry of calcium hydroxide (hydrated lime or slaked lime) according to Reaction [3.8.4]. The slaking process is often run in a continuous reactor but can be a batch process as well (European Commission, 2007). The slaked lime is put in contact with flue gases containing CO_2 (e.g., the kiln off-gas with 20-30% vol. of CO_2, or pure CO_2) leading to re-carbonation; calcium

carbonate reforms, and being insoluble in water, it precipitates as in Reaction [3.8.5] (discontinuous process). Separation of impurities from the milk of lime can be included (as shown in Figure 3.8.3) to ensure high purity PCC.

The precipitation Reaction [3.8.5] is capable of producing each of the three polymorphs (calcite, aragonite, and vaterite) depending on the applied reaction conditions. PCC characteristics can be tailored by regulating:

- temperature (milk of lime may be cooled or heated depending on the desired crystal type);
- CO_2 concentration and flow rate;
- stirring rate;
- particle size, impurities, and concentration of the hydrated lime slurry;
- additives.

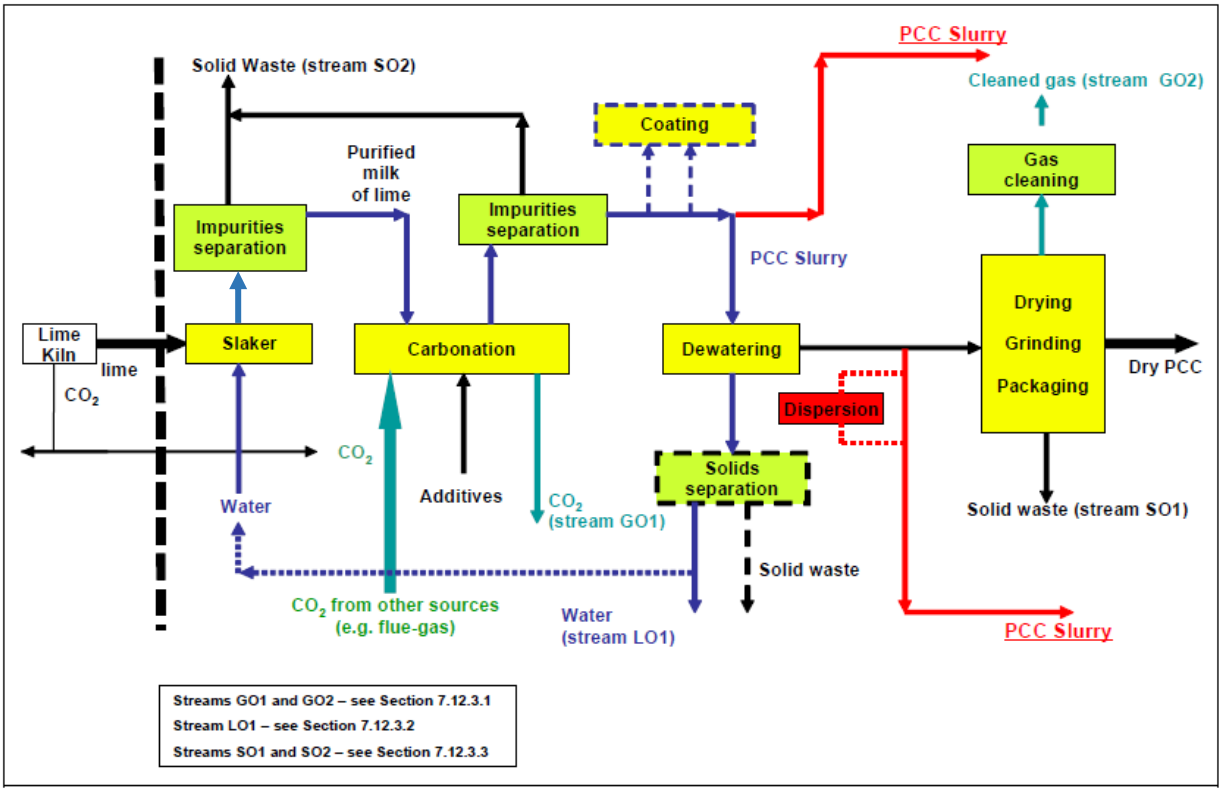


Figure 3.8.3. Process flow diagram of the conventional manufacturing of PCC. Source: BREF on Large Volume Inorganic Chemicals - Solids and Others Industry (European Commission, 2007).

PCC is then separated as a filter cake containing 50-60%w_t solids, while the solution is recirculated back to the slaking unit. Additional impurities can eventually be removed from the PCC slurry by washing. If the PCC is destined to go to a paper mill or a paint plant, the lower solids slurry may be used as it is, or processed to bring up the solids level (PCC "*satellite*" concept). If the PCC is to be used as a dry product, the slurry is dewatered, dried, milled, and packaged (PCC "*merchant*" concept).

The main input and output flows of conventional PCC manufacturing are presented in Table 3.8.4. These values are derived from the BREF on Large Volume Inorganic Chemicals-Solids and Others Industry (European Commission, 2007) and are related to actual PCC grades.

To produce one tonne of PCC, around 600-660 kg of raw lime is consumed and 440 kgCO_2/t PCC is stocked during lime carbonation (based on the stoichiometry).

Table 3.8.4. Major input and output data related to the conventional PCC production for the actual PCC grades. Source: BREF on Large Volume Inorganic Chemicals - Solids and Others Industry (European Commission, 2007).

Consumption/emission	per tonne PCC(*)	Location in the PCC process	Comment
Main raw material			
Raw lime	600 – 660 kg	Slaking	
CO_2	500 – 800 kg	Carbonation	(1)
Process water	2 – 10 m^3	Slaking	(11)
Energy			
Fuel	0 – 7.5 GJ	Carbonation, drying	(2)
Electricity	60 – 500 kWh		(3)
Emission to air			
CO_2 (4)	50 – 350 kg	Carbonation (GO1)	(1)
Dust	Not reported	Drying, grinding, packaging (GO2)	(5)
Emissions to water			
Chemical additives	Little	Dewatering (LO1)	(6)
pH	6.0 – 12.4	Plant effluent	(10)
Suspended solids	1 – 30 kg	Dewatering (LO1)	(7)
Solid wastes			
Fine particles (<100 micron)	<10 kg	Drying, grinding, packaging (SO1)	(8)
Coarse particles (1 mm – 50 mm)	2 – 100 kg	Slaking, carbonation (SO2)	(9)

(1) absorption efficiency can be low for some grades (depending of temperature, milk of lime viscosity, CO_2 flowrate, CO_2 content in the flue-gas, etc.)
(2) depending on the carbonation process and dewatering efficiency. Large range of fuel consumption is explained by different configuration of PCC plants. Most of the PCC plants produce PCC as slurry (fuel consumption around a low level; some PCC producers do not use fuel at all), while the PCC plants manufacturing dry PCC product (drying step involved) use much more fuel (fuel consumption around a high level)
(3) including CO_2 compression
(4) the PCC process is typically a net consumer of CO_2 (the difference between the used and emitted CO_2). The data do not include CO_2 related to energy consumption (cross-media effect)
(5) exhaust gases are filtered or washed
(6) additives (low quantities) can be used at the carbonation or coating step. Part of them can remain in water. Depends upon the process used.
(7) dewatering devices (filters, centrifuges, etc.) are designed to separate solids properly. In the case of ultrafine PCC production, too many ultrafine particles might remain in water. In this case, settling devices could be installed.
(8) out of grade PCC, leakages
(9) pieces of uncalcined limestone and sands from milk of lime purification; grids from PCC slurry purification
(10) effluent from the PCC plant located at a customer's site is typically discharged to the central waste water treatment plant at the site
(11) depending on the local situation, additional quantities of process water may be used.
(*) figures in this table are indicative ranges of annual averages based on various measurements or estimation techniques. Production of new grades (dimensions, shapes, coating, etc.) can have a certain impact on the process and for a change of input and output levels.

Efficiency of the process

The slow kinetic step which controls the overall reaction rate of the carbonation process is believed to be the rate of dissolution of calcium hydroxide in the slurry, so that calcium ions are available for reaction. The typical

saturated concentration is $2.16*10^{-2}$ molar (1.6 g/l) at 25°C (US 7,378,073 B2). Due to the low concentration, the reaction equilibria are such that, in the carbonation step, only about 30%-40% of the lime is converted to PCC at ambient temperature and pressure (US 7,378,073 B2; Othman et al., 2017). Therefore the carbonation process is slow, with low efficiency at ambient conditions. The low concentration level may also cause some difficulties once the conversion to PCC is completed during the separation step.

At the industrial scale, the rates of formation of carbonate CO_3^{2-} (from CO_2 solubilisation) and calcium ions Ca^{2+} (from dissolution of calcium hydroxide) are increased through pressurization of the carbonation reaction and/or by eventually using specific additives, in order to maximize the PCC yield.

Figure 3.8.4 shows the carbonation efficiency of a slurry of calcium hydroxide at different applied pressure (A) and at different CO_2 concentration (B), derived from the patent US 2002/0009410 A1 (Mathur, 2002); the achieved percentage of carbonation resulted in the range from 75% up to 100% depending on the applied conditions. For instance, at 2.1 bar and 38°C the overall carbonation efficiency was 95%.

(A) Effect of pressure (T=38°C, 20% CO_2)

(B) Effect of % CO_2 (T=38°C)

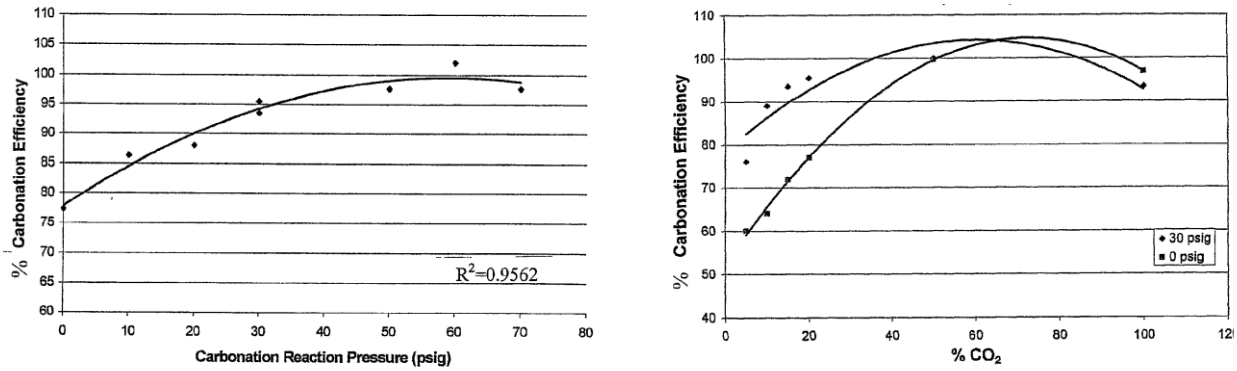


Figure 3.8.4. Effect of pressure (A) and %CO_2 gas (B) on the carbonation efficiency of $Ca(OH)_2$ slurry, from the US patent 2002/0009410 A1 (Mathur, 2002).

Since no detailed information is available on the type of process and operating conditions applied in the PCC plants, the flows reported in the BREF (600-660 kgCaO/tPCC, see Table 3.8.4) were taken as a reference to estimate the overall efficiency of the PCC production, which resulted in the range 85%-93% (computed with respect to the stoichiometric lime consumption of 560 kgCaO/tPCC); the estimated range is in line with the values previously presented.

Regarding the purity of PCC from the conventional carbonation process, it is strictly related to the purity of limestone feedstock and to the use of additives for increasing calcium extraction; in the latter case, PCC purification by washing is required. The major "contaminant" is generally magnesium carbonate, but it is very important that the limestone has a low content of manganese and iron, since these elements negatively affect the brightness of PCC products (Mattila, 2014; Sezer, 2013). Particularly the iron content should be lower than 0.1% for a commercial PCC product.

Carbonation rate of lime in the process

According to some authors (Schyvinck, 2012; Teir et al., 2012), the amount of CO_2 that is fixed in PCC products is equal to the amount of CO_2 that is released from limestone calcination; this means that, if the CO_2 emission from fuel consumption is omitted from the computation, a null balance for CO_2 can be assigned to the conventional process of PCC production. Despite the fact that the conventional method is energy intensive due to the high temperature required in the lime kiln and thus may produce noticeable amounts of CO_2 (e.g., +0.21 $kgCO_2/kgPCC$ assuming oil combustion for lime calcination, Teir et al., 2005), this approach does not take into consideration the "technical inefficiencies" of the calcination and carbonation processes, which imply dosages of raw materials greater than the stoichiometric values.

Referring to the average values reported in the BREF on Large Volume Inorganic Chemicals - Solids and Others Industry (2007), that are representative of the available technologies for PCC production in Europe, the process requires 600-660 kgCaO/tPCC (Table 3.8.4). Since the CO_2 stored in carbonates is 440 kg CO_2/tPCC but the use of lime in the PCC manufacturing implies a CO_2 emission of 471-518 $kgCO_2$/tPCC due to limestone calcination, a net CO_2 emission of 31-78 $kgCO_2$/tPCC should be assigned to the conventional manufacturing of PCC if the efficiencies of the different process steps are included (Figure 3.8.5).

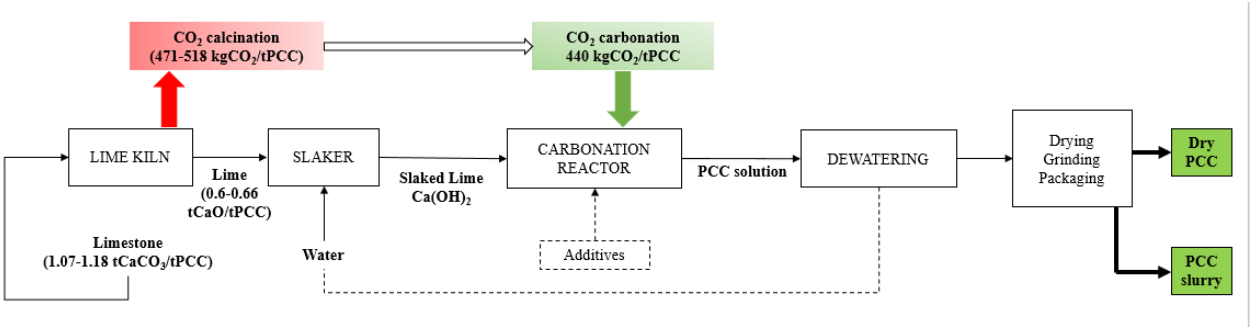


Figure 3.8.5. Mass balance of the conventional PCC production process estimated based on the BREF on Large Volume Inorganic Chemicals - Solids and Others Industry (European Commission, 2007), referring to 1 tonne of PCC produced.

3.8.3. PCC production via Indirect Carbonation of Alkaline Industrial Wastes

Introduction

Alternative methods for synthetizing PCC using different alkaline industrial wastes instead of natural limestone are being studied and/or developed (Bilen et al., 2018; Chang et al., 2014; Eloneva et al., 2009; Jimoh et al. 2017; Mattila et al., 2014; Said et al., 2013; Sundermann, 2016; Teir et al., 2016). These mineral carbonation methods are based on the reaction between CO_2 and metal oxide bearing minerals to form insoluble carbonates, which must be designed and optimized depending on the physical and chemical properties of the feedstock. The most common investigated alkaline wastes include iron and steel slags, waste cement (Jo et al., 2014; Katsuyama et al., 2005; Kunzler et al., 2011), oil shale ashes (Uibu et al., 2010; Velts et al., 2011; Velts et al., 2013), and coal fly ash (He et al., 2013).

The carbonation of alkaline materials can be performed in two different ways: direct or indirect.

The direct carbonation reaction occurs in only one step between the sample and the gas through dry or wet routes. The reaction kinetic of the dry gas-solid reaction at ambient pressure and temperature is too slow to be effective on a wide scale basis (Pan et al., 2015). The addition of water to the direct carbonation process in the so called aqueous-carbonation (or wet carbonation) accelerates the reaction rates; in this route, CO_2 is directly fed into the reactor containing a mixture of the mineral waste and the solvent solution. Despite this option requiring less process equipment compared to the indirect carbonation, it still needs further studies to address the quality and usefulness of PCC products (Mattila et al., 2012b).

The indirect carbonation process, depicted in Figure 3.8.6, is usually carried out in two main steps and has the advantage of producing purer carbonate. In the *lixiviation* or *dissolution step*, the calcium is selectively extracted from the materials using specific solvents (e.g. ammonium salt solutions, organic solvents, acids). Then, after separating the solid residues by filtration, the dissolved calcium is carbonated in a separated reactor by bubbling CO_2-containing flue gases into the calcium-rich solution (*carbonation step*). Naturally, the residue's particle size as well as the liquid to solid ratio and the solvent type and concentration significantly affect the Ca extraction efficiency and the selectivity of the dissolution process. Whereas in the carbonation step, the CO_2 flow rate and the operating conditions (temperature, CO_2 pressure, pH of solution) are crucial parameters for the process kinetics.

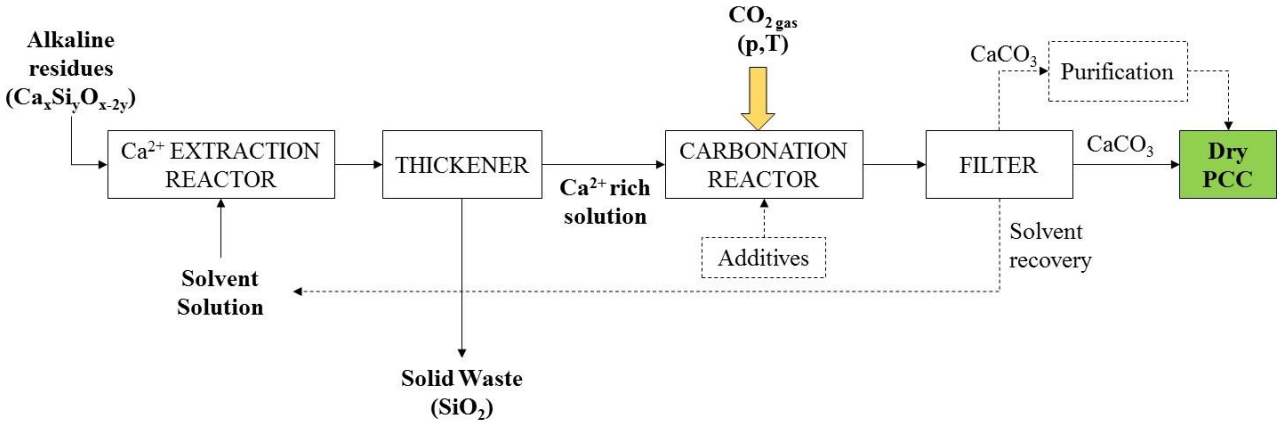


Figure 3.8.6. Overview of the PCC production from alkaline residues through the indirect carbonation method.

The precipitated calcium carbonate is then separated by filtration and eventually purified by washing it with water, whilst the solvent solution can be recirculated back to the extraction reactor (if no additives are used to favour precipitation), as depicted in Figure 3.8.6.

PCC production from alkaline materials allows the use of limestone and its calcination to be omitted, thus potentially lowering the CO_2 emission and preserving natural resources compared to conventional PCC production, even if it implies additional emissions due to solvent production and increased water and energy uses due to the PCC purification. Since the captured CO_2 can be taken from other sources (than the limestone calcination) these alternative PCC methods may allow negative CO_2 emission and can be considered as a carbon capture, utilization and storage technology (Mattila, 2014; Chang et al., 2017) whilst, at the same time, turning industrial wastes into value-added materials by controlling polymorphs and properties of the mineral carbonates.

The discontinuous reaction in the two steps carbonation has the advantage of ensuring a straight-forward adjustment of process parameters such as calcium concentration and gas flow rate which affect the solution (super)-saturation and product precipitation. Also, reaction time, temperature, solution pH and mixing properties can be accurately controlled so that the whole process can be steered to manufacture a product that fulfils the requirements set by the specific use (Mattila, 2014).

However, the challenge of using calcium-containing industrial wastes (e.g. steelmaking slag) is to guarantee similar product properties like in the conventional PCC production, especially in terms of material purity. Concerns exist around the potential impurities that may end up into the final PCC products originating from waste residues and solvent usage.

PCC production via carbonation of steel and iron slags: materials and methods of the review

The possibility of producing high purity PCC and the related efficiency, in terms of PCC yield and CO_2 removal, was investigated through a literature review focusing on iron and steelmaking slags that seem to be the most promising materials due to their high CaO content (30-60%) and large availability. In total, 16 papers published in scientific journals, a report, a US patent (US 8,603,428 B2/2013), 2 conference papers, a master and 2 doctoral theses were analysed. The list of all the documents analysed is reported in Table 3.8.5.

Table 3.8.5. List of the documents considered in the literature review on iron and steelmaking slags for the production of PCC.

Author	Type of residues/ tests	Title	Affiliation
		PEER REVIEWED PAPERS	
Bao et al., 2010*	Steelmaking slag (BOF)	Selective leaching of steelmaking slag for indirect CO_2 Mineral Sequestration	China
Bilen et al., 2018	Steelmaking slag	Evaluation of steelmaking slag for CO_2 fixation by leaching-carbonation process	Turkey
Chiang et al. 2014**	Blast Furnace slag	Towards zero-waste mineral carbon sequestration via two-way valorisation of ironmaking slag	Belgium Canada
Dri et al. 2013*	Steelmaking slag (BOF, SS)	Dissolution of steel slag and recycled concrete aggregate in ammonium bisulphate for CO_2 mineral carbonation	UK
Eloneva et al., 2008; Eloneva et al., 2009	Steel Converter Slag (BOF), Blast Furnace Slag, Desulphurization Slag, Ladle Slag	Steel Converter Slag as a Raw Material for Precipitation of Pure Calcium Carbonate for Production of Marketable Calcium Carbonate Reduction of CO_2 Emissions from Steel Plants by Using Steelmaking Slags for Production of Marketable Calcium Carbonate	Finland
Jo et al., 2017	Steel slag	Preparation of high-purity nano-$CaCO_3$ from steel slag	Korea
Kodama et al., 2008	Steelmaking slag (BOF)	Development of a new pH-swing CO_2 mineralization process with a recyclable reaction solution	Japan
Kunzler et al. 2011	Steelmaking slag and Concrete	CO_2 storage with indirect carbonation using industrial waste	Brazil
Mattila et al., 2012 (a)	Steel converter slag	Chemical kinetics modeling and process parameter sensitivity for precipitated calcium carbonate production from steelmaking slag	Finland
Noack et al., 2014	BOF, EAF, Desulphurization slag	Comparison of alkaline industrial wastes for aqueous mineral carbon sequestration through a parallel reactivity study	United States
Said et al., 2013 Said et al., 2016	Steel converter slag (Pilot plant)	Performance of separation processes for precipitated calcium carbonate produced with an innovative method from steelmaking slag and carbon dioxide Pilot-scale experimental work on carbon dioxide sequestration using steelmaking slag	Finland
Stolaroff et al., 2005	Steel and blast furnace slag	Using CaO- and MgO-rich industrial waste streams for carbon sequestration	United States

* only dissolution experiments. ** three stage process to simultaneously produce PCC and zeolitic materials from blast furnace slag.

Table 3.8.5 (continued). List of the documents considered in the literature review on iron and steelmaking slags for the production of PCC.

Author	Type of residues/ tests	Title	Affiliation
		PEER REVIEWED PAPERS	
Teir et al., 2007	Steelmaking slag	Dissolution of steelmaking slags in acetic acid for precipitated calcium carbonate production	Finland
Teir et al., 2016	Steel converter slag	Performance of separation processes for precipitated calcium carbonate produced with an innovative method from steelmaking slag and carbon dioxide	Finland
		REPORT	
Järvinen et al., 2010	Steelmaking slag	Success story on mineral carbonation of CO_2.	Finland
		PATENT	
Teir et al., 2013	Steelmaking slag	US 8,603,428 B2/ 2013	United States
		CONFERENCE PAPERS	
Eloneva et al., 2010	Steelmaking slag (BOF)	Feasibility study of a method utilizing carbon dioxide and steelmaking slags to produce precipitated calcium carbonate (PCC)	Finland
Mattila et al., 2012 (b)	Steelmaking slag (BOF)	Process efficiency and optimization of precipitated calcium carbonate (PCC) production from steel converter slag	Finland
		THESES	
Eloneva, 2010	Steelmaking slag (BOF)	Reduction of CO_2 emissions by mineral carbonation: steelmaking slags as raw material with a pure calcium carbonate end product	Finland
Mattila, 2014	Steelmaking slag (BOF)	Utilization of steelmaking waste materials for production of calcium carbonate ($CaCO_3$)	Finland
Sudermann, 2016	Steelmaking slag	Production of calcium carbonate from steelmaking slag and captured CO_2- Optimization of the carbonation process and product quality	Finland

PCC production from iron and steelmaking slags: characteristics of the process

Among the papers investigating PCC manufacture from iron and steelmaking slags, only three refer to blast furnace (BF) slag (Chiang et al., 2014; Eloneva et al., 2009; Stolaroff et al., 2005) while the majority focuses on steel converter slags. Among these papers, two investigate only the dissolution step (Bao et al., 2010; Dri et al., 2013) while, in all the others, experiments on both the Ca extraction and the precipitation step were performed and the optimum process conditions were outlined. Only 9 papers report quantitative data on PCC yield or CO_2 uptake, whereas almost all of them provide information about the morphology and purity of PCC products obtained from steel slag. A summary of the main process parameters, efficiency and quality of PCC products from the most relevant studies is reported in Table 3.8.6.

Since steelmaking slags contain, besides calcium, several other elements such as iron, silicon, magnesium, manganese, aluminium and vanadium, the success of the PCC production is strictly connected with the efficiency and selectivity of calcium separation from this complex matrix. Different solvents were tested through dissolution experiments by using acids (e.g. HCl, HNO_3, H_2SO_4, HF, CH_3COOH, etc.) or ammonium salt solutions (e.g., CH_3COONH_4, NH_4Cl, NH_4NO_3, etc.). Most of the recently published research has identified aqueous ammonium salt solutions, specifically ammonium acetate (CH_3COONH_4) and ammonium chloride (NH_4Cl) as the most selective and efficient solvents for dissolving calcium from steelmaking slags (Eloneva et al., 2009; Kodama et al., 2008; Mattila, 2014; Said et al., 2013; Said et al., 2016; Sudermann, 2016; Teir et al., 2016). Acid solutions (e.g. CH_3COOH or HCl) can dissolve calcium even more efficiently than ammonium salts, but other elements can be extracted from slags as well (Fe, Si, Mg, Al, etc.) thus lowering the purity of final PCC products (Bilen et al., 2018; Kunzler et al., 2011; Jo et al., 2017). Moreover, since acid solutions prevent efficient precipitation of calcium carbonate (required initial pH>9-10), there is a need to adjust the pH before carbonation (e.g., by adding NaOH); this makes more difficult to fully recover and reuse the solvent in the dissolution step (Eloneva, 2010).

Assuming the ammonium chloride as the solvent, the process chemistry evolves according to Reactions [3.8.6]-[3.8.9]. Of the calcium-containing phases in the steel slags, only free lime (CaO) and larnite (Ca_2SiO_4) react with the ammonium chloride to a large extent during the extraction step (Reactions [3.8.6] and [3.8.7]). After carbonation is completed (Reactions [3.8.8] and [3.8.9]), ammonium chloride in its original form is left (NH_4Cl) which can be easily recycled back to the extraction reactor once the calcium carbonate has been filtered from it.

$$CaO_{(s)} + 2\,NH_4Cl_{(aq)} + H_2O_{(l)} \rightarrow CaCl_{2\,(aq)} + 2\,NH_4OH_{(aq)} \quad [3.8.6]$$

$$Ca_2SiO_{4\,(s)} + 2\,NH_4Cl_{(aq)} + H_2O_{(l)} \rightarrow CaCl_{2\,(aq)} + CaSiO_{3\,(s)} + 2\,NH_4OH_{(aq)} \quad [3.8.7]$$

$$2\,NH_4OH_{(aq)} + CO_{2\,(g)} \rightarrow (NH_4)_2CO_{3\,(aq)} + H_2O_{(l)} \quad [3.8.8]$$

$$(NH_4)_2CO_{3\,(aq)} + CaCl_{2\,(aq)} \rightarrow CaCO_{3\,(s)} + 2\,NH_4Cl_{(aq)} \quad [3.8.9]$$

According to Mattila (2014), depending on the slag mineralogy, between 10-50% of the total calcium content in the slag can be dissolved by adding ammonium salt solutions; the author highlights that Ca extraction is more hindered in slags with large silicon, vanadium or iron fractions.

Likewise, Eloneva et al. (2009) observed high calcium dissolution for steel converter slag (50-80%) and desulphurization slag (50-60%) due to the higher free lime content (see Table 3.8.7), whereas in blast furnace slag and ladle slag the Ca dissolution efficiency is lower (<10% and <25%, respectively), since calcium is bound in silicates (e.g. larnite, which is prevalent in slowly cooled slags). Said et al. (2013) indicate a calcium extraction efficiency between 37-54% without grinding slags and up to 56-59% when the particle size of steel converter slag is reduced below 125 μm, using 1 M solution of NH_4Cl. Slightly higher performances were obtained by Said et al. (2016) in the Slag2PCC pilot plant; the Ca extraction efficiency was in the range 60-78% (depending on solvent cycles), reaching up to 94% in the two-stage dissolution process, while the carbonation efficiency resulted in the range 71%-91%. Due to the successful results, authors have supposed to realize a demonstration plant for pre-commercializing the technology by 2017.
In the US patent 8,603,428/2013 (Teir et al., 2013) about 60-85% of the calcium present in the waste can be extracted using ammonium acetate in concentration 0.5-2M.

Table 3.8.7. Major phases identified in the slags from XRD analysis (Source: Eloneva et al., 2010).

Slag type	**Phases identified (in descending apparent order of magnitude)**
Steel converter slag	Ca_2SiO_4, Ca_2FeAlO_5, FeO, CaO
Blast furnace slag	$Ca_2(Al(AlSi)O_7)$, $Ca_3Mg(SiO_4)_2$, $CaMgSiO_4$, $Ca_2(Mg_{0.5}Al_{0.5})$ $(Si_{1.5}Al_{0.5}O_7)$
Desulphurization slag	Ca_2SiO_4, CaO, Ca_2FeAlO_5, CaS, Fe_3O_4
Ladle slag	$Ca_3Al_{0.84}Fe_{1.16}Si_3O_{12}$, Ca_2SiO_4, MgO, SiO_2, Fe_3O_4, FeO

Despite ammonium salt solutions (especially NH_4Cl) being recognized as the most selective for extracting calcium ions (Eloneva et al., 2009; Kodama et al., 2008; Said et al., 2016; Sudermann, 2016; Teir et al., 2016), some authors advise against using high solvent concentrations (>1 M) since significant portions of other elements such as silicon, magnesium, or iron may dissolve, thus compromising the final purity of PCC products. Therefore, the process needs to be optimized in order to maximize Ca conversion and PCC purity.

Table 3.8.6. Main findings of the most relevant experimental studies on PCC production from iron and steel slags.

Study	Slag characteristics/ pre-treatment	Operating conditions		Process efficiency	PCC morphology	PCC purity	PCC yield [$kgCaCO_3/t_{SLAG}$]	CO_2 uptake [$kgCO_2/t_{SLAG}$]
		Dissolution step	Carbonation step					
Bao et al., 2010	Pre-dried at 60°C and milled < 297 μm [CaO] = 38.7%wt	Solution: Acetic acid in organic solvent TBP [0.6-1.2 M]; S/L= 25-200 g/l; Mixing rate=300-650 rpm; T=40-94°C; Time: 2-60 min.	Not Performed	Ca^{2+} extraction=80%; Selectivity = 100%	NM=Not Measured	NM	NM	NM
Bilen et al., 2018	Milled < 0.1 mm [CaO] = 48.8%wt	Solution: 0.7 M Acetic acid [0.1-1.0 M]. S/L= 65.4 g/l (38.5- 100 g/l); Mixing rate =700 rpm; T= 50°C (22-80°C); Time: 1.5 h (0.5-2.5 h)	Additive to neutralize pH: NaOH (Na/CH_3COO=0.93); T=50°C (30-70°C); CO_2 flow rate=22 l/min (5-22 l/min); pCO_2= 2 bar; Stirring rate= 600 rpm; Time=10' (2'-10')	Ca^{2+} extraction (optim.)= 61.5% (47%-67%) High selectivity at [CH_3COOH] ≤ 0.5M Carbonation effic. (optim.) = 89.7% (73.8%-97.1%). Overall effic.=57.2%	Scalenohedral calcite, particle size 1.8-5.8 μm at optimal conditions; uniformity 3.6	99.3%-99.7%	498.5 $kgCaCO_3/tSS$	219 $kgCO_2/tSS$
Chiang et al. 2014	Milled to a mean size of 138.3 μm [CaO] = 41%wt	Solution: Acetic acid [0.5-2 M] (added in 2 step); S/L= 137 g/l Mixing rate = 1000 rpm; Time: 1h; T=30°C	Additive to neutralize pH: $NaHCO_3$/ NaOH [same concentration as acetate] T= 90-120°C; pCO_2= 6-40 bar; CO_2 flow rate = NR; Stirring rate= 1000 rpm; Bubbling time: 1 h	Ca^{2+} extraction= 21% (at 0.5 M sol.); 47% (1M sol.); 90% (2M sol) Carbonation effic.= 96-99% for all tested conditions	Rhombohedral calcite + acicular aragonite + vaterite; Mean size < 20 μm	92.5-95.9% [<1 M sol.]; 86% [2M sol.]	335 kg $CaCO_3$/tBF**	147 $kgCO_2$/tBF**
Dri et al. 2013	Milled to 75-150 μm [CaO]= 38.44%wt	Solution: NH_4HSO_4 [1.3 M]. S/L= 50 g/l; Mixing rate =800 rpm; T=25-50-90°C; Time: 3 h	Not Performed	Ca^{2+} extraction= 5% due to precipitation as $CaSO_4$; High dissolution of Fe and Mg	NM	NM	NM	NM
Eloneva et al., 2008; Eloneva et al., 2009; Eloneva, 2010	BOF: [CaO]=45.9 %wt BF slag: [CaO]=34.5% wt DS: [CaO]=58.0% wt LS: [CaO]=49.4% wt Sieved: 74-125 μm	Tested solvent: 4 acids (acetic, propionic, nitric, sulfuric); 10 salts (sodium chloride, sodium acetate, ammonium chloride, ammonium acetate, ammonium nitrate, ammonium sulfate, ammonium di-hydrogen phosphate, ammonium hydrogen phosphate, aluminum sulfate, aluminum nitrate); sodium hydroxide; urea; Solvent concentrations: 0.1-0.2-0.3-0.5-1-2 M; S/L= 20 g/l; T≈20°C	Selected solution for carbonation: ammonium salts [0.5 M]; T=30-70°C; Stirring velocity=NR; CO_2 gas flow rate = 1 l/min (100% CO_2); Bubbling time: 1-2 h; Note: when acetic acid is used as solvent in the dissolution step, NaOH (20 g/l) was added before precipitation experiments	Ca^{2+} extraction (BOF, ammonium salts>0.5M)=50-80% Ca^{2+} extraction (BF, ammonium salts [0.5-2M]): <10%; poor selectivity; up to 80% with the use of acetic acid Ca^{2+} extraction (DS): 50-70% for NH_4NO_3 and CH_3COONH_4 [0.5-2M]; good selectivity Ca^{2+} extraction (LS) <25% for ammonium salts [0.5-2 M]; good selectivity Carbonation effic.= 50-70%	Rhombohedral calcite, particle size 5-30 μm	99.8% 63-89% (no PCC washing)	489 $kgCaCO_3$/tBOF	213 $kgCO_2$/tBOF

** estimated based on the stoichiometry, from the measured efficiencies of dissolution and carbonation processes and the [CaO] content in the slag.

Table 3.8.6 (continued). Main findings of the most relevant experimental studies on PCC production from iron and steel slags.

Study	Slag characteristics/ pre-treatment	Operating conditions		Process efficiency	PCC morphology	PCC purity	PCC yield [$kgCaCO_3/t_{SLAG}$]	CO_2 uptake [$kgCO_2/t_{SLAG}$]
		Dissolution step	Carbonation step					
Jo et al., 2017	Steel slag [CaO]=47%wt	Solution: [HCl]: 0.5-0.75-1M; S/L= 30-40-50-60 g/l; T =30°-50°-70° C; Time: 1h	Solution: 0.5M HCl (S/L=50 g/l); Additive to neutralize pH: NaOH [1M]; T=30°C; 100% CO_2, gas flow rate=NR; Time=NR	Ca^{2+} extraction=58.8% (0.5M) -82.7% (0.75M) -100% (1M). Poor selectivity (60% Mg extracted)	Rhombohedral calcite, 80-120 nm	98.5%	368-405 $kgCaCO_3/tSS$	162-178 $kgCO_2/tSS$
Kodama et al., 2008	Milled < 440 μm, calcinated at 950°C and sieved [CaO]= 44.5 %	Solution: 1M ammonium chloride (NH_4Cl); S/L= 63 g/l; Stirring rate: 300 rpm; T=80°C; Time: 1h	Additive to neutralize pH: none. Ca conc.=0.29 mol/l; Ti_n=40-90°C; CO_2 flow rate = 0.017 l/min (13%CO_2); Stirring rate = 1000 rpm; Bubbling time: 2 h	Ca^{2+} extraction=48.1% (mean) up to 59.5% (in fraction <63μm); Selectivity of Ca: 99.6% for NH_4Cl; Carbonation effic.=80% (40°C)	Cubic calcite (40°-60°C) Calcite + aragonite (80°-90°C) Size: NR	>98%	370 $kgCaCO_3/tSS$	162 $kgCO_2/tSS$
Kunzler et al., 2011	Pre-dried at 100°C, milled to 250-425 μm [CaO]=16% in SS	Solution: 0.29M HCl (range: 0-2M); S/L: 20-33.3-100 g/l; T= 25°C (range: 25-70°C); Time: 30'	Additive to neutralize pH: NaOH; T= 25°C; Ca conc. solution: 0.29 g/l; Gas flow rate:1 ml/min (100%CO_2); Bubbling time: 30'; Stirring rate: NR	Ca extraction: 76% (0.29 M sol., T=25°C) 85% (0.58 M sol., T=25°C) 88% (0.58 M sol., T=70°C); Poor selectivity at T>40°C Global efficiency (extraction + carbonation) = 83%	Cubic calcite Particle size: NR	> 98%	237 $kgCaCO_3/tSS$**	104 $kgCO_2/tSS$**
Mattila et al., 2012 (a), (b) Mattila 2014	Milled < 250 μm [CaO]=32.3-32.5%	Solvent tested: NH_4NO_3, NH_4Cl. Conc. NH_4Cl: 0.5-5 M; Conc. NH_4NO_3: 0.5-2 M; S/L=20-30-100-200 g/l; T=20°-70°C; Time: 1-2h; Stirring rate: 150-200 rpm	Additive to neutralize pH: none T= 20°-70°C; Ca conc. solution: 0.04-0.98 M; Gas flow rate: 0.5-1.0-2.0 l/min (100%CO_2); Bubbling time: 30'-90'; Stirring rate: NR	Ca extraction (1M NH_4Cl, 20°C, 200'): 33% one stage extraction - 46% in two extractors; Global efficiency= 42-45% (of reactive Ca); 16-28% of total Ca	NM	NM	170 $kgCaCO_3/tSS$	75 $kgCO_2/tSS$
Noack et al., 2014*	Ground < 1mm [CaO]=37-41%	Solvent tested: sodium bicarbonate/pure water; Solvent conc.= 0.5 M; S/L= 167 g/l; T=NR; Mixing rate=350-500 rpm; Time=1-4 h		Global efficiency= 24%	Calcite	NM	160 kg $CaCO_3/tSS$ **	70 $kgCO_2/tSS$**

** estimated based on the stoichiometry, from the measured efficiencies of dissolution and carbonation processes and the [CaO] content in the slag.

Table 3.8.6 (continued). Main findings of the most relevant experimental studies on PCC production from iron and steel slags.

Studies	Slag characteristics/ pre-treatment	Operating conditions		Process efficiency	PCC morphology	PCC purity	PCC yield [$kgCaCO_3/t_{SLAG}$]	CO_2 uptake [$kgCO_2/t_{SLAG}$]
		Dissolution step	Carbonation step					
Said et al., 2013	Milled and sieved: 74-125 μm; [CaO]= 44.9%	Tested solvent: NH_4NO_3, NH_4Cl, CH_3COONH_4. Conc.:0.5-2 M; S/L= 5 up to 100 g/l; T=30°C; Mixing Rate: 600 rpm; Time: 1h	No additive; T=30°C; CO_2 gas flow rate = 1 l/min; Mixing rate: 600 rpm	Ca^{2+} extraction (at S/L=20 g/l): 37-45% (NH_4Cl: 0.5-2M); 42-50% (NH_4NO_3: 0.5-2M); 41-50% (CH_3COONH_4: 0.5-2M)	Rhombohedral calcite, particle size < 10μm	NR	NR	NR
Said et al., 2016 (Pilot plant)	Milled <250 μm, [CaO]= 51.4 %	Solution: NH_4Cl [1M]; S/L= 100 g/l; T=20°C; Mixing rate: 200 rpm; Time: up to 1 h (solvent can be reused for more than 10 times)	No additive; T=25°-45°C; CO_2 gas flow rate=10-15 l/min (100% CO_2); Mixing rate: 170 rpm; Bubbling time: 1-2 h	Ca^{2+} extraction: 60% (recycled solvent) – 78% (fresh solvent); Overall estimated efficiency=55%	Rhombohedral calcite (25°C),size <30-40 μm; Aragonite/calcite (60/40) at 45°C, size <50 μm	>99.5%	≈500 $kgCaCO_3/tSS$	≈220 $kgCO_2/tSS$
Sudermann, 2016	[CaO]=25.40%	Solution: 1M NH_4Cl; S/L ≈ 100 g/l; Mixing rate = 200 rpm; Time: 1 h; Temperature 25°C	No additive; Tin=25°-45°C; CO_2 flow: 10 l/min; Time: 0.5-2 h; Mixing rate: NR	Ca^{2+} extraction (average): 35.2% at 25°C 39.7% at 40°C	Rhombohedral calcite (25°C), size 24-40 μm; Aragonite/Calcite (60/40) at 45°C, size 12-15 μm	Close to 100% for most of test conditions	NM	NM
Teir et al., 2016	Milled <250 μm; [CaO]=51.40%	Solution: 1.0M NH_4Cl; S/L= 100 g/l; T=20°C; Mixing rate = 200 rpm; Time: 1 h	No additive; T_{in}=20°C - 55°C; Gas flow rate: 13 l/min (100% CO_2); Bubbling time: 1h; Stirring velocity: 200 rpm	NM	Rhombohedral calcite at 20°C, size <84 μm; Aragonite at 55°C, size< 50 μm	NM	NM	NM

A purity of PCC up to 99.3%-99.9% may be achieved according to Bilen et al. (2018), Eloneva et al. (2009), Mattila (2014) and Said et al. (2016) from steelmaking slags using ammonium salt solutions as solvents; both rhombohedral and scalenohedral calcite can be produced, while pure and homogeneous aragonite has never been obtained, with the only exception of Teir et at., 2016 (Table 3.8.6). Sudermann (2016) indicates that pure calcite in the rhombohedral form and a mixture of aragonite/calcite can be successfully synthetized from steelmaking slag in the X2PCC pilot plant at temperature of 25°C and 40°C, respectively. Likewise, rhombohedral calcite with a diameter of 5-30 μm and a purity of 99.8% can be obtained from steel converter slag through the method described in the US patent number 8,603,428 (Tier et al., 2013). Slightly lower PCC purity (98%-98.5%) were attained from steel slags in the experimental works of Jo et al. (2017) and Kunzler et al. (2011), when HCl is used as solvent in the dissolution step and NaOH is added to adjust the pH of the carbonation solution.

Regarding the particle size of PCC obtained from steel slag, in almost all the experiments (Table 3.8.6) it was found larger than the typical particle size of commercial PCC (1-3 μm for filling applications, but nanometre scale is required in special cases) which implies the need for post-processing the PCC. The larger particle diameter observed in these experiments (Eloneva et al., 2008 and 2009; Said et al., 2013 and 2016; Teir et al., 2016) can be explained with the higher calcium concentration in the carbonation solution (up to 0.25 mol/l instead of 0.04 mol/l in traditional PCC production) due to the high solid to liquid ratio applied, the lower initial carbonation pH (9-10 instead of a typical pH=12-13 in traditional carbonation) and the longer precipitation time (1-2 h). Indeed, all these conditions seem to favour a rapid agglomeration of particles (Mattila, 2014).

In conclusion, results from the literature analysis indicate that steelmaking slags are suitable materials for synthetizing high purity PCC in line with the requirements for industrial applications, once all process parameters are optimized. The still critical aspects regard the particle size and morphology of PCC products (influencing their market values), the lifetime of the process solvent (i.e., the maximum reuse cycles assuring adequate PCC quality) and possible uses of solid residues (accounting for 88% of the steel slag used in the process). All these aspects directly affect the economic viability of the carbonation process at the industrial scale.

PCC production from iron and steelmaking slags: carbonation rate of lime

As shown in Table 3.8.6, there is a wide variation in the amount of PCC produced (160-500 $kgCaCO_3/t_{SLAG}$) and the CO_2 sequestration capacity (70-220 $kgCO_2/t_{SLAG}$) detected in the experiments, depending on the applied operating conditions and the initial characteristics of steelmaking slags. In some experiments, the PCC yield and the CO_2 capture were directly measured (Bilen et al., 2018; Eloneva et al., 2008; Eloneva et al., 2009; Jo et al., 2017; Kodama et al., 2008; Mattila et al., 2012 (a,b); Said et al., 2016); in three studies (Chiang et al., 2014; Kunzler et al., 2011; Noack et al., 2014) only data about the efficiencies of the calcium extraction and the carbonation steps and the initial [CaO] content in the slag were provided, thus the PCC production and the CO_2 uptake can be estimated based on those data. It is worth pointing out that this may lead to some

overestimating of the actual CO_2 uptake and PCC yield, because the mass losses during the filtration and purification steps cannot be included in the computation.

Based on the experimental data (9 studies), on average 153 (± 56) $kgCO_2/t_{SLAG}$ can be sequestered from indirect carbonation of steelmaking slag while producing 350 (± 128) $kgPCC/t_{SLAG}$. The CO_2 uptake per tonne of PCC produced from steelmaking slag resulted in 439 $kgCO_2$/tPCC, very close to the theoretical value of 440 $kgCO_2$/tPCC.

By considering the following assumptions for the BOF steel making route (see Chapter 3.1):

- an average production of 106 kg of slag / t crude steel;
- a specific lime addition of 30-67 kg / t of crude steel (JRC, 2013 a)

it results that approximately 334 kg of CO_2 can be sequestered in PCC per tonne of lime added to the steelmaking process.

Moreover, considering that the production of 1 tonne of lime releases in the atmosphere 786 kg of CO_2 (only from the calcination process, excluding the fuel consumption; JRC, 2013b), it results that, on average, 43% of the CO_2 emitted from the calcination process could be later on captured by the steel converter slag destined to the PCC production.

3.8.4. DISCUSSION AND CONCLUSIONS

Currently, the carbonation process is the most applied and cost-efficient method for PCC production in Europe. According to the BREF Document related to inorganic chemicals (EC, 2007), this process results in an almost null net CO_2 emission. About 85-93% of the added lime is, indeed, carbonated during the PCC manufacturing. In the second part of the chapter, also the production of PCC via indirect carbonation of the alkaline wastes was analysed. The focus was on iron and steel slags, the most promising material due to the high CaO content and the large availability. According to 9 literature studies, about 45% of the CO_2 emitted during the production of lime for the ferrous industry can be later captured by the slags destined to the PCC production. However, it should be stressed that this estimate derives only from tests performed at the lab-scale or at most in pilot plants. The particle size and morphology of the derived PCC, the lifetime of the extracting solvent (i.e., the maximum reuse cycles) and the disposal of significant quantity of solid residues (88% of the input slags) currently affect the economic viability of the process at the industrial scale.

REFERENCES

Ahn, J.-W., Kim, J.-H., Park, H.-S., Kim, J.-A., Han, C., Kim, H., 2005. *Synthesis of single phase aragonite precipitated calcium carbonate in $Ca(OH)_2$ -Na_2CO_3 -NaOH reaction system*. Korean Journal of Chemical Engineering 22(6), 852-856. DOI: https://doi.org/10.1007/BF02705664

Bao, W., Li, H., Zhang, Y., 2010. *Selective leaching of steelmaking slag for indirect CO_2 mineral sequestration*. Industrial & Engineering Chemistry Research 49(5), 2055-2063. DOI: https://doi.org/10.1021/ie801850s

Bilen, M., Altiner, M., Yildirim, M., 2018. *Evaluation of steelmaking slag for CO_2 fixation by leaching-carbonation process*. Particulate Science and Technology 36(3), 368-377. DOI: https://doi.org/10.1080/02726351.2016.1267285

Chang, R., Kim, S., Lee, S., Choi, S., Kim, M., Park, Y., 2017. *Calcium carbonate precipitation for CO_2 storage and utilization: a review of the carbonate crystallization and polymorphism*. Frontiers in Energy Research 10. DOI: 10.3389/fenrg.2017.00017

Chiang, Y.W., Santos, R.M., Elsen, J., Meesschaert, B., Martens, J.A., Van Gerven, T., 2014. *Towards zero-waste mineral carbon sequestration via two-way valorization of ironmaking slag*. Chemical Engineering Journal, 249, 260-269. DOI: http//dx.doi.org/10.1016/j.cej.2014.03.104

Dri, M., Sanna, A., Maroto-Valer, M.M., 2013. *Dissolution of steel slag and recycled concrete aggregate in ammonium bisulphate for CO_2 mineral carbonation*. Fuel Processing Technology 113, 114-122. DOI: https://doi.org/10.1016/j.fuproc.2013.03.034

Eloneva, S., Teir, S., Salminen, J., Fogelholm, C.-J., Zevenhoven, R., 2008. *Steel converter slag as a raw material for precipitation of pure calcium carbonate*. Industrial & Engineering Chemistry Research 47(18), 7104-7111. DOI: https://doi.org/10.1021/ie8004034

Eloneva, S., Teir, S.,Revitzer, H., Salminen, J., Said, A., Fogelholm, C.-J., Zevenhoven, R., 2009. *Reduction of CO_2 emissions from steel plants by using steelmaking slags for production of marketable calcium carbonate*. Process Metallurgy 80(6), 415-421. DOI: https://doi.org/10.2374/SRI09SP028|

Eloneva, S., 2010. *Reduction of CO_2 emissions by mineral carbonation: steelmaking slags as raw material with a pure calcium carbonate end product*. Doctoral thesis, Aalto University, Faculty of Engineering and Architecture, Department of Energy Technology. Available online: https://aaltodoc.aalto.fi/handle/123456789/4876

Eloneva, S., Said, A., Fogelholm, C.-J., Zevenhoven, R., 2010. *Feasibility study of a method utilizing carbon dioxide and steelmaking slags to produce precipitated calcium carbonate (PCC)*. In: Proceedings of the 2nd International Conference on Applied Energy (ICAE 2010). Singapore, 21-23 April 2010. Pages 169-178. https://www.researchgate.net/publication/267558532_Process_efficiency_and_optimisation_of_precipitated_calcium_carbonate_PCC_production_from_steel_converter_slag

Erdogan, N. and Eken, H.A., 2017. *Precipitated calcium carbonate production, synthesis and properties*. Physicochemical Problems of Mineral Processing 53(1), 57-68. DOI: http://dx.doi.org/10.5277/ppmp170105

European Commission, 2007. *Reference Document on Best Available Techniques (BREF) for the Manufacture of Large Volume Inorganic Chemicals - Solids and Others Industry*. Available online: https://eippcb.jrc.ec.europa.eu/reference/BREF/lvic-s_bref_0907.pdf

He, L., Yu, D., Lv, W., Wu, J., Xu, M., 2013. *A novel method for CO_2 sequestration via indirect carbonation of coal fly ash*. Industrial & Engineering Chemistry Research 52, 15138-15145. DOI: dx.doi.org/10.1021/ie4023644

Islam, M.S. and Quader, K.M.A., 2008. *Laboratory-scale production of commercial grade calcium carbonate from lime-soda process*. Chemical Engineering Research Bulletin 12, 1-6. DOI: https://doi.org/10.3329/cerb.v12i0.1490

Järvinen, M., Said, A., Zappa, W., Eloneva, S. Report from Aalto University, School of Engineering 2010. *Success story on mineral carbonation of CO_2*. Pushing academic research towards industrial scale through advanced modelling and piloting.

Jimoh, O.A., Otitoju, T.A., Hussin, H., Ariffin, K.S., Baharun, N., 2017. *Understanding the precipitated calcium carbonate (PCC) production mechanism and its characteristics in the liquid-gas system using milk of lime (MOL) suspension*. The South African Journal of Chemistry 70, 1-7. https://www.ajol.info/index.php/sajc/article/view/154848

Jo, H., Park, S.-H., Jang, Y.-N., Chae, S.-C., Lee, P.-K., Jo, H.Y., 2014. *Metal extraction and indirect mineral carbonation of waste cement material using ammonium salt solutions*. Chemical Engineering Journal 254, 313-323. DOI: https://doi.org/10.1016/j.cej.2014.05.129

Jo, H., Lee, M.-G., Park, J., Jung, K.-D., 2017. *Preparation of high-purity nano-$CaCO_3$ from steel slag*. Energy 120, 884-894. DOI: https://doi.org/10.1016/j.energy.2016.11.140

JRC, 2013a. *BREF document for iron and steel production*. Available online: https://eippcb.jrc.ec.europa.eu/reference/BREF/IS_Adopted_03_2012.pdf

JRC, 2013b. *BREF Document for the Production of cement, lime and magnesium oxide*. Available online: https://eippcb.jrc.ec.europa.eu/reference/BREF/CLM_Published_def.pdf

Katsuyama, Y., Yamasaki, A., Iizuka, A., Fujii, M., Kumagai, K., Yanagisawa, Y., 2005. *Development of a process for producing high-purity calcium carbonate ($CaCO_3$) from waste cement using pressurized CO_2*. Environmental Progress vol. 24/2, 162-170. DOI: https://doi.org/10.1002/ep.10080

Kodama, S., Nishimoto, T., Yamamoto, N., Yogo, K., Yamada, K., 2008. *Development of a new pH-swing CO_2 mineralization process with a recyclable reaction solution*. Energy 33(5), 776-784. DOI: https://doi.org/10.1016/j.energy.2008.01.005

Kunzler, C., Alves, N., Pereira, E., Nienczewski, J., Ligabue, R., Einloft, S., Dullius, J., 2011. *CO_2 storage with indirect carbonation using industrial waste*. Energy Procedia 4, 1010-1017. DOI: https://doi.org/10.1016/j.egypro.2011.01.149

Lei, M., Li, P.G., Sun, Z.B., Thang, W.H., 2006. *Effects of organic additives on the morphology of calcium carbonate particles in the presence of CTAB*. Materials Letters 60(9-10), 1261-1264. DOI: https://doi.org/10.1016/j.matlet.2005.11.023

Li, G., Li, Z., Ma, H., 2014. *Preparation of aragonite by carbonization in $CaCl_2$-NH_4Cl solution without any additives*. Monatshefte für Chemie - Chemical Monthly 145(1), 187-194. DOI: https://doi.org/10.1007/s00706-013-0995-6

Mattila, H.-P., Grigaliūnaite, I., Zevenhoven, R. 2012(a). *Chemical kinetics modelling and process parameter sensitivity for precipitated calcium carbonate production from steelmaking slags*. Chemical Engineering Journal 192, 77-89. DOI: https://doi.org/10.1016/j.cej.2012.03.068

Mattila, H.-P., Grigaliunaite, I., Said, A., Filppula, S., Fogelholm, C.-J., Zevenhoven, R., 2012(b). *Process efficiency and optimisation of precipitated calcium carbonate (PCC) production from steel converter slag*. In: Proceedings of ECOS 2012, 25th International Conference on Efficiency, Cost, Optimization, Simulation and Environmental Impact of Energy Systems, June 26-29, 2012, Perugia, Italy. Available online: https://pdfs.semanticscholar.org/581e/8b24ca9bae6386ca5f0bbd56e260c3f809e1.pdf

Mattila, H.P., 2014. *Utilization of steelmaking waste materials for production of calcium carbonate ($CaCO_3$)*. Doctoral thesis, Åbo Akademi University, Department of Chemical Engineering. Available online: https://www.doria.fi/handle/10024/99011

Mattila, H.P. and Zevenhoven, R., 2014. *Production of Precipitated Calcium Carbonate from steel converter slag and other calcium-containing industrial wastes and residues*. Advanced in Inorganic Chemistry, vol. 66, Chapter 10, 347-384. DOI: https://doi.org/10.1016/B978-0-12-420221-4.00010-X

Mattila, H.-P., Hudd, H., Zevenhoven, R., 2014. *Cradle-to-gate life cycle assessment of precipitated calcium carbonate production from steel converter slag*. Journal of Cleaner Production 84, 611-618. DOI: https://doi.org/10.1016/j.jclepro.2014.05.064

Mathur, V.K., 2002. *Precisely sized precipitated calcium carbonate (PCC) crystals of preselected crystal habit, manufactured using pressure carbonation*. Available online: https://patents.com/us-8936771.html

Noack, C.W., Dzombak, D.A., Nakles, D.V., Hawthorne, S.B., Heebink, L.V., Dando, N., Gershenzon, M., Ghosh, R.S., 2014. *Comparison of alkaline industrial wastes for aqueous mineral carbon sequestration through a parallel reactivity study*. Waste Management 34(10), 1815-1822. DOI: https://doi.org/10.1016/j.wasman.2014.03.009

Othman, A., Othman, R., Mohd Sabri, S.N, 2017. *Producing Precipitated Calcium Carbonate with and without terpineol*. Chemical Engineering Transactions 56, 421- 426. DOI: https://doi.org/10.3303/CET1756071

Pan, S.-Y., Chiang, A., Chang, E-E, Lin, Y.-P., Kim, H., Chiang, P.-C., 2015. *An innovative approach of integrated carbon mineralization and waste utilization: a review*. Aerosol and Air Quality Research 15(3), 1072-1091. DOI: 10.4209/aaqr.2014.10.0240

Patent US 7,378,073 B2. Inventor: de Pauw Gerlings, Martinus J.H., Date of publication: 27.05.2008. Available online: https://patentimages.storage.googleapis.com/d5/3a/7d/d9e101813df8a1/US7378073.pdf

Pohl, M., Rainer, C., Primosch, G., 2011. *Patent EP2371766A1*: *Process for obtaining precipitated calcium carbonate*. https://patents.google.com/patent/EP2371766A1/en?oq=+EP+2371766A1

Said, A., Mattila, H.-P., Järvinen, M., Zevenhoven, R., 2013. *Production of precipitated calcium carbonate (PCC) from steelmaking slag for fixation of CO_2*. Applied Energy 112, 765-771. DOI: https://doi.org/10.1016/j.apenergy.2012.12.042

Said, A., Laukkanen, T., Järvinen, M., 2016. *Pilot-scale experimental work on carbon dioxide sequestration using steelmaking slag*. Applied Energy 177, 602-611. DOI: https://doi.org/10.1016/j.apenergy.2016.05.136

Schyvinck, L., 2012. *Reducing CO_2 emissions*. Workshop on CO_2 reuse, October 24, 2012, Brussels.

Sezer, N., 2013. *Production of precipitated calcium carbonate from marble wastes*. Master Thesis in Mining Engineering, Middle East Technical University. Available online: http://etd.lib.metu.edu.tr/upload/12616347/index.pdf

Steinhauser, G., 2008. *Cleaner Production in the Solvay Process: general strategies and recent developments*. Journal of Cleaner Production 16(7), 833-841. DOI: https://doi.org/10.1016/j.jclepro.2007.04.005

Stolaroff, J.K., Lowry, G.V., Keith, D.W., 2005. *Using CaO- and MgO-rich industrial waste streams for carbon sequestration*. Energy Conversion and Management 46(5), 687-699. DOI: https://doi.org/10.1016/j.enconman.2004.05.009

Sundermann, C.M., 2016. *Production of calcium carbonate from steelmaking slag and captured CO_2-Optimization of the carbonation process and product quality*. Master Thesis in Innovative Sustainable Energy Engineering, Aalto University, Finland and Royal Institute of Technology, Sweden. Available online:https://aaltodoc.aalto.fi/bitstream/handle/123456789/23965/master_Sundermann_Carla_2016.pdf?sequence=1&isAllowed=y

Teir, S., Eloneva, S., Zevenhoven, R., 2005. *Production of precipitated calcium carbonate from calcium silicates and carbon dioxide*. Energy Conversion and Management 46(18-19), 2954-2979. DOI: https://doi.org/10.1016/j.enconman.2005.02.009

Teir, S., Eloneva, S., Fogelholm, C.-J., Zevenhoven, R., 2007. *Dissolution of steelmaking slags in acetic acid for precipitated calcium carbonate production*. Energy 32(4), 528-539. DOI: https://doi.org/10.1016/j.energy.2006.06.023

Teir, S., Eloneva, S., Revitzer, H., Zevenhoven, R., Salminen, J., Fogelholm, C.-J., Poylio, E., 2013. *Patent US 8,603,428 B2/2013. Method of producing calcium carbonate from waste and by-product*. Available online: https://patents.google.com/patent/US8603428B2/en

Teir, S., Auvinen, T., Said, A., Kotiranta, T., Peltola, H., 2016. *Performance of separation processes for precipitated calcium carbonate produced with an innovative method from steelmaking slag and carbon dioxide*. Frontiers in Energy Research 4, Article 6, 1-13. DOI: 10.3389/fenrg.2016.00006

Thriveni, T., Il, U.N., Ahn, J.W., 2013. *Aragonite precipitated calcium carbonate: a new versatile functional filler for light weight plastic*. In: Proceedings of the 8th Pacific Rim International Conference on Advanced

Materials and Processing. Edited by Fernand Marquis, The Minerals, Metals and Materials Society, 243-253. DOI: https://doi.org/10.1007/978-3-319-48764-9_31

Uibu, M., Velts, O., Kuusik, R., 2010. *Developments in CO_2 mineral carbonation of oil shale ash*. Journal of Hazardous Materials 174(1-3), 209-214. DOI: https://doi.org/10.1016/j.jhazmat.2009.09.038

Velts, O., Uibu, M., Kallas, J., Kuusik, R., 2011. *Waste oil shale ash as a novel source of calcium for precipitated calcium carbonate: carbonation mechanism, modelling, and product characterization*. Journal of Hazardous Materials 195, 139-146. DOI: 10.1016/j.jhazmat.2011.08.019

Velts, O., Uibu, M., Kallas, J., Kuusik, R., 2013. *CO_2 mineralisation: concept for co-utilization of oil shale energetics waste streams in $CaCO_3$ production*. Energy Procedia 37, 5921-5928. DOI: https://doi.org/10.1016/j.egypro.2013.06.518

Wardhani, S., Prasetia, F., Khunur, M.M., Purwonugroho, D., Prananto, Y.P., 2018. *Effect of CO_2 flow rate and carbonation temperature in the synthesis of crystalline precipitated calcium carbonate (PCC) from limestone*. Indonesian Journal of Chemistry 18(4), 573-579. DOI: 10.22146/ijc.26608

4. CONCLUSIONS OF THE LITERATURE REVIEW ON LIME CARBONATION

This work has assessed the potential of CO_2 uptake by carbonation during the use of lime products in multiple applications, according to Pillar 2 of 2050 EuLA vision, "Lime sector will be Carbon Negative by 2050" (EuLA 2020, Annual report. Pp. 31-33). This vision is consistent with the "European Green Deal" Communication and the consequent "Proposal for a Regulation of the European Parliament and of the Council establishing the framework for achieving climate neutrality and amending Regulation (EU) 2018/1999" which sets the climate neutrality around 2050 as long-term goal for the European Union, i.e. the balance between emissions and removals compensating not only the remaining emission of CO_2 but also of all greenhouse gases.

The carbonation can be seen as a permanent CO_2 removal process, since CO_2 is absorbed by lime and stored in the form of calcium carbonate ($CaCO_3$), that is the carbonation product. Thanks to carbonation, lime will partially or totally reabsorb (depending on the specific application) the CO_2 previously emitted during calcination, excluding the emission from fuel combustion. The ratio between the amount of CO_2 absorbed during carbonation and that emitted during calcination is the carbonation rate, expressed in percentage. This study has reviewed the literature on carbonation rate under both natural (i.e. when lime reacts with the ambient carbon dioxide) and enhanced conditions (i.e. when the carbonation is carried out under enhanced carbon dioxide concentration, but also by optimising other parameters such as the temperature, the relative humidity, the surface reactivity area, the pH and others, depending on the reaction matrix in the solid, water or gaseous phase).

The literature assessment about the carbonation potential of lime during its use phase has covered almost all the market sectors, in particular the ferrous (iron and steel) industry, the construction materials (sand lime bricks – SLB, light-weight lime concrete - autoclaved aerated concrete – AAC, mortars, hemp lime construction materials), the civil engineering (soil stabilisation and asphalt pavement), the environmental protection (flue gas treatment, treatment of drinking water, of wastewater, of biosolids and of dredging sediments), the agriculture, the chemical industry, other industries (non-ferrous industries) and pulp and paper. In Table 4.1 the distribution of lime in the different applications is reported for the year 2018, when the total lime production was around 20 million tonnes in Europe including UK.

Table 4.1. Distribution of lime (CaO) produced in Europe including UK between the different applications in 2018.

Lime applications (Adapted from EuLA database)	Lime sub-applications (Adapted from EuLA database)	Lime amount (thousands of tonnes of CaO)
Iron & Steel industry	Iron & Steel industry	**8,325**
Construction Materials	Sand lime brick (Silica brick)	**596**
	Light-weight lime concrete	**894**
	Pure air lime mortars	**86**
	Mixed air lime mortars (90%)	**588**
	Hemp-lime	**10**
	Other (paints, natural fibres...)	**318**
Civil Engineering	Soil stabilisation	**1,308**
	Asphalt pavements	**23**
Environmental Protection	Drinking water	**424**
	Wastewater treatment	**874**
	Sludge treatment	**593**
	Flue gas cleaning systems	**1,595**
	Other (Acid Mine Drainage – AMD, lake liming...)	**127**
Agriculture	Fertiliser	**331**
	Other (sanitation, aquafarming, ...)	**280**
Chemical Industry	Calcium carbide	**63**
	Soda	**19**
	Petrochemical	**318**
	Other (salts, leather tanning, ...)	**1,017**
Other Industrial Consumers	Sugar	**35**
	Glass	**158**
	Non-ferrous metal industry without aluminium	**315**
	Aluminium	**276**
	Other	**608**
Pulp & Paper	Pulp and Paper	**1,204**

The assessment is based on 668 documents, of which 197 are relevant, i.e. documents that provide quantitative and qualitative information useful for the evaluation of the carbonation rate in the specific lime applications.

Table 4.2 shows the main characteristics of the analysed literature, most of the relevant sources are peer-reviewed papers and the Best Available Techniques Reference documents (BREFs) which account for around 80% of the assessed literature. Documents are seldom related to full-scale experimental researches, especially for enhanced carbonation, that is mainly applied at the laboratory or at the pilot scale. Generally, European literature sources are available for each application, except for aluminium production, titanium dioxide production and AAC, for which mainly non-EU data sources were found.

Based on the findings, each application has been associated to a different colour-code according to the following clusters:

Applications with conclusive scientific data, where the amount of literature published on carbonation allows for statistical treatment or the results presented are consistent throughout these publications/reports to establish the carbonation rate being natural or enhanced.

Applications with less conclusive scientific data, where the amount of literature published on carbonation is insufficient to allow data comparability, thus the outcome is less conclusive to establish any carbonation rates (natural or enhanced).

Applications with no information available, where due to the low volume of lime in the application there are few studies on carbonation, and in particular no studies to estimate the carbonation rate.

Not assessed applications, where due to the low volume of lime in the application, there are no studies on carbonation. Thus, they are not covered in the scope of this literature review.

Table 4.3 reports the main literature findings about the carbonation rates in the different applications where lime is used. Each carbonation rate is expressed as the percentage of the CO_2 emitted during the production of lime excluding the fuel combustion emission (786 kg/t lime, according to the BREF Document for Cement, Lime and Magnesium Oxide Manufacturing Industries published by the European Commission pursuant to Emissions Directive 2010/75/EU (Integrated Pollution Prevention and Control). Based on this extensive literature review on carbonation, the conclusions reported in section 4.1-4.5 can be derived.

Based on the factors which affect enhanced carbonation reported in Table 4.4 and the assessed literature, the conditions for effective enhanced carbonation in conclusive applications is reported in Table 4.5.

4.1. Lime applications with conclusive scientific data on carbonation

Around 61% of the overall lime applications have relevant and consistent information in the literature allowing conclusive assessment on natural and enhanced carbonation rates as summarized in Table 4.6.

Steel slags' carbonation rate in the steel application, which is the major application of lime, can reach up to about 30% in natural conditions and about 60% when the operating conditions are optimized.

Among the other analysed sectors, a carbonation rate very close to 100% is reported for pure air lime mortars (80-92%), for the conventional production of precipitated calcium carbonate (PCC) in pulp and paper application (85-93%) and for the softening of water in drinking water application (100%).

In the building materials sector, information about the carbonation rate of mortars are robust. Pure air lime mortars show a relatively high carbonation rate in the long-term, i.e. 80-92% after 100 years, while mixed air lime mortars have a carbonation rate that is one fourth of pure air lime mortars (20-23%). The sector of hemp lime construction materials is also a conclusive application due to the extensive work and publications carried out particularly in UK and France, which show a good consistency around the value of 55% for hemp lime with similar composition.

Finally, the flue gas treatment and the ferrous and aluminium production sectors have in common the fact that under enhanced carbonation the solid residues can be used as a feedstock material for effective CO_2 sequestration. For Air Pollution Control Residues (APCR), a carbonation rate of about 30% is reported) the rate can reach up to about 60% when the operating conditions are optimized. The only exception is the red mud, i.e. the solid residue from the aluminium production, which shows a low carbonation rate for both natural ageing and enhanced carbonation. In this case, most of the CO_2 sequestration is due to the use of sodium hydroxide rather than lime. The literature about lime carbonation is quite abundant and results are promising; the limitation is related to the fact that so far only lab-scale tests have been performed, except for the APCR treatment. A strong push towards upscaling such processes to the industrial scale is then highly encouraged.

4.2 Lime applications with less conclusive scientific data on carbonation

Around 21% of the overall lime applications are less conclusive applications due to the low number of publications. The natural and enhanced carbonation rates of these applications are reported in Table 4.7.

For construction materials, not all the sub-applications have very robust studies available. In particular, for light-weight lime concrete (also called aerated autoclaved concrete – AAC) a 60% carbonation potential was recorded after 30 years of service life under natural conditions. However, this rate cannot be attributed only to the lime, since some free CaO is also present in the cement used as a raw material. Moreover, the data were collected in Japan (researchers by Matsushita et al.), which means they can be extrapolated only to the European areas with similar climate conditions. Regarding SLB, a 30% carbonation rate was reported during the service life (the age of the samples not being reported). However, this is based on one single literature source dating back 25 years ago (Eden et al., 1995). New analyses on samples taken from European buildings of different ages in terms of service life should be performed in order to confirm the amount of sequestered CO_2 previously indicated and to better understand the time evolution of the carbonation process in outdoor ambient conditions.

A similar conclusion can be drawn for the use of lime in the treatment of biosolids in the wastewater treatment plants (conditioning or sanitation after a dehydration unit). Two literature sources report a 40-50% carbonation rate for stocked biosolids, but the assessments were performed 25-30 years ago and moreover the time elapsed between the lime dosage and the sampling was not reported. When lime is used for the treatment of dredging sediments, the CO_2 permanently captured is 35% after 30 years. Neverthless this rate is highly uncertain because it is related to the application of lime to soils and not to sediments.

Further research is needed for confirming the carbonation rate of soil stabilisation and calcium carbide. Regarding the former, only one study provides a carbonation rate, while calcium carbide carbonation rate depends on the actual use of the carbide lime, which is the by-product of the main application of calcium carbide, i.e. the acetylene production. More information on the uses of carbide lime (i.e. how much of it is used for soil stabilization, PCC and others) and on soil stabilisation carbonation is necessary.

4.3. Lime applications with no available information on carbonation or not assessed

Lime applications with no available information on carbonation account for 6.3% of the European lime market in 2018, while applications not assessed account for 11.4%. Thus, all these applications account for around 18% of the European lime market in 2018.

Lime applications with no available information on carbonation are: agriculture, acid mine drainage, some sectors in the non-ferrous metallurgy without aluminium (production of base metals, of precious metals, and of lithium), asphalt pavements, soda and petrochemical. In all these applications the scientific literature on the topic is almost non-conclusive. In particular, for agriculture the existing literature focuses on the application of limestone and dolomite as liming materials, while for the treatment of sediments indications are available for the same reclamation technology (solidification and stabilization) but related to soil, a quite different material. In case of non-ferrous metals, no information was derived apart from the overall amount of calcium in the slags and/or tailings and its mineralogical composition.

Other minor applications in construction materials, chemical industry and other industrial consumers were not assessed since no information about lime carbonation was identified in the literature.

Table 4.2. Main information about the literature assessment: number of papers consulted per each application and relative characteristics. NC=natural carbonation; EC= enhanced carbonation. Caption: **applications with conclusive scientific data**, **applications with less conclusive scientific data** and **no information available**.

Lime application		N° total sources	Type of source	Type of test (field vs. lab-test)	Test duration	Geographical context
Iron and steel industry	Iron Slags	NC: 2	Peer-reviewed papers	Field tests	6 months - 100 years	1 paper: UK; 1 paper: USA
		EC:12	9 peer-reviewed papers + 1 BREF document + 2 websites (statistics about European steel and slags production)	Lab-tests	Generally 1 hour	4 papers: Europe (UK, Belgium, Poland, and Finland) 5 papers: Korea, Taiwan, China
	Steel slags	NC: 8	5 peer-reviewed papers + 1 BREF document + 2 websites	3 papers: field scale 1 paper: lab-scale 1 paper: both cases	Lab-scale: 1-12 weeks Field cases: 4-18 months	3 papers: Europe (Italy, Germany, and Spain) 2 papers: USA
		EC: 26	21 peer-reviewed papers + 1 master thesis + 1 report from ENEA + 1 BREF document + 2 websites	Lab-scale	1 minute - 12 weeks	All documents from Europe (mainly Italy, Belgium and the Netherlands) except for 6 papers (China, Taiwan, Canada, and USA)
Construction materials	Sand lime bricks	1	Report of the German Federal Association of Sand Lime Brick	Field test	Not available	Germany
	Light-weight lime concrete - Autoclaved aerated concrete	6	Peer-reviewed papers	Field tests	From 0 up to 33 years	5 papers: Japan 1 paper: Germany
	Pure air lime mortars	1	1 literature review (21 publications)	In the literature review is considered field and lab-scale tests	Different operating conditions tested	Valid for all contexts

Lime application			N° total sources	Type of source	Type of test (field vs. lab-test)	Test duration	Geographical context
	Mixed air-lime mortars		1	1 literature review (27 publications)	In the literature review is considered field and lab-scale tests	Different operating conditions tested	Valid for all contexts
Construction materials	Hemp lime		9	8 peer-reviewed papers; 1 meeting proceedings or seminars	5 documents: Life Cycle Assessment (LCA) 3 documents: lab-scale 1 document: lab and LCA	Lab-scale: 28 days – 10 months	8 documents: Europe (France, United Kingdom, Italy, Latvia) 1 document: India
Civil engineering	Soil stabilisation		6	2 peer-reviewed papers; 4 meeting proceedings or seminars	2 documents: field tests 1 document: lab-scale	Field tests: 3 – 34 years Lab-scale: 3 – 90 days	Germany; Virginia (USA); Belgium
	Asphalt pavements		0	7 documents but none reports information about carbonation rate of Hot Mix Asphalt	-	-	-
Environmental protection	Drinking water		2	2 peer-reviewed papers about water softening	Full-scale	-	Valid for all contexts
	Wastewater treatment		2	Peer-reviewed papers about biosolids	Field tests	Not available	Germany
	Sludge treatment - dredging sediments		2	Peer-reviewed papers	Field tests	From 3 to 34 years	Germany and USA
	Flue gas treatment	NC	5	4 peer-reviewed papers + 1 BREF document	4 full-scale tests	Few seconds	Europe (mainly Italy and UK)

Lime application			N° total sources	Type of source	Type of test (field vs. lab-test)	Test duration	Geographical context
		EC	18	14 peer reviewed papers; 1 website; 1 conference presentation; 1 patent document; 1 BREF document	11 documents related to lab-scale tests 6 documents about a full - scale experience	Lab-scale: 10 min-25 h Full-scale: 20 minutes	16 documents related to Europe (mainly UK and Italy), 1 document related to China
Environmental protection	Acid mine drainage		2	1 company website; 1 peer-reviewed paper	Full-scale treatment	Not reported	Valid for all contexts
Agriculture	Soil neutralisation		0	12 documents consulted but none reports useful indications	-	-	-
	Increment of soil organic carbon		2	Peer-reviewed papers	Field tests	70-80 years	Germany and France
Chemical industry	Calcium carbide		0	6 documents but none reports information about carbonation rate of carbide lime because it depends on its use	-	-	-
Non-ferrous applications	Base and precious metals, lithium		Many documents on the theme were consulted (Copper: 14 documents; Zinc-Lead: 22; Nickel: 14; Gold: 4; Platinum Group Metals: 4; Lithium: 13) but no relevant quantitative information was derived				
	TiO_2 production - Red gypsum		7	Peer-reviewed papers	Lab-scale tests in conditions of enhanced carbonation	5 minutes - 3 hours	6 papers: Malaysia 1 paper: Spain
	Aluminium production - Red mud		12	11 peer-reviewed papers 1 report from an industrial company	NC: field test AC: 10 lab-tests; 1 experience of full-scale	NC: not reported AC: 20'- 1 day	1 paper: Europe (Greece) 11 documents: contexts outside Europe, i.e. Australia, China, Canada, India, USA, and Korea

Lime application		N° total sources	Type of source	Type of test (field vs. lab-test)	Test duration	Geographical context
Pulp and paper – Precipitated Calcium Carbonate (PCC)	Traditional[1]	1	BREF Document	Real experience in EU	-	Europe
	Slag[2]	13	11 peer-reviewed papers; 2 university theses	12 documents: lab-scale 1 document: pilot plant	Different operating conditions tested	9 documents: Europe (Finland, Turkey, and Belgium) 4 documents: Brazil, Japan, Korea, and USA

[1] Traditional = production via carbonation of hydrated lime; [2] Slag = production via indirect carbonation of iron and steel slags.

Table 4.3. Literature-derived carbonation rate of lime in natural and enhanced conditions for each application. Caption: **applications with conclusive scientific data**, **applications with less conclusive scientific data** and **no information available**.

Lime application		Application share (%)	Natural carbonation rate (%)	Comments	Enhanced carbon. rate (%)	Comments
Iron and steel industry	Iron slags	41	Negligible even after 100 years	Ca and Mg are usually present in the form of silicates or in other low reactive compounds	7%-31%	Range derived only from lab-tests. Minimum value for the direct route, maximum value for the indirect route
	Steel slags		5% (4 months) - 28% (≈ 1 year)	1) 1 year is required for a good carbonation 2) huge piles of slag with low porosity should be avoided	39%-56% NOTE: ≈ 45% in the PCC application[1]	Range derived only from lab-tests. Values for direct route, slurry phase carbonation (most promising route)
Construction materials	Sand lime bricks	2.9	30% (age of samples not reported)	Value only from 1 document, of 25 years ago	-	-
	Light-weight lime concrete - Autoclaved aerated concrete	4.4	30% (10 years) - 60% (30 years)	1) The carbonation rate cannot be attributed all to lime due to the presence of CaO in the cement 2) Values from a Japanese research → use in European contexts with similar climate conditions	-	-
	Pure air lime mortars	0.4	80-92% after 100 years within 190 mm of depth	Low uncertainty	-	-
	Mixed air lime mortars	2.9	20-23% after 100 years within 190 mm of depth	Low uncertainty (considering one fourth of the pure air lime mortars value)	-	-
	Hemp -lime	0.1	55% after 91 days within 50 mm of depth	Good consistency among the data found. Uncertainty given by the influence of hemp lime composition on carbonation rate.	65%	Only one lab-scale study
Civil engineering	Soil stabilisation	6.4	37% after 34 years	Value from 1 field research study valid for a lime dosage of 2.5% and the German climate conditions	80%	Lab-test result on soil sample with 5% lime content after 3 days of curing

Lime application		Application share (%)	Natural carbonation rate (%)	Comments	Enhanced carbon. rate (%)	Comments
	Asphalt pavement – Hot Mix Asphalt	0.1	Not available	-	-	-
Environmental protection	Drinking water – softening process	2.1	100% presumably instantaneous	-	-	-
	Biosolids from wastewater treatment plants	4.3	Conditioning: 49% Post-stabilisation: 43%	Uncertainty due to: 1) values based only on 1 source, of 20-30 years ago 3) not reported the period of time between lime dosage and the analysis	-	-
	Dredging sediments (solidification/stabilisation)	2.9	35% after 30 years	High uncertainty → analyses related to the same reclamation technology, but applied to soil	-	Enhanced carbonation has been recently tested but data only related to the cement used as binder are available
	Flue gas cleaning systems	7.8	32% (lime reaction directly with the flue gas in few seconds)	Value derived from 16 tests performed in European plants	Carbonation of APCR 11-76% (lab-scale tests) 27-34% (full-scale experience)	The industrial experience is implemented in the UK by the society Carbon 8 Aggregates Ltd
	Acid mine drainage	0.6	Negligible	Indications from full-scale plants	-	-
Agriculture	Soil neutralization with liming materials	3.0	Not available	Focus only on limestone application	-	-
	Increment of soil organic carbon (SOC)		1-77 kgC/ha/year increment of SOC (after 70-80 years)	Uncertain range → It derives only from 2 studies	-	-

Lime application		Application share (%)	Natural carbonation rate (%)	Comments	Enhanced carbon. rate (%)	Comments
Chemical industry	Calcium carbide	0.3	Depending on the actual use of the carbide lime, e.g. equal to PCC carbonation rate when carbide lime is used for this use			
Non-ferrous applications	Base and precious metals, lithium	1.5	The literature on the theme is almost absent. Based on the little collected information, the carbonation processes interesting the solid residues (slags and/or tailings) should be modest			
	Titanium dioxide production - Red gypsum		No indications		Direct route: 10%-25% (first value for aqueous solution, second value for the adding of NH_4OH) Indirect route: 60%	Uncertainty due to: - documents on lab-scale tests - estimate based on the Ca content of the sample (not reported if it derives from lime or from limestone) - not considered the possible CO_2 emission from limestone during the neutralisation
	Aluminium production - Red mud	1.4	11.5% (fresh sample, no indication on the exact age)	The CO_2 sequestration is mainly due to its content of NaOH	11.5%	CO_2 uptake comparable to that of natural ageing → The limiting factor is the Ca content rather than the operating conditions of the carbonation process
Pulp and paper	Precipitated Calcium Carbonate (PCC)	5.9	85-93%	Not 100% rate due to lime impurities and technical inefficiencies of the calcination and the carbonation process	-	-

[1] In Chapter 3.4 related to PCC, a specific review about the production of PCC via indirect carbonation of steel converter slag was performed.

Table 4.4. Factors required for effective carbonation. Source: Pan, S.-Y., Chang, E. E., Chiang, P.-C., 2012. *CO_2 Capture by Accelerated Carbonation of Alkaline Wastes: A Review on Its Principles and Applications*. Aerosol and Air Quality Research, 12, 770–791. DOI: 10.4209/aaqr.2012.06.0149

	Solid Phase	Liquid Phase	Gas Phase
Physical Properties	· Particle size · Mineralogy · Specific surface area · Porosity · Permeability · Surface activities · Microstructure	· Temperature · L/S ratio	· Partial pressure · CO_2 flow rate · Relative humidity · Temperature
Chemical Properties	· Composition (e.g., Ca and f-CaO content, Ca/Si ratio, Ferrite/C_3A ratio) · Heavy Metals (e.g., Pb, Cd, Ni, Cr) · Free water content · Permeability	· Organics · Inorganic · Anions · Cations · pH · Permeability	· CO_2 Concentration · Organics · Inorganic · Particulate Matter

Table 4.5. Conditions for effective enhanced carbonation in conclusive applications.

Conclusive applications	**Conditions for effective enhanced carbonation**
Steel	Fine particle slags High contact with CO_2
Pure air lime and mixed air lime mortars	Lower wall thickness Contact with CO_2 Mortar composition (less cement higher carbonation rate)
Hemp lime	Composition Contact with CO_2
Drinking Water	Addition of coagulants and flocculating agents
Flue gas cleaning systems	CO_2 concentration Lower SOx concentration Relative humidity Temperature Reaction time
Aluminium	Composition of red mud Contact with CO_2
Pulp and paper	Contact with CO_2 No impurities in lime

4.4. Overall average carbonation rate for applications with conclusive and less conclusive scientific data

In Table 4.6, the amount of CO_2 emitted for producing lime excluding fuel combustion emission is reported, considering the emission factor of 786 kg CO_2/t lime. Then, the amount of CO_2 reabsorbed by lime through carbonation is calculated using the maximum natural carbonation, the minimum and the maximum enhanced carbonation rates, corresponding to 37%, 48% and 55% of the total CO_2 emitted by the conclusive applications, respectively. Therefore, the conclusive applications, which account for 61% of the European lime market in 2018, will reabsorb through natural carbonation about 23% of the process CO_2 emitted for producing the total amount of lime in 2018.

As a general assumption, where no information on enhanced carbonation was available, we assumed the minimum enhanced carbonation rate being equal to the maximum natural carbonation rate.

The information for less conclusive applications is reported in Table 4.7. Based on the previous assumption, the amount of CO_2 reabsorbed through maximum natural and minimum enhanced carbonation is the same and it accounts for 46% of the CO_2 emitted for producing the lime used in these applications. Therefore, the less conclusive applications, which account for 21% of the European lime market in 2018, will reabsorb around 10% of the total process CO_2 emitted.

In total, about 33% of the total CO_2 emitted will be reabsorbed through natural carbonation by the conclusive and less conclusive applications.

Table 4.6. Information about the amount of lime used in each conclusive application according to the lime market of 2018, the application share, CO_2 emission, natural and enhanced carbonation rate and the estimated amount of CO_2 absorbed through carbonation (rounded figures).

Application	Amount of lime (thousands of tonnes)	Application share (%)	Process emission (thousands of tonnes CO_2)	Natural Carbonation rate (%)		Enhanced Carbonation rate (%)		Total thousands of tonnes CO_2 carbonated		
				Min	Max	Min	Max	Max Natural Carbonation	Min Enhanced Carbonation	Max Enhanced Carbonation
Iron & Steel industry	8,325	40.7	6,543	5	28	39	56	1,832	2,552	3,664
Pure air lime Mortars[1]	86	0.4	68	80	92	92		62	62	-
Mixed air lime mortars[1]	588	2.9	462	20	23	23		106	106	-
Hemp -lime	10	0.1	8	20	55	-	65	4	-	5
Drinking Water[1]	424	2.1	333		100	100		333	333	-
Flue Gas Treatment[2]	1,595	7.8	1,254		32	59	66	401	740[2]	765[2]
Pulp & Paper	1,204	5.9	946	85	93	100	100	880	946	946
Aluminium	276	1.4	217		11.5	11.5	11.5	25	25	25
Total	**12,508**	**61**	**9,831**					**3,644**	**4,764**	**5,405**

[1]Since no information was found in the literature on enhanced carbonation, it is assumed that the minimum enhanced carbonation rate is equal to the maximum natural carbonation rate.

[2] Natural carbonation takes place inside the flue gas, while the enhanced carbonation on the APCR (Air Pollution Control Residues), allowing for a further increase by 27-34% of the carbonation rate. Then, for this specific application the natural and enhanced carbonation rates can be summed up, i.e. the potential total enhanced carbonation rate is 59-66%.

Table 4.7. Information about the amount of lime used in each less conclusive application according to the lime market of 2018, the application share, CO_2 emission, natural and enhanced carbonation rate and the estimated amount of CO_2 absorbed through carbonation (rounded figures).

Application	Amount of lime (thousands of tonnes)	Application share (%)	Process emission (thousands of tonnes CO_2)	Natural Carbonation rate (%)		Enhanced Carbonation rate (%)		Total thousands of tonnes CO_2 carbonated
				Min	Max	Min	Max	Max Natural Carbonation
Sand Lime Bricks[1]	596	2.9	468		30	30		141
Light-weight lime concrete[1]	894	4.4	703	30	60	60		422
Soil Stabilisation	1,308	6.4	1,028		37	-	80	380
Wastewater[1]	874	4.3	687	43	49	49		337
Sludge Treatment[1]	593	2.9	466	43	49	49		228
Calcium Carbide[1]	63	0.3	50	45	95	95		47
Total	**4,328**	**21**	**3,402**					**1,555**

[1]Since no information was found in the literature on enhanced carbonation, it is assumed that the minimum enhanced carbonation rate is equal to the maximum natural carbonation rate.

4.5. Carbonation rate over time for conclusive applications

The carbonation rate over time depends on the specific lime application. Lime used in flue gas treatment, drinking water, pulp and paper will carbonate instantaneously, while lime applied in construction materials (mortars and hemp_-lime) will carbonate during the whole lifetime of the building. From the assessed literature, the equation that links the carbonation rate to time for construction materials is the following:

$$CR = MCR \cdot {(K\sqrt{t})}/{depth}$$

where *CR* is the carbonation rate; *MCR* is the maximum carbonation rate; *K* is the carbonation constant; *t* is the time expressed in days and depth is the application thickness that carbonates after 100 years. For pure air lime mortars, *MCR* and *K* are equal to 80-92% and 1 $mm/\sqrt{day}$ respectively, while *K* of mixed air lime mortars is 0.25 $mm/\sqrt{day}$. In both cases, the depth is 191 mm. The carbonation rate in time of pure air lime mortars and mixed air lime mortars are reported in Figures 4.1 and 4.2.

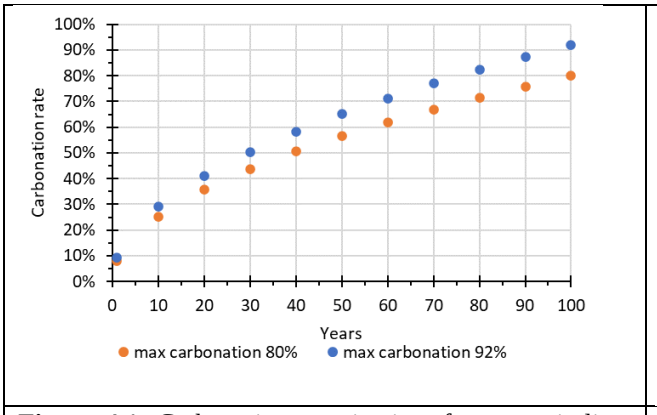


Figure 4.1. Carbonation rate in time for pure air lime mortars.

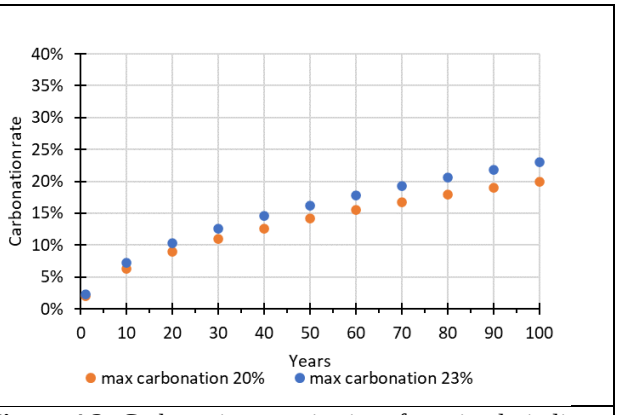


Figure 4.2. Carbonation rate in time for mixed air lime mortars.

Regarding hemp lime, *MCR* is 55% while *K* is 5.24 $mm/\sqrt{day}$ for a depth of 1001 mm and the carbonation rate in time is reported in Figure 4.3, while information about the carbonation time trend over time is not available for lime used in the aluminium industry.

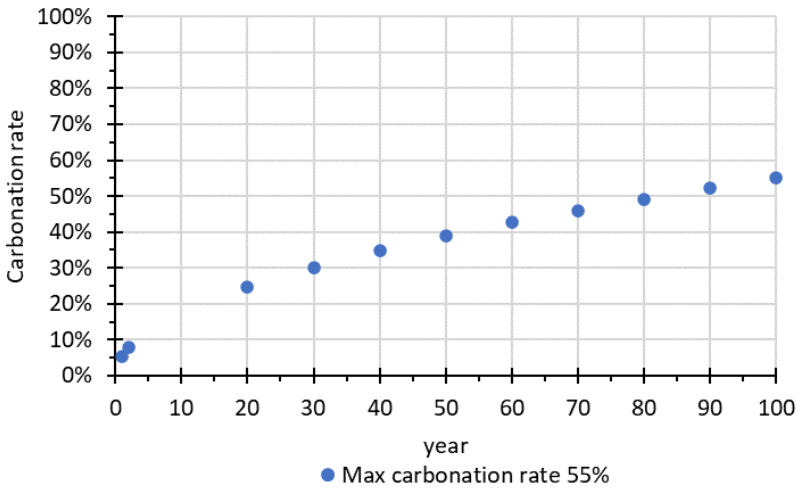


Figure 4.3. Carbonation rate in time for hemp lime.

In Figure 4.4 the carbonation rate in time for steel slags is reported. The estimated carbonation rate is calculated assuming that it is equal to the square rooted number of days multiplied by 0.0085 for the first 5 years of slags' storage and equal to 39% after the first 5 years. According to the equation, the minimum enhanced carbonation rate of 39% is reached after 5 years. The value is a little overestimated, considering that 2/3 of the free lime in steel slag will react within the first 5 years, whereas carbonation of calcium silicates and calcium aluminates will take more than 5 years, reaching a final carbonation degree of only 1/3. Thus, 39% can be considered as a theoretical maximum natural carbonation rate reached after 5 years or more likely later, since the carbonated surface of the slags' pile is less porous and consequently the CO_2 diffusion in the pile will decrease over time. However, it is to be mentioned that typically the steel slags are stored in the open-air for 3-6 months only.

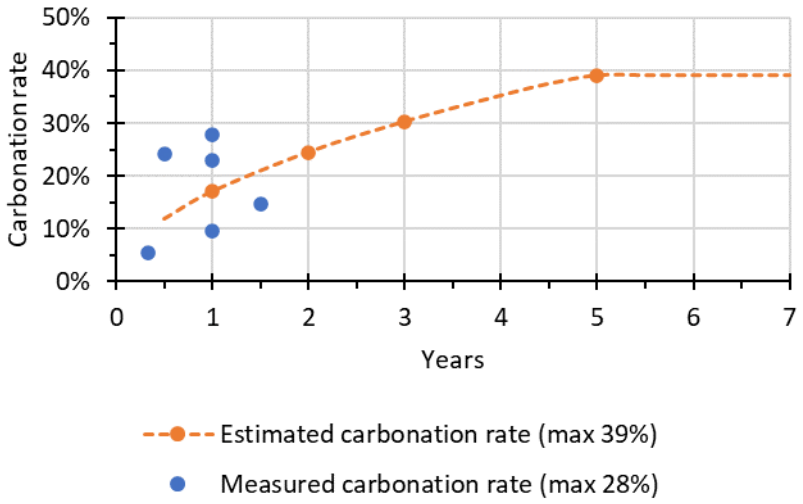


Figure 4.4. Carbonation rate in time for steel slags.

The calcination process emission and the CO_2 reabsorbed over a time period of 100 years for each conclusive application are reported in Table 4.8. For each application, the increase of the CO_2 reabsorbed through natural carbonation was calculated for each T with respect to the previous time step. Then, the total of the CO_2 reabsorbed at that T was calculated as the sum of all applications' increment at the same T, while the cumulative CO_2 carbonated is the sum of the total CO_2 reabsorbed at time T with the one at the previous time step. Finally, the ratio among the cumulative CO_2 carbonated and the CO_2 emitted during the calcination of the whole amount of lime used in all conclusive applications is reported in the last row. It can be noticed that the CO_2 reabsorbed through natural carbonation is the same as calculated in Table 4.6 and it is reached after 100 years on the basis of the assumptions made. However, 95% of the amount of CO_2 absorbed by the conclusive applications, which account for 61% of EuLA lime market in 2018, is already achieved after 1 year.

Table 4.8. CO_2 reabsorbed through natural carbonation over a time period of 100 years for conclusive applications according to the European lime market of 2018 (rounded figures).

Application	Amount of lime (thousands of tonnes)	Process emission (thousands of tonnes CO_2)	CO_2 reabsorbed through natural carbonation								Comments
			T=0	T=1 year	T=5 years	T=10 years	T=20 years	T=30 years	T=50 years	T=100 years	
Iron & Steel industry	8,325	6,543	0	1,832	0	0	0	0	0	0	Carbonation rate (CR) 28% after 1 year (Table 4.3) since open-air storage lasts 3-6 months
Pure air lime Mortars	86	68	0	6	8	6	8	6	10	18	Maximum natural CR 92%; 100 years
Mixed air lime mortars	588	462	0	11	13	10	14	11	17	31	Maximum natural CR 92%; 100 years
Hemp lime	10	8	0	0.4	0.5	0.4	0.6	0.4	0.7	1.3	Maximum natural CR 55%; 100 years
Drinking Water	424	333	333	0	0	0	0	0	0	0	Maximum natural CR 100%; instantly
Flue Gas Treatment	1,595	1,254	401	0	0	0	0	0	0	0	Maximum natural CR 32%; instantly
Pulp & Paper	1,204	946	880	0	0	0	0	0	0	0	Maximum natural CR 93%; instantly
Aluminium	276	217	0	0	0	0	0	0	0	25	Maximum natural CR 11.5%; assumed all at T=100 years as worst scenario since no information about time
Total	**12,508**	**9,831**	**1,614**	**1,849**	**22**	**16**	**23**	**17**	**28**	**75**	-
Cumulative CO_2 carbonated	-	-	**1,614**	**3,463**	**3,485**	**3,501**	**3,524**	**3,541**	**3,569**	**3,644**	-
Cumulative CO_2 carbonated/Process emission (%)	-	-	**16%**	**35%**	**35%**	**36%**	**36%**	**36%**	**36%**	**37%**	-

ANNEX A – APPLICATIONS WITH CONCLUSIVE INFORMATION ON CARBONATION

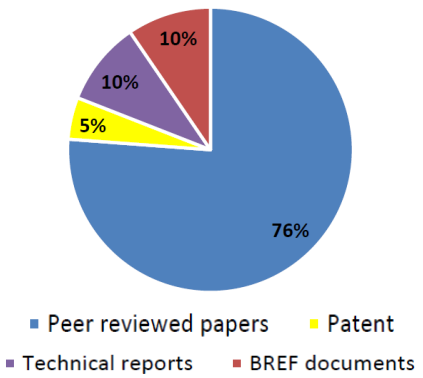
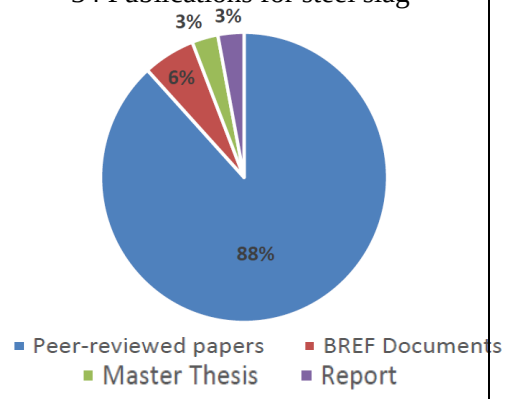
A.1 Carbonation in steel applications

Lime in steel making:

The presence of Ca-compounds in the steel slag is the consequence of the use of quicklime (CaO) or limestone ($CaCO_3$) during the iron and steel making processes. Quicklime is used in the hot metal desulphurization processes as well as in the BOF and EAF processes as a fluxing agent to create a basic slag that can neutralise acid-forming elements, remove sulphur, phosphorous, silica and alumina inclusions and protect the refractories. It is also used in a broad variety of secondary metallurgical processes for the removal of additional impurities and to prevent the reabsorption of impurities from the slag. In addition, quicklime can be used together with other materials, such as fluorspar, to form a synthetic slag, which is used as a flux to remove additional sulphur and phosphorus after the initial steel refining process. In the pig iron production process, quicklime is used far less, where it is mixed with limestone in a proportion of 1:6, mainly in the sintering process.

Natural carbonation occurs during the open-air storage of steel slag, because part of the $Ca(OH)_2$ in the slag reacts with the atmospheric CO_2. $Ca(OH)_2$ is the result of the complete hydration of free CaO remaining in the slag and this hydration is required for recycling slag as a construction material. Hydration of the slag takes place through open air exposure of slag piles, usually for 3-6 months.

Literature assessed to evaluate the carbonation rate:

Literature assessed	**72 publications**	
Relevant, reliable and adequate literature	21 publications for iron slag 	34 Publications for steel slag 
Natural carbonation rate[33]	Negligible even after 100 years	5% (4 months) - 28% (≈ 1 year)

Natural carbonation rate in steel is affected by:	Enhanced carbonation rate in steel is affected by:
Exposed surface area of the piles, low porosity of the piles preventing the contact with CO_2.	Particle size, Surface area contact with CO_2.

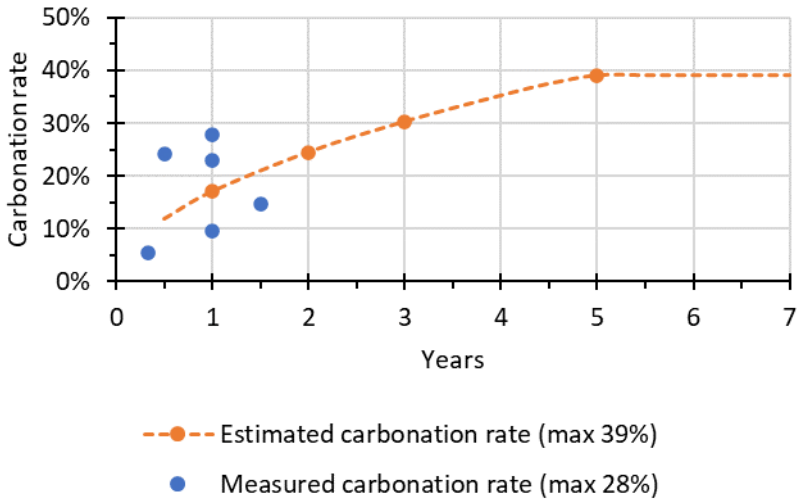
[33] The carbonation rate is the percentage of CO_2 emitted during lime calcination (excluding fuel combustion emission) which is reabsorbed through carbonation.

Here an illustrative graph of natural carbonation rate in time (expressed as months since the open-air storage of steel slags lasts in the order of months)

Carbonation rate = $0.0085\sqrt{number\ of\ days}$ for the first 5 years

Carbonation rate = 39% after the first 5 years

According to the equation, the minimum enhanced carbonation rate of 39% is potentially reached after 5 years. The value is a little overestimated, considering that 2/3 of the free lime in steel slag reacts within the first 5 years, whereas carbonation of calcium silicates and calcium aluminates takes more than 5 years, reaching a final carbonation degree of only 1/3. Thus, 39% can be considered as a theoretical maximum natural carbonation rate reached after 5 years or more likely later, since the carbonated surface of the slag pile is less porous and consequently the CO_2 diffusion in the pile decreases with time. Note that typically the steel slag open-air storage lasts for 3-6 months.



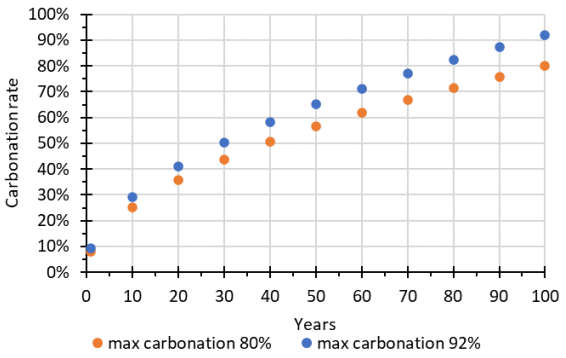
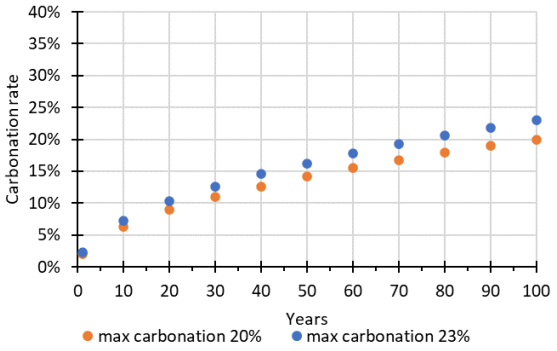
A.2 Carbonation in mortars applications

Lime in mortars:

Lime mortars have been used since ancient times. "Air lime" mortars are made of hydrated lime ($Ca(OH)_2$) and harden as a result of their exposure to atmospheric CO_2 and the formation calcium carbonate ($CaCO_3$). Thus, carbonation is the hardening process of air lime mortars Another type of mortar are a mix of lime and a strong hydraulic manufactured binder, e.g. Portland cement. These are sometime referred to as "mixed air lime" mortars.

Literature assessed to evaluate the carbonation rate:

Literature assessed	**100 publications** for "air lime" mortars	**90 publications** for "mixed air lime" mortars
Relevant, reliable and adequate literature	21 publications	27 publications
Natural carbonation rate[34]	80-92% after 100 years within 191 mm of depth	20-23% after 100 years within 191 mm of depth

Natural carbonation rate in "air lime" mortars is affected by:	Natural carbonation rate in "mixed air lime" mortars is affected by:
depth: from 0 to 191 mm below the mortar surface after 100 years, it is expected that the lime will be carbonated such that 80-92% of the calcination CO_2 emissions from lime will be reabsorbed.	the substitution rate of Portland cement in mortars because it reduces porosity and this decreases the carbonation rate
Natural carbonation rate in time for "air lime" mortars. Assumed equation: $[CR = NCR \cdot {K\sqrt{t}}/{depth}]$, where: *CR* is the carbonation rate (%); *NCR* is the natural carbonation rate (80-92%); *t* is time (day); *K* is the carbonation constant equal to 1 $mm/\sqrt{day}$; *depth* is the application thickness that carbonates after 100 years (191 mm). 	Natural carbonation rate in time for "mixed air lime" mortars. "Mixed air lime" mortars carbonation rate is one fourth of "air lime" ones, since the carbonation constant (*K*) is equal to 0.25 $mm/\sqrt{day}$ 

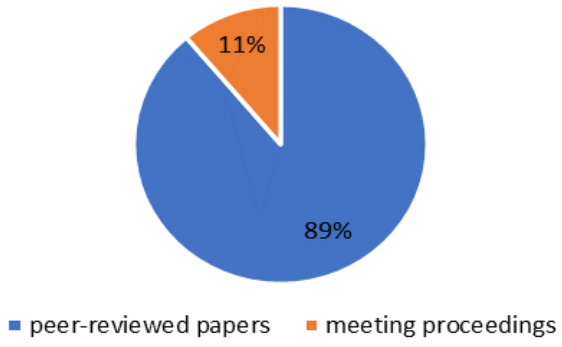
[34] The carbonation rate is the percentage of CO_2 emitted during lime calcination (excluding fuel combustion emission) which is reabsorbed through carbonation.

A.3 Carbonation in hemp lime application

Lime in hemp lime construction materials:

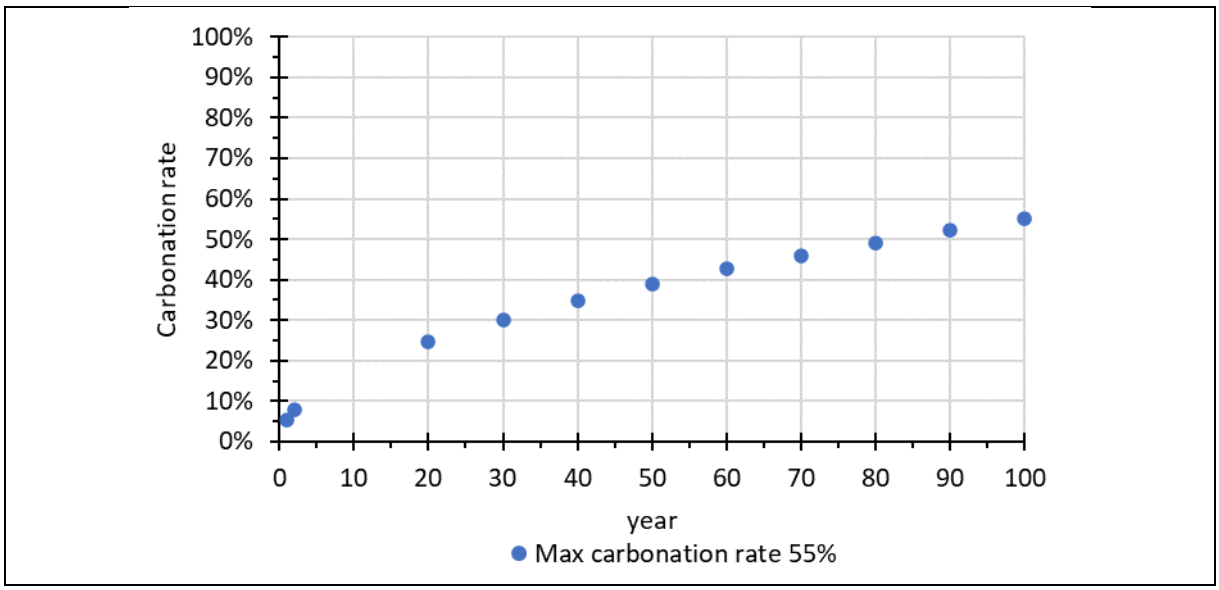
Hemp lime construction materials are mainly used in France and United Kingdom from where most publications are derived. The components of hemp lime material are hemp shiv, i.e. the chopped woody core of the stalks of the hemp plant (*Cannabis sativa*), and air lime binder with pozzolanic cementitious or hydraulic lime additives and in some cases surfactants. The air lime binder is hydrated lime ($Ca(OH)_2$) that, during the use phase of the hemp lime construction material, carbonates by reacting with atmospheric CO_2 and forming calcium carbonate ($CaCO_3$). Literature review shows the natural carbonation rate[35] is 55% and within 50 mm of carbonation depth, lime is fully carbonated after 91 days. Thus, the carbonation constant which measures the advance of carbonation depth over time is equal to 5.24 mm/√day given by the ratio of 50 mm over the square root of 91 days.

Literature assessed to evaluate the carbonation rate:

Literature assessed	**15 publications**
Relevant, reliable and adequate literature	Total: 9 publications 
Natural carbonation rate[1]	55% after 91 days within 50 mm of depth

Natural carbonation rate in hemp lime construction materials is affected by:
Binder composition
Natural carbonation rate in time for hemp lime. Assumed equation: $[CR = 55\% \cdot {K\sqrt{t}}/{depth}]$, where: *CR* is the carbonation rate (%); 55% is the natural carbonation rate; *t* is time (day); *K* is the carbonation constant equal to 5.24 $mm/\sqrt{day}$ and *depth*, i.e. the application thickness which carbonates after 100 years, is 1001 mm.

[35] The carbonation rate is the percentage of CO_2 emitted during lime calcination (excluding fuel combustion emission) which is reabsorbed through carbonation.


100%
90%
80%
70%
60%
50%
40%
30%
20%
10%
0%
Carbonation rate
0
10
20
30
40
50
60
70
80
90
100
year
Max carbonation rate 55%

A.4 Carbonation in drinking water application

Lime in drinking water:

Lime is used in the drinking water sector for many applications such as softening, pH adjustment, acid neutralisation, metals removal, alkalinity adjustment or removal of fluoride, phosphate, sulphate and nitrogen. One of the main applications is water softening, which aims to reduce the hardness of raw water (i.e. calcium and magnesium bicarbonates), alkalinity, and silica to avoid undesirable effects of scaling. The hard water is softened by using hydrated lime ($Ca(OH)_2$) and, if necessary, soda in order to precipitate the dissolved calcium and magnesium as insoluble calcium carbonate and magnesium hydroxide, respectively. These insoluble compounds are then removed by sedimentation and, usually, filtration. Lime used in water softening is considered fully carbonated, because CaO and $Ca(OH)_2$ are normally absent in the obtained sludge.

Literature assessed to evaluate the carbonation rate:

Literature assessed	**14 publications**
Relevant, reliable and adequate literature	2 peer-reviewed papers
Carbonation rate[36]	100% instantaneous

Natural carbonation rate in drinking water is affected by:
the low solubility of calcium carbonate and magnesium hydroxide. The addition of coagulants and flocculating agents accelerates the process. Alternatively, the addition of inert fine particles, such as sand or previously precipitated $CaCO_3$, that can act as nucleation centres, decreases the reaction time.
Natural carbonation rate in time for drinking water is not reported in the assessed literature, but it is presumably instantaneous, meaning that 100% of the process emissions is absorbed instantaneously in the use phase for the drinking water application.

[36] The carbonation rate is the percentage of CO_2 emitted during lime calcination (excluding fuel combustion emission) which is reabsorbed through carbonation.

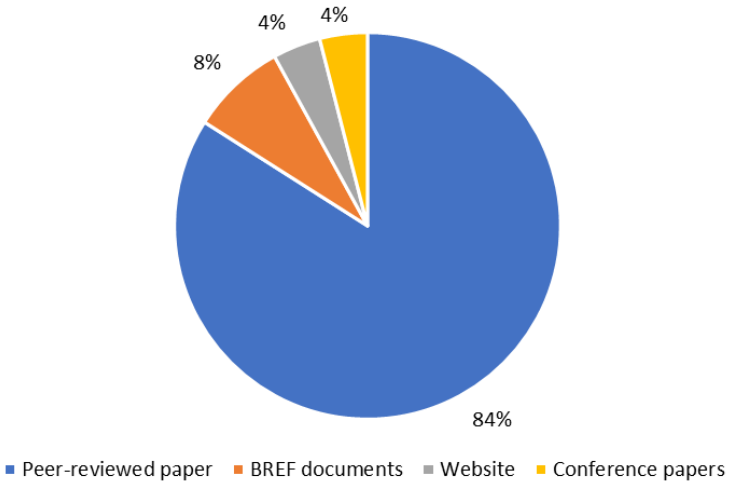
A.5 Carbonation in flue gas treatment applications

Lime in flue gas treatment:

Lime is used for removing the acid gases (HCl, SOx, HF) contained in flue gases generated from combustion plant, in particular coal-fired power plants and waste incineration facilities. Flue gas treatment process can be semi-dry or dry, depending on the form of lime used. In semi-dry processes, lime is supplied as aqueous solution or suspension, i.e. as milk of lime or as lime slurry solution. During the reaction with the flue gas, the water evaporates and the reaction products are dry. In dry processes, powder hydrated lime is directly supplied as sorbent. For both processes the reaction products are separated in a conventional dedusting unit (typically a baghouse filter). During the flue gas treatment, lime reacts with HCl, HF and SOx but also with CO_2, forming calcium carbonate.

Due to the short contact time between the lime sorbent and the pollutant gas, typically in the range of a few seconds, and the kinetic limits of the chemical reactions, lime is supplied in excess to the anticipated acid gases, commonly to a stoichiometric ratio of 1.4-2.5 (semi-dry) and 1.5-2.5 (dry). As a result, the solid residues generated by the process, generally referred to as Air Pollution Control Residues (APCR), contain high amount of free lime available for carbonation. Enhanced carbonation of APCR has been largely proposed as a technology to improve their chemical stability and their leaching behaviour before their final disposal or recycling. Furthermore, enhanced carbonation of APCR allows for a contextual CO_2 sequestration directly at a CO_2 point source emission where these residues are generated.

Literature assessed to evaluate the carbonation rate:

Literature assessed	**39 publications**
Relevant, reliable and adequate literature	Total: 23 publications 
Carbonation rate[37]	32% (natural); 27-34% (enhanced, applied to APCR) Total: 59-66% instantaneous

Natural carbonation rate in flue gas treatment is affected by:	Enhanced carbonation rate of APCR in flue gas treatment is affected by:
- the formation of an outer layer of calcium compounds, characterized by low porosity, which inhibits the CO_2 diffusion.	- the temperature when the liquid to solid (L/S) ratio is below the optimal value, otherwise its influence on the CO_2 uptake is negligible. The best operating temperature is 20-30°C (for

[37] The carbonation rate is the percentage of CO_2 emitted during lime calcination (excluding fuel combustion emission) which is reabsorbed through carbonation.

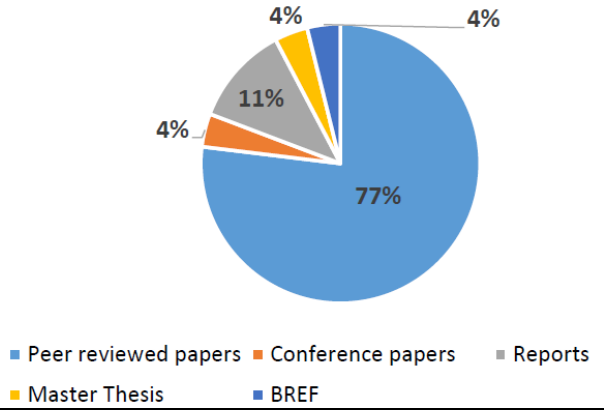
	aqueous-based carbonation) and above 350°C (for gas-solid carbonation). - In aqueous carbonation, adopted L/S ratios of 0.2-0.3. Too low L/S ratios hinder the solubilisation of CO_2 and Ca ions, while L/S ratio above the optimal value decreases the CO_2 uptake due to a higher resistance towards CO_2 diffusion. - The presence of SOx in the CO_2 enriched gas decreases the amount of CO_2 sequestered by the APCR, because SOx tends to clog the pores of the residue.
Natural carbonation rate in time for flue gas treatment is instantaneous, meaning that lime is carbonated at T=0 of the use phase	

A.6 Carbonation in aluminium applications

Lime in aluminium:

Lime in the form of quicklime or hydrated lime is used in Bayer process, the principal means of refining bauxite ore for alumina extraction. During the Bayer process, bauxite is digested in a caustic liquor of Na and Ca-hydroxides. This process produces two output streams, a liquor rich with alumina that is for alumina precipitation and subsequent aluminium production, and a solid residue, called red mud that is disposed of. This waste residue is an alkaline slurry with a water content of about 50-70% and a pH generally above 13 depending on its content of sodium and calcium compounds. Recent red mud disposal consists of dry stacking in order to thicken tailings until they reach a solid content of at least 48-55%, and then deposited in such a way that they consolidate and dry out. The natural carbonation of red mud slurry involves both pore water carbonation and solid phase reactions of tri-calcium aluminate (TCA) dissolution and calcite precipitation. To neutralize the mud, reducing its pH, different neutralization methods are proposed by means of seawater or BaseconTM® that uses artificial Ca and Mg rich brines. Another neutralization is based on CO_2, i.e. a carbonation under enhanced conditions. To improve CO_2 sequestration in a stable mineral phase, it was also proposed to use the addition of an external source of Ca or Mg.

Literature assessed to evaluate the carbonation rate:

Literature assessed	**41 publications**
Relevant, reliable and adequate literature	Total: 26 publications 
Carbonation rate[38]	11.5% (natural); 11.5% (enhanced) no information identified about the carbonation time

Natural carbonation rate in aluminium is affected by:	Enhanced carbonation rate in aluminium is affected by:
- the red mud composition; - the exposure time since dissolution of Ca-bearing minerals typically present in the red mud; - the amount of stirring during the storage of the red mud and consequently the number of surfaces exposed to the atmospheric CO_2.	- the same factors of natural carbonation since CO_2 partial pressure does not improve the carbonation rate.
Natural carbonation rate in time for aluminium is not reported in the assessed literature.	

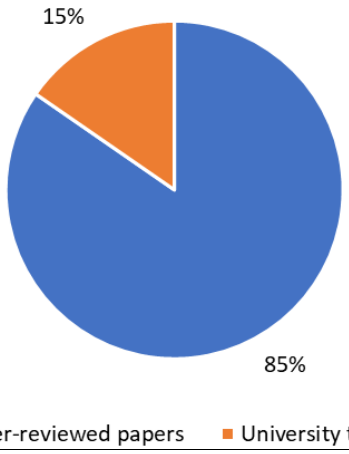
[38] The carbonation rate is the percentage of CO_2 emitted during lime calcination (excluding fuel combustion emission) which is reabsorbed through carbonation.

A.7 Carbonation in pulp and paper applications

Lime in pulp and paper:

Precipitated Calcium Carbonate (PCC), which is produced by a chemical route combining carbon dioxide (CO_2) with lime (CaO) under controlled operating conditions, is largely used as a coating pigment or filler in pulp and paper but also in other industrial applications. To produce PCC, a hydrated lime slurry is put in contact with flue gases containing CO_2, leading to re-carbonation of the lime. Thus, calcium carbonate reforms, and being insoluble in water, it precipitates. Separation of impurities from the lime slurry is used to ensure high purity PCC. The precipitation can produce each of the three crystalline forms (calcite, aragonite, and vaterite) depending on the reaction conditions. PCC characteristics can be tailored by regulating: the temperature; the CO_2 concentration and flow rate; the stirring rate; the particle size, the concentration of the hydrated lime slurry; and the use of additives. Since a CO_2-rich gas stream is required for the production of PCC, natural and enhanced carbonation are necessary in this sector.

Literature assessed to evaluate the carbonation rate:

Literature assessed	**52 publications**
Relevant, reliable and adequate literature	Total: 13 publications 
Carbonation rate[39]	85-93% during the manufacturing process

Natural carbonation rate in pulp and paper is affected by:
The rate of dissolution of calcium hydroxide in the slurry. To avoid excess dissolution and maximize the PCC yield, pressurization of the carbonation reaction and/or the use of specific additives are applied.
Natural carbonation rate in time for pulp and paper is instantaneous, meaning that 85-93% of the lime process emissions are carbonated at T=0 during the use phase for the pulp and paper making

[39] The carbonation rate is the percentage of CO_2 emitted during lime calcination (excluding fuel combustion emission) which is reabsorbed through carbonation.

ANNEX B - LIST OF OPTIMAL pH-RANGE IN SOIL

Table B.1. Optimal pH-range in arable soil depending on the soil type and the content of organic matter (CEN, 2006).

Type of soil	**Evaluated parameter**	**Organic matter content (% by mass)**				
		< 4	**4.1 - 8.0**	**8.1 - 15**	**15.1 - 30.0**	**> 30**
Sand	Optimal pH-range	5.4-5.8	5.0-5.4	4.7-5.1	4.3-4.7	-
Slightly loamy sand		5.8-6.3	5.4-5.9	5.0-5.5	4.6-5.1	-
Heavy loamy sand		6.1-6.7	5.6-6.2	5.2-5.8	4.8-5.4	-
Sandy silty loam		6.3-7.0	5.8-6.5	5.4-6.1	5.0-5.7	-
Clayey loam clay		6.4-7.2	5.9-6.7	5.5-6.3	5.1-5.9	-
Peat		-	-	-	-	4.3-4.7

Table B.2. Optimal pH-range in grassland depending on the soil type and the content of organic matter (CEN, 2006).

Type of soil	**Evaluated parameter**	**Organic matter content (% by mass)**		
		≤ 15	**15.1 - 30**	**> 30**
Sand	Optimal pH-range	4.7 - 5.2	4.3 - 4.7	
Slightly loamy sand		5.2 - 5.7	4.6 - 5.1	
Heavy loamy sand		5.4 - 6.0	4.8 - 5.4	
Sandy silty loam		6.3 - 7.0	5.6 - 6.3	
Clayey loam clay		5.7 - 6.5	5.1 - 5.9	
Peat		-	-	4.3

ANNEX C - LITERATURE REVIEW ABOUT THE EFFECT OF LIMING ON SOC LEVELS FOR THE EUROPEAN CONTEXT

Table C.1. list of field experiments: soil characteristics, liming dosage, and impacts on SOC. All the analysed cases are related to the European context.

Literature source	Geographical site	Type of soil and land use	Investigated soil horizon	Liming application		TOC (g/kg) or SOC stocks (t/ha)		Comments and conclusions
				Type of product	Amount (t/ha)	Limed plot	Un-limed plot	
Study 1 Persson et al. (1995)	Vållasen (Sweden)	Podzolized soil; Forest with norway spruce	Litter layer, humus layer, and mineral soil (0-50 cm)	$CaCO_3$	6 t/ha Sampling after 37 years	110.8 t/ha	129.4 t/ha	1) Liming significantly reduced the overall soil C stocks in all sites. AVERAGE L-U: -0.44 tC/ha/y 2) The reduction in limed plots was due to C losses from the litter and humus layers
	Dalby (Sweden)				9 t/ha Sampling after 42 years	82.2 t/ha	90.7 t/ha	
	Frodeparken, (Sweden)	Podzolized soil; Forest with European beech			10 t/ha Sampling after 38 years	96.3 t/ha	111.7 t/ha	
Study 2 Nilsson et al. (2001)	Hasslöv (south-western Sweden)	Typical Haplorthod soil; Forest with Norway spruces	Forest floor	Dolomite lime	8.75 t/ha were applied in the year 1984. Sampling was taken 10 years after the application	24.46 t/ha	27.68 t/ha	1) There were no significant treatment differences in C storage either in the individual soil layer or in the entire soil profile 2) In limed soil, the C storage tended to be smaller in the forest floor and higher in the mineral layer
			Mineral soil (0-40 cm)			133.24 t/ha	116.89 t/ha	

Literature source	Geographical site	Type of soil and land use	Investigated soil horizon	Liming application		TOC (g/kg) or SOC stocks (t/ha)		Comments and conclusions
				Type of product	Amount (t/ha)	Limed plot	Un-limed plot	
Study 3 Poulton et al. (2003)	Harpenden (southeast England)	Analysis on 2 old neighbouring arable sites that were reverted to woodlands: 1) acidic soil - deciduous wood 2) calcareous soil - oak dominated wood	Litter and mineral soil (0-69 cm)	$CaCO_3$	The specific amount of limestone was not reported. Sampling was made after 118 years	Net soil C change: 540 g/m^2/year	Net soil C change: 380 g/m^2/year	
Study 4 Šrámek et al. (2012)	Western Krušné hory Mts. Erzgebirge (Czech Republic)	Acid podzols and gleyic soils; acidophilous spruce forests	Humus layer	Dolomitic limestone (MgO > 18%)	A total dose of 3 tons. Sampling was taken 10 years after liming	38 g/kg	31 g/kg	1) The carbon concentration increased in a significant way ten years after liming 2) It is not possible to say whether this increment was due to liming or other factors
			Upper mineral layer (0-2 cm)			143 g/kg	108 g/kg	
			Lower mineral layer (2-30 cm)			51 g/kg	39 g/kg	
Study 5 Wellbrock et al. (2016)	National Inventory related to Germany	Forest soil (1,859 sampling points)	Organic layer	Dolomitic limestone (typically 2-5 t/ha)	The analysis was conducted in the period 2006-2008, 15 years after the previous inventory	Net variation in 15 years: -0.19 tC/ha/year	No significant variation in 15 years	1) In limed samples, C losses in the organic layer were more than compensated by the increment in the mineral layer 2) In limed samples, 9% C stocks increment compared to the previous inventory 3) In un-limed samples, 6% C stocks increment
			Mineral layer up to 90 cm			Net variation in 15 years: +0.84 tC/ha/year	Net variation in 15 years: +0.4 tC/ha/year	

Literature source	Geographical site	Type of soil and land use	Investigated soil horizon	Liming application		TOC (g/kg) or SOC stocks (t/ha)		Comments and conclusions
				Type of product	Amount (t/ha)	Limed plot	Un-limed plot	
Study 6 Grieve et al. (2005)	Bowmont valley (Scottish Borders)	Haplumbrept soil grassland	Humic horizon	$CaCO_3$ (39% Ca)	6 t/ha in 1999, 2000, and 2001. C_{org} concentrations (g/kg) are related to the year 1999 (first value) and 2001 (second value)	158.2 g/kg 111.9 g/kg	149.8 g/kg 104.6 g/kg	1) Over a 2-years period, the mean C_{org} concentration decreased (-30% in the humic horizon and -20% in the mineral horizon) 2) No significant difference from limed and un-limed plots was seen in terms of carbon concentration
			Ah mineral horizon			65.9 g/kg 54.5 g/kg	69.0 g/kg 53.2 g/kg	
Study 7 Mijangos et al. (2010)	Arraba area (Basque country, Spain)	Typical Dystrudept Calcareous grassland	0-10 cm depth	Burnt lime (92% CaO)	2.43 t/ha. Sampling was made six months after the application.	58 g/kg	52 g/kg	1) Liming did not result in any significant change in OC content 2) OC content in soil changes very slowly over the time (about 5-10 years are required to see possible significant changes
	Kurtzegan area (Basque country, Spain)	Aeric Humaquept Siliceous grassland				169 g/kg	186 g/kg	
Study 8 Fornara et al. (2011)	Rothamsted Hertfordshire (south-east of England)	Permanent pasture	Mineral soil 3-23 cm	$CaCO_3$	4 t/ha every four years starting from 1903. Data come from sampling in the period 1984-2005	No fertilization - net carbon change in soil		1) Net C_{org} sequestration measured in the mineral layer was significantly greater in limed than in un-limed plots 2) The increment was mainly due to higher C inputs being processed and incorporated into resistant soil organo-mineral pools
						+ 71 $gC/m^2/y$	- 25 $gC/m^2/y$	
						Yes fertilization - net carbon change in soil		

Literature source	Geographical site	Type of soil and land use	Investigated soil horizon	Liming application		TOC (g/kg) or SOC stocks (t/ha)		Comments and conclusions
				Type of product	Amount (t/ha)	Limed plot	Un-limed plot	
						+ 150 $gC/m^2/y$	+ 18 $gC/m^2/y$	
Study 9 Sochorová et al. (2016)	Eifel Mountains (Western Germany)	Pseudogley soil Nardetum grassland	0-10 cm depth	$Ca(OH)_2$	Scenario only lime: 715 kg Ca/ha/year (sampling taken after 70 years)	55.5 tC/ha	50.1 tC/ha	1) Positive liming-induced effects on soil C stocks are significantly reduced when lime is added together with key inorganic nutrient fertilizers such as N and P 2) Agricultural management practices aimed at the maximization of the hay production partly or fully negate the C sequestration potential of the grassland ecosystem as a whole
					Scenario combination of lime and N/P mineral fertilizers: 100 kg N/ha/year 35 kg P/ha/year 936 kg Ca/ha/year[1]	44.0 tC/ha	50.1 tC/ha	
Study 10 Šimek et al. (1999)	Libějovice (Czech Republic)	Sandy loam (cropland)	0-15 cm	1) Type of product not specified	1) 5 t/ha every 4 years 2) Lime is applied with manure (40 t/ha every 4 years) and inorganic fertilizers (160 N, 120 P_2O_5, 160 K_2O) 3) Sampling was made after 20 years	10.4 g/kg	9.4 g/kg[2] (7.1 g/kg)	1) The C_{org} content is greater for all the fertilized plots (with lime or not) compared to the un-limed plots 2) Increments of C were probably due to: - C addition from manure; - the increment of plant yield 3) The application of lime in combination with mineral fertilizers increases
	Jaroměřice (Czech Republic)	Loam (cropland)				11.8 g/kg	11.4 g/kg (10.0 g/kg)	

Literature source	Geographical site	Type of soil and land use	Investigated soil horizon	Liming application		TOC (g/kg) or SOC stocks (t/ha)		Comments and conclusions
				Type of product	Amount (t/ha)	Limed plot	Un-limed plot	
	Lípa (Czech Republich)	Sandy loam (cropland)				12.0 g/kg	10.9 g/kg (10.2 g/kg)	OC concentrations with respect to the addition of mineral fertilizers only (4-11% increase)
	Horažd'ovice (Czech Republic)	Sandy loam (cropland)				11.0 g/kg	10.5 g/kg (10.2 g/kg)	
Study 11 Paradelo et al. (2015)	Versailles (France)	Luvisol soil Bare fallow	0-20 cm	CaO	9 t/ha Sampling was taken after 80 years	1.5 t/ha	1.41 t/ha	1) Limed plots showed slightly higher SOC stocks than un-limed plots. In limed plots the aggregate stability was higher and the macrostructure better developed 2) The C protected by the gain in structure due to liming corresponded to a small gain in SOC stock

[1] Applied as Ca_3PO_4. In the same treatment the amount of lime was not reduced. [2] The first value refers to an un-limed fertilized soil (manure and inorganic fertilizers); the value within brackets refers to an un-limed, un-fertilized soil.

ANNEX D – CARBONATION OF CEMENT

D.1 INTRODUCTION

Cement is globally one of the most used construction materials with a wide range of applications. The most common is the Ordinary Portland Cement (OPC) or CEM I as defined by the European norm EN 197-1, that standardizes CEM I composition in 95%-100% of clinker and the remaining part of minor additional constituents. Clinker is a basic material for cement, produced from grinded limestone and clay as described below. Thus, lime in clinker is obtained from limestone in the cement production plant. In addition to CEM I, the norm EN 197-1 standardizes other 26 cement products whose clinker content is partly substituted by granulated blast furnace slag, pozzolanic materials, fly ashes, burnt shale, limestone, silica fume or a mix of them.

The main steps of dry cement production are represented in Figure D.1. The raw materials (limestone and clay) extracted from quarries are crushed and milled in order to obtain a fine powder called "raw meal". Then, the raw meal is pre-heated to 900°C through recovering the thermal energy of the hot kiln exhaust gases, typically by means of a cyclone tower. Subsequently, the hot raw meal is fed to a rotary kiln where the temperature reaches about 1450°C in order to melt the meal into clinker through chemical and physical reactions. The obtained clinker is then cooled, ground and blended with gypsum in order to control the setting time of the cement. Other components can be added to cement to deliver some specific properties, such as fly ash (FA), blast furnace slag (BFS) or fine limestone (Schorcht et al., 2013; IEA,2018).

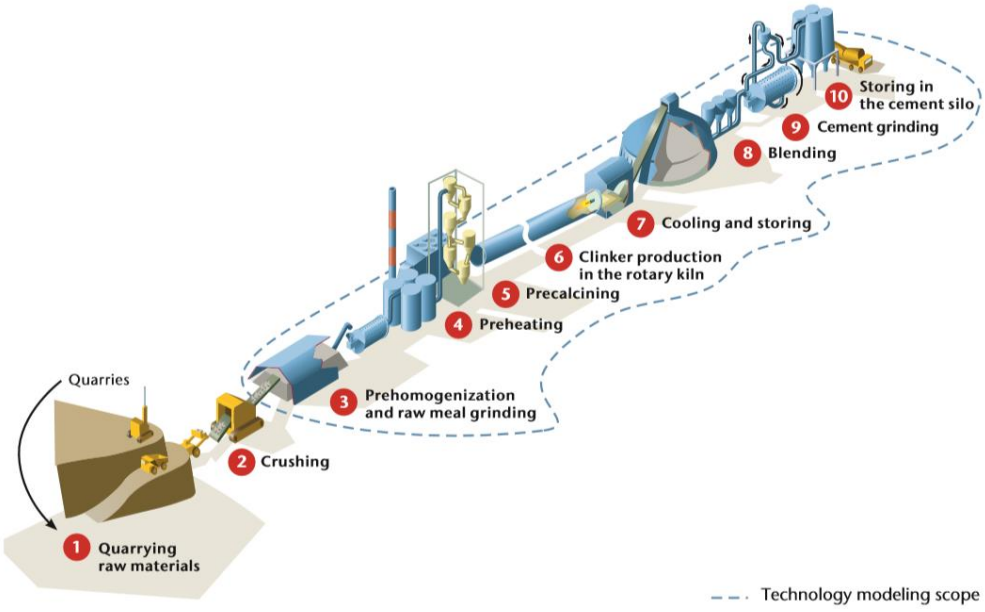


Figure D.1. Main phases of cement manufacturing (IEA,2018).

Among the reactions that occur in the kiln, the calcination of limestone [Reaction D.1] is one of the most important. The product of the calcination is quicklime or calcium oxide (CaO) obtained from the calcium carbonate ($CaCO_3$), with the release of carbon dioxide (CO_2). After CaO is formed, it reacts with Si and Al and Fe phases to form calcium silicates, calcium aluminate and calcium alumino-ferrites. The calcium content

in cement is generally expressed as calcium oxide CaO, and the same for the other elements (e.g. SiO_2, Al_2O_3, Fe_2O_3).

$$CaCO_3 \rightarrow CaO + CO_2 \quad [D.1]$$

Since calcination is highly endothermal, a huge amount of energy is delivered at that stage of the process (generally referred to as precalcination), the rest being used in the rotary kiln for clinkering. In 2014, 59% of the thermal energy necessary for cement production in Europe comes from conventional fossil fuels, while 37% from alternative fuels (e.g. tyres and plastics) and 4% from biomass (CEMBUREAU, 2016). As a result, cement production is one of the most CO_2 emitting activity, causing 8% of the global CO_2 emissions (Andrew, 2018). The *Best Available Techniques (BAT) Reference Document for the Production of Cement, Lime and Magnesium Oxide* stated that calcination CO_2 emission accounts for 62% of the cement production CO_2 emission, while the emission from fuels accounts for 38% (Schorcht et al., 2013).

Cement is used as binder in the construction materials: cement mortar and concrete. Cement mortar is composed of water, cement and fine aggregates, i.e. sand, and is used as bonding agent between building materials or for rendering of surfaces, while concrete is a mix of cement, water, fine and coarse aggregates like sand and gravel. Cement is used in steel reinforced concrete where hydrated lime ($Ca(OH)_2$ also called portlandite) is protecting the steel from the corrosion. During the hydration and setting of cement phases with water, some hydrated lime is generated which creates an alkaline layer (pH: 12 – 13) that forms a passivation layer around the steel. This protective film is endangered when ambient CO_2 diffuses in pore water of concrete and carbonation takes place, i.e. hydrated lime reacts with CO_2 and calcium carbonate precipitates [Reaction D.2]. In this way, carbonation of hydrated lime causes pH to drop below 9 and steel corrosion to occur, due to dissolution of the passivation layer (Durán-Herrera et al., 2013). Reinforcing steel corrosion affects the durability of the product. Another cause of steel corrosion due to pH decrease is chloride ion attack because of sea water and/or deicing salts (Gahari et al., 2016). However, natural carbonation allows to capture part of the CO_2 released during calcination in cement plant throughout the service life of the material.

$$Ca(OH)_2 + CO_2 \rightarrow CaCO_3 + H_2O \quad [D.2]$$

D.2 LITERATURE ASSESSMENT FOR CEMENT CARBONATION: MATERIAL AND METHODS

In the existing literature some studies are available about carbonation of cement (see Table D.1 for the complete list). Most of the studies assessed the carbonation of concrete, its consequences on concrete strength and its effects on life service of the reinforcing steel. In more recent studies (Ashraf, 2016; Andersson et al., 2019; McCord et al., 2018; McDonald et al., 2019; Xi et al., 2016) the carbonation of concrete is analysed as an option for capturing atmospheric CO_2.

From a total of 19 publications, seven studies (Andersson et al., 2019; Borges et al. 2010; Gajda, 2001; Jacobsen and Jahren, 2002; Pade and Guimaraes, 2007; Van den Heede et al., 2018; Xi et al., 2016) reported

a measure of the potential carbonation of concrete, as a percentage of the hydrated lime in concrete that is converted into calcium carbonate, or of the CO_2 calcination emission.

Table D.1. List of consulted documents for the literature review about the use of lime in concrete.

Peer-reviewed papers

1. Andersson et al., 2019. *Carbonation as a method to improve climate performance for cement based material*. In: Cement and Concrete Research, 124, 105819. DOI:10.1016/j.cemconres.2019.105819
2. Ashraf, 2016. *Carbonation of cement-based materials: Challenges and opportunities.* In: Construction and Building Materials, 120, 558-570. DOI: 10.1016/j.conbuildmat.2016.05.080
3. Borges et al., 2010. *Carbonation of CH and C-S-H in composite cement pastes containing high amounts of BFS.* In: Cement and Concrete Research, 40, 284-292. DOI: 10.1016/j.cemconres.2009.10.020
4. Durán-Herrera et al., 2013. *Accelerated and natural carbonation of concretes with internal curing and shrinkage /viscosity modifiers.* In: Materials and Structures. DOI: 10.1617/s11527-013-0226-y
5. Gajda, 2001. *Absorption of atmospheric carbon dioxide by Portland cement*. In: Portland Cement Association.
6. Ghahari et al., 2016. *An accelerated test method of simultaneous carbonation and chloride ion ingress: durability of silica fume concrete in severe environments.* In: Advances in Materials Science and Engineering, 2016, 1650979. DOI: 10.115/2016/1650979
7. Hussain et al., 2016. *An experimental investigation of accelerated carbonation on properties of concrete.* In: Engineering Journal, 20(2),30-38. DOI: 10.4186/ej.2016.20.2.29
8. McCord et al., 2018. *Mineralization Worked Examples for the TEA and LCA Guidelines for CO_2 Utilization*. In: CO2Chem Media and Publishing Ltd. DOI: 10.3998/2027.42/147467
9. McDonald et al., 2019. *A New, Carbon-Negative Precipitated Calcium Carbonate Admixture (PCC-A) for Low Carbon Portland Cements*. In: Materials, 12, 554. DOI:10.3390/ma12040554
10. Neves et al., 2012. *A method for the use of accelerated carbonation tests in durability design.* In: Construction and Building Materials, 36, 585-591. DOI: 10.1016/j.conbuildmat.2012.06.028
11. Pade and Guimaraes, 2007. *The CO_2 uptake of concrete in a 100 year perspective.* In: Cement and Concrete Research, 37, 1348-1356. DOI: 10.1016/j.cemconres.2007.06.009
12. Van den Heede et al., 2019. *Accelerated and natural carbonation of concrete high volume of fly ash: chemical, mineralogical and microstructural effects*. In: Royal Society open science, 6: 181665. DOI: 10.1098/rsos.181665
13. Véleva et al., 1998. *The corrosion performance of steel and reinforced concrete in a tropical humid climate.* In: Corrosion Reviews, 16(3), 235-284.
14. Visser, 2012. *Accelerated carbonation testing of mortar with supplementary cementing materials – Limitation of the acceleration due to drying.* In: HERON, 57(3), 231-247.
15. Xi et al., 2016. *Substantial global carbon uptake by cement carbonation.* In: Nature geoscience, 9, 880-883. DOI: 10.1038/NGEO2840
16. Yan et al., 2018. *Difference between natural and accelerated carbonation of concrete at 2% CO_2 and 20% CO_2.* In: Romanian Journal of Materials 2018, 48(1), 70-75.
17. You et al., 2013. *Effects of accelerated carbonation on physical properties of mortar.* In: Journal of Asian Architecture and Building Engineering, 13(1), 217-221.

Meeting proceedings or seminars

18. Jacobsen and Jahren, 2002. *Binding of CO_2 by carbonation of Norwegian OPC concrete*. In: CANMET/ACI International Conference on Sustainability and Concrete Technology, Lyon, November, 2002.
19. Moreno et al., 2011. *Accelerated carbonation of concrete specimens employing high-absorption limestone aggregate.* In: XII DBMC International Conference on Durability of Building Materials and Components, Porto – Portugal, April 12th-15th, 2011.

D.3 FUNDAMENTALS OF CEMENT CARBONATION

Carbonation of hydrated lime generated during cement production occurs naturally throughout the life of the material, due to the contact with CO_2 in the ambient air. The mechanism of carbonation involves many reactions. At first, CO_2 diffuses in the water present in the pore of the concrete and forms carbonic acid H_2CO_3 [Reaction D.3] that dissociates in HCO_3^- and CO_3^{2-}, whose concentrations depend on the pH of pore water. During the dissociation, H^+ ions are released and, as a result, the pH decreases. Then, calcium hydroxide dissolves in Ca^{2+} and hydroxyl ions. The released Ca^{2+} reacts with CO_3^{2-} forming $CaCO_3$ that precipitates, while hydroxyl ions buffer the H^+ released [Reaction D.4]. In this way, the pore water solution has constant pH. Since ambient CO_2 continues to diffuse in pore water, the pH lowers causing the further dissolution of calcium hydroxide. In addition to calcium hydroxide, calcium silicate hydrates (C-S-H) release calcium oxide which also leads to calcium carbonate [Reaction D.5] (Visser, 2012; Hussain, 2016). Indeed, Yan et al. (2018) found in their experiments that the calcium carbonate generated is more than the calcium hydroxide consumed. Thus, C-S-H and other phases give an important contribution to concrete carbonation. When all the calcium available for carbonation is consumed, the CO_2 concentration in the pore water reaches a new equilibrium with CO_2 concentration at the surface. As a consequence, the pH lowers (Visser, 2012). When the pH of the pore solution drops below 9, depassivation of the steel is imminent with consequences on the durability of reinforced steel (Durán-Herrera et al., 2013). Due to the destruction of the protective passive film, steel bar is more exposed to corrosion and cracking (Gahari, 2016).

$$CO_2 + H_2O \rightarrow H_2CO_3 \quad [D.3]$$

$$Ca(OH)_2 + H_2CO_3 \rightarrow CaCO_3 + 2H_2O \quad [D.4]$$

$$CaO + H_2CO_3 \rightarrow CaCO_3 + H_2O \quad [D.5]$$

The carbonation progresses from the surface of the concrete inwards, i.e. the carbon dioxide molecules penetrate further only after all carbonatable matter is consumed. For this reason, the carbonation depth is measured, i.e. the distance from the surface to where concrete is carbonated. The carbonation depth is measured

through phenolphthalein test[40] (Visser, 2012). The evolution of carbonation depth in time is defined through the Equation D.1, where CO_2 diffusion is modelled through the Fick's law (Neves et al., 2012).

$$x = K\sqrt{t} \qquad \text{[Equation D.1]}$$

where x is the carbonation depth; K is the carbonation coefficient or the carbonation rate (mm/year$^{-1/2}$) and t is the exposure time to CO_2 (year). Neves et al. (2012) defined K as the ratio among two parameters k_a and k_e:

$$K = {k_a}/{k_e} \qquad \text{[Equation D.2]}$$

where: k_a is the parameter related to intrinsic factors (e.g. resistance to accelerated carbonation) and k_e is the parameter related to environmental factors (exposure condition, e.g. rain sheltered environment or not).

Equation D.1 is useful to evaluate the service life of reinforced steel. Indeed, the time of corrosion initiation due to the carbonation is required to be longer than the service life. Since carbonation in natural environment occurs at a slow rate due to the low CO_2 concentration (about 0.04%), accelerated carbonation approach is used in laboratory, i.e. the accelerated carbonation tests occur in an environment with CO_2 concentration higher than in the ambient air. For OPC-based materials it is found that accelerated carbonation at 3% of CO_2 concentration is similar to natural carbonation and can be used to simulate a natural carbonation scenario (Ashraf, 2016).

Other parameters like temperature and relative humidity (RH) are controlled in laboratory tests. RH within the range of 50-70% is commonly used in experiments (Ashraf, 2016). Véleva et al. (1998) found that carbonation is favourable in tropical climate places due to the high humidity and temperature. In fact, water in concrete pores is necessary to dissolve CO_2 and consequently for carbonation, but at the same time CO_2 diffusion is lower in water than in the air. Thus, CO_2 diffusion is faster when the carbonated area is dried and at the same time the non-carbonated area is saturated. Since water is released when calcium carbonate precipitates from calcium hydroxide, this water needs to evaporate. In accelerated carbonation tests, it was found that at 65% RH, the pores can sufficiently dry out to allow carbonation. With higher RH, pore drying out is much slower and reduces the carbonation rate (Visser, 2012). At the same time, concrete with lower water/cement ratio has lower carbonation rate despite the high concrete porosity and higher corrosion rate are observed at higher water/cement ratio (Moreno et al., 2011).

Another effect of carbonation is the decreased porosity of carbonated concrete, since calcium carbonate occupies more volume than calcium hydroxide. As result, carbonation has some benefits like the enhancement of compressive strength and volume safety and at the same time, the reduction of porosity, permeability and chloride ion (You et al., 2013; Ashraf, 2016; Hussain et al.,2016). Hussain et al. (2016) observed also that the concrete porosity decreases with the increase of carbonation duration.

[40] Phenolphthalein is a chemical compound used as pH indicator which changes colour at a pH of 8.2. It is red when pH is higher than 8.2, colourless if below 8.2.

Supplementary Cementitious Materials (SCM), that are commonly added to cement in order to substitute a portion of clinker, have effects on carbonation resistance as summarized in Table D.2.

Table D.2. Effects of SCMs addition on carbonation resistance of concrete (Ashraf, 2016).

Types of SCM	Carbonation resistance	Proportion (%)
Fly ash	Decreases	10-70%
Pulverized fuel ash	Decreases	0-40%
Blast furnace slag	Decreases	0-85%
Silica fume	Decreases	0-20%
	Increases	5-10%
Nano and micro silica[41]	Increases	0-5%

McCord et al. (2018) and McDonald et al. (2019) assessed the avoided CO_2 emission using lime carbonation as a CO_2 capture process. In both cases, the calcium carbonate obtained from lime and CO_2 from the flue gas of two different processes is used as cement additive. McCord et al. (2018) assessed through Life Cycle Assessment methodology the environmental impacts of producing concrete containing calcium carbonate obtained from air pollution control residues, that are rich of unreacted lime from acid gas scrubber, and flue gas CO_2 both of them from a municipal solid waste incinerator plant. The greenhouse gas (GHG) emissions are compared with the emissions from the stabilization and landfilling of the residue of incinerator air pollution control facility combined with the production of concrete blocks. As result, the GHG emissions are estimated to be reduced by 34%. McDonald et al. (2019), meanwhile, evaluated the potentiality for reducing CO_2 emission of cement production blending OPC with carbon-negative Precipitated Calcium Carbonate Admixture (PCC-A), a carbon CAPture and CONversion (CAPCON) product of the Carbon Capture Machine (CCM). The PCC-A was obtained from CO_2-rich flue gas, where CO_2 was selectively dissolved at the point of emission in aqueous alkali (NaOH) solution. The solution was then mixed with calcium-containing brine to produce the PCC-A, after filtration, drying and contaminants (NaCl) removal. The final CO_2 sequestered is 100 gCO_2 per kilogram of PCC-A. Considering that the production of one kilogram of OPC clinker emits about 950g CO_2, a cement blended with 15% of PCC-A reduces CO_2 emissions by 27% compared to OPC.

[41] Nano and micro silica fume are not considered as SCM, but these materials take part in pozzolanic reaction.

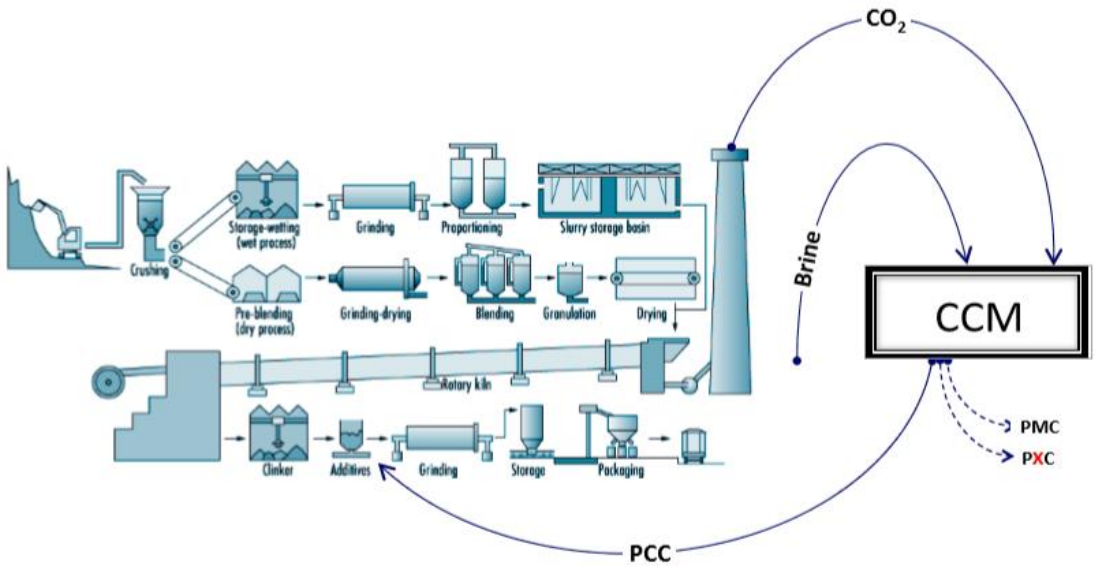


Figure D.2. Process proposed by McDonald et al. (2019) for producing blended OPC with PCC-A through Carbon Capture Machine (McDonald et al., 2019).

D.4 POTENTIAL CARBONATION RATE OF CEMENT

D.4.1 ACCELERATED CARBONATION

Borges et al. (2010) evaluated the carbonation of concrete that contains cement with Blast Furnace Slag (BFS) under accelerated conditions (5% CO_2, 60% RH and 25±5°C). The analysed samples have three different compositions, called 3S1C, 9S1C and 9S1CA. Formulation of samples 3S1C and 9S1C is 75% BFS with 25% OPC and 90% BFS with 10% OPC, respectively. 9S1CA has the same composition of 9S1C but activated with a sodium silicate solution (Na_2SiO_3). Lime content of OPC and BFS is 64.6% and 42.1%, respectively. All samples have water to solid ratio equal to 0.33. At first, some samples were cured under water for 90 days at 20°C and other samples at 60°C. Then, they were submitted to accelerated carbonation for 21 days. After 21 days, the carbonation degree is measured by means of a Thermogravimetric Analysis (TGA), i.e. the test samples were heated from 30°C to 1000°C at 10°C per minute under a nitrogen atmosphere. The weight loss was measured during heating. In the range 400-500°C, called the dehydroxylation region, the weight loss was ascribed to water evaporation as a consequence of calcium hydroxide decomposition in CaO and H_2O. The range 600-750°C is called the decarbonation region, because the weight loss was assumed only due to the CO_2 released and it corresponds to the amount of calcium hydroxide that is carbonated. At first, the initial $Ca(OH)_2$ content was estimated by heating the samples after the curing and it was assumed equal to the sum of two contributions: calcium hydroxide estimated by the weight loss generated in dehydroxilation range and calcium hydroxide estimated by the weight loss generated in decarbonation region because this calcium carbonate is generated by the carbonation of CaO in the paste during the curing time. After 21 days under accelerated carbonation, calcium hydroxide in 9S1C and 9S1CA samples are fully carbonated, while for the 3S1C samples, 59% and 51% of calcium hydroxide is carbonated when cured at 20°C and 60°C, respectively.

Van den Heede et al. (2018) evaluated through TGA the carbonation of cement with Fly Ash (FA) under accelerated carbonation – 1% (assumed similar as natural carbonation) and 10% CO_2, 60% RH, 20°C – for 16 weeks, i.e. 112 days. The analysed samples have three different compositions, called T(0.55), F50 and F40SF10, whose characteristics are summarized in Table D.3. The samples are cylindrical (diameter: 46 mm; height: 50 mm) and they were cured under water at 20±2°C for 28 days. Once the surface dries, the upper and lower surfaces of the cylinders were sealed with an impermeable aluminium tape leaving only the mantle surface for exposure. After the accelerated carbonation for 112 days, the samples were crushed into powder, that was used for assessing the carbonation degree of the samples through TGA. The samples were heated from 20°C to 1100°C at 10°C per minute under a nitrogen atmosphere. The initial $Ca(OH)_2$ content was estimated as in Borges et al. (2010). After the accelerated carbonation, the calcium hydroxide in the paste are fully carbonated for all samples. The calcium carbonate generated is higher than the calcium hydroxide consumed, because also the calcium in C-S-H takes part to carbonation, as explained in Section D.3. Then, small paste cylinders (diameter: 1-3 mm) were also subjected to natural carbonation – 0.03-0.04% CO_2, 60% RH, 20°C – for 112 days. All samples are fully carbonated also under natural carbonation except for F50 samples, where 92% of calcium hydroxide carbonates.

Table D.3. Characteristics of the samples in Van den Heede et al. (2018).

	T(0.55)	**F50**	**F40SF10**
Water to binder[42] ratio	0.55	0.35	0.35
Fly ash to binder[3] ratio	0	50	40
Silica fume to binder[3] ratio	0	0	10

D.4.2. NATURAL CARBONATION

The following studies seek to estimate the CO_2 uptake by the concrete during its lifecycle, i.e. from the production to the demolition and the crushing, expressed as a percentage of the calcination CO_2 emission, which is equal to the percentage of calcined limestone that carbonates.

The study of Pade and Guimaraes (2007) is based on theoretical work, laboratory studies, surveys and calculations based on concrete production in Nordic countries of Denmark, Iceland, Norway and Sweden. For the calculation of the CO_2 absorption by concrete, the concrete production in 2003 in Nordic countries was assumed, considering a lifetime of 100 years subdivided in 70 years of service life and 30 years of concrete disposal, i.e. demolition and crushing. Based on literature and experimental works, the main assumptions were that the CaO content in concrete is 65% and 75% of that is available for carbonation. The results are that 57%, 33%, 33% and 34% of CO_2 emitted during calcination is reabsorbed by the concrete in 100 years in Denmark, Norway, Sweden and Iceland, respectively. The difference among the countries is given by the fact that 90% of demolished concrete is crushed and recycled in Denmark. Crushing allows to expose a larger area of

[42] Binder is the solid mixture, composed of sand, gravel, OPC (CEM I 52.5 N), fly ash and silica fume.

concrete to ambient air and fosters the carbonation. Pade and Guimaraes compared their results with Gajda (2001) Jacobsen and Jahren (2002) studies. Both studies assumed that only the calcium hydroxide in concrete carbonates. Gajda estimated that 7.6% of the CO_2 emitted during calcination is reabsorbed during the life of concrete in US only from the calcium hydroxide phase without considering demolition and subsequent crushing, while Jacobsen and Jahren estimated that 16% of the CO_2 emitted during calcination is reabsorbed by concrete in Norway without surveying concrete uses. Furthermore, Jacobsen and Jahren used for calculations a hypothetical concrete element with average properties. Pade and Guimaraes instead, considered in their study the different concrete types and their different applications.

Based on experimental works and literature review, Xi et al. (2016) estimated that 17.6% of global CO_2 calcination emission is re-absorbed through carbonation during the entire lifecycle of concrete. In detail, 16.1% of the initial emissions are absorbed during the service life of concrete, 1.4% during the demolition and 0.1% during the disposal or the reuse of the concrete waste. Xi et al. assessed also that cement mortar reabsorbs 100% of calcination emission during its lifecycle, namely 97.9% during service life and 2.1% during the demolition stage. The higher carbon uptake is because mortar is applied in thin decorative layers to the exterior of building structures with larger areas exposed to the atmospheric CO_2.

Another approach for estimating the carbonation degree of concrete was presented by Andersson et al. (2019), who introduced three calculation methodologies for evaluating the annual CO_2 uptake by cement products, i.e. both concrete and mortars, during their lifetime based on many studies in literature, among them the one by Xi et al. The methodologies were built following the Intergovernmental Panel on Climate Change (IPCC) guidelines for emission inventories. The objective of the study is to include CO_2 uptake by existing cement-based products in countries emission inventories that already take into account the calcination CO_2 emissions. The simplified calculation methodology "Tier 1" assessed the annual CO_2 uptake by the existing cement products as a percentage of the annual calcination CO_2 emission, estimated at about 20%. This means that each year, 20% of the calcination annual CO_2 emission is reabsorbed by existing cement-based products, given that new cement products absorb more CO_2 than old ones. Furthermore, the linear proportionality between uptake and emission implies that when calcination emission increases in the years, also the uptake by cement increases. In addition to "Tier 1" method, other two more accurate calculation methodologies are under study.

Table D.4. Summary of the analysed literature reporting a carbonation degree for cement.

Reference	Geographical context	Type of work	Type of cement	Calcium oxide content	Carbonation condition[43]	Test duration	Carbonation degree	Notes
Borges et al. (2010)	United Kingdom	Lab-scale study	9S1C:90%BFS+ 10%OPC 3S1C:75%BFC+ 25%OPC	64.58% in OPC 42.10% in BFS	AC: 5% CO_2	21 days	100% (9S1C) 59-51% (3S1C)	Carbonation degree: % of $Ca(OH)_2$ that carbonates
Van den Heede et al. (2018)	Belgium	Lab-scale study	Cement + FA	-	AC: 1-10% CO_2 NC	112 days	100% AC; 92%-100% NC	Carbonation degree: % of $Ca(OH)_2$ that carbonates
Pade and Guimaraes (2007)	Denmark (DK); Iceland (IS); Norway (NO); Sweden (SE)	Survey and data processing	Concrete	65% in concrete	NC	100 years = 70 years of service life + 30 years of final disposal	57% DK; 33% NO and SE; 24% IS	Carbonation degree: % of CO_2 calcination that is reabsorbed
Gajda (2001)	United States	Survey and data processing	Concrete	-	NC	100 years of service life (no final disposal)	7.6%	Carbonation degree: % of CO_2 calcination that is reabsorbed
Jacobsen and Jahren (2002)	Norway	Survey and data processing	OPC	-	NC	Service life	16%	Carbonation degree: % of CO_2 calcination that is reabsorbed
Xi et al. (2016)	World	Survey and data processing	Concrete and cement mortar	-	NC	Entire life cycle	Concrete: 17.6% Cement mortar: 100%	Carbonation degree: % of CO_2 calcination that is reabsorbed
Andersson et al. (2019)	World	Survey and data processing	Concrete and cement mortar	-	NC	Entire life cycle	20%	Carbonation degree: annual uptake % of annual CO_2 calcination

[43] AC=Accelerated Carbonation; NC=Natural carbonation

D.5 CONCLUSIONS AND RECOMMENDATION ON FUTURE RESEARCH NEED FOR CEMENT CARBONATION

The carbonation process of calcium in concrete is well-known and the amount of calcium carbonate obtained can be measured through TGA. This analysis was used in the laboratory studies (Borges et al., 2010; Van den Heede et al., 2018) whose results were a full carbonation of calcium hydroxide in concrete under accelerated carbonation. But the calcium carbonate was generated during carbonation also from C-S-H. Since not all calcium phases in cement will carbonate, it would be useful to know the initial calcium content in cement components that is available for carbonation, in order to measure how much of the initial calcium in concrete carbonates and not only calcium hydroxide.

From the studies that investigated concrete carbonation during the whole lifecycle, it results that concrete can reabsorb from 17.6% (Xi et al., 2016) to 57% (Denmark case in Pade and Guimaraes, 2007) of the calcination CO_2 emission, meaning that 17.6% to 57% of calcium in the concrete is carbonated. Another result is that a relevant amount of calcium carbonate is generated when demolished concrete is crushed because a larger surface area is exposed to ambient air, that is favorable for carbonation. Further researches are necessary to evaluate the total carbonation degree by monitoring cement products along their lifecycle for a more accurate assessment the CO_2 uptake of concrete. Lastly, it should be noted that the interest for carbonation as a process for capturing and sequestering CO_2 is increasing.

REFERENCES

Andersson et al., 2019. *Carbonation as a method to improve climate performance for cement based material*. In: Cement and Concrete Research, 124, 105819. DOI:10.1016/j.cemconres.2019.105819

Andrew, 2018. *Global CO_2 emissions from cement production*. In: Earth System Science Data, 10, 195-217. DOI: 10.5194/essd-10-195-2018

Ashraf, 2016. *Carbonation of cement-based materials: Challenges and opportunities.* In: Construction and Building Materials, 120, 558-570. DOI: 10.1016/j.conbuildmat.2016.05.080

Borges et al., 2010. *Carbonation of CH and C-S-H in composite cement pastes containing high amounts of BFS.* In: Cement and Concrete Research, 40, 284-292. DOI: 10.1016/j.cemconres.2009.10.020

CEMBUREAU, 2016. *Cement, concrete & the circular economy.* Available online: https://cembureau.eu/media/1229/9062_cembureau_cementconcretecirculareconomy_coprocessing_2016-09-01-04.pdf

Durán-Herrera et al., 2013. *Accelerated and natural carbonation of concretes with internal curing and shrinkage /viscosity modifiers.* In: Materials and Structures. DOI: 10.1617/s11527-013-0226-y

Gajda, 2001. *Absorption of atmospheric carbon dioxide by Portland cement*. In: Portland Cement Association.

Ghahari et al., 2016. *An accelerated test method of simultaneous carbonation and chloride ion ingress: durability of silica fume concrete in severe environments.* In: Advances in Materials Science and Engineering, 2016, 1650979. DOI: 10.115/2016/1650979

Hussain et al., 2016. *An experimental investigation of accelerated carbonation on properties of concrete.* In: Engineering Journal, 20(2),30-38. DOI: 10.4186/ej.2016.20.2.29

IEA, 2018. *Technology Roadmap: Low-Carbon Transition in the Cement Industry.* Available online: https://www.wbcsd.org/Sector-Projects/Cement-Sustainability-Initiative/Resources/Technology-Roadmap-Low-Carbon-Transition-in-the-Cement-Industry

Jacobsen and Jahren, 2002. *Binding of CO_2 by carbonation of Norwegian OPC concrete*. In: CANMET/ACI International Conference on Sustainability and Concrete Technology, Lyon, November, 2002.

McCord et al., 2018. *Mineralization Worked Examples for the TEA and LCA Guidelines for CO_2 Utilization*. In: CO2Chem Media and Publishing Ltd. DOI: 10.3998/2027.42/147467

McDonald et al., 2019. *A New, Carbon-Negative Precipitated Calcium Carbonate Admixture (PCC-A) for Low Carbon Portland Cements*. In: Materials, 12, 554. DOI:10.3390/ma12040554

Moreno et al., 2011. *Accelerated carbonation of concrete specimens employing high-absorption limestone aggregate.* In: XII DBMC International Conference on Durability of Building Materials and Components, Porto – Portugal, April 12th-15th, 2011.

Neves et al., 2012. *A method for the use of accelerated carbonation tests in durability design.* In: Construction and Building Materials, 36, 585-591. DOI: 10.1016/j.conbuildmat.2012.06.028

Pade and Guimaraes, 2007. *The CO_2 uptake of concrete in a 100 year perspective.* In: Cement and Concrete Research, 37, 1348-1356. DOI: 10.1016/j.cemconres.2007.06.009

Frauke Schorcht et al., 2013. *Best Available Techniques (BAT) Reference Document for the Production of Cement, Lime and Magnesium Oxide*. In: Joint Research Centre (JRC) Reference Reports. Available online: https://eippcb.jrc.ec.europa.eu/sites/default/files/2019-11/CLM_Published_def_0.pdf

Van den Heede et al., 2019. *Accelerated and natural carbonation of concrete high volume of fly ash: chemical, mineralogical and microstructural effects*. In: Royal Society open science, 6: 181665. DOI: 10.1098/rsos.181665

Véleva et al., 1998. *The corrosion performance of steel and reinforced concrete in a tropical humid climate.* In: Corrosion Reviews, 16(3), 235-284.

Visser, 2012. *Accelerated carbonation testing of mortar with supplementary cementing materials – Limitation of the acceleration due to drying.* In: HERON, 57(3), 231-247.

Xi et al., 2016. *Substantial global carbon uptake by cement carbonation.* In: Nature geoscience, 9, 880-883. DOI: 10.1038/NGEO2840

Yan et al., 2018. *Difference between natural and accelerated carbonation of concrete at 2% CO_2 and 20% CO_2.* In: Romanian Journal of Materials 2018, 48(1), 70-75.

You et al., 2013. *Effects of accelerated carbonation on physical properties of mortar.* In: Journal of Asian Architecture and Building Engineering, 13(1), 217-221.